

Heat and Mass Transfer

Series Editors

Dieter Mewes
Franz Mayinger

For further volumes:
<http://www.springer.com/series/4247>

De-Yi Shang

Free Convection Film Flows and Heat Transfer

Models of Laminar Free Convection
with Phase Change for Heat and Mass
Transfer Analysis

Second Edition

 Springer

De-Yi Shang, Dr. (Tsinghua Univ., China)
Ottawa, ON
Canada
deyishang@yahoo.ca

ISSN 1860-4846 ISSN 1860-4854 (electronic)
ISBN 978-3-642-28982-8 ISBN 978-3-642-28983-5 (eBook)
DOI 10.1007/978-3-642-28983-5
Springer Heidelberg New York Dordrecht London

Library of Congress Control Number: 2012946183

© Springer-Verlag Berlin Heidelberg 2012

This work is subject to copyright. All rights are reserved by the Publisher, whether the whole or part of the material is concerned, specifically the rights of translation, reprinting, reuse of illustrations, recitation, broadcasting, reproduction on microfilms or in any other physical way, and transmission or information storage and retrieval, electronic adaptation, computer software, or by similar or dissimilar methodology now known or hereafter developed. Exempted from this legal reservation are brief excerpts in connection with reviews or scholarly analysis or material supplied specifically for the purpose of being entered and executed on a computer system, for exclusive use by the purchaser of the work. Duplication of this publication or parts thereof is permitted only under the provisions of the Copyright Law of the Publisher's location, in its current version, and permission for use must always be obtained from Springer. Permissions for use may be obtained through RightsLink at the Copyright Clearance Center. Violations are liable to prosecution under the respective Copyright Law.

The use of general descriptive names, registered names, trademarks, service marks, etc. in this publication does not imply, even in the absence of a specific statement, that such names are exempt from the relevant protective laws and regulations and therefore free for general use.

While the advice and information in this book are believed to be true and accurate at the date of publication, neither the authors nor the editors nor the publisher can accept any legal responsibility for any errors or omissions that may be made. The publisher makes no warranty, express or implied, with respect to the material contained herein.

Printed on acid-free paper

Springer is part of Springer Science+Business Media (www.springer.com)

Preface to the First Edition

Welcome to *Free Convection Film Flows and Heat Transfer*! Free convection film flows occur in many industrial processes. However, engineers still have to deal with many unresolved problems. This book systematically summarizes my recent research results that have been referred to and cited by many other researchers in this field. The purpose of this book is to provide a practical guide to university students, graduate students, design engineers, researchers and scientists who wish to further understand the characteristics of *Free Convection Film Flows and Heat Transfer*. I hope that this book will serve as a useful tool for them, as well as a guide to future research.

This book includes three related parts: (1) accelerating free convective boundary layers of Newtonian fluids; (2) accelerating free convection film boiling and condensation of Newtonian fluids, (3) accelerating film flows of non-Newtonian power-law fluids. These phenomena are all caused by buoyancy or gravity flows, and can be summed up in terms of the free convection film flows. In addition, the free convection film flows of Newtonian fluids can be taken as a special case of non-Newtonian power-law fluids.

In this book, I present my recent studies of *free convection film flows and heat transfer* on both vertical and inclined plates. Because of a lack of related books presenting the effects of variable thermophysical properties on heat and mass transfer, these effects are especially emphasized in this book with respect to free convection, free convection film boiling, and free convection film condensation of Newtonian fluids. A system of models for the treatment of variable thermophysical properties is introduced in this book, with an innovative temperature parameter method for gases and temperature-dependent models for liquids. A novel system of analysis and transformation models with an innovative velocity component method is applied throughout the book. This is a better alternative to the traditional Falkner–Skan-type transformation. The new analytical system and models lead to simplification for treatment of variable thermophysical properties of fluids, as well as hydrodynamics and heat transfer analysis. A system of reliable and rigorous computations solving the problems for two-point or three-point boundary values is provided in this book. In the analyses and calculations of the first two parts of this

book, I focus on clarifying the effects of variable thermophysical properties on heat and mass transfer. A system of numerical solutions is formulated to predict heat and mass transfer simply and reliably. In the last part of this book, heat and mass transfer of the accelerating film flows of Newtonian fluids are extended to that of non-Newtonian power-law fluids. So far, there has been a lack of such information and analysis for advanced heat and mass transfer of accelerating film flows of non-Newtonian power-law fluids.

In addition, a collection of novel terminologies has arisen in this book, e.g., *velocity component method, temperature parameter method, thermal conductivity parameter, viscosity parameter, specific heat parameter, overall temperature parameters, thermal physical property factors, boundary temperature ratio, buoyancy factor, wall superheated grade, wall subcooled grade, reference wall subcooled grade vapor bulk superheated grade, liquid bulk subcooled grade, computation for three-point boundary value problem, temperature gradient on the wall, velocity components at the interface, vapor film thickness, liquid film thickness, mass flow rate through the interface, mass flow rate parameter, Non-Newtonian power-law fluids, length of boundary layer region, boundary layer thickness, local Prandtl number, critical local Prandtl number, critical boundary layer thickness, and so on*. These terminologies reflect the recent developments on my study of *free convection film flows and heat transfer*. Therefore, I strongly urge readers to pay particular attention to the special physical significance of these terminologies. Readers will find them beneficial to understanding the essence of this book.

I am greatly indebted to Professor B.X. Wang, Academician of Chinese Academy of Science, and member of the Executive Committee of the International Center for Heat and Mass Transfer, who was my guide Professor for my Ph.D. studies of Tsinghua University, China. The recent developments devoted to Part 1 and Part 2 of this book relied on our long-term research cooperation. In addition, he carefully proofread the second chapter of this book and provided many valuable suggestions to the whole book. He even suggested the title of this book.

I am very grateful to Professor H. I. Andersson, Department for Energy and Process Engineering, Norwegian University of Science and Technology, Norway, for his highly effective cooperation related to the research developments shown in Part 3 of this book. As a distinguished researcher in the field of accelerating film flows of non-Newtonian fluids, his erudite and honorable character deeply impressed me. At the same time, I gratefully acknowledge the Norwegian Research Council for awarding me the very prestigious title of international scientist and providing financial support for my extensive research there in cooperation with Professor Andersson.

In addition, many friends and colleagues have contributed to this book. Here, I would particularly like to thank Professor Liangcai Zhong, Northeastern University, China, as well as some of my previous students, notably Yu Quan, Yang Wang, Yue Yuan, Hongyi Wang and Li Ren. They will see their contributions presented in the book. Without their collaborative research efforts this book would not have been possible.

I would like to offer my sincere gratitude to Professor Hongtan Liu, Department of Mechanical and Aerospace Engineering, University of Miami, USA, and Professor Ben Q. Li, School of Mechanical and Materials Engineering, Washington State University, USA. As good friends in my academic circles in North America, their warm encouragement gave me the full confidence to complete this book.

I would like to thank my respectable friend, Professor Pran Manga, School of Management, Department of Economy, University of Ottawa, who spent time going through parts of the manuscript. Owing to his generous help, this book could be completed in time.

Last and most of all, I offer a special word of thanks to my wife, Shihua Sun. During most of the past one and half years when I devoted to writing this book, she provided the loving family environment that offered me the tranquility and peace of mind that made writing it possible. This book is dedicated to her.

January, 2006

De-Yi Shang

Preface to the Second Edition

In the 5 years since the first edition of this book was published, its second edition has been published. During the past 5 years, we reported our extensive investigation results on heat and mass transfer of laminar free convection film condensation of vapour–gas mixture, with the following research developments: (i) a complete similarity mathematical model for convenient analysis and simultaneous numerical solution; (ii) a complete method for treatment of temperature- and concentration-dependent variable physical properties of vapour–gas mixture; (iii) an available method and procedure to resolve the challenge associated with obtaining the interfacial vapour saturations temperature; (iv) a system of analysis and calculation results on velocity and temperature fields, as well as heat and mass transfer of laminar free convection film condensation of vapour–mass mixture. Beyond my expectation, these new research developments are paid a particular attention by the “Global Thermal Fluids Central” who sent me a congratulations letter on the inclusion of my biographical sketch in the “Who’s Who in Thermal-Fluids”. These research developments have been collected in the existing second edition.

In addition, with an additional part “Theoretical Foundation”, a particular emphasis is laid on the theoretical description in the second edition. Two additional chapters are involved in this part. They are “New similarity analysis method for laminar free convection boundary layer and film flows” and “New Method for Treatment of Variable Physical Properties”. In the former chapter, a system of detailed theoretical analysis and derivation is provided for creation of the new similarity method and construction of the complete theoretical model. In the latter chapter, an advanced method and some comprehensive models are reported for treatment of temperature-dependent physical properties of gas and liquid, as well as concentration- and temperature-dependent physical properties of vapour–gas mixture. Since these models for treatments of variable physical properties are based on the typical experimental values, they will guarantee the research results provided in this book have the practical application values.

Furthermore, during the work on second edition of the book, a series of significant work was done for serious examination of the system of numerical results, and careful modification of the system of formulated equations proposed for

practical and reliable prediction of heat and mass transfer. Then, I expect the second edition would be obviously improved book based on its first edition. I welcome the comments on any aspect of it.

At last, I have found that it is necessary to change the expression on the author name of this book from “Deyi Shang” to “De-Yi Shang”, in order to match that in my numerous other publications. Although both of them are definitely same expression in Chinese Phonetic Alphabet, they have caused a big confusion for identification in English.

October, 2011

De-Yi Shang

Contents

1	Introduction	1
1.1	Scope	2
1.2	Application Backgrounds	3
1.3	Previous Developments of the Research	4
1.3.1	Laminar Free Convection Boundary Layers of Newtonian Fluids	4
1.3.2	Laminar Free Convection Film Boiling of Liquid	5
1.3.3	Laminar Free Convection Film Condensation of Pure Vapour	6
1.3.4	Laminar Free Convection Film Condensation of Vapour–Gas Mixture	7
1.3.5	Gravity-Driven Film Flow of Non-Newtonian Power-Law Fluids	7
1.4	Challenges Associated with Investigations of Laminar Free Convection and its Multi-phase Film Flows	9
1.4.1	Appropriate Theoretical Analysis Method	9
1.4.2	Consideration of Variable Physical Properties	9
1.4.3	Laminar Free Convection Boundary Layer	10
1.4.4	Laminar Free Convection Film Condensation and Boiling	10
1.4.5	Laminar Free Convection Film Condensation of Vapor–Gas Mixture	11
1.5	Developments in Recent Research	11
1.5.1	A New Similarity Analysis Method	12
1.5.2	A New System of Method on Treatment of Variable Physical Properties	13

- 1.5.3 Laminar Free Convection Boundary Layer of Gases with Consideration of Variable Physical Properties 14
- 1.5.4 Laminar Free Convection Boundary Layer of Liquids with Consideration of Variable Physical Properties 14
- 1.5.5 Laminar Free Convection Film Boiling and Film Condensation with Consideration of Variable Physical Properties 15
- 1.5.6 Laminar Free Convection Film Condensation of Vapor–Gas Mixture with Consideration of Variable Physical Properties 15
- 1.5.7 Hydrodynamics and Heat Transfer of Boundary Layer and Film Flows of Non-Newtonian Power-Law Fluids 17
- 1.5.8 Experimental Measurements of Velocity Field in Boundary Layer 18
- 1.6 Questions 19
- References 19

Part I Theoretical Foundation

- 2 Basic Conservation Equations for Laminar Free Convection 27**
 - 2.1 Continuity Equation 27
 - 2.2 Momentum Equation (Navier–Stokes Equations) 29
 - 2.3 Energy Equation 33
 - 2.4 Basic Equations of Laminar Free Convection Boundary Layer 37
 - 2.4.1 Continuity Equation 37
 - 2.4.2 Momentum Equations (Navier–Stokes Equations) 38
 - 2.4.3 Energy Equations 41
 - 2.5 Summary 44
 - 2.6 Exercises 44
- 3 Review of Falkner–Skan Transformation for Fluid Laminar Free Convection. 45**
 - 3.1 Introduction 45
 - 3.2 Falkner–Skan Transformation Related to Governing Equations Under Boussinesq Approximation 46
 - 3.3 Falkner–Skan Transformation Related to Governing Equations with Consideration of Variable Physical Properties 47

3.4	Limitations of the Falkner–Skan Type Transformation	49
3.5	Questions	50
	References	50
4	New Similarity Analysis Method for Laminar Free Convection Boundary Layer and Film Flows	53
4.1	Introduction	53
4.2	Governing Equations of Fluid Laminar Free Convection	54
4.3	Derivation on Dimensionless Physical Parameters	55
4.3.1	Select Whole Physical Variables Related to the Physical Phenomena	55
4.3.2	Select Basic Dimension System	56
4.3.3	Determine the Dimensionless Similarity Parameters	56
4.4	Investigation of Similarity Variables on Hydrodynamics	59
4.5	An Application Example of the New Similarity Analysis Method	63
4.5.1	Similarity Transformation of Eq. (4.1)	63
4.5.2	Similarity Transformation of Eq. (4.2)	64
4.5.3	Similarity Transformation of Eq. (4.3)	66
4.6	Summary	69
4.7	Remarks	69
4.8	Exercises	70
	References	71
5	New Method for Treatment of Variable Physical Properties	73
5.1	Introduction	74
5.2	Treatment of Temperature-Dependent Physical Properties of Gas	75
5.2.1	Temperature Parameter Method	75
5.2.2	For Monatomic and Diatomic Gases, Air and Water Vapour	76
5.2.3	For Polyatomic Gas	76
5.3	Treatment of Concentration- and Temperature-Dependent Physical Properties of Vapour–Gas Mixture	78
5.3.1	For Density	78
5.3.2	For Other Physical Properties	79
5.4	Treatment of Temperature-Dependent Physical Properties of Liquids	79
5.5	Physical Property Factor	79
5.5.1	For Gases	80
5.5.2	For Liquids	82
5.5.3	For Vapour–Gas Mixture	83

5.6	Summary	86
5.7	Remarks	86
5.8	Questions.	90
	References	91

Part II Laminar Free Convection with Consideration of Coupled Effects of Variable Physical Properties

6	Heat Transfer of Laminar Free Convection of Monatomic and Diatomic Gases, Air, and Water Vapor	95
6.1	Introduction	95
6.2	Governing Partial Differential Equations	97
6.3	Similarity Transformation of the Governing Equations	98
	6.3.1 Dimensionless Similarity Variables Based on the New Similarity Analysis Method	98
	6.3.2 Similarity Transformation of the Governing Equations	98
6.4	Heat Transfer Analysis	104
6.5	Numerical Results.	105
	6.5.1 Treatment of Variable Physical Properties	105
	6.5.2 Numerical Results.	107
6.6	Wall Dimensionless Temperature Gradient	110
6.7	Practical Prediction Equations on Heat Transfer.	111
6.8	Effect of Variable Physical Properties on Heat Transfer	112
6.9	Heat Transfer Under Boussinesq Approximation.	113
6.10	Summary	114
6.11	Remarks	114
6.12	Calculation Examples	114
6.13	Exercises	118
	References	118
7	Heat Transfer of Laminar Free Convection of Polyatomic Gas	121
7.1	Introduction	121
7.2	Variable Physical Properties of Polyatomic Gases.	122
7.3	Governing Differential Equations and Their Similarity Transformation	123
7.4	Treatment of Physical Property Factors	128
7.5	Heat Transfer Analysis	128
7.6	Numerical Solutions	129
7.7	Dimensionless Wall Temperature Gradient	133
7.8	Practical Prediction Equations on Heat Transfer.	136
7.9	Effect of Variable Physical Properties on Heat Transfer	137
7.10	Heat Transfer Under Boussinesq Approximation.	137

7.11	Summary	138
7.12	Remarks	141
7.13	Calculation Examples	141
7.14	Exercises	143
	References	144
8	Heat Transfer on Liquid Laminar Free Convection	145
8.1	Introduction	145
8.2	Governing Partial Differential Equations	147
8.3	Similarity Variables	147
8.4	Similarity Transformation	148
8.5	Treatment of Variable Physical Properties	150
	8.5.1 Variable Physical Properties of Liquids	150
	8.5.2 Physical Property Factors	150
8.6	Heat Transfer Analysis	151
8.7	Numerical Solutions	152
8.8	Approximation Equation on Wall Dimensionless Temperature Gradient	155
8.9	Approximation Equations on Heat Transfer	156
8.10	Summary	157
8.11	Remarks	159
8.12	Calculation Examples	159
8.13	Exercises	162
	References	162
9	Experimental Measurements of Free Convection with Large Temperature Difference	165
9.1	Introduction	165
9.2	Experimental Measurements of Velocity Field for Air Laminar Free Convection	167
	9.2.1 Experimental Devices and Instruments	167
	9.2.2 Measurement Results	168
	9.2.3 Governing Equations	169
	9.2.4 The Numerical Solutions	171
9.3	Experimental Measurements of Velocity Field for Water Laminar Free Convection	172
	9.3.1 Main Experimental Apparatus	172
	9.3.2 The Results of Experiment	173
	9.3.3 Governing Equations	174
	9.3.4 Numerical Solutions	178
9.4	Remarks	181
9.5	Questions	185
	References	185

10 Identical Laminar Free Convection for Inclined and Vertical Cases 187

10.1 Introduction 187

10.2 Fluid Laminar Free Convection on Inclined Plate 188

 10.2.1 Physical Model and Basic Equations 188

 10.2.2 Similarity Transformation of the Basic Equations 189

 10.2.3 Relationships of Momentum, Heat, and Mass Transfer Between Inclined and Vertical Cases 191

10.3 Gas Laminar Free Convection on Inclined Plate 194

10.4 Summary 200

10.5 Remarks 201

10.6 Calculation Example 201

10.7 Question 204

10.8 Exercise 204

References 210

Part III Laminar Free Convection Film Boiling and Condensation with Consideration of Coupled Effect of Variable Physical Properties

11 Complete Mathematical Models of Laminar Free Convection Film Boiling of Liquid 215

11.1 Introduction 215

11.2 Governing Partial Differential Equations 216

 11.2.1 For Vapor Film 217

 11.2.2 For Liquid Film 217

 11.2.3 For Boundary Conditions 217

11.3 Similarity Variables 218

 11.3.1 For Vapor Film 218

 11.3.2 For Liquid Film 219

11.4 Governing Ordinary Differential Equations 219

 11.4.1 For Vapor Film 219

 11.4.2 For Liquid Film 220

 11.4.3 For Boundary Conditions 221

11.5 Identical Mathematical Models of Laminar Free Convection Film Boiling of Saturated or Subcooled Liquid 221

11.6 Remarks 222

11.7 Exercises 223

References 236

12 Velocity and Temperature Fields of Laminar Free Convection

Film Boiling of Liquid 239

12.1 Introduction 239

12.2 Treatment of Variable Physical Properties 240

 12.2.1 For Variable Physical Properties of Vapor Film 240

 12.2.2 For Physical Property Factors of Vapor Film 240

 12.2.3 For Variable Physical Properties of Liquid Film 241

 12.2.4 For Physical Property Factors of Liquid Film 241

12.3 Numerical Calculation 242

 12.3.1 Calculation Procedure 242

 12.3.2 Numerical Results 242

12.4 Variation of Velocity and Temperature Fields 243

 12.4.1 For Velocity Fields of Vapour Film 243

 12.4.2 For Temperature Fields of Vapor Film 243

 12.4.3 For Velocity Fields of Liquid Film 243

12.5 Remarks 248

12.6 Exercises 249

References 249

13 Heat and Mass Transfer of Laminar Free Convection

Film Boiling of Liquid 251

13.1 Introduction 251

13.2 Heat Transfer Analysis 252

13.3 Wall Dimensionless Temperature Gradient 254

13.4 Practical Prediction Equations on Boiling Heat Transfer 257

13.5 Mass Transfer Analysis 259

13.6 Mass Flow Rate Parameter 261

 13.6.1 Vapor Film Thickness 261

 13.6.2 Interfacial Velocity Components 262

 13.6.3 Mass Flow Rate Parameter 263

13.7 Practical Prediction Equation on Boiling Mass Transfer 264

13.8 Summary 264

13.9 Remarks 271

13.10 Calculation Examples 272

13.11 Exercises 278

References 278

14 Complete Mathematical Model of Laminar Free Convection

Film Condensation of Pure Vapour 279

14.1 Introduction 279

14.2 Governing Partial Differential Equations 281

14.3 Similarity Variables 283

14.4 Governing Ordinary Differential Equations 284

14.5 Identical Governing Equations on Laminar Free Film
 Condensation of Saturated or Superheated Vapor 286

14.6 Remarks 286

14.7 Exercises 287

References 300

15 Velocity and Temperature Fields of Laminar Free Convection

Film Condensation of Pure Vapour 301

15.1 Introduction 301

15.2 Treatment of Variable Physical Properties 302

15.2.1 For Liquid Film 302

15.2.2 For Vapor Film. 303

15.3 Numerical Solutions 304

15.3.1 Calculation Procedure 304

15.3.2 Numerical Solution 304

15.4 Variations of Velocity and Temperature Fields. 305

15.4.1 For Velocity Fields of Liquid Film 305

15.4.2 For Temperature Fields of Liquid Film 310

15.4.3 For Velocity Fields of Vapor Film 310

15.5 Remarks 310

15.6 Exercises 311

References 312

16 Heat and Mass Transfer of Laminar Free Convection Film

Condensation of Pure Vapor 313

16.1 Introduction 314

16.2 Heat Transfer Analysis 314

16.3 Wall Dimensionless Temperature Gradient 315

16.4 Practical Prediction Equations on Condensation
 Heat Transfer 318

16.5 Mass Transfer Analysis 319

16.6 Mass Flow Rate Parameter. 321

16.6.1 Condensate Film Thickness and Velocity
 Components at the Interface 321

16.6.2 Interfacial Velocity Components 324

16.6.3 Condensate Mass Flow Rate Parameter 326

16.7 Practical Prediction Equations on Condensation
 Mass Transfer 328

16.8 Condensate Mass–Energy Transformation Equation 329

16.8.1 Theoretical Analysis on Condensate
 Mass–Energy Transformation 329

16.8.2 Condensate Mass–Energy
 Transformation Coefficient. 330

16.9 Summary 332

- 16.10 Remarks 340
- 16.11 Calculation Example 341
- 16.12 Exercises 349
- References 350

17 Effects of Various Physical Conditions on Heat Transfer

- of the Free Convection Film Condensation 351**
- 17.1 Introduction 351
- 17.2 Review of Governing Equations for Film Condensation
of Saturated Vapor 352
 - 17.2.1 Partial Differential Equations 353
 - 17.2.2 Similarity Variables 354
 - 17.2.3 Transformed Dimensionless
Differential Equations 355
- 17.3 Different Physical Assumptions 356
 - 17.3.1 Assumption a (with Boussinesq Approximation
of Condensate Film) 356
 - 17.3.2 Assumption b (Ignoring Shear Force
at Liquid–Vapor Interface) 358
 - 17.3.3 Assumption c (Ignoring Inertia Force
of the Condensate Film) 358
 - 17.3.4 Assumption d (Ignoring Thermal Convection
of the Condensate Film) 359
- 17.4 Effects of Various Physical Conditions on Velocity
and Temperature Fields 359
- 17.5 Effects of Various Physical Conditions on Heat Transfer . . . 360
- 17.6 Remarks 362
- 17.7 Exercises 365
- References 365

18 Complete Similarity Mathematical Models on Laminar

- Free Convection Film Condensation from Vapor–Gas Mixture . . 367**
- 18.1 Introduction 367
- 18.2 Governing Partial Differential Equations 368
- 18.3 Similarity Variables 371
 - 18.3.1 For Liquid Film 371
 - 18.3.2 For Vapor–Gas Mixture Film 372
- 18.4 Governing Ordinary Differential Equations 372
 - 18.4.1 For Liquid Film Flow 372
 - 18.4.2 For Vapor–Gas Mixture Film Flow 373
 - 18.4.3 For Boundary Conditions 374
- 18.5 Remarks 375
- 18.6 Exercises 375
- References 396

19	Velocity, Temperature, and Concentration Fields on Laminar Free Convection Film Condensation of Vapor–Gas Mixture	399
19.1	Introduction	399
19.2	Treatments of Variable Physical Properties	400
19.2.1	Treatment Methods	400
19.2.2	Treatment of Temperature-Dependent Physical Properties of Liquid Film	401
19.2.3	Treatment of Concentration-Dependent Densities of Vapor–Gas Mixture	402
19.2.4	Treatment of Other Concentration-Dependent Physical Properties of Vapor–Gas Mixture	403
19.2.5	Treatment of Temperature-Dependent Physical Properties of Vapor–Gas Mixture	405
19.3	Necessity for Satisfying Whole Interfacial Balance Conditions on Reliable Solution	405
19.4	Numerical Calculation Approach	406
19.5	Physical Property Data Applied for Numerical Calculation	407
19.6	Interfacial Vapor Saturation Temperature	407
19.7	Critical Bulk Vapor Mass Fraction with the Film Condensation	408
19.8	Velocity, Concentration, and Temperature Fields of the Two-Phase Film Flows	411
19.9	Variations of Velocity and Temperature Fields	412
19.9.1	Variation of Film Thicknesses	413
19.9.2	Variation of Velocity Fields of Condensate Liquid Film	415
19.9.3	Variation of Velocity Fields of Vapor–Gas Mixture Film	416
19.10	Remarks	416
19.11	Exercises	417
	References	418
20	Heat and Mass Transfer of Laminar Free Convection Film Condensation of Vapor–Gas Mixture	419
20.1	Introduction	420
20.2	Heat Transfer Analysis	420
20.3	Wall Temperature Gradient	422
20.4	Variation of Condensate Heat Transfer	425
20.5	Condensate Mass Transfer Analysis	428
20.6	Condensate Mass Flow Rate Parameter	430
20.7	Variation of Condensate Mass Flow Rate	435
20.8	Quite Different Film Condensations	441

20.9	Summary	443
20.10	Remarks	443
20.11	Calculation Examples	452
20.12	Exercises	456
	Reference	457

Part IV Gravity-Driven Film Flow of Non-Newtonian Fluids

21	Hydrodynamics of Falling Film Flow of Non-Newtonian Power-Law Fluids	461
21.1	Introduction	461
21.2	Principal Types of Power-Law Fluids	463
	21.2.1 Newtonian Fluids	463
	21.2.2 Power-Law Fluids	464
21.3	Physical Model and Governing Partial Differential Equations.	465
21.4	A New Similarity Transformation.	468
21.5	Numerical Solutions	471
21.6	Local Skin-Friction Coefficient.	472
21.7	Mass Flow Rate	474
21.8	Length of Boundary Layer Region	477
21.9	Critical Film Thickness	478
21.10	Effect of Wall Inclination	479
21.11	Summary	480
21.12	Remarks	480
21.13	Calculation Examples	482
	References	486
22	Pseudo-Similarity and Boundary Layer Thickness for Non-Newtonian Falling Film Flow	487
22.1	Introduction	487
22.2	Physical Model and Governing Partial Differential Equations.	489
22.3	Similarity Transformation	490
22.4	Local Prandtl Number	494
22.5	Pseudo-Similarity for Energy Equation	495
22.6	Critical Local Prandtl Number	497
22.7	Analysis of Boundary Layer Thickness	499
	22.7.1 Precautions for $Pr_x > Pr_x^*$	499
	22.7.2 Precautions for $Pr_x < Pr_x^*$	500
22.8	Remarks	502
	References	503

- 23 Heat Transfer of the Falling Film Flow of Non-Newtonian Power-Law Fluids 505**
- 23.1 Introduction 505
- 23.2 Governing Equations 506
- 23.3 Heat Transfer Analysis 508
- 23.4 Numerical Solution for Heat Transfer 510
- 23.5 Local Similarity Versus Local Pseudo-Similarity 515
- 23.6 Summary 516
- 23.7 Remarks 517
- 23.8 Calculation Examples 519
- References 522

- Appendix A: Tables with Physical Properties 525**

- Index 533**

Symbols

a	Thermal diffusive coefficient, m^2/s ; assumption for ignoring the variable thermophysical properties (or for Boussinesq approximation)
A	Area, m^2
b	Width of plate, m; assumption for ignoring the shear force at the liquid–vapor interface
c	Assumption for ignoring inertia force of condensate film
$C_{x,f}$	Local skin-friction coefficient of non-Newtonian power–law fluids, $2\text{Re}_x^{-1/(n+1)} \left[\left(\frac{dw_x}{d\eta} \right)_{\eta=0} \right]^n$
C_{mg}	Gas mass fraction in vapour–gas mixture
C_{mv}	Vapor mass fraction in vapour–gas mixture
$C_{mv,s}$	Interfacial vapor mass fraction
$C_{mv,\infty}$	Bulk vapor mass fraction
$C_{mv,\infty}^*$	Critical bulk vapor mass fraction (corresponding to the case for interfacial vapor saturation temperature $T_{s,int} \rightarrow T_W$)
c_p	Specific heat at constant pressure, $J/(kg\ K)$
c_{p_g}	Gas specific heat, $J/(kg\ K)$
c_{p_v}	Vapor specific heat, $J/(kg\ K)$
c_{p_m}	Specific heat of vapor–gas mixture, $J/(kg\ K)$
d	Assumption for ignoring the thermal convection of condensate film
D_v	Vapor mass diffusion coefficient in gas, m^2/s
e	Internal energy per unit mass, J/kg
E	Internal energy, J
\dot{E}	Internal energy per unit time in system, $\delta \dot{E} = \dot{Q} + \dot{W}_{out}$, W
ΔE	Increment of internal energy in a system, J
$\Delta \dot{E}$	Increment of internal energy per unit time in system, W
$E_{q_x}^*$	Deviation of heat transfer of free convection predicted by using Boussinesq approximation to that with considering variable physical properties

F	Force, N
F_m	Mass force acting on the control, N
F_s	Surface force acting on the control, N
\vec{F}	Surface force per unit mass, m/s^2
g	Gravity acceleration, m/s^2
\dot{G}	Momentum increment per unit time in system, $kg\ m/s^2$
Gr	Grashof number
Gr_x	Local Grashof number
$Gr_{x,\infty}$	Local Grashof number for gas laminar free convection, $\frac{g T_w/T_\infty-1 x^3}{v_\infty^2}$, local Grashof number for liquid laminar free convection, $\frac{g \rho_\infty/\rho_w-1 x^3}{v_\infty^2}$
$Gr_{xv,s}$	Local Grashof number of vapor film for film boiling, $\frac{g(\rho_{l,\infty}/\rho_{v,w}-1)x^3}{v_{v,s}^2}$
$Gr_{xl,\infty}$	Local Grashof number of liquid film for film boiling, $\frac{g(\rho_{l,\infty}/\rho_{l,s}-1)x^3}{v_{l,\infty}^2}$
$Gr_{xl,s}$	Local Grashof number of liquid film for film condensation of vapour, $\frac{g(\rho_{l,w}-\rho_{v,\infty})x^3}{v_{l,s}^2\rho_{l,s}}$
$Gr_{xv,\infty}$	Local Grashof number of vapour film for film condensation of vapour, $\frac{g(\rho_{v,s}/\rho_{v,\infty}-1)x^3}{v_{v,\infty}^2}$
$Gr_{xl,s}$	Local Grashof number of condensate liquid film for film condensation of vapour–gas mixture, $\frac{g(\rho_{l,w}-\rho_{m,\infty})x^3}{v_{l,s}^2\rho_{l,s}}$
$Gr_{xm,\infty}$	Local Grashof number of vapor–gas mixture film or film condensation of vapour–gas mixture, $\frac{g(\rho_{m,s}/\rho_{m,\infty}-1)x^3}{v_{m,\infty}^2}$
g_x	Local mass flow rate entering the vapor film at position x per unit area of the plate, $kg/(m^2\ s)$
G_x	Total mass flow rate entering the vapor film for position $x = 0$ to x with width of b of the plate, kg/s
$g(\eta, \zeta)$	Defined temperature gradient for pseudo-similarity case, $\frac{\partial\theta(\eta,\zeta)}{\partial\zeta}$
H	Enthalpy, $E + pV$, $c_p t$, J
h	Specific enthalpy (enthalpy per unit mass), $e + pv$, J/kg
h_{fg}	Latent heat of vaporization, J/kg
[J]	Basis dimension for quantity of heat
K	Coefficient of consistency of non-Newtonian power–law fluids, $kg\ s^{n-2}/m$
[K]	Basis dimension for temperature
[kg]	Basis dimension for mass
L	Reference length of plate, m
LDV	Laser Doppler Velocimeter
m	More complete condition
\dot{m}	Mass increment per unit time, kg/s

[m]	Basis dimension for length
n	Power law index; number of independent physical variables
n_λ	Thermal conductivity parameter
n_μ	Viscosity parameter
n_{c_p}	Specific heat parameter
$n_{\mu\lambda}$	Overall temperature parameter
$n_{\lambda,g}$	Thermal conductivity parameter of gas
$n_{\lambda,v}$	Thermal conductivity parameter of vapor
$n_{\mu,g}$	Viscosity parameter of gas
$n_{\mu,v}$	Viscosity parameter of vapour
$Nu_{x,w}$	Local Nusselt number with wall temperature t_w as reference temperature, $\alpha_{x,x}/\lambda_w$
$\overline{Nu}_{x,w}$	Average Nusselt number with wall temperature t_w as reference temperature, $\overline{\alpha}_{x,x}/\lambda_w$
p	Pressure, N/m^2
Pr	Randtl number
Pr_x	Local Prandtl number of falling film flow of non-Newtonian power-law fluids, $\frac{\lambda w_{x,\infty}}{a} Re_x^{-2/(n+1)}$
Pr_x^*	Critical Prandtl number of falling film flow of non-Newtonian power-law fluids
Pr_g	Gas Prandtl number
Pr_v	Vapor Prandtl number
Pr_m	Prandtl number of vapor-gas mixture
Q	Heat, J
\dot{Q}	Heat entering the system per unit time, W
Q_{in}	Heat transferred into the system from its surroundings, J
q_x	Local heat transfer rate at position x per unit area on the plate, W/m^2
q_x^*	Local heat transfer rate at position x per unit area on the plate under Boussinesq approximation, W/m^2
Q_x	Total heat transfer rate for position $x = 0$ to x with width of b on the plate, W
r	Number of basic dimension
Re_x	Local Reynolds number
[s]	Basis dimension for time
$Sc_{m,\infty}$	Local Schmidt number, defined as $Sc_{m,\infty} = \frac{v_{m,\infty}}{D_v}$
t	Temperature, °C
T	Absolute temperature, K
t_s	Saturation temperature of pure vapour, °C
t_w	Wall temperature, °C
Δt_w	Wall superheated temperature for film boiling, $t_w - t_s$; wall subcooled temperature for film condensation, $t_s - t_w$, °C

$\frac{\Delta t_w}{t_s}$	Wall superheated grade or film boiling, $\frac{t_w - t_s}{t_s}$, wall subcooled grade for film condensation of vapour, $\frac{t_s - t_w}{t_s}$
Δt_∞	Liquid subcooled temperature, for film boiling $t_s - t_\infty$, vapour superheated temperature, for film condensation of vapour, $t_\infty - t_s$, °C
$\frac{\Delta t_\infty}{t_s}$	Liquid subcooled temperature, for film boiling $\frac{t_s - t_\infty}{t_s}$, vapour superheated temperature for film condensation of vapour, $\frac{t_\infty - t_s}{t_s}$, °C
$t_{s,int}$	Interfacial vapor saturation temperature related to film condensation of vapour–gas mixture, °C
$t_{s,int} - t_w$	Wall subcooled temperature related to film condensation of vapour–gas mixture, °C
$t_{s,ref}$	Reference saturation temperature expressed by the saturation temperature of pure vapour with $C_{mv,\infty} = 1$ °C
$\frac{t_{s,ref} - t_w}{t_{s,ref}}$	Reference wall subcooled grade, °C
T_w/T_∞	Boundary temperature ratio for free convection
T_w/T_s	Film boundary temperature ratio for vapour film
V	Volume, m ³
v	Specific volume, m ³ /kg
w_x, w_y, w_z	Velocity components in x, y, z direction respectively, m/s
W_x, W_y, W_z	Dimensional velocity component in x, y, z direction respectively, respectively
w_{xl}, w_{yl}	Condensate liquid velocity components in x and y -coordinates, respectively, m/s
W_{xl}, W_{yl}	Dimensionless condensate liquid velocity components in x and y -coordinates, respectively
$w_{xl,s}, w_{yl,s}$	Condensate liquid velocity components at liquid–vapor interface in x and y -coordinates, respectively, m/s
$W_{xl,s}, W_{yl,s}$	Dimensionless condensate liquid velocity components at liquid–vapor interface in x and y -coordinates, respectively
w_{xv}, w_{yv}	Vapour velocity components in x and y -coordinates, respectively, m/s
W_{xv}, W_{yv}	Dimensionless vapour velocity components in x and y -coordinates, respectively
$w_{xv,s}, w_{yv,s}$	Vapour velocity components at liquid–vapor interface in x and y -coordinates, respectively, m/s
$W_{xv,s}, W_{yv,s}$	Dimensionless vapour velocity components at liquid–vapor interface in x and y -coordinates, respectively
w_{xm}, w_{ym}	Velocity components of vapor–gas mixture in x and y -coordinates, respectively, m/s
W_{xm}, W_{ym}	Dimensionless vapor–gas mixture velocity components in x and y -coordinates, respectively

$w_{xm,s}, w_{ym,s}$	Velocity components of vapor–gas mixture at liquid–vapor interface in x and y -coordinates, respectively, m/s
$W_{xm,s}, W_{ym,s}$	Dimensionless vapor–gas mixture velocity components at liquid–vapor interface in x and y -coordinates, respectively
$w_{x,\infty}$	Velocity component beyond the boundary layer
\vec{W}	Velocity, $w_x i + w_y j + w_z k$
\dot{W}	Work done per unit time, W
\dot{W}_{out}	Work per unit time acting on the system, J
x_0	Length of the boundary layer region, m
x, y, z	Dimensional coordinate variables
$-dw_x/dy$	Shear rate, 1/s

Greek Symbols

ρ	Density, kg/m ³
ρ_g	Gas density, kg/m ³
ρ_v	Density of vapor, kg/m ³
ρ_m	Density of vapour–gas mixture, kg/m ³
ρ_{mg}	Local density of gas in vapor–gas mixture, kg/m ³
ρ_{mv}	Local density of vapor in vapor–gas mixture, kg/m ³
λ	Thermal conductivity, W/(m K)
λ_g	Thermal conductivity of gas, W/(m K)
λ_v	Thermal conductivity of vapor, W/(m K)
λ_m	Thermal conductivity of vapor–gas mixture, W/(m K)
μ	Absolute viscosity, kg/(m s)
μ_g	Gas absolute viscosity, kg/(m s)
μ_v	Vapor absolute viscosity, kg/(m s)
μ_m	Absolute viscosity of vapor–gas mixture, kg/(m s)
$\mu_{l,s}$	Liquid absolute viscosity at the liquid–vapor interface
μ_a	The apparent viscosity, kg/(m s)
ν	Kinetic viscosity, m ² /s
β	Thermal volumetric expansion coefficient, K ⁻¹
τ	Shear stress, N/m ²
$\bar{\tau}$	Surface force acting on unit area; shear stress, N/m ²
ε	Deformation rate
[]	Symbol of tensor
{ }	Symbol of quantity grade
η	Dimensionless coordinate variable for boundary layer and film flow
$\eta_{v\delta}$	Dimensionless thickness of vapor film
η_l	Dimensionless co-ordinate variable of condensate liquid film
η_v	Dimensionless co-ordinate variable of vapour film
η_m	Dimensionless co-ordinate variable of vapor–gas mixture

$\eta_{l\delta}$	Dimensionless thickness for liquid film
η_{δ_l}	Dimensionless momentum boundary layer thickness
η_{δ_T}	Dimensionless thermal boundary layer thickness
$\eta_{\delta_l^*}$	Dimensionless critical boundary layer thickness
δ	Boundary layer thickness, m
δ_l	Condensate liquid film thickness, m
δ_v	Thickness of vapor film, m
δ_c	Concentration boundary layer thickness of vapor–gas mixture, m
δ_m	Momentum boundary layer thickness of vapor–gas mixture, m
$\delta_l(x)$	Boundary layer thickness at the x position, m
$\delta_l(x_0)$	Critical film thickness related to x_0 , m
Φ_s	Mass flow rate parameter
ψ	Flow function
α, γ	Inclined angle of surface
α_x	Local heat transfer coefficient, W/(m ² K)
$\bar{\alpha}_x$	Average heat transfer coefficient, W/(m ² K)
θ	Dimensionless temperature
θ_v	Dimensionless temperature of vapor film
θ_l	Dimensionless temperature of liquid film
θ_m	Dimensionless temperature of vapor–gas mixture film
$\theta(\eta, \zeta)$	Pseudo-similarity solution of dimensionless temperature
Γ_{mv}	Vapor relative mass fraction, $\frac{C_{mv} - C_{mv,\infty}}{C_{mv,s} - C_{mv,\infty}}$
$\left(\frac{d\theta}{d\eta}\right)_{\eta=0}$	Dimensionless temperature gradient on the plate
$\frac{1}{\rho} \frac{d\rho}{dx}$	Density factor
$\frac{1}{\rho_g} \frac{d\rho_g}{d\eta_m}$	Density factor of gas
$\frac{1}{\rho_v} \frac{d\rho_v}{d\eta_m}$	Density factor of vapor
$\frac{1}{\rho_m} \frac{d\rho_m}{d\eta_m}$	Density factor of vapor–gas mixture
$\frac{1}{\lambda} \frac{d\lambda}{d\eta}$	Thermal conductivity factor
$\frac{1}{\lambda_g} \frac{d\lambda_g}{d\eta_m}$	Thermal conductivity factor of gas
$\frac{1}{\lambda_v} \frac{d\lambda_v}{d\eta_m}$	Thermal conductivity factor of vapor
$\frac{1}{\lambda_m} \frac{d\lambda_m}{d\eta_m}$	Thermal conductivity factor of vapor–gas mixture
$\frac{1}{\mu} \frac{d\mu}{d\eta}$	Viscosity factor
$\frac{1}{\mu_g} \frac{d\mu_g}{d\eta_m}$	Viscosity factor of gas
$\frac{1}{\mu_v} \frac{d\mu_v}{d\eta_m}$	Viscosity factor of vapor

$\frac{1}{\mu_m} \frac{d\mu_m}{d\eta_m}$	Viscosity factor of vapor–gas mixture
$\frac{\nu_{v,s}}{\nu_v}$	Kinetic viscosity factor
$\psi(\text{Pr})$	Boussinesq solution
ζ	$\frac{x}{x_0}$

Subscripts

a	Assumption a
b	Assumption b
c	Assumption c
d	Assumption d
f	Film
g	Gas
i	Inclined case apply
int	Interfacial
l	Liquid
m	More complete condition
s	Surface force
v	Vertical case; vapour case
w	At wall
∞	Far from the wall surface
δ	Thickness of boundary layer
sub	Subcooling state

Part I
Theoretical Foundation

Chapter 2

Basic Conservation Equations for Laminar Free Convection

Abstract In this chapter, the basic conservation equations related to laminar free fluid flow conservation equations are introduced. For this purpose, the related general laminar free conservation equations on continuity equation, momentum equation, and energy equation are derived theoretically. On this basis, the corresponding conservation equations of mass, momentum, and energy for steady laminar free convection boundary layer are obtained by the quantities grade analysis.

2.1 Continuity Equation

The conceptual basis for the derivation of the continuity equation of fluid flow is the mass conservation law. The control volume for the derivation of continuity equation is shown in Fig. 2.1 in which the mass conservation principle is stated as

$$\dot{m}_{\text{increment}} = \dot{m}_{\text{in}} - \dot{m}_{\text{out}} \tag{2.1}$$

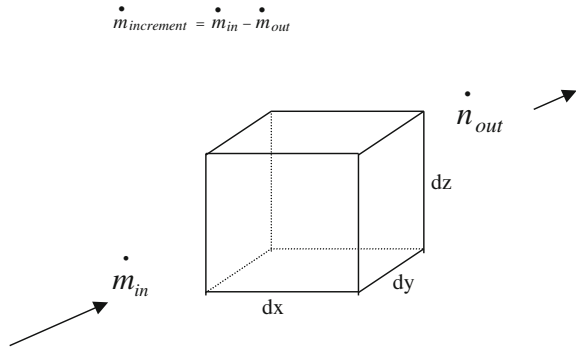
where $\dot{m}_{\text{increment}}$ expresses the mass increment per unit time in the control volume, \dot{m}_{in} represents the mass flowing into the control volume per unit time, and \dot{m}_{out} is the mass flowing out of the control volume per unit time. The dot notation signifies a unit time.

In the control volume, the mass of fluid flow is given by $\rho dx dy dz$, and the mass increment per unit time in the control volume can be expressed as

$$\dot{m}_{\text{increment}} = \frac{\partial \rho}{\partial \tau} dx dy dz. \tag{2.2}$$

The mass flowing into the control volume per unit time in the x direction is given by $\rho w_x dy dz$. The mass flowing out of the control volume in a unit time in the x direction is given by $[\rho w_x + \partial (\rho w_x) / \partial x \cdot dx] dy dz$. Thus, the mass increment per unit time

Fig. 2.1 Control volume for the derivation of the continuity equations



in the x direction in the control volume is given by $\frac{\partial(\rho w_x)}{\partial x} dx dy dz$. Similarly, the mass increments in the control volume in the y and z directions per unit time are given by $\frac{\partial(\rho w_y)}{\partial y} dy dx dz$ and $\frac{\partial(\rho w_z)}{\partial z} dz dx dy$, respectively. We, thus, obtain

$$\dot{m}_{out} - \dot{m}_{in} = \left(\frac{\partial(\rho w_x)}{\partial x} + \frac{\partial(\rho w_y)}{\partial y} + \frac{\partial(\rho w_z)}{\partial z} \right) dx dy dz. \quad (2.3)$$

Combining Eq. (2.1) with Eqs. (2.2) and (2.3), we obtain the following continuity equation in Cartesian coordinates:

$$\frac{\partial \rho}{\partial \tau} + \frac{\partial(\rho w_x)}{\partial x} + \frac{\partial(\rho w_y)}{\partial y} + \frac{\partial(\rho w_z)}{\partial z} = 0 \quad (2.4)$$

or in the vector notation

$$\frac{\partial \rho}{\partial \tau} + \nabla \cdot (\rho \vec{W}) = 0. \quad (2.5)$$

or

$$\frac{D\rho}{D\tau} + \rho \nabla \cdot (\vec{W}) = 0 \quad (2.6)$$

when ρ is constant and $\vec{W} = i w_x + j w_y + k w_z$ is the fluid velocity.

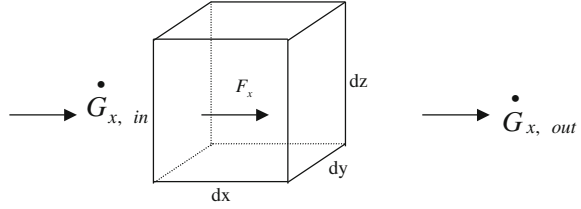
For steady state, the vector and Cartesian forms of the continuity equation are given by

$$\frac{\partial}{\partial x}(\rho w_x) + \frac{\partial}{\partial y}(\rho w_y) + \frac{\partial}{\partial z}(\rho w_z) = 0. \quad (2.7)$$

or

$$\nabla \cdot (\rho \vec{W}) = 0 \quad (2.8)$$

Fig. 2.2 Control volume for the derivation of momentum equations



2.2 Momentum Equation (Navier–Stokes Equations)

The control volume for the derivation of the momentum equation of fluid flow is shown in Fig. 2.2. Meanwhile, take an enclosed surface A that includes the control volume. According to momentum law, the momentum increment of the fluid flow per unit time equals the sum of the mass force and surface force acting on the fluid. The relationship is shown as below:

$$\dot{G}_{\text{increment}} = \vec{F}_m + \vec{F}_s \quad (2.9)$$

where \vec{F}_m and \vec{F}_s denote mass force and surface force, respectively.

In the system, the momentum increment $\dot{m}_{\text{increment}}$ of the fluid flow per unit time can be described as

$$\dot{G}_{\text{increment}} = \frac{D}{D\tau} \int_V \rho \vec{W} dV \quad (2.10)$$

In the system, the sum of mass force F_m and surface force F_s acting on the fluid is expressed as

$$F_m + F_s = \int_V \rho \vec{F} dV + \int_A \vec{\tau}_n dA \quad (2.11)$$

where V and A are volume and surface area of the system respectively, $\vec{\tau}_n$ is surface force acting on unit area.

Combining Eq. (2.9) with Eqs. (2.10) and (2.11), we have the following equation:

$$\frac{D}{D\tau} \int_V \rho \vec{W} dV = \int_V \rho \vec{F} dV + \int_A \vec{\tau}_n dA \quad (2.12)$$

According to tensor calculation, the right side of Eq. (2.12) is changed into the following form:

$$\int_V \rho \vec{F} dV + \int_A \vec{\tau}_n dA = \int_V \rho \vec{F} dV + \int_V \nabla \cdot [\tau] dV \quad (2.13)$$

where $\nabla \cdot [\tau]$ is divergence of the shear force tensor.

The left side of Eq. (2.12) can be rewritten as

$$\frac{D}{D\tau} \int_V \rho \vec{W} dV = \int_V \frac{D(\rho \vec{W})}{D\tau} dV \quad (2.14)$$

With Eqs. (2.13) and (2.14), Eq. (2.12) can be simplified as

$$\int_V \left\{ \frac{D(\rho \vec{W})}{D\tau} - \rho \vec{F} - \nabla \cdot [\tau] \right\} dV = 0 \quad (2.15)$$

Therefore,

$$\frac{D(\rho \vec{W})}{D\tau} = \rho \vec{F} + \nabla \cdot [\tau] \quad (2.16)$$

This is the Navier–Stokes equations of fluid flow. For Cartesian Coordinates, Eq. (2.16) can be expressed as

$$\frac{D(\rho w_x)}{D\tau} = \frac{\partial \tau_{xx}}{\partial x} + \frac{\partial \tau_{yx}}{\partial y} + \frac{\partial \tau_{zx}}{\partial z} + \rho g_x \quad (2.17)$$

$$\frac{D(\rho w_y)}{D\tau} = \frac{\partial \tau_{xy}}{\partial x} + \frac{\partial \tau_{yy}}{\partial y} + \frac{\partial \tau_{zy}}{\partial z} + \rho g_y \quad (2.18)$$

$$\frac{D(\rho w_z)}{D\tau} = \frac{\partial \tau_{xz}}{\partial x} + \frac{\partial \tau_{yz}}{\partial y} + \frac{\partial \tau_{zz}}{\partial z} + \rho g_z \quad (2.19)$$

where

$$\frac{D(\rho w_x)}{D\tau} = \frac{\partial(\rho w_x)}{\partial \tau} + \frac{(\partial \rho w_x)}{\partial x} w_x + \frac{(\partial \rho w_x)}{\partial y} w_y + \frac{(\partial \rho w_x)}{\partial z} w_z$$

$$\frac{D(\rho w_y)}{D\tau} = \frac{\partial(\rho w_y)}{\partial \tau} + \frac{(\partial \rho w_y)}{\partial x} w_x + \frac{(\partial \rho w_y)}{\partial y} w_y + \frac{(\partial \rho w_y)}{\partial z} w_z$$

$$\frac{D(\rho w_z)}{D\tau} = \frac{\partial(\rho w_z)}{\partial \tau} + \frac{(\partial \rho w_z)}{\partial x} w_x + \frac{(\partial \rho w_z)}{\partial y} w_y + \frac{(\partial \rho w_z)}{\partial z} w_z$$

In Eqs. (2.17)–(2.19), g_x , g_y , and g_z are gravity accelerations in x , y , and z directions, respectively, while the related shear forces are given below:

$$\begin{aligned}
\tau_{xx} &= - \left[p + \frac{2}{3} \mu \left(\frac{\partial w_x}{\partial x} + \frac{\partial w_y}{\partial y} + \frac{\partial w_z}{\partial z} \right) \right] + 2\mu \frac{\partial w_x}{\partial x} \\
\tau_{yy} &= - \left[p + \frac{2}{3} \mu \left(\frac{\partial w_x}{\partial x} + \frac{\partial w_y}{\partial y} + \frac{\partial w_z}{\partial z} \right) \right] + 2\mu \frac{\partial w_y}{\partial y} \\
\tau_{zz} &= - \left[p + \frac{2}{3} \mu \left(\frac{\partial w_x}{\partial x} + \frac{\partial w_y}{\partial y} + \frac{\partial w_z}{\partial z} \right) \right] + 2\mu \frac{\partial w_z}{\partial z} \\
\tau_{xy} &= \tau_{yx} = \mu \left(\frac{\partial w_y}{\partial x} + \frac{\partial w_x}{\partial y} \right) \\
\tau_{yz} &= \tau_{zy} = \mu \left(\frac{\partial w_z}{\partial y} + \frac{\partial w_y}{\partial z} \right) \\
\tau_{zx} &= \tau_{xz} = \mu \left(\frac{\partial w_x}{\partial z} + \frac{\partial w_z}{\partial x} \right)
\end{aligned}$$

Then, (2.17)–(2.19) are rewritten as follows, respectively:

$$\begin{aligned}
\frac{D(\rho w_x)}{D\tau} &= - \frac{\partial p}{\partial x} + 2 \frac{\partial}{\partial x} \left(\mu \frac{\partial w_x}{\partial x} \right) + \frac{\partial}{\partial y} \left[\mu \left(\frac{\partial w_x}{\partial y} + \frac{\partial w_y}{\partial x} \right) \right] \\
&\quad + \frac{\partial}{\partial z} \left[\mu \left(\frac{\partial w_x}{\partial z} + \frac{\partial w_z}{\partial x} \right) \right] - \frac{\partial}{\partial x} \left[\frac{2}{3} \mu \left(\frac{\partial w_x}{\partial x} + \frac{\partial w_y}{\partial y} + \frac{\partial w_z}{\partial z} \right) \right] + \rho g_x
\end{aligned} \tag{2.20}$$

Similarly, the momentum equations in the y and z directions are given by

$$\begin{aligned}
\frac{D(\rho w_y)}{D\tau} &= - \frac{\partial p}{\partial y} + \frac{\partial}{\partial x} \left[\mu \left(\frac{\partial w_x}{\partial y} + \frac{\partial w_y}{\partial x} \right) \right] + 2 \frac{\partial}{\partial y} \left(\mu \frac{\partial w_y}{\partial y} \right) \\
&\quad + \frac{\partial}{\partial z} \left[\mu \left(\frac{\partial w_y}{\partial z} + \frac{\partial w_z}{\partial y} \right) \right] - \frac{\partial}{\partial y} \left[\frac{2}{3} \mu \left(\frac{\partial w_x}{\partial x} + \frac{\partial w_y}{\partial y} + \frac{\partial w_z}{\partial z} \right) \right] + \rho g_y
\end{aligned} \tag{2.21}$$

$$\begin{aligned}
\frac{D(\rho w_z)}{D\tau} &= - \frac{\partial p}{\partial z} + \frac{\partial}{\partial x} \left[\mu \left(\frac{\partial w_x}{\partial z} + \frac{\partial w_z}{\partial x} \right) \right] + \frac{\partial}{\partial y} \left[\mu \left(\frac{\partial w_y}{\partial z} + \frac{\partial w_z}{\partial y} \right) \right] + 2 \frac{\partial}{\partial z} \left(\mu \frac{\partial w_z}{\partial z} \right) \\
&\quad - \frac{\partial}{\partial z} \left[\frac{2}{3} \mu \left(\frac{\partial w_x}{\partial x} + \frac{\partial w_y}{\partial y} + \frac{\partial w_z}{\partial z} \right) \right] + \rho g_z
\end{aligned} \tag{2.22}$$

For steady state, the momentum Eqs. (2.20)–(2.22) are given as follows respectively:

$$\begin{aligned}
\rho \left(\frac{\partial w_x}{\partial x} w_x + \frac{\partial w_x}{\partial y} w_y + \frac{\partial w_x}{\partial z} w_z \right) &+ w_x \left(w_x \frac{\partial \rho}{\partial x} + w_y \frac{\partial \rho}{\partial y} + w_z \frac{\partial \rho}{\partial z} \right) \\
&= - \frac{\partial p}{\partial x} + 2 \frac{\partial}{\partial x} \left(\mu \frac{\partial w_x}{\partial x} \right) + \frac{\partial}{\partial y} \left[\mu \left(\frac{\partial w_x}{\partial y} + \frac{\partial w_y}{\partial x} \right) \right] + \frac{\partial}{\partial z} \left[\mu \left(\frac{\partial w_x}{\partial z} + \frac{\partial w_z}{\partial x} \right) \right] \\
&\quad - \frac{\partial}{\partial x} \left[\frac{2}{3} \mu \left(\frac{\partial w_x}{\partial x} + \frac{\partial w_y}{\partial y} + \frac{\partial w_z}{\partial z} \right) \right] + \rho g_x
\end{aligned} \tag{2.23}$$

$$\begin{aligned}
& \rho \left(\frac{\partial w_y}{\partial x} w_x + \frac{\partial w_y}{\partial y} w_y + \frac{\partial w_y}{\partial z} w_z \right) + w_y \left(w_x \frac{\partial \rho}{\partial x} + w_y \frac{\partial \rho}{\partial y} + w_z \frac{\partial \rho}{\partial z} \right) \\
&= -\frac{\partial p}{\partial y} + \frac{\partial}{\partial x} \left[\mu \left(\frac{\partial w_x}{\partial y} + \frac{\partial w_y}{\partial x} \right) \right] + 2 \frac{\partial}{\partial y} \left(\mu \frac{\partial w_y}{\partial y} \right) + \frac{\partial}{\partial z} \left[\mu \left(\frac{\partial w_y}{\partial z} + \frac{\partial w_z}{\partial y} \right) \right] \\
&\quad - \frac{\partial}{\partial y} \left[\frac{2}{3} \mu \left(\frac{\partial w_x}{\partial x} + \frac{\partial w_y}{\partial y} + \frac{\partial w_z}{\partial z} \right) \right] + \rho g_y
\end{aligned} \quad (2.24)$$

$$\begin{aligned}
& \rho \left(\frac{\partial w_z}{\partial x} w_x + \frac{\partial w_z}{\partial y} w_y + \frac{\partial w_z}{\partial z} w_z \right) + w_z \left(w_x \frac{\partial \rho}{\partial x} + w_y \frac{\partial \rho}{\partial y} + w_z \frac{\partial \rho}{\partial z} \right) \\
&= -\frac{\partial p}{\partial z} + \frac{\partial}{\partial x} \left[\mu \left(\frac{\partial w_x}{\partial z} + \frac{\partial w_z}{\partial x} \right) \right] + \frac{\partial}{\partial y} \left[\mu \left(\frac{\partial w_y}{\partial z} + \frac{\partial w_z}{\partial y} \right) \right] + 2 \frac{\partial}{\partial z} \left(\mu \frac{\partial w_z}{\partial z} \right) \\
&\quad - \frac{\partial}{\partial z} \left[\frac{2}{3} \mu \left(\frac{\partial w_x}{\partial x} + \frac{\partial w_y}{\partial y} + \frac{\partial w_z}{\partial z} \right) \right] + \rho g_z
\end{aligned} \quad (2.25)$$

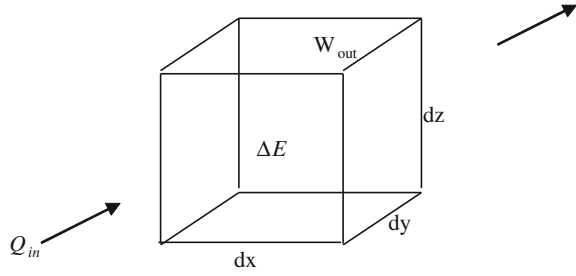
Let us compare term $\rho \left(\frac{\partial w_x}{\partial x} w_x + \frac{\partial w_x}{\partial y} w_y + \frac{\partial w_x}{\partial z} w_z \right)$ with term $w_x \left(w_x \frac{\partial \rho}{\partial x} + w_y \frac{\partial \rho}{\partial y} + w_z \frac{\partial \rho}{\partial z} \right)$. In general, derivatives $\frac{\partial w_x}{\partial x}$, $\frac{\partial w_x}{\partial y}$ and $\frac{\partial w_x}{\partial z}$ are much larger than the derivatives $\frac{\partial \rho_x}{\partial x}$, $\frac{\partial \rho_x}{\partial y}$ and $\frac{\partial \rho_x}{\partial z}$ respectively. In this case, the term $w_x \left(w_x \frac{\partial \rho}{\partial x} + w_y \frac{\partial \rho}{\partial y} + w_z \frac{\partial \rho}{\partial z} \right)$ is omitted, and (2.23) is rewritten as generally

$$\begin{aligned}
\rho \left(\frac{\partial w_x}{\partial x} w_x + \frac{\partial w_x}{\partial y} w_y + \frac{\partial w_x}{\partial z} w_z \right) &= -\frac{\partial p}{\partial x} + 2 \frac{\partial}{\partial x} \left(\mu \frac{\partial w_x}{\partial x} \right) \\
&\quad + \frac{\partial}{\partial y} \left[\mu \left(\frac{\partial w_x}{\partial y} + \frac{\partial w_y}{\partial x} \right) \right] \\
&\quad + \frac{\partial}{\partial z} \left[\mu \left(\frac{\partial w_x}{\partial z} + \frac{\partial w_z}{\partial x} \right) \right] \\
&\quad - \frac{\partial}{\partial x} \left[\frac{2}{3} \mu \left(\frac{\partial w_x}{\partial x} + \frac{\partial w_y}{\partial y} + \frac{\partial w_z}{\partial z} \right) \right] + \rho g_x
\end{aligned} \quad (2.23a)$$

Similarly, in general, (2.24) and (2.25) are rewritten as, respectively,

$$\begin{aligned}
\rho \left(\frac{\partial w_y}{\partial x} w_x + \frac{\partial w_y}{\partial y} w_y + \frac{\partial w_y}{\partial z} w_z \right) &= -\frac{\partial p}{\partial y} + \frac{\partial}{\partial x} \left[\mu \left(\frac{\partial w_x}{\partial y} + \frac{\partial w_y}{\partial x} \right) \right] \\
&\quad + 2 \frac{\partial}{\partial y} \left(\mu \frac{\partial w_y}{\partial y} \right) + \frac{\partial}{\partial z} \left[\mu \left(\frac{\partial w_y}{\partial z} + \frac{\partial w_z}{\partial y} \right) \right] \\
&\quad - \frac{\partial}{\partial y} \left[\frac{2}{3} \mu \left(\frac{\partial w_x}{\partial x} + \frac{\partial w_y}{\partial y} + \frac{\partial w_z}{\partial z} \right) \right] + \rho g_y
\end{aligned} \quad (2.24a)$$

Fig. 2.3 Control volume for derivation of the energy equations of fluid flow



$$\begin{aligned} \rho \left(\frac{\partial w_z}{\partial x} w_x + \frac{\partial w_z}{\partial y} w_y + \frac{\partial w_z}{\partial z} w_z \right) = & -\frac{\partial p}{\partial z} + \frac{\partial}{\partial x} \left[\mu \left(\frac{\partial w_x}{\partial z} + \frac{\partial w_z}{\partial x} \right) \right] \\ & + \frac{\partial}{\partial y} \left[\mu \left(\frac{\partial w_y}{\partial z} + \frac{\partial w_z}{\partial y} \right) \right] + 2 \frac{\partial}{\partial z} \left(\mu \frac{\partial w_z}{\partial x} \right) \\ & - \frac{\partial}{\partial z} \left[\frac{2}{3} \mu \left(\frac{\partial w_x}{\partial x} + \frac{\partial w_y}{\partial y} + \frac{\partial w_z}{\partial z} \right) \right] + \rho g_z \end{aligned} \tag{2.25a}$$

2.3 Energy Equation

The control volume for derivation of the energy equation of fluid flow is shown in Fig. 2.3. Meanwhile, take an enclosed surface A that includes the control volume. According to the first law of thermodynamics, we have the following equation:

$$\Delta \dot{E} = \dot{Q} + \dot{W}_{out} \tag{2.26}$$

where $\Delta \dot{E}$ is energy increment in the system per unit time, \dot{Q} is heat increment in the system per unit time, and \dot{W}_{out} denotes work done by the mass force and surface force on the system per unit time.

The energy increment per unit time in the system is described as

$$\Delta \dot{E} = \frac{D}{D\tau} \int_V \rho \left(e + \frac{W^2}{2} \right) dV \tag{2.27}$$

where τ denotes time, $\frac{W^2}{2}$ is the fluid kinetic energy, W is fluid velocity, and the symbol e represents the internal energy per unit mass.

The work done by the mass force and surface force on the system per unit time is expressed as

$$\dot{W}_{\text{out}} = \int_V \rho \vec{F} \cdot \vec{W} dV + \int_A \vec{\tau}_n \cdot \vec{W} dA \quad (2.28)$$

where \vec{F} is the mass force per unit mass, and $\vec{\tau}_n$ is surface force acting on unit area.

The heat increment entering into the system per unit time through thermal conduction is described by using Fourier's law as follows:

$$\dot{Q} = \int_A \lambda \frac{\partial t}{\partial n} dA \quad (2.29)$$

where n is normal line of the surface, and here the heat conduction is considered only.

With Eqs. (2.27)–(2.29), Eq. (2.26) is rewritten as

$$\frac{D}{D\tau} \int_V \rho \left(e + \frac{W^2}{2} \right) dV = \int_V \rho \vec{F} \cdot \vec{W} dV + \int_A \vec{\tau}_n \cdot \vec{W} dA + \int_A \lambda \frac{\partial t}{\partial n} dA \quad (2.30)$$

where

$$\frac{D}{D\tau} \int_V \rho \left(e + \frac{W^2}{2} \right) dV = \int_V \frac{D}{D\tau} \left[\rho \left(e + \frac{W^2}{2} \right) \right] dV \quad (2.31)$$

$$\int_A \vec{\tau}_n \cdot \vec{W} dA = \int_A \vec{n} [\tau] \cdot \vec{W} dA = \int_A \vec{n} ([\tau] \cdot \vec{W}) dA = \int_v \nabla \cdot ([\tau] \cdot \vec{W}) dV \quad (2.32)$$

$$\int_A \lambda \frac{\partial t}{\partial n} dA = \int_V \nabla \cdot (\lambda \nabla t) dV \quad (2.33)$$

With Eqs. (2.31)–(2.33), Eq. (2.30) is rewritten as

$$\int_V \frac{D}{D\tau} \left[\rho \left(e + \frac{W^2}{2} \right) \right] dV = \int_V \rho \vec{F} \cdot \vec{W} dV + \int_v \nabla \cdot ([\tau] \cdot \vec{W}) dV + \int_V \nabla \cdot (\lambda \nabla t) dV. \quad (2.34)$$

Then,

$$\frac{D}{D\tau} \left[\rho \left(e + \frac{W^2}{2} \right) \right] = \rho \vec{F} \cdot \vec{W} + \nabla \cdot ([\tau] \cdot \vec{W}) + \nabla \cdot (\lambda \nabla t) \quad (2.35)$$

where $[\tau]$ denotes tensor of shear force.

Equation (2.35) is the energy equation.

Through tensor and vector analysis, Eq. (2.35) can be further derived into the following form:

$$\frac{D(\rho e)}{D\tau} = [\tau] \cdot [\varepsilon] + \nabla \cdot (\lambda \nabla t) \quad (2.36)$$

Equation (2.36) is another form of the energy equation. Here, $[\tau] \cdot [\varepsilon]$ is the scalar quantity product of force tensor $[\tau]$ and deformation rate tensor $[\varepsilon]$, and represents the work done by fluid deformation surface force. The physical significance of Eq. (2.36) is that the internal energy increment of fluid with unit volume during the unit time equals the sum of the work done by deformation surface force of fluid with unit volume, $[\tau] \cdot [\varepsilon]$, and the heat entering the system.

The general Newtonian law is expressed as

$$[\tau] = 2\mu[\varepsilon] - \left(p + \frac{2}{3}\mu \nabla \cdot \vec{W} \right) [I] \quad (2.37)$$

where $[I]$ is unit tensor.

According to Eq. (2.37), the following equation can be obtained:

$$[\tau] \cdot [\varepsilon] = -p \nabla \cdot \vec{W} - \frac{2}{3}\mu (\nabla \cdot \vec{W})^2 + 2\mu[\varepsilon]^2 \quad (2.38)$$

Then, Eq. (2.36) can be rewritten as

$$\frac{D(\rho e)}{D\tau} = -p \nabla \cdot \vec{W} + \Phi + \nabla \cdot (\lambda \nabla t) \quad (2.39)$$

where $\Phi = -\frac{2}{3}\mu (\nabla \cdot \vec{W})^2 + 2\mu[\varepsilon]^2$ is viscous dissipation function, which is further described as

$$\begin{aligned} \Phi = \mu \left\{ 2 \left(\frac{\partial w_x}{\partial x} \right)^2 + 2 \left(\frac{\partial w_y}{\partial y} \right)^2 + 2 \left(\frac{\partial w_z}{\partial z} \right)^2 + \left(\frac{\partial w_x}{\partial y} + \frac{\partial w_y}{\partial x} \right)^2 \right. \\ \left. + \left(\frac{\partial w_y}{\partial z} + \frac{\partial w_z}{\partial y} \right)^2 + \left(\frac{\partial w_z}{\partial x} + \frac{\partial w_x}{\partial z} \right)^2 - \frac{2}{3} \left[\text{div}(\vec{W}) \right]^2 \right\} \end{aligned} \quad (2.40)$$

Equation (2.6) can be rewritten as

$$\nabla \cdot \vec{W} = -\frac{1}{\rho} \frac{D\rho}{D\tau} = \rho \frac{D}{D\tau} \left(\frac{1}{\rho} \right)$$

With the above equation, Eq. (2.39) is changed into the following form:

$$\left[\frac{D(\rho e)}{D\tau} + p\rho \frac{D}{D\tau} \left(\frac{1}{\rho} \right) \right] = \Phi + \nabla \cdot (\lambda \nabla t) \quad (2.41)$$

According to thermodynamics equation of fluid

$$\frac{D(\rho h)}{D\tau} = \frac{D(\rho e)}{D\tau} + p\rho \frac{D}{D\tau} \left(\frac{1}{\rho} \right) + \frac{Dp}{D\tau} \quad (2.42)$$

Equation (2.41) can be expressed as the following enthalpy form:

$$\frac{D(\rho h)}{D\tau} = \frac{Dp}{D\tau} + \Phi + \nabla \cdot (\lambda \nabla t) \quad (2.43)$$

or

$$\frac{D(\rho c_p t)}{D\tau} = \frac{Dp}{D\tau} + \Phi + \nabla \cdot (\lambda \nabla t) \quad (2.44)$$

where $h = c_p t$, while c_p is specific heat.

In Cartesian form, the energy Eq. (2.44) can be rewritten as

$$\begin{aligned} & \frac{\partial(\rho c_p t)}{\partial\tau} + w_x \frac{\partial(\rho c_p t)}{\partial x} + w_y \frac{\partial(\rho c_p t)}{\partial y} + w_z \frac{\partial(\rho c_p t)}{\partial z} \\ & = \frac{DP}{D\tau} + \frac{\partial}{\partial x} \left(\lambda \frac{\partial t}{\partial x} \right) + \frac{\partial}{\partial y} \left(\lambda \frac{\partial t}{\partial y} \right) + \frac{\partial}{\partial z} \left(\lambda \frac{\partial t}{\partial z} \right) + \Phi \end{aligned} \quad (2.45)$$

For steady state and nearly constant pressure processes, the viscous dissipation can be ignored, and then the Cartesian form of the energy equation (2.45) is changed into

$$w_x \frac{\partial(\rho c_p t)}{\partial x} + w_y \frac{\partial(\rho c_p t)}{\partial y} + w_z \frac{\partial(\rho c_p t)}{\partial z} = \frac{\partial}{\partial x} \left(\lambda \frac{\partial t}{\partial x} \right) + \frac{\partial}{\partial y} \left(\lambda \frac{\partial t}{\partial y} \right) + \frac{\partial}{\partial z} \left(\lambda \frac{\partial t}{\partial z} \right) \quad (2.46)$$

Above equation is usually approximately rewritten as

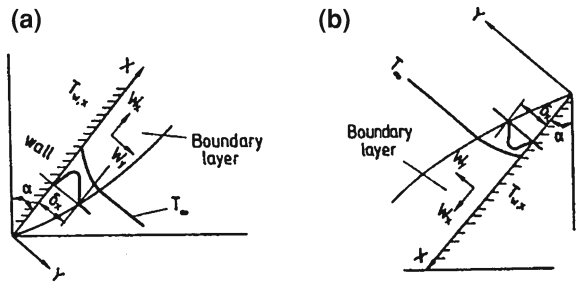
$$\rho \left[w_x \frac{\partial(c_p t)}{\partial x} + w_y \frac{\partial(c_p t)}{\partial y} + w_z \frac{\partial(c_p t)}{\partial z} \right] = \frac{\partial}{\partial x} \left(\lambda \frac{\partial t}{\partial x} \right) + \frac{\partial}{\partial y} \left(\lambda \frac{\partial t}{\partial y} \right) + \frac{\partial}{\partial z} \left(\lambda \frac{\partial t}{\partial z} \right) \quad (2.46a)$$

or

$$\rho c_p \left[w_x \frac{\partial t}{\partial x} + w_y \frac{\partial t}{\partial y} + w_z \frac{\partial t}{\partial z} \right] = \frac{\partial}{\partial x} \left(\lambda \frac{\partial t}{\partial x} \right) + \frac{\partial}{\partial y} \left(\lambda \frac{\partial t}{\partial y} \right) + \frac{\partial}{\partial z} \left(\lambda \frac{\partial t}{\partial z} \right) \quad (2.46b)$$

In fact, in (2.46a) the temperature-dependent density is ignored, and in (2.46b) both the temperature-dependent density and specific heat are ignored.

Fig. 2.4 Physical model and coordinate system of boundary layer of laminar free convection. **a** Ascending flow on the inclined surface ($t_w > t_\infty$). **b** Falling flow on the inclined surface ($t_w < t_\infty$)



2.4 Basic Equations of Laminar Free Convection Boundary Layer

In Fig. 2.4 the physical model and coordinate system of boundary layer with 2D laminar free convection are shown schematically. An inclined flat plate is suspended in fluid. The surface temperature is T_w and the fluid bulk temperature is T_∞ . If T_w is not equal to T_∞ , the laminar free convection can be produced on the inclined surface in both the cases as shown in Fig. 2.4a, b, respectively.

In the following sections, we will make quantitative grade analysis successively to investigate the governing equations of mass, momentum, and energy conservation for steady laminar free convection in the 2D boundary layer.

2.4.1 Continuity Equation

Based on the Eq. (2.7), the steady state 3D continuity equation is given by

$$\frac{\partial}{\partial x}(\rho w_x) + \frac{\partial}{\partial y}(\rho w_y) + \frac{\partial}{\partial z}(\rho w_z) = 0. \tag{2.47}$$

While, the steady state 2D continuity equation is given by

$$\frac{\partial}{\partial x}(\rho w_x) + \frac{\partial}{\partial y}(\rho w_y) + \frac{\partial}{\partial z}(\rho w_z) = 0 \tag{2.48}$$

In Eqs. (2.47) and (2.48), variable fluid density with temperature is considered.

Before the quantitative grade analysis, it is necessary to define its analytical standard. A normal quantitative grade is regarded as $\{1\}$, i.e., unit quantity grade, a very small quantitative grade is regarded as $\{\delta\}$, even very small quantitative grade is regarded as $\{\delta^2\}$, and so on. The ration of the quantities is easily defined, and some examples of ratios are introduced as follows:

$$\frac{\{1\}}{\{1\}} = \{1\}, \quad \frac{\{\delta\}}{\{\delta\}} = \{1\}, \quad \frac{\{1\}}{\{\delta\}} = \{\delta^{-1}\}, \quad \frac{\{1\}}{\{\delta^2\}} = \{\delta^{-2}\}$$

According to the theory of laminar free boundary layer, the quantities of the velocity component w_x and the coordinate x can be regarded as unity, i.e., $\{w_x\} = \{1\}$ and $\{x\} = \{1\}$. However, the quantities of the velocity component w_y and the coordinate y should be regarded as δ , i.e., $\{w_y\} = \{\delta\}$ and $\{y\} = \{\delta\}$.

For the terms of Eq. (2.48), the following ratios of quantity grade are obtained: $\frac{\{\rho w_x\}}{\{x\}} = \frac{\{1\}}{\{1\}} = \{1\}$ and $\frac{\{\rho w_y\}}{\{y\}} = \frac{\{\delta\}}{\{\delta\}} = \{1\}$. Therefore, both the two terms of Eq. (2.48) should be kept, and Eq. (2.48) can be regarded as the continuity equation of the steady state laminar 2D boundary layers. Of course, Eq. (2.48) is also suitable for the steady state 2D boundary layers with laminar free convection.

2.4.2 Momentum Equations (Navier–Stokes Equations)

According to Eqs. (2.23a) and (2.24a), the momentum equations for steady 2D convection are

$$\begin{aligned} \rho \left(w_x \frac{\partial w_x}{\partial x} + w_y \frac{\partial w_x}{\partial y} \right) &= -\frac{\partial p}{\partial x} + 2 \frac{\partial}{\partial x} \left(\mu \frac{\partial w_x}{\partial x} \right) \\ &+ \frac{\partial}{\partial y} \left[\mu \left(\frac{\partial w_x}{\partial y} + \frac{\partial w_y}{\partial x} \right) \right] - \frac{\partial}{\partial x} \left[\frac{2}{3} \mu \left(\frac{\partial w_x}{\partial x} + \frac{\partial w_y}{\partial y} \right) \right] + \rho g_x \end{aligned} \quad (2.49)$$

$$\begin{aligned} \rho \left(w_x \frac{\partial w_y}{\partial x} + w_y \frac{\partial w_y}{\partial y} \right) &= -\frac{\partial p}{\partial y} + \frac{\partial}{\partial x} \left[\mu \left(\frac{\partial w_x}{\partial y} + \frac{\partial w_y}{\partial x} \right) \right] \\ &+ 2 \frac{\partial}{\partial y} \left(\mu \frac{\partial w_y}{\partial y} \right) - \frac{\partial}{\partial y} \left[\frac{2}{3} \mu \left(\frac{\partial w_x}{\partial x} + \frac{\partial w_y}{\partial y} \right) \right] + \rho g_y \end{aligned} \quad (2.50)$$

According to the theory of boundary layer, the quantity grade of the pressure gradient $\frac{\partial p}{\partial x}$ can be regarded as unity, i.e., $\left\{ \frac{\partial p}{\partial x} \right\} = \{1\}$, but the quantity grade of the pressure gradient $\frac{\partial p}{\partial y}$ is only regarded as very small quantity grade, i.e., $\left\{ \frac{\partial p}{\partial y} \right\} = \{\delta\}$.

The quantity grades of the terms of Eqs. (2.49) and (2.50) are expressed as follows, respectively:

$$\begin{aligned} \rho \left(w_x \frac{\partial w_x}{\partial x} + w_y \frac{\partial w_x}{\partial y} \right) &= -\frac{\partial p}{\partial x} + 2 \frac{\partial}{\partial x} \left(\mu \frac{\partial w_x}{\partial x} \right) + \frac{\partial}{\partial y} \left[\mu \left(\frac{\partial w_x}{\partial y} + \frac{\partial w_y}{\partial x} \right) \right] \\ &- \frac{\partial}{\partial x} \left[\frac{2}{3} \mu \left(\frac{\partial w_x}{\partial x} + \frac{\partial w_y}{\partial y} \right) \right] + \rho g_x \\ \{1\} \left(\{1\} \frac{\{1\}}{\{1\}} + \{\delta\} \frac{\{1\}}{\{\delta\}} \right) &= \{1\} + \frac{\{1\}}{\{1\}} \{\delta^2\} \frac{\{1\}}{\{1\}} + \frac{\{1\}}{\{\delta\}} \{\delta^2\} \left(\frac{\{1\}}{\{\delta\}} + \frac{\{\delta\}}{\{1\}} \right) \\ &- \frac{\{1\}}{\{1\}} \delta^2 \left(\frac{\{1\}}{\{1\}} + \frac{\{\delta\}}{\{\delta\}} \right) + \{1\} \{1\} \end{aligned} \quad (2.49a)$$

$$\begin{aligned}
\rho \left(w_x \frac{\partial w_y}{\partial x} + w_y \frac{\partial w_y}{\partial y} \right) &= -\frac{\partial p}{\partial y} + \frac{\partial}{\partial x} \left[\mu \left(\frac{\partial w_x}{\partial y} + \frac{\partial w_y}{\partial x} \right) \right] + 2 \frac{\partial}{\partial y} \left(\mu \frac{\partial w_y}{\partial y} \right) \\
&\quad - \frac{\partial}{\partial y} \left[\frac{2}{3} \mu \left(\frac{\partial w_x}{\partial x} + \frac{\partial w_y}{\partial y} \right) \right] \\
+ \rho g_y \{1\} \left(\{1\} \frac{\{\delta\}}{\{1\}} + \{\delta\} \frac{\{\delta\}}{\{\delta\}} \right) &= \{\delta\} + \frac{\{1\}}{\{1\}} \{\delta^2\} \left(\frac{\{1\}}{\{\delta\}} + \frac{\{\delta\}}{\{1\}} \right) + \frac{\{1\}}{\{\delta\}} \{\delta^2\} \frac{\{\delta\}}{\{\delta\}} \\
&\quad - \frac{\{1\}}{\{\delta\}} \{\delta^2\} \left(\frac{\{1\}}{\{1\}} + \frac{\{\delta\}}{\{\delta\}} \right) + \{1\} \{\delta\}
\end{aligned} \tag{2.50a}$$

The quantity grades of Eqs.(2.49a) and (2.50a) are simplified as follows, respectively:

$$\begin{aligned}
\rho \left(w_x \frac{\partial w_x}{\partial x} + w_y \frac{\partial w_x}{\partial y} \right) &= -\frac{\partial p}{\partial x} + 2 \frac{\partial}{\partial x} \left(\mu \frac{\partial w_x}{\partial y} \right) + \frac{\partial}{\partial y} \left[\mu \left(\frac{\partial w_x}{\partial y} + \frac{\partial w_y}{\partial x} \right) \right] \\
&\quad - \frac{\partial}{\partial y} \left[\frac{2}{3} \mu \left(\frac{\partial w_x}{\partial x} + \frac{\partial w_y}{\partial y} \right) \right] + \rho g_x \\
\{1\}(\{1\} + \{1\}) &= \{1\} + \{\delta^2\} + \{1\} + \{\delta^2\} - (\{\delta^2\} + \{\delta^2\}) + \{1\}
\end{aligned} \tag{2.49b}$$

$$\begin{aligned}
\rho \left(w_x \frac{\partial w_y}{\partial x} + w_y \frac{\partial w_y}{\partial y} \right) &= -\frac{\partial p}{\partial y} + \frac{\partial}{\partial x} \left[\mu \left(\frac{\partial w_x}{\partial y} + \frac{\partial w_y}{\partial x} \right) \right] + 2 \frac{\partial}{\partial y} \left(\mu \frac{\partial w_y}{\partial y} \right) \\
&\quad - \frac{\partial}{\partial y} \left[\frac{2}{3} \mu \left(\frac{\partial w_x}{\partial x} + \frac{\partial w_y}{\partial y} \right) \right] + \rho g_y \\
\{1\}(\{\delta\} + \{\delta\}) &= \{\delta\} + (\{\delta\} + \{\delta^3\}) + \{\delta\} - (\{\delta\}(\{1\} + \{1\})) + \{\delta\}
\end{aligned} \tag{2.50b}$$

Observing the quantity grades in Eq. (2.49b), it is found that the terms $2 \frac{\partial}{\partial x} \left(\mu \frac{\partial w_x}{\partial y} \right)$, $\frac{\partial w_y}{\partial x}$ in term $\frac{\partial}{\partial y} \left[\mu \left(\frac{\partial w_x}{\partial y} + \frac{\partial w_y}{\partial x} \right) \right]$, and $\frac{\partial}{\partial x} \left[\frac{2}{3} \mu \left(\frac{\partial w_x}{\partial x} + \frac{\partial w_y}{\partial y} \right) \right]$ are very small and can be ignored from Eq. (2.49). Then, Eq. (2.49) is simplified as follows:

$$\rho \left(w_x \frac{\partial w_x}{\partial x} + w_y \frac{\partial w_x}{\partial y} \right) = -\frac{\partial p}{\partial x} + \frac{\partial}{\partial y} \left(\mu \left(\frac{\partial w_x}{\partial y} \right) \right) + \rho g_x \tag{2.51}$$

Comparing the quantity grades of Eq. (2.49b) with that of Eq. (2.50b), it is found that the quantity grades of Eq. (2.50b) are very small. Then, Eq. (2.50) can be ignored, and only Eq. (2.51) is taken as the momentum equation of 2D boundary layer.

From Fig. 2.4 it is found that for free convection on inclined plate the gravity acceleration component g_x is expressed as

$$g_x = g \cdot \cos \alpha \tag{2.52}$$

where g is gravity acceleration and α is the inclined angle of the plate.

With Eq. (2.52), Eq. (2.51) is rewritten as

$$\rho \left(w_x \frac{\partial w_x}{\partial x} + w_y \frac{\partial w_x}{\partial y} \right) = -\frac{\partial p}{\partial x} + \frac{\partial}{\partial y} \left(\mu \left(\frac{\partial w_x}{\partial y} \right) \right) + \rho g \cdot \cos \alpha \quad (2.53)$$

Suppose, the direction of $g \cdot \cos \alpha$ is reverse to that of the velocity component w_x , Eq. (2.53) can be rewritten as

$$\rho \left(w_x \frac{\partial w_x}{\partial x} + w_y \frac{\partial w_x}{\partial y} \right) = -\frac{\partial p}{\partial x} + \frac{\partial}{\partial y} \left(\mu \left(\frac{\partial w_x}{\partial y} \right) \right) - \rho g \cdot \cos \alpha \quad (2.54)$$

Beyond the boundary layer, where the effects of viscosity can be ignored, the momentum equation (2.54) is simplified into the following equation:

$$-\frac{dp}{dx} = \rho_\infty g \cdot \cos \alpha + \rho_\infty w_{x,\infty} \frac{dw_{x,\infty}}{dx} \quad (2.55)$$

where ρ_∞ and $w_{x,\infty}$ are fluid density and velocity component beyond the boundary layer.

With Eq. (2.55), Eq. (2.54) becomes

$$\rho \left(w_x \frac{\partial w_x}{\partial x} + w_y \frac{\partial w_x}{\partial y} \right) = \frac{\partial}{\partial y} \left(\mu \frac{\partial w_x}{\partial y} \right) + g(\rho_\infty - \rho) + \rho_\infty w_\infty \frac{dw_\infty}{dx} \quad (2.56)$$

For constant $w_{x,\infty}$ the Eq. (2.56) transforms to

$$\rho \left(w_x \frac{\partial w_x}{\partial x} + w_y \frac{\partial w_x}{\partial y} \right) = \frac{\partial}{\partial y} \left(\mu \frac{\partial w_x}{\partial y} \right) + g(\rho_\infty - \rho) \cos \alpha \quad (2.57)$$

This is the momentum equation of 2D boundary layer on an inclined plate with laminar free convection.

Equation (2.57) can be rewritten as

$$\rho \left(w_x \frac{\partial w_x}{\partial x} + w_y \frac{\partial w_x}{\partial y} \right) = \frac{\partial}{\partial y} \left(\mu \frac{\partial w_x}{\partial y} \right) + g |\rho_\infty - \rho| \cos \alpha \quad (2.57a)$$

In (2.57a), the absolute value of buoyancy factor $|\rho_\infty - \rho|$ shows that the buoyancy term $g |\rho_\infty - \rho| \cos \alpha$ has always positive sign no matter which one is larger between ρ and ρ_∞ . In this case, the buoyancy term $g |\rho_\infty - \rho| \cos \alpha$ and the velocity component w_x have same sign.

For the free convection of a perfect gas (ideal gas), the following simple power law can be used: $\frac{\rho_\infty}{\rho} = \frac{T}{T_\infty}$ where T denotes absolute temperature. In fact, for general real gas, this relation is also available. Therefore,

$$|\rho_\infty - \rho| \cos \alpha = \rho \left| \frac{T}{T_\infty} - 1 \right| \cos \alpha \quad (2.58)$$

Thus, for the laminar free convection of a perfect gas, Eq. (2.57) can be changed into

$$\rho \left(w_x \frac{\partial w_x}{\partial x} + w_y \frac{\partial w_x}{\partial y} \right) = \frac{\partial}{\partial y} \left(\mu \frac{\partial w_x}{\partial y} \right) + g\rho \left| \frac{T}{T_\infty} - 1 \right| \cos \alpha \quad (2.59)$$

If the temperature difference $|T_w - T_\infty|$ is very small, which will lead to a very small density difference $|\rho_\infty - \rho_w|$, the Boussinesq approximation can be applied. In this case, buoyancy factor in Eq. (2.57a) becomes $|\rho_\infty - \rho| = \rho\beta |T - T_\infty|$, and then, Eq. (2.57a) is changed to

$$w_x \frac{\partial w_x}{\partial x} + w_y \frac{\partial w_x}{\partial y} = \nu \frac{\partial^2 w_x}{\partial y^2} + g\beta |T - T_\infty| \cos \alpha \quad (2.57b)$$

where β is *Coefficient of expansion*.

2.4.3 Energy Equations

According to Eq. (2.46a), the energy equation for steady 2D convection is shown as follows:

$$\rho \left[w_x \frac{\partial(c_p t)}{\partial x} + w_y \frac{\partial(c_p t)}{\partial y} \right] = \frac{\partial}{\partial x} \left(\lambda \frac{\partial t}{\partial x} \right) + \frac{\partial}{\partial y} \left(\lambda \frac{\partial t}{\partial y} \right) \quad (2.60)$$

With the quantity grade analysis similar to that mentioned above, Eq. (2.60) can be changed into the following form for energy equation of 2D boundary layer.

$$\rho \left[w_x \frac{\partial(c_p t)}{\partial x} + w_y \frac{\partial(c_p t)}{\partial y} \right] = \frac{\partial}{\partial y} \left(\lambda \frac{\partial t}{\partial y} \right) \quad (2.61)$$

Up to now, it is the time to summarize the basic governing equations for description of mass, momentum, and energy conservation of 2D boundary layers with consideration of variable physical properties for laminar steady-state free convection as follows:

$$\frac{\partial}{\partial x}(\rho w_x) + \frac{\partial}{\partial y}(\rho w_y) + \frac{\partial}{\partial z}(\rho w_z) = 0 \quad (2.48)$$

$$\rho \left(w_x \frac{\partial w_x}{\partial x} + w_y \frac{\partial w_x}{\partial y} \right) = \frac{\partial}{\partial y} \left(\mu \frac{\partial w_x}{\partial y} \right) + g|\rho_\infty - \rho| \cos \alpha \quad (2.57a)$$

$$\rho \left[w_x \frac{\partial(c_p t)}{\partial x} + w_y \frac{\partial(c_p t)}{\partial y} \right] = \frac{\partial}{\partial y} \left(\lambda \frac{\partial t}{\partial y} \right) \quad (2.61)$$

For rigorous solutions of the governing equations, the fluid temperature-dependent properties, such as density ρ in mass equation and in buoyancy factor of momentum equation, absolute viscosity μ , specific heat c_p , and thermal conductivity λ will be considered in the successive chapters of this book.

The laminar free convection with two-dimensional boundary layer belongs to two-point boundary value problem, which is the basis of three-point boundary value problem, such as for film boiling and film condensation. For isothermal plate for example, the boundary conditions for the two-point boundary problem can be expressed as follows:

$$y = 0: \quad w_x = 0, \quad w_y = 0, \quad t = t_w \quad (2.62)$$

$$y \rightarrow \infty: \quad w_x \rightarrow 0, \quad t = t_\infty \quad (2.63)$$

where t_w is plate temperature, t_∞ is the fluid temperature beyond the boundary layer, and $w_{x,\infty}$ denotes the fluid velocity component in x -direction beyond the boundary layer.

The term $g |\rho_\infty - \rho| \cos \alpha$ in Eq.(2.57a) is regarded as buoyancy factor. For perfect gas, the buoyancy factor can be expressed as $g |\rho_\infty - \rho| \cos \alpha = \rho g \left| \frac{T}{T_\infty} - 1 \right| \cos \alpha$, then the basic governing equation for description of momentum conservation of 2D boundary layers with laminar steady state gas free convection can be expressed as

$$\rho \left(w_x \frac{\partial w_x}{\partial x} + w_y \frac{\partial w_x}{\partial y} \right) = \frac{\partial}{\partial y} \left(\mu \frac{\partial w_x}{\partial y} \right) + \rho g \left| \frac{T}{T_\infty} - 1 \right| \cos \alpha \quad (2.57b)$$

In addition, although the Eq.(2.57b) is originally for perfect gas, it is well known that it can be very accurately applied to free convection and film flows of general gases (Tables 2.1 and 2.2).

However, for Boussinesq approximation (in fact, only suitable for very small temperature difference of the boundary layer), the partial differential equations (2.48), (2.57) and (2.61) becomes

$$\frac{\partial}{\partial x} (\rho w_x) + \frac{\partial}{\partial y} (\rho w_y) = 0 \quad (2.48a)$$

$$w_x \frac{\partial w_x}{\partial x} + w_y \frac{\partial w_x}{\partial y} = \nu \left(\frac{\partial^2 w_x}{\partial y^2} \right) + g \beta |T - T_\infty| \cos \alpha \quad (2.57c)$$

$$w_x \frac{\partial t}{\partial x} + w_y \frac{\partial t}{\partial y} = \frac{\nu}{\text{Pr}} \frac{\partial^2 t}{\partial y^2} \quad (2.61a)$$

Table 2.1 Governing partial differential conservation equations in rectangular coordinate system for laminar free convection (with consideration of variable physical properties)

Mass equation	$\frac{\partial}{\partial x}(\rho w_x) + \frac{\partial}{\partial y}(\rho w_y) + \frac{\partial}{\partial z}(\rho w_z) = 0$
Momentum equation	$\rho \left(\frac{\partial w_x}{\partial x} w_x + \frac{\partial w_x}{\partial y} w_y + \frac{\partial w_x}{\partial z} w_z \right) = -\frac{\partial p}{\partial x} + 2 \frac{\partial}{\partial x} \left(\mu \frac{\partial w_x}{\partial x} \right)$ $+ \frac{\partial}{\partial y} \left[\mu \left(\frac{\partial w_x}{\partial y} + \frac{\partial w_y}{\partial x} \right) \right] + \frac{\partial}{\partial z} \left[\mu \left(\frac{\partial w_x}{\partial z} + \frac{\partial w_z}{\partial x} \right) \right]$ $- \frac{\partial}{\partial x} \left[\frac{2}{3} \mu \left(\frac{\partial w_x}{\partial x} + \frac{\partial w_y}{\partial y} + \frac{\partial w_z}{\partial z} \right) \right] + \rho g_x$ $\rho \left(\frac{\partial w_y}{\partial x} w_x + \frac{\partial w_y}{\partial y} w_y + \frac{\partial w_y}{\partial z} w_z \right) = -\frac{\partial p}{\partial y} + \frac{\partial}{\partial x} \left[\mu \left(\frac{\partial w_x}{\partial y} + \frac{\partial w_y}{\partial x} \right) \right]$ $+ 2 \frac{\partial}{\partial y} \left(\mu \frac{\partial w_y}{\partial y} \right) + \frac{\partial}{\partial z} \left[\mu \left(\frac{\partial w_y}{\partial z} + \frac{\partial w_z}{\partial y} \right) \right]$ $- \frac{\partial}{\partial y} \left[\frac{2}{3} \mu \left(\frac{\partial w_x}{\partial x} + \frac{\partial w_y}{\partial y} + \frac{\partial w_z}{\partial z} \right) \right] + \rho g_y$ $\rho \left(\frac{\partial w_z}{\partial x} w_x + \frac{\partial w_z}{\partial y} w_y + \frac{\partial w_z}{\partial z} w_z \right) = -\frac{\partial p}{\partial z} + \frac{\partial}{\partial x} \left[\mu \left(\frac{\partial w_x}{\partial z} + \frac{\partial w_z}{\partial x} \right) \right]$ $+ \frac{\partial}{\partial y} \left[\mu \left(\frac{\partial w_y}{\partial z} + \frac{\partial w_z}{\partial y} \right) \right] + 2 \frac{\partial}{\partial z} \left(\mu \frac{\partial w_z}{\partial z} \right)$ $- \frac{\partial}{\partial z} \left[\frac{2}{3} \mu \left(\frac{\partial w_x}{\partial x} + \frac{\partial w_y}{\partial y} + \frac{\partial w_z}{\partial z} \right) \right] + \rho g_z$
Energy equation	$\rho \left[w_x \frac{\partial(c_p \cdot t)}{\partial x} + w_y \frac{\partial(c_p \cdot t)}{\partial y} + w_z \frac{\partial(c_p \cdot t)}{\partial z} \right]$ $= \frac{\partial}{\partial x} \left(\lambda \frac{\partial t}{\partial x} \right) + \frac{\partial}{\partial y} \left(\lambda \frac{\partial t}{\partial y} \right) + \frac{\partial}{\partial z} \left(\lambda \frac{\partial t}{\partial z} \right) + \Phi$ $\Phi = \mu \left[2 \left(\frac{\partial w_x}{\partial x} \right)^2 + 2 \left(\frac{\partial w_y}{\partial y} \right)^2 + 2 \left(\frac{\partial w_z}{\partial z} \right)^2 + \left(\frac{\partial w_x}{\partial y} + \frac{\partial w_y}{\partial x} \right)^2 + \left(\frac{\partial w_y}{\partial z} + \frac{\partial w_z}{\partial y} \right)^2 \right.$ $\left. + \left(\frac{\partial w_z}{\partial x} + \frac{\partial w_x}{\partial z} \right)^2 \right] - \frac{2}{3} \left[\text{div}(\vec{W}) \right]^2$

Table 2.2 Governing partial differential equations in rectangular coordinate system for laminar free convection boundary layer

Governing partial differential equations for laminar free boundary layer (with consideration of variable physical properties)	
Mass equation	$\frac{\partial}{\partial x}(\rho w_x) + \frac{\partial}{\partial y}(\rho w_y) = 0$
Momentum equation	$\rho \left(w_x \frac{\partial w_x}{\partial x} + w_y \frac{\partial w_x}{\partial y} \right) = \frac{\partial}{\partial y} \left(\mu \frac{\partial w_x}{\partial y} \right) + g \rho_\infty - \rho \cos \alpha$ <p>(for fluid free convection)</p> $\rho \left(w_x \frac{\partial w_x}{\partial x} + w_y \frac{\partial w_x}{\partial y} \right) = \frac{\partial}{\partial y} \left(\mu \frac{\partial w_x}{\partial y} \right) + \rho g \left \frac{T}{T_\infty} - 1 \right \cos \alpha$ <p>(for gas free convection)</p>
Energy equation	$\rho \left[w_x \frac{\partial(c_p t)}{\partial x} + w_y \frac{\partial(c_p t)}{\partial y} \right] = \frac{\partial}{\partial y} \left(\lambda \frac{\partial t}{\partial y} \right)$
(with ignoring variable physical properties)	
Mass equation	$\frac{\partial w_x}{\partial x} + \frac{\partial w_y}{\partial y} = 0$
Momentum equation	$w_x \frac{\partial w_x}{\partial x} + w_y \frac{\partial w_x}{\partial y}$ $= \left(\nu \frac{\partial^2 w_x}{\partial y^2} \right) + g \beta T - T_\infty \cos \alpha$
Energy equation	$w_x \frac{\partial t}{\partial x} + w_y \frac{\partial t}{\partial y} = \frac{\nu}{\text{Pr}} \frac{\partial^2 t}{\partial y^2}$

2.5 Summary

Up to now the governing partial differential conservation equations for laminar free convection and those for laminar free boundary layer can be summarized as Table 2.1 and 2.2.

2.6 Exercises

1. Point out the advantages of inducing the boundary layer theory.
2. From the related governing equations, tell us the importance and necessity of consideration of variable physical properties in investigation of convection heat transfer, and point out the limitation with ignoring the variable physical properties.
3. Please review the governing partial differential conservation equations in rectangular coordinate system for laminar free convection (with consideration of variable physical properties), and use the quantitative grade analysis to derive out the related boundary layer governing ordinary differential equations with consideration of variable physical properties.

Chapter 3

Review of Falkner–Skan Transformation for Fluid Laminar Free Convection

Abstract In this chapter, the traditional Falkner–Skan type transformation for laminar free convection boundary layer is reviewed. The typical two-dimensional basic conservation equations for laminar free convection boundary layer are taken as example for derivation of the related similarity variables for Falkner–Skan type transformation. By means of the stream function and the procedure with the method of group theory, the similarity intermediate function variable $f(\eta)$ is induced. Then, the velocity components are transformed to the related functions with the similarity intermediate function variable ($f\eta$). On this basis, partial differential momentum equation of the free convection boundary layer is transformed to related ordinary equation. At last, the limitations of the Falkner–Skan type transformation are analyzed in detail.

3.1 Introduction

For solution of the laminar boundary layer problem, Falkner and Skan [1] proposed their similarity method in 1931. Up to now, the widely applied similarity analysis and transformation for the laminar convection boundary layer and film flows is based on the Falkner–Skan type transformation. So far, the Falkner–Skan type transformation has been collected in numerous publications, and only some of them such as [2–14] are listed here for saving space. So, before the presentation of my related new similarity analysis method in this book for laminar free convection and film flows, it is necessary here to review briefly the Falkner–Skan type similarity method.

3.2 Falkner–Skan Transformation Related to Governing Equations Under Boussinesq Approximation

Let us consider the governing equations of the boundary layer of steady state fluid laminar free convection. Based on Chap. 2, the governing equations of the boundary layer of steady state fluid laminar free convection are as follows for *Boussinesq approximation* (For convenient derivation, only vertical case is considered here):

$$\frac{\partial w_x}{\partial x} + \frac{\partial w_y}{\partial y} = 0. \quad (3.1)$$

$$w_x \frac{\partial w_x}{\partial x} + w_y \frac{\partial w_x}{\partial y} = \nu \frac{\partial^2 w_x}{\partial y^2} + g |\rho_\infty - \rho|. \quad (3.2)$$

$$\left(w_x \frac{\partial t}{\partial x} + w_y \frac{\partial t}{\partial y} \right) = \frac{\nu}{\text{Pr}} \frac{\partial^2 t}{\partial y^2}. \quad (3.3)$$

For rigorous solutions of the governing equations, the fluid temperature dependent properties, such as density, absolute viscosity, specific heat, and thermal conductivity will be considered in the successive chapters of this book.

The laminar free convection with two-dimensional boundary layer belongs to two-point boundary value problem. For isothermal flat plate for example, the boundary conditions for the two-point boundary problem can be expressed as follows:

$$y = 0 : \quad w_x = 0, \quad w_y = 0, \quad t = t_w. \quad (3.4)$$

$$y \rightarrow \infty : \quad w_{x,\infty} = 0, \quad t = t_\infty. \quad (3.5)$$

Here, w_x and w_y are velocity components of the fluids in x and y directions respectively, $w_{x,\infty}$ is constant main stream velocity, t is temperature. While, the subscript “ f ” is induced in the equations for inferring in particular to the constant physical properties with the average temperature of boundary layer, i.e., $t_f = \frac{t_w + t_\infty}{2}$ (Hereinafter the same). Here, Eqs. (3.1)–(3.3) will be taken as a basis for introduction of the Falkner–Skan type transformation method.

The detailed derivation for the related expressions of the Falkner–Skan transformation is omitted here, which need inducing the stream function $\psi(x, y)$ at first, and then requires a group theorem discussed at length by Hansen [15] and Na [16]. Meanwhile, the stream function is expressed by

$$w_x = \frac{\partial \psi}{\partial y}, \quad w_y = -\frac{\partial \psi}{\partial x}. \quad (3.6)$$

With Falkner–Skan transformation for fluid laminar free convection, we get the following variables for describing expressions for the stream function ψ and dimen-

sionless coordinate variable η :

$$\eta = \left(\frac{1}{4}\text{Gr}\right)^{1/4} \frac{y}{x}; \quad \psi = 4\nu \left(\frac{1}{4}\text{Gr}\right)^{1/4} f(\eta) \quad (3.7)$$

where Grashof number is expressed as

$$\text{Gr} = \frac{g\beta |T_w - T_\infty| x^3}{\nu_f^2}. \quad (3.8)$$

Combined with Eqs. (3.7) and (3.8), then, the dimensionless variables, w_x and w_y are derived from Eq. (3.6) respectively as follows:

$$w_x = \frac{4\nu}{x} \left(\frac{1}{4}\text{Gr}\right)^{1/2} f'(\eta), \quad (3.9)$$

$$w_y = \frac{\nu}{x} \left(\frac{1}{4}\text{Gr}\right)^{1/4} [(\eta)f'(\eta) - 3f(\eta)]. \quad (3.10)$$

Dimensionless temperature $\theta(\eta)$ is also given by

$$\theta(\eta) = \frac{t - t_\infty}{t_w - t_\infty}. \quad (3.11)$$

With Eqs. (3.9)–(3.11), Eqs. (3.1)–(3.3) lead to the following ordinary differential equations

$$f''' + 3f(\eta)f''(\eta) - 2(f'(\eta))^2 + \theta(\eta) = 0 \quad (3.12)$$

$$\theta''(\eta) + 3\text{Pr}f(\eta)\theta'(\eta) = 0 \quad (3.13)$$

with the boundary conditions

$$\eta = 0 : \quad f(\eta) = f'(\eta) = 0, \quad \theta(\eta) = 1 \quad (3.14)$$

$$\eta \rightarrow \infty : \quad f'(\eta) = 0, \quad \theta(\eta) = 0. \quad (3.15)$$

3.3 Falkner–Skan Transformation Related to Governing Equations with Consideration of Variable Physical Properties

Consider the boundary layer of the fluid laminar free convection from an isothermal vertical plate, the following governing partial differential equations of laminar free convection with consideration of variable physical properties are given by consulting

Eqs. (2.48), (2.57a) and (2.61):

$$\frac{\partial}{\partial x}(\rho w_x) + \frac{\partial}{\partial y}(\rho w_y) = 0 \quad (3.16)$$

$$\rho \left(w_x \frac{\partial w_x}{\partial x} + w_y \frac{\partial w_x}{\partial y} \right) = \frac{\partial}{\partial y} \left(\mu \frac{\partial w_x}{\partial y} \right) + g|\rho_\infty - \rho| \quad (3.17)$$

$$\rho c_p \left(w_x \frac{\partial t}{\partial x} + w_y \frac{\partial t}{\partial y} \right) = \frac{\partial}{\partial y} \left(\lambda \frac{\partial t}{\partial y} \right) \quad (3.18)$$

with the boundary conditions

$$y = 0 : \quad w_x = 0, \quad w_y = 0, \quad t = t_w \quad (3.19)$$

$$y \rightarrow \infty : \quad w_x \rightarrow 0, \quad t = t_\infty \quad (3.20)$$

where μ is the absolute viscosity, ρ is the density, λ is the thermal conductivity, g is the gravity acceleration, and t is temperature.

For variable physical properties, we set up following definition of the stream function ψ :

$$\frac{\rho}{\rho_w} w_x = \frac{\partial \psi}{\partial y}, \quad \frac{\rho}{\rho_w} w_y = -\frac{\partial \psi}{\partial x}. \quad (3.21)$$

For variable physical properties we can give expressions for stream function ψ and dimensionless coordinate variable η as defined by:

$$\eta = cx^{-1/4} \int_0^y \frac{\rho}{\rho_w} dy, \quad \psi = 4v_w \left(\frac{1}{4} \text{Gr}_{x,w} \right)^{1/4} f(\eta)$$

where

$$G_{x,w} = \frac{g|\rho_\infty/\rho_w - 1|x^3}{v_w^2}. \quad (3.22)$$

Dimensionless temperature $\theta(\eta)$ is defined by Eq. (3.11) too.

The function θ is a dimensionless temperature and f is related to the velocities in the following way

$$w_x = 4v_w c^2 x^{1/2} f'(\eta), \quad w_y = \left(\frac{\rho_w}{\rho} \right) \left(\frac{v_w c}{x^{1/4}} \right) (\eta f'(\eta) - 3f(\eta)) \quad (3.23)$$

where

$$C = \text{Gr}_{x,w} x^{-3/4}. \quad (3.24)$$

With the variables used in Eqs.(3.11), (3.21)–(3.24), Eqs.(3.16)–(3.18) are now transformed into the following equations:

$$\frac{d}{d\eta} \left[\frac{\rho\mu}{\rho_w\mu_w} f''(\eta) \right] + 3f(\eta)f''(\eta) - 2[f'(\eta)]^2 + \theta(\eta) = 0 \tag{3.25}$$

$$\frac{d}{d\eta} \left[\frac{\rho\lambda}{\rho_w\lambda_w} \theta'(\eta) \right] + 3Pr_w \left(\frac{c_p}{c_{p_w}} \right) f(\eta)\theta'(\eta) = 0 \tag{3.26}$$

where λ, ρ, c_p and Pr are thermal conductivity, density, specific heat and Prandtl number, respectively, while subscript w denotes the temperature on the wall.

The boundary conditions, (3.19) and (3.20) are transformed into

$$\eta = 0 : f(\eta) = f'(\eta) = 0, \quad \theta(\eta) = 1 \tag{3.27}$$

$$\eta \rightarrow \infty : f'(\eta) = 0, \quad \theta(\eta) = 0. \tag{3.28}$$

3.4 Limitations of the Falkner–Skan Type Transformation

From the similarity governing equations on laminar free convection boundary layer produced by Falkner–Skan type transformation, it is not difficult to find the disadvantages of this traditional similarity method.

By means of group theorem, obtaining the appropriate dimensional variables related to two-dimensional velocity components is complicated process, which has caused a restriction for application of the Falkner–Skan type transformation on extensive study of laminar free convection boundary layer and two-phase film flows.

By using the Falkner–Skan type similarity transformation, the dimensionless function $f(\eta)$ and its derivatives become the main dimensionless similarity variables of momentum field, and the velocity components are algebraic expressions with intermediate function $f(\eta)$ and its derivatives. Then, inconvenience is caused for investigation of the velocity field of laminar free convection and even for investigation of two-phase free film condensation and boiling.

With the Falkner–Skan transformation, a difficulty is encountered for similarity transformation of the governing equations for the laminar free convection with consideration of variable physical properties. It is because that derivation for obtaining an appropriate stream function expression as well as the expressions of the two-dimensional velocity components is difficult in particular consideration of variable physical properties. In addition, the velocity components can not easily be replaced by the stream function ψ . Furthermore, the great difficulty is encountered in the treatment of the variable physical properties in Eqs.(3.25) and (3.26), because the physical property factors $\frac{\rho\mu}{\rho_w\mu_w}, \frac{\rho\lambda}{\rho_w\lambda_w}$ and $\frac{c_p}{c_{p_w}}$ are function of temperature, and therefore are functions of η . Since rigorous consideration of variable physical properties is

closely related to the reliability of investigation of laminar free convection and two-phase film flows, such difficulty has hindered the research development of laminar free convection and its two-phase film flows.

To resolve the above problems caused by the traditional Falkner–Skan type transformation, in the following chapters, a related novel similarity analysis method will be presented for extensive investigation of laminar forced convection and two-phase film flows.

3.5 Questions

1. Please list all similarity variables for Falkner–Skan type transformation for laminar free convection boundary layer.
2. How to express the two-dimensional velocity components by using the Falkner–Skan type transformation for laminar free convection?
3. Can you point out the limitations of the Falkner–Skan type transformation in its application?
4. Suppose that the dimensionless coordinate variable η in Eq. (3.7) is replaced by the form $\eta = (\text{Gr})^{1/4} \frac{y}{x}$, and the forms of other similarity variables are kept, please try to transform similarly the governing partial differential equations (3.1) to (3.3) and the boundary condition equations (3.4) and (3.5) to the related ordinary differential equations.
5. From question 2, what relationship can you find between the similarity coordinate variable η and the transformed governing ordinary differential equations?

References

1. V.M. Falkner, S.W. Skan, Some approximate solutions of the boundary layer equations. *Phil. Mag.* **12**, 865 (1931)
2. E.M. Sparrow, J.L. Gregg, The variable fluid property problem in free convection. *Trans. ASME* **80**, 879–886 (1958)
3. B. Gebhart, Natural convection flow, instability, and transition. *J. Heat Transfer* **91**, 293–309 (1969)
4. E.R.G. Eckert, R.M. Drake, *Analysis of Heat and Mass Transfer* (McGraw-Hill, New York, 1972)
5. H. Schlichting, *Boundary Layer Theory* (trans: J. Kestin) (McGraw-Hill, New York, 1979), pp. 316–317
6. D.D. Gray, A. Giognini, The validity of the Boussinesq approximation for liquids and gases. *Int. J. Heat Mass Transfer* **19**, 545–551 (1977)
7. A.M. Clausing, S.N. Kempka, The influences of property variations on natural convection from vertical surfaces. *J. Heat Transfer* **103**, 609–612 (1981)
8. T. Cebeci, P. Bradshaw, *Physical and Computational Aspects of Convective Heat Transfer* (Springer, New York, 1984)
9. T. Fujii, *Theory of Laminar Film Condensation* (Springer, New York, 1991)
10. B. Louis et al., *Convective Heat Transfer*, 2nd edn. (Wiley, New York, 1993)

11. S. Kakac, Y. Yenner, *Convective Heat Transfer*, 2nd edn. (CRC Press, Boca Raton, 1995)
12. A. Bejan, *Convection Heat Transfer*, 2nd edn. (Wiley, New York, 1995)
13. I. Pop, D.B. Ingham, *Convective Heat transfer—Mathematical and Computational Modelling of Viscous Fluids and Porous Media* (Elsevier, Amsterdam, 2001)
14. T. Cebeci, *Convective Heat Transfer* 2nd edn. (Springer, Heidelberg, 2002)
15. A.G. Hansen, *Similarity analysis of boundary value problems in engineering* (Presentice-Hall, Englewood Cliffs, 1964)
16. T.Y. Na, *Computational methods in engineering boundary value problems* (Academic, New York, 1979)

Chapter 4

New Similarity Analysis Method for Laminar Free Convection Boundary Layer and Film Flows

Abstract A new similarity analysis method with a new set of dimensionless similarity variables is provided for complete similarity transformation of the governing partial differential equations of laminar free convection and two multi-phase film flows. The derivation of the Reynolds number together with the Nusselt number and Prandtl number is reviewed by means of Buckingham π -theorem and dimension analysis, where the Reynolds number is taken as the one of the new set of dimensionless analysis variables. The essential work focuses on derivation of equations for the dimensionless velocity components and the dimensionless coordinate variable, by means of a detailed analysis of quantity grade of the governing conservation partial differential equations of laminar free convection. On this basis, the new similarity analysis method is produced for complete similarity transformation of the conservation partial differential equations of laminar free convection and its film flows. With the novel dimensionless velocity components devoted in this chapter, the new similarity analysis method has obvious advantages compared with the Falkner–Skan transformation. These advantages are (i) more convenient for consideration and treatment of the variable physical properties, (ii) more convenient for analysis and investigation of the two-dimensional velocity field, and (iii) more convenient for satisfaction of the interfacial mass transfer matching conditions in the numerical calculation and for rigorous investigation of mass transfer for two-phase film flows with three-point boundary problem. These advantages will be found from the successive chapters.

4.1 Introduction

In Chap. 3 the traditional similarity analysis method, Falkner–Skan type transformation, for similarity transformation of governing partial differential equations of laminar convection was reviewed. With this method a flow function has to be induced at first, and then function $f(\eta)$ and its derivatives will become the unknown variables of the transformed dimensionless governing equations. Obviously, with

this method, it is not convenient for similarity transformation of the governing partial differential equations of laminar convection and film flows, never convenient to treat fluid variable thermophysical properties in the governing equations, and not easy to investigate heat and mass transfer, especially for multi-phase film flows, such as laminar film boiling and condensation.

To overcome these difficulties, a new similarity analysis method will be presented in this chapter. This method was at first reported in Ref. [1], and has been widely applied in our investigations on fluid laminar free convection [1–3], laminar free film boiling and condensation [4–6], and film flow of non-Newtonian fluids [7–9]. It has been found from these studies that, compared with the traditional Falkner–Skan transformation, the new similarity analysis method has obvious advantages on deep investigations on heat and mass transfer problems of free convection boundary layer and film flows, especially with consideration of variable physical properties.

In this chapter, we will take laminar free convection as an example to determine and derive a system of dimensionless similarity variables, such as local Grashof number, dimensionless coordinate variable, and dimensionless velocity components. In the derivation of the dimensionless similarity variables by using this method, it is never necessary to induce the flow function ψ , as well as the intermediate variable $f(\eta)$ and its derivatives in the transformed governing equation. In the following chapters of this book, it can be found that for investigation of fluid free convection, film boiling and condensation, and even falling film flow of non-Newtonian fluids, with this method, the treatment of fluid variable physical properties will be easier, and analysis of heat and mass transfer will become much more convenient than those based on Falkner–Skan type transformation.

4.2 Governing Equations of Fluid Laminar Free Convection

In this section, governing partial differential equations of fluid laminar free convection will be taken as example for investigation of the *new similarity analysis method*. Here, the key work is to derive and determine the related similarity variables, dimensionless coordinate variable, and dimensionless velocity components for similarity transformation of the governing partial differential equations. To this end, we take a fluid flow on a flat plate shown in Fig. 2.4 as the physical analysis model and co-ordinate system of laminar free convection.

According to Chap. 2 the present governing partial differential equations of fluid laminar free convection with Boussinesq approximation are expressed as follows:

$$\frac{\partial w_x}{\partial x} + \frac{\partial w_y}{\partial y} = 0 \quad (4.1)$$

$$w_x \frac{\partial w_x}{\partial x} + w_y \frac{\partial w_x}{\partial y} = \nu \frac{\partial^2 w_x}{\partial y^2} + g\beta |T - T_\infty| \cos \alpha \quad (4.2)$$

$$w_x \frac{\partial t}{\partial x} + w_y \frac{\partial t}{\partial y} = \frac{\nu}{\text{Pr}} \frac{\partial^2 t}{\partial y^2} \quad (4.3)$$

with the boundary conditions

$$y = 0 : W_x = 0, \quad W_y = 0, \quad t = t_w \quad (4.4)$$

$$y \rightarrow \infty : W_x \rightarrow 0, \quad t = t_\infty \quad (4.5)$$

where the values of the physical properties are mean values, for instance $\nu = (\nu_w + \nu_\infty)/2$ and $\text{Pr} = (\text{Pr}_w + \text{Pr}_\infty)/2$ for the Boussinesq approximation. The absolute value of buoyancy term $g\beta |T - T_\infty|$ shows that it has always positive sign no matter which one is larger between ρ and ρ_∞ . In this case, the buoyancy term $g\beta |T - T_\infty|$ and the velocity component w_x have the same sign.

Here, the plate temperature is isothermal, and the Boussinesq approximation is applied in the governing equations in order to simplify derivation of the similarity variables and the transformation of the governing partial differential equations.

The above equations will be used for derivation of similarity variables for transformation of the governing partial differential equations. For such purpose, Grashof number will be derived at first.

4.3 Derivation on Dimensionless Physical Parameters

There are different methods for derivation of the dimensionless physical parameters, such as Falkner–Skan analysis [10–12], differential equation analysis, and π -theorem [13] with dimension analysis. Here, the π -theorem with dimension analysis is applied to derive the dimensionless physical parameters.

4.3.1 Select Whole Physical Variables Related to the Physical Phenomena

The whole physical variables should be selected from the governing Eqs. (4.1)–(4.3), and then the following equation can be obtained in principle:

$$f(\lambda, L, \mu, g\beta |T_w - T_\infty| \cos \alpha, \alpha, \rho, c_p) = 0 \quad (4.6)$$

Here, L is reference length of the plate, λ , μ , ρ , and c_p are thermal conductivity, absolute viscosity, density and specific heat of the fluid, α is the heat transfer coefficient, and g is the gravity acceleration. While, $g\beta |T_w - T_\infty| \cos \alpha$ is related to the buoyancy. The above seven physical variables (i.e. $n = 7$) are independent, and decisive variables of fluid free convection.

4.3.2 Select Basic Dimension System

For investigation of the problem such as free convection heat transfer, the following five physical dimensions can be taken as basic ones: time [s], length [m], mass [kg], temperature [K], and quantity of heat, [J], where the symbols in square brackets [] express the basic physic dimensions. The above independent physical dimensions λ , L , μ , g , α , ρ and c_p can be derived from them, and expressed as $\left[\frac{\text{J}}{\text{m} \cdot \text{s} \cdot \text{K}}\right]$, [m], $\left[\frac{\text{kg}}{\text{m} \cdot \text{s}}\right]$, $\left[\frac{\text{m}}{\text{s}^2}\right]$, $\left[\frac{\text{J}}{\text{m}^2 \cdot \text{s} \cdot \text{K}}\right]$, $\left[\frac{\text{kg}}{\text{m}^3}\right]$ and $\left[\frac{\text{J}}{\text{kg} \cdot \text{K}}\right]$, respectively. Here, the basic physical dimensions [J] and [K] can be combined as an independent basic dimension $\left[\frac{\text{J}}{\text{K}}\right]$. In this case, the above five basic dimensions are changed to the following four basic dimension [s], [m], [kg], and [J/K] (i.e. $r = 4$).

Buckingham's π -theorem states that if a dependent variable Γ is completely determined by the values of a set of n independent variables, of which the basic dimensions with number of r involved, then a suitable dimensionless Γ_0 will be completely determined by $n-r$ dimensionless similarity parameters, i.e. the number of independent variables may be reduced by the number r .

Here, the number of independent physical variables is $n = 7$, the number of the related basic dimensions is $r = 4$. Then, the number of the related dimensionless similarity parameters should be $n - r = 7 - 4 = 3$. According to the π -theorem, the dimensional analysis thus yields the result

$$\Gamma_0 = f(\pi_1, \pi_2, \pi_3) \quad (4.7)$$

where π_1 , π_2 , and π_3 are dimensionless similarity parameters dependent on fluid free convection.

4.3.3 Determine the Dimensionless Similarity Parameters

According to the π -theorem, the dimensionless similarity parameters π_1 , π_2 and π_3 can be expressed as the following equations, respectively:

$$\pi_1 = \lambda^{a1} \times L^{b1} \times \mu^{c1} \times (g\beta |T_w - T_\infty| \cos \alpha)^{d1} \times \alpha = 0 \quad (4.8)$$

$$\pi_2 = \lambda^{a2} \times L^{b2} \times \mu^{c2} \times (g\beta |T_w - T_\infty| \cos \alpha)^{d2} \times \rho = 0 \quad (4.9)$$

$$\pi_3 = \lambda^{a3} \times L^{b3} \times \mu^{c3} \times (g\beta |T_w - T_\infty| \cos \alpha)^{d3} \times c_p = 0 \quad (4.10)$$

Then, the power indexes $a1$ to $d1$, $a2$ to $d2$, and $a3$ to $d3$ are determined as follows:

a. Determine the dimensionless similarity parameter π_1

By using dimensional analysis, the following dimensional equation is obtained for the dimensionless similarity parameter π_1 :

$$\left[\frac{\text{J}}{\text{s} \cdot \text{K} \cdot \text{m}} \right]^{a1} \cdot [\text{m}]^{b1} \cdot \left[\frac{\text{kg}}{\text{m} \cdot \text{s}} \right]^{c1} \cdot \left[\frac{\text{m}}{\text{s}^2} \right]^{d1} \cdot \left[\frac{\text{J}}{\text{s} \cdot \text{K} \cdot \text{m}^2} \right] = 0 \quad (4.11)$$

Obviously, the indexes $a1$ to $d1$ are suitable to the following equations:

$$\begin{aligned} \text{For dimension [kg] balance:} & \quad c1 = 0 \\ \text{For dimension [m] balance:} & \quad -a1 + b1 - c1 + d1 - 2 = 0 \\ \text{For dimension [s] balance:} & \quad -a1 - c1 - 2d1 - 1 = 0 \\ \text{For dimension [J/K]:} & \quad a1 + 1 = 0 \end{aligned}$$

$$\text{Their solutions are} \quad a1 = -1, b1 = 1, c1 = 0, d1 = 0$$

Then, the dimensionless similarity parameter π_1 is

$$\pi_1 = \frac{\alpha L}{\lambda} \quad (4.12)$$

Obviously, the dimensionless similarity parameter π_1 is *Nusselt number* Nu_L . Then, Eq. (4.12) is expressed as

$$\text{Nu}_L = \frac{\alpha L}{\lambda} \quad (4.13)$$

If the reference length L is replaced by the coordinate variable x , (4.13) becomes

$$\text{Nu}_x = \frac{\alpha x}{\lambda} \quad (4.13a)$$

where Nu_x is called local Nusselt number.

b. Determine the dimensionless similarity parameter π_2

By using dimensional analysis, the following dimensional equation is obtained for the dimensionless similarity parameter π_2 :

$$\left[\frac{\text{J}}{\text{s} \cdot \text{K} \cdot \text{m}} \right]^{a2} \cdot [\text{m}]^{b2} \cdot \left[\frac{\text{kg}}{\text{m} \cdot \text{s}} \right]^{c2} \cdot \left[\frac{\text{m}}{\text{s}^2} \right]^{d2} \cdot \left[\frac{\text{kg}}{\text{m}^3} \right] = 0 \quad (4.14)$$

Obviously, the indexes $a2$ to $d2$ are suitable to the following equations:

$$\begin{aligned} \text{For dimension [kg] balance:} & \quad c2 + 1 = 0 \\ \text{For dimension [m] balance:} & \quad -a2 + b2 - c2 + d2 - 3 = 0 \\ \text{For dimension [s] balance:} & \quad -a2 - c2 - 2d2 = 0 \\ \text{For dimension [J/K]:} & \quad a2 = 0 \end{aligned}$$

$$\text{They solutions are} \quad a2 = 0, b2 = 3/2, c2 = -1, d2 = 1/2$$

Then, we can obtain a following dimensionless parameter:

$$\pi_2 = \frac{[g\beta |T_w - T_\infty| \cos \alpha]^{1/2} \cdot L^{3/2} \rho}{\mu} = \frac{[g\beta |T_w - T_\infty| \cos \alpha]^{1/2} \cdot L^{3/2}}{\nu}$$

Set $\pi_{2a} = \pi_2^2$, we obtain the following expression for the dimensionless parameter π_2 :

$$\pi_{2a} = \frac{g\beta |T_w - T_\infty| \cos \alpha \cdot L^3}{\nu^2} \quad (4.15)$$

Obviously, the dimensionless similarity parameter π_{2a} is Grashof number Gr_L . Then, *local Grashof number* can be expressed as follows:

$$Gr_x = \frac{g\beta |T_w - T_\infty| \cos \alpha \cdot x^3}{\nu^2} \quad (4.16)$$

where Gr_x is called local Grashof number.

c. *Determine the dimensionless similarity parameter π_3*

By using dimensional analysis, the following dimensional equation is obtained for the dimensionless similarity parameter π_3 :

$$\left[\frac{\text{J}}{\text{s} \cdot \text{K} \cdot \text{m}} \right]^{a3} \cdot [\text{m}]^{b3} \cdot \left[\frac{\text{kg}}{\text{m} \cdot \text{s}} \right]^{c3} \cdot \left[\frac{\text{m}}{\text{s}^2} \right]^{d3} \cdot \left[\frac{\text{J}}{\text{kg} \cdot \text{K}} \right] = 0 \quad (4.17)$$

Obviously, the indexes $a3$ to $d3$ are suitable to the following equations:

For dimension [kg] balance:	$c3 - 1 = 0$
For dimension [m] balance:	$-a3 + b3 - c3 + d3 = 0$
For dimension [s] balance:	$-a3 - c3 - 2d3 = 0$
For dimension [J/K]:	$a3 + 1 = 0$
They solutions are	$a3 = -1, b3 = 0, c3 = 1, d3 = 0$

$$\pi'_3 = \frac{\mu \cdot c_p}{\lambda} \quad (4.18)$$

Obviously, the dimensionless similarity parameter π_3 is *Prandtl number* Pr. Then, Eq. (4.18) is expressed as

$$\text{Pr} = \frac{\mu \cdot c_p}{\lambda} \quad (4.19)$$

So far, we have derived three dimensionless similarity variables, *local Nusselt number* Nu_x , *local Grashof number* Gr_x , and *Prandtl number* Pr, respectively, for gas laminar free convection. While, the local Grashof number will be used for similarity transformation of its partial differential equations.

4.4 Investigation of Similarity Variables on Hydrodynamics

First of all, we assume the following equation for expression of dimensionless coordinate variable η :

$$\eta = \frac{y}{Kx^n} = \frac{y}{x} \frac{1}{K} x^{-n+1} \quad (4.20)$$

where variables K and index n need to be determined.

Now, we assume the dimensionless variable relayed to the velocity components w_x and w_y , respectively.

Obviously, the velocity component w_x in the boundary layer is caused by buoyancy. If we take a control volume with density ρ in the boundary layer, and assume the fluid density in the fluid bulk to be ρ_∞ , the kinetic energy $\frac{1}{2}Gw_x^2$ of the control volume is balanced to its following potential energy caused by the buoyancy:

$$\frac{1}{2}Gw_x^2 = Vgx |\rho_\infty - \rho| \cos \alpha$$

or

$$\frac{1}{2}Gw_x^2 = Vgx\beta |T - T_\infty| \cos \alpha \quad (a)$$

for Boussinesq approximation. Here, V and G are volume and mass of the control volume, respectively, and $G = \rho \cdot V$.

The above equation is simplified to

$$w_x = \sqrt{2gx \left| \frac{\rho_\infty - \rho}{\rho} \right| \cos \alpha}$$

For Boussinesq approximation. Equation (b) describes the velocity component w_x caused by the buoyancy.

The above equation can be expressed as

$$w_x = \sqrt{2gx\beta |T - T_\infty| \cos \alpha} \quad (b)$$

for Boussinesq approximation.

Equation (b) describes the velocity component w_x caused by the buoyancy.

According to Eq. (b), we induce the following equation:

$$w_x = 2\sqrt{gx\beta |T_w - T_\infty| \cos \alpha} \cdot W_x \quad (4.21)$$

Obviously, W_x is a dimensionless variable dependent on the velocity component w_x .

Meanwhile, the *velocity component* w_y is assumed as

$$w_y = 2\sqrt{gx\beta |T_w - T_\infty| \cos \alpha} \cdot Bx^p W_y \quad (4.22)$$

where W_y is *dimensionless velocity component* in y -coordinate, while, variable B and index p need to be determined.

From Eq. (4.20) we have

$$\frac{\partial \eta}{\partial x} = -n \frac{y}{Kx^{n+1}} \quad (4.23)$$

$$\frac{\partial \eta}{\partial y} = \frac{1}{Kx^n} \quad (4.24)$$

From Eq. (4.21) we have

$$\frac{\partial w_x}{\partial x} = \sqrt{\frac{g}{x} \beta |T_w - T_\infty| \cos \alpha} W_x + 2\sqrt{gx\beta |T_w - T_\infty| \cos \alpha} \frac{dW_x}{d\eta} \frac{\partial \eta}{\partial x}$$

With Eq. (4.23), the above equation becomes

$$\frac{\partial w_x}{\partial x} = \sqrt{\frac{g}{x} \beta |T_w - T_\infty| \cos \alpha} W_x - 2\sqrt{gx\beta |T_w - T_\infty| \cos \alpha} \cdot n \frac{y}{Kx^{n+1}} \frac{dW_x}{d\eta} \quad (4.25)$$

With Eq. (4.21) we have

$$\frac{\partial w_x}{\partial y} = 2\sqrt{gx\beta |T_w - T_\infty| \cos \alpha} \frac{dW_x}{d\eta} \frac{\partial \eta}{\partial y}$$

With Eq. (4.24) the above equation becomes

$$\frac{\partial w_x}{\partial y} = 2\sqrt{gx\beta |T_w - T_\infty| \cos \alpha} \frac{1}{Kx^n} \frac{dW_x}{d\eta} \quad (4.26)$$

Then,

$$\frac{\partial^2 w_x}{\partial y^2} = 2\sqrt{gx\beta |T_w - T_\infty| \cos \alpha} \frac{1}{K^2 x^{2n}} \frac{d^2 W_x}{d\eta^2} \quad (4.27)$$

With Eqs. (4.20)–(4.22), and (4.25)–(4.27), Eq. (4.2) is changed to

$$\begin{aligned} & 2\sqrt{gx\beta |T_w - T_\infty| \cos \alpha} \cdot W_x \left[\sqrt{\frac{g}{x} \beta |T_w - T_\infty| \cos \alpha} \cdot W_x \right. \\ & \quad \left. - 2\sqrt{gx\beta |T_w - T_\infty| \cos \alpha} \cdot n \frac{y}{Kx^{n+1}} \frac{dW_x}{d\eta} \right] \\ & + 2\sqrt{gx\beta |T_w - T_\infty| \cos \alpha} \cdot Bx^p W_y 2\sqrt{gx\beta |T_w - T_\infty| \cos \alpha} \frac{1}{Kx^n} \frac{dW_x}{d\eta} \\ & = 2v\sqrt{gx\beta |T_w - T_\infty| \cos \alpha} \frac{1}{K^2 x^{2n}} \frac{d^2 W_x}{d\eta^2} + g\beta |T - T_\infty| \cos \alpha \quad (4.28) \end{aligned}$$

Compare the two terms on the right side of the above equation. Their power indexes of variable x should be equal for the similarity transformation. Then,

$$\frac{1}{2} - 2n = 0$$

or

$$n = \frac{1}{4} \quad (4.29)$$

With Eq. (4.29), Eq. (4.20) is expressed as

$$\eta = \frac{y}{Kx^{1/4}} = \frac{y}{x} \frac{1}{K} x^{3/4}$$

Compared with Eq. (4.16), the above equation can be expressed as a quarter of the power of Grashof number as follows to keep the power of variable x :

$$\eta = \frac{y}{x} \left(\frac{1}{4} \text{Gr}_x \right)^{1/4} \quad (4.30)$$

where

$$K = \left[\frac{1}{4} \frac{g\beta |T_w - T_\infty| \cos \alpha}{\nu^2} \right]^{-1/4} \quad (4.31)$$

Compare the last terms on both sides of Eq. (4.28), and their power indexes of variable x should be equal then,

$$1 + p - n = 0$$

for similarity of the equation.

With Eq. (4.29), the above equation becomes

$$1 + p - \frac{1}{4} = 0$$

Then,

$$p = -\frac{3}{4} \quad (4.32)$$

With Eq. (4.32), Eq. (4.22) becomes

$$w_y = 2\sqrt{gx\beta |T_w - T_\infty| \cos \alpha} \cdot Bx^{-3/4} W_y$$

Compared with Eq. (4.16), the above equation can be expressed as follows with Grashof number Gr_x :

$$w_y = 2\sqrt{gx\beta |T_w - T_\infty| \cos \alpha} \cdot Bx^{-3/4} \left[\frac{1}{4} \frac{g\beta |T_w - T_\infty| \cos \alpha \cdot x^3}{\nu^2} \right]^{1/4} \left(\frac{1}{4} \text{Gr}_x \right)^{-1/4} W_y$$

or

$$w_y = 2\sqrt{gx\beta |T_w - T_\infty| \cos \alpha} \cdot B \left[\frac{1}{4} \frac{g\beta |T_w - T_\infty| \cos \alpha}{\nu^2} \right]^{1/4} \left(\frac{1}{4} \text{Gr}_x \right)^{-1/4} W_y$$

From the above equation, it is found that the factor $B \left[\frac{1}{4} \frac{g\beta |T_w - T_\infty| \cos \alpha}{\nu^2} \right]^{1/4}$ has zero dimension. For simplicity, we can set

$$B \left[\frac{1}{4} \frac{g\beta |T_w - T_\infty| \cos \alpha}{\nu^2} \right]^{1/4} = 1$$

Therefore,

$$w_y = 2\sqrt{gx\beta |T_w - T_\infty| \cos \alpha} \left(\frac{1}{4} \text{Gr}_x \right)^{-1/4} W_y \quad (4.33)$$

where

$$B = \left[\frac{1}{4} \frac{g\beta |T_w - T_\infty| \cos \alpha}{\nu^2} \right]^{-1/4} \quad (4.34)$$

So far, we have derived four similarity variables, i.e. local Grashof number Gr_x , dimensionless coordinate variable η , *dimensionless velocity components* W_x and W_y . From Eqs. (4.16), (4.21), (4.30), and (4.33), these dimensionless similarity variables can be summarized as follows:

$$\eta = \frac{y}{x} \left(\frac{1}{4} \text{Gr}_x \right)^{1/4} \quad (4.30)$$

$$\text{Gr}_x = \frac{g\beta |T_w - T_\infty| \cos \alpha \cdot x^3}{\nu^2} \quad (4.16)$$

$$W_x = \left[2\sqrt{gx\beta |T_w - T_\infty| \cos \alpha} \right]^{-1} w_x \quad (4.21)$$

$$W_y = \left[2\sqrt{gx\beta |T_w - T_\infty| \cos \alpha} \left(\frac{1}{4} \text{Gr}_x \right)^{-1/4} \right]^{-1} w_y \quad (4.33)$$

Additionally, for similarity transformation of the governing partial differential equations of fluid laminar free convection, it is also necessary to assume a *dimensionless temperature variable* θ as follows:

$$\theta(\eta) = \frac{t - t_\infty}{t_w - t_\infty} \quad (4.35)$$

where η denotes the *dimensionless coordinate variable*.

So far, five dimensionless similarity variables, dimensionless coordinate variable η , local Grashof number Gr_x , *dimensionless velocity components* W_x and W_y , and *dimensionless temperature variable* θ are presented. They form a new similarity analysis method for laminar free film convection and film flows. Among these dimensionless similarity variables, *dimensionless velocity components* W_x and W_y are new similarity variable, different from those, which inform the Falkner–Skan type transformation.

4.5 An Application Example of the New Similarity Analysis Method

For an application example of the new similarity analysis method, the above equations for *dimensionless variables* η , *local Grashof number* Gr_x , *dimensionless velocity components* W_x and W_y , and *dimensionless temperature* θ will be used to transform the governing partial differential equation (4.1)–(4.3) with their boundary condition equations, to the equivalent governing ordinary differential equations for laminar free convection. The related application processes of the new similarity analysis method are presented as follows:

4.5.1 Similarity Transformation of Eq. (4.1)

With Eq. (4.35), we have

$$\frac{\partial w_x}{\partial x} = \sqrt{\frac{g}{x} \beta |T_w - T_\infty| \cos \alpha} W_x + 2\sqrt{gx\beta |T_w - T_\infty| \cos \alpha} \frac{dW_x}{d\eta} \frac{\partial \eta}{\partial x} \quad (4.36)$$

With Eq. (4.30), we obtain

$$\begin{aligned} \frac{\partial \eta}{\partial x} &= -\frac{1}{4} x^{-\frac{5}{4}} y \left[\frac{1}{4} \frac{g\beta |T_w - T_\infty| \cos \alpha}{v^2} \right]^{1/4} \\ &= -\frac{1}{4} x^{-2} y \left[\frac{1}{4} \frac{g\beta |T_w - T_\infty| \cos \alpha \cdot x^3}{v^2} \right]^{1/4} \\ &= -\frac{1}{4} x^{-1} \frac{y}{x} \left[\frac{1}{4} \text{Gr}_x \right]^{1/4} \\ &= -\frac{1}{4} x^{-1} \eta \end{aligned} \quad (4.37)$$

Then,

$$\frac{\partial w_x}{\partial x} = \sqrt{\frac{g}{x}\beta |T_w - T_\infty| \cos \alpha} \cdot W_x - \frac{1}{2}\sqrt{gx\beta |T_w - T_\infty| \cos \alpha} \cdot x^{-1}\eta \frac{dW_x}{d\eta} \quad (4.38)$$

With Eq. (4.33), we have

$$\frac{\partial w_y}{\partial y} = 2\sqrt{gx\beta |T_w - T_\infty| \cos \alpha} \left(\frac{1}{4}\text{Gr}_x\right)^{-1/4} \frac{dW_y}{d\eta} \frac{\partial \eta}{\partial y} \quad (4.39)$$

With Eq. (4.30), we obtain

$$\frac{\partial \eta}{\partial y} = \frac{1}{x} \left(\frac{1}{4}\text{Gr}_x\right)^{1/4} \quad (4.40)$$

Then,

$$\begin{aligned} \frac{\partial w_y}{\partial y} &= 2\sqrt{gx\beta |T_w - T_\infty| \cos \alpha} \left(\frac{1}{4}\text{Gr}_x\right)^{-1/4} \frac{1}{x} \left(\frac{1}{4}\text{Gr}_x\right)^{1/4} \frac{dW_y}{d\eta} \\ &= 2\sqrt{gx\beta |T_w - T_\infty| \cos \alpha} \cdot x^{-1} \frac{dW_y}{d\eta} \end{aligned} \quad (4.41)$$

With Eqs. (4.38) and (4.41), Eq. (4.1) is changed to

$$\begin{aligned} &\sqrt{\frac{g}{x}\beta |T_w - T_\infty| \cos \alpha} \cdot W_x - \frac{1}{2}\sqrt{gx\beta |T_w - T_\infty| \cos \alpha} \cdot x^{-1}\eta \frac{dW_x}{d\eta} \\ &+ 2\sqrt{gx\beta |T_w - T_\infty| \cos \alpha} \cdot x^{-1} \frac{dW_y}{d\eta} = 0 \end{aligned}$$

The above equation is simplified to

$$2W_x - \eta \frac{dW_x}{d\eta} + 4 \frac{dW_y}{d\eta} = 0 \quad (4.42)$$

This is the dimensionless form of Eq. (4.1).

4.5.2 Similarity Transformation of Eq. (4.2)

With Eq. (4.21), we have

$$\frac{\partial w_x}{\partial y} = 2\sqrt{gx\beta |T_w - T_\infty| \cos \alpha} \frac{dW_x}{d\eta} \frac{\partial \eta}{\partial y}$$

With Eq. (4.40), the above equation becomes

$$\frac{\partial w_x}{\partial y} = 2\sqrt{gx\beta |T_w - T_\infty| \cos \alpha} \frac{1}{x} \left(\frac{1}{4} \text{Gr}_x \right)^{1/4} \frac{dW_x}{d\eta} \quad (4.43)$$

Then,

$$\frac{\partial^2 w_x}{\partial y^2} = 2\sqrt{gx\beta |T_w - T_\infty| \cos \alpha} \frac{1}{x^2} \left(\frac{1}{4} \text{Gr}_x \right)^{1/2} \frac{d^2 W_x}{d\eta^2} \quad (4.44)$$

Therefore, Eq. (4.2) is changed to

$$\begin{aligned} & 2\sqrt{gx\beta |T_w - T_\infty| \cos \alpha} \cdot W_x \left[\sqrt{\frac{g}{x} \beta |T_w - T_\infty| \cos \alpha} W_x \right. \\ & \quad \left. - \frac{1}{2} \sqrt{gx\beta |T_w - T_\infty| \cos \alpha} x^{-1} \eta \frac{dW_x}{d\eta} \right] \\ & + 4\sqrt{gx\beta |T_w - T_\infty| \cos \alpha} \left(\frac{1}{4} \text{Gr}_x \right)^{-1/4} \\ & \quad W_y \sqrt{gx\beta |T_w - T_\infty| \cos \alpha} \frac{1}{x} \left(\frac{1}{4} \text{Gr}_x \right)^{1/4} \frac{dW_x}{d\eta} \\ & = 2\nu \sqrt{gx\beta |T_w - T_\infty| \cos \alpha} \frac{1}{x^2} \left(\frac{1}{4} \text{Gr}_x \right)^{1/2} \frac{d^2 W_x}{d\eta^2} + g\beta |T - T_\infty| \cos \alpha \end{aligned}$$

With definition of local Grashof number in Eq. (4.16), the above equation is further simplified to

$$\begin{aligned} & 2\sqrt{gx\beta |T_w - T_\infty| \cos \alpha} W_x \left[\sqrt{\frac{g}{x} \beta |T_w - T_\infty| \cos \alpha} W_x \right. \\ & \quad \left. - \frac{1}{2} \sqrt{gx\beta |T_w - T_\infty| \cos \alpha} x^{-1} \eta \frac{dW_x}{d\eta} \right] \\ & + 4\sqrt{gx\beta |T_w - T_\infty| \cos \alpha} W_y \sqrt{gx\beta |T_w - T_\infty| \cos \alpha} \frac{1}{x} \frac{dW_x}{d\eta} \\ & = 2\nu \sqrt{gx\beta |T_w - T_\infty| \cos \alpha} \frac{1}{x^2} \left(\frac{1}{4} \frac{g\beta |T_w - T_\infty| \cos \alpha \cdot x^3}{\nu^2} \right)^{1/2} \\ & \quad \frac{d^2 W_x}{d\eta^2} + g\beta |T - T_\infty| \cos \alpha \end{aligned}$$

The above equation is divided by $g\beta |T_w - T_\infty| \cos \alpha$, and simplified to

$$2W_x \left[W_x - \frac{1}{2} \eta \frac{dW_x}{d\eta} \right] + 4W_y \frac{dW_x}{d\eta} = 2\nu \left(\frac{1}{4} \frac{1}{\nu^2} \right)^{1/2} \frac{d^2 W_x}{d\eta^2} + \theta$$

i.e.

$$W_x \left(2W_x - \eta \frac{dW_x}{d\eta} \right) + 4W_y \frac{dW_x}{d\eta} = \frac{d^2 W_x}{d\eta^2} + \theta \quad (4.45)$$

This is the dimensionless form of Eq. (4.2).

4.5.3 Similarity Transformation of Eq. (4.3)

From Eq. (4.35), we have

$$\frac{\partial t}{\partial x} = (t_w - t_\infty) \frac{d\theta}{d\eta} \frac{\partial \eta}{\partial x}$$

With Eq. (4.37), the above equation becomes

$$\frac{\partial t}{\partial x} = -\frac{1}{4}(t_w - t_\infty)x^{-1}\eta \frac{d\theta}{d\eta} \quad (4.46)$$

From Eq. (4.35), we have

$$\frac{\partial t}{\partial y} = (t_w - t_\infty) \frac{d\theta}{d\eta} \frac{\partial \eta}{\partial y}$$

With Eq. (4.40), the above equation becomes

$$\frac{\partial t}{\partial y} = (t_w - t_\infty) \frac{1}{x} \left(\frac{1}{4} Gr_x \right)^{1/4} \frac{d\theta}{d\eta} \quad (4.47)$$

Then,

$$\frac{\partial^2 t}{\partial y^2} = (t_w - t_\infty) \frac{1}{x^2} \left(\frac{1}{4} Gr_x \right)^{1/2} \frac{d^2 \theta}{d\eta^2} \quad (4.48)$$

Therefore, Eq. (4.3) is changed to

$$\begin{aligned} & 2\sqrt{g\alpha\beta |T_w - T_\infty| \cos \alpha} W_x \left(-\frac{1}{4}(t_w - t_\infty)x^{-1}\eta \frac{d\theta}{d\eta} \right) \\ & + 2\sqrt{g\alpha\beta |T_w - T_\infty| \cos \alpha} \left(\frac{1}{4} Gr_x \right)^{-1/4} W_y (t_w - t_\infty) \frac{1}{x} \left(\frac{1}{4} Gr_x \right)^{1/4} \frac{d\theta}{d\eta} \\ & = \frac{\lambda}{\rho c_p} (t_w - t_\infty) \frac{1}{x^2} \left(\frac{1}{4} Gr_x \right)^{1/2} \frac{d^2 \theta}{d\eta^2} \end{aligned}$$

With the definition of local Grashof number in Eq. (4.16), the above equation becomes

$$\begin{aligned}
& 2\sqrt{gx\beta |T_w - T_\infty| \cos \alpha} W_x \left(-\frac{1}{4}(t_w - t_\infty)x^{-1}\eta \frac{d\theta}{d\eta} \right) \\
& + 2\sqrt{gx\beta |T_w - T_\infty| \cos \alpha} W_y (t_w - t_\infty) \frac{1}{x} \frac{d\theta}{d\eta} \\
& = \frac{\lambda}{\rho c_p} (t_w - t_\infty) \frac{1}{x^2} \left(\frac{1}{4} \frac{g\beta |T_w - T_\infty| \cos \alpha \cdot x^3}{v^2} \right)^{1/2} \frac{d^2\theta}{d\eta^2}
\end{aligned}$$

The above equation is divided by $(t_w - t_\infty)\sqrt{gx\beta |T_w - T_\infty| \cos \alpha}$, and becomes

$$2W_x \left(-\frac{1}{4} \left(\eta \frac{d\theta}{d\eta} \right) \right) + 2W_y \frac{d\theta}{d\eta} = \frac{\lambda}{\rho c_p} \left(\frac{1}{4} \frac{1}{v^2} \right)^{1/2} \frac{d^2\theta}{d\eta^2}$$

The above equation is further simplified to

$$(-\eta W_x + 4W_y) \frac{d\theta}{d\eta} = \frac{1}{\text{Pr}} \frac{d^2\theta}{d\eta^2} \quad (4.49)$$

With Eqs. (4.20), (4.35)–(4.37), Eqs. (4.4) and (4.5) are transformed to as follows respectively:

$$\eta = 0 : W_x = 0, \quad W_y = 0, \quad \theta = 1 \quad (4.50)$$

$$\eta \rightarrow \infty : W_x = 0, \quad \theta = 0 \quad (4.51)$$

The transformed governing dimensionless equations of laminar free convection of gas with Boussinesq approximation are summarized as below:

$$2W_x - \eta \frac{dW_x}{d\eta} + 4 \frac{\partial W_y}{\partial \eta} = 0 \quad (4.42)$$

$$W_x \left(2W_x - \eta \frac{dW_x}{d\eta} \right) + 4W_y \frac{dW_x}{d\eta} = \frac{d^2W_x}{d\eta^2} + \theta \quad (4.45)$$

$$(-\eta W_x + 4W_y) \frac{d\theta}{d\eta} = \frac{1}{\text{Pr}} \frac{d^2\theta}{d\eta^2} \quad (4.49)$$

with the dimensionless boundary condition Eqs. (4.50) and (4.51).

From Chap. 3, it is seen that by using Falkner–Skan type transformation, the related unknown variables of transformed governing dimensionless equations are function $f(\eta)$ and its derivatives, except dimensionless temperature θ . While, in governing dimensionless equations transformed by the present transformation method, the related unknown variables are *dimensionless velocity components* W_x and W_y proportional to the related velocity components. Therefore, for differentiating the

Table 4.1 Summarization on application of the new similarity analysis method and Falkner–Skan transformation for laminar free convection with Boussinesq approximation

Term	Equation	With Falkner–Skan transformation
<i>Governing partial differential equations of laminar free convection (with Boussinesq approximation)</i>		
Mass equation	$\frac{\partial w_x}{\partial x} + \frac{\partial w_y}{\partial y} = 0$	
Momentum equation	$w_x \frac{\partial w_x}{\partial x} + w_y \frac{\partial w_x}{\partial y} = \nu \frac{\partial^2 w_x}{\partial y^2} + g\beta T - T_\infty \cos \alpha$	
Energy equation	$w_x \frac{\partial t}{\partial x} + w_y \frac{\partial t}{\partial y} = \frac{\lambda}{\rho c_p} \frac{\partial^2 t}{\partial y^2}$	
Boundary conditions	$y = 0 : W_x = 0, W_y = 0, t = t_w$ $y \rightarrow \infty : W_x \rightarrow 0, t = t_\infty$	
<i>Derived similarity variables</i>		
Dimensionless coordinate variable η	$\frac{y}{x} \left(\frac{1}{4} Gr_x\right)^{1/4}$	
Local Grashof number Gr_x	$\frac{g\beta T_w - T_\infty \cos \alpha x^3}{\nu^2}$	
Dimensionless temperature θ	$\theta = \frac{t - t_\infty}{t_w - t_\infty}$	
Velocity component w_x	$2\sqrt{gx\beta} T_w - T_\infty \cos \alpha W_x$	$\frac{4\nu}{x} \left(\frac{1}{4} Gr_x\right)^{1/2} f'(\eta)$
Velocity component w_y	$2\sqrt{gx\beta} T_w - T_\infty \cos \alpha \left(\frac{1}{4} Gr_x\right)^{-1/4} W_y$	$\frac{\nu}{x} \left(\frac{1}{4} Gr_x\right)^{1/2} [\eta \cdot f'(\eta) - 3f(\eta)]$
<i>Derived governing dimensionless equations (with Boussinesq approximation)</i>		
Mass equation	$2W_x - \eta \frac{dW_x}{d\eta} + 4 \frac{\partial W_y}{\partial \eta} = 0$	$f'''(\eta) + 3f(\eta)f''(\eta)f'(\eta) - 2(f'(\eta))^2 + \theta(\eta) = 0$
Momentum equation	$W_x \left(2W_x - \eta \frac{dW_x}{d\eta}\right) + 4W_y \frac{dW_x}{d\eta} = \frac{d^2 W_x}{d\eta^2} + \theta$	$\theta''(\eta) + 3Pr f(\eta)\theta'(\eta) = 0$
Energy equation	$(-\eta W_x + 4W_y) \frac{\partial \theta}{\partial \eta} = \frac{1}{Pr} \frac{\partial^2 \theta}{\partial \eta^2}$	$\eta = 0 : f(\eta) = f'(\eta) = 0, \theta(\eta) = 1$
Boundary conditions	$\eta \rightarrow \infty : W_x = 0, \theta = 0$	$\eta \rightarrow \infty : f'(\eta) = 0, \theta(\eta) = 0$

traditional Falkner–Skan type transformation, the present transformation method can be called as dimensionless velocity component method.

From the above successful verification, it is found that the derived *dimensionless coordinate variable* η , *local Grashof number* Gr_x , *dimensionless velocity components* W_x and W_y , and *dimensionless temperature* θ are validity of similarity analysis of fluid laminar free convection. It follows that the new similarity analysis method is available for the similarity analysis of fluid laminar free convection.

In the following chapters, the present new similarity analysis method will be used for the investigation of fluid laminar free convection, laminar free film boiling of liquid, laminar free film condensation of pure vapor, laminar free film condensation of vapor–gas mixture, and film flow of non-Newtonian power-law fluid. It will be seen that by using the new similarity analysis method, it will be more convenient for investigation of heat and mass transfer than that by using traditional Falkner–Skan type transformation, especially for consideration and treatment of variable physical properties.

4.6 Summary

In this chapter, taking governing partial differential equations of laminar free convection as example, we have derived the related local Grashof number Gr_x by using the π -theorem with dimension analysis, derived the expressions of similarity variables on hydrodynamics, such as dimensionless coordinate variable η , as well as dimensionless velocity components W_x and W_y by means of dimensional analysis of the governing partial differential equations. Furthermore, with these dimensionless variables, the governing partial differential equations of laminar free convection are transformed similarly to the related dimensionless equations. Then, the validity of the derived dimensionless similarity variables for the similarity transformation has been verified. The related governing partial differential equations, derived similarity variables, and the dimensionless governing equations transformed by the new similarity analysis method and Falkner–Skan transformation are summarized in Table 4.1.

4.7 Remarks

In this chapter, a new similarity analysis method, for laminar free convection boundary layer was presented in detail. Meanwhile, the approach for determination of a system of similarity parameters and variables, such as dimensionless coordinate variable η , local Grashof number Gr_x , dimensionless velocity components W_x and W_y were induced by means of the related examples for laminar free convection. The local Grashof number Gr_x is derived by means of π -theorem and dimension analysis, while, the dimensionless coordinate variable η and dimensionless velocity components W_x and W_y are derived by using the dimension analysis for the governing

partial differential equations. Finally, by using these derived similarity variables, the verifications were done by using the similarity transformation of the governing partial differential equations of laminar free convection. The verification results proved that these derived similarity variables are available, and the present similarity analysis method is reliable for similarity analysis of fluid laminar free convection.

In the following respects, the present new similarity analysis method is more convenient for application than the traditional Falkner–Skan type transformation:

For derivation of the similarity variables by using the new similarity analysis method, it is never necessary to induce the flow function. Then, it is more convenient to derive the similarity variables by using the present new similarity analysis method than that by Falkner–Skan transformation.

The obvious difference of the present new similarity analysis method from the traditional Falkner–Skan transformation lies in the similarity transformation of velocity components. For the former method, in the provided similarity expressions, the velocity components are proportional to the related dimensionless velocity components W_x and W_y , respectively. Then, the dimensionless velocity components W_x and W_y exist in the transformed dimensionless governing equations. While, for the latter transformation, in the provided similarity expressions, the velocity components are functions of induced **intermediate variable** $f(\eta)$ and its derivatives, respectively. Then, the intermediate variable $f(\eta)$ and its derivatives exist in the transformed dimensionless governing equations.

The dimensionless velocity components W_x and W_y have definite physical significance compared with the variable $f(\eta)$ and its derivatives. Then, the dimensionless governing equations transformed by using the new similarity analysis method demonstrate more obvious physical significance compare with those transformed by the Falkner–Skan type transformation.

In the successive chapters, we will find by using the new similarity analysis method that (i) it will be more convenient to treat variable physical properties of the governing equations, and (ii) it will be more convenient to investigate momentum field and mass transfer than that by means of the Falkner–Skan type transformation, especially for the investigation of multi-phase film flow problem.

4.8 Exercises

1. Please review the derivation for creating the present new similarity analysis method for laminar free convection boundary layer and film flows.
2. Please list all similarity variables for the new similarity analysis method on laminar free convection.
3. Please tell me the common grounds and differences of the similarity variables between the new similarity analysis method and Falkner–Skan type transformation for laminar free convection.
4. Can you list the advantages of the new similarity analysis method over the traditional Falkner–Skan type transformation in their application?

5. Suppose that the dimensionless coordinate variable η in Eq. (4.30) is replaced by the form $\eta = \frac{y}{x}(\text{Gr}_x)^{1/4}$, and the forms of other similarity variables are kept, please try to transform similarly the governing partial differential equations (4.1)–(4.3) and the boundary condition Eqs. (4.4) and (4.5) to the related ordinary differential forms.
6. From question 2, what relationship can you find between the similarity coordinate variable η and the transformed governing ordinary differential equations?

References

1. D.Y. Shang, B.X. Wang, Effect of variable thermophysical properties on laminar free convection of gas. *Int. J. Heat Mass Transf.* **33**(7), 1387–1395 (1990)
2. D.Y. Shang, B.X. Wang, Effect of variable thermophysical properties on laminar free convection of polyatomic gas. *Int. J. Heat Mass Transf.* **34**(3), 749–755 (1991)
3. D.Y. Shang, B.X. Wang, Y. Wang, Y. Quan, Study on liquid laminar free convection with consideration of variable thermophysical properties. *Int. J. Heat Mass Transf.* **36**(14), 3411–3419 (1993)
4. D.Y. Shang, B.X. Wang, L.C. Zhong, A study on laminar film boiling of Liquid along an isothermal vertical plates in a pool with consideration of variable thermophysical properties. *Int. J. Heat Mass Transf.* **37**(5), 819–828 (1994)
5. D.Y. Shang, T. Adamek, Study on laminar film condensation of saturated steam on a vertical flat plate for consideration of various physical factors including variable thermophysical properties. *Wärme- und Stoffübertragung* **30**, 89–100 (1994)
6. D.Y. Shang, B.X. Wang, An extended study on steady-state laminar film condensation of a superheated vapor on an isothermal vertical plate. *Int. J. Heat Mass Transf.* **40**(4), 931–941 (1997)
7. H.I. Andersson, D.Y. Shang, An extended study of hydrodynamics of gravity-driven film flow of power-law fluids. *Fluid Dyn. Res.* **22**, 345–357 (1998)
8. D.Y. Shang, H. Andersson, Heat transfer in gravity-driven film flow of power-law fluids. *Int. J. Heat Mass Transf.* **42**(11), 2085–2099 (1999)
9. D.Y. Shang, J. Gu, Analyses of pseudo-similarity and boundary layer thickness for non-Newtonian falling film flow. *Heat Mass Transf.* **41**(1), 44–50 (2004)
10. V.M. Falkner, S.W. Skan, Some approximate solutions of the boundary layer equations. *Phil. Mag.* **12**, 865 (1931)
11. H. Schlichting, *Boundary Layer Theory* (translated by J. Kestin). (McGraw Hill, New York, 1979), pp. 316–317
12. T. Cebeci, P. Bradshaw, *Physical and Computational Aspects of Convective Heat Transfer* (Springer, New York, 1984)
13. E. Buckingham, *Phys. Rev.* **4**, 345–376 (1914)

Chapter 5

New Method for Treatment of Variable Physical Properties

Abstract The advanced method reported in this chapter for treatment of fluid variable physical properties involves temperature parameter method for treatment of temperature-dependent physical properties of gases, theoretical equation method for treatment of concentration- and temperature-dependent density of vapour-gas mixture, weighted sum method for treatment of other concentration- and temperature-dependent physical properties of vapour-gas mixture and polynomial method for treatment of temperature-dependent physical properties of liquids. These methods are taken as a theoretical foundation of this book for extensive investigation of hydrodynamics and heat transfer of free convection of gases, free convection of liquids, free convection film boiling of liquid and free convection film condensation of pure vapour or vapour-gas mixture with consideration of coupled effects of variable physical properties. For the temperature parameter method based on the simple power-law of the temperature-dependent physical properties of gases, a system of the temperature parameters such as n_μ , n_λ and n_{c_p} are reported. From these temperature parameters, it is seen that the specific heat parameter is much small, and then, it follows that the variable temperature will have more obvious effects on viscosity, thermal conductivity and density of gases than that of the specific heat. Since the determination of the temperature parameter is based on the typical experimental data, with the provided temperature parameters, the temperature-variable physical properties of gases can be stimulated very well by using the temperature parameter method. Furthermore, with the temperature parameter method the treatment of variable physical properties of vapour or gas becomes very simple and convenient. Taking water as an example, the temperature-dependent polynomials of the density, thermal conductivity and viscosity are introduced for liquid variable physical properties, while the specific heat at constant pressure is so small that it can be disregarded generally with variation of temperature. These polynomials are reliable, since the related typical experimental data. The concentration-dependent density equations of vapour-gas mixture are reported through the rigorously theoretical derivation, while the other concentration-dependent physical properties of vapour-gas mixture are expressed as the weighted sum of the physical properties of the involved vapour and gas with their

concentrations (mass fraction). Since the involved vapour and gas are temperature-dependent, the physical properties of the vapour-gas mixture are concentration- and temperature-dependent.

5.1 Introduction

The study of laminar free convection of gases with variable physical properties can be traced back to the perturbation analysis of Hara [1] for air free convection. The solution is applicable for small values of the perturbation parameter, $\varepsilon_H = (T_w - T_\infty)/T_\infty$. Later, Tataev [2] investigated the free convection of a gas with variable viscosity. A well-known analysis of the variable fluid property problem for laminar free convection on an isothermal vertical flat plate has been presented by Sparrow and Gregg [3], giving solutions of the boundary layer equations for five assumed gases. They proposed a reference temperature and suggested that with it the problem of variable physical properties can be treated as a constant property problem, i.e. using the Boussinesq approximation. Gray and Giorgini [4] discussed the validity of the Boussinesq approximation and proposed a method for analysing natural convection flow with fluid properties assumed to be a linear function of temperature and pressure. Clausing and Kempka [5] reported their experimental study of the influence of property variations on natural convection and showed that, for the laminar region, Nu_f is a function of $Ra_f (= Gr_f Pr_f)$ only, with the reference temperature T_f taken as the average temperature in the boundary layer. Herwig [6] expanded the functions describing the temperature dependence of the fluid properties as Taylor series to analyse the influence of variable properties on laminar fully developed pipe flow. Pozzi and Lupo [7] assumed viscosity and thermal conductivity to depend on temperature in a polynomial form to analyse the variable property effects in free convection. In this chapter, I will present a temperature parameter method proposed in our Ref. [8, 9] for treatment of variable physical properties of gases, and a polynomial method provided in Ref. [10] for treatment of variable physical properties of liquids. Both of the methods were applied respectively in our series of studies for investigation of effects of variable physical properties on gas free convection [8, 9], liquid free convection [10], free convection film convection boiling [11], free convection film condensation of pure gas [12, 13], and free convection film condensation of vapour-gas mixture [14], as well as were partially applied in investigation for my recent book [15].

5.2 Treatment of Temperature-Dependent Physical Properties of Gas

5.2.1 Temperature Parameter Method

For *treatment of variable physical properties*, a *temperature parameter method* developed in [8, 9] is presented here, which is based on a *simple power-law* of gases. According to the measurement values of physical properties of gases, it is found that at constant pressure the physical properties of gases such as density, viscosity, thermal conductivity and specific heat with absolute temperature, very closely follow a simple power-law, i.e. $\rho \approx T^{-1}$, $\mu \approx T^{n_\mu}$, $\lambda \approx T^{n_\lambda}$ and $c_p \approx T^{n_{c_p}}$, where n_μ , n_λ and n_{c_p} are *temperature parameters*, respectively called **viscosity parameter**, **thermal conductivity parameter** and **specific heat parameter**. Obviously, different gases have different temperature parameters. Then, for *absolute temperatures* T_1 and T_2 , we have

$$\frac{\mu_1}{\mu_2} = \left(\frac{T_1}{T_2} \right)^{n_\mu} \quad (5.1)$$

$$\frac{\lambda_1}{\lambda_2} = \left(\frac{T_1}{T_2} \right)^{n_\lambda} \quad (5.2)$$

$$\frac{c_{p1}}{c_{p2}} = \left(\frac{T_1}{T_2} \right)^{n_{c_p}} \quad (5.3)$$

While the change of density with absolute temperature at constant pressure can be expressed as

$$\frac{\rho_1}{\rho_2} = \left(\frac{T_1}{T_2} \right)^{-1} \quad (5.4)$$

While, the dimensionless exponents n_μ , n_λ and n_{c_p} are exponents of absolute temperature, and then named temperature parameter here. Obviously, the different gases have different temperature parameter n_μ , n_λ and n_{c_p} .

For practical issues of free convection and its film flows, the *absolute temperature* T_1 is usually replaced by any temperature T in the boundary layer or film flows, and T_2 is usually replaced by T_∞ which is located at the boundary of the boundary layer or film flows. Then, the above equations become the following ones respectively:

$$\frac{\mu}{\mu_\infty} = \left(\frac{T}{T_\infty} \right)^{n_\mu} \quad (5.5)$$

$$\frac{\lambda}{\lambda_\infty} = \left(\frac{T}{T_\infty} \right)^{n_\lambda} \quad (5.6)$$

Table 5.1 The value of parameters n_μ , n_λ and n_{c_p} for several monatomic and diatomic gases, and also for air and water vapour, cited from Shang and Wang [8]

Gas	T_∞ (K)	n_μ	Temperature range (K)	n_λ	Temperature range (K)	n_{c_p}	Temperature range (K)	Recommended Pr
Ar	273	0.72	220–1500	0.73	210–1500	0.01	220–1500	0.622
He	273	0.66	273–873	0.725	273–873	0.01	273–873	0.675
H ₂	273	0.68	80–1000	0.8	220–700	0.042	220–700	0.68
Air	273	0.68	220–1400	0.81	220–1000	0.078	230–1000	0.7
CO	273	0.71	230–1500	0.83	220–600	0.068	220–600	0.72
N ₂	273	0.67	220–1500	0.76	220–1200	0.07	220–1200	0.71
O ₂	273	0.694	230–2000	0.86	220–600	0.108	230–600	0.733
Water vapour	380	1.04	380–1500	1.185	380–800	0.003	380–800	1

$$\frac{c_p}{c_{p\infty}} = \left(\frac{T}{T_\infty} \right)^{n_\lambda} \quad (5.7)$$

$$\frac{\rho}{\rho_\infty} = \left(\frac{T}{T_\infty} \right)^{-1} \quad (5.8)$$

5.2.2 For Monatomic and Diatomic Gases, Air and Water Vapour

According to the experimental values for several *monatomic and diatomic gases*, and also for air and water vapour, reported by Hisenrath et al. [16], n_μ , n_λ and n_{c_p} values are given in Table 5.1, with the percentage deviations for predicted values of μ and λ predicted from Eqs. (5.5) and (5.6).

The *Prandtl number* is defined as $\text{Pr} = \mu c_p / \lambda$. Strictly speaking, Pr should also depend on temperature. However, it is well known that $\text{Pr} \approx 0.72$ for a diatomic gas, $\text{Pr} \approx 0.7$ for air and $\text{Pr} \approx 1$ for water vapour. Hence, Pr can be taken as a constant for monatomic and diatomic gases, and for air and water vapour in the related temperature ranges from T to T_∞ .

It can be found from Table 5.1 that the values of the specific heat parameter n_{c_p} are around 0.01 for monatomic gases, and lower than 0.11 for diatomic gases, air and water vapour. For the case $1/2 \leq (T/T_\infty) \leq 2$, it is possible to treat c_p as a constant value for these gases, so as to simplify the analysis but still suit the needs of engineering application.

5.2.3 For Polyatomic Gas

According to the summarised experimental values of μ , λ and c_p for several *polyatomic gases* reported in Refs. [17–20], the temperature parameters n_λ , n_μ and n_{c_p}

Table 5.2 The values of temperature parameters n_λ , n_μ and n_{cp} , cited from Shang and Wang [9]

Gas	T_0 (K)	n_μ	Temperature range (K)	Deviation (%)	n_λ	Temperature range (K)	Deviation (%)	n_{cp}	Temperature range (K)	Deviation (%)
Gas mixture	273	0.75	273–1173	±3	1.02	273–1473	±1	0.134	273–1473	±2.5
CO ₂	273	0.88	220–700	±2	1.3	220–720	±2	0.34	230–810	±1
C ₂ H ₄	273	0.853	210–900	±3	1.71	220–600	±3	0.73	273–922	±1.5
CH ₄	273	0.78	220–1000	±3	1.29	230–1000	±3.6	0.534	273–1033	±4.2
CCl ₄	273	0.912	270–500	±1	1.29	260–400	±1	0.28	270–700	±2
SO ₂	273	0.91	200–1250	±4	1.323	250–900	±4.5	0.257	273–1200	±3
H ₂ S	273	1	270–500	±1	1.29	260–400	±1	0.18	230–700	±2
NH ₃	273	1.04	220–1000	±1	1.375	250–900	±2	0.34	230–1033	±0.36
C ₂ H ₅ OH	273	0.925	270–600	±0.6	1.95	260–430	±4	0.59	250–922	±0.25

Note Components of the gas mixture: CO₂ = 0.13, watervapour = 0.11 and N₂ = 0.76 [21]

and the deviation of μ , λ and c_p arising from the corresponding experimental data are listed in Table 5.2.

5.3 Treatment of Concentration- and Temperature-Dependent Physical Properties of Vapour–Gas Mixture

Treatment of variable physical properties of vapour-gas mixture is more complicated work than that of gas since the concentration-dependent physical properties should be first taken into account, and on this basis, the temperature-dependent physical properties are considered.

5.3.1 For Density

Take ρ_m as density of vapour-gas mixture, ρ_{mv} and ρ_{mg} as *local densities* of vapour and gas in the *vapour-gas mixture*, and ρ_v and ρ_g as densities of vapour and gas, respectively, then, we will have the following equations for their relations:

$$\rho_m = \rho_{mv} + \rho_{mg}$$

$$C_{mv}\rho_m = \rho_{mv}$$

$$\frac{\rho_{mv}}{\rho_v} + \frac{\rho_{mg}}{\rho_g} = 1$$

The solutions of the above group of equations are

$$\rho_m = \frac{\rho_v \rho_g}{(1 - C_{mv})\rho_v + C_{mv}\rho_g} \quad (5.9)$$

$$\rho_{mv} = \frac{C_{mv}\rho_v \rho_g}{(1 - C_{mv})\rho_v + C_{mv}\rho_g} \quad (5.10)$$

$$\rho_{mg} = \frac{(1 - C_{mv})\rho_v \rho_g}{(1 - C_{mv})\rho_v + C_{mv}\rho_g} \quad (5.11)$$

where C_{mv} is the *vapour mass fraction* of the vapour-gas mixture, ρ_m is vapour-gas mixture density, ρ_{mv} is local vapour density, and ρ_{mg} is local gas density and ρ_v and ρ_g are vapour and gas density respectively. Although, Eqs. (5.9)–(5.11) seem for expression of concentration-dependent densities of the vapour-gas mixture, they actually cover the concentration- and temperature-dependent densities, because the vapour and gas densities ρ_v and ρ_g are *temperature-dependent*, and need to be further treated by the temperature parameter method.

5.3.2 For Other Physical Properties

According to equations recommended by [15], the other concentration-dependent physical properties, such as μ_m , λ_m , c_{p_m} and Pr_m of vapour-gas mixture are assumed as following weighted sum formulae:

$$\mu_m = C_{mv}\mu_v + (1 - C_{mv})\mu_g \quad (5.12)$$

$$\lambda_m = C_{mv}\lambda_v + (1 - C_{mv})\lambda_g \quad (5.13)$$

$$c_{p_m} = C_{mv}c_{p_v} + (1 - C_{mv})c_{p_g} \quad (5.14)$$

$$Pr_m = C_{mv}Pr_v + (1 - C_{mv})Pr_g \quad (5.15)$$

where μ_m , λ_m , c_{p_m} and Pr_m denote the related physical properties of vapour-gas mixture.

Since the vapour physical properties μ_v , λ_v , c_{p_v} and Pr_v , as well as gas physical properties μ_g , λ_g , c_{p_g} and Pr_g are temperature-dependent physical properties, and need to be further treated by using the temperature parameter method, Eqs. (5.12)–(5.15) actually cover for treatment of the concentration- and temperature-dependent physical properties μ_m , λ_m , c_{p_m} and Pr_m of vapour-gas mixture.

5.4 Treatment of Temperature-Dependent Physical Properties of Liquids

For treatment of variable physical properties of liquids, Ref. [10] suggested a *polynomial method*. Now we take water at atmospheric pressure as an example, the temperature-dependent expressions of density and thermal conductivity with the temperature range between 0 and 100 °C are expressed with polynomial as

$$\rho = -4.48 \times 10^{-3}t^2 + 999.9 \quad (5.16)$$

$$\lambda = -8.01 \times 10^{-6}t^2 + 1.94 \times 10^{-3}t + 0.563 \quad (5.17)$$

The deviation predicted is less than 0.35 % by Eq. (5.16) and less than 0.18 % by Eq. (5.17), compared with *the typical experimental data* shown in appendix of this book.

For the absolute viscosity of water, the following expression described in Ref. [22] is applied:

$$\mu = 10^{-3} \exp \left[-1.6 - \frac{1150}{T} + \left(\frac{690}{T} \right)^2 \right] \quad (5.18)$$

The deviation predicted by Eq. (5.18) is less than 1.8 %, as compared with the experimental data shown in appendix of this book.

In addition, for a lot of liquid, the specific heat varies very little with temperature, and can be regarded as constant.

5.5 Physical Property Factor

It will be found in the successive chapters that the variable physical properties always exist as the related physical property factors in the dimensionless ordinary partial differential equations of laminar free convection. In fact, there are two types of *physical property factors*, the temperature-dependent physical property factors for gases and liquids such as $\frac{1}{\rho} \frac{d\rho}{d\eta}$, $\frac{1}{\mu} \frac{d\mu}{d\eta}$, $\frac{1}{\lambda} \frac{d\lambda}{d\eta}$, $\frac{1}{c_p} \frac{dc_p}{d\eta}$ and $\frac{v_\infty}{v}$ and the concentration-dependent physical property factors such as $\frac{1}{\rho_m} \frac{d\rho_m}{d\eta_m}$, $\frac{1}{\mu_m} \frac{d\mu_m}{d\eta_m}$ and $\frac{1}{\lambda_m} \frac{d\lambda_m}{d\eta_m}$. Here, η is the dimensional coordinate variable for gas and liquid, η_m denotes the dimensional coordinate variable for vapour-gas mixture, and the subscript denotes vapour-gas mixture. These physical property factors are presented as follows respectively:

5.5.1 For Gases

Transformation of the density factor $\left(\frac{1}{\rho} \frac{d\rho}{d\eta}\right)$:

With Eq. (5.8) we obtain

$$\frac{1}{\rho} \frac{d\rho}{d\eta} = \frac{1}{\rho} \frac{d}{d\eta} \left(\rho_\infty \frac{T_\infty}{T} \right).$$

Suppose T_w and T_∞ are boundary temperatures of the boundary layer, i.e. water temperature and fluid bulk temperature respectively, they can express a *dimensionless temperature* variable

$$\theta = \frac{T - T_\infty}{T_w - T_\infty} \quad \text{or} \quad \theta = \frac{t - t_\infty}{t_w - t_\infty} \quad (5.19)$$

i.e.

$$T = (T_w - T_\infty)\theta + T_\infty \quad \text{or} \quad t = (t_w - t_\infty)\theta + t_\infty$$

Therefore,

$$\begin{aligned} \frac{1}{\rho} \frac{d\rho}{d\eta} &= \frac{\rho_\infty}{\rho} \frac{d}{d\eta} \left[\frac{T_\infty}{(T_w - T_\infty)\theta + T_\infty} \right] \\ &= \frac{T}{T_\infty} \frac{d}{d\eta} \left[\frac{1}{(T_w/T_\infty - 1)\theta + 1} \right] \\ &= -[(T_w/T_\infty - 1)\theta + 1] \frac{(T_w/T_\infty - 1) \frac{d\theta}{d\eta}}{[(T_w/T_\infty - 1)\theta + 1]^2} \end{aligned}$$

Then,

$$\frac{1}{\rho} \frac{d\rho}{d\eta} = -\frac{(T_w/T_\infty - 1)}{(T_w/T_\infty - 1)\theta + 1} \cdot \frac{d\theta}{d\eta} \quad (5.20)$$

Transformation of the viscosity factor $\frac{1}{\mu} \frac{d\mu}{d\eta}$:

With Eq. (5.5) we get

$$\begin{aligned} \frac{1}{\mu} \frac{d\mu}{d\eta} &= \frac{1}{\mu} \frac{d}{d\eta} \left[\mu_\infty \left(\frac{T}{T_\infty} \right)^{n_\mu} \right] \\ &= \frac{\mu_\infty}{\mu} \frac{d}{d\eta} \left[\left(\frac{T}{T_\infty} \right)^{n_\mu} \right] \\ &= \left(\frac{T}{T_\infty} \right)^{-n_\mu} \frac{d}{d\eta} \left[\left(\frac{(T_w - T_\infty)\theta + T_\infty}{T_\infty} \right)^{n_\mu} \right] \\ &= ((T_w/T_\infty - 1)\theta + 1)^{-n_\mu} \frac{d}{d\eta} ((T_w/T_\infty - 1)\theta + 1)^{n_\mu} \\ &= ((T_w/T_\infty - 1)\theta + 1)^{-n_\mu} n_\mu ((T_w/T_\infty - 1)\theta + 1)^{n_\mu - 1} (T_w/T_\infty - 1) \frac{d\theta}{d\eta} \end{aligned}$$

Then, the *viscosity factor* is described as

$$\frac{1}{\mu} \frac{d\mu}{d\eta} = \frac{n_\mu (T_w/T_\infty - 1)}{(T_w/T_\infty - 1)\theta + 1} \cdot \frac{d\theta}{d\eta} \quad (5.21)$$

Transformation of the thermal conductivity factor $\frac{1}{\lambda} \frac{d\lambda}{d\eta}$:

With a derivation similar to that for the factor $\left(\frac{1}{\mu} \frac{d\mu}{d\eta}\right)$ we can obtain the following equation for description of the thermal conductivity factor:

$$\frac{1}{\lambda} \frac{d\lambda}{d\eta} = \frac{n_\lambda (T_w/T_\infty - 1)}{(T_w/T_\infty - 1)\theta + 1} \cdot \frac{d\theta}{d\eta} \quad (5.22)$$

Transformation of physical factor $\frac{v_\infty}{v}$

The physical factor $\frac{v_\infty}{v}$ can be expressed as

$$\frac{v_\infty}{v} = \frac{\frac{\mu_\infty}{\rho_\infty}}{\frac{\mu}{\rho}} = \frac{\mu_\infty}{\mu} \cdot \frac{\rho}{\rho_\infty}$$

By using Eqs. (5.5) and (5.8), we have

$$\frac{v_\infty}{v} = \left(\frac{T_\infty}{T} \right)^{n_\mu} \cdot \left(\frac{T_\infty}{T} \right) = \left(\frac{T_\infty}{T} \right)^{n_\mu + 1}$$

i.e.

$$\frac{v_{\infty}}{v} = \left(\frac{T_{\infty}}{(T_w - T_{\infty})\theta + T_{\infty}} \right)^{n_{\mu}+1}$$

Therefore,

$$\frac{v_{\infty}}{v} = [(T_w/T_{\infty} - 1)\theta + 1]^{-(n_{\mu}+1)} \quad (5.23)$$

5.5.2 For Liquids

Taking water as an example, the above temperature-dependent *physical property factors* are described as

Transformation for density factor $\frac{1}{\rho} \frac{d\rho}{d\eta}$

At first, the *density factor* $\frac{1}{\rho} \frac{d\rho}{d\eta}$ is expressed as

$$\frac{1}{\rho} \frac{d\rho}{d\eta} = \frac{1}{\rho} \frac{d\rho}{dt} \frac{dt}{d\eta}$$

where with Eq.(5.16) the following equation is obtained

$$\frac{d\rho}{dt} = -2 \times 4.48 \times 10^{-3} t$$

With Eq.(5.19) we obtain

$$\frac{dt}{d\eta} = (t_s - t_{\infty}) \frac{d\theta}{d\eta}$$

Therefore,

$$\frac{1}{\rho} \frac{d\rho}{d\eta} = \frac{1}{\rho} (-2 \times 4.48 \times 10^{-3} t) (t_s - t_{\infty}) \frac{d\theta}{d\eta}$$

Then,

$$\frac{1}{\rho} \frac{d\rho}{d\eta} = \frac{(-2 \times 4.48 \times 10^{-3} t) (t_s - t_{\infty})}{-4.48 \times 10^{-3} t^2 + 999.9} \cdot \frac{d\theta}{d\eta} \quad (5.24)$$

Transformation for viscosity factor $\frac{1}{\mu} \frac{d\mu}{d\eta}$

With (5.18) we have

$$\mu = \exp \left[-1.6 - \frac{1150}{T} + \left(\frac{690}{T} \right)^2 \right] \times 10^{-3}$$

$$\frac{1}{\mu} \frac{d\mu}{d\eta} = \frac{1}{\mu} \frac{d}{d\eta} \left\{ \exp \left[-1.6 - \frac{1150}{T} + \left(\frac{690}{T} \right)^2 \right] \times 10^{-3} \right\}$$

$$= \frac{\mu}{\mu} \left[\frac{1150}{T^2} - 2 \times \frac{690^2}{T^3} \right] \frac{dT}{d\eta}$$

where,

$$\frac{dT}{d\eta} = (T_w - T_\infty) \frac{d\theta}{d\eta}$$

Then,

$$\frac{1}{\mu} \frac{d\mu}{d\eta} = \left(\frac{1150}{T^2} - 2 \times \frac{690^2}{T^3} \right) (T_w - T_\infty) \frac{d\theta}{d\eta} \quad (5.25)$$

Transformation for thermal conductivity factor $\frac{1}{\lambda} \frac{d\lambda}{d\eta}$

With Eq.(5.17) we have

$$\frac{1}{\lambda} \frac{d\lambda}{d\eta} = \frac{1}{\lambda} \frac{d}{d\eta} (-8.01 \times 10^{-6} t^2 + 1.94 \times 10^{-3} t + 0.563)$$

i.e.

$$\frac{1}{\lambda} \frac{d\lambda}{d\eta} = \frac{1}{\lambda} (-8.01 \times 2 \times 10^{-6} t + 1.94 \times 10^{-3}) \frac{dt}{d\eta}$$

where,

$$\frac{dt}{d\eta} = (t_w - t_\infty) \frac{d\theta}{d\eta}$$

Then,

$$\frac{1}{\lambda} \frac{d\lambda}{d\eta} = \frac{(-8.01 \times 2 \times 10^{-6} t + 1.94 \times 10^{-3})(t_w - t_\infty)}{-8.01 \times 10^{-6} t^2 + 1.94 \times 10^{-3} t + 0.563} \frac{d\theta}{d\eta} \quad (5.26)$$

5.5.3 For Vapour–Gas Mixture

Transformation for density factor $\frac{1}{\rho_m} \frac{d\rho_m}{d\eta_m}$

With Eq.(5.9), the *density factor of the vapour-gas mixture* in the governing dimensional differential equations will be derived as

$$\frac{1}{\rho_m} \frac{d\rho_m}{d\eta_m} = \frac{1}{\rho_m} \frac{d}{d\eta_m} \left[\frac{\rho_v \rho_g}{(1 - C_{mv}) \rho_v + C_{mv} \rho_g} \right]$$

Then,

$$\frac{1}{\rho_m} \frac{d\rho_m}{d\eta_m} = \frac{1}{\rho_m} \left[\frac{\rho_v \frac{d\rho_g}{d\eta_m} + \rho_g \frac{d\rho_v}{d\eta_m}}{(1 - C_{mv})\rho_v + C_{mv}\rho_g} - \frac{\rho_v \rho_g}{((1 - C_{mv})\rho_v + C_{mv}\rho_g)^2} \cdot \right. \\ \left. (1 - C_{mv}) \frac{d\rho_v}{d\eta_m} - \rho_v \frac{dC_{mv}}{d\eta_m} + C_{mv} \frac{d\rho_g}{d\eta_m} + \rho_g \frac{dC_{mv}}{d\eta_m} \right]$$

With Eq.(5.9) we have

$$\frac{1}{\rho_m} \frac{d\rho_m}{d\eta_m} = \frac{1}{\rho_g} \frac{d\rho_g}{d\eta_m} + \frac{1}{\rho_v} \frac{d\rho_v}{d\eta_m} - \frac{1}{(1 - C_{mv})\rho_v + C_{mv}\rho_g} \cdot \\ \left[(1 - C_{mv}) \frac{d\rho_v}{d\eta_m} - \rho_v \frac{dC_{mv}}{d\eta_m} + C_{mv} \frac{d\rho_g}{d\eta_m} + \rho_g \frac{dC_{mv}}{d\eta_m} \right]$$

The above equation is further changed to

$$\frac{1}{\rho_m} \frac{d\rho_m}{d\eta_m} = \frac{1}{\rho_g} \frac{d\rho_g}{d\eta_m} + \frac{1}{\rho_v} \frac{d\rho_v}{d\eta_m} - \frac{1}{(1 - C_{mv})\rho_v + C_{mv}\rho_g} \cdot \\ \left[(1 - C_{mv}) \frac{d\rho_v}{d\eta_m} + C_{mv} \frac{d\rho_g}{d\eta_m} - (\rho_v - \rho_g) \frac{dC_{mv}}{d\eta_m} \right]$$

or

$$\frac{1}{\rho_m} \frac{d\rho_m}{d\eta_m} = \frac{1}{\rho_g} \frac{d\rho_g}{d\eta_m} + \frac{1}{\rho_v} \frac{d\rho_v}{d\eta_m} - \frac{C_{mv}(\rho_v - \rho_g)}{(1 - C_{mv})\rho_v + C_{mv}\rho_g} \cdot \\ \left[\frac{1 - C_{mv}}{C_{mv}} \cdot \frac{\rho_v}{\rho_v - \rho_g} \cdot \frac{1}{\rho_v} \frac{d\rho_v}{d\eta_m} + \frac{\rho_g}{\rho_v - \rho_g} \cdot \frac{1}{\rho_g} \frac{d\rho_g}{d\eta_m} - \frac{1}{C_{mv}} \frac{dC_{mv}}{d\eta_m} \right]$$

Now, we introduce the *vapour relative mass fraction* Γ_{mv} as

$$\Gamma_{mv} = \frac{C_{mv} - C_{mv,\infty}}{C_{mv,s} - C_{mv,\infty}}$$

where $C_{mv,s}$ and $C_{mv,\infty}$ are vapour mass fractions at the liquid–vapour interface and in vapour-gas bulk respectively,

Then, we have

$$\frac{1}{\rho_m} \frac{d\rho_m}{d\eta_m} = \frac{1}{\rho_g} \frac{d\rho_g}{d\eta_m} + \frac{1}{\rho_v} \frac{d\rho_v}{d\eta_m} - \frac{C_{mv}(\rho_v - \rho_g)}{(1 - C_{mv})\rho_v + C_{mv}\rho_g} \cdot \left[\frac{1 - C_{mv}}{C_{mv}} \cdot \frac{\rho_v}{\rho_v - \rho_g} \cdot \right. \\ \left. \frac{1}{\rho_v} \frac{d\rho_v}{d\eta_m} + \frac{\rho_g}{\rho_v - \rho_g} \cdot \frac{1}{\rho_g} \frac{d\rho_g}{d\eta_m} - \frac{C_{mv} - C_{mv,\infty}}{C_{mv}} \frac{d\Gamma_{mv}}{d\eta_m} \right] \quad (5.27)$$

Transformation for viscosity factor $\frac{1}{\mu_m} \frac{d\mu_m}{d\eta_m}$

With Eq. (5.12) the **viscosity factor** $\frac{1}{\mu_m} \frac{d\mu_m}{d\eta_m}$ is

$$\begin{aligned} \frac{1}{\mu_m} \frac{d\mu_m}{d\eta_m} &= \frac{1}{\mu_m} \frac{d}{d\eta_m} [C_{mv}\mu_v + (1 - C_{mv})\mu_g] \\ &= \frac{1}{\mu_m} \left[C_{mv} \frac{d\mu_v}{d\eta_m} + \mu_v \frac{dC_{mv}}{d\eta_m} + (1 - C_{mv}) \frac{d\mu_g}{d\eta_m} - \mu_g \frac{dC_{mv}}{d\eta_m} \right] \end{aligned}$$

i.e.

$$\frac{1}{\mu_m} \frac{d\mu_m}{d\eta_m} = \frac{1}{\mu_m} \left[C_{mv} \frac{d\mu_v}{d\eta_m} + (1 - C_{mv}) \frac{d\mu_g}{d\eta_m} + (\mu_v - \mu_g) \frac{dC_{mv}}{d\eta_m} \right]$$

Then, we have

$$\frac{1}{\mu_m} \frac{d\mu_m}{d\eta_m} = C_{mv} \frac{\mu_v}{\mu_m} \frac{1}{\mu_v} \frac{d\mu_v}{d\eta_m} + (1 - C_{mv}) \frac{\mu_g}{\mu_v \mu_g} \frac{1}{\mu_g} \frac{d\mu_g}{d\eta_m} + \frac{\mu_v - \mu_g}{\mu_m} \cdot \frac{dC_{mv}}{d\eta_m}$$

With definition of *vapour relative mass fraction* Γ_{mv} we have

$$\frac{1}{\mu_m} \frac{d\mu_m}{d\eta_m} = C_{mv} \frac{\mu_v}{\mu_m} \frac{1}{\mu_v} \frac{d\mu_v}{d\eta_m} + (1 - C_{mv}) \frac{\mu_g}{\mu_m \mu_g} \frac{1}{\mu_g} \frac{d\mu_g}{d\eta_m} + \frac{\mu_v - \mu_g}{\mu_m} (C_{mv,s} - C_{mv,\infty}) \frac{d\Gamma_{mv}}{d\eta_m} \quad (5.28)$$

Thus, it is seen that the viscosity factor $\frac{1}{\mu_m} \frac{d\mu_m}{d\eta_m}$ of vapour-gas mixture is dominated by the concentration C_{mv} , as well as the gas and vapour viscosity factors $\frac{1}{\mu_g} \frac{d\mu_g}{d\eta_m}$ and $\frac{1}{\mu_v} \frac{d\mu_v}{d\eta_m}$ respectively. Since $\frac{1}{\mu_g} \frac{d\mu_g}{d\eta_m}$ and $\frac{1}{\mu_v} \frac{d\mu_v}{d\eta_m}$ are temperature-dependent, the viscosity factor $\frac{1}{\mu_m} \frac{d\mu_m}{d\eta_m}$ of vapour-gas mixture is concentration- and temperature-dependent.

Transformation for thermal conductivity factor $\frac{1}{\lambda_m} \frac{d\lambda_m}{d\eta_m}$

Similar to derivation for Eq. (5.28), the viscosity factor $\frac{1}{\mu_m} \frac{d\mu_m}{d\eta_m}$ of vapour-gas mixture the thermal conductivity factor $\frac{1}{\lambda_m} \frac{d\lambda_m}{d\eta_m}$ of the vapour-gas mixture can be expressed as

The *concentration-dependent thermal conductivity factor* is described as

$$\frac{1}{\lambda_m} \frac{d\lambda_m}{d\eta_m} = C_{mv} \frac{\lambda_v}{\lambda_m} \frac{1}{\lambda_v} \frac{d\lambda_v}{d\eta_m} + (1 - C_{mv}) \frac{\lambda_g}{\lambda_m \lambda_g} \frac{1}{\lambda_g} \frac{d\lambda_g}{d\eta_m} + \frac{\lambda_v - \lambda_g}{\lambda_m} (C_{mv,s} - C_{mv,\infty}) \frac{d\Gamma_{mv}}{d\eta_m} \quad (5.29)$$

Similar to the analysis on the viscosity factor $\frac{1}{\mu_m} \frac{d\mu_m}{d\eta_m}$ of vapour-gas mixture, the thermal conductivity factor $\frac{1}{\lambda_m} \frac{d\lambda_m}{d\eta_m}$ of the vapour-gas mixture is concentration- and temperature-dependent also.

It is seen that the concentration-dependent physical property factors are function of the temperature-dependent physical property factors.

Eqs. (5.1)–(5.29) consist of the theoretical foundation for treatment of variable physical properties of gas, liquid and vapour-gas mixture for this book. These models will be used in the successive related chapters for serious investigation of heat and mass transfer on laminar free convection and two-phase free convection film boiling and condensation.

5.6 Summary

So far, it is time to summarise the models for treatment of fluid variable physical properties in Table 5.3.

5.7 Remarks

The advanced method for treatment of variable physical properties of fluids is proposed. This method involves temperature parameter method for treatment of temperature-dependent physical properties of gases, weighted sum method for treatment of concentration- and temperature-dependent physical properties of vapour-gas mixture and polynomial method for treatment of temperature-dependent physical properties of liquids. These methods for treatment of variable physical properties of fluids will be taken as a theoretical foundation of this book for extensive investigation of hydrodynamics and heat transfer of free convection of gases, free convection of liquids, free convection film boiling of liquid, free convection film condensation of pure vapour and free convection film condensation of vapour-gas mixture with consideration of coupled effects of variable physical properties.

The fundamentals of the temperature parameter method for treatment of variable physical properties of gases come from the simple power-law for description of the temperature-dependent physical properties of gases. The temperature parameters are representatives of the power-law indexes. A series of values of the temperature parameters n_μ , n_λ and n_{c_p} are reported based on the typical experimental results. For monatomic and diatomic gases, air and water vapour the value of n_μ varies from autoedited 10.64 to 1.04, while the value of n_λ varies from 0.71 to 1.185. Additionally, the density of gases is inversely proportion to its absolute temperature. Compared with the viscosity and thermal conductivity parameters, the specific heat parameter is much small. Therefore, the variable temperature will have more obvious effects on viscosity, thermal conductivity and density of gases than the specific heat. Since the determination of the temperature parameter is based on the typical experimental data, the simple power-law can simulate well the temperature-variable physical properties of gases. Obviously, with the temperature parameter method the treatment of variable

Table 5.3 Models for treatment of fluid variable physical properties

Term	Equations
Treatment of gas temperature-dependent physical properties	<p data-bbox="238 467 262 943"><i>Temperature-dependent physical property equations:</i></p> $\frac{\rho}{\rho_\infty} = \left(\frac{T}{T_\infty}\right)^{-1}$ $\frac{\mu}{\mu_\infty} = \left(\frac{T}{T_\infty}\right)^{n_\mu}$ $\frac{\lambda}{\lambda_\infty} = \left(\frac{T}{T_\infty}\right)^{n_\lambda}$ $\frac{c_p}{c_{p\infty}} = \left(\frac{T}{T_\infty}\right)^{n_{c_p}}$ <p data-bbox="556 411 579 943"><i>Temperature-dependent physical property factor equations:</i></p> $\frac{1}{\rho} \frac{d\rho}{d\eta} = -\frac{(T_w - T_\infty)}{(T_w - T_\infty)\theta} \frac{d\theta}{d\eta}$ $\frac{1}{\mu} \frac{d\mu}{d\eta} = \frac{n_\mu(T_w/T_\infty - 1)}{(T_w/T_\infty - 1)\theta + 1} \frac{d\theta}{d\eta}$ $\frac{1}{\lambda} \frac{d\lambda}{d\eta} = \frac{n_\lambda(T_w/T_\infty - 1)}{T_w/T_\infty - \theta + 1} \frac{d\theta}{d\eta}$ $\frac{1}{c_p} \frac{dc_p}{d\eta} = \frac{n_{c_p}(T_w/T_\infty - 1)}{(T_w/T_\infty - 1)\theta + 1} \frac{d\theta}{d\eta}$ $\frac{v_\infty}{y} = [(T_w/T_\infty - 1)\theta + 1]^{-(n_\mu + 1)}$ <p data-bbox="873 149 932 943">where η is the dimensionless coordinate variable, T_w and T_∞ are boundary temperature of the boundary layer and θ is dimensionless temperature, where $\theta = \frac{T - T_\infty}{T_w - T_\infty}$ or $\theta = \frac{t - t_\infty}{t_w - t_\infty}$</p>

Term	Equations
Treatment of liquid temperature-dependent properties (taking water as example)	<p data-bbox="209 469 224 940"><i>Temperature-dependent physical property equations:</i></p> $\rho = -4.48 \times 10^{-3}t^2 + 999.9$ $\lambda = -8.01 \times 10^{-6}t^2 + 1.94 \times 10^{-3}t + 0.563$ $\mu = 10^{-3} \exp \left[-1.6 - \frac{1150}{T} + \left(\frac{690}{T} \right)^2 \right]$
	specific heat c_p can be regarded as constant for atmospheric pressure
	<i>Temperature-dependent physical property factor equations:</i>
	$\frac{1}{\lambda} \frac{d\rho}{d\eta} = \frac{-4.48 \times 10^{-3}t^2 + 999.9}{(-2 \times 4.48 \times 10^{-3}t)(t_s - t_\infty)} \cdot \frac{d\theta}{d\eta}$ $\rho \frac{d\eta}{d\mu} = \left(\frac{1150}{T^2} - 2 \times \frac{690^2}{T^3} \right) (T_w - T_\infty) \frac{d\theta}{d\eta}$ $\frac{\mu}{\lambda} \frac{d\lambda}{d\eta} = \frac{-8.01 \times 2 \times 10^{-6}t + 1.94 \times 10^{-3}}{-8.01 \times 10^{-6}t^2 + 1.94 \times 10^{-3}t + 0.563} \cdot \frac{d\theta}{d\eta}$
Treatment of concentration- and temperature-dependent properties of vapour-gas mixture	<p data-bbox="616 451 631 940"><i>Equations on concentration-dependent physical properties of vapour-gas mixture:</i></p> $\rho_{mv} = \frac{C_{mv}\rho_v\rho_g}{(1 - C_{mv})\rho_v + C_{mv}\rho_g}$ $\rho_{mg} = \frac{\rho_v\rho_g}{(1 - C_{mv})\rho_v + C_{mv}\rho_g}$ $\rho_m = \frac{(1 - C_{mv})\rho_v + C_{mv}\rho_g}{C_{mv}\mu_v + (1 - C_{mv})\mu_g}$ $\mu_m = C_{mv}\lambda_v + (1 - C_{mv})\lambda_g$ $\lambda_m = C_{mv}c_{p_v} + (1 - C_{mv})c_{p_g}$ $Pr_m = C_{mv}Pr_v + (1 - C_{mv})Pr_g$ <p data-bbox="921 451 937 940"><i>Equations on concentration-dependent density factors:</i></p> $\frac{1}{\rho_m} \frac{d\rho_m}{d\eta_m} = \frac{1}{\rho_g} \frac{d\rho_g}{d\eta_m} + \frac{1}{\rho_v} \frac{d\rho_v}{d\eta_m}$

(continued)

Table 5.3 (continued)

Term	Equations
	$-\frac{C_{mv}(\rho_v - \rho_g)}{(1 - C_{mv})\rho_v + c_{mv}\rho_g} \left[\frac{(1 - c_{mv})}{C_{mv}} \rho_v \frac{1}{\rho_v - \rho_g} \frac{d\rho_v}{d\eta_m} + \frac{\rho_g}{(\rho_v - \rho_g)} \frac{1}{\rho_g} \frac{d\rho_g}{d\eta_m} - \frac{C_{mv,s} - C_{mv,\infty}}{C_{mv}} \frac{d\Gamma_{mv}}{d\eta_m} \right]$
	<p>where, the involved temperature-dependent density factors:</p>
	$\frac{1}{\rho_v} \frac{d\rho_v}{d\eta_m} = -\frac{(T_{s,int}/T_\infty - 1)d\theta_m/d\eta_m}{(T_{s,int}/T_\infty - 1)\theta_m + 1}$
	$\frac{\rho_v}{\rho_g} \frac{d\eta_m}{d\rho_g} = -\frac{(T_{s,int}/T_\infty - 1)\theta_m + 1}{(T_{s,int}/T_\infty - 1)d\theta_m/d\eta_m}$
	$\rho_g \frac{d\eta_m}{d\rho_g} = \frac{(T_{s,int}/T_\infty - 1)\theta_m + 1}{(T_{s,int}/T_\infty - 1)d\theta_m/d\eta_m}$
	<p>where $T_{s,int}$ is liquid–vapour interfacial temperature</p>
	<p><i>Concentration-dependent viscosity factor equation:</i></p>
	$\frac{1}{\mu_m} \frac{d\mu_m}{d\eta_m} = \frac{\mu_v}{\mu_m} \frac{1}{\mu_v} \frac{d\mu_v}{d\eta_m} + (1 - C_{mv}) \frac{\mu_g}{\mu_m} \frac{1}{\mu_g} \frac{d\mu_g}{d\eta_m} + (C_{mv,s} - C_{mv,\infty}) \frac{\mu_v - \mu_g}{\mu_m} \frac{d\Gamma_{mv}}{d\eta_m}$
	<p>where $\Gamma_{mv} = \frac{C_{mv} - C_{mv,\infty}}{C_{mv,s} - C_{mv,\infty}}$ is vapour relative mass fraction and the involved vapour and gas temperature-dependent viscosity factors are respectively</p>
	$\frac{1}{\mu_v} \frac{d\mu_v}{d\eta_m} = \frac{n_{\mu v}(T_{s,int}/T_\infty - 1)d\theta_m/d\eta_m}{(T_{s,int}/T_\infty - 1)\theta_m + 1}$
	$\frac{\mu_v}{\mu_g} \frac{d\eta_m}{d\mu_g} = \frac{n_\mu(T_{s,int}/T_\infty - 1)d\theta_m/d\eta_m}{(T_{s,int}/T_\infty - 1)\theta_m + 1}$
	$\mu_g \frac{d\eta_m}{d\mu_g} = \frac{(T_{s,int}/T_\infty - 1)\theta_m + 1}{(T_{s,int}/T_\infty - 1)d\theta_m/d\eta_m}$
	<p><i>Concentration-dependent viscosity factor equation:</i></p>
	$\frac{1}{\lambda_m} \frac{d\lambda_m}{d\eta_m} = \frac{\lambda_v}{\lambda_m} \frac{1}{\lambda_v} \frac{d\lambda_v}{d\eta_m} + (1 - C_{mv}) \frac{\lambda_g}{\lambda_m} \frac{1}{\lambda_g} \frac{d\lambda_g}{d\eta_m} + \frac{\lambda_v - \lambda_g}{\lambda_m} (C_{mv,s} - C_{mv,\infty}) \frac{d\Gamma_{mv}}{d\eta_m}$
	<p>where the involved temperature-dependent thermal conductivity factors:</p>
	$\frac{1}{\lambda_v} \frac{d\lambda_v}{d\eta_m} = \frac{n_\lambda(T_s/T_\infty - 1)\theta_v + 1}{n_\lambda(T_{s,int}/T_\infty - 1)d\theta_m/d\eta_m}$
	$\frac{\lambda_v}{\lambda_g} \frac{d\eta_m}{d\lambda_g} = \frac{(T_{s,int}/T_\infty - 1)\theta_m + 1}{(T_{s,int}/T_\infty - 1)d\theta_m/d\eta_m}$

physical properties of vapour or gas is not only reliable, but also very simple and convenient for heat transfer application.

Taking water as an example, the temperature-dependent polynomials of the density, thermal conductivity and viscosity are introduced for liquids, while the specific heat at constant pressure varies so small with variation of temperature that it can be disregarded. These polynomials are reliable since they are based on the typical experimental data.

The concentration-dependent density equations of vapour-gas mixture are reported through the rigorously theoretical derivation, while the other concentration-dependent physical properties of vapour-gas mixture are expressed as the weighted sum of the physical properties of the involved vapour and gas with their concentrations (mass fraction). Since the involved vapour and gas are temperature-dependent, the physical properties of the vapour-gas mixture are concentration- and temperature-dependent.

5.8 Questions

1. Please explain the meanings of the temperature-dependent physical properties, concentration-dependent physical properties and concentration- and temperature-dependent physical properties?
2. Please tell me the advantages of the temperature parameter method for description of temperature-dependent physical properties of gas? Do you know how the temperature parameters of gases reported in Tables 5.1 and 5.2 were obtained?
3. Which kind of fluid is suggested to use the polynomial expression method for describing the temperature-dependent physical properties? please tell me how the polynomials were obtained for description of water temperature-dependent physical properties?
4. Please explain why the physical properties of vapour-gas mixture are concentration- and temperature-dependent?
5. How are the physical properties of vapour-gas mixture concentration- and temperature-dependent?
6. What is the relationship between the temperature-dependent physical properties and the concentration-dependent physical properties for vapour-gas mixture?
7. Please derive out Eqs. (5.9)–(5.11) on the densities related to the vapour-gas mixture.
8. From equations for gas temperature-dependent physical properties, water temperature-dependent physical properties and concentration- and temperature-dependent physical properties, please analyze the necessity and importance of treatment of variable physical properties on laminar free convection and film flows.

References

1. T. Hara, The free-convection flow about a heated vertical plate in air. *Trans. Jpn. Soc. Mech. Eng.* **20**, 517–520 (1954)
2. A.A. Tataev, Heat exchange in condition of free laminar movement of gas with variable viscosity at a vertical wall. *Zh. Tekh. Fiz.* **26**, 2714–2719 (1956)
3. E.M. Sparrow, J.L. Gregg, The variable fluid-property problem in free convection. *Trans. ASME* **80**, 879–886 (1958)
4. D.D. Gray, A. Giogini, The validity of the Boussinesq approximation for liquids and gases. *Int. J. Heat Mass Trans.* **19**, 546–577 (1977)
5. A.M. Clausing, S.N. Kempka, The influences of property variations on natural convection from vertical surfaces. *J. Heat Transfer* **103**, 609–612 (1981)
6. H. Herwig, The effect of variable properties on momentum and heat transfer in a tube with constant heat flux across the wall. *Int. J. Heat Mass Transf.* **28**(2), 423–431 (1985)
7. A. Pozzi, M. Lupo, Variable-property effects in free convection. *Int. J. Heat Fluid Flow* **11**(2), 135–141 (1990)
8. D.Y. Shang, B.X. Wang, Effect of variable thermophysical properties on laminar free convection of gas. *Int. J. Heat Mass Transf.* **33**(7), 1387–1395 (1990)
9. D.Y. Shang, B.X. Wang, Effect of variable thermophysical properties on laminar free convection of polyatomic gas. *Int. J. Heat Mass Transf.* **34**(3), 749–755 (1991)
10. B.X. Shang, Y. Wang, Wang, Y. Quan, Study on liquid laminar free convection with consideration of variable thermophysical properties. *Int. J. Heat Mass Transf.* **36**(14), 3411–3419 (1993)
11. D.Y. Shang, B.X. Wang, L.C. Zhong, A study on laminar film boiling of liquid along an isothermal vertical plates in a pool with consideration of variable thermophysical properties. *Int. J. Heat Mass Transfer* **37**(5), 819–828 (1994)
12. D.Y. Shang, T. Adamek, Study on laminar film condensation of saturated steam on a vertical flat plate for consideration of various physical factors including variable thermophysical properties. *Wärme- und Stoffübertragung* **30**, 89–100 (1994)
13. D.Y. Shang, B.X. Wang, An extended study on steady-state laminar film condensation of a superheated vapor on an isothermal vertical plate. *Int. J. Heat Mass Transf.* **40**(4), 931–941 (1997)
14. D.Y. Shang, L.C. Zhong, Extensive study on laminar free film condensation from vapor-gas mixture. *Int. J. Heat Mass Transf.* **51**, 4300–4314 (2008)
15. D.Y. Shang, *Theory of heat transfer with forced convection film flows* (Springer, Heiderberg, 2010)
16. J. Hisenrath et al., *Tables of Thermodynamic and Transport Properties* (National Bureau of Standards, Washington, 1955)
17. Y.S. Touloukian, S.C. Saxena, P. Hestermans, *Thermophysical Properties of Matter. Viscosity*, vol. 2 (IFI/Plenum, New York, 1970)
18. Y.S. Touloukian, P.E. Liley, S.C. Saxena, *Thermophysical Properties of Matter. Thermal Conductivity, Non-Metallic Liquids and Gases*, vol. 3 (IFI/Plenum, New York, 1970)
19. Y.S. Touloukian, T. Makita, *Thermophysical Properties of Matter. Specific Heat, Non-Metallic Liquids and Gases*, vol. 6 (IFI/Plenum, New York, 1970)
20. VDI—Wärmeatlas, *Berechnungsblätter für den Wärmeübertragung*, 5, erweiterte edn. (VDI Verlage GmbH, Düsseldorf, 1988)
21. S.M. Yang, *Heat Transfer*, 2nd edn. (Higher Education Press, 1987), pp. 443
22. J.Q. Chang, *Real Fluid Mechanics* (Tsinghua University Press, Beijing, 1986)

Part II
Laminar Free Convection with
Consideration of Coupled Effects of
Variable Physical Properties

Chapter 6

Heat Transfer of Laminar Free Convection of Monatomic and Diatomic Gases, Air, and Water Vapor

Abstract The new similarity analysis method is used to replace the traditional Falkner-Skan type transformation for creating similarity governing models of laminar free convection. With this method, the velocity components are directly transformed into the corresponding dimensionless velocity components. Then, it is more convenient to equivalently transform the governing partial differential equations into the related ordinary differential ones, without inducing stream function and the intermediate function variable required by the traditional Falkner-Skan type transformation. Furthermore, with this method, it is more convenient for treatment of variable physical properties. The temperature parameter method is used for treatment of variable physical properties of gases. With this method the physical property factors coupled with the governing ordinary differential equations are transformed to the functions of the Prandtl number, temperature parameters, and the boundary temperature ratio for simultaneous solution. There are obvious effects of variable physical properties on velocity and temperature fields, as well as heat transfer of free convection of gas. Based on the heat transfer analysis and related rigorous numerical results, the prediction equations of gas free convection heat transfer is created. Since the Prandtl number and temperature parameters of gases are based on the experimental data, these prediction equations of gas free convection heat transfer are reliable and then have practical application value.

6.1 Introduction

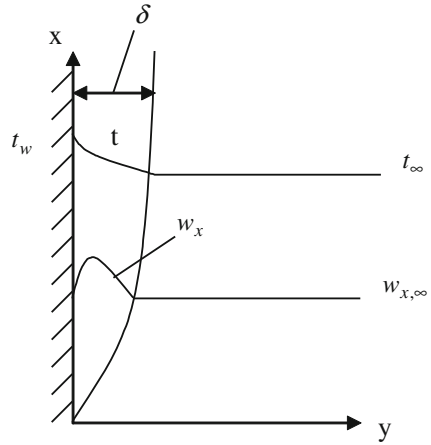
The study of laminar free convection of gases with variable thermophysical properties can be traced back to the perturbation analysis of Hara [1] for air free convection. The solution is applicable for small values of the perturbation parameter, $\varepsilon_H = (T_w - T_\infty)/T_\infty$. Later, Tataev [2] investigated the free convection of a gas with variable viscosity. A well-known analysis of the variable fluid property problem for laminar free convection on an isothermal vertical flat plate has been presented by

Sparrow and Gregg [3], giving solutions of the boundary layer equations for five assumed gases. They proposed a reference temperature and suggested that with it the problem of variable thermophysical properties can be treated as a constant property problem, i.e., using the Boussinesq approximation. Gray and Giogini [4] discussed the validity of the Boussinesq approximation and proposed a method for analyzing natural convection flow with fluid properties assumed to be a linear function of temperature and pressure. Clausing and Kempka [5] reported their experimental study of the influence of property variations on natural convection and showed that, for the laminar region, Nu_f is a function of $Ra_f (= Gr_f Pr_f)$ only, with the reference temperature T_f taken as the average temperature in the boundary layer.

In this chapter and Chap. 7 I will present respectively our recent studies [6, 7], for effect of variable physical properties on laminar free convection of different kind of gases. In this chapter, the gases involved are monatomic and diatomic gases as well as air and water vapor. The variation of specific heat of these gases is very small, and so can be neglected when considering variable physical properties. In this chapter, the gases involved are polyatomic gases in which the variation of specific heat cannot be neglected. In these studies a recently developed dimensionless velocity component method provided in Chap. 4 is provided for the similarity transformation of the governing partial differential equations of the laminar boundary layer, to replace the traditional Falkner-Skan transformations.

Additionally, a temperature parameter method for the treatment of a gas with variable thermophysical properties is proposed. With this method, the thermal conductivity, dynamic viscosity and specific heat of gases are assumed to vary with absolute temperature according to a simple power law. The parameters of thermal conductivity, absolute viscosity, and specific heat are proposed and the corresponding values are provided from the typical experimental data of the thermophysical properties. The density is taken to be inversely proportional to the absolute temperature at constant pressure, while the Prandtl number is assumed to be constant. The governing equations for the laminar free convection of gas are transformed into the dimensionless ordinary equations by using the dimensionless velocity component method, and meanwhile the variable thermophysical properties are treated by employing the temperature parameter method. The governing ordinary differential equations with the boundary conditions are solved for various boundary temperature ratios for the various gases mentioned above, and the rigorous numerical results are provided. These numerical results have shown that there are different velocity and temperature distributions for different boundary temperature ratios, as well as for different gases. Curve-fit formulas for the temperature gradient at the wall with very good agreement to the numerical solutions are provided, which facilitate rapid and yet accurate estimates of the heat transfer coefficient and the Nusselt number together with various boundary temperature ratios T_w/T_∞ and different gases.

Fig. 6.1 Physical model and coordinate system of boundary layer for laminar free convection



6.2 Governing Partial Differential Equations

The physical analytical model and co-ordinate system used for laminar free convection of gas on an isothermal vertical flat plate is shown in Fig. 6.1. The boundary layer is laminar when *Raleigh number*, $Ra (= Gr Pr)$ is less than 10^9 [8].

According to the presentation in Chap. 2 the governing partial differential equations for mass, momentum and energy for a steady laminar flow in the boundary layer for gas laminar vertical free convection with consideration of variable physical properties can be given by

$$\frac{\partial}{\partial x}(\rho w_x) + \frac{\partial}{\partial y}(\rho w_y) = 0 \tag{6.1}$$

$$\rho \left(w_x \frac{\partial w_x}{\partial x} + w_y \frac{\partial w_x}{\partial y} \right) = \frac{\partial}{\partial y} \left(\mu \frac{\partial w_x}{\partial y} \right) + g\rho \left| \frac{T}{T_\infty} - 1 \right| \tag{6.2}$$

$$\rho c_p \left(w_x \frac{\partial T}{\partial x} + w_y \frac{\partial T}{\partial y} \right) = \frac{\partial}{\partial y} \left(\lambda \frac{\partial T}{\partial y} \right). \tag{6.3}$$

The absolute value of buoyancy term $\rho g |T/T_\infty - 1|$ shows that it has always positive sign no matter which one is larger between T and T_∞ . In this case, the buoyancy term $\rho g |T/T_\infty - 1|$ and the velocity component w_x have the same sign. The boundary conditions are,

$$y = 0: w_x = 0, \quad w_y = 0, \quad T = T_w \tag{6.4}$$

$$y \rightarrow \infty: w_x \rightarrow 0, \quad T = T_\infty. \tag{6.5}$$

6.3 Similarity Transformation of the Governing Equations

6.3.1 Dimensionless Similarity Variables Based on the New Similarity Analysis Method

According to Chap. 4 for the dimensionless similarity variables based on the new similarity analysis method, the related dimensionless similarity variables are assumed as follows, respectively, for laminar free convection of gases on a vertical flat plate with consideration of variable physical properties:

The dimensionless coordinate variable is expressed as

$$\eta = \frac{y}{x} \left(\frac{1}{4} \text{Gr}_{x,\infty} \right)^{1/4} \quad (6.6)$$

where the local Grashof number $\text{Gr}_{x,\infty}$ is defined as

$$\text{Gr}_{x,\infty} = \frac{g |T_w/T_\infty - 1| x^3}{\nu_\infty^2} \quad (6.7)$$

Here, kinematic viscosity ν has the subscript ∞ . It means that the physical property to be considered is related to boundary temperature t_∞ for consideration of variable physical properties.

A dimensionless temperature variable is defined as

$$\theta = \frac{T - T_\infty}{T_w - T_\infty}. \quad (6.8)$$

Dimensionless velocity components for consideration of variable physical properties are assumed to be:

$$W_x = \left[2\sqrt{gx |T_w/T_\infty - 1|} \right]^{-1} w_x \quad (6.9)$$

$$W_y = \left[2\sqrt{gx |T_w/T_\infty - 1|} \left(\frac{1}{4} \text{Gr}_{x,\infty} \right)^{-1/4} \right]^{-1} w_y. \quad (6.10)$$

6.3.2 Similarity Transformation of the Governing Equations

With the above assumed dimensionless variables the governing partial differential equations governing partial differential equations can be transformed similarly as follows:

For Eq. (6.1)

Equation (6.1) is initially changed into

$$\rho \left(\frac{\partial w_x}{\partial x} + \frac{\partial w_y}{\partial y} \right) + w_x \frac{\partial \rho}{\partial x} + w_y \frac{\partial \rho}{\partial y} = 0 \quad (6.11)$$

With the dimensionless variables assumed in Eqs. (6.6), (6.7), (6.9) and (6.10) we obtain the following relations:

$$\frac{\partial w_x}{\partial x} = \left[2\sqrt{gx} |T_w/T_\infty - 1|^{1/2} \right] \frac{dW_x}{d\eta} \frac{\partial \eta}{\partial x} + \frac{1}{2} x^{-\frac{1}{2}} \left[2\sqrt{g} |T_w/T_\infty - 1|^{1/2} \right] W_x,$$

where

$$\begin{aligned} \frac{\partial \eta}{\partial x} &= \frac{\partial}{\partial x} \left[\frac{y}{x} \left(\frac{1}{4} \text{Gr}_{x,\infty} \right)^{1/4} \right] \\ &= \frac{\partial}{\partial x} \left[y \left(\frac{1}{4} \frac{g |T_w/T_\infty - 1| x^{-1}}{v_\infty^2} \right)^{1/4} \right] \\ &= -\frac{1}{4} \left[y \left(\frac{1}{4} \frac{g |T_w/T_\infty - 1|}{v_\infty^2} \right)^{1/4} \right] x^{-\frac{5}{4}} \\ &= -\frac{1}{4} \left[y \left(\frac{1}{4} \frac{g |T_w/T_\infty - 1| x^3}{v_\infty^2} \right)^{1/4} \right] x^{-2} \\ &= -\frac{1}{4} x^{-1} \eta. \end{aligned}$$

Then,

$$\begin{aligned} \frac{\partial w_x}{\partial x} &= \left[2\sqrt{gx} |T_w/T_\infty - 1|^{1/2} \right] \frac{dW_x}{d\eta} \left(-\frac{1}{4} x^{-1} \eta \right) \\ &\quad + \frac{1}{2} x^{-\frac{1}{2}} \left[2\sqrt{g} |T_w/T_\infty - 1|^{1/2} \right] W_x \\ &= -\frac{1}{2} \left[\sqrt{\frac{g}{x}} |T_w/T_\infty - 1|^{1/2} \right] \eta \frac{dW_x}{d\eta} + \left[\sqrt{\frac{g}{x}} |T_w/T_\infty - 1|^{1/2} \right] W_x \\ &= \sqrt{\frac{g}{x}} |T_w/T_\infty - 1|^{1/2} \left(W_x - \frac{1}{2} \eta \frac{dW_x}{d\eta} \right) \quad (6.12) \\ \frac{\partial w_y}{\partial y} &= \left[2\sqrt{gx} |T_w/T_\infty - 1|^{1/2} \left(\frac{1}{4} \text{Gr}_{x,\infty} \right)^{-1/4} \right] \frac{dW_y}{d\eta} \frac{\partial \eta}{\partial y} \end{aligned}$$

$$\begin{aligned}
&= \left[2\sqrt{gx} |T_w/T_\infty - 1|^{1/2} \left(\frac{1}{4} \text{Gr}_{x,\infty} \right)^{-1/4} \right] \frac{dW_y}{d\eta} \frac{1}{x} \left(\frac{1}{4} \text{Gr}_{x,\infty} \right)^{1/4} \\
&= 2\sqrt{\frac{g}{x}} |T_w/T_\infty - 1|^{1/2} \frac{dW_y}{d\eta} \tag{6.13}
\end{aligned}$$

$$\frac{\partial \rho}{\partial x} = \frac{d\rho}{d\eta} \frac{\partial \eta}{\partial x} = -\frac{1}{4} x^{-1} \eta \frac{d\rho}{d\eta} \tag{6.14}$$

$$\frac{\partial \rho}{\partial y} = \frac{d\rho}{d\eta} \frac{\partial \eta}{\partial y} = \frac{1}{x} \left(\frac{1}{4} \text{Gr}_{x,\infty} \right)^{1/4} \frac{d\rho}{d\eta}. \tag{6.15}$$

By using Eqs. (6.12)–(6.15), Eq. (6.12) can be changed to

$$\begin{aligned}
\rho &\left[\sqrt{\frac{g}{x}} |T_w/T_\infty - 1|^{1/2} \left(W_x - \frac{1}{2} \eta \frac{dW_y}{d\eta} \right) + 2\sqrt{\frac{g}{x}} |T_w/T_\infty - 1|^{1/2} \frac{dW_y}{d\eta} \right] \\
&+ 2\sqrt{gx} |T_w/T_\infty - 1|^{1/2} W_x \left(-\frac{1}{4} \eta x^{-1} \frac{d\rho}{d\eta} \right) + 2\sqrt{gx} |T_w/T_\infty - 1|^{1/2} \\
&\times \left(\frac{1}{4} \text{Gr}_{x,\infty} \right)^{-1/4} W_y \frac{d\rho}{d\eta} \left(\frac{1}{4} \text{Gr}_{x,\infty} \right)^{1/4} x^{-1} = 0 \tag{6.16}
\end{aligned}$$

Equation (6.16) is divided by $|T_w/T_\infty - 1|^{1/2} \sqrt{\frac{g}{x}}$ and transformed into

$$\rho \left[\left(W_x - \frac{1}{2} \eta \frac{dW_y}{d\eta} \right) + 2 \frac{dW_y}{d\eta} \right] + 2W_x \left(-\frac{1}{4} \eta \frac{d\rho}{d\eta} \right) + 2W_y \frac{d\rho}{d\eta} = 0 \tag{6.17}$$

or

$$2W_x - \eta \frac{dW_x}{d\eta} + 4 \frac{dW_y}{d\eta} - \frac{1}{\rho} \frac{d\rho}{d\eta} (\eta W_x - 4W_y) = 0 \tag{6.18}$$

For Eq. (6.2)

Equation (6.2) can be rewritten as

$$\rho \left(w_x \frac{\partial w_x}{\partial x} + w_y \frac{\partial w_x}{\partial y} \right) = \mu \frac{\partial^2 w_x}{\partial y^2} + \frac{\partial w_x}{\partial y} \frac{\partial \mu}{\partial y} + \rho g (T/T_\infty - 1). \tag{6.19}$$

The absolute value of buoyancy factor $|T/T_\infty - 1|$ shows that the buoyancy term $\rho g |T/T_\infty - 1|$ has always positive sign no matter which one is larger between T and T_∞ . In this case, the buoyancy term $\rho g |T/T_\infty - 1|$ and the velocity component w_x have same sign.

With the dimensionless variables assumed in Eqs. (6.6), (6.7), (6.9), and (6.10) we obtain the following equations:

$$\frac{\partial w_x}{\partial y} = 2\sqrt{gx} |T_w/T_\infty - 1|^{1/2} \frac{dW_x}{d\eta} \frac{\partial \eta}{\partial y},$$

where

$$\frac{\partial \eta}{\partial y} = x^{-1} \left(\frac{1}{4} \text{Gr}_{x,\infty} \right)^{1/4}.$$

Then,

$$\frac{\partial w_x}{\partial y} = 2\sqrt{gx} |T_w/T_\infty - 1|^{1/2} \frac{dW_x}{d\eta} x^{-1} \left(\frac{1}{4} \text{Gr}_{x,\infty} \right)^{1/4} \quad (6.20)$$

$$\begin{aligned} \frac{\partial^2 w_x}{\partial y^2} &= 2\sqrt{gx} |T_w/T_\infty - 1|^{1/2} \frac{d^2 W_x}{d\eta^2} x^{-1} \left(\frac{1}{4} \text{Gr}_{x,\infty} \right)^{1/4} \frac{\partial \eta}{\partial y} \\ &= 2\sqrt{gx} |T_w/T_\infty - 1|^{1/2} \frac{d^2 W_x}{d\eta^2} x^{-1} \left(\frac{1}{4} \text{Gr}_{x,\infty} \right)^{1/4} x^{-1} \left(\frac{1}{4} \text{Gr}_{x,\infty} \right)^{1/4} \\ &= 2\sqrt{gx} |T_w/T_\infty - 1|^{1/2} \frac{d^2 W_x}{d\eta^2} \left(\frac{1}{4} \text{Gr}_{x,\infty} \right)^{1/2} x^{-2} \end{aligned} \quad (6.21)$$

$$\frac{\partial \mu}{\partial y} = \frac{d\mu}{d\eta} \frac{\partial \eta}{\partial y} = \frac{d\mu}{d\eta} \left(\frac{1}{4} \text{Gr}_{x,\infty} \right)^{1/4} x^{-1}. \quad (6.22)$$

Using Eqs. (6.9), (6.10), (6.12), (6.20)–(6.22), Eq. (6.19) becomes

$$\begin{aligned} \rho &\left[2\sqrt{gx} |T_w/T_\infty - 1|^{1/2} W_x \sqrt{\frac{g}{x}} |T_w/T_\infty - 1|^{1/2} \left(W_x - \frac{1}{2} \eta \frac{dW_x}{d\eta} \right) \right. \\ &\quad \left. + 2\sqrt{gx} |T_w/T_\infty - 1|^{1/2} \left(\frac{1}{4} \text{Gr}_{x,\infty} \right)^{-1/4} W_y \right. \\ &\quad \left. \times \left(2\sqrt{gx} |T_w/T_\infty - 1|^{1/2} \frac{dW_x}{d\eta} x^{-1} \left(\frac{1}{4} \text{Gr}_{x,\infty} \right)^{1/4} \right) \right] \\ &= 2\mu \sqrt{gx} |T_w/T_\infty - 1|^{1/2} \frac{d^2 W_x}{d\eta^2} \left(\frac{1}{4} \text{Gr}_{x,\infty} \right)^{1/2} x^{-2} \\ &\quad + 2\sqrt{gx} |T_w/T_\infty - 1|^{1/2} \frac{dW_x}{d\eta} x^{-1} \left(\frac{1}{4} \text{Gr}_{x,\infty} \right)^{1/4} \\ &\quad \times \frac{d\mu}{d\eta} \left(\frac{1}{4} \text{Gr}_{x,\infty} \right)^{1/4} x^{-1} + \rho g |T/T_\infty - 1| \end{aligned} \quad (6.23)$$

Equation (6.23) is divided by $\rho g (T_w/T_\infty - 1)$, meanwhile, the definition of local Grashof number $\text{Gr}_{x,\infty}$ is considered, and then, Eq. (6.23) is simplified to

$$\begin{aligned}
& 2W_x \left(W_x - \frac{1}{2}\eta \frac{dW_x}{d\eta} \right) + 2W_y \left(2 \frac{dW_x}{d\eta} \right) \\
& = 2\nu \frac{d^2 W_x}{d\eta^2} \left(\frac{1}{4} \frac{1}{\nu_\infty^2} \right)^{1/2} + 2 \frac{1}{\rho} \frac{dW_x}{d\eta} \frac{d\mu}{d\eta} \left(\frac{1}{4} \frac{1}{\nu_\infty^2} \right)^{1/2} + \theta
\end{aligned}$$

or

$$2W_x \left(W_x - \frac{1}{2}\eta \frac{dW_x}{d\eta} \right) + 2W_y \left(2 \frac{dW_x}{d\eta} \right) = \frac{\nu}{\nu_\infty} \frac{d^2 W_x}{d\eta^2} + \frac{1}{\rho} \frac{dW_x}{d\eta} \frac{d\mu}{d\eta} \frac{1}{\nu_\infty} + \theta. \quad (6.24)$$

Equation (6.24) is multiplied by $\frac{\nu_\infty}{\nu}$ and is simplified to

$$\frac{\nu_\infty}{\nu} \left[W_x \left(2W_x - \eta \frac{dW_x}{d\eta} \right) + 4W_y \frac{dW_x}{d\eta} \right] = \frac{d^2 W_x}{d\eta^2} + \frac{1}{\mu} \frac{d\mu}{d\eta} \frac{dW_x}{d\eta} + \frac{\nu_\infty}{\nu} \theta \quad (6.25)$$

For Eq. (6.3)

Finally, Eq. (6.3) can be rewritten as:

$$\rho c_p \left(w_x \frac{\partial T}{\partial x} + w_y \frac{\partial T}{\partial y} \right) = \lambda \frac{\partial^2 T}{\partial y^2} + \frac{\partial \lambda}{\partial y} \frac{\partial T}{\partial y}, \quad (6.26)$$

where

$$\begin{aligned}
T & = (T_w - T_\infty)\theta + T_\infty \\
\frac{\partial T}{\partial x} & = -(T_w - T_\infty) \frac{d\theta}{d\eta} \frac{\partial \eta}{\partial x} = -(T_w - T_\infty) \frac{d\theta}{d\eta} \left(\frac{1}{4} \right) \eta x^{-1} \quad (6.27)
\end{aligned}$$

$$\frac{\partial T}{\partial y} = (T_w - T_\infty) \frac{d\theta}{d\eta} \frac{\partial \eta}{\partial y} = (T_w - T_\infty) \frac{d\theta}{d\eta} \left(\frac{1}{4} \text{Gr}_{x,\infty} \right)^{1/4} x^{-1} \quad (6.28)$$

$$\begin{aligned}
\frac{\partial^2 T}{\partial y^2} & = (T_w - T_\infty) \left(\frac{1}{4} \text{Gr}_{x,\infty} \right)^{1/4} x^{-1} \frac{d^2 \theta}{d\eta^2} \frac{\partial \eta}{\partial y} \\
& = (T_w - T_\infty) \frac{d^2 \theta}{d\eta^2} \left(\frac{1}{4} \text{Gr}_{x,\infty} \right)^{1/2} x^{-2} \quad (6.29)
\end{aligned}$$

$$\frac{\partial \lambda}{\partial y} = \frac{d\lambda}{d\eta} \frac{\partial \eta}{\partial y} = \frac{d\lambda}{d\eta} \left(\frac{1}{4} \text{Gr}_{x,\infty} \right)^{1/4} x^{-1}. \quad (6.30)$$

Then, Eq. (6.26) will be transformed into

$$\begin{aligned}
\rho c_p \left(2\sqrt{gx} |T_w/T_\infty - 1|^{1/2} W_x (-1)(T_w - T_\infty) \frac{d\theta}{d\eta} \left(\frac{1}{4} \right) \eta x^{-1} \right. \\
\left. + 2\sqrt{gx} |T_w/T_\infty - 1|^{1/2} \left(\frac{1}{4} \text{Gr}_{x,\infty} \right)^{-1/4} W_y (T_w - T_\infty) \right)
\end{aligned}$$

$$\begin{aligned}
& \frac{d\theta}{d\eta} \left(\frac{1}{4} \text{Gr}_{x,\infty} \right)^{1/4} x^{-1} \\
&= \lambda (T_w - T_\infty) \frac{d^2\theta}{d\eta^2} \left(\frac{1}{4} \text{Gr}_{x,\infty} \right)^{1/2} x^{-2} \\
&+ \frac{d\lambda}{d\eta} \left(\frac{1}{4} \text{Gr}_{x,\infty} \right)^{1/4} x^{-1} (T_w - T_\infty) \frac{d\theta}{d\eta} \left(\frac{1}{4} \text{Gr}_{x,\infty} \right)^{1/4} x^{-1}. \quad (6.31)
\end{aligned}$$

Equation (6.31) is divided by $(T_w - T_\infty) |T_w/T_\infty - 1|^{1/2} \sqrt{\frac{g}{x}}$, meanwhile, the definition of local Grashof number $\text{Gr}_{x,\infty}$ is considered, and then, Eq. (6.31) is simplified to

$$\rho c_p \left(2W_x(-1) \frac{d\theta}{d\eta} \left(\frac{1}{4} \right) \eta + 2W_y \frac{d\theta}{d\eta} \right) = \lambda \frac{d^2\theta}{d\eta^2} + \left(\frac{1}{4} \frac{1}{v_\infty^2} \right)^{1/2} \frac{d\lambda}{d\eta} \frac{d\theta}{d\eta} \left(\frac{1}{4} \frac{1}{v_\infty^2} \right)^{1/2}$$

or

$$\rho c_p \left(-2W_x \frac{d\theta}{d\eta} \left(\frac{1}{4} \right) \eta + 2W_y \frac{d\theta}{d\eta} \right) = \frac{1}{2v_\infty} \lambda \frac{d^2\theta}{d\eta^2} + \frac{1}{2v_\infty} \frac{d\lambda}{d\eta} \frac{d\theta}{d\eta}. \quad (6.32)$$

Equation is multiplied by $\frac{2v_\infty}{\lambda}$ and simplified into

$$\text{Pr} \frac{v_\infty}{\nu} (-\eta W_x + 4W_y) \frac{d\theta}{d\eta} = \frac{d^2\theta}{d\eta^2} + \frac{1}{\lambda} \frac{d\lambda}{d\eta} \frac{d\theta}{d\eta}. \quad (6.33)$$

The governing ordinary differential equations can be summarized as follows:

$$\left(2W_x - \eta \frac{dW_x}{d\eta} + 4 \frac{dW_y}{d\eta} \right) - \frac{1}{\rho} \frac{d\rho}{d\eta} (\eta W_x - 4W_y) = 0 \quad (6.18)$$

$$\frac{v_\infty}{\nu} \left[W_x \left(2W_x - \eta \frac{dW_x}{d\eta} \right) + 4W_y \frac{dW_y}{d\eta} \right] = \frac{d^2W_x}{d\eta^2} + \frac{1}{\mu} \frac{d\mu}{d\eta} \frac{dW_x}{d\eta} + \frac{v_\infty}{\nu} \theta \quad (6.25)$$

$$\text{Pr} \frac{v_\infty}{\nu} (-\eta W_x + 4W_y) \frac{d\theta}{d\eta} = \frac{d^2\theta}{d\eta^2} + \frac{1}{\lambda} \frac{d\lambda}{d\eta} \frac{d\theta}{d\eta} \quad (6.33)$$

With the assumed dimensionless variables the following dimensionless boundary conditions are easily obtained from Eqs. (6.4) and (6.5):

$$\eta = 0: W_x = 0, W_y = 0, \theta = 1 \quad (6.34)$$

$$\eta \rightarrow \infty: W_x \rightarrow 0, \theta \rightarrow 0. \quad (6.35)$$

6.4 Heat Transfer Analysis

The local heat transfer rate q_x at position x per unit area from the surface of the plate to the gas can be calculated by Fourier's law as

$$q_x = -\lambda_w \left(\frac{\partial T}{\partial y} \right)_{y=0}$$

with Eq. (5.28) we have

$$\left(\frac{\partial T}{\partial y} \right)_{y=0} = (T_w - T_\infty) \left(\frac{d\theta}{d\eta} \right) \left(\frac{1}{4} \text{Gr}_{x,\infty} \right)^{1/4} x^{-1}$$

Then,

$$q_x = -\lambda_w (T_w - T_\infty) \left(\frac{1}{4} \text{Gr}_{x,\infty} \right)^{1/4} x^{-1} \left(\frac{d\theta}{d\eta} \right)_{\eta=0}. \quad (6.36)$$

The local heat transfer coefficient α_x , defined as $q_x = \alpha_x (T_w - T_\infty)$, will be given by

$$\alpha_x = \lambda_w \left(\frac{1}{4} \text{Gr}_{x,\infty} \right)^{1/4} x^{-1} \left(-\frac{d\theta}{d\eta} \right)_{\eta=0}. \quad (6.37)$$

The local Nusselt number defined by $\text{Nu}_{x,w} = \frac{\alpha_x x}{\lambda_w}$ will be

$$\text{Nu}_{x,w} = \lambda_w \left(\frac{1}{4} \text{Gr}_{x,\infty} \right)^{1/4} x^{-1} \left(-\frac{d\theta}{d\eta} \right)_{\eta=0} \frac{x}{\lambda_w}$$

i.e.

$$\text{Nu}_{x,w} = \left(\frac{1}{4} \text{Gr}_{x,\infty} \right)^{1/4} \left(-\frac{d\theta}{d\eta} \right)_{\eta=0}. \quad (6.38)$$

Total heat transfer rate for position $x = 0$ to x with width of b on the plate is a integration $Q_x = \int \int_A q_x dA = \int_0^x q_x b dx$, and hence

$$Q_x = \lambda_w b (T_w - T_\infty) \left(-\frac{d\theta}{d\eta} \right)_{\eta=0} \int_0^x \left(\frac{1}{4} \text{Gr}_{x,\infty} \right)^{1/4} x^{-1} dx,$$

with Eq. (5.7) for definition of local Grashof number $\text{Gr}_{x,\infty}$ we obtain

$$Q_x = \frac{4}{3} b \lambda_w (T_w - T_\infty) \left(\frac{1}{4} \text{Gr}_{x,\infty} \right)^{1/4} \left(-\frac{d\theta}{d\eta} \right)_{\eta=0}. \quad (6.39)$$

The average heat transfer rate, defined as $\overline{Q}_x = Q_x/(b \times x)$ is given by

$$\overline{Q}_x = \frac{4}{3}x^{-1}\lambda_w(T_w - T_\infty) \left(\frac{1}{4}\text{Gr}_{x,\infty}\right)^{1/4} \left(-\frac{d\theta}{d\eta}\right)_{\eta=0}. \quad (6.40)$$

The average heat transfer coefficient $\overline{\alpha}_x$ defined as $\overline{Q}_x = \overline{\alpha}_x(T_w - T_\infty)$ is expressed as

$$\overline{\alpha}_x = \frac{4}{3}\lambda_w \left(\frac{1}{4}\text{Gr}_{x,\infty}\right)^{1/4} x^{-1} \left(-\frac{d\theta}{d\eta}\right)_{\eta=0}. \quad (6.41)$$

The average Nusselt number is defined as $\overline{\text{Nu}}_{x,w} = \frac{\overline{\alpha}_x x}{\lambda_w}$, and hence

$$\overline{\text{Nu}}_{x,w} = \frac{4}{3}\lambda_w \left(\frac{1}{4}\text{Gr}_{x,\infty}\right)^{1/4} x^{-1} \left(-\frac{d\theta}{d\eta}\right)_{\eta=0} \frac{x}{\lambda_w}$$

i.e.

$$\overline{\text{Nu}}_{x,w} = \frac{4}{3} \left(\frac{1}{4}\text{Gr}_{x,\infty}\right)^{1/4} \left(-\frac{d\theta}{d\eta}\right)_{\eta=0}. \quad (6.42)$$

It is seen that, for practical calculation of heat transfer, only wall dimensionless temperature gradient $\left(-\frac{d\theta}{d\eta}\right)_{\eta=0}$ dependent on numerical solution is no-given variable.

6.5 Numerical Results

6.5.1 Treatment of Variable Physical Properties

According to the temperature parameter of gases demonstrated in Chap. 5, the gas variable physical properties can be described by the following equations for laminar free convection:

$$\frac{\mu}{\mu_\infty} = \left(\frac{T}{T_\infty}\right)^{n_\mu} \quad (5.5)$$

$$\frac{\lambda}{\lambda_\infty} = \left(\frac{T}{T_\infty}\right)^{n_\lambda} \quad (5.6)$$

$$\frac{c_p}{c_{p_\infty}} = \left(\frac{T}{T_\infty}\right)^{n_{c_p}} \quad (5.7)$$

$$\frac{\rho}{\rho_\infty} = \left(\frac{T}{T_\infty}\right)^{-1} \quad (5.8)$$

where several values of the temperature parameter of monatomic and diatomic gases, and also for air and water vapor can be seen in Table 5.1.

It is seen that the temperature-dependent physical property factors $\frac{1}{\rho} \frac{d\rho}{d\eta}$, $\frac{1}{\mu} \frac{d\mu}{d\eta}$, $\frac{1}{\lambda} \frac{d\lambda}{d\eta}$, and $\frac{\nu_\infty}{\nu}$ are coupled in governing ordinary differential equations (6.18), (6.25), and (6.33). These factors tend to greatly increase the difficulty of getting a solution of the governing equations. However, with the provided gas temperature parameters, the physical property factors can be transformed into the functions of temperature θ . Then, the governing dimensionless equations can be solved. The transformation of these physical property factors is expressed as follows:

Transformation of the density factor $\left(\frac{1}{\rho} \frac{d\rho}{d\eta}\right)$:

With Eq. (5.8) we obtain

$$\frac{1}{\rho} \frac{d\rho}{d\eta} = \frac{1}{\rho} \frac{d}{d\eta} \left(\rho_\infty \frac{T_\infty}{T} \right).$$

By using Eq. (6.8) we have

$$T = (T_w - T_\infty)\theta + T_\infty$$

Then,

$$\begin{aligned} \frac{1}{\rho} \frac{d\rho}{d\eta} &= \frac{\rho_\infty}{\rho} \frac{d}{d\eta} \left[\frac{T_\infty}{(T_w - T_\infty)\theta + T_\infty} \right] \\ &= \frac{T}{T_\infty} \frac{d}{d\eta} \left[\frac{1}{(T_w/T_\infty - 1)\theta + 1} \right] \\ &= -[(T_w/T_\infty - 1)\theta + 1] \frac{(T_w/T_\infty - 1) \frac{d\theta}{d\eta}}{[(T_w/T_\infty - 1)\theta + 1]^2} \end{aligned}$$

i.e. the density factor is expressed as

$$\frac{1}{\rho} \frac{d\rho}{d\eta} = -\frac{(T_w/T_\infty - 1) \frac{d\theta}{d\eta}}{(T_w/T_\infty - 1)\theta + 1}. \quad (6.43)$$

Transformation of the viscosity factor $\left(\frac{1}{\mu} \frac{d\mu}{d\eta}\right)$:

With Eq. (5.5) we get

$$\begin{aligned} \frac{1}{\mu} \frac{d\mu}{d\eta} &= \frac{\mu_\infty}{\mu} \frac{d}{d\eta} \left(\frac{T}{T_\infty} \right)^{n_\mu} \\ &= \left(\frac{T}{T_\infty} \right)^{-n_\mu} \frac{d}{d\eta} \left[\frac{(T_w - T_\infty)\theta + T_\infty}{T_\infty} \right]^{n_\mu} \end{aligned}$$

$$\begin{aligned}
&= ((T_w/T_\infty - 1)\theta + 1)^{-n_\mu} \frac{d}{d\eta} ((T_w/T_\infty - 1)\theta + 1)^{n_\mu} \\
&= ((T_w/T_\infty - 1)\theta + 1)^{-n_\mu} n_\mu ((T_w/T_\infty - 1)\theta + 1)^{n_\mu - 1} (T_w/T_\infty - 1) \frac{d\theta}{d\eta}.
\end{aligned}$$

Then, the viscosity factor is described as

$$\frac{1}{\mu} \frac{d\mu}{d\eta} = \frac{n_\mu (T_w/T_\infty - 1) d\theta/d\eta}{(T_w/T_\infty - 1)\theta + 1}. \quad (6.44)$$

Transformation of the thermal conductivity factor $\left(\frac{1}{\lambda} \frac{d\lambda}{d\eta}\right)$

With a derivation similar to that for the factor $\left(\frac{1}{\mu} \frac{d\mu}{d\eta}\right)$ we can obtain the following equation for description of the *thermal conductivity factor*:

$$\frac{1}{\lambda} \frac{d\lambda}{d\eta} = \frac{n_\lambda (T_w/T_\infty - 1) d\theta/d\eta}{(T_w/T_\infty - 1)\theta + 1}. \quad (6.45)$$

Transformation of factor $\left(\frac{v_\infty}{v}\right)$

By using Eqs. (5.5) and (5.8), we have

$$\frac{v_\infty}{v} = [(T_w/T_\infty - 1)\theta + 1]^{-(n_\mu + 1)}. \quad (6.46)$$

6.5.2 Numerical Results

It is obvious that the velocity and temperature fields can be obtained from the solution of the governing ordinary differential equations (6.18), (6.25) and (6.33) with boundary conditions, Eqs. (6.34) and (6.35), combined with the property factor Eqs. (5.13)–(5.15), and (5.17). It is expected that, for the case of constant properties, the dimensionless velocity field w_x and dimensionless temperature field θ will be functions of Pr only. But for the case of variable properties, both the dimensionless velocity field and the dimensionless temperature field will depend not only on Pr but also on the temperature parameters n_μ and n_λ , and the boundary temperature ratio T_w/T_∞ .

The nonlinear two-point boundary value problem defined by Eqs. (6.18), (6.25), and (6.33) were solved, and calculations were carried out numerically by using a shooting method. First, Eqs. (6.18), (6.25), and (6.33) were written as a system of five first-order differential equations, which were solved by means of fifth-order Runge-Kuta iteration iteration.

The Runge–Kutta integration scheme, along with Newton–Raphson shooting method is one of the most commonly used techniques for the solution of such two-point boundary value problem. Although this method provides satisfactory result for such type of problems, it may fail when applied to problems in which the differential equations are very sensitive to the choice of the missing initial conditions.

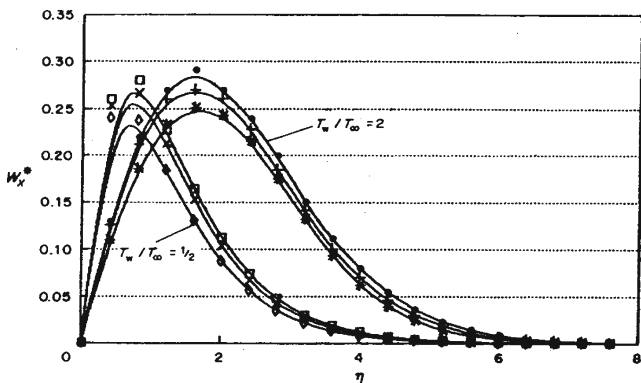


Fig. 6.2 Comparison of velocity profiles for free convection of different gases, cited from Shang and Wang [6] ●—●, □—□, Ar ($Pr = 0.622, n_\lambda \approx n_\mu \approx n_{\mu\lambda}$), +—+, ×—×, O_2 ($Pr = 0.733, n_{\mu\lambda} = 0.79$), *—*, ◇—◇, Water vapour ($Pr = 1, n_{\mu\lambda} = 1.12$)

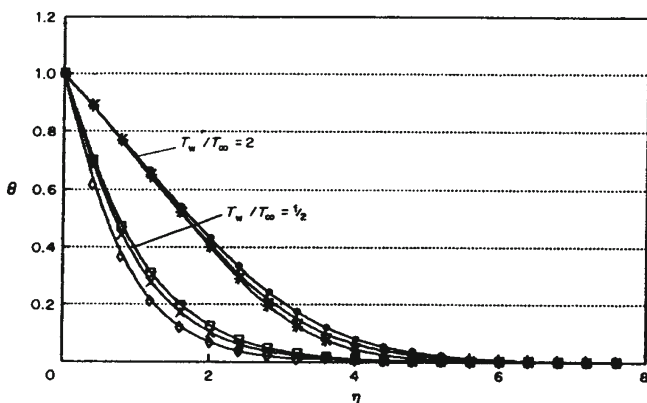


Fig. 6.3 Comparison of temperature profiles for free convection of different gases, cited from Shang and Wang [6] ●—●, □—□, Ar ($Pr = 0.622, n_\lambda \approx n_\mu \approx n_{\mu\lambda}$), +—+, ×—×, O_2 ($Pr = 0.733, n_{\mu\lambda} = 0.79$), *—*, ◇—◇, Water vapour ($Pr = 1, n_{\mu\lambda} = 1.12$)

Moreover, another serious difficulty which may be encountered in the boundary-value problems is in linear instability. Difficulty also arises in the case in which one end of the range of integration is at infinity. The end-point of integration is usually approximated by assigning a finite value to this point, and by estimating a value at this point the solution will reach its asymptotic state. The computing time for integrating differential equations sometimes depends critically on the quality of the initial guesses of the unknown boundary conditions and the initial end-point.

Then, a Newton iteration procedure was employed to satisfy the outer boundary equations. The present fifth-order scheme utilizes variable grid spacing. The typical results for the velocity and temperature field together with different boundary temperature ratios T_w/T_∞ are plotted in Figs. 6.2, 6.3, 6.4, and 6.5 for compari-

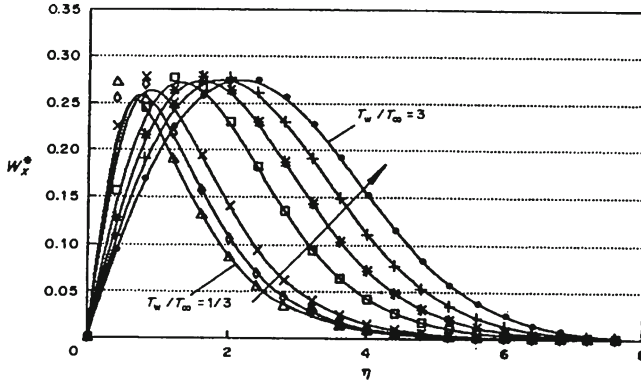


Fig. 6.4 Comparison of velocity profiles for free convection of air ($Pr = 0.7, n_{\mu\lambda} = 0.79$) with different T_w/T_∞ , cited from Shang and Wang [6]

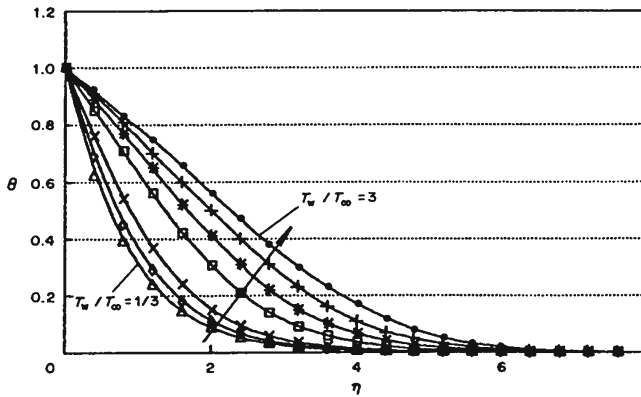


Fig. 6.5 Comparison of temperature profiles for free convection of air ($Pr = 0.7, n_{\mu\lambda} = 0.79$) with different temperature ratio T_w/T_∞ , cited from Shang and Wang [6]

son of velocity and temperature profiles with different gases and different boundary temperature ratios T_w/T_∞ , respectively.

It is found that both the *velocity and temperature fields* of argon laminar free convection are higher than those of oxygen laminar free convection, while, both the velocity fields of oxygen free convection are higher than those of water vapor laminar free convection. It follows that with increasing the temperature parameters n_μ and n_∞ the level both of the velocity and temperature fields of free convection will decrease.

Additionally, it is seen that with increasing the boundary temperature ratio T_w/T_∞ , the temperature field will raise and the maximum of velocity field will increase and shift far from the plate.

Furthermore, from the numerical calculations it is found that, even for the diatomic gases, air and water vapor, the modifications using n_μ and n_λ by $n_{\mu\lambda}$ are unnecessary, because the numerical results obtained either with the actual n_μ and n_λ values or with the modified $n_{\mu\lambda}$ values are almost the same.

6.6 Wall Dimensionless Temperature Gradient

From the heat transfer analysis we find that the wall dimensionless temperature gradient $\left(\frac{d\theta}{d\eta}\right)_{\eta=0}$ is only one variable which depends on numerical solution for prediction of heat transfer coefficient.

The numerical solution $\left(\frac{d\theta}{d\eta}\right)_{\eta=0}$ of the governing equations (6.18), (6.25) and (6.33) for some monatomic and diatomic gases, air and water vapor are obtained. Some solutions $\left(\frac{d\theta}{d\eta}\right)_{\eta=0}$ are listed in Table 6.1 and plotted in Fig. 6.6 for laminar free convection of different gases. By using curve-fitting method, Shang and Wang [7] obtained the following formulated equations for simple and reliable prediction of the

Table 6.1 Calculated results of $\left(-\frac{d\theta}{d\eta}\right)_{\eta=0}$

T_w/T_∞		Ar	H ₂	Air	N ₂	CO	O ₂	Water vapor
		Pr = 0.622	Pr = 0.68	Pr = 0.7	Pr = 0.71	Pr = 0.72	Pr = 0.733	Pr = 1
		$n_\mu = 0.72$	$n_\mu = 0.68$	$n_\mu = 0.68$	$n_\mu = 0.67$	$n_\mu = 0.71$	$n_\mu = 0.694$	$n_\mu = 1.04$
		$n_\lambda = 0.73$	$n_\lambda = 0.8$	$n_\lambda = 0.81$	$n_\lambda = 0.76$	$n_\lambda = 0.83$	$n_\lambda = 0.86$	$n_\lambda = 1.185$
3	A	0.1940	0.1974	0.1987	0.2043	0.1973	0.1973	0.1738
	B	0.1935	0.1975	0.1988	0.2044	0.1975	0.1975	0.1738
5/2	A	0.2256	0.2300	0.2316	0.2374	0.2306	0.2307	0.2110
	B	0.2249	0.2300	0.2318	0.2374	0.2308	0.2311	0.2115
2	A	0.2714	0.2772	0.2794	0.2852	0.2792	0.2796	0.2679
	B	0.2703	0.2772	0.2796	0.2850	0.2794	0.2801	0.2689
3/2	A	0.3438	0.3526	0.3557	0.3609	0.3570	0.3582	0.3651
	B	0.3427	0.3527	0.3561	0.3609	0.3575	0.3590	0.3665
5/4	A	0.3990	0.4105	0.4144	0.4188	0.4172	0.4193	0.4448
	B	0.3983	0.4109	0.4151	0.4191	0.4179	0.4201	0.4459
→ 1	A	0.4784	0.4943	0.4995	0.5021	0.5046	0.5079	0.5671
	B	0.4787	0.4953	0.5007	0.5033	0.5059	0.5092	0.5670
3/4	A	0.6035	0.6276	0.6351	0.6336	0.6446	0.6507	0.7775
	B	0.6011	0.6247	0.6333	0.6312	0.6423	0.6479	0.7761
1/2	A	0.8344	0.8774	0.8898	0.8776	0.9093	0.9225	1.2181
	B	0.8285	0.8666	0.8786	0.8684	0.8993	0.9098	1.2081
1/3	A	1.1492	1.2247	1.2448	1.2124	1.2812	1.3075	1.9198
	B	1.1419	1.2022	1.2209	1.1949	1.2591	1.2774	1.8805

Note A. numerical solution, B. evaluated by Eq. (6.47) with Eqs. (6.48)–(6.50), cited from Shang and Wang [6]

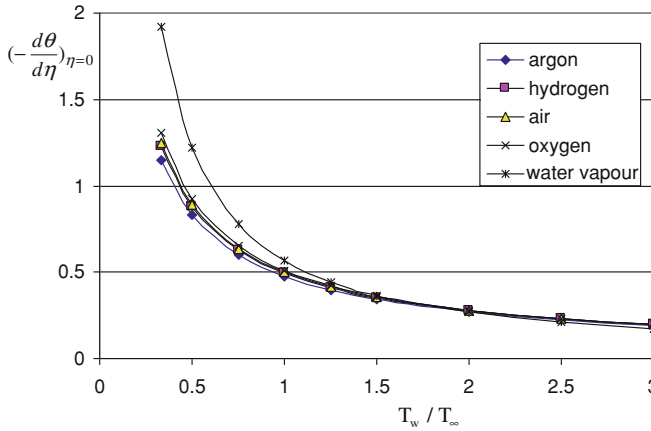


Fig. 6.6 Numerical solutions of temperature gradient $\left(-\frac{d\theta}{d\eta}\right)_{\eta=0}$ for laminar free convection of argon, hydrogen, air, oxygen and water vapour

values $\left(\frac{d\theta}{d\eta}\right)_{\eta=0}$ for laminar free convection of monatomic and diatomic gases, air, and water vapor:

$$\left(-\frac{d\theta}{d\eta}\right)_{\eta=0} = \psi(\text{Pr}) \left(\frac{T_w}{T_\infty}\right)^{-m} \tag{6.47}$$

where

$$\psi(\text{Pr}) = 0.567 + 0.186 \times \ln(\text{Pr}) \quad (0.6 \leq \text{Pr} \leq 1) \tag{6.48}$$

$$m = 0.35n_\lambda + 0.29n_\mu + 0.36 \quad (T_w/T_\infty > 1) \tag{6.49}$$

$$m = 0.42n_\lambda + 0.34n_\mu + 0.24 \quad (T_w/T_\infty < 1). \tag{6.50}$$

The predicted results $\left(-\frac{d\theta}{d\eta}\right)_{\eta=0}$ of Eqs. (6.47) with (6.48) to (6.50) are compared with those of the numerical results shown in Table 6.1. The agreement is quite good.

6.7 Practical Prediction Equations on Heat Transfer

By using Eq. (6.47) with Eqs. (6.48)–(6.50), Eqs. (6.36)–(6.42) are available for prediction of heat transfer on laminar gas free convection on vertical flat plate with consideration of coupled effect of variable physical properties, for example:

The local heat transfer rate q_x at position x per unit area from the surface of the plate to the gas is expressed as

$$q_x = \lambda_w(T_w - T_\infty) \left(\frac{1}{4} \text{Gr}_{x,\infty} \right)^{1/4} x^{-1} \psi(\text{Pr}) \left(\frac{T_w}{T_\infty} \right)^{-m}. \quad (6.36^*)$$

The local Nusselt number defined by $\text{Nu}_{x,w} = \frac{\alpha_{x,w}}{\lambda_w}$ will be

$$\text{Nu}_{x,w} = \left(\frac{1}{4} \text{Gr}_{x,\infty} \right)^{1/4} \psi(\text{Pr}) \left(\frac{T_w}{T_\infty} \right)^{-m}. \quad (6.38^*)$$

Total heat transfer rate for position $x = 0$ to x with width of b on the plate will be

$$Q_x = \frac{4}{3} b \lambda_w (T_w - T_\infty) \left(\frac{1}{4} \text{Gr}_{x,\infty} \right)^{1/4} \psi(\text{Pr}) \left(\frac{T_w}{T_\infty} \right)^{-m}. \quad (6.39^*)$$

The average Nusselt number is defined as $\overline{\text{Nu}}_{x,w} = \frac{\overline{\alpha_{x,w}}}{\lambda_w}$, will be

$$\overline{\text{Nu}}_{x,w} = \frac{4}{3} \left(\frac{1}{4} \text{Gr}_{x,\infty} \right)^{1/4} \psi(\text{Pr}) \left(\frac{T_w}{T_\infty} \right)^{-m}, \quad (6.42^*)$$

where

$$\psi(\text{Pr}) = 0.567 + 0.186 \times \ln(\text{Pr}) \quad (0.6 \leq \text{Pr} \leq 1) \quad (6.48)$$

$$m = 0.35n_\lambda + 0.29n_\mu + 0.36 \quad (T_w/T_\infty > 1) \quad (6.49)$$

$$m = 0.42n_\lambda + 0.34n_\mu + 0.24 \quad (T_w/T_\infty < 1). \quad (6.50)$$

It is indicated that Eqs. (6.36*)–(6.42*) will be reliable for prediction of heat transfer on laminar free convection on a vertical flat plate with consideration of coupled effect of variable physical properties. It is reason that these prediction equations come from the theoretical equations on heat transfer coupled with the formulated equation of the solution of governing equations (6.1)–(6.5), the wall dimensionless temperature gradient $\left(-\frac{d\theta}{d\eta} \right)_{\eta=0}$. While, Eqs. (6.1)–(6.5) as well as (6.43)–(6.46) have well simulated the practical laminar free convection by means of the rigorous consideration and treatment of variable physical properties.

6.8 Effect of Variable Physical Properties on Heat Transfer

From the theoretical equations (6.36*)–(6.42*), it is seen that effect of variable physical properties on heat transfer is dominated by the factor $\psi(\text{Pr}) \left(\frac{T_w}{T_\infty} \right)^{-m}$, which demonstrates the effect of Prandtl number Pr , boundary temperature ratio $\frac{T_w}{T_\infty}$ and temperature parameters of gas. If we change the factor to $\psi(\text{Pr}) \left(\frac{T_w}{T_\infty} \right)^{-m} =$

Table 6.2 Effects of $Pr, n_\mu, n_\lambda,$ and T_w/T_∞ on heat transfer of laminar free convection of monatomic and diatomic gases, air, and water vapor

Term	Heat transfer	
	for $T_w/T_\infty > 1$	for $T_w/T_\infty < 1$
For effect of Pr	Heat transfer increases with increase of Pr	
For effect of T_w/T_∞	Heat transfer increases with increase of T_w/T_∞	
For effect of Temperature parameter n_μ or n_λ	Heat transfer decreases with increase of $T_w/T_\infty, n_\mu$ or n_λ	

$\psi(Pr) \left(\frac{T_\infty}{T_w}\right)^m$, we can easily see that with increasing the Prandtl number Pr or boundary temperature ratio T_w/T_∞ , heat transfer will increase. However, for $T_w/T_\infty > 1$, heat transfer will decrease with increasing the temperature parameters of gas. While, for $T_w/T_\infty < 1$ heat transfer will increase with increasing the temperature parameters of gas.

The numerical solutions on temperature gradient $-\left(\frac{d\theta}{d\eta}\right)_{\eta=0}$ can be briefly summarized in Table 6.1 for laminar free convection of monatomic and diatomic gases, air, and water vapor, with effect of $Pr, n_\mu, n_\lambda,$ and T_w/T_∞ (Table 6.2).

6.9 Heat Transfer Under Boussinesq Approximation

Obviously, when boundary temperature ratio T_w/T_∞ is very close to unity, i.e., $T_w/T_\infty \rightarrow 1$, the free convection is corresponding to Boussinesq approximation. In this case, the effect of variable physical properties will not need to be considered, and then the temperature gradient $\left(-\frac{d\theta}{d\eta}\right)_{\eta=0}$ only depends on Pr , i.e.,

$$\left(-\frac{d\theta}{d\eta}\right)_{\eta=0} = \psi(Pr) = 0.567 + 0.186 \times \ln(Pr) \quad (0.6 \leq Pr \leq 1) \quad (6.51)$$

where $\psi(Pr)$ expresses the well-known Boussinesq solution.

With Eqs.(6.51), (6.36)–(6.42) become the equations on heat transfer under Boussinesq approximation, for example:

$$q_x = \lambda_w(T_w - T_\infty) \left(\frac{1}{4}Gr_{x,\infty}\right)^{1/4} x^{-1} \psi(Pr) \quad (6.36^{**})$$

$$Nu_{x,w} = \left(\frac{1}{4}Gr_{x,\infty}\right)^{1/4} \psi(Pr) \quad (6.38^{**})$$

6.10 Summary

So far, the governing equations for laminar free convection of monatomic and diatomic gases, air, and water vapor and expressions related to heat transfer can be summarized in Table 6.3 with consideration of variable physical properties.

6.11 Remarks

In this chapter, a novel system of analysis and transformation models is introduced by using the new similarity analysis method to transform the governing partial differential equations of laminar free convection. With the new similarity analysis method, the velocity components are directly transformed into the corresponding dimensionless velocity components, so that it is not necessary to induce the flow function as well as the intermediate function variable with Falkner-Skan transformation. In addition, with the new analysis and transformation models based on the new similarity analysis method, a convenience is provided to treat the variable physical properties for free convection and film flows.

The temperature parameter method is used for treatment of variable physical properties of gases. With this method the physical property factors coupled with the governing ordinary differential equations are transformed to the functions with the dimensionless temperature and the related temperature parameters for convenient simultaneous solution.

It is seen from the calculated results that there are obvious effects of variable physical properties on velocity and temperature fields, as well as heat transfer of free convection of gases, and such effects depend on the boundary temperature ratio T_w/T_∞ , the temperature parameter n_μ and n_λ as well as the Prandtl number of gases. The prediction equations on gas free convection heat transfer are created based on the heat transfer analysis and the related numerical solutions. It is found that the gas temperature parameters, Prandtl number, and boundary temperature ratio dominate the heat transfer of gas laminar free convection. Since the temperature parameters are based on the experimental data, such prediction equations of gas free convection heat transfer are reliable, and have practical application value.

6.12 Calculation Examples

Question:

A flat plate with $b = 2$ m in width and $x = 0.25$ m in length is suspended vertically in air. The ambient temperature is $t_\infty = 20^\circ\text{C}$. Calculate the free convection heat transfer of the plate for boundary temperature ratio $T_w/T_\infty = 1.1, 1.2, 1.4, 1.7$ and 2.1 .

Table 6.3 Governing equations for laminar free convection of monatomic and diatomic gases, air and water vapor and expressions related to heat transfer

Term	Expression
<i>Governing partial differential equations</i>	
Mass equation	$\frac{\partial}{\partial x} (\rho w_x) + \frac{\partial}{\partial y} (\rho w_y) = 0$
Momentum equation	$\rho \left(w_x \frac{\partial w_x}{\partial x} + w_y \frac{\partial w_x}{\partial y} \right) = \frac{\partial}{\partial y} \left(\mu \frac{\partial w_x}{\partial y} \right) + \rho g \frac{T - T_\infty}{T_\infty}$
Energy equation	$\rho c_p \left(w_x \frac{\partial T}{\partial x} + w_y \frac{\partial T}{\partial y} \right) = \frac{\partial}{\partial y} \left(\lambda \frac{\partial T}{\partial y} \right)$
Boundary conditions	$y = 0: w_x = 0, w_y = 0, T = T_w$ $y \rightarrow \infty: w_x \rightarrow 0, T = T_\infty$
<i>Assumed similarity variables</i>	
η	$\frac{y}{x} \left(\frac{1}{4} Gr_{x,\infty} \right)^{1/4}$
$Gr_{x,\infty}$	$(Gr_{x,\infty})_v = \frac{g T_w - T_\infty x^3}{\nu_\infty^2}$
θ	$\theta = \frac{T - T_\infty}{T_w - T_\infty}$
W_x	$(2\sqrt{g\bar{x}} T_w - T_\infty - 1)^{1/2} w_x$
W_y	$(2\sqrt{g\bar{x}} T_w - T_\infty - 1)^{1/2} \left(\frac{1}{4} Gr_{x,\infty} \right)^{-1/4} w_y$
<i>Governing ordinary differential equations</i>	
Mass equations	$2W_x - \eta \frac{dW_x}{d\eta} + 4 \frac{dW_y}{d\eta} - \frac{1}{\rho} \frac{d\rho}{d\eta} (\eta W_x - 4W_y) = 0$
Momentum Equation	$\frac{\nu_\infty}{\nu} \left(W_x \left(2W_x - \eta \frac{dW_x}{d\eta} \right) + 4W_y \frac{dW_x}{d\eta} \right) = \frac{d^2 W_x}{d\eta^2} + \frac{1}{\mu} \frac{d\mu}{d\eta} \frac{dW_x}{d\eta} + \frac{\nu_\infty}{\nu} \theta$
Energy equation	$Pr \frac{\nu_\infty}{\nu} (-\eta W_x + 4W_y) \frac{d\theta}{d\eta} = \frac{1}{\lambda} \frac{d\lambda}{d\eta} \frac{d\theta}{d\eta} + \frac{d^2 \theta}{d\eta^2}$
Boundary conditions	$\eta = 0: W_x = 0, W_y = 0, \theta = 1;$ $\eta \rightarrow \infty: W_x = 0, \theta = 0$
<i>Boussinesq solution</i>	
$\left(-\frac{d\theta}{d\eta} \right)_{\eta=0} = \psi(Pr) = 0.567 + 0.186 \times \ln(Pr) \quad (0.6 \leq Pr \leq 1)$	
<i>Heat transfer under Boussinesq approximation</i>	
Local heat transfer rate	$q_x = \lambda_w (T_w - T_\infty) \left(\frac{1}{4} Gr_{x,\infty} \right)^{1/4} x^{-1} \psi(Pr)$
Local heat transfer coefficient defined by $Nu_{x,w} = \frac{\alpha_{x,w}}{\lambda_w}$	$\alpha_x = \lambda_w \left(\frac{1}{4} Gr_{x,\infty} \right)^{1/4} x^{-1} \psi(Pr)$
Local Nusselt number defined by $Nu_{x,w} = \frac{\alpha_{x,w}}{\lambda_w}$	$Nu_{x,w} = \left(\frac{1}{4} Gr_{x,\infty} \right)^{1/4} \psi(Pr)$
Total heat transfer rate $Q_x = \int \int_A q_x dA = \int_0^x q_x b dx$	$Q_x = \frac{4}{3} b \lambda_w (T_w - T_\infty) \left(\frac{1}{4} Gr_{x,\infty} \right)^{1/4} \psi(Pr)$

(continued)

Table 6.3 (continued)

Average heat transfer coefficient $\bar{\alpha}_x$ defined as $\bar{Q}_x = \bar{\alpha}_x(T_w - T_\infty)$	$\bar{\alpha}_x = \frac{4}{3}\lambda_w \left(\frac{1}{4}\text{Gr}_{x,\infty}\right)^{1/4} x^{-1}\psi(\text{Pr})$
Average Nusselt number is defined as $\bar{\text{Nu}}_{x,w} = \frac{\bar{\alpha}_x x}{\lambda_w}$	$\bar{\text{Nu}}_{x,w} = \frac{4}{3} \left(\frac{1}{4}\text{Gr}_{x,\infty}\right)^{1/4} \psi(\text{Pr})$
Wall dimensionless temperature gradient $\left(-\frac{d\theta}{d\eta}\right)_{\eta=0} = \psi(\text{Pr}) \left(\frac{T_w}{T_\infty}\right)^{-m}$	$(0.6 \leq \text{Pr} \leq 1)$
where $\psi(\text{Pr}) = 0.567 + 0.186 \times \ln(\text{Pr})$ $m = 0.35n_\lambda + 0.29n_\mu + 0.36$ $(T_w/T_\infty > 1)$ $m = 0.42n_\lambda + 0.34n_\mu + 0.24$ $(T_w/T_\infty < 1)$	
<i>Heat transfer for consideration of coupled effect of variable physical properties variable</i>	
Local heat transfer rate	$q_x = \lambda_w(T_w - T_\infty) \left(\frac{1}{4}\text{Gr}_{x,\infty}\right)^{1/4} x^{-1}\psi(\text{Pr}) \left(\frac{T_w}{T_\infty}\right)^{-m}$
Local heat transfer coefficient defined by $\text{Nu}_{x,w} = \frac{\alpha_x x}{\lambda_w}$	$\alpha_x = \lambda_w \left(\frac{1}{4}\text{Gr}_{x,\infty}\right)^{1/4} x^{-1}\psi(\text{Pr}) \left(\frac{T_w}{T_\infty}\right)^{-m}$
Local Nusselt number defined by $\text{Nu}_{x,w} = \frac{\alpha_x x}{\lambda_w}$	$\text{Nu}_{x,w} = \left(\frac{1}{4}\text{Gr}_{x,\infty}\right)^{1/4} \psi(\text{Pr}) \left(\frac{T_w}{T_\infty}\right)^{-m}$
Total heat transfer rate $Q = \int \int_A q_x dA = \int_0^x q_x b dx$	$Q_x = \frac{4}{3}b\lambda_w(T_w - T_\infty) \left(\frac{1}{4}\text{Gr}_{x,\infty}\right)^{1/4} \psi(\text{Pr}) \left(\frac{T_w}{T_\infty}\right)^{-m}$
Average heat transfer rate, defined as $\bar{Q}_x = Q_x/(b \times x)$	$\bar{Q}_x = \frac{4}{3}x^{-1}\lambda_w(T_w - T_\infty) \left(\frac{1}{4}\text{Gr}_{x,\infty}\right)^{1/4} \psi(\text{Pr}) \left(\frac{T_w}{T_\infty}\right)^{-m}$
Average heat transfer coefficient $\bar{\alpha}_x$ defined as $\bar{Q}_x = \bar{\alpha}_x(T_w - T_\infty)$	$\bar{\alpha}_x = \frac{4}{3}\lambda_w \left(\frac{1}{4}\text{Gr}_{x,\infty}\right)^{1/4} x^{-1}\psi(\text{Pr}) \left(\frac{T_w}{T_\infty}\right)^{-m}$
Average Nusselt number is defined as $\bar{\text{Nu}}_{x,w} = \frac{\bar{\alpha}_x x}{\lambda_w}$	$\bar{\text{Nu}}_{x,w} = \frac{4}{3} \left(\frac{1}{4}\text{Gr}_{x,\infty}\right)^{1/4} \psi(\text{Pr}) \left(\frac{T_w}{T_\infty}\right)^{-m}$

Solution:

From $t_\infty = 20^\circ\text{C}$ and $T_w/T_\infty = 1.1, 1.2, 1.4, 1.7, 2.1$, we obtain $T_w = 322.3, 351.6, 410.2, 498.1, 615.3\text{K}$ or $t_w = 49.3, 78.6, 137.2, 225.1, 342.3^\circ\text{C}$. The air physical properties are as follows:

$\nu_\infty = 15.06 \times 10^{-6}\text{m}^2/\text{s}$ for air $t_\infty = 20^\circ\text{C}$; $\lambda_w = 2.825 \times 10^{-2}, 3.037 \times 10^{-2}, 3.4675 \times 10^{-2}, 4.1007 \times 10^{-2}$ and $4.8622 \times 10^{-2}\text{W}/(\text{m}^\circ\text{C})$ for air at $t_w = 49.3, 78.6, 137.2, 225.1$ and 342.3°C respectively. From Tables 6.1 and 6.3, we obtain $n_\mu = 0.68, n_\lambda = 0.81$ and $\text{Pr} = 0.7$ for air.

Then,

$$\psi(\text{Pr}) = 0.567 + 0.186 \times \ln 0.7 = 0.50066$$

m is evaluated as below with T_w/T_∞

Table 6.4 Calculated results

T_w/T_∞	1.1	1.2	1.4	1.7	2.1
t_w (°C)	49.3	78.6	137.2	225.1	342.3
t_∞ (°C)	20	20	20	20	20
λ_w [W/(m°C)]	2.825×10^{-2}	3.037×10^{-2}	3.4675×10^{-2}	4.1007×10^{-2}	4.8622×10^{-2}
$-\left(\frac{d\theta}{d\eta}\right)_{\eta=0}$	0.4621	0.4295	0.3773	0.3205	0.2683
$Gr_{x,\infty}$	6.75×10^7	1.35×10^8	2.7×10^8	4.73×10^8	7.43×10^8
$\overline{Nu}_{x,w}$	39.4927	43.652	45.602	44.550	41.761
$\overline{\alpha}_x$ [W/(m ² K)]	4.46237	5.3026	6.3247	7.3074	8.1218
Q (W)	65.3782	154.37	370.63	749.38	1308.83

$$\begin{aligned}
 m &= 0.35n_\lambda + 0.29n_\mu + 0.36 \\
 &= 0.35 \times 0.81 + 0.29 \times 0.68 + 0.36 = 0.8407.
 \end{aligned}$$

In this case, the dimensionless temperature gradient $\left(-\frac{d\theta}{d\eta}\right)_{\eta=0}$ can be evaluated as

$$\begin{aligned}
 \left(-\frac{d\theta}{d\eta}\right)_{\eta=0} &= \psi(\text{Pr}) \left(\frac{T_w}{T_\infty}\right)^{-m} \\
 &= 0.50066 \times \left(\frac{T_w}{T_\infty}\right)^{-0.8407}.
 \end{aligned}$$

The evaluated values of $\left(-\frac{d\theta}{d\eta}\right)_{\eta=0}$ are plotted in Table 6.4 for different temperature ratios.

Also

$$\begin{aligned}
 Gr_{x,\infty} &= \frac{g \left| T_w/T_\infty - 1 \right| x^3}{\nu_\infty^2} \\
 &= \frac{9.8 \times |T_w/T_\infty - 1| \times 0.25^3}{(15.06 \times 10^{-6})^2}
 \end{aligned}$$

The calculated values of $Gr_{x,\infty}$ are plotted in Table 6.4.

With Eq. (4.53) the average Nusselt number can expressed as

$$\overline{Nu}_{x,w} = -\frac{4}{3} \left(\frac{1}{4} Gr_{x,\infty}\right)^{1/4} \left(\frac{d\theta}{d\eta}\right)_{\eta=0}$$

Then, the average Nusselt number $\overline{Nu}_{x,w}$ are evaluated with the calculated values of $Gr_{x,\infty}$ and $\left(-\frac{d\theta}{d\eta}\right)_{\eta=0}$ and then, plotted in Table 6.4.

From the definition of the average Nusselt number $\overline{\text{Nu}}_{x,w} = \frac{\overline{\alpha_x} x}{\lambda_w}$, the average heat transfer coefficient can be calculated as

$$\overline{\alpha_x} = \frac{\lambda_w}{x} \overline{\text{Nu}}_{x,w} = \frac{\lambda_w}{0.25} \overline{\text{Nu}}_{x,w}$$

The average heat transfer coefficient $\overline{\alpha_x}$ are calculated with the related $\overline{\text{Nu}}_{x,w}$ and λ_w , and plotted in Table 6.4 also.

Finally, heat transfer Q_x is calculated as

$$Q_x = \overline{\alpha_x} (t_w - t_\infty) x \times b = \overline{\alpha_x} (t_w - t_\infty) \times 0.25 \times 2$$

The values of Q_x is calculated with the related values of $\overline{\alpha_x}$ and $t_w - t_\infty$, and plotted in Table 6.4.

6.13 Exercises

1. From this chapter, tell me the importance for consideration of variable physical properties on laminar free convection.
2. Please explain the necessity and importance of consideration of variable physical properties for deep investigation of laminar free convection.
3. Can you tell me if Eqs. (6.36*)–(6.42*) are qualified for reliable prediction of heat transfer of laminar free convection? Why?
4. Follow the question of calculation example, only change air to water vapour as the ambient gas, and keep other conditions, and calculate the average heat transfer coefficients and free convection heat transfer on the plate.
5. Please calculate the question of exercise 4 by using the related empirical equation.
6. Compare the calculated results in exercises 4 and 5, and tell me which calculated result is more reliable for practical application, why?
7. Do you think the treatment of variable physical properties in this chapter is reliable? Why?
8. Compare the governing similarity models (6.18), (6.25) and (6.33), to (3.25) and (3.26), respectively transformed by the new similarity analysis method and Falkner-Skan type transformation, please find out which model is more convenient for consideration of variable physical properties.

References

1. T. Hara, The free-convection flow about a heated vertical plate in air. *Trans. Jpn. Soc. Mech. Eng.* **20**, 517–520 (1954)
2. A.A. Tataev, Heat exchange in condition of free laminar movement of gas with Variable viscosity at a vertical wall. *Zh. Tekh. Fiz.* **26**, 2714–2719 (1956)

3. E.M. Sparrow, J.L. Gregg, The variable fluid-property problem in free convection. *Trans. ASME* **80**, 879–886 (1958)
4. D.D. Gray, A. Giogni, The validity of the Boussinesq approximation for liquids and gases. *Int. J. Heat Mass Transf.* **19**, 546–577 (1977)
5. A.M. Clausing, S.N. Kempka, The influences of property variations on natural convection from vertical surfaces. *J. Heat Transf.* **103**, 609–612 (1981)
6. D.Y. Shang, B.X. Wang, Effect of variable thermophysical properties on laminar free convection of gas. *Int. J. Heat Mass Transf.* **33**(7), 1387–1395 (1990)
7. D.Y. Shang, B.X. Wang, Effect of variable thermophysical properties on laminar free convection of polyatomic gas. *Int. J. Heat Mass Transf.* **34**(3), 749–755 (1991)
8. E.R.G. Eckert, R.M. Drake, *Analysis of Heat and Mass Transfer* (McGraw-Hill, New York, 1972)

Chapter 7

Heat Transfer of Laminar Free Convection of Polyatomic Gas

Abstract Based on the study of Chap. 6, the temperature-dependent specific heat is further considered for investigation of laminar free convection of polyatomic gases with consideration of variable physical properties. The viscosity, thermal conductivity, and specific heat parameters are provided for a series of polyatomic gases. The governing energy ordinary differential equation is further derived out for consideration of temperature-dependent specific heat, by using the new similarity analysis method. A system of numerical solutions are obtained for variation of the temperature parameters n_μ , n_λ , and n_{c_p} , Prandtl number, and the boundary temperature ratio. It is seen from the numerical results that there are obvious effects of variable physical properties on velocity and temperature fields, as well as heat transfer of free convection of polyatomic gases. The theoretical equations of heat transfer of polyatomic gas free convection created based on the heat transfer analysis contain a only one no-given variable, the wall temperature gradient. Based on the system of numerical solutions on the wall dimensionless temperature gradient, the prediction equation of the wall temperature gradient is created by means of a curve-fitting method, and then, the theoretical equations on heat transfer are available for prediction of heat transfer. It is found that the gas temperature parameters, Prandtl number, and the boundary temperature ratio dominate the heat transfer of laminar free convection of polyatomic gases. Because the temperature parameters are based on the typical experimental data, these equations on heat transfer are reliable for engineering prediction of laminar free convection of polyatomic gas.

7.1 Introduction

In Chap. 6, the new similarity analysis method and temperature parameter method were introduced for the similarity transformation of the governing partial differential equations of laminar free convection of monatomic and diatomic gases, air, and water vapor with consideration of variable physical properties. The temperature parameter method, density, thermal conductivity, and absolute viscosity of the

gases are assumed to vary with absolute temperature according to a simple power law. The temperature parameters of thermal conductivity and the absolute viscosity are proposed and the corresponding values are provided according to the typical experimental data of the corresponding physical properties. The density is taken as inversely proportional to absolute temperature at constant pressure, while the Prandtl number is assumed constant. Since the variation of specific heat for these gases with temperature is very small, it is taken as constant for the treatment of variable physical properties.

However, for polyatomic gases, the variation of specific heat is not so small, and then it cannot be taken as constant. In this Chapter I focus on the presentation of free convection of polyatomic gases along an isothermal vertical flat plate with large temperature difference [1]. For this purpose the governing equations for laminar free convection of gas are also transformed to dimensionless ordinary equations by the new similarity analysis method. For treatment of variable physical properties the temperature parameter method is used to further treat variation of specific heat with temperature. Not only the density, thermal conductivity, and dynamic viscosity but also the specific heat is assumed to vary with absolute temperature according to the simple power law. The temperature parameters n_λ , n_μ and n_{c_p} are further introduced and the corresponding values are proposed according to the typical experimental results for polyatomic gases. On this basis, heat transfer of laminar free convection of polyatomic gas will be further presented in this chapter for laminar free convection of polyatomic gases.

7.2 Variable Physical Properties of Polyatomic Gases

The effect of the variable physical properties on laminar free convection and heat transfer of monatomic and diatomic gases, air and water vapor along an isothermal vertical flat plate has been reported in Chap. 6. However, for the polyatomic gases the variation of specific heat with temperature is more obvious. For this reason, an additional equation for specific heat has to be added to the equations based on Chap. 6 in order to further considerate variable physical properties of polyatomic gases. Thus, for polyatomic gas, the equations of viscosity, thermal conductivity, density, and specific heat with temperature are described as follows:

$$\frac{\mu}{\mu_\infty} = \left(\frac{T}{T_\infty} \right)^{n_\mu} \quad (7.1)$$

$$\frac{\lambda}{\lambda_\infty} = \left(\frac{T}{T_\infty} \right)^{n_\lambda} \quad (7.2)$$

$$\frac{c_p}{c_{p_\infty}} = \left(\frac{T}{T_\infty} \right)^{n_{c_p}} \quad (7.3)$$

$$\frac{\rho}{\rho_\infty} = \left(\frac{T}{T_\infty} \right)^{-1} \quad (7.4)$$

$$c_p/c_{p_\infty} = (T/T_\infty)^{n_{cp}} \quad (7.5)$$

According to the summarized experimental values of μ , λ and c_p for several polyatomic gases reported in Refs. [2–5], the temperature parameters n_λ , n_μ and n_{c_p} and arising from the corresponding experimental data are listed in Table 5.2.

7.3 Governing Differential Equations and Their Similarity Transformation

The physical analytical model and co-ordinate system used for laminar free convection of monatomic and diatomic gases, as well as air and water vapor on an isothermal vertical flat plate is also shown in Fig. 6.1. Then, we can express the following governing partial differential equations for continuity, momentum, and energy conservations and their boundary conditions for laminar free convection of polyatomic gases along an isothermal vertical plate:

$$\frac{\partial}{\partial x}(\rho w_x) + \frac{\partial}{\partial y}(\rho w_y) = 0 \quad (7.6)$$

$$\rho \left(w_x \frac{\partial w_x}{\partial x} + w_y \frac{\partial w_x}{\partial y} \right) = \frac{\partial}{\partial y} \left(\mu \frac{\partial w_x}{\partial y} \right) + g\rho \left| \frac{T}{T_\infty} - 1 \right| \quad (7.7)$$

$$\rho \left(w_x \frac{\partial (c_p T)}{\partial x} + w_y \frac{\partial (c_p T)}{\partial y} \right) = \frac{\partial}{\partial y} \left(\lambda \frac{\partial T}{\partial y} \right) \quad (7.8)$$

$$y = 0: w_x = 0, \quad w_y = 0, \quad T = T_w \quad (7.9)$$

$$y \rightarrow \infty: w_x \rightarrow 0, \quad T = T_\infty \quad (7.10)$$

where the temperature-dependent specific heat of polyatomic gas is considered in the energy equation.

For similarity transformation of the governing Eqs. (7.6)–(7.8) we use the new similarity analysis method and assume the following dimensionless variables, which are same as those for laminar free convection of monatomic and diatomic gases, air, and water vapor in Chapter 6:

$$\eta = \frac{y}{x} \left(\frac{1}{4} \text{Gr}_{x,\infty} \right)^{1/4} \quad (7.11)$$

$$\text{Gr}_{x,\infty} = \frac{g |T_w/T_\infty - 1| x^3}{\nu_\infty^2} \quad (7.12)$$

$$\theta = \frac{T - T_\infty}{T_w - T_\infty} \quad (7.13)$$

$$W_x = \left[2\sqrt{gx} |T_w/T_\infty - 1|^{1/2} \right]^{-1} w_x \quad (7.14)$$

$$W_y = \left[2\sqrt{gx} |T_w/T_\infty - 1|^{1/2} \left(\frac{1}{4} \text{Gr}_{x,\infty} \right)^{-1/4} \right]^{-1} w_y \quad (7.15)$$

According to the derivation similar to that in Chap. 6, the corresponding governing dimensionless equations of Eqs. (7.6)–(7.7) should be

$$2W_x - \eta \frac{dW_x}{d\eta} + 4 \frac{dW_y}{d\eta} - \frac{1}{\rho} \frac{d\rho}{d\eta} (\eta W_x - 4W_y) = 0 \quad (7.16)$$

$$\frac{\nu_\infty}{\nu} \left(W_x \left(2W_x - \eta \frac{dW_x}{d\eta} \right) + 4W_y \frac{dW_x}{d\eta} \right) = \frac{d^2 W_x}{d\eta^2} + \frac{1}{\mu} \frac{d\mu}{d\eta} \frac{dW_x}{d\eta} + \frac{\nu_\infty}{\nu} \theta \quad (7.17)$$

However, because the variation of specific heat of the polyatomic gases with temperature must be considered, the similarity transformation for Eq. (7.8) should be done.

At first, Eq. (7.8) can be further expressed as

$$\rho c_p \left(w_x \frac{\partial T}{\partial x} + w_y \frac{\partial T}{\partial y} \right) + \rho T \left(w_x \frac{\partial(c_p)}{\partial x} + w_y \frac{\partial(c_p)}{\partial y} \right) = \frac{\partial \lambda}{\partial y} \frac{\partial T}{\partial y} + \lambda \frac{\partial^2 T}{\partial y^2}$$

or

$$\left[\rho c_p w_x \frac{\partial T}{\partial x} + \rho T w_x \frac{\partial(c_p)}{\partial x} \right] + \left[\rho c_p w_y \frac{\partial T}{\partial y} + \rho T w_y \frac{\partial(c_p)}{\partial y} \right] = \frac{\partial \lambda}{\partial y} \frac{\partial T}{\partial y} + \lambda \frac{\partial^2 T}{\partial y^2} \quad (7.18)$$

According to Chap. 6, we have

$$\frac{\partial \lambda}{\partial y} = \frac{d\lambda}{d\eta} \left(\frac{1}{4} \text{Gr}_{x,\infty} \right)^{1/4} x^{-1} \quad (7.19)$$

$$\frac{\partial T}{\partial x} = -(T_w - T_\infty) \frac{d\theta}{d\eta} \left(\frac{1}{4} \right) \eta x^{-1} \quad (7.20)$$

$$\frac{\partial T}{\partial y} = (T_w - T_\infty) \frac{d\theta}{d\eta} \left(\frac{1}{4} \text{Gr}_{x,\infty} \right)^{1/4} x^{-1} \quad (7.21)$$

$$\frac{\partial^2 T}{\partial y^2} = (T_w - T_\infty) \frac{d^2 \theta}{d\eta^2} \left(\frac{1}{4} \text{Gr}_{x,\infty} \right)^{1/2} x^{-2} \quad (7.22)$$

Similar to Eq. (7.14) we have

$$\frac{\partial c_\rho}{\partial x} = -\frac{1}{4} \eta x^{-1} \eta \frac{dc_\rho}{d\eta} \quad (7.23)$$

Similar to Eq. (6.22) we have

$$\frac{\partial c_\rho}{\partial y} = \frac{dc_\rho}{d\eta} \left(\frac{1}{4} \text{Gr}_{x,\infty} \right)^{1/4} x^{-1} \quad (7.24)$$

where

$$T = (T_w - T_\infty)\theta + T_\infty \quad (7.25)$$

Then, Eq. (7.18) is changed to

$$\begin{aligned} & 2\rho\sqrt{g\bar{x}} |T_w/T_\infty - 1|^{1/2} W_x \left[T \left(-\frac{1}{4} \eta x^{-1} \frac{dc_p}{d\eta} \right) + c_p \times \left(-(T_w - T_\infty) \frac{d\theta}{d\eta} \left(\frac{1}{4} \right) \eta x^{-1} \right) \right] \\ & + 2\rho\sqrt{g\bar{x}} |T_w/T_\infty - 1|^{1/2} \left(\frac{1}{4} \text{Gr}_{x,\infty} \right)^{-1/4} \times W_y \left[T \frac{dc_p}{d\eta} \left(\frac{1}{4} \text{Gr}_{x,\infty} \right)^{1/4} x^{-1} \right. \\ & \left. + c_p \times (T_w - T_\infty) \frac{d\theta}{d\eta} \left(\frac{1}{4} \text{Gr}_{x,\infty} \right)^{1/4} x^{-1} \right] \\ & = \frac{d\lambda}{d\eta} \left(\frac{1}{4} \text{Gr}_{x,\infty} \right)^{1/4} x^{-1} (T_w - T_\infty) \frac{d\theta}{d\eta} \left(\frac{1}{4} \text{Gr}_{x,\infty} \right)^{1/4} \\ & \quad \times x^{-1} + \lambda (T_w - T_\infty) \frac{d^2 \theta}{d\eta^2} \left(\frac{1}{4} \text{Gr}_{x,\infty} \right)^{1/2} x^{-2} \end{aligned} \quad (7.26)$$

With the definition of Local Grashof number, the above equation is simplified to

$$\begin{aligned} & 2\rho\sqrt{g\bar{x}} |T_w/T_\infty - 1|^{1/2} W_x \left[T \left(-\frac{1}{4} \eta x^{-1} \frac{dc_p}{d\eta} \right) + c_p \left(-(T_w - T_\infty) \frac{d\theta}{d\eta} \left(\frac{1}{4} \right) \eta x^{-1} \right) \right] \\ & + 2\rho\sqrt{g\bar{x}} |T_w/T_\infty - 1|^{1/2} W_y \left[T \frac{dc_p}{d\eta} x^{-1} + c_p (T_w - T_\infty) \frac{d\theta}{d\eta} x^{-1} \right] \\ & = \frac{d\lambda}{d\eta} x^{-1} (T_w - T_\infty) \frac{d\theta}{d\eta} \left(\frac{g |T_w/T_\infty - 1| x^3}{4\nu_\infty^2} \right)^{1/2} x^{-1} + \lambda (T_w - T_\infty) \frac{d^2 \theta}{d\eta^2} \\ & \quad \times \left(\frac{g |T_w/T_\infty - 1| x^3}{4\nu_\infty^2} \right)^{1/2} x^{-2} \end{aligned} \quad (7.27)$$

The above equation is divided by $\sqrt{\frac{g}{x}} |T_w/T_\infty - 1|^{1/2} (T_w - T_\infty)$ and this leads to

$$\begin{aligned}
& 2\rho W_x \left[\frac{T}{T_w - T_\infty} \left(-\frac{1}{4}\eta \frac{dc_p}{d\eta} \right) + c_p \left(-\frac{d\theta}{d\eta} \left(\frac{1}{4}\eta \right) \right) \right] + 2\rho W_y \left[\frac{T}{T_w - T_\infty} \frac{dc_p}{d\eta} + c_p \frac{d\theta}{d\eta} \right] \\
& = \frac{d\lambda}{d\eta} \frac{d\theta}{d\eta} \left(\frac{1}{4\nu_\infty^2} \right)^{1/2} + \lambda \frac{d^2\theta}{d\eta^2} \left(\frac{1}{4\nu_\infty^2} \right)^{1/2}
\end{aligned} \tag{7.28}$$

The above equation is multiplied by $\frac{2\nu_\infty}{\lambda}$ and is simplified, then

$$\begin{aligned}
& \frac{\nu_\infty}{\lambda} \rho W_x \left[\frac{T}{T_w - T_\infty} \left(-\eta \frac{dc_p}{d\eta} \right) - c_p \left(\frac{d\theta}{d\eta} \eta \right) \right] \\
& + 4 \frac{\nu_\infty}{\lambda} \rho W_y \left[\frac{T}{T_w - T_\infty} \frac{dc_p}{d\eta} + c_p \frac{d\theta}{d\eta} \right] = \frac{1}{\lambda} \frac{d\lambda}{d\eta} \frac{d\theta}{d\eta} + \frac{d^2\theta}{d\eta^2}
\end{aligned}$$

Since $\frac{\nu_\infty}{\lambda} c_p \rho = \text{Pr} \frac{\nu_\infty}{\nu}$, the above equation can be simplified to

$$\begin{aligned}
& -\text{Pr} \frac{\nu_\infty}{\nu} \eta W_x \left[\frac{T}{T_w - T_\infty} \left(\frac{1}{c_p} \frac{dc_p}{d\eta} \right) + \left(\frac{d\theta}{d\eta} \right) \right] + 4\text{Pr} \frac{\nu_\infty}{\nu} W_y \left(\frac{T}{T_w - T_\infty} \frac{1}{c_p} \frac{dc_p}{d\eta} + \frac{d\theta}{d\eta} \right) \\
& = \frac{1}{\lambda} \frac{d\lambda}{d\eta} \frac{d\theta}{d\eta} + \frac{d^2\theta}{d\eta^2}
\end{aligned}$$

or

$$\text{Pr} \frac{\nu_\infty}{\nu} (-\eta W_x + 4W_y) \left(\frac{d\theta}{d\eta} + \frac{T}{T_w - T_\infty} \frac{1}{c_p} \frac{dc_p}{d\eta} \right) = \frac{1}{\lambda} \frac{d\lambda}{d\eta} \frac{d\theta}{d\eta} + \frac{d^2\theta}{d\eta^2} \tag{7.29}$$

Now we simplify $\frac{T}{T_w - T_\infty} \frac{1}{c_p} \frac{dc_p}{d\eta}$. From Eqs. (7.5) and (7.25) we obtain the following equation:

$$\begin{aligned}
\frac{dc_p}{d\eta} & = c_{p\infty} \frac{d \left(\frac{(T_w - T_\infty)\theta + T_\infty}{T_\infty} \right)^{n_{c_p}}}{d\eta} \\
& = c_{p\infty} n_{c_p} \left(\frac{(T_w - T_\infty)\theta + T_\infty}{T_\infty} \right)^{n_{c_p}-1} \frac{T_w - T_\infty}{T_\infty} \frac{d\theta}{d\eta} \\
& = c_{p\infty} n_{c_p} \left(\frac{T}{T_\infty} \right)^{n_{c_p}-1} \frac{T_w - T_\infty}{T_\infty} \frac{d\theta}{d\eta}
\end{aligned}$$

Then

$$\begin{aligned}
\frac{T}{T_w - T_\infty} \frac{1}{c_p} \frac{dc_p}{d\eta} &= \frac{c_{p\infty}}{c_p} n_{c_p} \left(\frac{T}{T_\infty} \right)^{n_{c_p}-1} \frac{T}{T_\infty} \frac{d\theta}{d\eta} \\
&= \left(\frac{T}{T_\infty} \right)^{-n_{c_p}} n_{c_p} \left(\frac{T}{T_\infty} \right)^{n_{c_p}-1} \frac{T}{T_\infty} \frac{d\theta}{d\eta} \\
&= n_{c_p} \frac{d\theta}{d\eta}
\end{aligned}$$

Consequently Eq. (7.29) is changed as

$$\text{Pr} \frac{\nu_\infty}{\nu} (-\eta W_x + 4W_y) \left(\frac{d\theta}{d\eta} + n_{c_p} \frac{d\theta}{d\eta} \right) = \frac{1}{\lambda} \frac{d\lambda}{d\eta} \frac{d\theta}{d\eta} + \frac{d^2\theta}{d\eta^2}$$

i.e.

$$(1 + n_{c_p}) \text{Pr} \frac{\nu_\infty}{\nu} (-\eta W_x + 4W_y) \frac{d\theta}{d\eta} = \frac{1}{\lambda} \frac{d\lambda}{d\eta} \frac{d\theta}{d\eta} + \frac{d^2\theta}{d\eta^2} \quad (7.30)$$

Now we summarize the transformed dimensionless equations for the laminar free convection of polyatomic gases as follows:

$$2W_x - \eta \frac{dW_x}{d\eta} + 4 \frac{dW_y}{d\eta} - \frac{1}{\rho} \frac{d\rho}{d\eta} (\eta W_x - 4W_y) = 0 \quad (7.16)$$

$$\frac{\nu_\infty}{\nu} \left(W_x \left(2W_x - \eta \frac{dW_x}{d\eta} \right) + 4W_y \frac{dW_x}{d\eta} \right) = \frac{d^2W_x}{d\eta^2} + \frac{1}{\mu} \frac{d\mu}{d\eta} \frac{dW_x}{d\eta} + \frac{\nu_\infty}{\nu} \theta \quad (7.17)$$

$$(1 + n_{c_p}) \text{Pr} \frac{\nu_\infty}{\nu} (-\eta W_x + 4W_y) \frac{d\theta}{d\eta} = \frac{1}{\lambda} \frac{d\lambda}{d\eta} \frac{d\theta}{d\eta} + \frac{d^2\theta}{d\eta^2} \quad (7.30)$$

with boundary conditions

$$\eta = 0, W_x = 0, W_y = 0, \theta = 1 \quad (7.31)$$

$$\eta \rightarrow \infty, W_x \rightarrow 0, \theta \rightarrow 0 \quad (7.32)$$

It is obvious that when $n_{c_p} = 0$ the Eq. (7.30) will turn back to Eq. (6.33) for laminar free convection of monatomic and diatomic gases, air, and water vapor. Therefore, the energy equation of laminar free convection of monatomic and diatomic gases, air and water vapour is a special case of that of the polyatomic gas laminar free convection with $n_{c_p} = 0$.

7.4 Treatment of Physical Property Factors

According to Chap. 5, the physical property factors for gases coupled with the governing ordinary differential equations are expressed as following equations respectively:

$$\frac{1}{\rho} \frac{d\rho}{d\eta} = -\frac{\left(\frac{T_w}{T_\infty} - 1\right)}{\left(\frac{T_w}{T_\infty} - 1\right)\theta + 1} \frac{d\theta}{d\eta} \quad (7.33)$$

$$\frac{1}{\mu} \frac{d\mu}{d\eta} = \frac{n_\mu \left(\frac{T_w}{T_\infty} - 1\right)}{\left(\frac{T_w}{T_\infty} - 1\right)\theta + 1} \frac{d\theta}{d\eta} \quad (7.34)$$

$$\frac{1}{\lambda} \frac{d\lambda}{d\eta} = \frac{n_\lambda \left(\frac{T_w}{T_\infty} - 1\right)}{\left(\frac{T_w}{T_\infty} - 1\right)\theta + 1} \frac{d\theta}{d\eta} \quad (7.35)$$

$$\frac{v_\infty}{v} = \left(\left(\frac{T_w}{T_\infty} - 1 \right) \theta + 1 \right)^{-(n_\mu + 1)} \quad (7.36)$$

Combined with the physical property factor Eqs. (7.33)–(7.36), and Eqs. (7.16), (7.17), and (7.30) with boundary conditions, (7.31) and (7.32) can be solved for the velocity and temperature fields. It will be expected that, with consideration of variable physical properties, the dimensionless velocity field and the dimensionless temperature field depend on $\frac{T_w}{T_\infty}$, Pr, n_λ , n_μ and n_{c_p} for the laminar free convection of polyatomic gases.

7.5 Heat Transfer Analysis

With the same heat transfer analysis as that in Chap. 6, the analytical expressions on heat transfer for laminar free convection of polyatomic gases are as follows:

The local heat transfer rate q_x at position x per unit area from the surface of the plate to the gas will be expressed as

$$q_x = \lambda_w (T_w - T_\infty) \left(\frac{1}{4} \text{Gr}_{x,\infty} \right)^{1/4} x^{-1} \left(-\frac{d\theta}{d\eta} \right)_{\eta=0} \quad (7.37)$$

The local heat transfer coefficient α_x , defined as $q_x = \alpha_x (T_w - T_\infty)$, will be given by

$$\alpha_x = \lambda_w \left(\frac{1}{4} \text{Gr}_{x,\infty} \right)^{1/4} x^{-1} \left(-\frac{d\theta}{d\eta} \right)_{\eta=0} \quad (7.38)$$

The local Nusselt number defined by $\text{Nu}_{x,w} = \frac{\alpha_x x}{\lambda_w}$ will be

$$\text{Nu}_{x,w} = \left(\frac{1}{4} \text{Gr}_{x,\infty} \right)^{1/4} \left(-\frac{d\theta}{d\eta} \right)_{\eta=0} \quad (7.39)$$

Total heat transfer rate for position $x = 0$ to x with width of b on the plate is a integration $Q_x = \int_A q_x dA = \int_0^x q_x b dx$, and hence

$$Q_x = \frac{4}{3} b \lambda_w (T_w - T_\infty) \left(\frac{1}{4} \text{Gr}_{x,\infty} \right)^{1/4} \left(-\frac{d\theta}{d\eta} \right)_{\eta=0} \quad (7.40)$$

The average heat transfer rate, defined as $\bar{Q}_x = Q_x / (b \times x)$ is given by

$$\bar{Q}_x = \frac{4}{3} x^{-1} \lambda_w (T_w - T_\infty) \left(\frac{1}{4} \text{Gr}_{x,\infty} \right)^{1/4} \left(-\frac{d\theta}{d\eta} \right)_{\eta=0} \quad (7.41)$$

The average heat transfer coefficient $\bar{\alpha}_x$ defined as $\bar{Q}_x = \bar{\alpha}_x (T_w - T_\infty)$ is expressed as

$$\bar{\alpha}_x = \frac{4}{3} \lambda_w \left(\frac{1}{4} \text{Gr}_{x,\infty} \right)^{1/4} x^{-1} \left(-\frac{d\theta}{d\eta} \right)_{\eta=0} \quad (7.42)$$

The average Nusselt number is defined as $\overline{\text{Nu}}_{x,w} = \frac{\bar{\alpha}_x x}{\lambda_w}$ hence

$$\overline{\text{Nu}}_{x,w} = \frac{4}{3} \left(\frac{1}{4} \text{Gr}_{x,\infty} \right)^{1/4} \left(-\frac{d\theta}{d\eta} \right)_{\eta=0} \quad (7.43)$$

Obviously, in the above theoretical equations on heat transfer, only the wall dimensionless temperature gradient $\left(-\frac{d\theta}{d\eta} \right)_{\eta=0}$ dependent on numerical solution is no-given variable.

7.6 Numerical Solutions

The governing dimensionless Eqs. (7.16), (7.17) and (7.30) with the boundary condition Eqs. (7.31) and (7.32) were calculated numerically combined with the physical property factor Eqs. (7.33)–(7.36) for the velocity and temperature fields. The calculations were carried out by the shooting method presented in Chap. 6. The typical results for the velocity and temperature field were obtained with different Pr, n_λ , n_μ and n_{c_p} at different boundary temperature ratios $\frac{T_w}{T_\infty}$. Some of the solutions were plotted in Figs. 7.1, 7.2, 7.3, and 7.4. Meanwhile, the solutions of dimensionless temperature gradient $\left(-\frac{d\theta}{d\eta} \right)_{\eta=0}$, for laminar free convection of several polyatomic

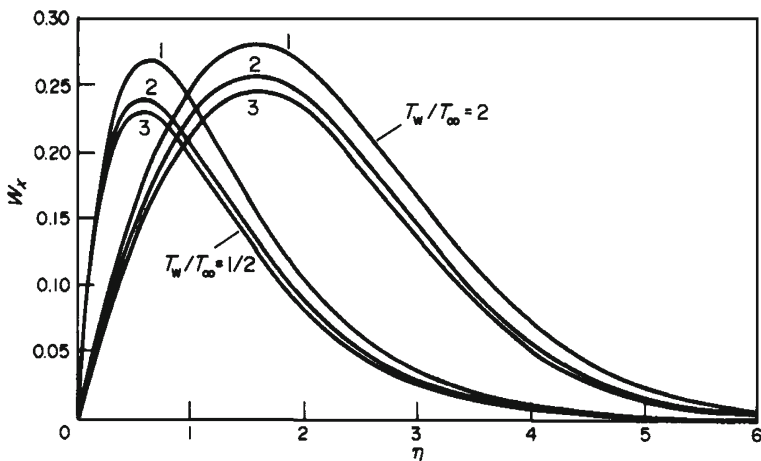


Fig. 7.1 Velocity profiles for free convection of different polyatomic gases, cited from Shang and Wang [1]. 1 gas mixture ($\text{CO}_2 = 0.13, \text{H}_2\text{O} = 0.11, \text{N}_2 = 0.76$); 2 SO_2 ; 3 NH_3

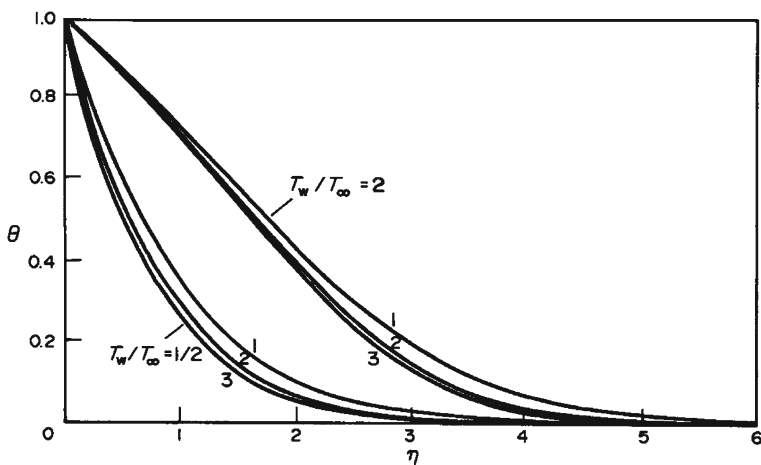


Fig. 7.2 Temperature profiles for free convection of different polyatomic gases, cited from Shang and Wang [1]. 1 gas mixture ($\text{CO}_2 = 0.13, \text{H}_2\text{O} = 0.11, \text{N}_2 = 0.76$); 2 SO_2 ; 3 NH_3

gases with the related $\text{Pr}, n_\lambda, n_\mu$ and n_{c_p} at various boundary temperature ratios $\frac{T_w}{T_\infty}$ are shown in Table 7.1 and plotted in Fig. 7.5. These solutions describe the effects of $\text{Pr}, n_\lambda, n_\mu$ and n_{c_p} on velocity and temperature fields as well as heat transfer of polyatomic gas laminar free convection. It is found that the effects of Pr, n_λ and n_μ with the boundary temperature ratios $\frac{T_w}{T_\infty}$ on the velocity and temperature fields of polyatomic laminar free convection are same as those on the velocity and tempera-

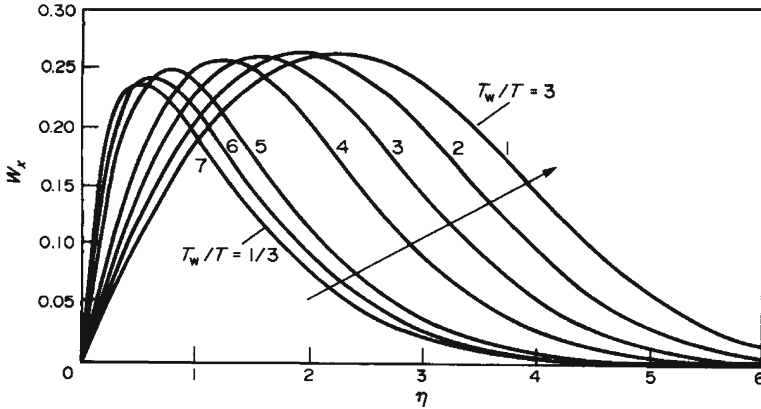


Fig. 7.3 Velocity profiles for free convection of CO₂ with different boundary temperature ratios, cited from Shang and Wang [1]. 1 $\frac{T_w}{T_\infty} = 3$; 2 $\frac{T_w}{T_\infty} = \frac{5}{2}$; 3 $\frac{T_w}{T_\infty} = 2$; 4 $\frac{T_w}{T_\infty} = \frac{3}{2}$; 5 $\frac{T_w}{T_\infty} = \frac{3}{4}$; 6 $\frac{T_w}{T_\infty} = \frac{1}{2}$; 7 $\frac{T_w}{T_\infty} = \frac{1}{3}$

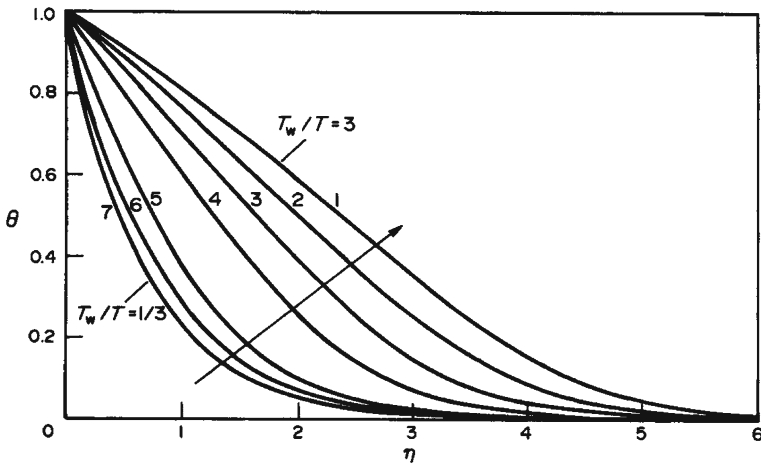


Fig. 7.4 Temperature profiles for free convection of CO₂ with different boundary temperature ratios, cited from Shang and Wang [1]. 1 $\frac{T_w}{T_\infty} = 3$; 2 $\frac{T_w}{T_\infty} = \frac{5}{2}$; 3 $\frac{T_w}{T_\infty} = 2$; 4 $\frac{T_w}{T_\infty} = \frac{3}{2}$; 5 $\frac{T_w}{T_\infty} = \frac{3}{4}$; 6 $\frac{T_w}{T_\infty} = \frac{1}{2}$; 7 $\frac{T_w}{T_\infty} = \frac{1}{3}$

ture fields of laminar free convection of monatomic and diatomic gases, air and water vapor. The effect of Pr , n_μ , n_λ , n_{c_p} and T_w/T_∞ on temperature gradient $-\left(\frac{d\theta}{d\eta}\right)_{\eta=0}$ can be briefly summarized in Table 7.3 for laminar free convection of polyatomic gases.

For consideration of variation of specific heat of the monatomic and diatomic gases, air, and water vapor with temperature, the corresponding numerical solutions

Table 7.1 Calculated results of wall temperature gradient $\left(-\frac{d\theta}{dr}\right)_{r=0}$ for consideration of temperature-dependent density, viscosity, thermal conductivity, and specific heat, cited from Shang and Wang [1]

$\frac{T_w}{T_\infty}$	Gas mixture Pr = 0.63 $n_\mu = 0.75$ $n_\lambda = 1.02$ $n_{cp} = 0.134$	CO ₂ Pr = 0.73 $n_\mu = 0.88$ $n_\lambda = 1.3$ $n_{cp} = 0.34$	CH ₄ Pr = 0.74 $n_\mu = 0.78$ $n_\lambda = 1.29$ $n_{cp} = 0.534$	CCl ₄ Pr = 0.8 $n_\mu = 0.912$ $n_\lambda = 1.29$ $n_{cp} = 0.28$	SO ₂ Pr = 0.81 $n_\mu = 0.91$ $n_\lambda = 1.323$ $n_{cp} = 0.257$	H ₂ S Pr = 0.85 $n_\mu = 1$ $n_\lambda = 1.29$ $n_{cp} = 0.18$	NH ₃ Pr = 0.87 $n_\mu = 1.04$ $n_\lambda = 1.375$ $n_{cp} = 0.34$
3	A	0.1805	0.1744	0.1908	0.1760	0.1696	0.1709
	B	0.1792	0.1729	0.1896	0.1747	0.1687	0.1699
5/2	A	0.2136	0.2107	0.2289	0.2130	0.2104	0.2093
	B	0.2125	0.2102	0.2291	0.2125	0.2100	0.2093
2	A	0.2626	0.2664	0.2870	0.2696	0.2669	0.2690
	B	0.2618	0.2669	0.2880	0.2702	0.2676	0.2700
3/2	A	0.3435	0.3619	0.3860	0.3670	0.3644	0.3733
	B	0.3426	0.3631	0.3892	0.3682	0.3659	0.3752
5/4	A	0.4076	0.4408	0.4674	0.4475	0.4452	0.4608
	B	0.4062	0.4413	0.4703	0.4480	0.4461	0.4621
3/4	A	0.6613	0.7751	0.8095	0.7783	0.7902	0.8415
	C	0.6602	0.7745	0.8105	0.7889	0.7903	0.8448
1/2	A	0.9752	1.2291	1.2700	1.2504	1.2625	1.3751
	C	0.9757	1.2223	1.2594	1.2483	1.2573	1.3805
1/3	A	1.4434	1.9722	2.0185	2.0274	2.0429	2.2802
	C	1.4420	1.9289	1.9569	1.9753	2.0274	2.2558

Note: Component of the gas mixture: CO₂ = 0.13, water vapour = 0.11 and N₂ = 0.76 A. The numerical solution. B. From Eq. (7.45) with Eqs. (7.46) and (7.47). C. From Eq. (7.45) with Eqs. (7.46) and (6.48)

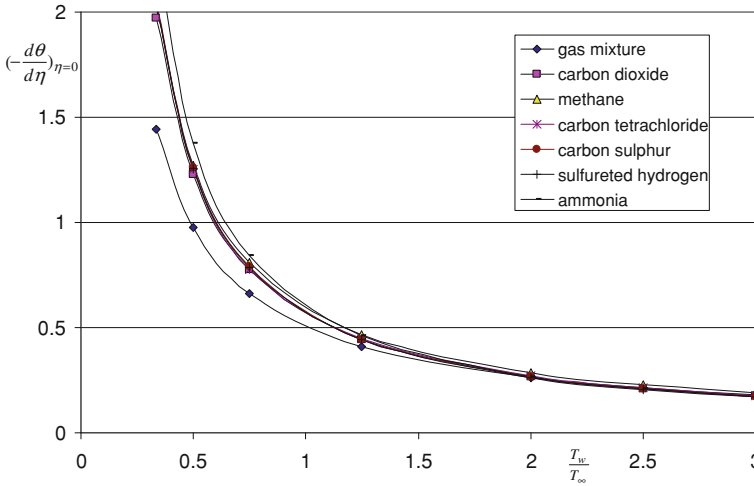


Fig. 7.5 Numerical solutions of temperature gradient $\left(-\frac{d\theta}{d\eta}\right)_{\eta=0}$ for laminar free convection of polyatomic gas

are calculated by Eqs. (7.16), (7.17) and (7.30) with the boundary condition Eqs. (7.31) and (7.32) as well as Eqs. (7.33)–(7.37) for the physical property factors, and listed in Table 7.2. It is found that these numerical solutions are very identical to the related numerical solutions without consideration of variation of specific heat. Then, it follows that it is acceptable to neglect the effect of the specific heat for calculation of the free convection heat transfer coefficient of the monatomic and diatomic gases, air, and water vapor.

7.7 Dimensionless Wall Temperature Gradient

With the system of numerical solutions wall dimensionless temperature gradient $\left(-\frac{d\theta}{d\eta}\right)_{\eta=0}$, the only one no-given physical variable in the above heat transfer theoretically analytical equations, a curve-fit formula of $\left(-\frac{d\theta}{d\eta}\right)_{\eta=0}$ was obtained by Shang and Wang [1], and shown as follows for laminar free convection of polyatomic gases with consideration of variable physical properties:

$$-\left(\frac{d\theta}{d\eta}\right)_{\eta=0} = (1 + 0.3n_{c_p})\psi(\text{Pr})\left(\frac{T_w}{T_\infty}\right)^{-m} \tag{7.44}$$

where $\psi(\text{Pr})$ is Boussinesq approximation solution in the range of gas *Prandtl number*, and is expressed as follows:

Table 7.2 Calculated results of wall temperature gradient $\left(-\frac{d\theta}{dr}\right)_{r=0}$ for consideration of temperature-dependent density, viscosity, thermal conductivity, and specific heat, cited from Shang and Wang [1]

$\frac{T_w}{T_\infty}$		H ₂	Air	N ₂	CO	O ₂	Water vapour
3	A	Pr = 0.68 $n_\mu = 0.68$ $n_\lambda = 0.8$ $n_{cp} = 0.042$	Pr = 0.7 $n_\mu = 0.68$ $n_\lambda = 0.81$ $n_{cp} = 0.078$	Pr = 0.71 $n_\mu = 0.67$ $n_\lambda = 0.76$ $n_{cp} = 0.07$	Pr = 0.72 $n_\mu = 0.71$ $n_\lambda = 0.83$ $n_{cp} = 0.068$	Pr = 0.73 $n_\mu = 0.694$ $n_\lambda = 0.86$ $n_{cp} = 0.108$	Pr = 1 $n_\mu = 1.04$ $n_\lambda = 1.185$ $n_{cp} = 0.003$
	B	0.2004	0.2042	0.2094	0.2020	0.2047	0.1740
5/2	A	0.1974	0.1987	0.2043	0.1973	0.2973	0.1738
	B	0.2334	0.2380	0.2433	0.2362	0.2394	0.2113
2	A	0.2300	0.2316	0.2374	0.2306	0.2307	0.2110
	B	0.2814	0.2871	0.2923	0.2859	0.2901	0.2682
3/2	A	0.22772	0.2794	0.2852	0.2792	0.2796	0.2679
	B	0.3579	0.3655	0.3699	0.3556	0.3716	0.3655
→ 1	A	0.3526	0.3557	0.3609	0.3570	0.3590	0.3651
	B	0.4943	0.4995	0.5021	0.5046	0.5079	0.5671
5/4	A	0.4943	0.4995	0.5021	0.5046	0.5079	0.5671
	B	0.4167	0.4258	0.4292	0.4272	0.4384	0.4453
3/4	A	0.4105	0.4144	0.4188	0.4172	0.4193	0.4448
	B	0.6370	0.6525	0.6492	0.6601	0.6751	0.7783
1/2	A	0.6276	0.6351	0.6336	0.6446	0.6507	0.7775
	B	0.8906	0.9141	0.8992	0.9311	0.9569	1.2194
1/3	A	0.8774	0.8898	0.8776	0.9003	0.9225	1.2181
	B	1.2431	1.2789	1.2420	1.3116	1.3560	1.9208
		1.2247	1.2448	1.2124	1.2812	1.3075	1.9198

A. Numerical solution with consideration of temperature-dependent density, viscosity, thermal conductivity, and specific heat. B. Numerical solution with consideration of temperature-dependent density, viscosity, thermal conductivity, but without temperature-dependent specific heat

Table 7.3 Effects of Pr, n_μ , n_λ , T_w/T_∞ and T_w/T_∞ on temperature gradient $-\left(\frac{d\theta}{d\eta}\right)_{\eta=0}$ for laminar free convection of polyatomic gases

Term	Heat transfer	
	for $T_w/T_\infty > 1$	for $T_w/T_\infty < 1$
For effect of Pr	Heat transfer increases with increase of Pr	
For effect of T_w/T_∞	Heat transfer increases with increase of T_w/T_∞	
For effect of Temperature parameter n_μ , n_λ , or η_{c_p}	Heat transfer decreases with increase of n_μ , n_λ , or η_{c_p}	

$$\psi(\text{Pr}) = 0.567 + 0.186 \times \ln \text{Pr} \quad (0.6 \leq \text{Pr} \leq 1) \tag{6.48}$$

While,

$$m = 0.35n_\lambda + 0.29n_\mu + 0.36 \quad (T_w/T_\infty > 1) \tag{7.45}$$

$$m = 0.42n_\lambda + 0.34n_\mu + 0.28 \quad (T_w/T_\infty < 1) \tag{7.46}$$

Some results of temperature gradient $\left(-\frac{d\theta}{d\eta}\right)_{\eta=0}$ for laminar free convection of different polyatomic gases predicted by using above equations are listed in Table 7.1 also, where it is found that these predicted results are well identical to the related numerical solutions.

On the other hand, it is clear from the curve-fitting formulae to see that the effect of Prandtl number Pr, the temperature parameters n_μ , n_λ , and n_{c_p} , and the boundary temperature ratio T_w/T_∞ on the wall temperature gradient $\left(-\frac{d\theta}{d\eta}\right)_{\eta=0}$. Such effect regulation is summarized in Table 7.3. Obviously, these effect regulations are same both for laminar free convection of all gases.

Also, if boundary temperature ratio T_w/T_∞ tends to unity, the specific heat parameter n_{c_p} will be regarded as zero, and Eq. (7.44) is transformed to

$$-\left(\frac{d\theta}{d\eta}\right)_{\eta=0} = \psi(\text{Pr}) \tag{7.47}$$

It is identical to Boussinesq approximation, while $\psi(\text{Pr})$ expresses well-known Boussinesq solution.

7.8 Practical Prediction Equations on Heat Transfer

By using Eq. (7.44) with Eqs. (6.48), (7.45) and (7.46), Eqs. (7.37)–(7.43) are available for prediction of heat transfer, and become the following corresponding equations for reliable prediction of heat transfer on laminar gas free convection on vertical flat plate with consideration of coupled effect of variable physical properties:

The local heat transfer rate q_x at position x per unit area from the surface of the plate to the gas is expressed as

$$q_x = \lambda_w(T_w - T_\infty) \left(\frac{1}{4} \text{Gr}_{x,\infty} \right)^{1/4} x^{-1} (1 + 0.3n_{c_p}) \psi(\text{Pr}) \left(\frac{T_w}{T_\infty} \right)^{-m} \quad (7.37^*)$$

The local heat transfer coefficient α_x , defined as $q_x = \alpha_x(T_w - T_\infty)$, will be given by

$$\alpha_x = \lambda_w \left(\frac{1}{4} \text{Gr}_{x,\infty} \right)^{1/4} x^{-1} (1 + 0.3n_{c_p}) \psi(\text{Pr}) \left(\frac{T_w}{T_\infty} \right)^{-m} \quad (7.38^*)$$

The local Nusselt number defined by $\text{Nu}_{x,w} = \frac{\alpha_x x}{\lambda_w}$ will be

$$\text{Nu}_{x,w} = \left(\frac{1}{4} \text{Gr}_{x,\infty} \right)^{1/4} (1 + 0.3n_{c_p}) \psi(\text{Pr}) \left(\frac{T_w}{T_\infty} \right)^{-m} \quad (7.39^*)$$

Total heat transfer rate for position $x = 0$ to x with width of b on the plate will be

$$Q_x = \frac{4}{3} b \lambda_w (T_w - T_\infty) \left(\frac{1}{4} \text{Gr}_{x,\infty} \right)^{1/4} (1 + 0.3n_{c_p}) \psi(\text{Pr}) \left(\frac{T_w}{T_\infty} \right)^{-m} \quad (7.40^*)$$

The average heat transfer rate, defined as $\bar{Q}_x = Q_x / (b \times x)$ is given by

$$\bar{Q}_x = \frac{4}{3} x^{-1} \lambda_w (T_w - T_\infty) \left(\frac{1}{4} \text{Gr}_{x,\infty} \right)^{1/4} (1 + 0.3n_{c_p}) \psi(\text{Pr}) \left(\frac{T_w}{T_\infty} \right)^{-m} \quad (7.41^*)$$

The average heat transfer coefficient $\bar{\alpha}_x$ defined as $\bar{Q}_x = \bar{\alpha}_x(T_w - T_\infty)$ is expressed as)

$$\bar{\alpha}_x = \frac{4}{3} \lambda_w \left(\frac{1}{4} \text{Gr}_{x,\infty} \right)^{1/4} x^{-1} (1 + 0.3n_{c_p}) \psi(\text{Pr}) \left(\frac{T_w}{T_\infty} \right)^{-m} \quad (7.42^*)$$

The average Nusselt number is defined as $\overline{\text{Nu}}_{x,w} = \frac{\bar{\alpha}_x x}{\lambda_w}$, will be

$$\overline{Nu_{x,w}} = \frac{4}{3} \left(\frac{1}{4} Gr_{x,\infty} \right)^{1/4} (1 + 0.3n_{c_p}) \psi(\text{Pr}) \left(\frac{T_w}{T_\infty} \right)^{-m} \tag{7.43*}$$

where

$$\psi(\text{Pr}) = 0.567 + 0.186 \times \ln(\text{Pr}) \quad (0.6 \leq \text{Pr} \leq 1) \tag{6.48}$$

$$m = 0.35n_\lambda + 0.29n_\mu + 0.36 \quad (T_w/T_\infty > 1) \tag{7.45}$$

$$m = 0.42n_\lambda + 0.34n_\mu + 0.28 \quad (T_w/T_\infty < 1) \tag{7.46}$$

Obviously, Eqs. (6.37*)–(6.43*) will be reliable for prediction of heat transfer on laminar free convection of polyatomic gas on a vertical flat plate with consideration of coupled effect of variable physical properties. It is reason that these prediction equations come from the theoretical equations on heat transfer coupled with the formulated equation of the solution of governing Eqs. (7.16), (7.17), and (7.30), which have very well simulated the practical laminar free convection of polyatomic gas by means of the rigorous consideration and treatment of variable physical properties.

7.9 Effect of Variable Physical Properties on Heat Transfer

From the theoretical Eqs. (7.37*)–(7.43*), it is seen that *effect of variable physical properties* on heat transfer is dominated by the factor $(1 + 0.3n_{c_p}) \psi(\text{Pr}) \left(\frac{T_w}{T_\infty} \right)^{-m}$, which demonstrates the effect of Prandtl number Pr, boundary temperature ratio $\frac{T_w}{T_\infty}$ and temperature parameters of gas. If we change the factor to $(1 + 0.3n_{c_p}) \psi(\text{Pr}) \left(\frac{T_w}{T_\infty} \right)^{-m} = (1 + 0.3n_{c_p}) \psi(\text{Pr}) \left(\frac{T_\infty}{T_w} \right)^m$, we can easily see that with increasing the Prandtl number Pr, heat transfer will increase. However, for $T_w/T_\infty > 1$, heat transfer will decrease with increasing the temperature parameters of gas. While, for $T_w/T_\infty < 1$ heat transfer will increase with increasing the temperature parameters of gas.

The above analysis on effect regulation Pr, n_μ , n_λ , and T_w/T_∞ on temperature gradient $-\left(\frac{d\theta}{d\eta} \right)_{\eta=0}$ can be briefly summarized in Table 7.3 for laminar free convection of polyatomic gases.

7.10 Heat Transfer Under Boussinesq Approximation

Obviously when boundary temperature ratio T_w/T_∞ is very close to unity, i.e. $T_w/T_\infty \rightarrow 1$, the effect of all physical properties on laminar free convection will never exist. In this case, n_{c_p} will be regarded as zero. Then, from Eqs. (7.45) and (6.49), we have the same equation on Boussinesq solution for laminar free convec-

tion of polyatomic gas as that in Chap. 6:

$$\left(-\frac{d\theta}{d\eta}\right)_{\eta=0} = \psi(\text{Pr}) = 0.567 + 0.186 \times \ln(\text{Pr}) \quad (0.6 \leq \text{Pr} \leq 1) \quad (7.51)$$

In this case, we have the same equations as those in Chap. 6 for heat transfer of laminar free convection of polyatomic gas on vertical flat plate under Boussinesq approximation:

$$q_x = \lambda_w(T_w - T_\infty) \left(\frac{1}{4}\text{Gr}_{x,\infty}\right)^{1/4} x^{-1} \psi(\text{Pr}) \quad (7.37^{**})$$

$$\alpha_x = \lambda_w \left(\frac{1}{4}\text{Gr}_{x,\infty}\right)^{1/4} x^{-1} \psi(\text{Pr}) \quad (7.38^{**})$$

$$\text{Nu}_{x,w} = \left(\frac{1}{4}\text{Gr}_{x,\infty}\right)^{1/4} \psi(\text{Pr}) \quad (7.39^{**})$$

$$Q_x = \frac{4}{3} b \lambda_w (T_w - T_\infty) \left(\frac{1}{4}\text{Gr}_{x,\infty}\right)^{1/4} \psi(\text{Pr}) \quad (7.40^{**})$$

$$\bar{Q}_x = \frac{4}{3} x^{-1} \lambda_w (T_w - T_\infty) \left(\frac{1}{4}\text{Gr}_{x,\infty}\right)^{1/4} \psi(\text{Pr}) \quad (7.41^{**})$$

$$\bar{\alpha}_x = \frac{4}{3} \lambda_w \left(\frac{1}{4}\text{Gr}_{x,\infty}\right)^{1/4} x^{-1} \psi(\text{Pr}) \quad (7.42^{**})$$

$$\bar{\text{Nu}}_{x,w} = \frac{4}{3} \left(\frac{1}{4}\text{Gr}_{x,\infty}\right)^{1/4} \psi(\text{Pr}) \quad (7.43^{**})$$

7.11 Summary

Comparing the analyses and results in Chap. 4 with that in this chapter, it is obvious to find that laminar free convection and heat transfer of the monatomic and diatomic gases, air, and water vapor can be regarded as a special case of that of polyatomic gases. In fact, the results of free convection heat transfer of polyatomic gases are very well identical to those of the monatomic and diatomic gases, air and water vapor. So far, the governing equations of laminar free convection for general gases and expressions related to heat transfer can be summarized in Table 7.4.

Table 7.4 Summary of the governing equations of laminar free convection for gases and the expressions related to heat transfer

Term	Expression
<i>Governing partial differential equations</i>	
Mass equation	$\frac{\partial}{\partial x}(\rho w_x) + \frac{\partial}{\partial y}(\rho w_y) = 0$
Momentum equation	$\rho \left(w_x \frac{\partial w_x}{\partial x} + w_y \frac{\partial w_x}{\partial y} \right) = \frac{\partial}{\partial y}(\mu \frac{\partial w_x}{\partial y}) + \rho g \frac{T - T_\infty}{T_\infty}$
Energy equation	$\rho \left(w_x \frac{\partial(c_p T)}{\partial x} + w_y \frac{\partial(c_p T)}{\partial y} \right) = \frac{\partial}{\partial y}(\lambda \frac{\partial T}{\partial y})$
Boundary conditions	$y = 0: w_x = 0, w_y = 0, T = T_w$ $y \rightarrow \infty: w_x \rightarrow 0, T = T_\infty$
<i>Assumed similarity variables</i>	
η	$\frac{y}{x} \left(\frac{1}{4} \text{Gr}_{x,\infty} \right)^{1/4}$
$\text{Gr}_{x,\infty}$	$(\text{Gr}_{x,\infty})_v = \frac{g T_w/T_\infty - 1 x^3}{\nu_\infty^2}$
θ	$\theta = \frac{T - T_\infty}{T_w - T_\infty}$
W_x	$(2\sqrt{g x} T_w/T_\infty - 1 ^{1/2})^{-1} w_x$
W_y	$(2\sqrt{g x} T_w/T_\infty - 1 ^{1/2} (\frac{1}{4} \text{Gr}_{x,\infty})^{-1/4})^{-1} w_y$
<i>Governing ordinary differential equations</i>	
Mass equations	$2W_x - \eta \frac{dW_x}{d\eta} + 4 \frac{dW_y}{d\eta} - \frac{1}{\rho} \frac{d\rho}{d\eta} (\eta W_x - 4W_y) = 0$
Momentum equation	$\frac{\nu_\infty}{v} \left(W_x \left(2W_x - \eta \frac{dW_x}{d\eta} \right) + 4W_y \frac{dW_x}{d\eta} \right) = \frac{d^2 W_x}{d\eta^2} + \frac{1}{\mu} \frac{d\mu}{d\eta} \frac{dW_x}{d\eta} + \frac{\nu_\infty \theta}{v}$
Energy equation	$(1 + n_{c_p}) \text{Pr} \frac{\nu_\infty}{v} (-\eta W_x + 4W_y) \frac{d\theta}{d\eta} = \frac{1}{\lambda} \frac{d\lambda}{d\eta} \frac{d\theta}{d\eta} + \frac{d^2 \theta}{d\eta^2}$
Boundary conditions	$\eta = 0: W_x = 0, W_y = 0, \theta = 1;$ $\eta \rightarrow \infty: W_x = 0, \theta = 0$
<i>Boussinesq solution</i>	
$\left(-\frac{d\theta}{d\eta} \right)_{\eta=0} = \psi(\text{Pr}) = 0.567 + 0.186 \times \ln(\text{Pr}) \quad (0.6 \leq \text{Pr} \leq 1)$	
<i>Heat transfer under Boussinesq approximation</i>	
Local heat transfer rate	$q_x = \lambda_w (T_w - T_\infty) \left(\frac{1}{4} \text{Gr}_{x,\infty} \right)^{1/4} x^{-1} \psi(\text{Pr})$
Local heat transfer coefficient defined by $\text{Nu}_{x,w} = \frac{q_{x,x}}{z_w}$	$\alpha_x = \lambda_w \left(\frac{1}{4} \text{Gr}_{x,\infty} \right)^{1/4} x^{-1} \psi(\text{Pr})$

Term	Expression
Local Nusselt number local Nusselt number defined by $Nu_{x,w} = \frac{\bar{\alpha}_x x}{\lambda_w}$	$Nu_{x,w} = \left(\frac{1}{4} Gr_{x,\infty}\right)^{1/4} \psi(\text{Pr})$
Total heat transfer rate $Q = \iint_A q_x dA = \int_0^x q_x b dx$	$Q_x = \frac{4}{3} b \lambda_w (T_w - T_\infty) \left(\frac{1}{4} Gr_{x,\infty}\right)^{1/4} \psi(\text{Pr})$
Average heat transfer rate, defined as $\bar{Q}_x = Q_x / (b \times x)$	$\bar{Q}_x = \frac{4}{3} x^{-1} \lambda_w (T_w - T_\infty) \left(\frac{1}{4} Gr_{x,\infty}\right)^{1/4}$
Average heat transfer coefficient $\bar{\alpha}_x$ defined as $\bar{Q}_x = \bar{\alpha}_x (T_w - T_\infty)$	$\bar{\alpha}_x = \frac{4}{3} \lambda_w \left(\frac{1}{4} Gr_{x,\infty}\right)^{1/4} x^{-1} \psi(\text{Pr})$
Average Nusselt number average Nusselt number is defined as $\overline{Nu}_{x,w} = \frac{\bar{\alpha}_x x}{\lambda_w}$	$\overline{Nu}_{x,w} = \frac{4}{3} \left(\frac{1}{4} Gr_{x,\infty}\right)^{1/4} \psi(\text{Pr})$
Wall dimensionless temperature gradient with consideration of variable physical properties $\left(-\frac{d\theta}{d\eta}\right)_{\eta=0} = (1 + 0.3n_{cp}) \psi \left(\frac{T_w}{T_\infty}\right)^{-m}$	$(0.6 \leq \text{Pr} \leq 1)$
where $\psi(\text{Pr}) = 0.567 + 0.186 \times \ln(\text{Pr})$	$(T_w/T_\infty > 1)$
$m = 0.35n_x + 0.29n_\mu + 0.36$	$(T_w/T_\infty < 1)$
$m = 0.42n_x + 0.34n_\mu + 0.28$	
Heat transfer for consideration of coupled effect of variable physical properties variable	
Local heat transfer rate	$q_x = \lambda_w (T_w - T_\infty) \left(\frac{1}{4} Gr_{x,\infty}\right)^{1/4} x^{-1} (1 + 0.3n_{cp}) \psi \left(\text{Pr}\right) \left(\frac{T_w}{T_\infty}\right)^{-m}$
Local heat transfer coefficient defined by $Nu_{x,w} = \frac{\alpha_x x}{\lambda_w}$	$\alpha_x = \lambda_w \left(\frac{1}{4} Gr_{x,\infty}\right)^{1/4} x^{-1} (1 + 0.3n_{cp}) \psi \left(\text{Pr}\right) \left(\frac{T_w}{T_\infty}\right)^{-m}$
Local Nusselt number defined by $Nu_{x,w} = \frac{\alpha_x x}{\lambda_w}$	$Nu_{x,w} = \left(\frac{1}{4} Gr_{x,\infty}\right)^{1/4} (1 + 0.3n_{cp}) \psi \left(\text{Pr}\right) \left(\frac{T_w}{T_\infty}\right)^{-m}$
Total heat transfer rate $Q = \iint_A q_x dA = \int_0^x q_x b dx$	$Q_x = \frac{4}{3} b \lambda_w (T_w - T_\infty) \left(\frac{1}{4} Gr_{x,\infty}\right)^{1/4} (1 + 0.3n_{cp}) \psi \left(\text{Pr}\right) \left(\frac{T_w}{T_\infty}\right)^{-m}$
Average heat transfer rate, defined as $\bar{Q}_x = Q_x / (b \times x)$	$\bar{Q}_x = \frac{4}{3} x^{-1} \lambda_w (T_w - T_\infty) \left(\frac{1}{4} Gr_{x,\infty}\right)^{1/4} (1 + 0.3n_{cp}) \psi \left(\text{Pr}\right) \left(\frac{T_w}{T_\infty}\right)^{-m}$
Average heat transfer coefficient $\bar{\alpha}_x$ defined as $\bar{Q}_x = \bar{\alpha}_x (T_w - T_\infty)$	$\bar{\alpha}_x = \frac{4}{3} \lambda_w \left(\frac{1}{4} Gr_{x,\infty}\right)^{1/4} x^{-1} (1 + 0.3n_{cp}) \psi \left(\text{Pr}\right) \left(\frac{T_w}{T_\infty}\right)^{-m}$
Average Nusselt number is defined as $\overline{Nu}_{x,w} = \frac{\bar{\alpha}_x x}{\lambda_w}$	$\overline{Nu}_{x,w} = \frac{4}{3} \left(\frac{1}{4} Gr_{x,\infty}\right)^{1/4} (1 + 0.3n_{cp}) \psi \left(\text{Pr}\right) \left(\frac{T_w}{T_\infty}\right)^{-m}$

7.12 Remarks

On the basis of study of Chap. 6, the temperature-dependent specific heat is further considered for investigation of laminar free convection of polyatomic gases with consideration of variable physical properties. The temperature parameters, such as viscosity, thermal conductivity, and specific heat parameters are presented for a series of polyatomic gases. The governing energy ordinary differential equation is derived out for further consideration of temperature-dependent specific heat. With the temperature parameter method, the physical property factors coupled with the governing ordinary differential equations are transformed to the functions with the dimensionless temperature and the related temperature parameters for convenient simultaneous solution. A system of solutions is obtained numerically. It is seen from the calculated results that there are obvious effects of variable physical properties on velocity and temperature fields, as well as heat transfer of free convection of polyatomic gases. The theoretical equations of heat transfer of polyatomic gas free convection are created based on the heat transfer analysis, where the wall dimensionless temperature gradient is the only one no-given variable. Then, the system of numerical solutions on the wall temperature gradient is formulated into a prediction equation. Then, it is found that the gas temperature parameters n_μ , n_λ and n_{c_p} , Prandtl number, and the boundary temperature ratio dominate the heat transfer of laminar free convection of polyatomic gases. Since the temperature parameters are based on the experimental data, the heat transfer prediction equations are reliable for practical application. The method proposed in this chapter, for analyzing the laminar free convection of polyatomic gases along a vertical isothermal flat plate can be suitable for laminar free convection for all gases, and could yield reliable results.

7.13 Calculation Examples

Example 1:

An plate with uniform temperature $t_w = 0^\circ\text{C}$, width $b = 2$ m and height $x = 0.9$ m is suspended in a gas mixture with temperature $t_\infty = 500^\circ\text{C}$. The kinetic viscosity of the gas mixture is $\nu_\infty = 7.63 \times 10^{-5} \text{ m}^2/\text{s}$ at $t_\infty = 500^\circ\text{C}$, and the thermal conductivity of the gas mixture is $\lambda_w = 0.0228 \text{ W}/(\text{m}^\circ\text{C})$ at $t_w = 0^\circ\text{C}$. The temperature parameters of the gas mixture are $n_\mu = 0.75$, $n_\lambda = 1.02$ and $n_{c_p} = 0.134$ respectively. The gas mixture Prandtl number is $\text{Pr} = 0.63$. Suppose the free convection is laminar.

Please calculate the average heat transfer coefficients and free convection heat transfer on the plate.

Solution:

The temperature ratio T_w/T_∞ of the gas laminar free convection is

$$T_w/T_\infty = 273/(500 + 273) = 0.35317$$

Since $T_w/T_\infty < 1$ from Eq. (5.46) we have

$$\begin{aligned} m &= 0.42\eta_\lambda + 0.34\eta_\mu + 0.28 \\ &= 0.42 \times 1.02 + 0.34 \times 0.75 + 0.28 \\ &= 0.9634 \end{aligned}$$

Also

$$\begin{aligned} \psi(\text{Pr}) &= 0.567 + 0.186 \times \ln \text{Pr} \\ &= 0.567 + 0.186 \times \ln(0.63) \\ &= 0.48106 \end{aligned}$$

Then, temperature gradient $-\left(\frac{d\theta}{d\eta}\right)_{\eta=0}$ is evaluated as

$$\begin{aligned} -\left(\frac{d\theta}{d\eta}\right)_{\eta=0} &= (1 + 0.3\eta_{c_p})\psi(\text{Pr})\left(\frac{T_w}{T_\infty}\right)^{-m} \\ &= (1 + 0.3 \times 0.134) \times 0.48106 \times 0.35317^{-0.9634} \\ &= 1.3639 \end{aligned}$$

Then, local Grashof number is calculated as

$$\begin{aligned} \text{Gr}_{x,\infty} &= \frac{g |T_w/T_\infty - 1| x^3}{\nu_\infty^2} \\ &= \frac{9.8 \times |0.35317 - 1| \times 0.9^3}{(7.63 \times 10^{-5})^2} \\ &= 793770003 \\ &= 0.79377 \times 10^9 \end{aligned}$$

In this case, average Nusselt number $\overline{\text{Nu}}_{x,w}$ can be calculated as follows by using Eq. (7.42):

$$\begin{aligned} \overline{\text{Nu}}_{x,w} &= \frac{4}{3} \left(\frac{d\theta}{d\eta}\right)_{\eta=0} \left(\frac{1}{4}\text{Gr}_{x,\infty}\right)^{1/4} \\ &= \frac{4}{3} \times 1.3639 \times \left(\frac{1}{4} \times 793770003\right)^{1/4} \\ &= 215.84 \end{aligned}$$

With the definition of $\overline{Nu}_{x,w}$, $\overline{Nu}_{x,w} = \frac{\overline{\alpha_x x}}{\lambda_w}$, the average heat transfer coefficient $\overline{\alpha_x}$ is expressed as

$$\overline{\alpha_x} = \frac{\overline{Nu}_{x,w} \cdot \lambda_w}{x} = \frac{215.84 \times 0.0228}{0.9} = 5.468 \text{ W}/(\text{m}^2 \cdot ^\circ \text{C})$$

Then, total heat transfer rate on the plate is

$$\begin{aligned} Q_x &= \overline{\alpha_x}(T_w - T_\infty)x \times b \\ &= 5.468 \times (0 - 500) \times 0.9 \times 2 \\ &= -4921.2 \text{ W} \end{aligned}$$

where the negative sign implies that the total heat transfer rate Q_x is from gas mixture to the plate.

7.14 Exercises

1. Please analyze the relation of the energy equations of Chaps. 6 and 7. What does it mean?
2. Can you tell me if Eqs. (7.37*)–(7.43*) with Eqs. (6.48), (7.45) and (7.46) are qualified for practical prediction of heat transfer of laminar gas free convection? Why?
3. Follow the example 1 of calculation examples, only change gas mixture to CO₂ air, and water vapour as the ambient gas, and keep other conditions.
 - (i) Calculate the average heat transfer coefficients and free convection heat transfer of the plate for boundary temperature ratio $T_w/T_\infty = 1.1, 1.2, 1.4, 1.7$ and 2.1 .
 - (ii) Calculate the free convection heat transfer of the plate under Boussinesq approximation.
 - (iii) From the above calculated results on heat transfer, which conclusions will be obtain?
4. Please calculate the questions (i) and (ii) of exercise 3 by using the related empirical equation.
5. Compare the calculated results in exercises 3 and 4, and tell me which calculated result is more reliable for practical application, why?
6. Do you think the treatment of variable physical properties in this chapter is reliable? Why?

References

1. D.Y. Shang, B.X. Wang, Effect of variable thermophysical properties on laminar free convection of polyatomic gas. *Int. J. Heat Mass Transf.* **34**(3), 749–755 (1991)
2. Y.S. Touloukian, S.C. Saxena, P. Hestermans, *Thermophysical Properties of Matter*, vol. 2, viscosity, (IFI/Plenum, New York, 1970)
3. Y.S. Touloukian, P.E. Liley, S.C. Saxena, *Thermophysical Properties of Matter*, vol. 3, Thermal conductivity, Non-metallic liquids and gases, (IFI/Plenum, New York, 1970)
4. Y.S. Touloukian, T. Makita, *Thermophysical Properties of Matter*, vol. 6, Specific heat, Non-metallic liquids and gases, (IFI/Plenum, New York, 1970)
5. S.M. Yang, *Heat Transfer*, 2nd edn., (Higher Education Press, Metals Park, Ohio, 1987), p. 443

Chapter 8

Heat Transfer on Liquid Laminar Free Convection

Abstract The new similarity analysis method is used to transform the governing partial differential equations of laminar free convection of liquid into the corresponding governing dimensionless system, which are identical to the corresponding governing dimensionless system of gas laminar free convection, except different treatment of variable physical properties. Due to the different variable physical properties from gases, the polynomial approach is suggested for treatment of temperature-dependent physical properties of liquid. Taking water as an example, the polynomial approach is applied for expressions of temperature-dependent density, thermal conductivity, and viscous. These expressions are reliable because they are based on the typical experimental values of the physical properties. By means of the equations of the physical property factors coupled with the governing ordinary differential equations of liquid laminar free convection created by the new similarity analysis method, the non-linear governing equations with corresponding boundary conditions are simultaneously solved numerically. The effect of variable physical properties on water laminar free convection along an isothermal vertical plate is investigated. It is found that the wall temperature gradient is the only one no-given condition for prediction of heat transfer. Compared with wall temperature, the bulk temperature dominates heat transfer of laminar free convection. By means of the curve-fitting equation on the wall temperature gradient, the heat transfer analysis equations based on the new similarity analysis model become those with the practical application value for heat transfer prediction.

8.1 Introduction

The theoretical analysis of laminar free convection of liquid along an isothermal vertical flat plate was also started by means of Boussinesq approximation. For the case of larger temperature difference, the effects of variable physical properties should be taken into consideration, as those in Refs. [1–9]. In Ref. [1] Fuji et al. used two

methods of correlating to examine the effects of variable physical properties on heat transfer for free convection from vertical surfaces in liquids. The first method of correlating the data consisted of using the constant property correlations for Nusselt number and evaluating all properties at a reference temperature, $T_r = T_w - (T_w - T_\infty)/4$. They noted that the choice of the reference temperature agrees with the solution provided by two previous studies of Fujii [2] and Akage [3]. The second method that they used to correlate their data in oils was first proposed by Akagi [3] and applies only to liquids for which viscosity variation is dominant. Piau [4] treated the similarity analysis of variable property effects in free convection from vertical surfaces in high Prandtl number liquids. It was indicated that the main property variations in water at moderate temperature levels are in the viscosity, μ and the volumetric coefficient of thermal expansion, β and that for higher Prandtl number liquids, the variation of β is often negligible. In Ref. [5], Piau included the effect of thermal stratification of the ambient fluid in an analysis, which also include variables μ and β for water. Brown [6] used an integral method and studied the effect of the coefficient of volumetric expansion on laminar free convection heat transfer. Carey and Mollendorf [7] have shown the mathematical forms of viscosity variation with temperature, which results in similarity solutions for laminar free convection from a vertical isothermal surface in liquids with temperature-dependent viscosity. Sabhapathy and Cheng [8] studied the effects of temperature-dependent viscosity and coefficient of thermal expansion on the stability of laminar free convection boundary-layer flow of a liquid along an isothermal, vertical surface, employing linear stability theory for Prandtl numbers between 7 and 10. Qureshi and Gebhart [9] studied the stability of vertical thermal buoyancy-induced flow in cold and saline water. They indicated that the anomalous density behavior of cold water, for example, a density extremum at about 4 °C in pure water at atmospheric pressure, commonly has very large effects on flow and transport. However, the results reported are so far not convenient for heat transfer prediction due to difficulty of treating the variable thermophysical properties in governing equations.

In this chapter, an advanced development [10] of laminar free convection of liquid with large temperature difference is introduced. The new similarity analysis method, i.e. velocity component method for similarity transformation presented in this book is used here for similarity transformation of the governing partial differential equations of liquid free convection. Meanwhile, the polynomial equations are suggested to express the variable physical properties of a liquid. For example, polynomial equations of the density and thermal conductivity of water are proposed, and expression of absolute viscosity of water is also based on a polynomial. A typical example of the laminar free convection of water was provided. It is concluded that the Nusselt number could be predicted by local Grashof number and the dimensionless temperature gradient on the wall. Furthermore, a reliable curve-fit formula of the dimensionless temperature gradient is presented for simple and accurate prediction of water free convection with large temperature difference.

8.2 Governing Partial Differential Equations

The physical analytical model and co-ordinate system used for laminar free convection of liquid on an isothermal vertical flat plate is shown in Fig. 6.1 also. According to the presentation in Chap. 2, the conservation equation for mass, momentum, and energy of steady laminar free convection of liquid in the boundary layer are

$$\frac{\partial}{\partial x}(\rho w_x) + \frac{\partial}{\partial y}(\rho w_y) = 0 \quad (8.1)$$

$$\rho \left(w_x \frac{\partial w_x}{\partial x} + w_y \frac{\partial w_x}{\partial y} \right) = \frac{\partial}{\partial y} \left(\mu \frac{\partial w_x}{\partial y} \right) + g |\rho_\infty - \rho| \quad (8.2)$$

$$\rho c_p \left(w_x \frac{\partial t}{\partial x} + w_y \frac{\partial t}{\partial y} \right) = \frac{\partial}{\partial y} \left(\lambda \frac{\partial t}{\partial y} \right) \quad (8.3)$$

The boundary conditions are

$$y = 0 : w_x = 0, \quad w_y = 0, \quad t = t_w \quad (8.4)$$

$$y \rightarrow \infty : w_x \rightarrow 0, \quad t = t_\infty \quad (8.5)$$

where the variable physical properties are considered except the specific heat. In fact, such treatment for physical properties is suitable for a lot of liquids. Additionally, the absolute value of buoyancy term $g |\rho_\infty - \rho|$ in Eq. (7.2) shows that it has always positive sign no matter which one is larger between ρ and ρ_∞ . In this case, the buoyancy term $g |\rho_\infty - \rho|$ and the velocity component w_x have the same sign.

8.3 Similarity Variables

For *similarity transformation* of the governing partial differential equations for the laminar free convection of liquid, the velocity component method is also used. Consulting the assumed dimensionless variables in Chap. 6 for the similarity transformation of the governing partial differential equations of gas laminar free convection, the following dimensionless transformation variables can be assumed for the transformation of governing equations of liquid laminar free convection:

$$\eta = \frac{y}{x} \left(\frac{1}{4} \text{Gr}_{x,\infty} \right)^{1/4} \quad (8.6)$$

$$\theta = \frac{t - t_\infty}{t_w - t_\infty} \quad (8.7)$$

$$W_x = \left[2\sqrt{gx} \left| \frac{\rho_\infty}{\rho_w} - 1 \right|^{\frac{1}{2}} \right]^{-1} w_x \quad (8.8)$$

$$W_y = \left[2\sqrt{gx} \left| \frac{\rho_\infty}{\rho_w} - 1 \right|^{-\frac{1}{2}} \left(\frac{1}{4} \text{Gr}_{x,\infty} \right)^{-\frac{1}{4}} \right]^{-1} w_y \quad (8.9)$$

$$\text{Gr}_{x,\infty} = \frac{g |\rho_\infty / \rho_w - 1| x^3}{\nu_\infty^2} \quad (8.10)$$

8.4 Similarity Transformation

For convenience of similarity transformation, it is necessary to rewrite the governing Eqs. (8.1)–(8.3) into the following format respectively:

$$\rho \left(\frac{\partial w_x}{\partial x} + \frac{\partial w_y}{\partial y} \right) + w_x \frac{\partial \rho}{\partial x} + w_y \frac{\partial \rho}{\partial y} = 0 \quad (8.1a)$$

$$\rho \left(w_x \frac{\partial w_x}{\partial x} + w_y \frac{\partial w_x}{\partial y} \right) = \mu \frac{\partial^2 w_x}{\partial y^2} + \frac{\partial w_x}{\partial y} \frac{\partial \mu}{\partial y} + g |\rho_\infty - \rho| \quad (8.2a)$$

$$\rho c_p \left(w_x \frac{\partial t}{\partial x} + w_y \frac{\partial t}{\partial y} \right) = \lambda \frac{\partial^2 t}{\partial y^2} + \frac{\partial \lambda}{\partial y} \frac{\partial t}{\partial y} \quad (8.3a)$$

Similar to the derivation of the related partial differential equations in Chap. 6, the related derivatives by means of Eqs. (8.6)–(8.10) are obtained and expressed as follows:

$$\frac{\partial w_x}{\partial x} = \sqrt{\frac{g}{x}} \left| \frac{\rho_\infty}{\rho_w} - 1 \right|^{1/2} \left(W_x - \frac{1}{2} \eta \frac{dW_x}{d\eta} \right) \quad (8.11)$$

$$\frac{\partial w_y}{\partial y} = 2\sqrt{\frac{g}{x}} \left| \frac{\rho_\infty}{\rho_w} - 1 \right|^{1/2} \frac{dW_y}{d\eta} \quad (8.12)$$

$$\frac{\partial \rho}{\partial x} = -\frac{1}{4} \eta x^{-1} \frac{d\rho}{d\eta} \quad (8.13)$$

$$\frac{\partial \rho}{\partial y} = \frac{d\rho}{d\eta} \left(\frac{1}{4} \text{Gr}_{x,\infty} \right)^{1/4} x^{-1} \quad (8.14)$$

$$\frac{\partial w_x}{\partial y} = 2\sqrt{gx} \left| \frac{\rho_\infty}{\rho_w} - 1 \right|^{1/2} \frac{dW_x}{d\eta} x^{-1} \left(\frac{1}{4} \text{Gr}_{x,\infty} \right)^{1/4} \quad (8.15)$$

$$\frac{\partial^2 w_x}{\partial y^2} = 2\sqrt{gx} \left| \frac{\rho_\infty}{\rho_w} - 1 \right|^{1/2} \frac{d^2 W_x}{d\eta^2} x^{-2} \left(\frac{1}{4} \text{Gr}_{x,\infty} \right)^{1/2} \quad (8.16)$$

$$\frac{\partial \mu}{\partial y} = \frac{d\mu}{d\eta} x^{-1} \left(\frac{1}{4} \text{Gr}_{x,\infty} \right)^{1/4} \quad (8.17)$$

$$\frac{\partial t}{\partial x} = -(t_w - t_\infty) \frac{d\theta}{d\eta} \left(\frac{1}{4}\right) \eta x^{-1} \quad (8.18)$$

$$\frac{\partial t}{\partial y} = (t_w - t_\infty) \frac{d\theta}{d\eta} \left(\frac{1}{4} \text{Gr}_{x,\infty}\right)^{\frac{1}{4}} x^{-1} \quad (8.19)$$

$$\frac{\partial^2 t}{\partial y^2} = (t_w - t_\infty) \frac{d^2\theta}{d\eta^2} \left(\frac{1}{4} \text{Gr}_{x,\infty}\right)^{\frac{1}{2}} x^{-2} \quad (8.20)$$

$$\frac{\partial \lambda}{\partial y} = \frac{d\lambda}{d\eta} \left(\frac{1}{4} \text{Gr}_{x,\infty}\right)^{\frac{1}{4}} x^{-1} \quad (8.21)$$

where

$$t = (t_w - t_\infty)\theta + t_\infty \quad (8.22)$$

Similar to the derivations in Chap. 6, by using Eqs. (8.11)–(8.22), the following governing ordinary differential equations can be obtained from the Eqs. (8.1a)–(8.3a):

$$2W_x - \eta \frac{dW_x}{d\eta} + 4 \frac{dW_y}{d\eta} - \frac{1}{\rho} \frac{d\rho}{d\eta} (\eta W_x - 4W_y) = 0 \quad (8.23)$$

$$\frac{\nu_\infty}{\nu} \left(W_x \left(2W_x - \eta \frac{dW_x}{d\eta} \right) + 4W_y \frac{dW_x}{d\eta} \right) = \frac{d^2 W_x}{d\eta^2} + \frac{1}{\mu} \frac{d\mu}{d\eta} \frac{dW_x}{d\eta} + \frac{\nu_\infty}{\nu} \frac{\frac{\rho_\infty}{\rho} - 1}{\frac{\rho_\infty}{\rho_w} - 1} \quad (8.24)$$

$$\text{Pr} \frac{\nu_\infty}{\nu} (-\eta W_x + 4W_y) \frac{d\theta}{d\eta} = \frac{1}{\lambda} \frac{d\lambda}{d\eta} \frac{d\theta}{d\eta} + \frac{d^2\theta}{d\eta^2} \quad (8.25)$$

with boundary conditions

$$\eta = 0, \quad W_x = 0, \quad W_y = 0, \quad \theta = 1 \quad (8.26)$$

$$\eta \rightarrow \infty, \quad W_x \rightarrow 0, \quad \theta \rightarrow 0 \quad (8.27)$$

Equations (8.23)–(8.27) are dimensionless governing equations and the boundary conditions of laminar free convection of liquid.

In fact, the buoyancy factor $\frac{\frac{\rho_\infty}{\rho} - 1}{\frac{\rho_\infty}{\rho_w} - 1}$ in Eq. (8.24) is suitable for all fluid, i.e., both liquid and gas. For gas, the buoyancy factor can be rewritten as follows by using the simple power law of gas:

$$\frac{\frac{\rho_\infty}{\rho} - 1}{\frac{\rho_\infty}{\rho_w} - 1} = \frac{\frac{T}{T_\infty} - 1}{\frac{T_w}{T_\infty} - 1} = \frac{T - T_\infty}{T_w - T_\infty} = \theta \quad (8.28)$$

8.5 Treatment of Variable Physical Properties

8.5.1 Variable Physical Properties of Liquids

We take water as an example to introduce the *treatment of variable physical properties* of liquid. According to Chap. 5, the temperature-dependent expressions of density, thermal conductivity, and absolute viscosity of water at atmospheric pressure with the temperature range between 0 and 100°C are, respectively, expressed by polynomials as

$$\rho = -4.48 \times 10^{-3}t^2 + 999.9 \quad (5.16)$$

$$\lambda = -8.01 \times 10^{-6}t^2 + 1.94 \times 10^{-3}t + 0.563 \quad (5.17)$$

$$\mu = \exp \left[-1.6 - \frac{1150}{T} + \left(\frac{690}{T} \right)^2 \right] \times 10^{-3} \quad (5.18)$$

Meanwhile, specific heat of water can be regarded as constant with temperature variation.

8.5.2 Physical Property Factors

According to the derivation of Chap. 5, the dimensionless *physical property factors* $\frac{1}{\rho} \frac{d\rho}{d\eta}$, $\frac{1}{\mu} \frac{d\mu}{d\eta}$, and $\frac{1}{\lambda} \frac{d\lambda}{d\eta}$ in the transformed dimensionless governing Eqs. (8.23)–(8.25) for water laminar free convection with consideration of the variable physical properties can be derived out and shown as:

$$\frac{1}{\rho} \frac{d\rho}{d\eta} = \frac{-2 \times 4.48 \times 10^{-3}t(t_w - t_\infty)d\theta}{-4.48 \times 10^{-3}t^2 + 999.9d\eta} \quad (5.24)$$

$$\frac{1}{\mu} \frac{d\mu}{d\eta} = \left(\frac{1150}{T^2} - 2 \times \frac{690^2}{T^3} \right) (t_w - t_\infty) \frac{d\theta}{d\eta} \quad (5.25)$$

$$\frac{1}{\lambda} \frac{d\lambda}{d\eta} = \frac{(-2 \times 8.01 \times 10^{-6}t + 1.94 \times 10^{-3})(t_w - t_\infty) \frac{d\theta}{d\eta}}{-8.01 \times 10^{-6}t^2 + 1.94 \times 10^{-3}t + 0.563} \quad (5.26)$$

where $t = (t_s - t_\infty)\theta + t_\infty$ and $T = t + 273$.

In addition, for water and a lot of liquids in the special temperature range for engineering application, it is known that the physical factor $\text{Pr} \frac{\nu_\infty}{\nu}$ can be expressed as

$$\text{Pr} \frac{\nu_\infty}{\nu} = \text{Pr}_\infty \frac{\rho}{\rho_\infty} \frac{\lambda_\infty}{\lambda}$$

Up to now, the physical property factors of Eqs. (8.26)–(8.28) have been transformed to the functions with the dimensionless temperature for convenient simultaneous solution of the governing equations.

8.6 Heat Transfer Analysis

Consulting the heat transfer analysis in Chap. 6 for gas laminar film free convection, the analytic expressions related to heat transfer of liquid laminar free convection are obtained as follows:

The *local heat transfer rate* q_x at position x per unit area from the surface of the plate to the gas will be expressed as

$$q_x = \lambda_w(t_w - t_\infty) \left(\frac{1}{4} \text{Gr}_{x,\infty} \right)^{1/4} x^{-1} \left(-\frac{d\theta}{d\eta} \right)_{\eta=0} \quad (8.29)$$

The *local heat transfer coefficient* α_x , defined as $q_x = \alpha_x(T_w - T_\infty)$, will be given by

$$\alpha_x = \lambda_w \left(\frac{1}{4} \text{Gr}_{x,\infty} \right)^{1/4} x^{-1} \left(-\frac{d\theta}{d\eta} \right)_{\eta=0} \quad (8.30)$$

The local Nusselt number defined by $\text{Nu}_{x,w} = \frac{\alpha_x}{x} \lambda_w$ will be

$$\text{Nu}_{x,w} = \left(\frac{1}{4} \text{Gr}_{x,\infty} \right)^{1/4} \left(-\frac{d\theta}{d\eta} \right)_{\eta=0} \quad (8.31)$$

Total heat transfer rate for position $x = 0$ to x with width of b on the plate is a integration $Q_x = \int \int_A q_x dA = \int_0^x q_x b dx$ and hence

$$Q_x = \frac{4}{3} b \lambda_w (t_w - t_\infty) \left(\frac{1}{4} \text{Gr}_{x,\infty} \right)^{1/4} \left(-\frac{d\theta}{d\eta} \right)_{\eta=0} \quad (8.32)$$

The *average heat transfer rate*, defined as $\bar{Q}_x = Q_x / (b \times x)$ is given by

$$\bar{Q}_x = \frac{4}{3} x^{-1} \lambda_w (T_w - T_\infty) \left(\frac{1}{4} \text{Gr}_{x,\infty} \right)^{1/4} \left(-\frac{d\theta}{d\eta} \right)_{\eta=0} \quad (8.33)$$

The *average heat transfer coefficient* $\bar{\alpha}_x$ defined as $\bar{Q}_x = \bar{\alpha}_x(T_w - T_\infty)$ is expressed as

$$\bar{\alpha}_x = \frac{4}{3} \lambda_w \left(\frac{1}{4} \text{Gr}_{x,\infty} \right)^{1/4} x^{-1} \left(-\frac{d\theta}{d\eta} \right)_{\eta=0} \quad (8.34)$$

The *average Nusselt number* is defined as $\overline{Nu}_{x,w} = \frac{\overline{\alpha_x x}}{\lambda_w}$, and hence

$$\overline{Nu}_{x,w} = \frac{4}{3} \left(\frac{1}{4} Gr_{x,\infty} \right)^{1/4} \left(-\frac{d\theta}{d\eta} \right)_{\eta=0} \quad (8.35)$$

Obviously, for practical calculation of heat transfer, only the wall dimensionless temperature gradient $\left(-\frac{d\theta}{d\eta} \right)_{\eta=0}$ dependent on the solution of governing equations is no-given variable.

8.7 Numerical Solutions

As a typical liquid laminar free convection, the water laminar free convection can be taken as an example for presentation of the numerical calculation.

The shooting method has been adopted to solve numerically the nonlinear governing Eqs. (8.23)–(8.25) with the boundary conditions (8.26) and (8.27) at different temperature conditions t_w and t_∞ . The water physical property values of ρ_∞ , ρ_w , ν_∞ , λ_∞ , and Pr_∞ at different temperatures are taken directly from the appendix of this book. The typical results for velocity and temperature fields of the boundary layer are plotted as Figs. 8.1, 8.2, 8.3 and 8.4, respectively. The corresponding solutions for the dimensionless temperature gradient $\left(-\frac{d\theta}{d\eta} \right)_{\eta=0}$ are described in Table 8.1 and plotted in Fig. 8.5. The velocity and temperature profiles show clearly the effects of the variable physical properties on velocity and temperature distributions as well as heat transfer of the water free convection. The related influences are presented as follows:

Effects of bulk temperature t_∞ :

The bulk temperature t_∞ causes a great effect on the velocity and temperature profiles. With increase of bulk temperature t_∞ , the velocity W_x and the temperature θ obviously increase, meanwhile, the maximum of w_x shifts further from the plate. While, with increase of bulk temperature t_∞ , the temperature gradient $\left(-\frac{d\theta}{d\eta} \right)_{\eta=0}$ decreases obviously.

Fig. 8.1 The velocity profiles at $t_w = 40^\circ\text{C}$ (corresponding to $Pr_w = 4.42$) with different t_∞ (1→5 cited from Shang et al. [10]) Note $t_\infty = 20, 39.99, 60, 80, \text{ and } 100^\circ\text{C}$, (corresponding to $Pr_\infty = 7.164, 4.42, 3.019, 2.232$ and 1.758, respectively)

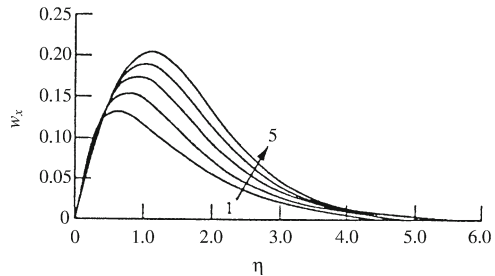


Fig. 8.2 The velocity profiles at $t_\infty = 40^\circ\text{C}$ and different surface temperatures t_w , (1 \rightarrow 5: $t_w = 20, 39.99, 60, 80,$ and 100°C), cited from Shang et al. [10]

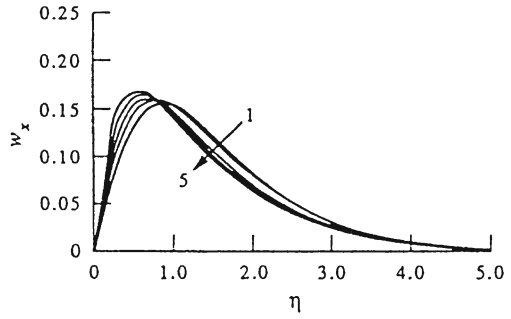


Fig. 8.3 The temperature profiles at $t_w = 40^\circ\text{C}$ and different t_∞ , (1 \rightarrow 5: $t_\infty = 20, 39.99, 60, 80,$ and 100°C), cited from Shang et al. [10]

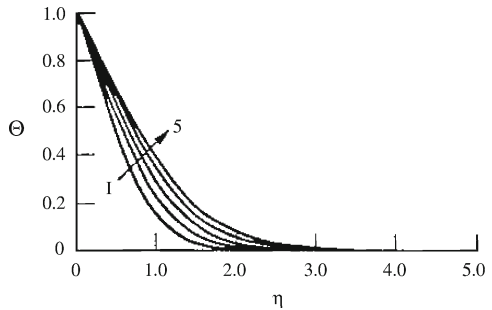
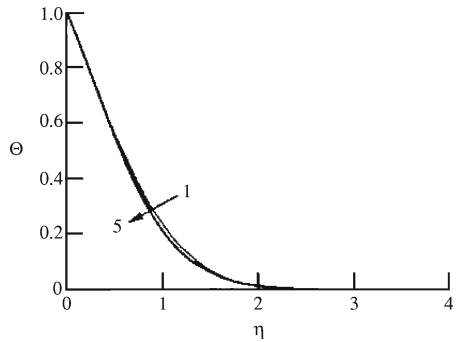


Fig. 8.4 The temperature profiles at $t_\infty = 40^\circ\text{C}$ and different surface temperatures t_w , (1 \rightarrow 5: $t_w = 20, 39.99, 60, 80,$ and 100°C), cited from Shang et al. [10]



Effects of wall temperature t_w :

The effects of wall temperature t_w on the velocity W_x and temperature θ are much less than those of wall temperature t_∞ . With the increase of wall temperature t_w , the maximum velocity of W_x increases and shifts slightly close to the plate. Generally, the effects of wall temperature t_w on the temperature θ and temperature gradient $\left(-\frac{d\theta}{d\eta}\right)_{\eta=0}$ are slightly. With increasing bulk temperature t_∞ , the effects of wall temperature t_w on the temperature θ and temperature gradient $\left(-\frac{d\theta}{d\eta}\right)_{\eta=0}$ will decrease.

Table 8.1 The typical numerical solutions of dimensionless temperature gradient $\left(-\frac{d\theta}{d\eta}\right)_{\eta=0}$ for water laminar free convection along a vertical plate, cited from Shang et al. [10]

t_∞ (°C)	Pr_∞	t_w (°C)							
		5	10	20	30	40	60	80	100
		Pr_w							
		11.207	9.565	7.164	5.547	4.420	3.019	2.232	1.758
		$\left(-\frac{d\theta}{d\eta}\right)_{\eta=0}$							
5	11.207	1.21	1.169	1.156	1.164	1.179	1.212	1.245	1.275
10	9.565	1.153	1.137	1.13	1.131	1.139	1.162	1.187	1.211
20	7.164	1.076	1.063	1.05	1.051	1.054	1.068	1.083	1.1
30	5.547	0.989	0.983	0.977	0.971	0.977	0.988	0.999	1.012
40	4.420	0.917	0.913	0.91	0.91	0.914	0.92	0.929	0.938
60	3.019	0.809	0.808	0.807	0.809	0.81	0.814	0.821	0.827
80	2.232	0.733	0.732	0.733	0.734	0.735	0.739	0.74	0.746
100	1.758	0.679	0.679	0.6790	0.68	0.681	0.683	0.685	0.686

Note The number with mark corresponding to Boussinesq approximation solutions

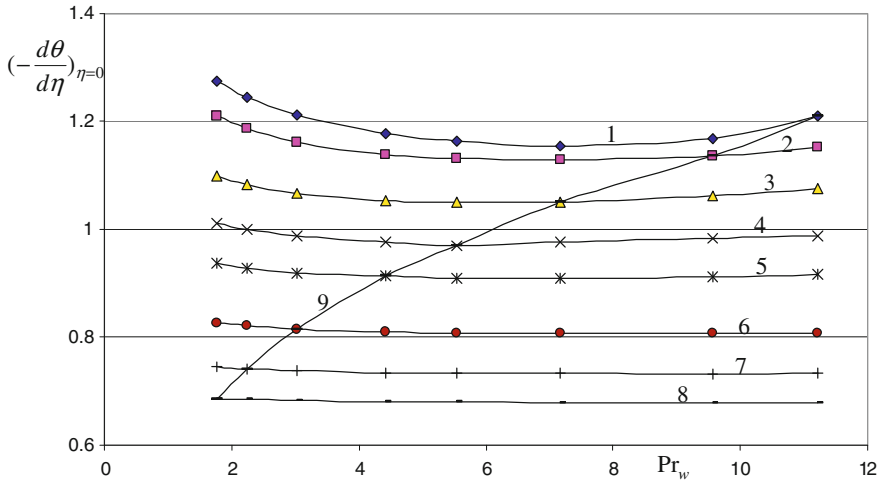


Fig. 8.5 Numerical solutions of dimensionless temperature gradient $\left(-\frac{d\theta}{d\eta}\right)_{\eta=0}$ for water laminar free convection along vertical plate. Note Lines 1 → 8 for $t_\infty = 5, 10, 20, 30, 40, 60, 80$ and 100 °C (corresponding to $Pr_\infty = 11.207, 9.565, 7.164, 5.547, 4.42, 3.019, 2.232$ and 1.758 , respectively). Line 9 for $Pr_w \rightarrow Pr_\infty$ (identical to Boussinesq approximation solution)

Furthermore, compared with wall temperature t_w , temperature t_∞ dominates the velocity and temperature fields, as well as the wall temperature gradient $\left(-\frac{d\theta}{d\eta}\right)_{\eta=0}$. Due to the reason that only the wall dimensionless temperature gradient $\left(-\frac{d\theta}{d\eta}\right)_{\eta=0}$ is no-given variable from Eqs. (8.29)–(8.35), the temperature dominates heat transfer prediction of the laminar liquid free convection.

The velocity and temperature profiles show the large differences between the momentum and temperature boundary layer thicknesses for laminar free convection of liquid due to $Pr \gg 1$. Therefore, it is very difficult to make a solution of the governing equations for liquid free convection, especially for consideration of variable thermophysical properties.

8.8 Approximation Equation on Wall Dimensionless Temperature Gradient

Boussinesq approximation could be obtained from Table 8.1 in which the plate temperature t_w is very close to the bulk temperature t_∞ .

Then, a curve-fit formula (8.36) is obtained for prediction of the solutions of liquid laminar free convection under the *Boussinesq approximation*.

$$\left(-\frac{d\theta}{d\eta}\right)_{\eta=0}^* = 0.5812Pr^{0.301} \quad (1.7 < Pr < 11.3) \quad (8.36)$$

It can be seen from the predicted values in Table 8.1 that Eq. (8.36) can very accurately simulate the related Boussinesq solutions.

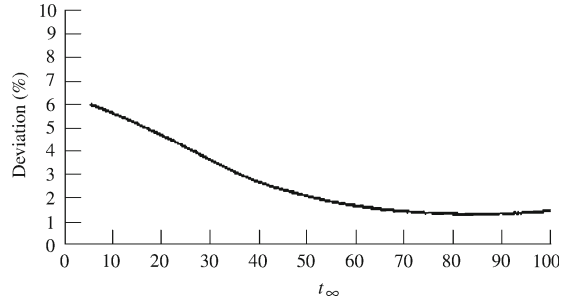
From the typical solutions for temperature gradient $\left(-\frac{d\theta}{d\eta}\right)_{\eta=0}$ in Table 8.1 it is found that the effect of t_w on temperature gradient $\left(-\frac{d\theta}{d\eta}\right)_{\eta=0}$ is not obvious generally, but the temperature t_∞ dominates the effect on the temperature gradient $\left(-\frac{d\theta}{d\eta}\right)_{\eta=0}$. On this basis, if the Prandtl number Pr in Eq. (8.36) for Boussinesq approximation solutions is replaced by a reference Prandtl number Pr_∞ as Eq. (8.37), the maximal deviation for prediction of the temperature gradient $\left(-\frac{d\theta}{d\eta}\right)_{\eta=0}$ of water laminar free convection is less than 6% for t_∞ range from 5 to 100 °C with consideration of variable physical properties. However, the maximal deviation will be less than 2% for t_∞ from 50 to 100 °C, as shown in Fig. 8.6.

$$\left(-\frac{d\theta}{d\eta}\right)_{\eta=0} = 0.5812Pr_\infty^{0.301} \quad (1.7 < Pr_\infty < 11.3) \quad (8.37)$$

where Pr_∞ is Prandtl number at bulk temperature t_∞ .

Then, Eq. (8.37) is suggested as *an approximation equation on wall dimensionless temperature gradient on an isothermal vertical flat plate*.

Fig. 8.6 Maximum calculated deviation of $\left(-\frac{d\theta}{d\eta}\right)_{\eta=0}$ by Eq. (6.52), cited from Shang et al. [10]



8.9 Approximation Equations on Heat Transfer

Therefore, combining Eq. (8.37) with Eqs. (8.29)–(8.35), we have the following *approximation equations on heat transfer* of laminar free convection of water on an isothermal vertical flat plate:

$$q_x = 0.5812\lambda_w(t_w - t_\infty) \left(\frac{1}{4}\text{Gr}_{x,\infty}\right)^{1/4} x^{-1}\text{Pr}_\infty^{0.301} \quad (8.29^*)$$

$$\alpha_x = 0.5812\lambda_w \left(\frac{1}{4}\text{Gr}_{x,\infty}\right)^{1/4} x^{-1}\text{Pr}_\infty^{0.301} \quad (8.30^*)$$

$$\text{Nu}_{x,w} = 0.5812 \left(\frac{1}{4}\text{Gr}_{x,\infty}\right)^{1/4} \text{Pr}_\infty^{0.301} \quad (8.31^*)$$

$$Q_x = 0.5812 \times \frac{4}{3} b\lambda_w(t_w - t_\infty) \left(\frac{1}{4}\text{Gr}_{x,\infty}\right)^{1/4} \text{Pr}_\infty^{0.301} \quad (8.32^*)$$

$$\bar{Q}_x = 0.5812 \times \frac{4}{3} x^{-1}\lambda_w(T_w - T_\infty) \left(\frac{1}{4}\text{Gr}_{x,\infty}\right)^{1/4} \text{Pr}_\infty^{0.301} \quad (8.33^*)$$

$$\bar{\alpha}_x = 0.5812 \times \frac{4}{3} \lambda_w \left(\frac{1}{4}\text{Gr}_{x,\infty}\right)^{1/4} x^{-1}\text{Pr}_\infty^{0.301} \quad (8.34^*)$$

$$\bar{\text{Nu}}_x = 0.5812 \times \frac{4}{3} \left(\frac{1}{4}\text{Gr}_{x,\infty}\right)^{1/4} \text{Pr}_\infty^{0.301} \quad (8.35^*)$$

Equations (8.29*)–(8.35*) are used for prediction of laminar free convection of water on an isothermal vertical flat plate with the prediction deviations between 6 and 2% from $t_\infty = 5$ to 50°C , and lower than 2% between $t_\infty = 50$ and 100°C . Anyway, the prediction deviation decreases with increasing the bulk temperature t_∞ increases.

Table 8.2 Summary of the governing equations of liquid laminar free convection and the equations related to heat transfer

Term	Expression
<i>Governing partial deferential equations</i>	
Mass equation	$\frac{\partial}{\partial x} (\rho w_x) + \frac{\partial}{\partial y} (\rho w_y) = 0$
Momentum equation	$\rho \left(w_x \frac{\partial w_x}{\partial x} + w_y \frac{\partial w_x}{\partial y} \right) = \frac{\partial}{\partial y} \left(\mu \frac{\partial w_x}{\partial y} \right) + g \rho_\infty - \rho $
Energy equation	$\rho c_p \left(w_x \frac{\partial T}{\partial x} + w_y \frac{\partial T}{\partial y} \right) = \frac{\partial}{\partial y} \left(\lambda \frac{\partial T}{\partial y} \right)$
Boundary conditions	$y = 0 : w_x = 0, w_y = 0, T = T_w$ $y \rightarrow \infty : w_x \rightarrow 0, T = T_\infty$
<i>Similarity variables</i>	
η	$\frac{y}{x} \left(\frac{1}{4} Gr_{x,\infty} \right)^{1/4}$
$Gr_{x,\infty}$	$\frac{g \rho_\infty / \rho_w - 1 x^3}{\nu_\infty^2}$
θ	$\frac{T - T_\infty}{T_w - T_\infty}$
W_x	$\left[2\sqrt{gx} \left \frac{\rho_\infty}{\rho_w} - 1 \right ^{\frac{1}{2}} \right]^{-1} w_x$
W_y	$\left[2\sqrt{gx} \left \frac{\rho_\infty}{\rho_w} - 1 \right ^{-\frac{1}{2}} \left(\frac{1}{4} Gr_{x,\infty} \right)^{-\frac{1}{4}} \right]^{-1} w_y$
<i>Governing ordinary differential equations</i>	
Mass equations	$2W_x - \eta \frac{dW_x}{d\eta} + 4 \frac{dW_x}{d\eta} - \frac{1}{\rho} \frac{d\rho}{d\eta} (\eta W_x - 4W_y) = 0$
Momentum Equation	$\frac{\nu_\infty}{\nu} \left(W_x \left(2W_x - \eta \frac{dW_x}{d\eta} \right) + 4W_y \frac{dW_x}{d\eta} \right)$ $= \frac{d^2 W_x}{d\eta^2} + \frac{1}{\mu} \frac{d\mu}{d\eta} \frac{dW_x}{d\eta} + \frac{\nu_\infty}{\nu} \frac{\frac{\rho_\infty}{\rho} - 1}{\frac{\rho_\infty}{\rho_w} - 1}$
Energy equation	$Pr \frac{\nu_\infty}{\nu} (-\eta W_x + 4W_y) \frac{d\theta}{d\eta} = \frac{1}{\lambda} \frac{d\lambda}{d\eta} \frac{d\theta}{d\eta} + \frac{d^2 \theta}{d\eta^2}$
Boundary condition	$\eta = 0 : W_x = 0, W_y = 0, \theta = 1$ $\eta \rightarrow \infty : W_x = 0, \theta = 0$

(continued)

8.10 Summary

So far, the governing equations of liquid laminar free convection and the equations related to heat transfer can be summarized in Table 8.2.

Table 8.2 (continued)

Term	Expression
<i>Treatment of variable physical properties</i>	
Temperature-dependent properties	Take water as example for polynomial expressions $\rho = -4.48 \times 10^{-3}t^2 + 999.9$ $\lambda = -8.01 \times 10^{-6}t^2 + 1.94 \times 10^{-3}t + 0.563$ $\mu = \exp \left[-1.6 - \frac{1150}{T} + \left(\frac{690}{T} \right)^2 \right] \times 10^{-3}$
Physical property factors	Take water as example for polynomial expressions $\frac{1}{\rho} \frac{d\rho}{d\eta} = \frac{-2 \times 4.48 \times 10^{-3}t(t_w - t_\infty)}{-4.48 \times 10^{-3}t^2 + 999.9} \frac{d\theta}{d\eta}$ $\frac{1}{\mu} \frac{d\mu}{d\eta} = \left(\frac{1150}{T^2} - 2 \times \frac{690^2}{T^3} \right) (t_w - t_\infty) \frac{d\theta}{d\eta}$ $\frac{1}{\lambda} \frac{d\lambda}{d\eta} = \frac{(-2 \times 8.01 \times 10^{-6}t + 1.94 \times 10^{-3})(t_w - t_\infty) \frac{d\theta}{d\eta}}{-8.01 \times 10^{-6}t^2 + 1.94 \times 10^{-3}t + 0.563}$
Wall dimensionless temperature gradient	$\left(-\frac{d\theta}{d\eta} \right)_{\eta=0}$ (for water free convection)
For Boussinesq solution	$\left(-\frac{d\theta}{d\eta} \right)_{\eta=0}^* = 0.5812 \text{Pr}^{0.301} \quad (1.7 < \text{Pr} < 11.3)$
Approximation equation for consideration of variable physical properties	$\left(-\frac{d\theta}{d\eta} \right)_{\eta=0} = 0.5812 \text{Pr}_\infty^{0.301} \quad (1.7 < \text{Pr} < 11.3)$
<i>Approximation equations on heat transfer for water free convection with consideration of variable physical properties (for water free convection)</i>	
q_x (defined as $-\lambda_w \left(\frac{\partial T}{\partial y} \right)_{y=0}$)	$q_x = 0.5812 \text{Pr}_\infty^{0.301} \lambda_w (t_w - t_\infty) \left(\frac{1}{4} \text{Gr}_{x,\infty} \right)^{1/4} x^{-1} \text{Pr}_\infty^{0.301}$
α_x (defined as $\frac{q_x}{(T_w - T_\infty)}$)	$\alpha_x = 0.5812 \text{Pr}_\infty^{0.301} \lambda_w \left(\frac{1}{4} \text{Gr}_{x,\infty} \right)^{1/4} x^{-1} \text{Pr}_\infty^{0.301}$
Q_x (defined as $\int_0^x q_x b dx$)	$Q_x = 0.5812 \times \frac{4}{3} b \lambda_w (t_w - t_\infty) \left(\frac{1}{4} \text{Gr}_{x,\infty} \right)^{1/4} \text{Pr}_\infty^{0.301}$
\bar{Q}_x , defined as $Q_x / (b \times x)$	$\bar{Q}_x = 0.5812 \times \frac{4}{3} x^{-1} \lambda_w (T_w - T_\infty) \left(\frac{1}{4} \text{Gr}_{x,\infty} \right)^{1/4} \text{Pr}_\infty^{0.301}$
$\bar{\alpha}_x$ (defined as $\frac{Q_x}{(T_w - T_\infty) b x}$)	$\bar{\alpha}_x = 0.5812 \times \frac{4}{3} \lambda_w \left(\frac{1}{4} \text{Gr}_{x,\infty} \right)^{1/4} x^{-1} \text{Pr}_\infty^{0.301}$
$\text{Nu}_{x,w}$ (defined as $\frac{\alpha_x x}{\lambda_w}$)	$\text{Nu}_{x,w} = 0.5812 \times \left(\frac{1}{4} \text{Gr}_{x,\infty} \right)^{1/4} \text{Pr}_\infty^{0.301}$
$\bar{\text{Nu}}_{x,w}$ (defined as $\frac{\bar{\alpha}_x x}{\lambda_w}$)	$\bar{\text{Nu}}_{x,w} = 0.5812 \times \frac{4}{3} \left(\frac{1}{4} \text{Gr}_{x,\infty} \right)^{1/4} \text{Pr}_\infty^{0.301}$

8.11 Remarks

In this chapter, laminar free convection of liquids is extensively investigated. The new similarity analysis method is used conveniently to transform the governing partial differential equations of laminar free convection of liquid into the corresponding dimensionless system. Taking water as an example, the polynomial is used for expressions of temperature-dependent density, thermal conductivity, and viscous, while the specific heat at constant pressure is taken as constant with maximum possible deviation of 0.45 % only. These expressions are reliable because they are based on the typical experimental data of the physical properties.

By means of the provided equations on the physical property factors coupled with the governing ordinary differential equations, the non-linear governing equations with corresponding boundary conditions can be simultaneously solved numerically for velocity and temperature fields. Taking water laminar free convection along an isothermal vertical plate as an example, the coupled effect of variable physical properties was investigated. It is found that compared with the wall temperature, the effect of bulk temperature dominates heat transfer of laminar free convection. By means of heat transfer analysis based on the new similarity analysis model, it is found that the wall temperature gradient $\left(-\frac{d\theta}{d\eta}\right)_{\eta=0}$ is the only one no-given condition for prediction of heat transfer. The approximation equation for prediction of the temperature gradient $\left(-\frac{d\theta}{d\eta}\right)_{\eta=0}$ of laminar water free convection is presented for consideration of coupled effect of variable physical properties. Then, the equations for practical prediction of heat transfer of laminar water free convection are provided.

8.12 Calculation Examples

Example 1:

A flat plate with $b = 1$ m in width and $x = 0.25$ m in length is suspended vertically in the space of water. The ambient temperature is $t_{\infty} = 5^{\circ}\text{C}$, and the plate temperature is $t_w = 60^{\circ}\text{C}$. The water properties are as follows:

$$\nu_{\infty} = 1.5475 \times 10^{-6} \text{ m}^2/\text{s}, \text{Pr}_{\infty} = 11.16 \text{ and } \rho_{\infty} = 999.8 \text{ kg/m}^3 \text{ at } t_{\infty} = 5^{\circ}\text{C}; \lambda_w = 0.659 \text{ W/(m}^{\circ}\text{C)} \text{ and } \rho_w = 983.3 \text{ kg/m}^3 \text{ at } t_w = 60^{\circ}\text{C}.$$

Suppose the free convection is laminar, please calculate the free convection heat transfer on the plate.

Solution:

With the definition of local Grashof number shown in Eq. (8.10), we have

$$\begin{aligned}
 \text{Gr}_{x,\infty} &= \frac{g |\rho_\infty / \rho_w - 1| x^3}{\nu_\infty^2} \\
 &= \frac{9.8 \times |999.8/983.8 - 1| \times 0.25^3}{(1.5475 \times 10^{-6})^2} \\
 &= 1.04 \times 10^9
 \end{aligned}$$

The flow of free convection can be regarded as laminar flow.

With Eq. (8.37), the dimensionless temperature gradient $\left(-\frac{d\theta}{d\eta}\right)_{\eta=0}$ for water laminar free convection can be calculated by the following equation:

$$\begin{aligned}
 \left(-\frac{d\theta}{d\eta}\right)_{\eta=0} &= 0.5812 \text{Pr}_\infty^{0.301} \\
 &= 0.5812 \times 11.207^{0.301} \\
 &= 1.202879
 \end{aligned}$$

On this basis, the following average Nusselt number $\overline{\text{Nu}}_{x,w}$ can be obtained as

$$\begin{aligned}
 \overline{\text{Nu}}_{x,w} &= -\frac{4}{3} \left(\frac{1}{4} \text{Gr}_{x,\infty}\right)^{1/4} \left(\frac{d\theta}{d\eta}\right)_{\eta=0} \\
 &= (4/3) \times (0.25 \times 1.04 \times 10^9)^{1/4} \times 1.202879 \\
 &= 203.6
 \end{aligned}$$

With the definition of average Nusselt number, $\overline{\text{Nu}}_{x,w} = \frac{\bar{\alpha}_x X}{\lambda_w}$, the following average heat transfer coefficient can be calculated as

$$\bar{\alpha}_x = \overline{\text{Nu}}_{x,w} \frac{\lambda_w}{x} = 203.6 \times \frac{0.659}{0.25} = 536.7 \text{ W}/(\text{m}^2 \cdot ^\circ\text{C})$$

With the definition of the average heat transfer coefficient, $Q_x = \bar{\alpha}_x (t_w - t_\alpha) \times x \times b$, we obtain the following total free convection heat transfer on the plate

$$\begin{aligned}
 Q_x &= \bar{\alpha}_x (t_w - t_\alpha) \times x \times b \\
 &= 536.7 \times (60 - 5) \times 0.25 \times 1 \\
 &= 7379.6 \text{ W} \\
 &= 7.3796 \text{ kW}
 \end{aligned}$$

Example 2:

For the flat plate of question 1, if the plate height is changed into 0.11 m, and temperatures are changed into $t_\infty = 60^\circ\text{C}$ and $t_w = 5^\circ\text{C}$, please calculate the corresponding heat transfer.

The water physical properties are as follows:

kinematic viscosity $\nu_\infty = 0.478 \times 10^{-6} \text{ m}^2/\text{s}$, Prandtl number $\text{Pr}_\infty = 3$, and the density at $\rho_\infty = 983.1 \text{ kg/m}^3$ at $t_\infty = 60^\circ\text{C}$ thermal conductivity $\lambda_w = 0.5625$ and density $\rho_w = 999.8 \text{ kg/m}^3$ at $t_w = 5^\circ\text{C}$.

Solution:

With the definition of local Grashof number shown in Eq. (8.10), we get

$$\begin{aligned} \text{Gr}_{x,\infty} &= \frac{g |\rho_\infty/\rho_w - 1| x^3}{\nu_\infty^2} \\ &= \frac{9.8 \times |983.1/999.8 - 1| \times 0.11^3}{(0.478 \times 10^{-6})^2} \\ &= 0.95357 \times 10^9 \end{aligned}$$

The free convection can be regarded as laminar flow.

With Eq. (8.37), the dimensionless temperature gradient $\left(-\frac{d\theta}{d\eta}\right)_{\eta=0}$ will be

$$\begin{aligned} \left(-\frac{d\theta}{d\eta}\right)_{\eta=0} &= 0.5812 \text{Pr}_\infty^{0.301} \\ &= 0.5812 \times 3.019^{0.301} \\ &= 0.810521 \end{aligned}$$

On this basis, with Eq. (8.49) the following average Nusselt number, $\overline{\text{Nu}}_{x,w}$, can be obtained as

$$\begin{aligned} \overline{\text{Nu}}_{x,w} &= -\frac{4}{3} \left(\frac{1}{4} \text{Gr}_{x,\infty}\right)^{1/4} \left(\frac{d\theta}{d\eta}\right)_{\eta=0} \\ &= (4/3) \times (0.25 \times 0.95357 \times 10^9)^{1/4} \times 0.810521 \\ &= 133.5482 \end{aligned}$$

With the definition of average Nusselt number, $\overline{\text{Nu}}_{x,w} = \frac{\bar{\alpha}_x X}{\lambda_w}$, the following mean heat transfer coefficient can be calculated as

$$\bar{\alpha}_x = \overline{\text{Nu}}_{x,w} \frac{\lambda_w}{x} = 133.5482 \times \frac{0.5625}{0.11} = 682.9169 \text{ W/m}^2 \text{ }^\circ\text{C}$$

With the definition of the average heat transfer coefficient $\bar{\alpha}_x$, $Q_x = \bar{\alpha}_x (t_w - t_\infty) \times x \times b$, we have the following free convection heat transfer on the plate

$$\begin{aligned}
 Q_x &= \bar{\alpha}_x(t_w - t_\infty) \times x \times b \\
 &= 682.9169 \times (5 - 60) \times 0.11 \times 1 \\
 &= -4131.65 \text{ W} \\
 &= -4.131615 \text{ kW}
 \end{aligned}$$

The negative sign denotes the heat flux is to the plate from the liquid.

8.13 Exercises

1. Please give a detailed derivation for obtaining the governing ordinary differential Eqs. (8.23)–(8.25) for liquid laminar free convection.
2. Please analyze the identity of the similarity mathematical models of laminar free convection of liquid and gas.
3. Please explain the reason to, respectively, investigate laminar free convection of liquid and gas with consideration of variable physical properties.
4. Please give out the related derivations for obtaining the heat transfer analysis Eqs. (8.29)–(8.35) for liquid laminar free convection.
5. Please point out the effect of wall temperature on velocity and temperature fields of laminar liquid free convections.
6. Please point out the effect of bulk temperature on velocity and temperature fields of laminar liquid free convection.
7. How do you know the bulk temperature dominates heat transfer of laminar liquid free convection?
8. Follow example 1. Only the ambient temperature is $t_\infty = 60^\circ\text{C}$, and the plate temperature is $t_w = 5^\circ\text{C}$. Suppose the free convection is laminar.
 - (i) Please calculate the free convection heat transfer on the plate.
 - (ii) Please calculate the free convection heat transfer on the plate under Boussinesq approximation.
9. Please calculate the questions (i) and (ii) of exercise 9 by using the related empirical equation.
10. Do you think the treatment of variable physical properties in this chapter is reliable?

References

1. T. Fujii et al., Experiments on natural convection heat transfer from the outer surface of a vertical cylinder to liquids. *Int. J. Heat Mass Transf.* **13**, 753–787 (1970)
2. T. Fujii, Heat transfer from a vertical flat surface by laminar free convection—The case where the physical constants of fluids depend on the temperature and the surface has an arbitrary

- temperature distribution in the vertical direction. *Trans. Japan. Soc. Mech. Eng.* **24**, 964–972 (1958)
3. S. Akagi, Free convection heat transfer in viscous oil. *Trans. Jpn. Soc. Mech. Eng.* **30**, 624–635 (1964)
 4. J.M. Piau, in *Convection Natural Laminaire en Regime Permanent dans les Liquids*, ed. by C.R. Hebd. Influence des Variations des Proprieties Physique avec la Temperature, vol. 271 (Seanc Acad Sci., Paris, 1970), pp. 935–956
 5. J.M. Piau, Influence des variations des proprieties physiques et la stratification en convection naturelle. *Int. J. Heat Mass Transf.* **17**, 465–476 (1974)
 6. A. Brown, The effect on laminar free convection heat transfer of temperature dependence of the coefficient of volumetric expansion. *Trans. ASME Ser. C J. Heat Transf.* **97**, 133–135 (1975)
 7. V.P. Carey, J.C. Mollendorf, Natural convection in liquids with temperature dependence viscosity, in *Proceedings of the Sixth International Heat Transfer Conference*, Toronto, 1978. NC-5, vol. 2 (Hemisphere, Washington, DC, 1978), pp. 211–217
 8. P. Sabhapathy, K.C. Cheng, The effect of temperature-dependent viscosity and coefficient of thermal expansion on the stability of laminar, natural convective flow along an isothermal, vertical surface. *Int. J. Heat Mass Transf.* **29**, 1521–1529 (1986)
 9. Z.H. Qureshi, B. Gebhart, The stability of vertical thermal buoyancy induced flow in cold pure and saline water. *Int. J. Heat Mass Transf.* **29**, 1383–1392 (1986)
 10. D.Y. Shang, B.X. Wang, Y. Wang, Y. Quan, Study on liquid laminar free convection with consideration of variable thermophysical properties. *Int. J. Heat Mass Transf.* **36**(14), 3411–3419 (1993)

Chapter 9

Experimental Measurements of Free Convection with Large Temperature Difference

Abstract Experimental investigations were carried out to verify the results of the previous chapters for effects of variable physical properties on laminar free convection of air and water. By increasing the wall temperature for the liquid laminar free convection or increasing the boundary temperature ratio for gas laminar free convection of gas, the velocity component of the free convection increases, and the velocity profile moves to the direction of the flat plate. Consequently, the thickness of the velocity boundary layer decreases. With an increase of the plate height x , the velocity component of water or air free convection increases, and the velocity profile moves toward to the fluid bulk. As a result, the thickness of velocity boundary layer increases. It is found that the agreement between the measured and calculated velocity fields is good, thus it is confirmed that the results in Chaps. 6–8 are reliable.

9.1 Introduction

The classical measurement of the velocity field for free convection of air along an isothermal vertical plate was originally made by Schmidt and Beckman [1]. Their results showed excellent agreement with the corresponding numerical results for the Boussinesq approximation calculated by Pohlhausen [2] shown in Fig. 9.1. It is further seen that the velocity and thermal boundary-layer thicknesses are proportional to $x^{1/4}$.

However, in their experimental measurements only small differences between the surface and the ambient temperatures were considered, since there has been a shortage of accurate measuremental results for consideration of the larger temperature differences. The reasons of this shortage are twofold: (i) the lower velocity of free convection and (ii) the restriction of the measuring devices. First of all, the fluid velocity in free convection is typically much slower. In consequence of this, the experimental measurements become more difficult and less reliable due to the increasing influence of various interferences. In addition, due to the weak flow of

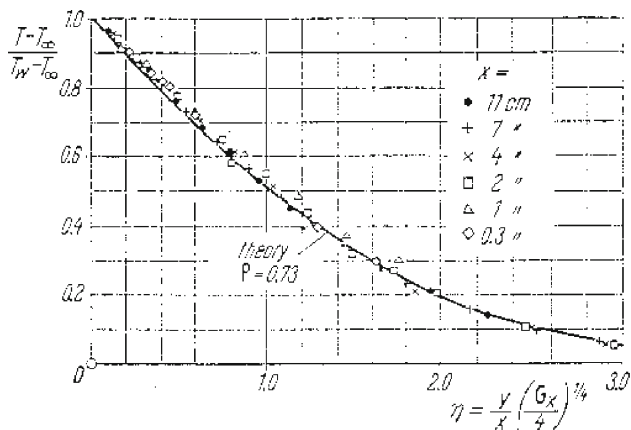
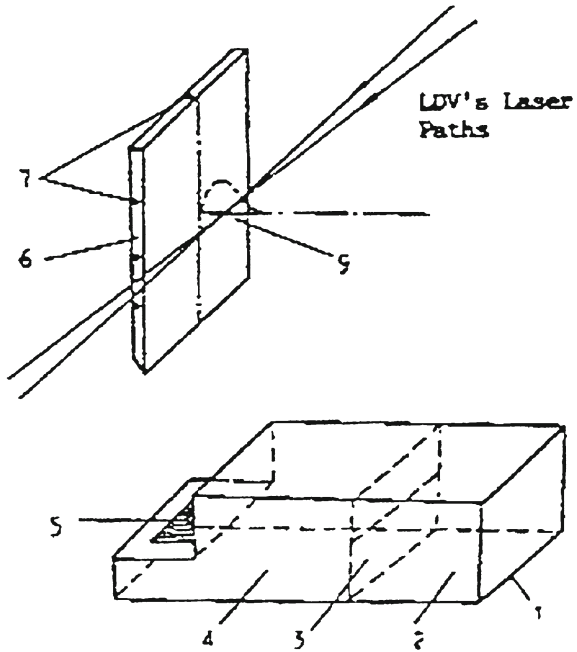


Fig. 9.1 Velocity distribution in the laminar boundary layer on a hot vertical flat plate in natural convection of air, as measured by Schmidt and Beckmann [1] (From Schlichting [3])

free convection, the pressure gradients are also quite small and the measuremental techniques based on pressure differences, such as the Pitot tube, cannot be used very accurately. The hot-wire anemometer has been used in velocity measurements, but its basic principle is heat transfer from a heated wire. The heat transfer from the wire is dependent on the flow velocity. However, the major problem that easily produces deviation for the measurement in free convection is the small magnitude of the velocity. Additionally, since the velocity boundary layer for the free convection is very thin, with the above instrument, the interference, which cannot be negligible, will be manifest in the measurement.

Fortunately, the laser doppler velocimeter (LDV) has been developed in recent years. The LDV demonstrates higher accuracy for the measurement of fluid velocity. An instrument, which does not contact the flow field, will not produce any interference in the velocity field. It can measure very low velocity flow. All these features give LDV great advantage over hot-wire anemometers. With consideration of variable thermophysical properties, two experimental results of the laminar free convection for air and water for larger temperature differences, which were provided by Shang and Wang [4–6], are introduced in this chapter. The experimental results were verified by the calculation methods with consideration of variable thermophysical properties introduced in Chaps. 6 and 8 respectively. In this chapter we discuss the measurements of the velocity fields in the laminar boundary layer for free convection of air and water studied with the LDV. Large temperature differences were considered in the experimental measurements for the free convection. The experimental results were verified by the corresponding numerical solutions, and it is shown that the experimental results agreed well with the corresponding numerical solutions for variable thermophysical properties.

Fig. 9.2 Schematic diagram of experimental device, cited from Shang and Wang [4]: 1 particulate generator, 2 chamber of mosquito-repellent incense, 3 spacer, 4 storage smoke chamber, 5 wire net of copper, 6 isothermal flat plate, 7. thermocouples, 8 focus of lasers



9.2 Experimental Measurements of Velocity Field for Air Laminar Free Convection

9.2.1 Experimental Devices and Instruments

The experimental device established is shown schematically in Fig. 9.2. It consists essentially of three parts: an isothermal vertical testing plate, LDV, and a particulate generator.

Isothermal testing plate. This is a flat copper plate with a polished surface, 300 mm in height, 195 mm in width, and 7 mm in thickness. A sharp angle is made at the bottom of the plate to minimize the possible distortion of the measured velocity field for air free convection. A thin film heater is embedded in the testing plate, the electric power supplied to the heater being adjusted by a current transformer. ϕ 0.1 mm Cu–Constantan thermocouples are installed in the plate to monitor and measure the temperature.

LDV. The short wavelength LDV at Northeastern University was used to measure the velocity field of air free convection. The velocity measured with this LDV is so small that it is suitable for detecting the air velocity field being studied.

Particulate generator. The experimental measurement of the velocity field by the LDV requires a particulate generator with an ability to track the air convection. The particulate generator, as shown in Fig. 9.2, consists of a chamber for burning

Table 9.1 The measurement conditions with the related thermophysical properties for air free convection

Heights (m)	Temperature conditions (K)	$\nu_{\infty} \times 10^6$ (m ² /s)
$x = 0.025$	$T_w/T_{\infty} = 1.1$ and $T_{\infty} = 291$	14.88
	$T_w/T_{\infty} = 1.5$ and $T_{\infty} = 293$	15.06
	$T_w/T_{\infty} = 1.8$ and $T_{\infty} = 287$	14.52
$x = 0.05$	$T_w/T_{\infty} = 1.1$ and $T_{\infty} = 291$	14.88
	$T_w/T_{\infty} = 1.5$ and $T_{\infty} = 293$	15.06
	$T_w/T_{\infty} = 1.8$ and $T_{\infty} = 287$	14.52
$x = 0.1$	$T_w/T_{\infty} = 1.1$ and $T_{\infty} = 291$	14.88
	$T_w/T_{\infty} = 1.5$ and $T_{\infty} = 293$	15.06
	$T_w/T_{\infty} = 1.8$ and $T_{\infty} = 287$	14.52
$x = 0.15$	$T_w/T_{\infty} = 1.1$ and $T_{\infty} = 291$	14.88
	$T_w/T_{\infty} = 1.5$ and $T_{\infty} = 293$	15.06
	$T_w/T_{\infty} = 1.8$ and $T_{\infty} = 287$	14.52

mosquito-repellent incense, a storage chamber of smoke, and a net made of copper wire. The mosquito-repellent incense is burnt in the burning chamber and the smoke produced enters into the storage chamber through the upper gap of the spacer. The smoke cools down in a storage chamber, and then, diffuses through a copper-wire net into the air stream. The velocity of the smoke through the net is very small, and consequently it will disturb the velocity field only to a very small extent.

9.2.2 Measurement Results

Experiments were conducted at three temperature conditions: $T_w/T_{\infty} = 1.1$ and $T_{\infty} = 291$ K; $T_w/T_{\infty} = 1.5$ and $T_{\infty} = 293$ K; and $T_w/T_{\infty} = 1.8$ and $T_{\infty} = 287$ K. For each case, the measurements were made at four heights counted from the bottom edge of the testing plate, i.e. $x = 25$ mm, $x = 50$ mm, $x = 100$ mm and $x = 150$ mm. The measurement conditions with the related thermophysical properties for air are listed in Table 9.1. Measured velocities w_x are plotted in Figs. 9.3, 9.4 and 9.5. It is clear from each of the figures that, w_x would increase along x , and simultaneously, the position for maximum w_x shifts far away from the surface. Comparing the results shown in Figs. 9.3–9.5, it is also seen that, for the same height, x , the larger the boundary temperature ratio T_w/T_{∞} the thinner the thickness of boundary layer would be, and so, the position of maximum w_x will be closer to the plate surface with an increased value of maximum w_x . Additionally, the dimensionless velocity component w_x transformed by using Eqs. (9.1) and (9.2) are plotted in Figs. 9.6, 9.7, and 9.8, respectively.

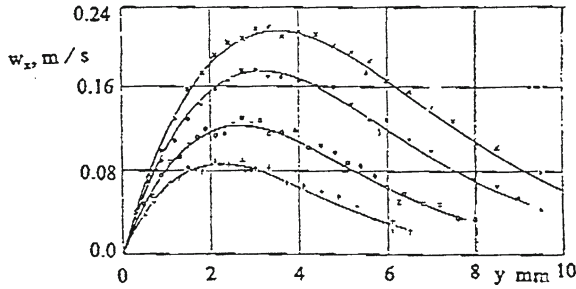


Fig. 9.3 Measured and calculated values for the dimensional velocity of air free convection for conditions $T_w/T_\infty = 1.1$ and $T_\infty = 291$ K, cited from Shang and Wang [4]; +, $x = 0.025$ m; ■, $x = 0.050$ m; □, $x = 0.100$ m; ×, $x = 0.150$ m; — numerical prediction

Fig. 9.4 Measured and calculated values for dimensional velocity of air free convection for conditions $T_w/T_\infty = 1.5$ and $T_\infty = 293$ K, cited from Shang and Wang [4]; +, $x = 0.025$ m; ■, $x = 0.050$ m; □, $x = 0.100$ m; ×, $x = 0.150$ m; — numerical prediction

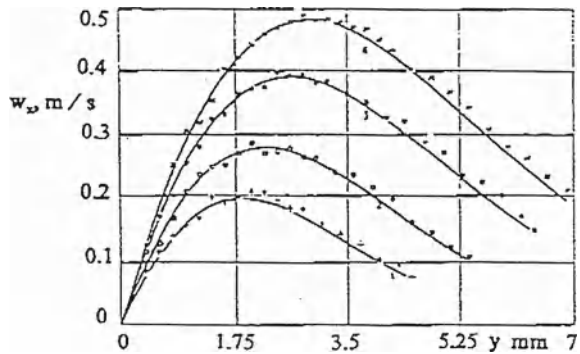
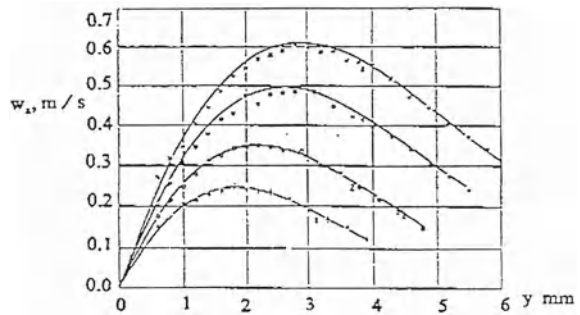


Fig. 9.5 Measured and calculated values for dimensional velocity of air free convection for condition $T_w/T_\infty = 1.8$ and $T_\infty = 287$ K, cited from Shang and Wang [4]; +, $x = 0.025$ m; ■, $x = 0.050$ m; □, $x = 0.100$ m; ×, $x = 0.150$ m; — numerical prediction



9.2.3 Governing Equations

The governing partial differential equations of gas laminar free convection and their boundary conditions are shown as Eqs. (6.1)–(6.5) in Chapter 6. According to Chap. 6, the related defined similarity variables are shown as

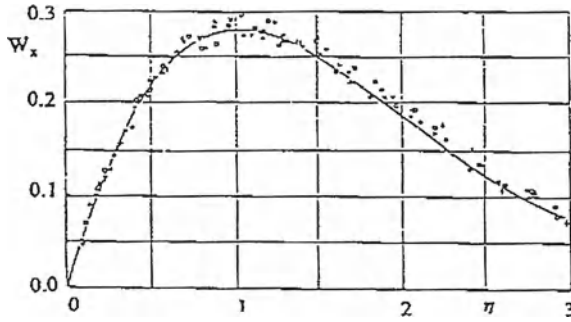


Fig. 9.6 Measured and calculated values for dimensionless velocity of air free convection for condition $T_w/T_\infty = 1.1$ and $T_\infty = 291$ K, cited from Shang and Wang [4]: +, $x = 0.025$ m; ■, $x = 0.050$ m; □, $x = 0.100$ m; ×, $x = 0.150$ m; — numerical prediction

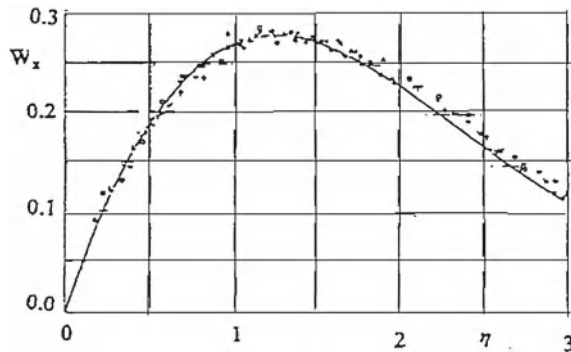


Fig. 9.7 Measured and calculated values for dimensionless velocity of air free convection for condition $T_w/T_\infty = 1.5$ and $T_\infty = 293$ K, cited from Shang and Wang [4]: +, $x = 0.025$ m; ■, $x = 0.050$ m; □, $x = 0.100$ m; ×, $x = 0.150$ m; — numerical prediction

$$\eta = \frac{y}{x} \left(\frac{1}{4} Gr_{x,\infty} \right)^{1/4} \quad Gr_{x,\infty} = \frac{g(T_w/T_\infty - 1)x^3}{\nu_\infty^2} \tag{9.1}$$

$$W_x = \left[2\sqrt{gx}(T_w/T_\infty - 1)^{1/2} \right]^{-1} w_x \tag{9.2}$$

$$W_y = \left[2\sqrt{gx} |T_w/T_\infty - 1|^{1/2} \left(\frac{1}{4} Gr_{x,\infty} \right)^{-1/4} \right]^{-1} w_y \tag{9.3}$$

and the transformed dimensionless governing equations and boundary conditions are

$$\left(2W_x - \eta \frac{dW_x}{d\eta} + 4 \frac{dW_y}{d\eta} \right) - \frac{1}{\rho} \frac{d\rho}{d\eta} (\eta W_x - 4W_y) = 0 \tag{9.4}$$

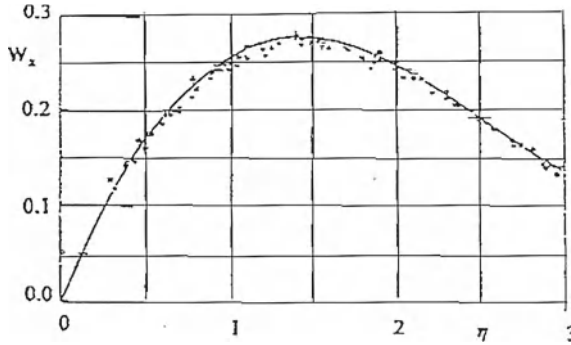


Fig. 9.8 Measured and calculated values for dimensionless velocity of air free convection for condition $T_w/T_\infty = 1.8$ and $T_\infty = 287\text{ K}$, cited from Shang and Wang [4]: +, $x = 0.025\text{ m}$; ■, $x = 0.050\text{ m}$; □, $x = 0.100\text{ m}$; ×, $x = 0.150\text{ m}$; — numerical prediction

$$\frac{\nu_\infty}{\nu} \left[W_x \left(2W_x - \eta \frac{dW_x}{d\eta} \right) + 4W_y \frac{dW_x}{d\eta} \right] = \frac{d^2 W_x}{d\eta^2} + \frac{1}{\mu} \frac{d\mu}{d\eta} \frac{dW_x}{d\eta} + \frac{\nu_\infty}{\nu} \theta \quad (9.5)$$

$$\text{Pr} \frac{\nu_\infty}{\nu} \left(-\eta W_x + 4W_y \right) \frac{d\theta}{d\eta} = \frac{d^2 \theta}{d\eta^2} + \frac{1}{\lambda} \frac{d\lambda}{d\eta} \frac{d\theta}{d\eta} \quad (9.6)$$

$$\eta = 0, \quad W_x = 0, \quad W_y = 0, \quad \theta = 1 \quad (9.7)$$

$$\eta \rightarrow \infty, \quad W_x \rightarrow 0, \quad \theta \rightarrow 0 \quad (9.8)$$

for the gas laminar free convection.

9.2.4 The Numerical Solutions

By using the shooting method, the governing dimensionless differential equations (9.4)–(9.6) with their boundary conditions are solved for $T_w/T_\infty = 1.1$ and $T_\infty = 291\text{ K}$; $T_w/T_\infty = 1.5$ and $T_\infty = 293\text{ K}$; and $T_w/T_\infty = 1.8$ and $T_\infty = 287\text{ K}$, respectively, for the air free convection ($n_\mu = 0.68$, $n_\lambda = 0.81$). The numerical solutions for dimensionless velocity components W_x are plotted also in Figs. 9.3, 9.4, and 9.5. The dimensionless numerical solutions transformed by using Eq. (9.1) and (9.2) are plotted in Figs. 9.6–9.8, respectively. It can be seen that the measured results agree very well with the predicted results.

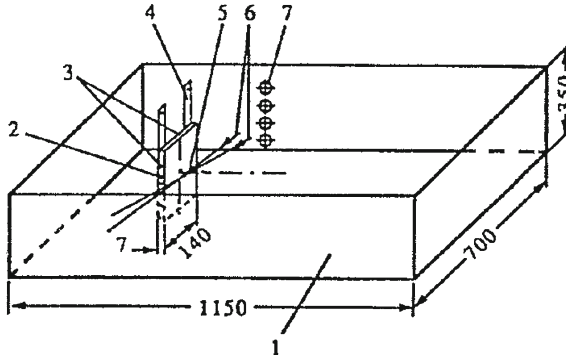


Fig. 9.9 Schematic diagram of the device used in the experiment of water free convection, cited from Shang et al. [6]: 1 water tank, 2 isothermal vertical flat plate, 3 thermocouples, 4 metal plate, 5 focus of laser, 6 laser paths, 7 drilled hole for laser path

9.3 Experimental Measurements of Velocity Field for Water Laminar Free Convection

9.3.1 Main Experimental Apparatus

An isothermal vertical flat plate, a LDV, and a water tank (see Fig.9.9) constitute the main experimental apparatus.

Isothermal vertical flat plate. The isothermal vertical flat plate (called here the plate) made of copper, is 250 mm in length, 140 mm in width and 7 mm in thickness. The surface of the plate is well polished. In the Plate, a Nickel–Chromium wire of 0.5 mm in diameter and 389 m in length is uniformly inserted. The Nickel–Chromium wire serves as an electrical heat source, and it is insulated. A sharp angle is made in the bottom of the plate so that the velocity field would not be influenced by the free convection near to the bottom surface. Thermocouples are installed in the Plate and are very close to the surface. By controlling the electric current passing through the Nickel–Chromium wire, the temperature at the surface of the Plate will be maintained at a certain level. On the top of the plate, two metal plates with 150 mm in length and 3 mm in thickness are welded. The upper part of both metal plates is drilled so that the Plate can be suspended on the frame.

LDV. The equipment used to measure the velocity field of the water free convection on the plate is the LDV of the 606 Institute in Shenyang. In order to measure very small velocities such as that of water free convection, the technique of frequency-deviation-shift is applied to the LDV.

Water tank. The water tank is rectangular in shape. It is made of organic glass plate with 8 mm thickness. The top of the water tank is open. The tank is 1.1 m in length, 0.7 m in width and 0.35 m in height. With such a large space the water tank can efficiently keep away the free convection near to the surface of the plate

Table 9.2 The measurement conditions

Heights (m)	Temperature (°C)
$x = 0.05$	$t_w = 40$ and $t_\infty = 20$
	$t_w = 50$ and $t_\infty = 20$
	$t_w = 60$ and $t_\infty = 20$
$x = 0.10$	$t_w = 40$ and $t_\infty = 20$
	$t_w = 50$ and $t_\infty = 20$
	$t_w = 60$ and $t_\infty = 20$
$x = 0.15$	$t_w = 40$ and $t_\infty = 20$
	$t_w = 50$ and $t_\infty = 20$
	$t_w = 60$ and $t_\infty = 20$
$x = 0.20$	$t_w = 40$ and $t_\infty = 20$
	$t_w = 50$ and $t_\infty = 20$
	$t_w = 60$ and $t_\infty = 20$

face from any disturbing influences. In the side of the tank are drilled four drill ways of 20 mm diameter each. The drilled ways serve as paths of laser light. Through the drill ways the laser will reach the surface of the plate to measure the velocity field of the water free convection. The distance between each two centers of the drilled ways is 50 mm, which just matches the measured heights. The locations of the drilled ways are covered with the thin organic glass, 1 mm in thickness, so that the laser power wasted though the organic glass can be minimized.

9.3.2 The Results of Experiment

At the start of this experiment the surface of the plate should be heated slowly so that the temperature of the plate rises slowly. For this purpose the voltage and electricity current through the Nickel–Chromium wire is increased slowly by means of a voltage regulator. After the temperature of the measured surface is raised to given level, the temperature is stabilized for three minutes, and then the measurements commenced.

In this experiment, the measurements are carried out under three temperature conditions: $t_w = 40^\circ\text{C}$ and $t_\infty = 20^\circ\text{C}$, $t_w = 50^\circ\text{C}$ and $t_\infty = 20^\circ\text{C}$, $t_w = 60^\circ\text{C}$ and $t_\infty = 20^\circ\text{C}$, respectively. For each condition the measurements are made at four heights from the bottom of the Plate, i.e., $x = 0.05\text{ m}$, $x = 0.10\text{ m}$, $x = 0.15\text{ m}$ and $x = 0.20\text{ m}$. The measurement conditions are listed in Table 9.2 in detail. The measured values of the velocity components w_x are described in Tables 9.4–9.6 and plotted in Figs. 9.10–9.12, respectively. The measured values w_x and the corresponding co-ordinate variable x are further transformed to the dimensionless values by using the expressions (9.9)–(9.11), described in Tables 9.4–9.6 and Figs. 9.13–9.15, respectively.

Table 9.3 Water property values

t (°C)	20	40	50	60
ρ (kg/m ³)	998.3	992.3	988.1	983.2
λ [W/(mK)]	0.5996	–	–	–
$\nu \times 10^{-6}$ [kg/(ms)]	1.004	–	–	–
Pr	6.99	–	–	–

9.3.3 Governing Equations

The governing partial differential equations of liquid laminar free convection and their boundary conditions are shown as Eqs. (8.1)–(8.5) in Chapter 8. According to Chapter 8, the related defined similarity variables for liquid laminar free convection are shown as

$$\eta = \left(\frac{1}{4} \text{Gr}_{x,\infty} \right)^{1/4} \frac{y}{x}, \quad \text{Gr}_{x,\infty} = \frac{g |\rho_\infty / \rho_w - 1| x^3}{\nu_\infty^2} \quad (9.9)$$

$$W_x = \left(2\sqrt{gx} |\rho_\infty / \rho_w - 1|^{1/2} \right)^{-1} w_x \quad (9.10)$$

$$W_y = \left[2\sqrt{gx} \left| \frac{\rho_\infty}{\rho} - 1 \right|^{-\frac{1}{2}} \left(\frac{1}{4} \text{Gr}_{x,\infty} \right)^{-\frac{1}{4}} \right]^{-1} w_y \quad (9.11)$$

The transformed dimensionless governing equations and boundary conditions for liquid laminar free convection are

$$2W_x - \eta \frac{dW_x}{d\eta} + 4 \frac{dW_y}{d\eta} - \frac{1}{\rho} \frac{d\rho}{d\eta} (\eta W_x - 4W_y) = 0 \quad (9.12)$$

$$\frac{\nu_\infty}{\nu} \left(W_x \left(2W_x - \eta \frac{dW_x}{d\eta} \right) + 4W_y \frac{dW_x}{d\eta} \right) = \frac{d^2 W_x}{d\eta^2} + \frac{1}{\mu} \frac{d\mu}{d\eta} \frac{dW_x}{d\eta} + \frac{\nu_\infty}{\nu} \frac{\frac{\rho_\infty}{\rho} - 1}{\frac{\rho_\infty}{\rho_w} - 1} \quad (9.13)$$

$$\text{Pr} \frac{\nu_\infty}{\nu} (-\eta W_x + 4W_y) \frac{d\theta}{d\eta} = \frac{1}{\lambda} \frac{d\lambda}{d\eta} \frac{d\theta}{d\eta} + \frac{d^2 \theta}{d\eta^2} \quad (9.14)$$

with boundary conditions

$$\eta = 0, \quad W_x = 0, \quad W_y = 0, \quad \theta = 1 \quad (9.15)$$

$$\eta \rightarrow \infty, \quad W_x \rightarrow 0, \quad \theta \rightarrow 0 \quad (9.16)$$

Table 9.4 The measurement results for velocities w_x and the transformed values of W_x for water laminar free convection at $t_w = 40^\circ\text{C}$ and $t_\infty = 20^\circ\text{C}$, cited from Shang et al. [6]

$x = 0.05\text{ m}$				$x = 0.10\text{ m}$			
$y\text{ (mm)}$	η	$w_x\text{ (m/s)}$	W_x	$y\text{ (mm)}$	η	$w_x\text{ (m/s)}$	W_x
0.2	0.147	0.007	0.0707	0.2	0.124	0.007	0.0500
0.3	0.221	0.0093	0.0854	0.3	0.186	0.0119	0.0773
0.4	0.294	0.0115	0.1056	0.4	0.248	0.0135	0.0877
0.5	0.368	0.0129	0.1185	0.5	0.309	0.0156	0.1013
0.6	0.441	0.0136	0.1249	0.6	0.371	0.0182	0.1182
0.7	0.515	0.0143	0.1313	0.7	0.433	0.0190	0.1234
0.8	0.589	0.0150	0.1377	0.8	0.495	0.0193	0.1253
0.9	0.662	0.0142	0.1304	0.9	0.557	0.0195	0.1266
1.0	0.736	0.0139	0.1276	1.0	0.619	0.0209	0.1357
1.2	0.883	0.0129	0.1185	1.3	0.804	0.0185	0.1201
1.4	1.030	0.0126	0.1157	1.5	0.928	0.0182	0.1182
1.5	1.104	0.0118	0.1084	1.7	1.052	0.0161	0.1104
1.7	1.251	0.0111	0.1019	1.9	1.176	0.0160	0.1039
1.9	1.398	0.0096	0.0882	2.1	1.299	0.0141	0.0916
2.1	1.545	0.0089	0.0817	2.4	1.485	0.0142	0.0922
2.4	1.766	0.0078	0.0716	2.7	1.671	0.0107	0.0695
2.6	1.913	0.0061	0.0560	3.0	1.856	0.0105	0.0682
2.8	2.060	0.0056	0.0514	3.3	2.042	0.0085	0.0552
$x = 0.15\text{ m}$				$x = 0.20\text{ m}$			
$y\text{ (mm)}$	η	$w_x\text{ (m/s)}$	W_x	$y\text{ (mm)}$	η	$w_x\text{ (m/s)}$	W_x
0.2	0.112	0.0109	0.0578	0.2	0.104	0.0120	0.0551
0.3	0.168	0.0136	0.0721	0.3	0.156	0.0168	0.0771
0.4	0.224	0.0168	0.0890	0.4	0.208	0.0190	0.0872
0.5	0.280	0.0201	0.1065	0.5	0.260	0.0206	0.0946
0.7	0.391	0.0226	0.1198	0.7	0.364	0.0247	0.1134
0.9	0.503	0.0239	0.1267	0.9	0.468	0.0270	0.1240
1.1	0.615	0.0249	0.1320	1.1	0.572	0.0278	0.1276
1.3	0.727	0.0252	0.1335	1.2	0.624	0.0294	0.1350
1.4	0.783	0.0237	0.1229	1.3	0.676	0.0297	0.1364
1.6	0.894	0.0229	0.1214	1.4	0.728	0.0278	0.1276
1.8	1.056	0.0217	0.1130	1.6	0.832	0.0270	0.1240
2.0	1.118	0.0216	0.1145	1.8	0.937	0.0260	0.1194
2.2	1.230	0.0197	0.1044	2.0	1.041	0.0250	0.1148
2.4	1.342	0.0185	0.0980	2.3	1.197	0.0229	0.1051
2.6	1.453	0.0182	0.0964	2.6	1.353	0.0206	0.0946
2.8	1.565	0.0163	0.0864	2.9	1.509	0.0180	0.0826
3.1	1.733	0.0123	0.0650	3.1	1.613	0.0167	0.0767
3.4	1.901	0.0116	0.0615	3.4	1.719	0.0146	0.0670

Table 9.5 The measurement results for velocities w_x and the transformed value W_x for water laminar free Convection at $t_w = 50^\circ\text{C}$ and $t_\infty = 20^\circ\text{C}$, cited from Shang et al. [6]

$x = 0.05\text{ m}$				$x = 0.10\text{ m}$			
$y\text{ (mm)}$	η	$w_x\text{ (m/s)}$	W_x	$y\text{ (mm)}$	η	$w_x\text{ (m/s)}$	W_x
0.2	0.168	0.0116	0.0819	0.2	0.141	0.0146	0.0729
0.3	0.252	0.0148	0.1045	0.3	0.212	0.0184	0.0919
0.4	0.336	0.0162	0.1144	0.4	0.282	0.0221	0.1103
0.5	0.419	0.0174	0.1229	0.5	0.353	0.0249	0.1243
0.6	0.503	0.0184	0.1299	0.6	0.423	0.0259	0.1293
0.7	0.587	0.0188	0.1328	0.8	0.565	0.0266	0.1328
0.8	0.671	0.0187	0.1321	1.0	0.706	0.0263	0.1313
1.0	0.839	0.0172	0.1215	1.1	0.776	0.0256	0.1278
1.1	0.923	0.0168	0.1186	1.4	0.988	0.0234	0.1168
1.3	1.091	0.0155	0.1095	1.6	1.129	0.0206	0.1028
1.4	1.174	0.0148	0.1045	1.7	1.200	0.0209	0.1043
1.5	1.258	0.0141	0.0996	1.8	1.270	0.0196	0.0979
1.7	1.426	0.0122	0.0862	2.0	1.411	0.0180	0.0899
1.8	1.510	0.0118	0.0833	2.1	1.482	0.0167	0.0834
2.0	1.678	0.0107	0.0756	2.3	1.623	0.0151	0.0754
2.2	1.846	0.0086	0.0607	2.5	1.764	0.0133	0.0664
2.4	2.013	0.0081	0.0572	2.6	1.835	0.0126	0.0629
2.6	2.181	0.0064	0.0452	2.9	2.047	0.0102	0.0509
$x = 0.15\text{ m}$				$x = 0.20\text{ m}$			
$y\text{ (mm)}$	η	$w_x\text{ (m/s)}$	W_x	$y\text{ (mm)}$	η	$w_x\text{ (m/s)}$	W_x
0.2	0.127	0.0167	0.0681	0.2	0.119	0.0194	0.0685
0.3	0.191	0.0219	0.0893	0.3	0.178	0.0264	0.0932
0.4	0.255	0.0242	0.0987	0.4	0.237	0.0294	0.1028
0.5	0.319	0.0277	0.1129	0.5	0.297	0.0321	0.1133
0.6	0.382	0.0309	0.1260	0.6	0.356	0.0340	0.1201
0.7	0.446	0.0310	0.1264	0.7	0.415	0.0360	0.1271
0.9	0.574	0.0334	0.1362	0.9	0.534	0.0384	0.1356
1.0	0.637	0.0332	0.1353	1.0	0.593	0.0389	0.1374
1.2	0.765	0.0315	0.1284	1.1	0.652	0.0372	0.1314
1.3	0.828	0.0312	0.1272	1.3	0.771	0.0365	0.1289
1.4	0.892	0.0301	0.1227	1.5	0.890	0.0342	0.1208
1.5	0.956	0.0293	0.1194	1.7	1.008	0.0317	0.1119
1.6	1.020	0.0281	0.1151	2.9	1.127	0.0304	0.1073
1.8	1.147	0.0255	0.1040	2.2	1.305	0.0272	0.0960
2.0	1.275	0.0233	0.0950	2.5	1.483	0.0239	0.0844
2.3	1.466	0.0208	0.0848	2.9	1.720	0.0193	0.0682
2.8	1.784	0.0168	0.0685	3.2	1.898	0.0174	0.0614
3.3	2.103	0.0125	0.0510	3.4	2.017	0.0161	0.0569

Table 9.6 The measurement results for velocities w_x and the transformed values W_x for water laminar free convection at $t_w = 60^\circ\text{C}$ and $t_\infty = 20^\circ\text{C}$ cited from Shang et al. [6]

$x = 0.05\text{ m}$				$x = 0.10\text{ m}$			
$y\text{ (mm)}$	η	$w_x\text{ (m/s)}$	W_x	$y\text{ (mm)}$	η	$w_x\text{ (m/s)}$	W_x
0.2	0.186	0.0149	0.0858	0.2	0.156	0.0208	0.0847
0.3	0.279	0.0200	0.1152	0.3	0.234	0.0258	0.1051
0.4	0.371	0.0220	0.1267	0.4	0.313	0.0299	0.1218
0.5	0.464	0.0234	0.1348	0.5	0.391	0.0315	0.1283
0.6	0.557	0.0236	0.1359	0.6	0.469	0.0321	0.1308
0.7	0.650	0.0235	0.1354	0.7	0.547	0.0340	0.1385
0.9	0.836	0.0206	0.1187	0.8	0.625	0.0328	0.1336
1.0	0.929	0.0200	0.1152	0.9	0.703	0.0317	0.1291
1.1	1.021	0.0197	0.1135	1.1	0.859	0.0298	0.1214
1.2	1.114	0.0196	0.1129	1.2	0.938	0.0289	0.1177
1.3	1.207	0.0178	0.1025	1.3	1.016	0.0279	0.1136
1.4	1.300	0.0161	0.0927	1.4	1.094	0.0267	0.1088
1.5	1.393	0.0151	0.0870	1.5	1.172	0.0254	0.1035
1.6	1.486	0.0145	0.0835	1.7	1.328	0.0230	0.0937
1.8	1.671	0.0121	0.0697	1.8	1.406	0.0213	0.0868
2.0	1.857	0.0104	0.0599	2.0	1.563	0.0183	0.0745
2.1	1.950	0.0105	0.0605	2.4	1.875	0.0145	0.0591
2.3	2.136	0.0095	0.0547	2.9	2.266	0.0112	0.0456
$x = 0.15\text{ m}$				$x = 0.20\text{ m}$			
$y\text{ (mm)}$	η	$w_x\text{ (m/s)}$	W_x	$y\text{ (mm)}$	η	$w_x\text{ (m/s)}$	W_x
0.2	0.141	0.0230	0.0765	0.2	0.131	0.0243	0.0700
0.3	0.212	0.0299	0.0994	0.3	0.197	0.0336	0.0968
0.4	0.282	0.0353	0.1174	0.4	0.263	0.0379	0.1092
0.5	0.353	0.0384	0.1277	0.5	0.329	0.0420	0.1210
0.7	0.494	0.0408	0.1357	0.7	0.460	0.0460	0.1325
0.9	0.635	0.0405	0.1347	0.9	0.591	0.0470	0.1354
1.1	0.776	0.0393	0.1307	1.1	0.723	0.0455	0.1310
1.3	0.917	0.0355	0.1181	1.2	0.788	0.0449	0.1293
1.4	0.988	0.0342	0.1137	1.3	0.854	0.0425	0.1224
1.6	1.129	0.0314	0.1044	1.7	1.117	0.0364	0.1048
1.8	1.270	0.0290	0.0964	2.0	1.314	0.0319	0.0919
2.0	1.411	0.0264	0.0878	2.2	1.445	0.0294	0.0847
2.1	1.482	0.0249	0.0828	2.4	1.577	0.0258	0.0743
2.3	1.623	0.0220	0.0732	2.6	1.708	0.0243	0.0700
2.5	1.764	0.0196	0.0652	2.8	1.840	0.0219	0.0631
2.7	1.905	0.0175	0.0582	2.9	1.905	0.0201	0.0579
3.0	2.117	0.0152	0.0505	3.1	2.037	0.0188	0.0541
3.3	2.329	0.0126	0.0419	3.4	2.234	0.0157	0.0452

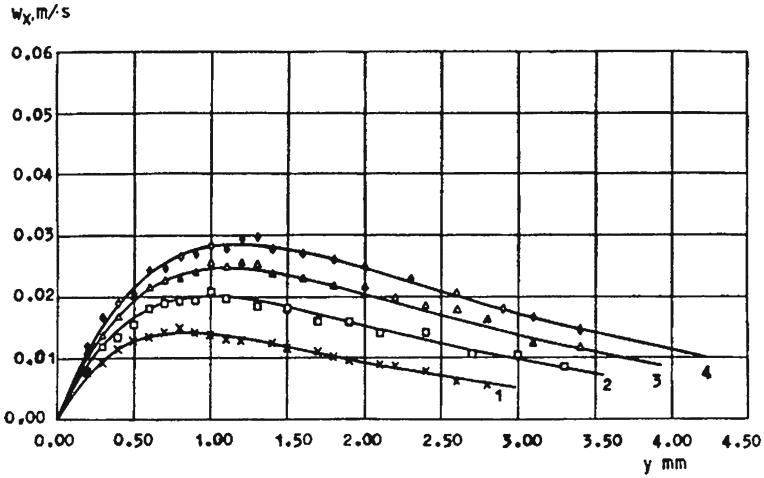


Fig. 9.10 Measured and numerical values of velocity w_x of water laminar free convection for $t_w = 40^\circ\text{C}$ and $t_\infty = 20^\circ\text{C}$, cited from Shang et al. [6]; Full line numerical solution, symbol corresponding measured value: 1. \times , $x = 0.05\text{ m}$; 2. \square , $x = 0.10\text{ m}$; 3. \triangle , $x = 0.15\text{ m}$; and 4. \diamond , $x = 0.20\text{ m}$

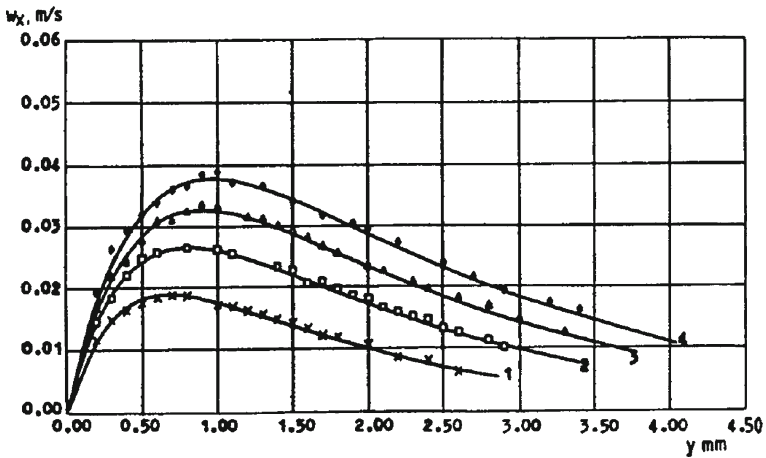


Fig. 9.11 Measured and numerical values of velocity w_x of water laminar free convection for $t_w = 50^\circ\text{C}$ and $t_\infty = 20^\circ\text{C}$, cited from Shang et al. [6]; full line numerical solution, symbol corresponding measured value: 1. \times , $x = 0.05\text{ m}$; 2. \square , $x = 0.10\text{ m}$; 3. \triangle , $x = 0.15\text{ m}$; and 4. \diamond , $x = 0.20\text{ m}$

9.3.4 Numerical Solutions

As the analysis in Chap. 8, if the specific heat c_p of water is substituted by c_{p_∞} , i.e., at the temperature at infinity, the maximum predicted deviation will be less than

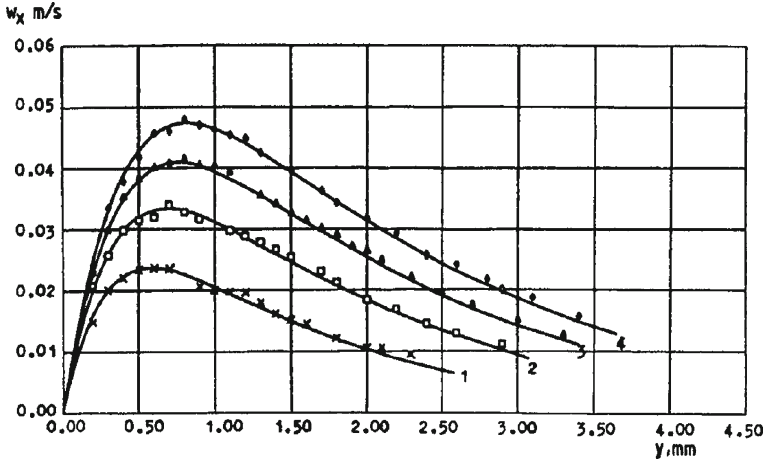


Fig. 9.12 Measured and numerical values for velocity w_x of water laminar free convection for $t_w = 60^\circ\text{C}$ and $t_\infty = 20^\circ\text{C}$, cited from Shang et al. [6]: *full line* numerical solution, *symbol* corresponding measured value: 1. \times , $x = 0.05$ m; 2. \square , $x = 0.10$ m; 3. Δ , $x = 0.15$ m; and 4. \diamond , $x = 0.20$ m

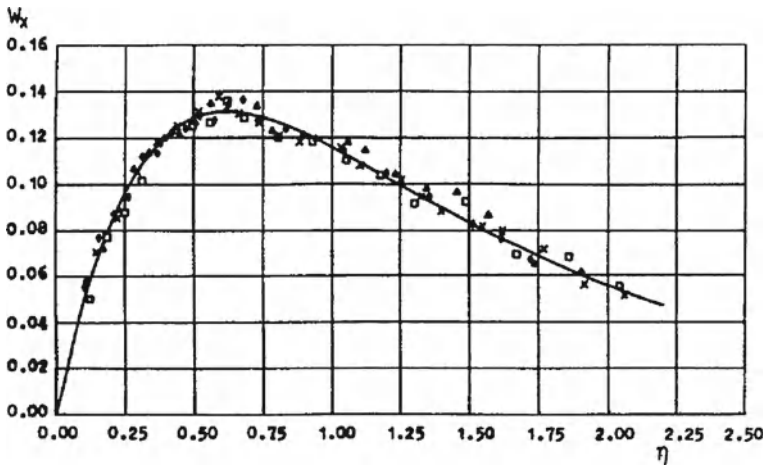


Fig. 9.13 Measured and calculated values of the dimensionless velocity W_x of water laminar free convection, for $t_w = 40^\circ\text{C}$ and $t_\infty = 20^\circ\text{C}$ cited from Shang et al. [6]: *full line* numerical solution, *symbol* corresponding measured value: 1. \times , $x = 0.05$ m; 2. \square , $x = 0.10$ m; 3. Δ , $x = 0.15$ m; and 4. \diamond , $x = 0.20$ m

0.455% for the temperature range from 0 to 100°C according to typical experiment values [8]. Such small deviation is allowed for the treatment of variable physical properties. Consequently, property factor $\text{Pr} \frac{\nu_\infty}{\nu}$ of Eq. 9.14 can be changed to the following form for water laminar free convection:

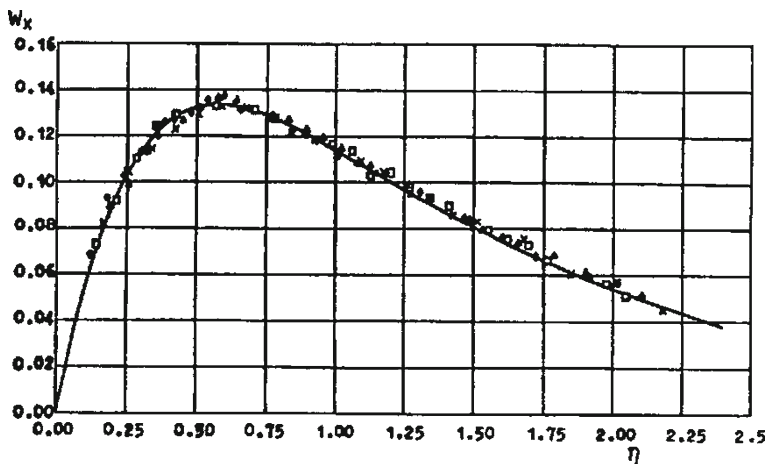


Fig. 9.14 Measured and calculated values for dimensionless velocity W_x of water laminar free convection, for $t_w = 50^\circ\text{C}$ and $t_\infty = 20^\circ\text{C}$, cited from Shang et al. [6]: full line numerical solution, symbol corresponding measured value: 1. \times , $x = 0.05\text{ m}$; 2. \square , $x = 0.10\text{ m}$; 3. Δ , $x = 0.15\text{ m}$; and 4. \diamond , $x = 0.20\text{ m}$

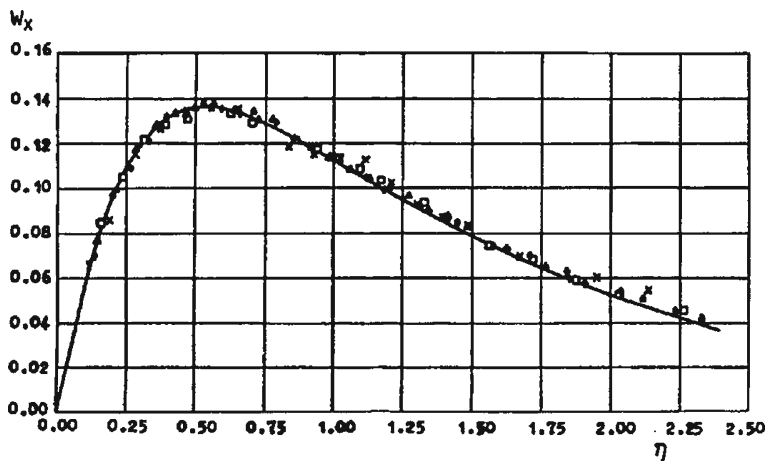


Fig. 9.15 Measured and calculated values for dimensionless velocity W_x of water laminar free convection, for condition $t_w = 60^\circ\text{C}$ and $t_\infty = 20^\circ\text{C}$, cited from Shang et al. [6]: full line numerical solution, symbol corresponding measured value: 1. \times , $x = 0.05\text{ m}$; 2. \square , $x = 0.10\text{ m}$; 3. Δ , $x = 0.15\text{ m}$; and 4. \diamond , $x = 0.20\text{ m}$

$$\text{Pr} \frac{\nu_\infty}{\nu} = \text{Pr}_\infty \frac{\lambda_\infty \rho}{\lambda \rho} \tag{9.17}$$

The physical property values of ρ , μ , ν , λ , and Pr are taken from those listed in Chapter 8. For convenience some specimen values of the physical properties for the experiment are listed in Table 9.3.

According to the approach of the numerical calculation of Chapter 8, the solutions for water laminar free convection are obtained from the governing ordinary differential equations (9.12)–(9.14) with Eq. (9.17) and the boundary conditions (9.15) and (9.16) by shooting method, respectively, for $t_w = 40^\circ\text{C}$ and $t_\infty = 20^\circ\text{C}$, $t_w = 50^\circ\text{C}$ and $t_\infty = 20^\circ\text{C}$, $t_w = 60^\circ\text{C}$ and $t_\infty = 20^\circ\text{C}$. While, the water physical properties such as ρ , λ and ν are described, respectively, by Eqs. (5.16)–(5.18). Meanwhile Eqs. (5.24)–(5.26) are applied for describing the related water physical property factors of the governing equations. The numerical solutions for velocity component w_x obtained for the water laminar free convection are listed in Tables 9.4, 9.5 and 9.6 and plotted in Figs. 9.10, 9.11, and 9.12, respectively. In addition, these numerical solutions w_x are transformed into the corresponding dimensional ones W_x by means of Eqs. (9.9) and (9.10). The transformed dimensionless solutions are described in Tables 9.4–9.6 and plotted in Figs. 9.13–9.15, respectively. It can be seen that the measured results agree very well with the predicted results.

$$\rho = 4.48 \times 10^{-3} t^2 + 999.9 \quad (5.16)$$

$$\lambda = -8.01 \times 10^{-6} t^2 + 1.94 \times 10^{-3} t + 0.563 \quad (5.17)$$

$$\mu = \exp \left[-1.6 - \frac{1150}{T} + \left(\frac{690}{T} \right)^2 \right] \times 10^{-3} \quad (5.18)$$

9.4 Remarks

Experimental investigations were carried out to study effects of variable physical properties on laminar free convection of air and water and to further verify the results of the previous chapters, Chaps. 6 and 8. The following points are made.

By increasing the temperature t_w for the liquid laminar free convection or with increasing the boundary temperature ratio T_w/T_∞ for gas laminar free convection of gas, the velocity component w_x of the free convection increases, and the velocity profile moves to the direction of the flat plate. Consequently, the thickness of the velocity boundary layer decreases.

With an increase of the height x , the velocity component w_x of water or air free convection increases, and the velocity profile moves toward the fluid bulk. As a result the thickness of velocity boundary layer increases.

It is found that the agreement between the measured and calculated velocity fields is good, thus confirming that the results in Chaps. 6, 7 and 8 are reliable.

Table 9.7 The numerical solutions of velocity components w_x and W_x at $t_w = 40^\circ\text{C}$ and $t_\infty = 20^\circ\text{C}$, cited from Shang et al. [6]

$x = 0.05\text{ m}$				$x = 0.10\text{ m}$			
η	$y\text{ (mm)}$	W_x	$w_x\text{ (m/s)}$	η	$y\text{ (mm)}$	W_x	$w_x\text{ (m/s)}$
0	0	0	0	0	0	0	0
0.075	0.102	0.0378	0.0041	0.075	0.121	0.0378	0.0058
0.150	0.204	0.0674	0.0073	0.150	0.242	0.0674	0.0104
0.225	0.306	0.0898	0.0098	0.225	0.364	0.0898	0.0138
0.300	0.408	0.1063	0.0116	0.300	0.485	0.1063	0.0164
0.375	0.510	0.1178	0.0128	0.375	0.606	0.1178	0.0181
0.450	0.612	0.1253	0.0136	0.450	0.727	0.1253	0.0193
0.525	0.713	0.1297	0.0141	0.525	0.848	0.1297	0.0200
0.600	0.815	0.1314	0.0143	0.600	0.970	0.1314	0.0202
0.700	0.951	0.1308	0.0142	0.700	1.131	0.1308	0.0201
0.800	1.087	0.1277	0.0139	0.800	1.293	0.1277	0.0197
0.900	1.223	0.1231	0.0134	0.900	1.454	0.1231	0.0190
1.050	1.427	0.1143	0.0124	1.050	1.700	0.1143	0.0176
1.200	1.631	0.1046	0.0114	1.200	1.939	0.1046	0.0161
1.350	1.835	0.0948	0.0103	1.350	2.182	0.0948	0.0146
1.500	2.039	0.0853	0.0093	1.500	2.424	0.0853	0.0131
1.800	2.446	0.0681	0.0074	1.800	2.909	0.0681	0.0105
2.100	2.854	0.0536	0.0058	2.100	3.394	0.0536	0.0083
$x = 0.15\text{ m}$				$x = 0.20\text{ m}$			
η	$y\text{ (mm)}$	W_x	$w_x\text{ (m/s)}$	η	$y\text{ (mm)}$	W_x	$w_x\text{ (m/s)}$
0	0	0	0	0	0	0	0
0.075	0.134	0.0378	0.0071	0.075	0.144	0.0378	0.0082
0.150	0.268	0.0674	0.0127	0.150	0.288	0.0674	0.0147
0.225	0.403	0.0898	0.0169	0.225	0.432	0.0898	0.0196
0.300	0.537	0.1063	0.0201	0.300	0.577	0.1063	0.0232
0.375	0.671	0.1178	0.0222	0.375	0.721	0.1178	0.0257
0.450	0.805	0.1253	0.0236	0.450	0.865	0.1253	0.0273
0.525	0.939	0.1297	0.0245	0.525	1.009	0.1297	0.0282
0.600	1.073	0.1314	0.0248	0.600	1.153	0.1314	0.0286
0.700	1.252	0.1308	0.0247	0.700	1.345	0.1308	0.0285
0.800	1.431	0.1277	0.0241	0.800	1.538	0.1277	0.0278
0.900	1.610	0.1231	0.0232	0.900	1.730	0.1231	0.0268
1.050	1.878	0.1143	0.0216	1.050	2.018	0.1143	0.0249
1.200	2.147	0.1046	0.0197	1.200	2.306	0.1046	0.0228
1.350	2.415	0.0948	0.0179	1.350	2.595	0.0948	0.0206
1.500	2.684	0.0853	0.0161	1.500	2.883	0.0853	0.0186
1.800	3.220	0.0681	0.0129	1.800	2.460	0.0681	0.0148
2.100	3.757	0.0536	0.0101	2.100	4.036	0.0536	0.0117

Table 9.8 The numerical solutions of velocity components w_x and W_x at $t_w = 50^\circ\text{C}$ and $t_\infty = 20^\circ\text{C}$, cited from Shang et al. [6]

$x = 0.05\text{ m}$				$x = 0.10\text{ m}$			
η	$y\text{ (mm)}$	W_x	$w_x\text{ (m/s)}$	η	$y\text{ (mm)}$	W_x	$w_x\text{ (m/s)}$
0	0	0	0	0	0	0	0
0.075	0.089	0.0416	0.0059	0.075	0.106	0.0416	0.0083
0.150	0.179	0.0732	0.0104	0.150	0.213	0.0732	0.0147
0.225	0.268	0.0964	0.0137	0.225	0.319	0.0964	0.0193
0.300	0.358	0.1127	0.0160	0.300	0.425	0.1127	0.0226
0.375	0.447	0.1235	0.0175	0.375	0.531	0.1235	0.0247
0.450	0.536	0.1300	0.0184	0.450	0.638	0.1300	0.0260
0.525	0.626	0.1331	0.0188	0.525	0.744	0.1331	0.0267
0.600	0.715	0.1337	0.0189	0.600	0.850	0.1337	0.0268
0.700	0.834	0.1317	0.0186	0.700	0.992	0.1317	0.0264
0.800	0.954	0.1274	0.0180	0.800	1.134	0.1274	0.0255
0.900	1.073	0.1219	0.0173	0.900	1.275	0.1219	0.0244
1.050	1.252	0.1123	0.0159	1.050	1.488	0.1123	0.0225
1.200	1.430	0.1022	0.0145	1.200	1.700	0.1022	0.0205
1.350	1.609	0.0922	0.0131	1.350	1.913	0.0922	0.0185
1.650	1.967	0.0740	0.0105	1.650	2.338	0.0740	0.0148
1.950	2.324	0.0586	0.0083	1.950	2.763	0.0586	0.0117
2.250	2.682	0.0459	0.0065	2.250	3.188	0.0459	0.0092
$x = 0.15\text{ m}$				$x = 0.20\text{ m}$			
η	$y\text{ (mm)}$	W_x	$w_x\text{ (m/s)}$	η	$y\text{ (mm)}$	W_x	$w_x\text{ (m/s)}$
0	0	0	0	0	0	0	0
0.075	0.118	0.0416	0.0102	0.075	0.126	0.0416	0.0118
0.150	0.235	0.0732	0.0180	0.150	0.253	0.0732	0.0207
0.225	0.353	0.0964	0.0236	0.225	0.379	0.0964	0.0273
0.300	0.471	0.1127	0.0276	0.300	0.506	0.1127	0.0319
0.375	0.588	0.1235	0.0303	0.375	0.632	0.1235	0.0350
0.450	0.706	0.1300	0.0319	0.450	0.759	0.1300	0.0368
0.525	0.824	0.1331	0.0326	0.525	0.885	0.1331	0.0377
0.600	0.941	0.1337	0.0328	0.600	1.012	0.1337	0.0379
0.700	1.098	0.1317	0.0323	0.700	1.180	0.1317	0.0373
0.800	1.255	0.1274	0.0313	0.800	1.349	0.1274	0.0361
0.900	1.412	0.1219	0.0299	0.900	1.517	0.1219	0.0345
1.050	1.647	0.1123	0.0275	1.050	1.770	0.1123	0.0318
1.200	1.883	0.1022	0.0251	1.200	2.023	0.1022	0.0289
1.350	2.118	0.0922	0.0226	1.350	2.276	0.0922	0.0261
1.650	2.589	0.0740	0.0182	1.650	2.782	0.0740	0.0210
1.950	3.064	0.0586	0.0144	1.950	3.288	0.0586	0.0166
2.250	3.530	0.0459	0.0113	2.250	3.794	0.0459	0.0130

Table 9.9 The numerical solutions of velocities components w_x and W_x at $t_w = 60^\circ\text{C}$ and $t_\infty = 20^\circ\text{C}$, cited from Shang et al. [6]

$x = 0.05\text{ m}$				$x = 0.10\text{ m}$			
η	$y\text{ (mm)}$	W_x	$w_x\text{ (m/s)}$	η	$y\text{ (mm)}$	W_x	$w_x\text{ (m/s)}$
0	0	0	0	0	0	0	0
0.075	0.081	0.0454	0.0079	0.075	0.096	0.0454	0.0111
0.150	0.162	0.0789	0.0137	0.150	0.192	0.0789	0.0194
0.225	0.242	0.1028	0.0178	0.225	0.288	0.1028	0.0252
0.300	0.323	0.1189	0.0206	0.300	0.384	0.1189	0.0292
0.375	0.404	0.1290	0.0224	0.375	0.480	0.1290	0.0317
0.450	0.485	0.1345	0.0233	0.450	0.576	0.1345	0.0330
0.525	0.565	0.1365	0.0237	0.525	0.672	0.1365	0.0335
0.600	0.646	0.1360	0.0236	0.600	0.768	0.1360	0.0334
0.700	0.754	0.1326	0.0230	0.700	0.896	0.1326	0.0326
0.800	0.862	0.1273	0.0221	0.800	1.024	0.1273	0.0313
0.900	0.969	0.1209	0.0210	0.900	1.152	0.1209	0.0297
1.050	1.131	0.1106	0.0192	1.050	1.344	0.1106	0.0272
1.200	1.292	0.1001	0.0174	1.200	1.536	0.1001	0.0246
1.350	1.454	0.0901	0.0156	1.350	1.728	0.0901	0.0221
1.650	1.777	0.0721	0.0125	1.650	2.112	0.0721	0.0177
1.950	2.100	0.0570	0.0099	1.950	2.496	0.0570	0.0140
2.250	2.423	0.0446	0.0077	2.250	2.880	0.0446	0.0109
$x = 0.15\text{ m}$				$x = 0.20\text{ m}$			
η	$y\text{ (mm)}$	W_x	$w_x\text{ (m/s)}$	η	$y\text{ (mm)}$	W_x	$w_x\text{ (m/s)}$
0	0	0	0	0	0	0	0
0.075	0.106	0.0454	0.0137	0.075	0.114	0.0454	0.0158
0.150	0.213	0.0789	0.0237	0.150	0.228	0.0789	0.0274
0.225	0.319	0.1028	0.0309	0.225	0.342	0.1028	0.0357
0.300	0.425	0.1189	0.0358	0.300	0.457	0.1189	0.0413
0.375	0.531	0.1290	0.0388	0.375	0.571	0.1290	0.0448
0.450	0.638	0.1345	0.0404	0.450	0.685	0.1345	0.0467
0.525	0.744	0.1365	0.0410	0.525	0.799	0.1365	0.0474
0.600	0.850	0.1360	0.0409	0.600	0.913	0.1360	0.0472
0.700	0.992	0.1326	0.0399	0.700	1.065	0.1326	0.0464
0.800	1.134	0.1273	0.0383	0.800	1.218	0.1273	0.0442
0.900	1.275	0.1209	0.0364	0.900	1.370	0.1209	0.0420
1.050	1.488	0.1106	0.0333	1.050	1.598	0.1106	0.0384
1.200	1.700	0.1001	0.0301	1.200	1.827	0.1001	0.0348
1.350	1.913	0.0901	0.0271	1.350	2.055	0.0901	0.0313
1.650	2.338	0.0721	0.0217	1.650	2.511	0.0721	0.0250
1.950	2.763	0.0570	0.0171	1.950	2.968	0.0570	0.0198
2.250	3.188	0.0446	0.0134	2.250	3.425	0.0446	0.0155

9.5 Questions

1. What is proved through the experimental measurement results in this chapter?
2. Do you think the measurement by using LDV is the best way to obtain the velocity field of fluid flow? Why?

References

1. E. Schmidt, W. Beckman, Ads temperature-und Geschwindigkeitsfeld von einer wärme abgebenden senkrechten plätte bei natürlicher konvection. *Forsch. Ing. Wes.* **1**, 391 (1930)
2. E. Pohlhausen, Der Wärmesustausch zwischen festen Körpern und Flüssigkeiten mit kleiner Reibung und kleiner Wärmeleitung. *Z. Angew. Math. Mech.* **1**, 115–121 (1921)
3. H. Schlichting, *Boundary-Layer Theory*, 6th edn. (McGraw-Hill, New York, 1968)
4. D.Y. Shang, B.X. Wang, Measurement on velocity of laminar boundary layer for gas free convection along an isothermal vertical flat plate, in Anonymous (ed.), *Institution of Chemical Engineers Symposium Series*, vol. 1(12), 3rd UK National Conference Incorporating 1st European Conference on Thermal Sciences, Birmingham, 16–18 Sept. 1992. (Hemisphere, New York, 1992), pp. 484–489
5. D.Y. Shang, B.X. Wang, Y. Wang, Y. Quan, Study on liquid laminar free convection with consideration of variable thermophysical properties. *Int. J. Heat Mass Transf.* **36**(14), 3411–3419 (1993)
6. D.Y. Shang, B.X. Wang, H.S. Takhar, Measurements of the velocity field of the malinar boundary layer for eater free convection along an isothermal vertical flat plate. *App. Mech. Eng.* **3**(4), 553–570 (1998)
7. D.Y. Shang, B.X. Wang, Effect of variable thermophysical properties on laminar free convection of gas. *Int. J. Heat Mass Transf.* **33**(7), 1387–1395 (1990)
8. VDI-Wärmeatlas, *Berechnungsblätter für den Wärmeübertragung*, vol. 5 erweiterte edn. (VDI Verlage GmbH, Düsseldorf, 1988)

Chapter 10

Identical Laminar Free Convection for Inclined and Vertical Cases

Abstract The new similarity analysis method is applied to the similarity transformation of the governing partial differential equations of laminar free convection on inclined plate. It is seen that the transformed governing ordinary differential equations on the inclined plate are same as those on the vertical plate. Then, it follows that there are identical governing ordinary differential equations and dimensionless prediction equations on heat transfer both for inclined and vertical cases of laminar convection. In this case, the vertical case can only be regarded as a special example of the inclined case. Therefore, the numerical solutions and prediction equations on heat transfer for vertical case can be directly used for the inclined case. Finally, the simple and direct correlations for describing the transformation of the velocity components and heat transfer from the vertical case to the inclined case for the free convection are derived.

10.1 Introduction

It was Rich [1] who first suggested theoretically the procedure for obtaining the heat transfer rate from an inclined surface. According to his procedure, the problem of free convection on an inclined surface is identical to that of flow over a vertical surface except that g is replaced by $g \cos \gamma$, and therefore, a replacement of g by $g \cos \gamma$ in all the relationships derived earlier. This implies using $Gr_x \cos \gamma$ for Gr_x . As a result, his experimental data are in general agreement with the anticipated values. The data obtained by Vliet [2] for a uniform-flux, heated surface in air and in water indicate the validity of the procedure mentioned above up to inclination angles as large as 60° . Detailed experimental results on this were obtained by Fujii and Imura [3]. They also discuss the separation of the boundary layer for the inclined surface facing upward.

However, so far, there has been a shortage of theoretically rigorous derivations to support the above conclusions by means of a replacement of g with $g \cos \gamma$

for all the relationships, and there is a shortage of clear correlations in describing the transformations of heat transfer, momentum transfer, and mass flow rate drawn from the vertical case to the inclined case for the free convection. As we know, the traditional method for the treatment of similarity transformation of the governing equations for laminar free convection is the Falkner–Skan transformation [4–6]. It is difficult with the traditional Falkner–Skan transformation to realize such a derivation.

Fortunately, the new similarity analysis method presented in Chap. 4 [7–9] for similarity transformation of the governing partial differential equations of fluid laminar boundary layer has provided the possibility to realize such derivation. It is shown that in these studies the velocity component method has its advantages over the Falkner–Skan transformation for the treatment of variable thermophysical properties and other various physical factors. On this basis, Shang and Takhar [10] clarified the relationships of heat, momentum, and mass transfer of laminar fluid free convection between inclined and vertical cases for consideration of variable thermophysical properties.

In this chapter, I will introduce the exact relationships of heat, momentum, and mass transfer between inclined and vertical cases with consideration of variable thermophysical properties in order to satisfy the requirement in industrial applications. To this end, the governing equations of laminar free convection of fluid in the inclined case are transformed by means of a developed similarity transformation approach, viz, the velocity component method, instead of traditional Falkner–Skan type of transformation. Meanwhile, the suitable forms of some dimensionless variables such as an appropriate suitable local Grashof number $Gr_{x,\infty}$ and suitable dimensionless velocity components for the free convection are proposed. It will be found that the formation of the transformed dimensionless governing equations for the inclined case is fully same as those for the corresponding vertical cases. Then, it is obvious that, except the different assumption of local Grashof number and dimensionless velocity components, the prediction correlations of heat transfer, momentum transfer, and mass flow rate for fluid laminar free convection for the vertical case presented in the previous chapters can be completely taken as those for the related inclined case.

10.2 Fluid Laminar Free Convection on Inclined Plate

10.2.1 Physical Model and Basic Equations

The physical model and co-ordinate system are shown schematically in Fig. 10.1. An isothermal inclined flat plate is suspended in a quiescent liquid. The surface temperature is t_w and the fluid bulk temperature is t_∞ . It is assumed that t_w is not equal to t_∞ , so that laminar free convection can be produced easily on the inclined surface in both the cases as shown in Fig. 10.1a, b, respectively. The governing partial differential equations for mass, momentum, and energy for consideration of variable thermophysical properties applied to the liquid laminar free convection on

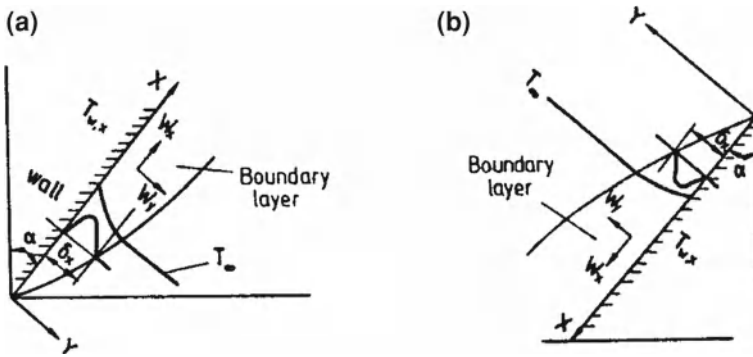


Fig. 10.1 Physical model and coordinate system. **a** Ascending flow on the inclined surface ($t_w > t_\infty$). **b** Falling flow on the inclined surface ($t_w < t_\infty$)

the inclined surface are

$$\frac{\partial}{\partial x} [\rho(w_x)_i] + \frac{\partial}{\partial y} [\rho(w_y)_i] = 0 \tag{10.1}$$

$$\rho \left[(w_x)_i \frac{\partial (w_x)_i}{\partial x} + (w_y)_i \frac{\partial (w_x)_i}{\partial y} \right] = \frac{\partial}{\partial y} \left[\mu \frac{\partial (w_x)_i}{\partial y} \right] + g |\rho_\infty - \rho| \cos \gamma \tag{10.2}$$

$$\rho c_p \left[(w_x)_i \frac{\partial t}{\partial x} + (w_y)_i \frac{\partial t}{\partial y} \right] = \frac{\partial}{\partial y} \left(\lambda \frac{\partial t}{\partial y} \right) \tag{10.3}$$

where γ expresses the inclined angle of the plate. Here, the buoyancy fact $|\rho_\infty - \rho|$ is taken as the absolute value because its direction is same as that of the velocity component $(w_x)_i$.

The boundary conditions are

$$y = 0 : (w_x)_i = 0, (w_y)_i = 0, t = t_w \tag{10.4}$$

$$y \rightarrow \infty : (w_x)_i = 0, t = t_\infty \tag{10.5}$$

10.2.2 Similarity Transformation of the Basic Equations

For similarity transformation of the basic equations, we use the velocity component method which was developed in Refs. [7–9] and presented in Chaps. 5–7. If subscripts i and v are taken to express the case on the isothermal inclined and vertical surfaces, respectively, for laminar free convection, we assume the following dimensionless co-ordinate variables for similarity transformation of the above governing partial differential equations of liquid laminar free convection on inclined plate:

$$\eta_i = \frac{y}{x} \left[\frac{1}{4} (Gr_{x,\infty})_i \right]^{1/4} \quad (10.6)$$

where η_i is the dimensionless co-ordinate variable for boundary layer. The local Grashof number $(Gr_{x,\infty})_i$ can be assumed to be

$$(Gr_{x,\infty})_i = \frac{g \cos \gamma |\rho_\infty / \rho_w - 1| x^3}{\nu_\infty^2} \quad (10.7)$$

The dimensionless temperature is given by

$$\theta = \frac{t - t_\infty}{t_w - t_\infty} \quad (10.8)$$

The dimensionless velocity components are assumed to be

$$(W_x)_i = \left(2\sqrt{g \cos \gamma x} |\rho_\infty / \rho_w - 1|^{1/2} \right)^{-1} (w_x)_i \quad (10.9)$$

$$(W_y)_i = \left\{ 2\sqrt{g \cos \gamma x} |\rho_\infty / \rho_w - 1|^{1/2} \left[\frac{1}{4} (Gr_{x,\infty})_i \right]^{-1/4} \right\}^{-1} (w_y)_i \quad (10.10)$$

With the above similarity variables defined in Eqs. (10.6)–(10.10), Eqs. (10.1)–(10.3) with the boundary conditions (10.4) and (10.5) can be transformed into the following governing ordinary differential equations:

$$2(W_x)_i - \eta \frac{d(W_x)_i}{d\eta_i} + 4 \frac{d(W_y)_i}{d\eta_i} - \frac{1}{\rho} \frac{d\rho}{d\eta_i} [\eta_i (W_x)_i - 4(W_y)_i] = 0 \quad (10.11)$$

$$\begin{aligned} & \frac{\nu_\infty}{\nu} \left[(W_x)_i \left(2(W_x)_i - \eta_i \frac{d(W_x)_i}{d\eta_i} \right) + 4(W_y)_i \frac{d(W_x)_i}{d\eta_i} \right] \\ & = \frac{d^2(W_x)_i}{d\eta_i^2} + \frac{1}{\mu} \frac{d\mu}{d\eta_i} \frac{d(W_x)_i}{d\eta_i} + \frac{\nu_\infty}{\nu} \frac{\frac{\rho_\infty}{\rho} - 1}{\frac{\rho_\infty}{\rho_w} - 1} \end{aligned} \quad (10.12)$$

$$\text{Pr} \frac{\nu_\infty}{\nu} [-\eta_i (W_x)_i + 4(W_y)_i] \frac{d\theta}{d\eta_i} = \frac{d^2\theta}{d\eta_i^2} + \frac{1}{\lambda} \frac{d\lambda}{d\eta_i} \frac{d\theta}{d\eta_i} \quad (10.13)$$

$$\eta_i = 0 : (W_x)_i = 0, \quad (W_y)_i = 0, \quad \theta = 1 \quad (10.14)$$

$$\eta_i \rightarrow 0 : (W_x)_i = 0, \quad \theta = 0 \quad (10.15)$$

The derivation processes for Eqs. (10.11)–(10.13) are described in Appendix A in detail.

10.2.3 Relationships of Momentum, Heat, and Mass Transfer Between Inclined and Vertical Cases

For heat transfer

Equations (10.11)–(10.13) and their boundary conditions Eqs. (10.14)–(10.15) are dimensionless forms of the equations of liquid laminar free convection in the inclined case. They are completely identical to Eqs. (8.23)–(8.27) for the vertical case in Chap. 8. Therefore, for same fluid laminar free convection with same boundary temperature conditions t_w and t_∞ , we have

$$-\left[\left(\frac{d\theta}{d\eta}\right)_{\eta=0}\right]_i = -\left[\left(\frac{d\theta}{d\eta}\right)_{\eta=0}\right]_v. \quad (10.16)$$

With the same derivation as that in Chap. 6, the correlation for $\left[\left(\frac{d\theta}{d\eta}\right)_{\eta=0}\right]_i$ in the following form for water laminar free convection can be taken for consideration of variable thermophysical properties:

$$-\left[\left(\frac{d\theta}{d\eta}\right)_{\eta=0}\right]_i = -\left[\left(\frac{d\theta}{d\eta}\right)_{\eta=0}\right] = 0.5812\text{Pr}_\infty^{0.301} \quad (1.7 < \text{Pr}_\infty < 11.3) \quad (10.17)$$

where the liquid bulk temperature t_∞ is defined as that of reference Prandtl number Pr_∞ .

In addition, the heat transfer equations for laminar free convection on vertical flat plate can be followed as those on inclined plate, i.e.,

The local heat transfer rate q_x at position x per unit area from the surface of the plate to the gas will be

$$(q_x)_i = -\lambda_w(t_w - t_\infty) \left(\frac{1}{4}Gr_{x,\infty}\right)_i^{1/4} x^{-1} \left(\frac{d\theta}{d\eta}\right)_{\eta=0} \quad (8.29i)$$

The local heat transfer coefficient α_x , defined as $q_x = \alpha_x(T_w - T_\infty)$, will be given by

$$(\alpha_x)_i = -\lambda_w \left(\frac{1}{4}Gr_{x,\infty}\right)_i^{1/4} x^{-1} \left(\frac{d\theta}{d\eta}\right)_{\eta=0} \quad (8.30i)$$

The local Nusselt number defined by $Nu_{x,w} = \frac{\alpha_x x}{\lambda_w}$ will be

$$(Nu_{x,w})_i = \left(\frac{1}{4}Gr_{x,\infty}\right)_i^{1/4} \left(-\frac{d\theta}{d\eta}\right)_{\eta=0} \quad (8.31i)$$

Total heat transfer rate for position $x = 0$ to x with width of b on the plate is an integration $Q_x = \int \int_A q_x dA = \int_0^x q_x b dx$, and hence

$$(Q_x)_i = \frac{4}{3} b \lambda_w (t_w - t_\infty) \left(\frac{1}{4} Gr_{x,\infty} \right)_i^{1/4} \left(-\frac{d\theta}{d\eta} \right)_{\eta=0} \quad (8.32i)$$

The average heat transfer rate, defined as $\overline{Q}_x = Q_x / (b \times x)$ is given by

$$(\overline{Q}_x)_i = \frac{4}{3} b \lambda_w (T_w - T_\infty) \left(\frac{1}{4} Gr_{x,\infty} \right)_i^{1/4} \left(-\frac{d\theta}{d\eta} \right)_{\eta=0} \quad (6.33i)$$

The average heat transfer coefficient $\overline{\alpha}_x$ defined as $Q_x = \overline{\alpha}_x (T_w - T_\infty)$ is expressed as

$$(\overline{\alpha}_x)_i = \frac{4}{3} \lambda_w \left(\frac{1}{4} Gr_{x,\infty} \right)_i^{1/4} x^{-1} \left(-\frac{d\theta}{d\eta} \right)_{\eta=0} \quad (8.34i)$$

The average Nusselt number is defined as $\overline{Nu}_{x,w} = \frac{\overline{\alpha}_x x}{\lambda_w}$, and hence

$$(\overline{Nu}_{x,w})_i = \frac{4}{3} \left(\frac{1}{4} Gr_{x,\infty} \right)_i^{1/4} \left(-\frac{d\theta}{d\eta} \right)_{\eta=0} \quad (8.35i)$$

Obviously, for practical calculation of heat transfer, only the wall dimensionless temperature gradient $\left(-\frac{d\theta}{d\eta} \right)_{\eta=0}$ dependent on the solution of governing equations is no-given variable.

While, the corresponding practical prediction equations on heat transfer of water laminar free convection on an inclined flat plate will be, respectively,

$$(q_x)_i = 0.5812 \lambda_w (t_w - t_\infty) \left(\frac{1}{4} Gr_{x,\infty} \right)_i^{1/4} x^{-1} \text{Pr}_\infty^{0.301} \quad (8.29iw)$$

$$(\alpha_x)_i = 0.5812 \lambda_w \left(\frac{1}{4} Gr_{x,\infty} \right)_i^{1/4} x^{-1} \text{Pr}_\infty^{0.301} \quad (8.30iw)$$

$$(Nu_{x,w})_i = 0.5812 \left(\frac{1}{4} Gr_{x,\infty} \right)_i^{1/4} \text{Pr}_\infty^{0.301} \quad (8.31iw)$$

$$(Q_x)_i = 0.5812 \times \frac{4}{3} b \lambda_w (t_w - t_\infty) \left(\frac{1}{4} Gr_{x,\infty} \right)_i^{1/4} \text{Pr}_\infty^{0.301} \quad (8.32iw)$$

$$(\overline{Q}_x)_i = 0.5812 \times \frac{4}{3} x^{-1} \lambda_w (T_w - T_\infty) \left(\frac{1}{4} Gr_{x,\infty} \right)_i^{1/4} \text{Pr}_\infty^{0.301} \quad (8.33iw)$$

$$(\bar{\alpha}_x)_i = 0.5812 \times \frac{4}{3} \lambda_w \left(\frac{1}{4} Gr_{x,\infty} \right)_i^{1/4} x^{-1} Pr_\infty^{0.301} \quad (8.34iw)$$

$$(\overline{Nu}_x)_i = 0.5812 \times \frac{4}{3} \left(\frac{1}{4} Gr_{x,\infty} \right)_i^{1/4} Pr_\infty^{0.301} \quad (8.35iw)$$

From definitions of local Grashof number for the inclined and vertical cases defined in Eqs. (10.7) and (8.10), respectively, we obtain the following equation:

$$\frac{(Gr_{x,\infty})_i}{(Gr_{x,\infty})_v} = \cos \gamma \quad (10.18)$$

From the definition of local Nusselt number of laminar free convection, we have

$$\frac{(Nu_{x,w})_i}{(Nu_{x,w})_v} = \frac{-\left(\frac{1}{4} Gr_{x,\infty}\right)_i^{1/4} \left[\left(\frac{d\theta}{d\eta} \right)_{\eta=0} \right]_i}{-\left(\frac{1}{4} Gr_{x,\infty}\right)_v^{1/4} \left[\left(\frac{d\theta}{d\eta} \right)_{\eta=0} \right]_v} = \cos^{1/4} \gamma \quad (10.19)$$

For momentum transfer

Since the dimensionless governing Eqs. (10.11)–(10.13) are completely identical to Eqs. (8.23)–(8.25), the solutions for dimensionless velocity components both for the inclined and vertical cases for liquid laminar free convection are identical, i.e.,

$$(W_x)_i = (W_x)_v \quad (10.20)$$

$$(W_y)_i = (W_y)_v \quad (10.21)$$

Combining Eq. (10.20) with Eqs. (10.9) and (8.8), we have

$$\left(2\sqrt{g \cos \gamma x} |\rho_\infty / \rho_w - 1|^{1/2} \right)^{-1} (w_x)_i = \left[2\sqrt{g x} \left| \frac{\rho_\infty}{\rho_w} - 1 \right|^{1/2} \right]^{-1} (w_x)_v$$

i.e.

$$\frac{(w_x)_i}{(w_x)_v} = \cos^{1/2} \gamma \quad (10.22)$$

Combining Eq. (10.21) with Eqs. (10.10) and (8.9), we have

$$\begin{aligned} & \left\{ 2\sqrt{g \cos \gamma x} |\rho_\infty / \rho_w - 1|^{1/2} \left[\frac{1}{4} (Gr_{x,\infty})_i \right]^{-1/4} \right\}^{-1} (w_y)_i \\ &= \left[2\sqrt{g x} \left| \frac{\rho_\infty}{\rho_w} - 1 \right|^{-1/2} \left(\frac{1}{4} Gr_{x,\infty} \right)^{-1/4} \right]^{-1} (w_y)_v \end{aligned}$$

$$\begin{aligned} \frac{(w_y)_i}{(w_y)_v} &= \left\{ 2\sqrt{g \cos \gamma x} |\rho_\infty / \rho_w - 1|^{1/2} \left[\frac{1}{4} (Gr_{x,\infty})_i \right]^{-1/4} \right\} \\ &\quad \times \left[2\sqrt{gx} \left| \frac{\rho_\infty}{\rho_w} - 1 \right|^{-\frac{1}{2}} \left(\frac{1}{4} Gr_{x,\infty} \right)^{-\frac{1}{4}} \right]^{-1} \\ \frac{(w_y)_i}{(w_y)_v} &= \frac{2\sqrt{g \cos \gamma x} |\rho_\infty / \rho_w - 1|^{1/2} \left[\frac{1}{4} (Gr_{x,\infty})_i \right]^{-1/4}}{2\sqrt{gx} \left| \frac{\rho_\infty}{\rho_w} - 1 \right|^{-\frac{1}{2}} \left(\frac{1}{4} Gr_{x,\infty} \right)^{-\frac{1}{4}}} \\ \frac{(w_y)_i}{(w_y)_v} &= \frac{\sqrt{\cos \gamma} [(Gr_{x,\infty})_i]^{-1/4}}{(Gr_{x,\infty})_v^{-\frac{1}{4}}} \\ \frac{(w_y)_i}{(w_y)_v} &= \frac{\sqrt{\cos \gamma} [(Gr_{x,\infty})_v]^{-1/4}}{(Gr_{x,\infty})_i^{-\frac{1}{4}}} \end{aligned}$$

i.e

$$\frac{(w_y)_i}{(w_y)_v} = \cos^{1/4} \gamma \quad (10.23)$$

The governing basic equations and relationships of momentum and heat transfer between the inclined and vertical cases for liquid laminar free convection are summarized in Table 10.1.

10.3 Gas Laminar Free Convection on Inclined Plate

In principle, the governing equations of laminar free convection of liquid are completely suitable to those of gas. Then, the relationship equations between the inclined and vertical for liquid laminar free convection derived in Sect. 10.2 are completely suitable to those of gas laminar free convection.

However, for convenience, it is necessary to use the temperature parameter method for the expression of gas density variation with absolute temperature, i.e.,

$$\frac{\rho}{\rho_\infty} = \frac{T_\infty}{T} \quad (10.24)$$

to rewrite the equations for buoyancy factor, local Grashof number, and velocity components as follows for gas laminar free convection.

For inclined case:

The buoyancy force is expressed as

$$g |\rho_\infty - \rho| \cos \gamma = \rho g \left| \frac{T - T_\infty}{T_\infty} \right| \cos \gamma \quad (10.25)$$

Table 10.1 Governing equations of fluid laminar free convection both with the vertical and inclined cases, and the relationships for heat, momentum, and mass transfer between the vertical and inclined cases

Term	On vertical surface	On inclined surface
<i>Governing partial differential equations</i>		
Mass equation	$\frac{\partial}{\partial x}(\rho w_x) + \frac{\partial}{\partial y}(\rho w_y) = 0$	
Momentum equation	$\rho \left[(w_x)_v \frac{\partial(w_x)_v}{\partial x} + (w_y)_v \frac{\partial(w_x)_v}{\partial y} \right] = \frac{\partial}{\partial y} \left[\mu \frac{\partial(w_x)_v}{\partial y} \right] + g \rho_\infty - \rho $	$\rho \left[(w_x)_i \frac{\partial(w_x)_i}{\partial x} + (w_y)_i \frac{\partial(w_x)_i}{\partial y} \right] = \frac{\partial}{\partial y} \left[\mu \frac{\partial(w_x)_i}{\partial y} \right] + g \rho_\infty - \rho \cos \gamma$
Energy equation	$(\rho c_p (\rho_\infty - \rho) = \rho g \frac{T - T_\infty}{T_\infty} \text{ for gas laminar free convection})$ $\rho c_p \left(w_x \frac{\partial t}{\partial x} + w_y \frac{\partial t}{\partial y} \right) = \frac{\partial}{\partial y} \left(\lambda \frac{\partial t}{\partial y} \right)$	$(g(\rho_\infty - \rho) \cos \gamma = \rho g \frac{T - T_\infty}{T_\infty} \cos \gamma \text{ for gas laminar free convection})$
<i>Boundary conditions</i>		
$y = 0$	$w_x = 0, \quad w_y = 0, \quad T = T_w$	
$y \rightarrow \infty$	$w_x \rightarrow 0, \quad T = T_\infty$	
<i>Similarity variables</i>		
η	$\eta = \frac{y}{x} \left[\frac{1}{4} (Gr_{x,\infty})_v \right]^{1/4}$	$\eta = \frac{y}{x} \left[\frac{1}{4} (Gr_{x,\infty})_i \right]^{1/4}$
$Gr_{x,\infty}$	For general fluid laminar free convection $(Gr_{x,\infty})_v = \frac{g \rho_\infty/\rho_w - 1 x^3}{\nu_\infty^2}$	For general fluid laminar free convection $(Gr_{x,\infty})_i = \frac{g \cos \gamma \rho_\infty/\rho_w - 1 x^3}{\nu_\infty^2}$
θ	Refer in particular to for gas laminar free convection $(Gr_{x,\infty})_v = \frac{g T_w/T_\infty - 1 x^3}{\nu_\infty^2}$	Refer in particular to for gas laminar free convection $(Gr_{x,\infty})_i = \frac{g \cos \gamma T_w/T_\infty - 1 x^3}{\nu_\infty^2}$
W_x	For general fluid laminar free convection $(W_x)_v = (2\sqrt{g\bar{x}} \rho_\infty/\rho_w - 1 ^{1/2})^{-1} (w_x)_v$	For general fluid laminar free convection $(W_x)_i = (2\sqrt{g\bar{x} \cos \gamma} \rho_\infty/\rho_w - 1 ^{1/2})^{-1} (w_x)_i$
	Refer in particular to for gas laminar free convection $(W_x)_v = (2\sqrt{g\bar{x}} T_w/T_\infty - 1 ^{1/2})^{-1} (w_x)_v$	Refer in particular to for gas laminar free convection $(W_x)_i = (2\sqrt{g\bar{x} \cos \gamma} T_w/T_\infty - 1 ^{1/2})^{-1} w_x$

(continued)

Table 10.1 (continued)

Term	On vertical surface	On inclined surface
W_y	<p>For general fluid laminar free convection</p> $(W_y)_v = \left(2\sqrt{g\bar{x}} \rho_\infty/\rho_w - 1 ^{1/2} \left(\frac{1}{4}Gr_{x,\infty}\right)_v^{-1/4}\right)^{-1} (w_y)_v$ <p>Refer in particular to for gas laminar free convection</p> $W_y = \left(2\sqrt{g\bar{x}} T_w/T_\infty - 1 ^{1/2} \left(\frac{1}{4}Gr_{x,\infty}\right)_i^{-1/4}\right)^{-1} (w_y)_v$	$(W_y)_i = \left(2\sqrt{g\bar{x}\cos\gamma} \rho_\infty/\rho_w - 1 ^{1/2} \left(\frac{1}{4}Gr_{x,\infty}\right)_i^{-1/4}\right)^{-1} (w_y)_i$ $W_y = \left(2\sqrt{g\bar{x}\cos\gamma} T_w/T_\infty - 1 ^{1/2} \left(\frac{1}{4}Gr_{x,\infty}\right)_i^{-1/4}\right)^{-1} (w_y)_i$
<i>Governing ordinary differential equations</i>		
Mass equation	$2W_x - \eta \frac{dW_x}{d\eta} + 4 \frac{dW_y}{d\eta} - \frac{1}{\rho} \frac{d\rho}{d\eta} (\eta W_x - 4W_y) = 0$	
Momentum equation	$\frac{\nu_\infty}{v} \left(W_x \left(2W_x - \eta \frac{dW_x}{d\eta} \right) + 4W_y \frac{dW_y}{d\eta} \right) = \frac{d^2W_x}{d\eta^2} + \frac{1}{\mu} \frac{d\mu}{d\eta} \frac{dW_x}{d\eta} + \frac{\nu_\infty}{v} \frac{\rho}{\rho_\infty} - 1$	$\frac{\nu_\infty}{\rho_w} \frac{\rho}{\rho_\infty} - 1$
Energy equations	(Refer in particular to gas laminar free convection the buoyancy factor	$\frac{\rho}{\rho_w} \frac{\rho_\infty - 1}{\rho_w} = \theta$)
Boundary conditions	$Pr \frac{\nu_\infty}{v} (-\eta W_x + 4W_y) \frac{d\theta}{d\eta} = \frac{d^2\theta}{d\eta^2} + \frac{1}{\lambda} \frac{d\lambda}{d\eta} \frac{d\theta}{d\eta}$	
θ	$\eta = 0 : W_x = 0, W_y = 0, \theta = 1$ $\eta \rightarrow \infty : W_x = 0, \theta = 0$	
<i>Relationships of similarity variables related to vertical and inclined cases</i>		
$Gr_{x,\infty}$	$\frac{(Gr_{x,\infty})_i}{(Gr_{x,\infty})_v} = \cos \gamma$	
W_x	$(W_x)_i = (W_x)_v$ (Then, $\frac{(w_x)_i}{(w_x)_v} = \cos^{1/2} \gamma$)	
W_y	$(W_y)_i = (W_y)_v$ (Then, $\frac{(w_y)_i}{(w_y)_v} = \cos^{1/4} \gamma$)	
θ	$\theta_i = \theta_v$	
<i>Temperature gradient</i>		
$\left(\frac{d\theta}{d\eta}\right)_{\eta=0}$	For water laminar free convection: $\left[\left(\frac{d\theta}{d\eta}\right)_{\eta=0}\right]_i = -\left[\left(\frac{d\theta}{d\eta}\right)_{\eta=0}\right]_v = 0.5812Pr_{\infty}^{0.301}$	$(1.7 < Pr_\infty < 11.3)$

Term	On vertical surface	On inclined surface
	<p>Refer in particular to laminar free convection of diatomic gas, air and water vapor</p> $[-(\frac{d\theta}{dt})_{\eta=0}]_i = -[(\frac{d\theta}{dt})_{\eta=0}] = \psi(\text{Pr}) (\frac{T_w}{T_\infty})^{-m}$ $\psi(\text{Pr}) = (0.567 + 0.186 \cdot \text{Ln}(\text{Pr}))$ $m = 0.35n_\lambda + 0.29n_\mu + 0.36 \quad \text{for } T_w/T_\infty > 1$ $m = 0.42n_\lambda + 0.34n_\mu + 0.24 \quad \text{for } T_w/T_\infty < 1$	
<i>Heat transfer</i>		
For general free convection	$(q_x)_v = \lambda_w(t_w - t_\infty) (\frac{1}{4} Gr_{x,\infty})_v^{1/4} x^{-1} [(-\frac{d\theta}{dt})_{\eta=0}]_v$ $(\alpha_x)_v = \lambda_w (\frac{1}{4} Gr_{x,\infty})_v^{1/4} x^{-1} [(-\frac{d\theta}{dt})_{\eta=0}]_v$ $(Nu_{x,w})_v = (\frac{1}{4} Gr_{x,\infty})_v^{1/4} [(-\frac{d\theta}{dt})_{\eta=0}]_v$ $(Q_x)_v = -\frac{4}{3} b\lambda_w(t_w - t_\infty) (\frac{1}{4} Gr_{x,\infty})_v^{1/4} [(-\frac{d\theta}{dt})_{\eta=0}]_v$ $(\overline{Q_x})_v = \frac{4}{3} x^{-1} \lambda_w(T_w - T_\infty) (\frac{1}{4} Gr_{x,\infty})_v^{1/4} [(-\frac{d\theta}{dt})_{\eta=0}]_v$ $(\overline{\alpha_x})_v = \frac{4}{3} \lambda_w (\frac{1}{4} Gr_{x,\infty})_v^{1/4} x^{-1} [(-\frac{d\theta}{dt})_{\eta=0}]_v$ $(\overline{Nu_{x,w}})_v = \frac{4}{3} (\frac{1}{4} Gr_{x,\infty})_v^{1/4} [(-\frac{d\theta}{dt})_{\eta=0}]_v$	$(q_x)_i = \lambda_w(t_w - t_\infty) (\frac{1}{4} Gr_{x,\infty})_i^{1/4} x^{-1} [(-\frac{d\theta}{dt})_{\eta=0}]_i$ $(\alpha_x)_i = \lambda_w (\frac{1}{4} Gr_{x,\infty})_i^{1/4} x^{-1} [(-\frac{d\theta}{dt})_{\eta=0}]_i$ $(Nu_{x,w})_i = (\frac{1}{4} Gr_{x,\infty})_i^{1/4} [(-\frac{d\theta}{dt})_{\eta=0}]_i$ $(Q_x)_i = -\frac{4}{3} b\lambda_w(t_w - t_\infty) (\frac{1}{4} Gr_{x,\infty})_i^{1/4} [(-\frac{d\theta}{dt})_{\eta=0}]_i$ $(\overline{Q_x})_i = \frac{4}{3} x^{-1} \lambda_w(T_w - T_\infty) (\frac{1}{4} Gr_{x,\infty})_i^{1/4} [(-\frac{d\theta}{dt})_{\eta=0}]_i$ $(\overline{\alpha_x})_i = \frac{4}{3} \lambda_w (\frac{1}{4} Gr_{x,\infty})_i^{1/4} x^{-1} [(-\frac{d\theta}{dt})_{\eta=0}]_i$ $(\overline{Nu_{x,w}})_i = \frac{4}{3} (\frac{1}{4} Gr_{x,\infty})_i^{1/4} [(-\frac{d\theta}{dt})_{\eta=0}]_i$

The local Grashof number is expressed as

$$(Gr_{x,\infty})_i = \frac{g \cos \gamma |T_w/T_\infty - 1| x^3}{\nu_\infty^2} \quad (10.26)$$

The dimensionless velocity components are

$$(W_x)_i = \left(2\sqrt{g \cos \gamma x} |T_w/T_\infty - 1|^{1/2} \right)^{-1} (w_x)_i \quad (10.27)$$

$$(W_y)_i = \left\{ 2\sqrt{g \cos \gamma x} |T_w/T_\infty - 1|^{1/2} \left[\frac{1}{4} (Gr_{x,\infty})_i \right]^{-1/4} \right\}^{-1} (w_y)_i \quad (10.28)$$

For vertical case:

The buoyancy force is expressed as

$$g(\rho_\infty - \rho) = \rho g \frac{T - T_\infty}{T_\infty} \quad (10.29)$$

The local Grashof number is expressed as

$$(Gr_{x,\infty})_v = \frac{g |T_w/T_\infty - 1| x^3}{\nu_\infty^2} \quad (10.30)$$

The dimensionless velocity components are

$$(W_x)_v = \left(2\sqrt{gx} |T_w/T_\infty - 1|^{1/2} \right)^{-1} (w_x)_v \quad (10.31)$$

$$(W_y)_v = \left\{ 2\sqrt{gx} |T_w/T_\infty - 1|^{1/2} \left[\frac{1}{4} (Gr_{x,\infty})_v \right]^{-1/4} \right\}^{-1} (w_y)_v \quad (10.32)$$

Furthermore, with the simple power law of gas, the buoyancy factor $\frac{\frac{\rho_\infty}{\rho_w} - 1}{\frac{\rho_\infty}{\rho_w} - 1}$ can be transformed into

$$\frac{\frac{\rho_\infty}{\rho} - 1}{\frac{\rho_\infty}{\rho_w} - 1} = \frac{\frac{T}{T_\infty} - 1}{\frac{T_w}{T_\infty} - 1} = \frac{T - T_\infty}{T_w - T_\infty} = \theta$$

Then, Eq. (10.12) is transformed into equation

$$\begin{aligned} & \frac{\nu_\infty}{\nu} \left[(W_x)_i \left(2(W_x)_i - \eta_i \frac{d(W_x)_i}{d\eta_i} \right) + 4(W_y)_i \frac{d(W_x)_i}{d\eta_i} \right] \\ & = \frac{d^2(W_x)_i}{d\eta_i^2} + \frac{1}{\mu} \frac{d\mu}{d\eta_i} \frac{d(W_x)_i}{d\eta_i} + \frac{\nu_\infty \theta}{\nu} \end{aligned} \quad (10.33)$$

The dimensionless governing Eqs. (10.11), (10.13), and (10.33) for fluid laminar free convection for inclined case are completely identical to those for vertical case for gas laminar free convection. Then, the following curve-fitting formulae of dimensionless temperature gradient are suitable both to inclined and vertical cases for laminar free convection of diatomic gases, air, and water vapor:

$$\left[\left(\frac{d\theta}{d\eta} \right)_{\eta=0} \right]_i = \left[\left(\frac{d\theta}{d\eta} \right)_{\eta=0} \right]_v = \psi(\text{Pr}) \left(\frac{T_w}{T_\infty} \right)^{-m} \quad (10.34)$$

where

$$\psi(\text{Pr}) = (0.567 + 0.186 \cdot \text{Ln}(\text{Pr})) \quad (6.48)$$

$$m = 0.35n_\lambda + 0.29n_\mu + 0.36 \quad \text{for } T_w/T_\infty > 1 \quad (6.49)$$

$$m = 0.42n_\lambda + 0.34n_\mu + 0.24 \quad \text{for } T_w/T_\infty > 1 \quad (6.50)$$

Obviously, the heat transfer Eqs. (8.29i)–(8.35i) for laminar free convection on vertical flat plate will also be followed, respectively, as those for gas laminar free convection on inclined plate, i.e.,

$$(q_x)_i = \lambda_w(t_w - t_\infty) \left(\frac{1}{4} Gr_{x,\infty} \right)_i^{1/4} x^{-1} \left[\left(-\frac{d\theta}{d\eta} \right)_{\eta=0} \right]_i \quad (8.29i)$$

$$(\alpha_x)_i = \lambda_w \left(\frac{1}{4} Gr_{x,\infty} \right)_i^{1/4} x^{-1} \left[\left(-\frac{d\theta}{d\eta} \right)_{\eta=0} \right]_i \quad (8.30i)$$

$$(Nu_{x,w})_i = \left(\frac{1}{4} Gr_{x,\infty} \right)_i^{1/4} \left[\left(-\frac{d\theta}{d\eta} \right)_{\eta=0} \right]_i \quad (8.31i)$$

$$(Q_x)_i = -\frac{4}{3} b \lambda_w (t_w - t_\infty) \left(\frac{1}{4} Gr_{x,\infty} \right)_i^{1/4} \left[\left(-\frac{d\theta}{d\eta} \right)_{\eta=0} \right]_i \quad (8.32i)$$

$$(\bar{Q}_x)_i = \frac{4}{3} x^{-1} \lambda_w (T_w - T_\infty) \left(\frac{1}{4} Gr_{x,\infty} \right)_i^{1/4} \left[\left(-\frac{d\theta}{d\eta} \right)_{\eta=0} \right]_i \quad (8.33i)$$

$$(\bar{\alpha}_x)_i = \frac{4}{3} \lambda_w \left(\frac{1}{4} Gr_{x,\infty} \right)_i^{1/4} x^{-1} \left[\left(-\frac{d\theta}{d\eta} \right)_{\eta=0} \right]_i \quad (8.34i)$$

$$(\overline{Nu}_{x,w})_i = \frac{4}{3} \left(\frac{1}{4} Gr_{x,\infty} \right)_i^{1/4} \left[\left(-\frac{d\theta}{d\eta} \right)_{\eta=0} \right]_i \quad (8.35i)$$

While, the corresponding practical prediction Eqs. (6.36*)–(6.42*) on heat transfer of gas laminar free convection on a vertical flat plate will be, respectively, followed as those on inclined flat plate, i.e.,

$$(\alpha_x)_i = \lambda_w(T_w - T_\infty) \left(\frac{1}{4} Gr_{x,\infty} \right)_i^{1/4} x^{-1} \psi(\text{Pr}) \left(\frac{T_w}{T_\infty} \right)^{-m} \quad (6.36^*)$$

$$(\alpha_x)_i = -\lambda_w \left(\frac{1}{4} Gr_{x,\infty} \right)_i^{1/4} x^{-1} \psi(\text{Pr}) \left(\frac{T_w}{T_\infty} \right)^{-m} \quad (6.37^*)$$

$$(Nu_{x,w})_i = \left(\frac{1}{4} Gr_{x,\infty} \right)_i^{1/4} \psi(\text{Pr}) \left(\frac{T_w}{T_\infty} \right)^{-m} \quad (6.38^*)$$

$$(Q_x)_i = \frac{4}{3} b \lambda_w (T_w - T_\infty) \left(\frac{1}{4} Gr_{x,\infty} \right)_i^{1/4} \psi(\text{Pr}) \left(\frac{T_w}{T_\infty} \right)^{-m} \quad (6.39^*)$$

$$\overline{Q_x} = \frac{4}{3} b \lambda_w (T_w - T_\infty) \left(\frac{1}{4} Gr_{x,\infty} \right)^{1/4} \psi(\text{Pr}) \left(\frac{T_w}{T_\infty} \right)^{-m} \quad (6.40^*)$$

$$(\overline{\alpha_x})_i = \frac{4}{3} \lambda_w \left(\frac{1}{4} Gr_{x,\infty} \right)_i^{1/4} x^{-1} \psi(\text{Pr}) \left(\frac{T_w}{T_\infty} \right)^{-m} \quad (6.41^*)$$

$$\overline{(Nu_{x,w})}_i = \frac{4}{3} \left(\frac{1}{4} Gr_{x,\infty} \right)_i^{1/4} \psi(\text{Pr}) \left(\frac{T_w}{T_\infty} \right)^{-m} \quad (6.42^*)$$

where

$$\psi(\text{Pr}) = 0.567 + 0.186 \times \ln(\text{Pr}) \quad (0.6 \leq \text{Pr} \leq 1) \quad (6.48)$$

$$m = 0.64n_{\mu\lambda} + 0.36 = 0.35n_\lambda + 0.29n_\mu + 0.36 \quad (T_w/T_\infty > 1) \quad (6.49)$$

$$m = 0.76n_{\mu\lambda} + 0.24 = 0.42n_\lambda + 0.34n_\mu + 0.24 \quad (T_w/T_\infty < 1) \quad (6.50)$$

10.4 Summary

So far, the governing equations of fluid laminar free convection both with the vertical and inclined cases, and the relationships for heat, momentum, and mass transfer between the vertical and inclined cases are summarized in Table 10.1.

10.5 Remarks

In this chapter, the new similarity analysis method is applied to the similarity transformation of the governing partial differential equations of laminar free convection on inclined plate. Such transformed governing ordinary differential equations are same as those of the corresponding equations on the vertical plate; then, they have the same numerical solutions and prediction equations on heat transfer. Finally, the following simple and direct correlations for describing the transformations of the velocity components, heat transfer, and mass flow rate from the vertical case into the inclined case for the free convection are derived:

$$\frac{(w_x)_i}{(w_x)_v} = \cos^{1/2} \gamma, \quad \frac{(w_y)_i}{(w_y)_v} = \cos^{1/4} \gamma, \quad \frac{(Nu_{x,w})_i}{(Nu_{x,w})_v} = \cos^{1/4} \gamma \quad \text{and} \quad \frac{(G_x)_i}{(G_x)_v} = \cos^{1/4} \gamma$$

The successful derivation for the relationships of heat, momentum, and mass transfer for laminar free convection between the inclined and vertical plates, in this chapter, once again reveals the advantage of the new similarity analysis method over the traditional Falkner–Skan transformation, for studying laminar boundary layer problems.

10.6 Calculation Example

Question:

A flat plate with $b = 1$ m in width and $x = 0.3$ m in length is suspended vertically in air. The ambient temperature is $t_\infty = 20^\circ\text{C}$. Calculate the free convection heat transfer of the plate for the temperature ratio $T_w/T_\infty = 1.7$. What is its heat transfer rate, if the plate's inclined angle is 45° .

Solution:

From $t_\infty = 20^\circ\text{C}$ and $T_w/T_\infty = 1.7$, we have $T_w = 498.1$ K or $T_w = 225.1^\circ\text{C}$.

The air physical properties are as follows: kinetic viscosity is $\nu_\infty = 15.06 \times 10^{-6}$ m²/s at $t_\infty = 20^\circ\text{C}$, $\lambda_w = 4.07 \times 10^{-2}$ W/(m °C) at $T_w = 225.1^\circ\text{C}$. From Tables 4.1 and 4.3, we get $n_\mu = 0.68$, $n_\lambda = 0.81$, and $\text{Pr} = 0.7$ for air.

1. *For vertical case:*

From Eq. (5.51), the local Nusselt number is expressed as

$$(Nu_{x,w})_v = - \left(\frac{1}{4} Gr_{x,\infty} \right)_v^{1/4} \left(\frac{d\theta}{d\eta} \right)_{\eta=0}$$

where $(Nu_{x,w})_v$ is defined as

$$(Nu_{x,w})_v = \frac{(\alpha_x)_v x}{\lambda_w}$$

The local Grashof number is evaluated as

$$\begin{aligned} (Gr_{x,\infty})_v &= \frac{g |T_w/T_\infty - 1| x^3}{\nu_\infty^2} \\ &= \frac{9.8 \times |(498.1/293 - 1)| \times 0.3^3}{(15.06 \times 10^{-6})^2} \\ &= 0.81665 \times 10^9 < 10^9 \end{aligned}$$

Then, the flow is laminar free convection.

According to Eqs. (5.54) and (5.55), the temperature gradient is expressed as

$$-\left(\frac{d\theta}{d\eta}\right)_{\eta=0} = \psi(\text{Pr}) \left(\frac{T_w}{T_\infty}\right)^{-m}$$

where parameter m is expressed as

$$\begin{aligned} m &= 0.35n_\lambda + 0.29n_\mu + 0.36 \\ &= 0.35 \times 0.81 + 0.29 \times 0.68 + 0.36 = 0.8407 \end{aligned}$$

for $T_w/T_\infty > 1$. Then,

$$-\left(\frac{d\theta}{d\eta}\right)_{\eta=0} = \psi(\text{Pr}) \left(\frac{T_w}{T_\infty}\right)^{-m} = 0.32048$$

On these bases, $(Nu_{x,w})_v$ can be evaluated as follows:

$$\begin{aligned} (Nu_{x,w})_v &= -\left(\frac{1}{4}Gr_{x,\infty}\right)_v^{1/4} \left(\frac{d\theta}{d\eta}\right)_{\eta=0} \\ &= \left(\frac{1}{4} \times (0.81665 \times 10^9)\right)^{1/4} \times 0.32048 \\ &= 38.3085 \end{aligned}$$

With the definition of local Nusselt number for vertical case, $Nu_{x,w} = \frac{\alpha_x x}{\lambda_w}$, the local heat transfer coefficient for vertical case can be calculated as

$$\begin{aligned} (\alpha_x)_v &= (Nu_{x,w})_v \frac{\lambda_w}{x} \\ &= 38.3085 \times \frac{0.0407}{0.3} \\ &= 5.197 \text{ W}/(\text{m}^2 \text{ K}) \end{aligned}$$

The average heat transfer coefficient can be calculated as

$$\begin{aligned}\overline{(\alpha_x)_v} &= \frac{4}{3}(\alpha_x)_v \\ &= \frac{4}{3} \times 5.197 \\ &= 6.9296 \text{ W}/(\text{m}^2 \text{ K})\end{aligned}$$

The heat transfer rate of the free convection on the vertical plate is

$$\begin{aligned}(Q_x)_v &= \overline{(\alpha_x)_v} \times (T_w - T_\infty) \times bx \\ &= 6.9296 \times (498.1 - 293) \times 1 \times 0.3 \\ &= 426.38 \text{ W}\end{aligned}$$

2. *For inclined case:*

From Table 9.2, the local Nusselt number for inclined case can be expressed as

$$\begin{aligned}(Nu_{x,w})_i &= (Nu_{x,w})_v \cdot \cos^{1/4} \gamma \\ &= 38.3085 \times \cos^{1/4}(45^\circ) \\ &= 35.129\end{aligned}$$

With the definition of local Nusselt number for inclined case, $Nu_{x,w} = \frac{\alpha_x x}{\lambda_w}$, the local heat transfer coefficient for inclined case can be calculated as

$$\begin{aligned}(\alpha_x)_i &= (Nu_{x,w})_i \frac{\lambda_w}{x} \\ &= 35.129 \times \frac{4.07 \times 10^{-2}}{0.3} \\ &= 4.7658 \text{ W}/(\text{m}^2 \text{ K})\end{aligned}$$

The average heat transfer coefficient can be calculated as

$$\begin{aligned}\overline{(\alpha_x)_i} &= \frac{4}{3}(\alpha_x)_i \\ &= \frac{4}{3} \times 4.7658 \\ &= 6.3544 \text{ W}/(\text{m}^2 \text{ K})\end{aligned}$$

The heat transfer rate of the free convection on the inclined plate is

$$\begin{aligned}
 (Q_x)_i &= \overline{(\alpha_x)}_i \times (T_w - T_\infty) \times bx \\
 &= 6.3544 \times (498.1 - 293) \times 1 \times 0.3 \\
 &= 391 \text{ W}
 \end{aligned}$$

10.7 Question

1. How to understand the identity of laminar free convection for inclined and vertical gases?

10.8 Exercise

1. Please explain the identity of the governing mathematical models between the laminar free convection on the inclined and vertical cases.

Appendix A Derivation of Eqs. (10.1)–(10.3)

A1. Derivation of Eq. (10.1)

Equation (10.1) can be changed to

$$\rho \left[\frac{\partial (w_x)_i}{\partial x} + \frac{\partial (w_y)_i}{\partial x} \right] + (w_x)_i \frac{\partial \rho}{\partial x} + (w_y)_i \frac{\partial \rho}{\partial y} = 0 \quad (10.1a)$$

With the dimensionless variables assumed in Eqs. (10.6), (10.7), (10.9), and (10.10), the following correlations are obtained:

$$\begin{aligned}
 \frac{\partial (w_x)_i}{\partial x} &= \left[2\sqrt{gx} \left| \frac{\rho_\infty}{\rho_w} - 1 \right|^{1/2} \right] \frac{d(W_x)_i}{d\eta_i} \frac{\partial \eta_i}{\partial x} \cos \gamma \\
 &\quad + \frac{1}{2} x^{-1/2} \left[2\sqrt{g} \left| \frac{\rho_\infty}{\rho_w} - 1 \right|^{1/2} \right] (W_x)_i \cos^{1/2} \gamma
 \end{aligned}$$

where

$$\frac{\partial \eta_i}{\partial x} = \frac{\partial}{\partial x} \left[\frac{y}{x} \left(\frac{1}{4} Gr_{x,\infty} \right)_i^{1/4} \right]$$

$$\begin{aligned}
&= \frac{\partial}{\partial x} \left[y \left(\frac{1}{4} \frac{g \left| \frac{\rho_\infty}{\rho_w} - 1 \right| x^{-1}}{v_\infty^2} \right)^{1/4} \right] \\
&= -\frac{1}{4} \left[y \left(\frac{1}{4} \frac{g \left| \frac{\rho_\infty}{\rho_w} - 1 \right|}{v_\infty^2} \right)^{1/4} \right]_{x=\frac{5}{4}} \\
&= -\frac{1}{4} \left[y \left(\frac{1}{4} \frac{g \left| \frac{\rho_\infty}{\rho_w} - 1 \right| x^3}{v_\infty^2} \right)^{1/4} \right]_{x=2} \\
&= -\frac{1}{4} x^{-1} \eta_i
\end{aligned}$$

Then,

$$\begin{aligned}
\frac{\partial(w_x)_i}{\partial x} &= \left[2\sqrt{gx} \frac{\rho_\infty}{\rho_w} - 1^{1/2} \right] \frac{d(W_x)_i}{d\eta_i} \left(-\frac{1}{4} x^{-1} \eta_i \right) \cos^{1/2} \gamma \\
&\quad + \frac{1}{2} x^{-\frac{1}{2}} \left[2\sqrt{g} \left| \frac{\rho_\infty}{\rho_w} - 1 \right|^{1/2} \right] (W_x)_i \cos^{1/2} \gamma \\
&= -\frac{1}{2} \left[\sqrt{\frac{g}{x}} \left| \frac{\rho_\infty}{\rho_w} - 1 \right|^{1/2} \right] \eta \frac{d(W_x)_i}{d\eta_i} \cos^{1/2} \gamma \\
&\quad + \left[\sqrt{\frac{g}{x}} \left| \frac{\rho_\infty}{\rho_w} - 1 \right|^{1/2} \right] (W_x)_i \cos^{1/2} \gamma \\
&= \sqrt{\frac{g}{x}} \left| \frac{\rho_\infty}{\rho_w} - 1 \right|^{1/2} \cos^{1/2} \gamma \left((W_x)_i - \frac{1}{2} \eta_i \frac{d(W_x)_i}{d\eta_i} \right) \quad (A1)
\end{aligned}$$

$$\frac{\partial(w_y)_i}{\partial y} = 2\sqrt{\frac{g}{x}} \left| \frac{\rho_\infty}{\rho_w} - 1 \right|^{1/2} \cos^{1/2} \gamma \frac{d(W_y)_i}{d\eta} \quad (A2)$$

$$\frac{\partial \rho}{\partial x} = \frac{d\rho}{d\eta_i} \frac{\partial \eta_i}{\partial x} = -\frac{1}{4} \eta_i x^{-1} \frac{d\rho}{d\eta_i} \quad (A3)$$

$$\frac{\partial \rho}{\partial y} = \frac{d\rho}{d\eta_i} \frac{\partial \eta_i}{\partial y} = \frac{d\rho}{d\eta_i} \left[\frac{1}{4} (Gr_{x,\infty})_i \right]^{1/4} x^{-1} \quad (A4)$$

With Eqs. (A1)–(A4), Eq. (10.1a) can be transformed into

$$\begin{aligned}
& \rho \left[\sqrt{\frac{g}{x}} \left| \frac{\rho_\infty}{\rho_w} - 1 \right|^{1/2} \cos^{1/2} \gamma \left((W_x)_i - \frac{1}{2} \eta_i \frac{d(W_x)_i}{d\eta_i} \right) \right. \\
& \quad \left. + 2 \sqrt{\frac{g}{x}} \left| \frac{\rho_\infty}{\rho_w} - 1 \right|^{1/2} \cos^{1/2} \gamma \frac{d(W_y)_i}{d\eta_i} \right] \\
& \quad + 2 \sqrt{gx \cos \gamma} |\rho_\infty / \rho_w - 1|^{1/2} (W_x)_i \left(-\frac{1}{4} \eta_i x^{-1} \frac{d\rho}{d\eta} \right) \\
& \quad + 2 \sqrt{gx \cos \gamma} |\rho_\infty / \rho_w - 1|^{1/2} \left[\frac{1}{4} (Gr_{x,\infty})_i \right]^{-1/4} (W_y)_i \frac{d\rho}{d\eta_i} \left(\frac{1}{4} Gr_{x,\infty} \right)_i^{1/4} x^{-1} \\
& = 0 \tag{A5}
\end{aligned}$$

Equation (A5) is divided by $\sqrt{\frac{g \cos \gamma}{x}} \left| \frac{\rho_\infty}{\rho_w} - 1 \right|^{1/2}$ then it is simplified to

$$2(W_x)_i - \eta \frac{d(W_x)_i}{d\eta_i} + 4 \frac{d(W_y)_i}{d\eta_i} - \frac{1}{\rho} \frac{d\rho}{d\eta_i} [\eta_i (W_x)_i - 4(W_y)_i] = 0 \tag{10.11}$$

This is the dimensionless continuity equation of fluid laminar free convection for inclined case.

A2. Derivation of Eq. (10.2)

Equation (10.2) is rewritten as

$$\rho \left[(w_x)_i \frac{\partial (w_x)_i}{\partial x} + (w_y)_i \frac{\partial (w_x)_i}{\partial y} \right] = \mu \frac{\partial^2 (w_x)_i}{\partial x^2} + \frac{\partial (w_x)_i}{\partial y} \frac{\partial \mu}{\partial y} + g |\rho_\infty - \rho| \cos \gamma \tag{10.2a}$$

where

$$\begin{aligned}
\frac{\partial (w_x)_i}{\partial y} &= \frac{d(W_x)_i}{d\eta_i} \frac{\partial \eta_i}{\partial y} = 2 \sqrt{gx} \left| \frac{\rho_\infty}{\rho_w} - 1 \right|^{1/2} \frac{d(W_x)_i}{d\eta_i} \frac{\partial \eta_i}{\partial y} \cos^{1/2} \gamma \\
\frac{\partial \eta_i}{\partial y} &= x^{-1} \left[\frac{1}{4} (Gr_{x,\infty})_i \right]^{1/4}
\end{aligned}$$

Then,

$$\frac{\partial (w_x)_i}{\partial y} = 2 \sqrt{gx} \left| \frac{\rho_\infty}{\rho_w} - 1 \right|^{1/2} \frac{d(W_x)_i}{d\eta_i} x^{-1} \left[\frac{1}{4} (Gr_{x,\infty})_i \right]^{1/4} \cos^{1/2} \gamma \tag{A6}$$

$$\begin{aligned}
\frac{\partial^2 w_x}{\partial y^2} &= 2\sqrt{gx} \left| \frac{\rho_\infty}{\rho_w} - 1 \right|^{1/2} \frac{d^2(W_x)_i}{d\eta_i^2} x^{-1} \left[\frac{1}{4} (Gr_{x,\infty})_i \right]^{1/4} \frac{\partial \eta_i}{\partial y} \cos^{1/2} \gamma \\
&= 2\sqrt{gx} \left| \frac{\rho_\infty}{\rho_w} - 1 \right|^{1/2} \frac{d^2(W_x)_i}{d\eta_i^2} x^{-1} \left[\frac{1}{4} (Gr_{x,\infty})_i \right]^{1/4} x^{-1} \\
&\quad \times \left[\frac{1}{4} (Gr_{x,\infty})_i \right]^{1/4} \cos^{1/2} \gamma \\
&= 2\sqrt{gx} \left| \frac{\rho_\infty}{\rho_w} - 1 \right|^{1/2} \frac{d^2(W_x)_i}{d\eta_i^2} \left(\frac{1}{4} Gr_{x,\infty} \right)_i^{1/2} x^{-2} \cos^{1/2} \gamma
\end{aligned} \tag{A7}$$

$$\begin{aligned}
\frac{\partial \mu}{\partial y} &= \frac{d\mu}{d\eta_i} \frac{\partial \eta_i}{\partial y} \\
&= \frac{d\mu}{d\eta_i} \left(\frac{1}{4} Gr_{x,\infty} \right)_i^{1/4} x^{-1}
\end{aligned} \tag{A8}$$

With (A6)–(A8), Eq. (10.2a) is changed into

$$\begin{aligned}
&\rho \left[2\sqrt{gx \cos \gamma} \left| \rho_\infty / \rho_w - 1 \right|^{1/2} (W_x)_i \sqrt{\frac{g}{x}} \left| \frac{\rho_\infty}{\rho_w} - 1 \right|^{1/2} \right. \\
&\quad \left. \cos^{1/2} \gamma \left((W_x)_i - \frac{1}{2} \eta \frac{d(W_x)_i}{d\eta} \right) + 2\sqrt{gx \cos \gamma} \left| \rho_\infty / \rho_w - 1 \right|^{1/2} \left[\frac{1}{4} (Gr_{x,\infty})_i \right]^{-1/4} \right. \\
&\quad \left. \times (W_y)_i 2\sqrt{gx} \left| \frac{\rho_\infty}{\rho_w} - 1 \right|^{1/2} \frac{d(W_x)_i}{d\eta_i} x^{-1} \left[\frac{1}{4} (Gr_{x,\infty})_i \right]^{1/4} \cos^{1/2} \gamma \right] \\
&= 2\mu \sqrt{gx} \left| \frac{\rho_\infty}{\rho_w} - 1 \right|^{1/2} \frac{d^2(W_x)_i}{d\eta^2} \left[\frac{1}{4} (Gr_{x,\infty})_i \right]^{1/2} x^{-2} \cos^{1/2} \gamma \\
&\quad + 2\sqrt{gx} \left| \frac{\rho_\infty}{\rho_w} - 1 \right|^{1/2} \frac{d(W_x)_i}{d\eta_i} x^{-1} \left[\frac{1}{4} (Gr_{x,\infty})_i \right]^{1/4} \cos^{1/2} \gamma \frac{d\mu}{d\eta_i} \\
&\quad \times \left[\frac{1}{4} (Gr_{x,\infty})_i \right]^{1/4} x^{-1} + g \left| \rho_\infty - \rho \right| \cos \gamma
\end{aligned} \tag{A9}$$

With definition of $(Gr_{x,\infty})_i$, Eq. (A9) is rewritten as

$$\begin{aligned}
&\rho \left[2\sqrt{gx \cos \gamma} \left| \rho_\infty / \rho_w - 1 \right|^{1/2} (W_x)_i \sqrt{\frac{g}{x}} \left| \frac{\rho_\infty}{\rho_w} - 1 \right|^{1/2} \cos^{1/2} \gamma \right. \\
&\quad \times \left((W_x)_i - \frac{1}{2} \eta \frac{d(W_x)_i}{d\eta} \right) + 2\sqrt{gx \cos \gamma} \left| \rho_\infty / \rho_w - 1 \right|^{1/2} \\
&\quad \left. \times (W_y)_i 2\sqrt{gx} \left| \frac{\rho_\infty}{\rho_w} - 1 \right|^{1/2} \frac{d(W_x)_i}{d\eta_i} x^{-1} \cos^{1/2} \gamma \right]
\end{aligned}$$

$$\begin{aligned}
&= 2\mu\sqrt{gx} \left| \frac{\rho_\infty}{\rho_w} - 1 \right|^{1/2} \frac{d^2 W_x}{d\eta_i^2} \left[\frac{1}{4} \frac{g \cos \gamma |\rho_\infty/\rho_w - 1| x^3}{v_\infty^2} \right]^{1/2} x^{-2} \cos^{1/2} \gamma \\
&+ 2\sqrt{gx} \left| \frac{\rho_\infty}{\rho_w} - 1 \right|^{1/2} \frac{d(W_x)_i}{d\eta_i} x^{-1} \left[\frac{1}{4} \left(\frac{g \cos \gamma |\rho_\infty/\rho_w - 1| x^3}{v_\infty^2} \right) \right]_i^{1/2} \\
&\times \cos^{1/2} \gamma \frac{d\mu}{d\eta_i} x^{-1} + g |\rho_\infty - \rho| \cos \gamma \tag{A10}
\end{aligned}$$

Equation (A10) is divided by $\rho g \left| \frac{\rho_\infty}{\rho_w} - 1 \right| \cos \gamma$, and simplified to

$$\begin{aligned}
&\left[2\sqrt{x}(W_x)_i \sqrt{\frac{1}{x}} \left((W_x)_i - \frac{1}{2} \eta \frac{d(W_x)_i}{d\eta_i} \right) + 2\sqrt{x}(W_y)_i 2\sqrt{x} \frac{d(W_x)_i}{d\eta_i} x^{-1} \right] \\
&= 2v\sqrt{x} \frac{d^2(W_x)_i}{d\eta_i^2} \left[\frac{1}{4} \frac{x^3}{v_\infty^2} \right]^{1/2} x^{-2} + \frac{2}{\rho} \sqrt{x} \frac{d(W_x)_i}{d\eta_i} x^{-1} \left[\frac{1}{4} \left(\frac{x^3}{v_\infty^2} \right) \right]_i^{1/2} \\
&\times \frac{d\mu}{d\eta_i} x^{-1} + \frac{\rho_w}{\rho} \left| \frac{\rho_\infty - \rho}{\rho_\infty - \rho_w} \right|
\end{aligned}$$

The above equation is divided by $\frac{v}{v_\infty}$, and simplified to

$$\begin{aligned}
&\frac{v_\infty}{v} \left[2(W_x)_i \left((W_x)_i - \frac{1}{2} \eta_i \frac{d(W_x)_i}{d\eta_i} \right) + 2(W_y)_i 2 \frac{d(W_x)_i}{d\eta_i} \right] \\
&= \frac{d^2(W_x)_i}{d\eta_i^2} + \frac{2}{\rho} \frac{v_\infty}{v} \frac{d(W_x)_i}{d\eta_i} \left[\frac{1}{4} \left(\frac{1}{v_\infty^2} \right) \right]_i^{1/2} \frac{d\mu}{d\eta_i} + \frac{v_\infty}{v} \frac{\rho_w}{\rho} \left| \frac{\rho_\infty - \rho}{\rho_\infty - \rho_w} \right|
\end{aligned}$$

i.e.,

$$\begin{aligned}
&\frac{v_\infty}{v} \left[(W_x)_i (2(W_x)_i - \eta_i \frac{d(W_x)_i}{d\eta_i}) + 4(W_y)_i \frac{d(W_x)_i}{d\eta_i} \right] \\
&= \frac{d^2(W_x)_i}{d\eta_i^2} + \frac{1}{\mu} \frac{d(W_x)_i}{d\eta_i} \frac{d\mu}{d\eta_i} + \frac{v_\infty}{v} \frac{\rho_w}{\rho} \left| \frac{\rho_\infty - \rho}{\rho_\infty - \rho_w} \right| \tag{A11}
\end{aligned}$$

Because $\frac{\rho_\infty - \rho}{\rho_\infty - \rho_w}$ is always positive, the above equation is rewritten as

$$\begin{aligned}
&\frac{v_\infty}{v} \left[(W_x)_i (2(W_x)_i - \eta_i \frac{d(W_x)_i}{d\eta_i}) + 4(W_y)_i \frac{d(W_x)_i}{d\eta_i} \right] \tag{10.12} \\
&= \frac{d^2(W_x)_i}{d\eta_i^2} + \frac{1}{\mu} \frac{d\mu}{d\eta_i} \frac{d(W_x)_i}{d\eta_i} + \frac{v_\infty}{v} \frac{\frac{\rho_\infty}{\rho} - 1}{\frac{\rho_\infty}{\rho_w} - 1}
\end{aligned}$$

This is the dimensionless momentum equation of fluid laminar free convection for inclined case.

A3. Derivation of Eq. (10.3)

Equation (10.3) is rewritten as

$$\rho c_p \left[(w_x)_i \frac{\partial t}{\partial x} + (w_y)_i \frac{\partial t}{\partial y} \right] = \lambda \frac{\partial^2 t}{\partial y^2} + \frac{\partial \lambda}{\partial y} \frac{\partial t}{\partial y} \quad (\text{A12})$$

where

$$t = (t_w - t_\infty)\theta + t_\infty \quad (\text{A13})$$

$$\frac{\partial t}{\partial x} = -(t_w - t_\infty) \frac{d\theta}{d\eta_i} \left(\frac{1}{4} \right) \eta_i x^{-1} \quad (\text{A14})$$

$$\frac{\partial t}{\partial y} = (t_w - t_\infty) \frac{d\theta}{d\eta_i} \left(\frac{1}{4} Gr_{x,\infty} \right)_i^{1/4} x^{-1} \quad (\text{A15})$$

$$\frac{\partial^2 t}{\partial y^2} = (t_w - t_\infty) \frac{d^2\theta}{d\eta_i^2} \left(\frac{1}{4} Gr_{x,\infty} \right)_i^{1/2} x^{-2} \quad (\text{A16})$$

$$\frac{\partial \lambda}{\partial y} = \frac{d\lambda}{d\eta_i} \left(\frac{1}{4} Gr_{x,\infty} \right)_i^{1/4} x^{-1} \quad (\text{A17})$$

With Eqs. (A13)–(A17), Eq. (A12) becomes

$$\begin{aligned} & \rho c_p \left[-2\sqrt{g \cos \gamma x} |\rho_\infty / \rho_w - 1|^{1/2} (W_x)_i (t_w - t_\infty) \frac{d\theta}{d\eta_i} \left(\frac{1}{4} \right) \eta_i x^{-1} \right. \\ & \quad \left. + 2\sqrt{g \cos \gamma x} |\rho_\infty / \rho_w - 1|^{1/2} \left(\frac{1}{4} Gr_{x,\infty} \right)_i^{-1/4} \right. \\ & \quad \left. \times (W_y)_i (t_w - t_\infty) \frac{d\theta}{d\eta_i} \left(\frac{1}{4} Gr_{x,\infty} \right)_i^{1/4} x^{-1} \right] \\ & = \lambda (t_w - t_\infty) \frac{d^2\theta}{d\eta_i^2} \left(\frac{1}{4} Gr_{x,\infty} \right)_i^{1/2} x^{-2} + \frac{d\lambda}{d\eta_i} \left(\frac{1}{4} Gr_{x,\infty} \right)_i^{1/4} \\ & \quad \times x^{-1} (t_w - t_\infty) \frac{d\theta}{d\eta_i} \left(\frac{1}{4} Gr_{x,\infty} \right)_i^{1/4} x^{-1} \quad (\text{A18}) \end{aligned}$$

Equation(A18) is divided by $(t_w - t_\infty)$, simplified to the following form by consideration of the definition of Grashof number, $Gr_{x,\infty}$:

$$\begin{aligned} & \rho c_p \left[-2\sqrt{g \cos \gamma x} |\rho_\infty/\rho_w - 1|^{1/2} (W_x)_i \frac{d\theta}{d\eta_i} \left(\frac{1}{4}\right) \eta_i x^{-1} \right. \\ & \quad \left. -2\sqrt{g \cos \gamma x} |\rho_\infty/\rho_w - 1|^{1/2} (W_y)_i \frac{d\theta}{d\eta_i} x^{-1} \right] \\ & = \lambda \frac{d^2\theta}{d\eta_i^2} \left(\frac{1}{4} \frac{g \cos \gamma |\rho_\infty/\rho_w - 1| x^3}{v_\infty^2} \right)_i^{1/2} x^{-2} \\ & \quad + \frac{d\lambda}{d\eta_i} \left(\frac{1}{4} \frac{g \cos \gamma |\rho_\infty/\rho_w - 1| x^3}{v_\infty^2} \right)_i^{1/2} x^{-1} \frac{d\theta}{d\eta_i} x^{-1} \end{aligned}$$

The above equation is divided by $|\frac{\rho_\infty}{\rho_w} - 1|^{1/2} \sqrt{\frac{g \cos \gamma}{x}}$, then, we get

$$\begin{aligned} & \rho c_p \left[-2(W_x)_i \frac{d\theta}{d\eta_i} \left(\frac{1}{4}\right) \eta_i + 2(W_y)_i \frac{d\theta}{d\eta_i} \right] \\ & = \lambda \frac{d^2\theta}{d\eta_i^2} \left(\frac{1}{4} \frac{1}{v_\infty^2}\right)_i^{1/2} + \frac{d\lambda}{d\eta_i} \left(\frac{1}{4} \frac{1}{v_\infty^2}\right)_i^{1/2} \frac{d\theta}{d\eta_i} \end{aligned} \quad (A19)$$

This equation is multiplied by $\frac{2v_\infty}{\lambda}$ and on simplification, finally becomes

$$\frac{v_\infty}{\lambda} \rho c_p \left[-(W_x)_i \frac{d\theta}{d\eta_i} \eta_i + 4(W_y)_i \frac{d\theta}{d\eta_i} \right] = \frac{d^2\theta}{d\eta_i^2} + \frac{1}{\lambda} \frac{d\lambda}{d\eta_i} \frac{d\theta}{d\eta_i}$$

i.e.,

$$\text{Pr} \frac{v_\infty}{\nu} \left[-\eta_i (W_x)_i + 4(W_y)_i \right] \frac{d\theta}{d\eta_i} = \frac{d^2\theta}{d\eta_i^2} + \frac{1}{\lambda} \frac{d\lambda}{d\eta_i} \frac{d\theta}{d\eta_i} \quad (10.13)$$

This is the dimensionless energy equation of fluid laminar free convection for inclined case.

References

1. B.R. Rich, An investigation of heat transfer from an inclined flat plate in free convection. Trans. ASME **75**, 489–499 (1953)
2. G.C. Vliet, Natural convection local heat transfer on constant heat flux inclined surface. J. Heat Transfer **9**, 511–516 (1969)
3. T. Fujii, H. Imura, Natural convection from a plate with arbitrary inclination Int. J. Heat Mass Transfer **15**, 755–767 (1972)

4. V.M. Falkner, S.W. Skan, Some approximate solutions of the boundary layer equations. *Phil. Mag* **12**, 865 (1931)
5. H. Schlichting, *Boundary Layer Theory*, translated by J. Kestin (McGraw-Hill, New York, 1979), pp. 316–317
6. T. Cebeci, P. Bradshaw, *Physical and Computational Aspects of Convective Heat Transfer* (Springer-Verlag, New York, 1984)
7. D.Y. Shang, B.X. Wang, Effect of variable thermophysical properties on laminar free convection of gas. *Int. J. Heat Mass Transfer* **33**(7), 1387–1395 (1990)
8. D.Y. Shang, B.X. Wang, Effect of variable thermophysical properties on laminar free convection of polyatomic gas. *Int. J. Heat Mass Transfer* **34**, 749–755 (1991)
9. D.Y. Shang, B.X. Wang, Y. Wang, Y. Quan, Study on liquid laminar free convection with consideration of variable thermophysical properties. *Int. J. Heat Mass Transfer* **36**(14), 3411–3419 (1993)
10. D.Y. Shang, H.S. Takhar, Extended study on relationships of heat, momentum, and mass transfer for laminar free convection between inclined and vertical plates. *J. Theor. Appl. Fluid Mech.* **1**(1), 16–32 (1995)

Part III
Laminar Free Convection Film Boiling
and Condensation with Consideration
of Coupled Effect of Variable Physical
Properties

Chapter 11

Complete Mathematical Models of Laminar Free Convection Film Boiling of Liquid

Abstract The new similarity analysis method is successfully applied for complete similarity transformation of the governing partial differential equations of laminar free film boiling of subcooled liquid with consideration of coupled effects of variable physical properties, where the laminar free film boiling of saturated liquid is only regarded as its special case. The dimensionless velocity components as the solutions for vapor and liquid films have definite physical meanings. It follows that the new similarity analysis method is appropriate for extensive investigation of the two-phase boundary layer problems with consideration of coupled effects of variable physical properties, such as the temperature-dependent density, thermal conductivity, and absolute viscosity of the medium of vapor and liquid films. The interfacial balance equations between the vapor and liquid films are considered in detail, such as mass flow rate balance, velocity component balance, shear force balance, temperature balance, and energy balance.

11.1 Introduction

Bromley [1] first treated the laminar film boiling heat transfer of saturated liquid from a horizontal cylinder, using a simple theoretical model. Later, analytical investigations [2–7] were made to analyze pool film boiling from a vertical plate, in which only a few researches [5] and [7] took into account temperature-dependence of fluid physical properties. McFadden and Grosh [5] developed the analysis of saturated film boiling where the temperature-dependence of density and specific heat were taken into account. Nishikawa, Ito, and Matsumoto [7] made an analysis of pool film boiling as a variable property problem on the basis of the two-phase boundary layer theory, but only the effect of variation of vapor's physical properties with temperature was examined in the range of lower degree of subcooling ($T_s - T_\infty = 0, 20, 40^\circ\text{C}$).

However, in film boiling, the temperature difference between the heating surface and bulk liquid is very large, where large superheated degrees on the surface and

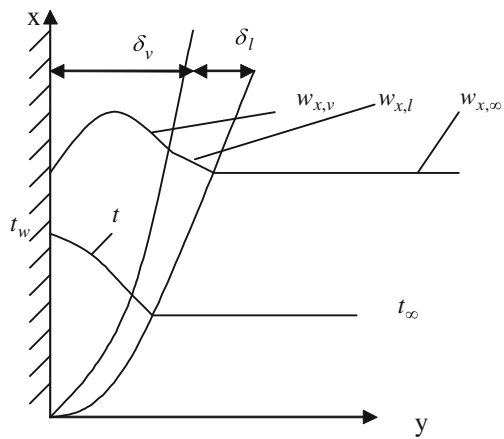
large subcooled degrees of liquid are often included. In Chaps. 6–8 it is shown that the physical property variations of gas and liquid with temperature have great influences on their free convection. Of course, they have definitely great effect on the film boiling of liquid. Therefore, from now on, two chapters will be devoted in this book to introduce the recent studies of Shang, Wang, and Zhong [8–10] on the film boiling of liquid, respectively. In this chapter, the rigorous theoretical models for film boiling of liquid along an isothermal vertical plate are established by means of the new similarity analysis method. The purpose of this chapter is to set up a theoretical foundation for the laminar free film boiling of subcooled liquid, and the related boiling of saturated liquid is regarded as its special case.

11.2 Governing Partial Differential Equations

The analytical model and coordinating system used in laminar free film boiling of liquid are shown in Fig. 11.1. The heated plate with uniform temperature T_w is submerged vertically in stagnant liquid whose temperature is higher than the liquid saturated temperature T_s . The bulk liquid temperature is less than the liquid saturated temperature T_s . We assume that the heating surface of the plate is covered with continuous laminar vapor film, which moves upward with the vapor. Thus, a two-phase boundary layer is formed. Heat flux produced from the heating surface of the plate transfers through the two-phase boundary layer to the bulk liquid. Meanwhile, mass transfer is produced at the vapor–liquid interface due to the film boiling of liquid.

The governing conservation equations of mass, momentum, and energy conservation for steady laminar free convection of the laminar free film boiling of subcooled liquid can be described as

Fig. 11.1 Physical model and coordinate system of film boiling of subcooled liquid



11.2.1 For Vapor Film

The governing conservation equations of mass, momentum, and energy conservation of *vapor film* for steady laminar free convection of the laminar free film boiling of subcooled liquid can be described as follows with consideration of variable physical properties of vapor medium:

$$\frac{\partial}{\partial x}(\rho_v w_{xv}) + \frac{\partial}{\partial y}(\rho_v w_{yv}) = 0 \quad (11.1)$$

$$\rho_v \left(w_{xv} \frac{\partial w_{xv}}{\partial x} + w_{yv} \frac{\partial w_{xv}}{\partial y} \right) = \frac{\partial}{\partial y} \left(\mu_v \frac{\partial w_{xv}}{\partial y} \right) + g(\rho_{l,\infty} - \rho_v) \quad (11.2)$$

$$\rho_v c_{pv} \left(w_{xv} \frac{\partial T_v}{\partial x} + w_{yv} \frac{\partial T_v}{\partial y} \right) = \frac{\partial}{\partial y} \left(\lambda_v \frac{\partial T_v}{\partial y} \right) \quad (11.3)$$

11.2.2 For Liquid Film

For the laminar free film boiling of subcooled liquid, the thermal boundary layer of liquid appears together besides the velocity boundary layer. Also, the variable physical properties must be considered in the following mass, momentum, and energy governing partial differential equations for the *liquid film*:

$$\frac{\partial}{\partial x}(\rho_l w_{xl}) + \frac{\partial}{\partial y}(\rho_l w_{yl}) = 0 \quad (11.4)$$

$$\rho_l \left(w_{xl} \frac{\partial w_{xl}}{\partial x} + w_{yl} \frac{\partial w_{xl}}{\partial y} \right) = \frac{\partial}{\partial y} \left(\mu_l \frac{\partial w_{xl}}{\partial y} \right) + g(\rho_{l,\infty} - \rho_l) \quad (11.5)$$

$$\rho_l c_{pl} \left(w_{xl} \frac{\partial t_l}{\partial x} + w_{yl} \frac{\partial t_l}{\partial y} \right) = \frac{\partial}{\partial y} \left(\lambda_l \frac{\partial t_l}{\partial y} \right) \quad (11.6)$$

11.2.3 For Boundary Conditions

The boundary conditions of the laminar free convection film boiling of subcooled liquid are as follows with consideration of variable physical properties of both liquid and vapor films:

$$y = 0 : w_{xv} = 0, \quad w_{yv} = 0, \quad T_v = T_w \quad (11.7)$$

$$y = \delta_v : w_{xv,s} = w_{xl,s} \quad (11.8)$$

$$\rho_{v,s} \left(w_{xv} \frac{\partial \delta_v}{\partial x} - w_{yv} \right)_s = \rho_{l,s} \left(w_{xl} \frac{\partial \delta_l}{\partial x} - w_{yl} \right)_s \quad (11.9)$$

$$\mu_{v,s} \left(\frac{\partial w_{xv}}{\partial y} \right)_s = \mu_{l,s} \left(\frac{\partial w_{xl}}{\partial y} \right)_s \quad (11.10)$$

$$-\lambda_{v,s} \left(\frac{\partial T_v}{\partial y} \right)_{y=\delta_v} = h_{fg} \rho_{l,s} \left(w_{xl} \frac{\partial \delta_l}{\partial x} - w_{yl} \right)_s - \lambda_{l,s} \left(\frac{\partial t_l}{\partial y} \right)_{y=\delta_v} \quad (11.11)$$

$$T = T_s, \quad (11.12)$$

$$y \rightarrow \infty: w_{xl} \rightarrow 0, \quad t_l \rightarrow t_\infty \quad (11.13)$$

Here, Eqs. (11.7)–(11.11) express physical matching conditions of the continuities of velocity, mass flow rate, shear force, heat flux, and temperature at the vapor–liquid interface.

In order to solve easily the governing partial differential equations, it is better to transform them into the related identical dimensionless forms. In this purpose, the present new similarity analysis method is carried out for their similarity transformation. At first, we introduce the following similarity variables:

11.3 Similarity Variables

Due to the two-phase boundary layer, there should be two sets of the transformation variables: the transformation variables for vapor and liquid films.

11.3.1 For Vapor Film

For *similarity transformation* of the governing equations of the vapor film, the following *similarity variables* are up:

η_v is set up at first as the dimensionless coordinate variable, i.e.,

$$\eta_v = \left(\frac{1}{4} \text{Gr}_{xv,s} \right)^{1/4} \frac{y}{x} \quad (11.14)$$

where the local Grashof number $\text{Gr}_{xv,s}$ is defined as

$$\text{Gr}_{xv,s} = \frac{g(\rho_{l,\infty}/\rho_{v,w} - 1)x^3}{\nu_{v,s}^2} \quad (11.15)$$

The dimensionless temperature is given as

$$\theta_v = \frac{T_v - T_s}{T_w - T_s} \quad (11.16)$$

The dimensionless velocity components are given as

$$W_{xv} = (2\sqrt{gx}(\rho_{1,\infty}/\rho_{v,w} - 1)^{1/2})^{-1} w_{xv} \quad (11.17)$$

$$W_{yv} = \left(2\sqrt{gx}(\rho_{1,\infty}/\rho_{v,w} - 1)^{1/2} \left(\frac{1}{4} \text{Gr}_{xv,s} \right)^{-1/4} \right)^{-1} w_{yv} \quad (11.18)$$

11.3.2 For Liquid Film

For similarity transformation of the governing equation for *liquid film*, the following similarity variables are set up:

For liquid film, the *dimensionless coordinate variable* η_l is defined at first as follows:

$$\eta_l = \left(\frac{1}{4} \text{Gr}_{x1,\infty} \right)^{1/4} \frac{y}{x} \quad (11.19)$$

where the *local Grashof number* $\text{Gr}_{x1,\infty}$ is defined as

$$\text{Gr}_{x1,\infty} = \frac{g(\rho_{1,\infty}/\rho_{l,s} - 1)x^3}{\nu_{l,\infty}^2} \quad (11.20)$$

The *dimensionless temperature* is given as

$$\theta_l = \frac{t_l - t_\infty}{t_s - t_\infty} \quad (11.21)$$

The *dimensionless velocity components* are defined as

$$W_{x1} = (2\sqrt{gx}(\rho_{1,\infty}/\rho_{l,s} - 1)^{1/2})^{-1} w_{x1} \quad (11.22)$$

$$W_{y1} = \left(2\sqrt{gx}(\rho_{1,\infty}/\rho_{l,s} - 1)^{1/2} \left(\frac{1}{4} \text{Gr}_{x1,\infty} \right)^{-1/4} \right)^{-1} w_{y1} \quad (11.23)$$

11.4 Governing Ordinary Differential Equations

11.4.1 For Vapor Film

Consulting the derivations in Chap. 6 for laminar free convection of gas, respectively, the governing partial differential Eqs.(11.1)–(11.3) for laminar free film boiling

of liquid can be equivalently transformed into the following governing ordinary differential equations (see the detailed transformation in Appendix A):

$$2W_{xv} - \eta_v \frac{dW_{xv}}{d\eta_v} + 4 \frac{dW_{yv}}{d\eta_v} - \frac{1}{\rho_v} \frac{d\rho_v}{d\eta_v} (\eta_v W_{xv} - 4W_{yv}) = 0 \quad (11.24)$$

$$\begin{aligned} & \frac{\nu_{v,s}}{\nu_v} \left[W_{xv} \left(2W_{xv} - \eta_v \frac{dW_{xv}}{d\eta_v} \right) + 4W_{yv} \frac{dW_{xv}}{d\eta_v} \right] \\ &= \frac{d^2 W_{xv}}{d\eta_v^2} + \frac{1}{\mu_v} \frac{d\mu_v}{d\eta_v} \frac{dW_{xv}}{d\eta_v} + \frac{\nu_{v,s}}{\nu_v} \frac{\rho_{v,w}}{\rho_v} \frac{\rho_{l,\infty} - \rho_v}{\rho_{l,\infty} - \rho_{v,w}} \end{aligned} \quad (11.25)$$

$$\text{Pr}_v \frac{\nu_{v,s}}{\nu_v} (-\eta_v W_{xv} + 4W_{yv}) \frac{d\theta_v}{d\eta_v} = \frac{d^2 \theta_v}{d\eta_v^2} + \frac{1}{\lambda_v} \frac{d\lambda_v}{d\eta_v} \frac{d\theta_v}{d\eta_v} \quad (11.26)$$

where Eqs. (11.24)–(11.26), respectively, express the mass, momentum and energy equations of vapour film.

11.4.2 For Liquid Film

Consulting the derivations in Chap. 8 for laminar free convection of liquid, respectively, the governing partial differential Eqs. (11.4)–(11.6) for laminar free convection film boiling of liquid can be equivalently transformed into the following governing ordinary differential equations (see the detailed transformation in Appendix A):

$$2W_{xl} - \eta_l \frac{dW_{xl}}{d\eta_l} + 4 \frac{dW_{yl}}{d\eta_l} - \frac{1}{\rho_l} \frac{d\rho_l}{d\eta_l} (\eta_l W_{xl} - 4W_{yl}) = 0 \quad (11.27)$$

$$\begin{aligned} & \frac{\nu_{l,\infty}}{\nu_l} \left[W_{xl} \left(2W_{xl} - \eta_l \frac{dW_{xl}}{d\eta_l} \right) + 4W_{yl} \frac{dW_{xl}}{d\eta_l} \right] \\ &= \frac{d^2 W_{xl}}{d\eta_l^2} + \frac{1}{\mu_l} \frac{d\mu_l}{d\eta_l} \frac{dW_{xl}}{d\eta_l} + \frac{\nu_{l,\infty}}{\nu_l} \frac{\left(\frac{\rho_{l,\infty}}{\rho_l} - 1 \right)}{\left(\frac{\rho_{l,\infty}}{\rho_{l,s}} - 1 \right)} \end{aligned} \quad (11.28)$$

$$\text{Pr}_l \frac{\nu_{l,\infty}}{\nu_l} (-\eta_l W_{xl} + 4W_{yl}) = \frac{d\theta_l}{d\eta_l^2} + \frac{1}{\lambda_l} \frac{d\lambda_l}{d\eta_l} \frac{d\theta_l}{d\eta_l} \quad (11.29)$$

where Eqs. (11.27)–(11.29), respectively, express the mass, momentum, and energy equations of liquid film.

11.4.3 For Boundary Conditions

With the corresponding assumed variable equations mentioned above, the physical boundary conditions (11.7)–(11.13) for the laminar free film boiling of subcooled liquid are transformed equivalently to the following ones, respectively (see Appendix B):

$$\eta_v = 0: W_{xv} = 0, \quad W_{yv} = 0, \quad \theta_v = 1 \quad (11.30)$$

$$\eta_v = \eta_{v\delta}(\eta_l = 0): W_{xl,s} = \left(\frac{\rho_{l,\infty}}{\rho_{v,w}} - 1 \right)^{1/2} \left(\frac{\rho_{l,\infty}}{\rho_{l,s}} - 1 \right)^{-1/2} W_{xv,s} \quad (11.31)$$

$$\begin{aligned} -W_{yl} &= \frac{1}{4} \frac{\rho_{v,s}}{\rho_{l,s}} \left(\frac{v_{v,s}}{v_{l,\infty}} \right)^{1/2} (\rho_{l,\infty}/\rho_{v,w} - 1)^{1/4} (\rho_{l,\infty}/\rho_{l,s} - 1)^{-1/4} \\ &\quad \times (\eta_{v\delta} W_{xv} - 4W_{yv}) \end{aligned} \quad (11.32)$$

$$\begin{aligned} \left(\frac{dW_{xl}}{d\eta_l} \right)_{\eta_l=0} &= \frac{\mu_{v,s}}{\mu_{l,s}} \left(\frac{v_{l,\infty}}{v_{v,s}} \right)^{1/2} (\rho_{l,\infty}/\rho_{v,w} - 1)^{3/4} \\ &\quad \times (\rho_{l,\infty}/\rho_{l,s} - 1)^{-3/4} \left(\frac{dW_{xv}}{d\eta_v} \right)_s \end{aligned} \quad (11.33)$$

$$\begin{aligned} -\lambda_{v,s}(T_w - T_s) \left(\frac{d\theta_v}{d\eta_v} \right)_{\eta_v=\eta_{v\delta}} &\left(\frac{v_{l,\infty}}{v_{v,s}} \right)^{1/2} (\rho_{l,\infty}/\rho_{v,w} - 1)^{1/4} \\ &\quad \times (\rho_{l,\infty}/\rho_{l,s} - 1)^{-1/4} + 4h_{fg}\rho_{l,s}v_{l,\infty}W_{yl,s} \\ \left(\frac{d\theta_l}{d\eta_l} \right)_{\eta_l=0} &= \frac{\quad}{-\lambda_{l,s}(t_s - t_\infty)} \end{aligned} \quad (11.34)$$

$$\theta_v = 0, \quad \theta_l = 1 \quad (11.35)$$

$$\eta_l \rightarrow \infty: W_{xl} \rightarrow 0, \quad \theta_l \rightarrow 0 \quad (11.36)$$

For vapor film where Eqs. (11.31)–(11.35) express the physical matching conditions such as velocity, local mass flux, shear force, heat flux, and temperature balances at the vapor–liquid interface, respectively, Eqs. (11.30) and (11.36) express the related conditions at the wall and bulk, respectively.

11.5 Identical Mathematical Models of Laminar Free Convection Film Boiling of Saturated or Subcooled Liquid

The laminar free convection film boiling of saturated liquid with the subcooled temperature $\Delta t_\infty = t_s - t_\infty = 0$ can be regarded as a special case of that of the film boiling of subcooled liquid. It follows that such two boiling have identical mathematical

model, and the above mathematical model of the laminar free convection film boiling of subcooled liquid is completely suitable for that of saturated liquid, if the following simplifications are done:

- (i) The energy equation of liquid film Eq. (11.6) is omitted. Then, its related dimensionless form, i.e., Eq. (11.29) is ignored.
- (ii) The defined dimensionless temperature variable in Eq. (11.21) for liquid film is omitted.
- (iii) The liquid film heat conduction in the boundary condition Eq. (11.11) for energy balance at the vapor–liquid interface is ignored as follows:

$$-\lambda_{v,s} \left(\frac{\partial T_v}{\partial y} \right)_{y=\delta_v} = h_{fg} \rho_{v,s} \left(w_{xv} \frac{\partial \delta_{xv}}{\partial x} - w_{yv} \right)_s \tag{11.11sat}$$

Then, its corresponding dimensionless form, Eq. (11.34), should be simplified to

$$-\lambda_{v,s}(T_w - T_s) \left(\frac{d\theta_v}{d\eta_v} \right)_s \left(\frac{\nu_{l,\infty}}{\nu_{v,s}} \right)^{1/2} (\rho_{l,\infty}/\rho_{v,w} - 1)^{1/4} \\ \times (\rho_{l,\infty}/\rho_{l,s} - 1)^{-1/4} + 4h_{fg}\rho_{l,s}\nu_{l,\infty}W_{y1,s} = 0 \tag{11.34sat.}$$

Strictly speaking, the defined similarity variable $Gr_{x1,\infty}$ in Eq.(11.20) should be zero for laminar free convection film boiling of saturated liquid, since the liquid density $\rho_{l,\infty}$ at t_∞ is equal to $\rho_{l,s}$ at t_s for the saturated situation. If so, it will be never possible to do all above similarity transformation. For solving this problem, the temperature t_∞ can be regarded very close to t_s , so that the value of $\rho_{l,\infty}$ is very close to the value of $\rho_{l,s}$. For example, if the temperature relative deviation $(t_s - t_\infty)/t_s$ is less than an arbitrary small number ε , the film boiling of subcooled liquid will be very close to that of saturated liquid. Such arbitrary number ε can be found out by using an asymptotic approach.

The advantage of the above treatment is that the mathematical models of the laminar free film boiling of subcooled and saturated liquids become identical.

11.6 Remarks

The new similarity analysis method is successfully applied for similarity transformation of the governing partial differential equations of laminar free film boiling of subcooled liquid with consideration of coupled effects of variable physical properties. The governing partial differential equations of the laminar free film boiling of saturated liquid are only their special case. The provided dimensionless velocity components of vapor and liquid films have definite physical meanings, and then as the solutions of the governing models, they can be understood easily. It follows that the new similarity analysis method is appropriate for the treatment of the two-phase boundary layer problems with consideration of variable physical properties.

In this extensive investigation of the laminar free film boiling of liquid, the temperature-dependent physical properties, such as density, thermal conductivity, and absolute viscosity of the medium of vapor and liquid films are seriously taken into account. Meanwhile, the interfacial balance equations between the vapor and liquid films are considered in detail, such as mass flow rate balance, velocity component balance, shear force balance, temperature balance, and energy balance.

11.7 Exercises

1. Which boundary conditions are considered at the vapor–liquid interface of laminar free film boiling of subcooled liquid?
2. How do you know that the mathematical model of laminar free film boiling of subcooled liquid covers the case for the saturated liquid?
3. Point out the physical property factors coupled with the governing ordinary differential equations of laminar free film boiling of liquid.
4. Please point out the relation and difference of the laminar free film boiling of liquid from laminar free convection boundary layers of liquid or gas.
5. How to use the system of governing mathematical model on laminar free convection film boiling of subcooled liquid to treat the issue on laminar free film boiling of saturated liquid?

Appendix A Similarity Transformation for Eqs. (11.1)–(11.6)

Similarity transformation of partial differential equations of laminar free film boiling of liquid is given below:

A1 For vapor film

Transformation of Eq. (11.1):

At first, Eq. (11.1) is rewritten as

$$\rho_v \left(\frac{\partial w_{xv}}{\partial x} + \frac{\partial w_{yv}}{\partial y} \right) + w_{xv} \frac{\partial \rho_v}{\partial x} + w_{yv} \frac{\partial \rho_v}{\partial y} = 0 \quad (\text{A1})$$

With Eqs. (11.14), (11.15), (11.17), and (11.18), we can obtain the following correlations:

$$\frac{\partial w_{xv}}{\partial x} = \sqrt{\frac{g}{x}} (\rho_{1,\infty}/\rho_{v,w} - 1)^{1/2} \left(W_{xv} - \frac{1}{2} \eta_v \frac{dW_{xv}}{d\eta} \right) \quad (\text{A1})$$

$$\frac{\partial w_{yv}}{\partial y} = 2\sqrt{\frac{g}{x}} (\rho_{1,\infty}/\rho_{v,w} - 1)^{1/2} \left(\frac{dW_{yv}}{d\eta_v} \right) \quad (\text{A2})$$

$$\frac{\partial \rho_v}{\partial x} = -\frac{1}{4} \eta_v x^{-1} \frac{d\rho_v}{d\eta_v} \quad (\text{A3})$$

$$\frac{\partial \rho_v}{\partial y} = \frac{d\rho_v}{d\eta_v} \left(\frac{1}{4} \text{Gr}_{xv,s} \right)^{1/4} x^{-1} \quad (\text{A4})$$

With Eqs. (11.17), (11.18), and (A1)–(A4), the Eq. (A1) can be changed to

$$\begin{aligned} \rho_v \left[\sqrt{\frac{g}{x}} (\rho_{1,\infty}/\rho_{v,w} - 1)^{1/2} \left(W_{xv} - \frac{1}{2} \eta_v \frac{dW_{xv}}{d\eta} \right) + 2\sqrt{\frac{g}{x}} (\rho_{1,\infty}/\rho_{v,w} - 1)^{1/2} \frac{dW_{yv}}{d\eta_v} \right] \\ + 2\sqrt{gx} (\rho_{1,\infty}/\rho_{v,w} - 1)^{1/2} W_{x1} \left(-\frac{1}{4} \eta_v x^{-1} \frac{d\rho_v}{d\eta_v} \right) \\ + 2\sqrt{gx} (\rho_{1,\infty}/\rho_{v,w} - 1)^{1/2} \left(\frac{1}{4} \text{Gr}_{x1,\infty} \right)^{-1/4} W_{y1} \frac{d\rho_v}{d\eta_v} \left(\frac{1}{4} \text{Gr}_{x1,\infty} \right)^{-1/4} x^{-1} = 0 \end{aligned}$$

The above equation is divided by $(\rho_{1,\infty}/\rho_{v,w} - 1)^{1/2} \sqrt{\frac{g}{x}}$ and is simplified to

$$2W_{xv} - \eta_v \frac{dW_{xv}}{d\eta_v} + 4 \frac{dW_{yv}}{d\eta_v} - \frac{1}{\rho_v} \frac{d\rho_v}{d\eta_v} (\eta_v W_{xv} - 4W_{yv}) = 0 \quad (\text{11.24})$$

Transformation of Eq. (11.2):

The Eq. (11.2) is rewritten as

$$\rho_v \left(w_{xv} \frac{\partial w_{xv}}{\partial x} + w_{yv} \frac{\partial w_{xv}}{\partial y} \right) = \mu_v \frac{\partial^2 w_{xv}}{\partial y^2} + \frac{\partial w_{xv}}{\partial y} \frac{\partial \mu_v}{\partial y} + g(\rho_{1,\infty} - \rho_v) \quad (\text{A6})$$

With the dimensionless transformation variables assumed in Eqs. (11.14), (11.15), (11.17), and (11.18), we get

$$\frac{\partial w_{xv}}{\partial y} = 2\sqrt{gx} (\rho_{1,s}/\rho_{v,w} - 1)^{1/2} \frac{dW_{xv}}{d\eta_v} x^{-1} \left(\frac{1}{4} \text{Gr}_{xv,s} \right)^{1/4} \quad (\text{A7})$$

$$\begin{aligned} \frac{\partial^2 w_{xv}}{\partial y^2} &= 2\sqrt{gx} (\rho_{1,s}/\rho_{v,w} - 1)^{1/2} \frac{d^2 W_{xv}}{d\eta_v^2} x^{-1} \left(\frac{1}{4} \text{Gr}_{xv,s} \right)^{1/4} \left(\frac{1}{4} \text{Gr}_{xv,s} \right)^{1/4} x^{-1} \\ &= 2\sqrt{gx} (\rho_{1,\infty}/\rho_{v,w} - 1)^{1/2} \frac{d^2 W_{xv}}{d\eta_v^2} \left(\frac{1}{4} \text{Gr}_{xv,s} \right)_{1/2} x^{-2} \end{aligned} \quad (\text{A8})$$

$$\frac{\partial \mu_v}{\partial y} = \frac{d\mu_v}{d\eta_v} \left(\frac{1}{4} \text{Gr}_{xv,s} \right)^{1/4} x^{-1} \quad (\text{A9})$$

With Eqs. (11.17), (11.18), and (A7)–(A9), Eq. (A6) will be changed to

$$\begin{aligned} & \rho_v \left[2\sqrt{g\bar{x}}(\rho_{1,\infty}/\rho_{v,w} - 1)^{1/2} W_{xv} \sqrt{\frac{g}{x}} (\rho_{1,\infty}/\rho_{v,w} - 1)^{1/2} \left(W_{xv} - \frac{1}{2}\eta_v \frac{dW_{xv}}{d\eta} \right) \right. \\ & \quad + 2\sqrt{g\bar{x}}(\rho_{1,\infty}/\rho_{v,w} - 1)^{1/2} \left(\frac{1}{4} \text{Gr}_{xv,s} \right)^{-1/4} W_{yv} 2\sqrt{g\bar{x}} \\ & \quad \left. \times (\rho_{1,\infty}/\rho_{v,w} - 1)^{1/2} \frac{dW_{xv}}{d\eta_v} x^{-1} \left(\frac{1}{4} \text{Gr}_{xv,s} \right)^{1/4} \right] \\ & = \mu_v 2\sqrt{g\bar{x}}(\rho_{1,\infty}/\rho_{v,w} - 1)^{1/2} \frac{d^2 W_{xv}}{d\eta_v^2} \left(\frac{1}{4} \text{Gr}_{xv,s} \right)^{1/2} x^{-2} \\ & \quad + 2\sqrt{g\bar{x}}(\rho_{1,\infty}/\rho_{v,w} - 1)^{1/2} \frac{dW_{xv}}{d\eta_v} x^{-1} \left(\frac{1}{4} \text{Gr}_{xv,s} \right)^{1/4} \frac{d\mu_v}{d\eta_v} \\ & \quad \times \left(\frac{1}{4} \text{Gr}_{xv,s} \right)^{1/4} x^{-1} + g(\rho_{1,\infty} - \rho_v) \end{aligned}$$

The above equation is divided by $g(\rho_{1,\infty}/\rho_{v,w} - 1)$ and with the definition of $\text{Gr}_{xv,s}$, the equation is further simplified to

$$\begin{aligned} & \rho_v \left[2W_{xv} \left(W_{xv} \frac{1}{2}\eta_v \frac{dW_{xv}}{d\eta} \right) + 4W_{yv} \frac{dW_{xv}}{d\eta_v} \right] \\ & = \mu_v \frac{d^2 W_{xv}}{d\eta_v^2} \frac{1}{\nu_{v,s}} + \frac{dW_{xv}}{d\eta_v} \frac{1}{\nu_{v,s}} \frac{d\mu_v}{d\eta_v} + \frac{\rho_{1,\infty} - \rho_v}{\rho_{1,\infty}/\rho_{v,w} - 1} \end{aligned}$$

The above equation is multiplied by $\frac{1}{\rho_v} \frac{\nu_{v,s}}{\nu_v}$ and further simplified to

$$\begin{aligned} & \frac{\nu_{v,s}}{\nu_v} \left[W_{xv} \left(2W_{xv} - \eta_v \frac{dW_{xv}}{d\eta} \right) + 4W_{yv} \frac{dW_{xv}}{d\eta_v} \right] \\ & = \frac{d^2 W_{xv}}{d\eta_v^2} + \frac{1}{\mu_v} \frac{d\mu_v}{d\eta_v} \frac{dW_{xv}}{d\eta_v} + \frac{\nu_{v,s}}{\nu_v} \frac{\rho_{v,w}}{\rho_v} \frac{\rho_{1,\infty} - \rho_{\infty}}{\rho_v - \rho_{v,w}} \end{aligned} \quad (\text{11.25})$$

Transformation of Eq. (11.3):

Equation (11.3) is first rewritten as

$$\rho_v c_{p_v} \left(w_{xv} \frac{\partial T_v}{\partial x} + w_{yv} \frac{\partial T_v}{\partial y} \right) = \lambda_v \frac{\partial^2 T_v}{\partial y^2} + \frac{\partial \lambda_v}{\partial y} \frac{\partial T_v}{\partial y} \quad (\text{A10})$$

where

$$T_v = (T_w - T_s)\theta_v + T_s \quad (\text{A11})$$

$$\frac{\partial T_v}{\partial x} = -(T_w - T_s) \frac{d\theta_v}{d\eta_v} \left(\frac{1}{4}\right) \eta_{v,v} x^{-1} \quad (\text{A12})$$

$$\frac{\partial T_v}{\partial y} = -(T_w - T_s) \frac{d\theta_v}{d\eta_v} \left(\frac{1}{4} \text{Gr}_{xv,s}\right)^{1/4} x^{-1} \quad (\text{A13})$$

$$\frac{\partial T_v}{\partial y} = -(T_w - T_s) \frac{d\theta_v}{d\eta_v} \left(\frac{1}{4} \text{Gr}_{xv,s}\right)^{1/2} x^{-2} \quad (\text{A14})$$

$$\frac{\partial T_v}{\partial x} = \frac{d\lambda_v}{d\eta_v} \left(\frac{1}{4} \text{Gr}_{xv,s}\right)^{1/4} x^{-1} \quad (\text{A15})$$

With Eqs. (11.17), (11.18), and (A11)–(A15), Eq. (A10) will become

$$\begin{aligned} & \rho_v c_{p_v} \left\{ 2\sqrt{g\bar{x}}(\rho_{1,\infty}/\rho_{v,w} - 1)^{1/2} W_{xv} \left[-(T_w - T_s) \frac{d\theta_v}{d\eta_v} \left(\frac{1}{4}\right) \eta_{v,v} x^{-1} \right] \right. \\ & \quad \left. + 2\sqrt{g\bar{x}}(\rho_{1,\infty}/\rho_{v,w} - 1)^{1/2} \left(\frac{1}{4} \text{Gr}_{xv,s}\right)^{-1/4} W_{yv} \right. \\ & \quad \left. \times \left[(T_w - T_s) \frac{d\theta_v}{d\eta_v} \left(\frac{1}{4} \text{Gr}'_{xv,s}\right)^{1/4} x^{-1} \right] \right\} \\ & = \lambda_{v,v} (T_w - T_s) \frac{d^2\theta_v}{d\eta_v^2} \left(\frac{1}{4} \text{Gr}_{xv,s}\right)^{1/2} x^{-2} + \frac{d\lambda_v}{d\eta_v} \left(\frac{1}{4} \text{Gr}_{xv,s}\right)^{1/4} x^{-1} \\ & \quad \times \left[(T_w - T_s) \frac{d\theta_v}{d\eta_v} \left(\frac{1}{4} \text{Gr}'_{xv,s}\right)^{1/4} x^{-1} \right] \end{aligned}$$

The above equation is divided by $(T_w - T_s)$ and is further simplified to

$$\begin{aligned} & \rho_v c_{p_v} \left\{ 2\sqrt{g\bar{x}}(\rho_{1,\infty}/\rho_{v,w} - 1)^{1/2} W_{xv} \left[-\frac{d\theta_v}{d\eta_v} \left(\frac{1}{4}\right) \eta_{v,v} x^{-1} \right] \right. \\ & \quad \left. + 2\sqrt{g\bar{x}}(\rho_{1,\infty}/\rho_{v,w} - 1)^{1/2} W_{yv} \left[\frac{d\theta_v}{d\eta_v} x^{-1} \right] \right\} \\ & = \lambda_v \frac{d^2\theta_v}{d\eta_v^2} \left(\frac{1}{4} \text{Gr}_{xv,s}\right)^{1/2} x^{-2} + \frac{d\lambda_v}{d\eta_v} \left(\frac{1}{4} \text{Gr}_{xv,s}\right)^{1/2} x^{-2} \left[\frac{d\theta_v}{d\eta_v} \right] \end{aligned}$$

The above equation is divided by $\sqrt{\frac{g}{x}}(\rho_{1,s}/\rho_{v,w} - 1)^{1/2}$, and then is simplified to the following form with consideration of the definition of $\text{Gr}_{xv,s}$:

$$\rho_v c_{p_v} \left\{ W_{xv} \left[-\frac{d\theta_v}{d\eta_v} \eta_v \right] + 4W_{yv} \left[\frac{d\theta_v}{d\eta_v} \right] \right\} = \lambda_v \frac{d^2\theta_v}{d\eta_v^2} \left(\frac{1}{\nu_{v,s}} \right) + \frac{d\lambda_v}{d\eta_v} \left(\frac{1}{\nu_{v,s}} \right) \left[\frac{d\theta_v}{d\eta_v} \right]$$

The above equation is multiplied by $\frac{\nu_{v,s}}{\lambda_v}$ and simplified to

$$\text{Pr}_v \frac{\nu_{v,s}}{\nu_v} (-\eta_v W_{xv} + 4W_{yv}) \frac{d\theta_v}{d\eta_v} = \frac{d^2\theta_v}{d\eta_v^2} + \frac{1}{\lambda_v} \frac{d\lambda_v}{d\eta_v} \frac{d\theta_v}{d\eta_v} \quad (11.26)$$

where Pr_v is, vapor Prandtl number, defined as $\text{Pr}_v = \frac{\mu_v c_{p_v}}{\lambda_v}$

A2 For liquid film

After the assumptions of the dimensionless variables, the similarity transformations of the governing partial differential equations for liquid will be done as below:

Transformation of Eq. (11.4):

The similarity transformation of Eq. (11.4) is done, initially yielding

$$\rho_l \left(\frac{\partial w_{x1}}{\partial x} + \frac{\partial W_{y1}}{\partial y} \right) + w_{x1} \frac{\partial \rho_l}{\partial x} + w_{y1} \frac{\partial \rho_l}{\partial y} = 0 \quad (A16)$$

With the similarity variables assumed in Eqs. (11.19), (11.20), (11.22), and (11.23), we can obtain the following correlations:

$$\frac{\partial w_{x1}}{\partial x} = \sqrt{\frac{g}{x}} (\rho_{l,\infty}/\rho_{l,s} - 1)^{1/2} \left(W_{x1} - \frac{1}{2} \eta_l \frac{dW_{x1}}{d\eta_l} \right) \quad (A17)$$

$$\frac{\partial w_{y1}}{\partial y} = 2\sqrt{\frac{g}{x}} (\rho_{l,\infty}/\rho_{l,s} - 1)^{1/2} \left(\frac{dW_{y1}}{d\eta_l} \right) \quad (A18)$$

$$\frac{\partial \rho_l}{\partial x} = -\frac{1}{4} \eta_l x^{-1} \frac{d\rho_l}{d\eta_l} \quad (A19)$$

$$\frac{\partial \rho_l}{\partial y} = \frac{d\rho_l}{d\eta_l} \left(\frac{1}{4} \text{Gr}_{x1,\infty} \right)^{1/4} x^{-1} \quad (A20)$$

With the above Eqs. (A17)–(A20), (A16) can be changed to

$$\begin{aligned} & \rho_l \left[\sqrt{\frac{g}{x}} (\rho_{l,\infty}/\rho_{l,s} - 1)^{1/2} \left(W_{x1} - \frac{1}{2} \eta_l \frac{dW_{x1}}{d\eta_l} \right) + 2\sqrt{\frac{g}{x}} (\rho_{l,\infty}/\rho_{l,s} - 1)^{1/2} \frac{dW_{y1}}{d\eta_l} \right] \\ & + 2\sqrt{gx} (\rho_{l,\infty}/\rho_{l,s} - 1)^{1/2} W_{x1} \left(\frac{1}{4} \eta_l x^{-1} \frac{d\rho_l}{d\eta_l} \right) \\ & + 2\sqrt{gx} (\rho_{l,\infty}/\rho_{l,s} - 1)^{1/2} \left(\frac{1}{4} \text{Gr}_{x1,\infty} \right)^{1/4} W_{y1} \frac{d\rho_l}{d\eta_l} \left(\frac{1}{4} \text{Gr}_{x1,\infty} \right)^{1/4} x^{-1} = 0 \end{aligned}$$

The above equation is divided by $\sqrt{\frac{g}{x}} (\rho_{l,\infty}/\rho_{l,s} - 1)^{1/2}$ and is further simplified to

$$2W_{xl} - \eta_1 \frac{dW_{xl}}{d\eta_1} + 4 \frac{dW_{yl}}{d\eta_1} - \frac{1}{\rho_1} \frac{d\rho_1}{d\eta_1} (\eta_1 W_{xl} - 4W_{yl}) = 0 \quad (11.27)$$

Transformation of Eq. (11.5):

Equation (11.5) is first rewritten as

$$\rho_1 \left(w_{xl} \frac{\partial w_{xl}}{\partial x} + w_{yl} \frac{\partial w_{xl}}{\partial y} \right) = \mu_1 \frac{\partial^2 w_{xl}}{\partial y^2} + \frac{\partial w_{xl}}{\partial y} \frac{\partial \mu_1}{\partial y} + g(\rho_{1,\infty} - \rho_1) \quad (A21)$$

With the similarity variables assumed in Eqs. (11.19), (11.20), (11.22), and (11.23) we can obtain the following correlations:

$$\frac{\partial w_{xl}}{\partial y} = 2\sqrt{gx}(\rho_{1,\infty}/\rho_{1,s} - 1)^{1/2} \frac{dW_{xl}}{d\eta_1} x^{-1} \left(\frac{1}{4} \text{Gr}_{xl,\infty} \right)^{1/4} \quad (A22)$$

$$\begin{aligned} \frac{\partial^2 w_{xl}}{\partial y^2} &= 2\sqrt{gx}(\rho_{1,\infty}/\rho_{1,s} - 1)^{1/2} \frac{d^2 W_{xl}}{d\eta_1^2} x^{-1} \left(\frac{1}{4} \text{Gr}_{xl,\infty} \right)^{1/4} \left(\frac{1}{4} \text{Gr}_{xl,\infty} \right)^{1/4} x^{-1} \\ &= 2\sqrt{gx}(\rho_{1,\infty}/\rho_{1,s} - 1)^{1/2} \frac{d^2 W_{xl}}{d\eta_1^2} \left(\frac{1}{4} \text{Gr}_{xl,\infty} \right)^{1/2} x^{-2} \end{aligned} \quad (A23)$$

$$\frac{\partial \mu_1}{\partial y} = \frac{d\mu_1}{d\eta_1} \left(\frac{1}{4} \text{Gr}_{xl,\infty} \right)^{1/4} x^{-1} \quad (A24)$$

With Eqs. (11.19), (11.20), (11.22), (11.23), and (A22)–(A24), Eq. (A21) becomes

$$\begin{aligned} &\rho_1 \left[2\sqrt{gx}(\rho_{1,\infty}/\rho_{1,s} - 1)^{1/2} W_{xl} \sqrt{\frac{g}{x}} (\rho_{1,\infty}/\rho_{1,s} - 1)^{1/2} \left(W_{xl} - \frac{1}{2} \eta_1 \frac{dW_{xl}}{d\eta_1} \right) \right. \\ &\quad \left. + 2\sqrt{gx}(\rho_{1,\infty}/\rho_{1,s} - 1)^{1/2} \left(\frac{1}{4} \text{Gr}_{xl,\infty} \right)^{-1/4} W_{yl} 2\sqrt{gx} \right. \\ &\quad \left. \times (\rho_{1,\infty}/\rho_{1,s} - 1)^{1/2} \frac{dW_{xl}}{d\eta_1} x^{-1} \left(\frac{1}{4} \text{Gr}_{xl,\infty} \right)^{1/4} \right] \\ &= \mu_1 2\sqrt{gx}(\rho_{1,\infty}/\rho_{1,s} - 1)^{1/2} \frac{d^2 W_{xl}}{d\eta_1^2} \left(\frac{1}{4} \text{Gr}_{xl,\infty} \right)^{1/2} x^{-2} \\ &\quad + 2\sqrt{gx}(\rho_{1,\infty}/\rho_{1,s} - 1)^{1/2} \frac{dW_{xl}}{d\eta_1} x^{-1} \left(\frac{1}{4} \text{Gr}_{xl,\infty} \right)^{1/4} \frac{d\mu_1}{d\eta_1} \\ &\quad \times \left(\frac{1}{4} \text{Gr}_{xl,\infty} \right)^{1/4} x^{-1} + g(\rho_{1,\infty} - \rho_1) \end{aligned}$$

With the definition of $\text{Gr}_{xl,\infty}$, the above equation is simplified to

$$\begin{aligned}
& \rho_l \left[2\sqrt{g\bar{x}}(\rho_{1,\infty}/\rho_{1,s} - 1)^{1/2} W_{xl} \sqrt{\frac{g}{x}} (\rho_{1,\infty}/\rho_{1,s} - 1)^{1/2} \left(W_{xl} - \frac{1}{2} \eta_l \frac{dW_{xl}}{d\eta_l} \right) \right. \\
& \quad \left. + 2\sqrt{g\bar{x}}(\rho_{1,\infty}/\rho_{1,s} - 1)^{1/2} W_{yl} 2\sqrt{g\bar{x}}(\rho_{1,\infty}/\rho_{1,s} - 1)^{1/2} \frac{dW_{xl}}{d\eta_l} x^{-1} \right] \\
& = \mu_l 2\sqrt{g\bar{x}}(\rho_{1,\infty}/\rho_{1,s} - 1)^{1/2} \frac{d^2 W_{xl}}{d\eta_l^2} \left(\frac{1}{4} \frac{g(\rho_{1,\infty}/\rho_{1,s} - 1)x^3}{v_{1,\infty}^2} \right)^{1/2} x^{-2} \\
& \quad + 2\sqrt{g\bar{x}}(\rho_{1,\infty}/\rho_{1,s} - 1)^{1/2} \frac{dW_{xl}}{d\eta_l} x^{-1} \frac{d\mu_l}{d\eta_l} \left(\frac{1}{4} \frac{g(\rho_{1,\infty}/\rho_{1,s} - 1)x^3}{v_{1,\infty}^2} \right)^{1/2} x^{-1} \\
& \quad + g(\rho_{1,\infty} - \rho_l)
\end{aligned}$$

The above equation is divided by $g(\rho_{1,\infty}/\rho_{1,s} - 1)$ and simplified to

$$\begin{aligned}
& \rho_l \left[2W_{xl} \left(W_{xl} - \frac{1}{2} \eta_l \frac{dW_{xl}}{d\eta_l} \right) + 4W_{yl} \frac{dW_{xl}}{d\eta_l} \right] \\
& = \mu_l \frac{d^2 W_{xl}}{d\eta_l^2} \frac{1}{v_{1,\infty}} + \frac{dW_{xl}}{d\eta_l} \frac{d\mu_l}{d\eta_l} \left(\frac{1}{v_{1,\infty}} \right) + \rho_{1,s} \frac{(\rho_{1,\infty} - \rho_l)}{(\rho_{1,\infty} - \rho_{1,s})}
\end{aligned}$$

The above equation is multiplied by $\frac{v_{1,\infty}}{\mu_l}$ and simplified to

$$\begin{aligned}
& \frac{v_{1,\infty}}{v_l} \left[W_{xl} \left(2W_{xl} - \eta_l \frac{dW_{xl}}{d\eta_l} \right) + 4W_{yl} \frac{dW_{xl}}{d\eta_l} \right] \\
& = \frac{d^2 W_{xl}}{d\eta_l^2} + \frac{1}{\mu_l} \frac{d\mu_l}{d\eta_l} \frac{dW_{xl}}{d\eta_l} + \frac{v_{1,\infty}}{v_l} \frac{\left(\frac{\rho_{1,\infty}}{\rho_l} - 1 \right)}{\left(\frac{\rho_{1,\infty}}{\rho_{1,s}} - 1 \right)}
\end{aligned} \tag{11.28}$$

For transformation of Eq. (11.6):

Equation (11.6) is first rewritten as

$$\rho_l c_{pl} \left(w_{xl} \frac{\partial t_1}{\partial x} + w_{yl} \frac{\partial t_1}{\partial y} \right) = \lambda_1 \frac{\partial^2 t_1}{\partial y^2} + \frac{\partial \lambda_1}{\partial y} \frac{\partial t_1}{\partial y} \tag{A25}$$

With the similarity variables assumed in Eqs. (11.19)–(11.23), the following correlations are produced:

$$t_1 = (t_s - t_\infty)\theta_1 + t_\infty \tag{A26}$$

$$\frac{\partial t_1}{\partial x} = -(t_s - t_\infty) \frac{d\theta_1}{d\eta_l} \left(\frac{1}{4} \right) \eta_l x^{-1} \tag{A27}$$

$$\frac{\partial t_1}{\partial y} = (t_s - t_\infty) \frac{d\theta_l}{d\eta_l} \left(\frac{1}{4} \text{Gr}_{x1,\infty} \right)^{1/4} x^{-1} \quad (\text{A28})$$

$$\frac{\partial^2 t_1}{\partial y^2} = (t_s - t_\infty) \frac{d^2\theta_l}{d\eta_l^2} \left(\frac{1}{4} \text{Gr}_{x1,\infty} \right)^{1/2} x^{-2} \quad (\text{A29})$$

$$\frac{\partial \lambda_1}{\partial y} = \frac{d\lambda_1}{d\eta} \left(\frac{1}{4} \text{Gr}_{x1,\infty} \right)^{1/4} x^{-1} \quad (\text{A30})$$

With Eqs. (11.19), (11.20), and (A26)–(A30), the Eq. (A25) is transformed into

$$\begin{aligned} & \rho_1 c_{p1} \left[2\sqrt{g\bar{x}}(\rho_{1,\infty}/\rho_{1,s} - 1)^{1/2} W_{x1} \left(-(t_s - t_\infty) \frac{d\theta_l}{d\eta_l} \left(\frac{1}{4} \right) \eta_1 x^{-1} \right) \right. \\ & \quad \left. + 2\sqrt{g\bar{x}}(\rho_{1,\infty}/\rho_{1,s} - 1)^{1/2} \left(\frac{1}{4} \text{Gr}_{x1,\infty} \right)^{-1/4} W_{y1}(t_s - t_\infty) \frac{d\theta_l}{d\eta_l} \right. \\ & \quad \left. \times \left(\frac{1}{4} \text{Gr}_{x1,\infty} \right)^{-1/4} x^{-1} \right] \\ & = \lambda_1 (t_s - t_\infty) \frac{d^2\theta_l}{d\eta_l^2} \left(\frac{1}{4} \text{Gr}_{x1,\infty} \right)^{1/2} x^{-2} \\ & \quad + \frac{d\lambda_l}{d\eta} \left(\frac{1}{4} \text{Gr}_{x1,\infty} \right)^{-1/4} x^{-1} (t_s - t_\infty) \frac{d\theta_l}{d\eta_l} \left(\frac{1}{4} \text{Gr}_{x1,\infty} \right)^{1/4} x^{-1} \end{aligned}$$

With the definition of $\text{Gr}_{x1,\infty}$, the above equation is simplified to

$$\begin{aligned} & \rho_1 c_{p1} \left[2\sqrt{g\bar{x}}(\rho_{1,\infty}/\rho_{1,s} - 1)^{1/2} W_{x1} \left(-(t_s - t_\infty) \frac{d\theta_l}{d\eta_l} \left(\frac{1}{4} \right) \eta_1 x^{-1} \right) \right. \\ & \quad \left. + 2\sqrt{g\bar{x}}(\rho_{1,\infty}/\rho_{1,s} - 1)^{1/2} W_{x1}(t_s - t_\infty) \frac{d\theta_l}{d\eta_l} x^{-1} \right] \\ & = \lambda_1 (t_s - t_\infty) \frac{d^2\theta_l}{d\eta_l^2} \left(\frac{1}{4} \frac{g(\rho_{1,\infty}/\rho_{1,s} - 1)x^3}{\nu_{1,\infty}} \right)^{1/2} x^{-2} \\ & \quad + \frac{d\lambda_l}{d\eta} x^{-1} (t_s - t_\infty) \frac{d\theta_l}{d\eta_l} \left(\frac{1}{4} \frac{g(\rho_{1,\infty}/\rho_{1,s} - 1)x^3}{\nu_{1,\infty}} \right)^{1/2} x^{-1} \end{aligned}$$

The above equation is divided by $\sqrt{\frac{g}{x}}(\rho_{1,\infty}/\rho_{1,s} - 1)^{1/2}(t_s - t_\infty)$, and simplified to

$$\rho_1 c_{p1} \left[-W_{x1} \left(\frac{d\theta_l}{d\eta_l} \eta_1 \right) + 4W_{y1} \frac{d\theta_l}{d\eta_l} \right] = \lambda_1 \frac{d^2\theta_l}{d\eta_l} + \frac{l}{\nu_{1,\infty}^2} + \frac{d\lambda_l}{d\eta} \frac{d\theta_l}{d\eta_l} \frac{1}{\nu_{1,\infty}}$$

This equation is multiplied by $\frac{v_{l,\infty}}{\lambda_l}$ and simplified to

$$\text{Pr}_l \frac{v_{l,\infty}}{v_l} (-\eta W_{x1} + 4W_{y1}) \frac{d\theta_l}{d\eta_1} = \frac{d^2\theta_l}{d\eta_1^2} + \frac{1}{\lambda_l} \frac{d\lambda_l}{d\eta_1} \frac{d\theta_l}{d\eta_1} \quad (11.29)$$

Appendix B Similarity Transformation for Boundary Condition Equations

With the corresponding transformation variables the physical boundary conditions (11.7)–(11.13) are transformed equivalently to the following ones, respectively:

Derivation of Eq. (11.7)

With the related defined variables in Eqs. (11.14), (11.16)–(11.18), Eq. (11.7) can be easily derived to

$$\eta_1 = 0: W_{xv} = 0, \quad W_{xv} = 0, \quad \theta_l = 0 \quad (11.30)$$

Derivation of Eq. (11.8)

With Eqs. (11.17) and (11.22), Eq. (11.8) can be easily changed to

$$2\sqrt{g\bar{x}}(\rho_{l,\infty}/\rho_{v,w} - 1)^{1/2} W_{xv} = 2\sqrt{g\bar{x}}(\rho_{l,\infty}/\rho_{l,s} - 1)^{1/2} W_{x1}$$

i.e.,

$$W_{x1} = (\rho_{l,\infty}/\rho_{v,w} - 1)^{1/2} (\rho_{l,\infty}/\rho_{l,s} - 1)^{-1/2} W_{xv} \quad (11.31)$$

Derivation of Eq. (11.9)

With Eqs. (11.17), (11.18), (11.22) and (11.23), Eq. (11.9) is changed to

$$\begin{aligned} \rho_{v,s} & \left[2\sqrt{g\bar{x}}(\rho_{l,\infty}/\rho_{v,w} - 1)^{1/2} W_{xv} \frac{\partial \delta_v}{\partial \bar{x}} \right. \\ & \quad \left. - 2\sqrt{g\bar{x}}(\rho_{l,\infty}/\rho_{v,w} - 1)^{1/2} \left(\frac{1}{4} \text{Gr}_{xv,s} \right)^{-1/4} W_{yv} \right]_s \\ & = \rho_{l,s} \left[2\sqrt{g\bar{x}}(\rho_{l,\infty}/\rho_{l,s} - 1)^{1/2} W_{x1} \frac{\partial \delta_l}{\partial \bar{x}} \right. \\ & \quad \left. - 2\sqrt{g\bar{x}}(\rho_{l,\infty}/\rho_{l,s} - 1)^{1/2} \left(\frac{1}{4} \text{Gr}_{x1,\infty} \right)^{-1/4} W_{y1} \right]_s \end{aligned} \quad (B1)$$

With Eq. (11.14), the following equations will be obtained, respectively:

$$\delta_v = \eta_v \delta \left(\frac{1}{4} \text{Gr}_{xv,s} \right)^{1/4} x$$

By using the definition of $\text{Gr}_{xv,s}$, we have

$$\frac{d\delta_v}{dx} = \frac{1}{4} \eta_{v\delta} \left(\frac{1}{4} \text{Gr}_{xv,s} \right)^{-1/4} \tag{B2}$$

Similarly, we have

$$\frac{d\delta_l}{dx} = \frac{1}{4} \eta_{l\delta} \left(\frac{1}{4} \text{Gr}_{xl,\infty} \right)^{-1/4} \tag{B3}$$

With Eqs. (B2) and (B3), Eq. (B1) is changed to

$$\begin{aligned} & \rho_{v,s} \left[2\sqrt{g\bar{x}}(\rho_{1,\infty}/\rho_{v,w} - 1)^{1/2} W_{xv} \left(\frac{1}{4} \eta_{v\delta} \left(\frac{1}{4} \text{Gr}_{xv,s} \right)^{-1/4} \right) \right. \\ & \quad \left. - 2\sqrt{g\bar{x}}(\rho_{1,\infty}/\rho_{v,w} - 1)^{1/2} \left(\frac{1}{4} \text{Gr}_{xv,s} \right)^{-1/4} W_{yv} \right]_s \\ & = \rho_{l,s} \left[2\sqrt{g\bar{x}}(\rho_{1,\infty}/\rho_{l,s} - 1)^{1/2} W_{xl} \left(\frac{1}{4} \eta_{l\delta} \left(\frac{1}{4} \text{Gr}_{xl,\infty} \right)^{-1/4} \right) \right. \\ & \quad \left. - 2\sqrt{g\bar{x}}(\rho_{1,\infty}/\rho_{l,s} - 1)^{1/2} \left(\frac{1}{4} \text{Gr}_{xl,\infty} \right)^{-1/4} W_{yl} \right]_s \end{aligned} \tag{B4}$$

At the liquid–vapor interface, $\eta_{l\delta} = 0$, then, the above equation is changed to

$$\begin{aligned} & \rho_{v,s} \left[2\sqrt{g\bar{x}}(\rho_{1,\infty}/\rho_{v,w} - 1)^{1/2} W_{xv} \left(\frac{1}{4} \eta_{v\delta} \left(\frac{1}{4} \text{Gr}_{xv,s} \right)^{-1/4} \right) \right. \\ & \quad \left. - 2\sqrt{g\bar{x}}(\rho_{1,\infty}/\rho_{v,w} - 1)^{1/2} \left(\frac{1}{4} \text{Gr}_{xv,s} \right)^{-1/4} W_{yv} \right]_s \\ & = \rho_{l,s} \left[-2\sqrt{g\bar{x}} \left(\rho_{1,\infty}/\rho_{l,s} - 1 \right)^{1/2} \left(\frac{1}{4} \text{Gr}_{xl,\infty} \right)^{-1/4} W_{yl} \right]_s \end{aligned}$$

With the definitions of $\text{Gr}_{xv,s}$ and $\text{Gr}_{xl,\infty}$, we have the following equations, respectively:

$$\rho_{1,\infty}/\rho_{v,w} - 1 = \frac{v_{v,s}^2}{g\bar{x}^3} \text{Gr}_{xv,s} \tag{B5}$$

$$\rho_{1,\infty}/\rho_{1,s} - 1 = \frac{\nu_{1,\infty}^2}{gx^3} \text{Gr}_{x1,\infty} \quad (\text{B6})$$

With Eqs. (B5) and (B6), Eq. (B4) is changed to

$$\begin{aligned} & \rho_{v,s} \left[2\sqrt{gx} \left(\frac{\nu_{v,s}^2}{gx^3} \text{Gr}_{xv,s} \right)^{1/2} W_{xv} \left(\frac{1}{4} \eta_{v\delta} \left(\frac{1}{4} \text{Gr}_{xv,s} \right)^{-1/4} \right) \right. \\ & \quad \left. - 2\sqrt{gx} \left(\frac{\nu_{v,s}^2}{gx^3} \text{Gr}_{xv,s} \right)^{1/2} \left(\frac{1}{4} \text{Gr}_{xv,s} \right)^{-1/4} W_{yv} \right]_s \\ & = \rho_{1,s} \left[-2\sqrt{gx} \left(\frac{\nu_{1,\infty}^2}{gx^3} \text{Gr}_{x1,\infty} \right)^{1/2} \left(\frac{1}{4} \text{Gr}_{x1,\infty} \right)^{-1/4} W_{y1} \right]_s \end{aligned}$$

i.e.,

$$\begin{aligned} & \rho_{v,s} \left[2\sqrt{gx} \left(\frac{\nu_{v,s}^2}{gx^3} \right)^{1/2} W_{xv} \left(\frac{1}{4} \eta_{v\delta} \left(\frac{1}{4} \right)^{-1/4} \text{Gr}_{xv,s}^{1/4} \right) \right. \\ & \quad \left. - 2\sqrt{gx} \left(\frac{\nu_{v,s}^2}{gx^3} \right)^{1/2} \left(\frac{1}{4} \right)^{-1/4} W_{yv} \text{Gr}_{xv,s}^{1/4} \right]_s \\ & = \rho_{1,s} \left[-2\sqrt{gx} \left(\frac{\nu_{1,\infty}^2}{gx^3} \right)^{1/2} \left(\frac{1}{4} \right)^{-1/4} \text{Gr}_{x1,\infty}^{1/4} W_{y1} \right]_s \end{aligned}$$

The above equation can be simplified to

$$\rho_{v,s} \left[\nu_{v,s} W_{xv} \left(\frac{1}{4} \eta_{v\delta} \right) - \nu_{v,s} W_{yv} \right]_s \text{Gr}_{xv,s}^{1/4} = \rho_{1,s} [-\nu_{1,\infty} W_{y1}]_s \text{Gr}_{x1,\infty}^{1/4}$$

i.e.,

$$-\frac{\rho_{v,s}}{\rho_{1,s}} \frac{\nu_{v,s}}{\nu_{1,\infty}} \left[\frac{1}{4} \eta_{v\delta} W_{xv} - W_{yv} \right]_s \left(\frac{\text{Gr}_{xv,s}}{\text{Gr}_{x1,\infty}} \right)^{1/4} = W_{y1}$$

With definitions of $\text{Gr}_{xv,s}$ and $\text{Gr}_{x1,\infty}$, we have

$$\begin{aligned} -W_{y1} & = \frac{\rho_{v,s}}{\rho_{1,s}} \frac{\nu_{v,s}}{\nu_{1,\infty}} \left[\frac{1}{4} \eta_{v\delta} W_{xv} - W_{yv} \right]_s \left(\frac{\nu_{1,\infty}}{\nu_{v,s}} \right)^{1/2} \\ & \quad \times (\rho_{1,\infty}/\rho_{v,w} - 1)^{1/4} (\rho_{1,\infty}/\rho_{1,s} - 1)^{-1/4} \end{aligned}$$

i.e.,

$$-W_{yl} = \frac{1}{4} \frac{\rho_{v,s}}{\rho_{l,s}} \left(\frac{v_{v,s}}{v_{l,\infty}} \right)^{1/2} (\rho_{l,\infty}/\rho_{v,w} - 1)^{1/4} (\rho_{l,\infty}/\rho_{l,s} - 1)^{-1/4} (\eta_{v\delta} W_{xv} - 4W_{yv}) \quad (11.32)$$

Derivation of Eq. (11.10)

Equation (11.10) is changed to

$$\begin{aligned} \mu_{v,s} \left[2\sqrt{gx} (\rho_{l,\infty}/\rho_{v,w} - 1)^{1/2} \left(\frac{dW_{xv}}{d\eta_v} \right)_s x^{-1} \left(\frac{1}{4} \text{Gr}_{xv,s} \right)^{1/4} \right]_s \\ = \mu_{l,s} \left[2\sqrt{gx} (\rho_{l,\infty}/\rho_{l,s} - 1)^{1/2} \left(\frac{dW_{xl}}{d\eta_l} \right)_s x^{-1} \left(\frac{1}{4} \text{Gr}_{xl,\infty} \right)^{1/4} \right]_s \end{aligned}$$

The above equation is simplified to

$$\left(\frac{dW_{xl}}{d\eta_l} \right)_s = \frac{\mu_{v,s}}{\mu_{l,s}} (\rho_{l,\infty}/\rho_{l,s} - 1)^{-1/2} \left(\frac{dW_{xv}}{d\eta_v} \right)_s \left(\frac{\text{Gr}_{xv,s}}{\text{Gr}_{xl,\infty}} \right)^{1/4}$$

With the definitions of $\text{Gr}_{xv,s}$ and $\text{Gr}_{xl,\infty}$, the above equation is simplified to

$$\begin{aligned} \left(\frac{dW_{xl}}{d\eta_l} \right)_s &= \frac{\mu_{v,s}}{\mu_{l,s}} (\rho_{l,\infty}/\rho_{v,w} - 1)^{1/2} (\rho_{l,\infty}/\rho_{l,s} - 1)^{-1/2} \left(\frac{dW_{xv}}{d\eta_v} \right)_s \left(\frac{\text{Gr}_{xv,s}}{\text{Gr}_{xl,\infty}} \right)^{1/4} \\ \left(\frac{dW_{xl}}{d\eta_l} \right)_s &= \frac{\mu_{v,s}}{\mu_{l,s}} \left(\frac{v_{l,\infty}}{v_{v,s}} \right)^{1/2} (\rho_{l,\infty}/\rho_{v,w} - 1)^{1/2} (\rho_{l,\infty}/\rho_{l,s} - 1)^{-1/2} \left(\frac{dW_{xv}}{d\eta_v} \right)_s \\ &\quad \times (\rho_{l,\infty}/\rho_{v,w} - 1)^{1/2} (\rho_{l,\infty}/\rho_{l,s} - 1)^{-1/2} \left(\frac{\text{Gr}_{xv,s}}{\text{Gr}_{xl,\infty}} \right)^{1/4} \end{aligned}$$

i.e.,

$$\left(\frac{dW_{xl}}{d\eta_l} \right)_s = \frac{\mu_{v,s}}{\mu_{l,s}} \left(\frac{v_{l,\infty}}{v_{v,s}} \right)^{1/2} (\rho_{l,\infty}/\rho_{v,w} - 1)^{3/4} (\rho_{l,\infty}/\rho_{l,s} - 1)^{-3/4} \left(\frac{dW_{xv}}{d\eta_v} \right)_s \quad (11.33)$$

Derivation of Eq. (11.11)

Equation (11.11) is changed to

$$\begin{aligned} -\lambda_{v,s} (T_w - T_s) \left(\frac{d\theta_v}{d\eta_v} \right)_s \left(\frac{1}{4} \text{Gr}'_{xv,s} \right)^{1/4} x^{-1} \\ = h_{fg} \rho_{l,s} \left[2\sqrt{gx} (\rho_{l,\infty}/\rho_{l,s} - 1)^{1/2} W_{xl,s} \frac{1}{4} \eta_{l\delta} \left(\frac{1}{4} \text{Gr}_{xl,\infty} \right)^{-1/4} \right] \end{aligned}$$

$$\begin{aligned}
& -2\sqrt{gx}(\rho_{l,\infty}/\rho_{l,s} - 1)^{1/2} \left(\frac{1}{4}\text{Gr}_{x1,\infty} \right)^{-1/4} \left. W_{y1,s} \right]_s \\
& - \lambda_{l,s}(t_s - t_\infty) \left(\frac{d\theta_l}{d\eta_l} \right)_s \left(\frac{1}{4}\text{Gr}_{x1,\infty} \right)^{1/4} x^{-1}
\end{aligned}$$

Since $\eta_{l\delta} = 0$ at the vapor-liquid interface, the above equation is simplified as follows:

$$\begin{aligned}
& - \lambda_{v,s}(T_w - T_s) \left(\frac{d\theta_v}{d\eta_v} \right)_s \left(\frac{1}{4}\text{Gr}_{xv,s} \right)^{1/4} x^{-1} \\
& = -h_{fg}\rho_{l,s} \left[2\sqrt{gx}(\rho_{l,\infty}/\rho_{l,s} - 1)^{1/2} \left(\frac{1}{4}\text{Gr}_{x1,\infty} \right)^{-1/4} \left. W_{y1,s} \right]_s \\
& - \lambda_{l,s}(t_s - t_\infty) \left(\frac{d\theta_l}{d\eta_l} \right)_s \left(\frac{1}{4}\text{Gr}_{x1,\infty} \right)^{1/4} x^{-1}
\end{aligned}$$

With $\text{Gr}_{x1,\infty}$ definition, $\text{Gr}_{x1,\infty} = \frac{g(\rho_{l,\infty}/\rho_{l,s}-1)x^3}{\nu_{l,\infty}^2}$, the above equation is changed to

$$\begin{aligned}
& - \lambda_{v,s}(T_w - T_s) \left(\frac{d\theta_v}{d\eta_v} \right)_s \left(\frac{1}{4}\text{Gr}'_{xv,s} \right)^{1/4} x^{-1} \\
& = -h_{fg}\rho_{l,s} \left[2\sqrt{gx} \left(\frac{\nu_{l,\infty}^2}{gx^3} \text{Gr}_{x1,\infty} \right)^{1/2} \left(\frac{1}{4}\text{Gr}_{x1,\infty} \right)^{-1/4} \left. W_{y1,s} \right]_s \\
& - \lambda_{l,s}(t_s - t_\infty) \left(\frac{d\theta_l}{d\eta_l} \right)_s \left(\frac{1}{4}\text{Gr}_{x1,\infty} \right)^{1/4} x^{-1}
\end{aligned}$$

i.e.,

$$\begin{aligned}
& - \lambda_{v,s}(T_w - T_s) \left(\frac{d\theta_v}{d\eta_v} \right)_s \left(\frac{1}{4}\text{Gr}'_{xv,s} \right)^{1/4} x^{-1} \\
& = -h_{fg}\rho_{l,s} \left[2\sqrt{gx} \left(\frac{\nu_{l,\infty}^2}{gx^3} \right)^{1/2} 2 \left(\frac{1}{4}\text{Gr}_{x1,\infty} \right)^{1/4} \left. W_{y1,s} \right]_s \\
& - \lambda_{l,s}(t_s - t_\infty) \left(\frac{d\theta_l}{d\eta_l} \right)_s \left(\frac{1}{4}\text{Gr}_{x1,\infty} \right)^{1/4} x^{-1}
\end{aligned}$$

With definitions of $\text{Gr}_{xv,s}$ and $\text{Gr}_{x1,\infty}$, the above equation is changed to

$$\begin{aligned}
& -\lambda_{v,s}(T_w - T_s) \left(\frac{d\theta_v}{d\eta_v} \right)_s \left(\frac{1}{4} \frac{g(\rho_{1,\infty}/\rho_{v,w} - 1)x^3}{\nu_{v,s}^2} \right)^{1/4} x^{-1} \\
& = -h_{fg}\rho_{1,s} \left[2\sqrt{gx} \left(\frac{\nu_{1,\infty}^2}{gx^3} \right)^{1/2} 2 \left(\frac{1}{4} \frac{g(\rho_{1,\infty}/\rho_{1,s} - 1)x^3}{\nu_{1,\infty}^2} \right)^{1/4} W_{y1,s} \right]_s \\
& -\lambda_{1,s}(t_s - t_\infty) \left(\frac{d\theta_1}{d\eta_1} \right)_s \left(\frac{1}{4} \frac{g(\rho_{1,\infty}/\rho_{1,s} - 1)x^3}{\nu_{1,\infty}^2} \right)^{1/4} x^{-1}
\end{aligned}$$

The above equation is divided by $g^{1/4}x^{-1/4}$, and simplified to

$$\begin{aligned}
& -\lambda_{v,s}(T_w - T_s) \left(\frac{d\theta_v}{d\eta_v} \right)_s \left(\frac{(\rho_{1,\infty}/\rho_{v,w} - 1)}{\nu_{v,s}^2} \right)^{1/4} \\
& + h_{fg}\rho_{1,s} \left[2 \left(\frac{\nu_{1,\infty}^2}{1} \right)^{1/2} 2 \left(\frac{(\rho_{1,\infty}/\rho_{1,s} - 1)}{\nu_{1,\infty}^2} \right)^{1/4} W_{y1,s} \right]_s \\
& = -\lambda_{1,s}(t_s - t_\infty) \left(\frac{d\theta_1}{d\eta_1} \right)_s \left(\frac{(\rho_{1,\infty}/\rho_{1,s} - 1)}{\nu_{1,\infty}^2} \right)^{1/4}
\end{aligned}$$

i.e.,

$$\left(\frac{d\theta_1}{d\eta_1} \right)_s = \frac{-\lambda_{v,s}(T_w - T_s) \left(\frac{d\theta_v}{d\eta_v} \right)_s \left(\frac{\nu_{1,\infty}}{\nu_{v,s}} \right)^{1/2} (\rho_{1,\infty}/\rho_{v,w} - 1)^{1/4} \times (\rho_{1,\infty}/\rho_{1,s} - 1)^{-1/4} + 4h_{fg}\rho_{1,s}\nu_{1,\infty}W_{y1,s}}{-\lambda_{1,s}(t_s - t_\infty)} \quad (11.34)$$

In addition, Eqs. (11.12) and (11.13) can be easily be changed to

$$\theta_v = 0, \quad \theta_l = 1 \quad (11.35)$$

$$\eta_1 \rightarrow \infty: \quad W_{x1} \rightarrow 0, \quad \theta_1 = 0 \quad (11.36)$$

References

1. L. Bromley, Heat transfer in stable film boiling. *Chem. Eng. Prog.* **46**(5), 221–227 (1950)
2. J.C.H. Koh, Analysis of film boiling on vertical surface. *J. Heat Transf.* **84C**(1), 55–62 (1962)
3. R.D. Cess, Analysis of laminar film boiling from a vertical flat plate. Research report 405 FF 340–R2-x, Westinghouse Research Laboratory, Pittsburgh, Pa., March 1959. (Surface J. Heat Transfer).
4. E.M. Sparrow, R.D. Cess, The effect of subcooled liquid on laminar film boiling. *J. Heat Transf.* **84C**(2), 149–156 (1962)

5. P.M. McFadden, R.J. Grosh, An analysis of laminar film boiling with variable properties. *Int. J. Heat Mass Transf.* **1**(4), 325–335 (1961)
6. K. Nishikawa, T. Ito, Two-phase boundary-layer treatment of free convection film boiling. *Int. J. Heat Mass Transf.* **9**(2), 103–115 (1966)
7. K. Nishikawa, T. Ito, K. Matsumoto, Investigation of variable thermophysical property problem concerning pool film boiling from vertical plate with prescribed uniform temperature. *Int. J. Heat Mass Transf.* **19**(10), 1173–1182 (1976)
8. D.Y. Shang, L.C. Zhong, B.X. Wang, in *Study of film boiling of water with variable thermo-physical properties along a vertical plate, transfer phenomena*, ed. by B.X. Wang, Science and Technology, (Higher Education press, New York, 1992), pp. 427–432
9. L.C. Zhong, D.Y. Shang, B.X. Wang, Effect of variable thermophysical properties on film boiling of liquid. *J. Northeas. Univ.* **15**(88), 6–11 (1994)
10. D.Y. Shang, B.X. Wang, L.C. Zhong, A study on laminar film boiling of liquid along an isothermal vertical plates in a pool with consideration of variable thermophysical properties. *Int. J. Heat Mass Transf.* **37**(5), 819–828 (1994)

Chapter 12

Velocity and Temperature Fields of Laminar Free Convection Film Boiling of Liquid

Abstract Physical property factors coupled with the theoretical and mathematical models of the laminar free convection film boiling of liquids are treated into the functions of dimensionless temperature, for simultaneous solutions with the three-point boundary values conditions of the two-phase film flow. Then, the numerical solutions of momentum and temperature fields at different wall superheated grades and liquid bulk subcooled grades are theoretically reliable, because the variable physical properties are treated rigorously. On this basis, a system of rigorous numerical solutions for momentum and temperature fields of the two-phase film flows are calculated with taking the film of boiling water as the example, in which the related boiling of saturated water is only the special case. The numerical procedure presented here is reliable for rigorous solutions of the theoretical models of three-point boundary value problem with the two-phase flow. The dimensionless velocity components have definite physical meanings; then, the corresponding solutions of the models can be easily understood. With increasing the wall superheated grades, the maximum of velocity field of vapor film will increase and shift far away from the plate. The velocity of vapor film will decrease with increasing the liquid subcooled grade. With increasing the liquid subcooled degree, the thickness of liquid film will increase, and the velocity profile level of liquid film will decrease slower and slower. Furthermore, with increasing wall superheated grade, the effect of wall superheated grade on the velocity field of liquid film will decrease.

12.1 Introduction

In Chap. 11, the complete similarity mathematical model was derived for laminar free convection film boiling of subcooled liquid, where the model of the film boiling of saturated liquid are regarded as its special case.

On the basis of Chap. 11, in this chapter, the mathematical model with the governing ordinary differential equations and the complete boundary conditions are solved by a successively iterative procedure at different wall superheated degrees and

different liquid subcooled degrees. Meanwhile, the temperature parameter method and polynomial formulae are used for treatment of the variable thermophysical properties of the vapor and liquid films, respectively. The distributions of velocity and temperature fields of the laminar free convection film boiling of liquid are rigorously determined.

12.2 Treatment of Variable Physical Properties

For solution of the dimensionless governing equations of the laminar free convection film boiling, the treatment of variable physical properties for vapor and liquid films must be, respectively, performed. To this end, the approach reported in Chap. 5 for treatment of variable physical properties will be used as follows.

12.2.1 For Variable Physical Properties of Vapor Film

The temperature parameter method [1] will be used for description of the temperature-dependent physical properties of gas. In this case, the boundary temperature T_∞ (the bulk temperature) should be replaced by T_s (the saturation temperature), and then, the simple power law equations (5.5)–(5.8) become

$$\frac{\mu_v}{\mu_{v,s}} = \left(\frac{T}{T_s} \right)^{n_\mu} \quad (12.1)$$

$$\frac{\lambda_v}{\lambda_{v,s}} = \left(\frac{T}{T_s} \right)^{n_\lambda} \quad (12.2)$$

$$\frac{\rho_v}{\rho_{v,s}} = \left(\frac{T}{T_s} \right)^{-1} \quad (12.3)$$

Here we omit the equation for specific heat. With Eqs. (12.1) and (12.3), we have

$$\frac{\nu_v}{\nu_{v,s}} = \left(\frac{T}{T_{v,s}} \right)^{n_\mu+1} \quad (12.4)$$

where the subscript v denotes vapor and the subscript s denotes saturation temperature, respectively.

12.2.2 For Physical Property Factors of Vapor Film

In the governing ordinary differential equations (11.24) to (11.26) for vapor film the physical property factors $\frac{1}{\rho_v} \frac{d\rho_v}{d\eta_v}$, $\frac{1}{\mu_v} \frac{d\mu_v}{d\eta_v}$, $\frac{1}{\lambda_v} \frac{d\lambda_v}{d\eta_v}$, and $\frac{\nu_{v,s}}{\nu_v}$ are involved. In order

to solve these equations, these physical property factors must be transformed in the form of temperature and temperature gradient. Consulting Eqs. Chapter 5, we have the following equations for description of the vapour physical property factors $\frac{1}{\rho_v} \frac{d\rho_v}{d\eta_v}$, $\frac{1}{\mu_v} \frac{d\mu_v}{d\eta_v}$, $\frac{1}{\lambda_v} \frac{d\lambda_v}{d\eta_v}$, and $\frac{\nu_{v,s}}{\nu_v}$, respectively:

$$\frac{1}{\rho_v} \frac{d\rho_v}{d\eta_v} = -\frac{(T_w/T_s - 1)d\theta_v/d\eta_v}{(T_w/T_s - 1)\theta_v + 1} \quad (12.5)$$

$$\frac{1}{\mu_v} \frac{d\mu_v}{d\eta_v} = \frac{n_\mu(T_w/T_s - 1)d\theta_v/d\eta_v}{(T_w/T_s - 1)\theta_v + 1} \quad (12.6)$$

$$\frac{1}{\lambda_v} \frac{d\lambda_v}{d\eta_v} = \frac{n_\lambda(T_w/T_s - 1)d\theta_v/d\eta_v}{(T_w/T_s - 1)\theta_v + 1} \quad (12.7)$$

$$\frac{\nu_{v,s}}{\nu_v} = [(T_w/T_s - 1)\theta_v + 1]^{-(n_\mu+1)} \quad (12.8)$$

12.2.3 For Variable Physical Properties of Liquid Film

For treatment of variable physical properties of liquid, the polynomial method suggested in Chap. 5 will be used for description of the temperature-dependent physical properties of liquid. For example, for water the temperature-dependent expressions of density, thermal conductivity, and absolute viscosity can be expressed as follows:

$$\rho_l = -4.48 \times 10^{-3} t^2 + 999.9 \quad (12.9)$$

$$\lambda_l = -8.01 \times 10^{-6} t^2 + 1.94 \times 10^{-3} t + 0.563 \quad (12.10)$$

$$\mu_l = \exp \left[-1.6 - \frac{1150}{T} + \left(\frac{690}{T} \right)^2 \right] \times 10^{-3} \quad (12.11)$$

12.2.4 For Physical Property Factors of Liquid Film

Consulting Chapter 5 (5.24) to (5.26) the physical property factors $\frac{1}{\rho_l} \frac{d\rho_l}{d\eta_l}$, $\frac{1}{\mu_l} \frac{d\mu_l}{d\eta_l}$, and $\frac{1}{\lambda_l} \frac{d\lambda_l}{d\eta_l}$ in governing Eqs. (11.27) to (11.29) become the following equations at atmospheric pressure for water film flow of laminar free convection film boiling of liquid:

$$\frac{1}{\rho_l} \frac{d\rho_l}{d\eta_l} = \frac{-2 \times 4.48 \times 10^{-3} t (t_s - t_\infty) \frac{d\theta_l}{d\eta_l}}{-4.48 \times 10^{-3} t^2 + 999.9} \quad (12.12)$$

$$\frac{1}{\mu_l} \frac{d\mu_l}{d\eta_l} = \left(\frac{1150}{T^2} - 2 \times \frac{690^2}{T^3} \right) (t_s - t_\infty) \frac{d\theta_l}{d\eta_l} \quad (12.13)$$

$$\frac{1}{\lambda_l} \frac{d\lambda_l}{d\eta_l} = \frac{(-2 \times 8.01 \times 10^{-6}t + 1.94 \times 10^{-3})(t_s - t_\infty) \frac{d\theta_l}{d\eta_l}}{-8.01 \times 10^{-6}t^2 + 1.94 \times 10^{-3}t + 0.563} \quad (12.14)$$

12.3 Numerical Calculation

12.3.1 Calculation Procedure

The present numerical calculation for the laminar free convection film boiling of liquid belongs to a three-point boundary value problem. The general procedure of the calculation with the theoretical model for the film boiling of liquid is described as follows: first the values of $\eta_{v\delta}$ and $W_{xv,s}$ of the vapor film at the vapor–liquid interface are guessed. The two values combined with Eqs. (11.30) and (11.35) as the boundary conditions allow us to solve the governing equations (11.24) to (11.26) for vapor film by using the shooting method. The solutions include the values $W_{yv,s}$, $(dW_{xv}/d\eta_v)_s$ and $\left(\frac{d\theta_v}{d\eta_v}\right)_s$ at the vapor–liquid interface. With the values $\eta_{v\delta}$, $W_{xv,s}$ and $W_{yv,s}$, the values of $W_{xl,s}$ and $W_{yl,s}$ can be calculated from the corresponding boundary condition equations, (11.31) and (11.32). Then, the values $W_{xl,s}$ and $W_{yl,s}$ together with the boundary conditions (11.35) and (11.36) are used to solve the governing equations for liquid film (11.27) to (11.29) by using the shooting method again. The solutions will yield the values of $(dW_{xl}/d\eta_l)_s$ and $\left(\frac{d\theta_l}{d\eta_l}\right)_s$. Equations (11.33) and (11.34) are taken to adjudge the convergence of the solutions for the two-phase boundary governing equations. Thus, the calculation is successively iterated by changing the values of $\eta_{v\delta}$ and $W_{xv,s}$.

12.3.2 Numerical Results

As an example of application for solving the theoretical and mathematical mode of laminar free convection film boiling of water on an isothermal vertical plate, the numerical calculation was carried out. The film boiling of saturated water is taken as its special case. From Chap. 5 we know that the temperature parameters n_μ , n_λ and n_{c_p} of water vapor are 1.04, 1.185, and 0.003. Such low value of n_{c_p} make it possible to actually treat n_{c_p} of water vapor as zero, i.e., c_p is taken as constant. By using the above procedure, the numerical calculations have been done by using the shooting method for solving the three-point values problem at wall superheated grade $\frac{\Delta t_w}{t_s} = \frac{t_w - t_s}{t_s} = 2.77, 3.77, 4.77, 5.77$ and 7.27 °C as well as water subcooled grade $\frac{\Delta t_\infty}{t_s} = \frac{t_s - t_\infty}{t_s} = 0, 0.1, 0.3$ and 1 respectively. The densities of water vapor at the above specified temperatures, the physical values of saturated water vapor and water needed in the calculations are taken from Ref. [2]. A system of numerical

results of velocity and temperature profiles for the two-phase flow films are shown in Figs. 12.1, 12.2, 12.3, 12.4 respectively. From these numerical results, the following phenomena are found:

12.4 Variation of Velocity and Temperature Fields

From these numerical results, the following variations of velocity and temperature fields are found together with wall superheated grade and liquid subcooled grade.

12.4.1 For Velocity Fields of Vapour Film

From Figs. 12.1a, 12.2a, 12.3a and 12.4a, it is seen that the velocity of vapor film will increase with increasing wall superheated grades $\frac{\Delta t_w}{t_s} \left(= \frac{t_w - t_s}{t_s} \right)$. With increasing the wall superheated grades $\frac{\Delta t_w}{t_s} \left(= \frac{t_w - t_s}{t_s} \right)$, the maximum of velocity field will increase and shift far away from the plate. In addition, the velocity of vapour film will decrease with increasing the water subcooled grade, $\frac{\Delta t_\infty}{t_s} \left(= \frac{t_s - t_\infty}{t_s} \right)$.

12.4.2 For Temperature Fields of Vapor Film

From Figs. 12.1b, 12.2b, 12.3b and 12.4b, it is seen that the temperature profiles of vapor film will increase with increasing wall superheated grade, $\frac{\Delta t_w}{t_s} \left(= \frac{t_w - t_s}{t_s} \right)$, and decrease with increasing water subcooled grade, $\frac{\Delta t_\infty}{t_s} \left(= \frac{t_s - t_\infty}{t_s} \right)$. Furthermore, the temperature profile level will decrease slower and slower with increasing the water subcooled degree $\frac{\Delta t_\infty}{t_s} \left(= \frac{t_s - t_\infty}{t_s} \right)$.

12.4.3 For Velocity Fields of Liquid Film

From Figs. 12.1c, 12.2c, 12.3c, and 12.4c, it is seen that the velocity of liquid film will increase with increasing the wall superheated grades $\frac{\Delta t_w}{t_s} \left(= \frac{t_w - t_s}{t_s} \right)$, and decrease with increasing water subcooled grade, $\frac{\Delta t_\infty}{t_s} \left(= \frac{t_s - t_\infty}{t_s} \right)$. Furthermore, with increasing the water subcooled degree $\frac{\Delta t_\infty}{t_s} \left(= \frac{t_s - t_\infty}{t_s} \right)$, the thickness of liquid film will increase, and the velocity profile level of liquid film will decrease slower and slower.

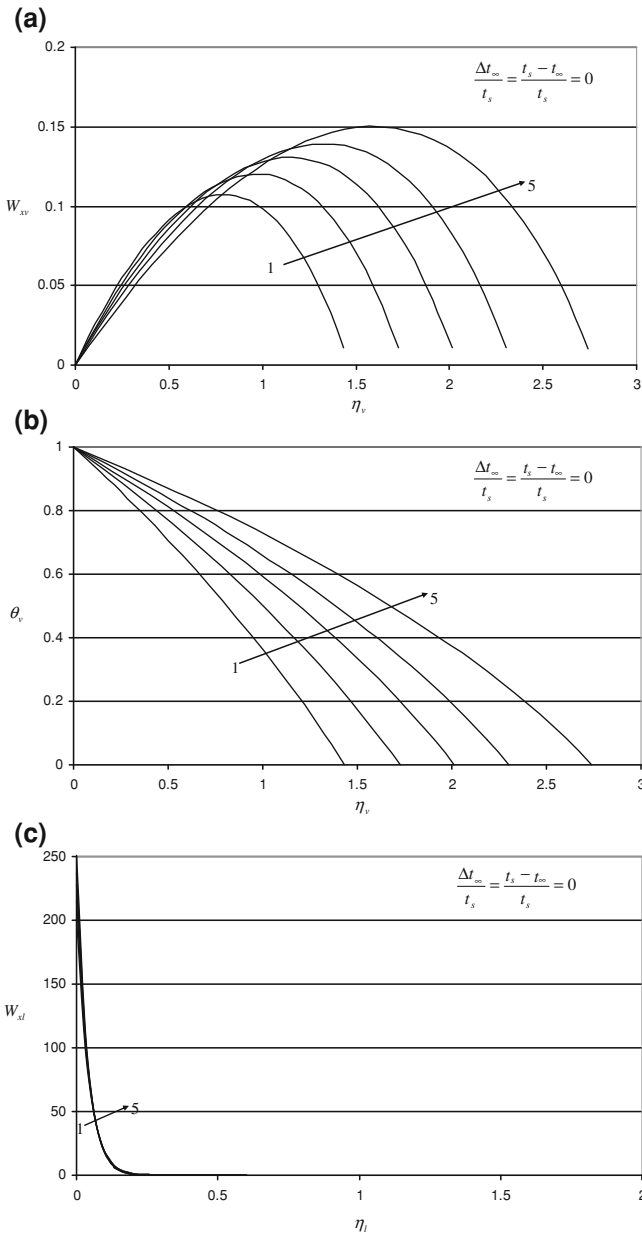


Fig. 12.1 Numerical results on **a** velocity profiles of vapour film, W_{xv} , and **b** temperature profiles of vapour film, θ_v , as well as **c** velocity profiles of liquid film, W_{xl} , for laminar free convection film boiling of water at $\frac{\Delta t_{\infty}}{t_s} \left(= \frac{t_s - t_{\infty}}{t_s} \right) = 0$ and different $\frac{\Delta t_w}{t_s} = \frac{t_w - t_s}{t_s}$. Lines 1–5: $\frac{\Delta t_w}{t_s} = \frac{t_w - t_s}{t_s} = 2.77, 3.77, 4.77, 5.77$ and 7.27°C respectively

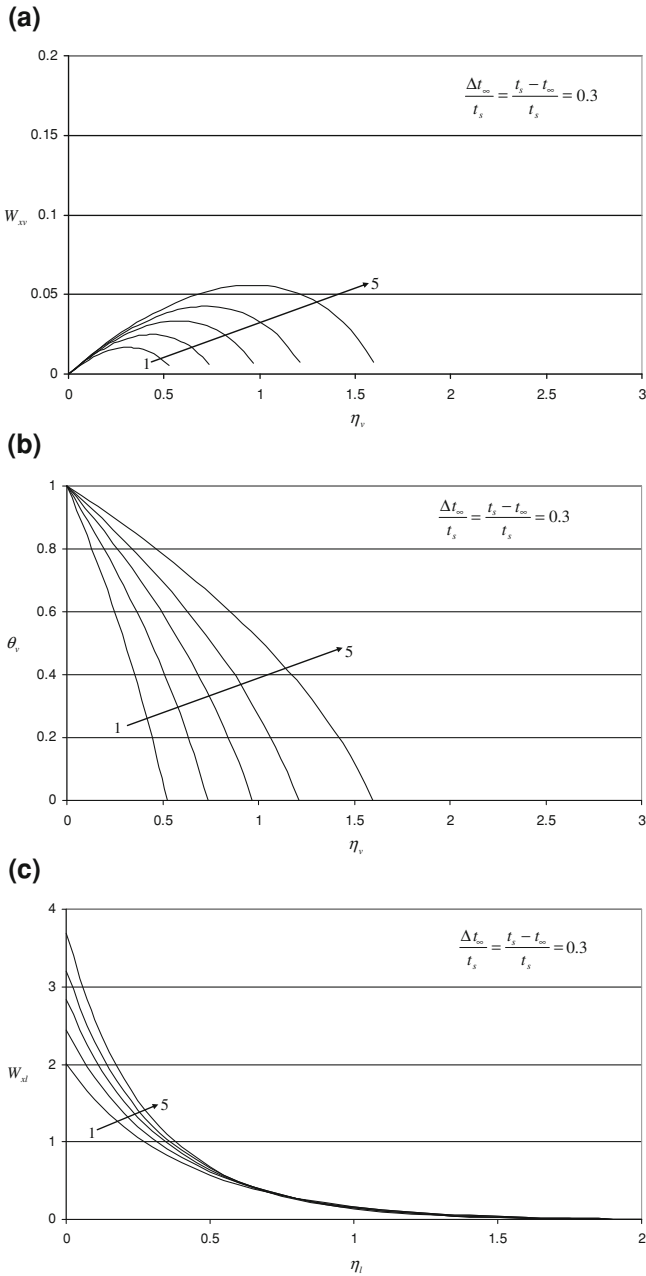


Fig. 12.2 Numerical results on **a** velocity profiles of vapor film, W_{xv} , and **b** temperature profiles of vapor film, θ_v , as well as **c** velocity profiles of liquid film, W_{xl} , for laminar convection film boiling of water at $\frac{\Delta t_{\infty}}{t_s} (= \frac{t_s - t_{\infty}}{t_s}) = 0.3$ and different $\frac{\Delta t_w}{t_s} = \frac{t_w - t_s}{t_s}$. Lines 1–5: $\frac{\Delta t_w}{t_s} = \frac{t_w - t_s}{t_s} = 2.77, 3.77, 4.77, 5.77$ and 7.27 °C, respectively

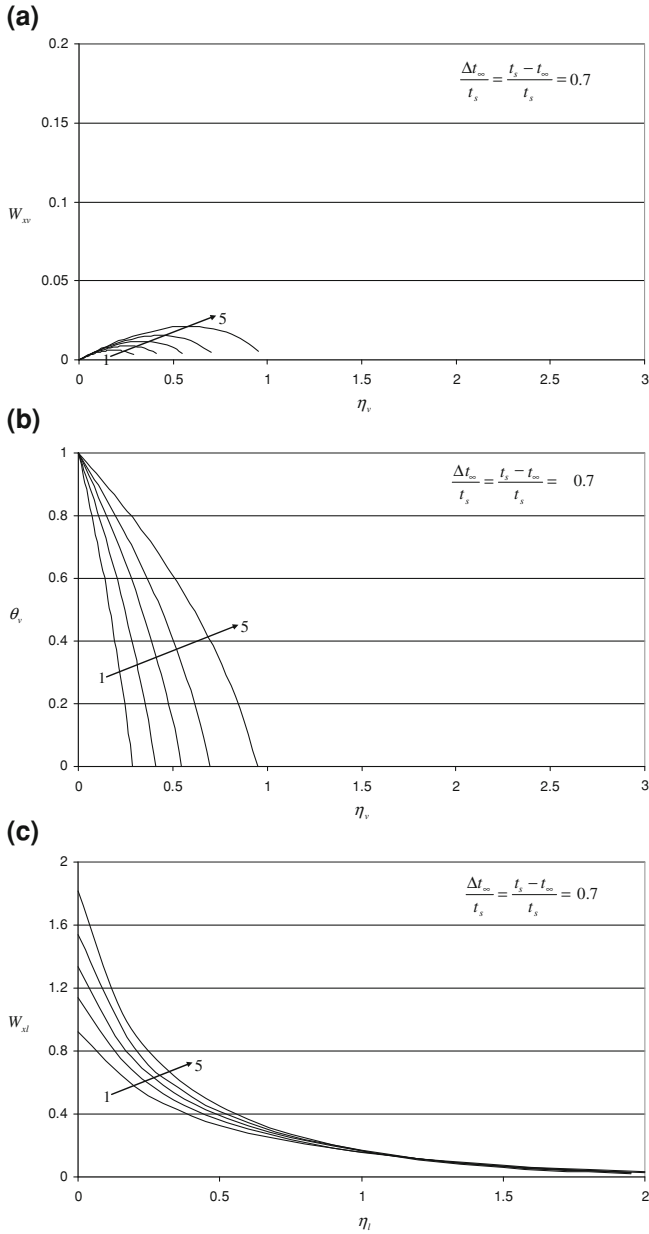


Fig. 12.3 Numerical results on **a** velocity profiles of vapor film, W_{xv} , and **b** temperature profiles of vapor film, θ_v , as well as **c** velocity profiles of liquid film, W_{xl} , for laminar free convection film boiling of water at $\frac{\Delta t_{\infty}}{t_s} (= \frac{t_s - t_{\infty}}{t_s}) = 0.7$ and different $\frac{\Delta t_w}{t_s} = \frac{t_w - t_s}{t_s}$. Lines 1–5: $\frac{\Delta t_w}{t_s} = \frac{t_w - t_s}{t_s} = 2.77, 3.77, 4.77, 5.77$ and 7.27 °C respectively

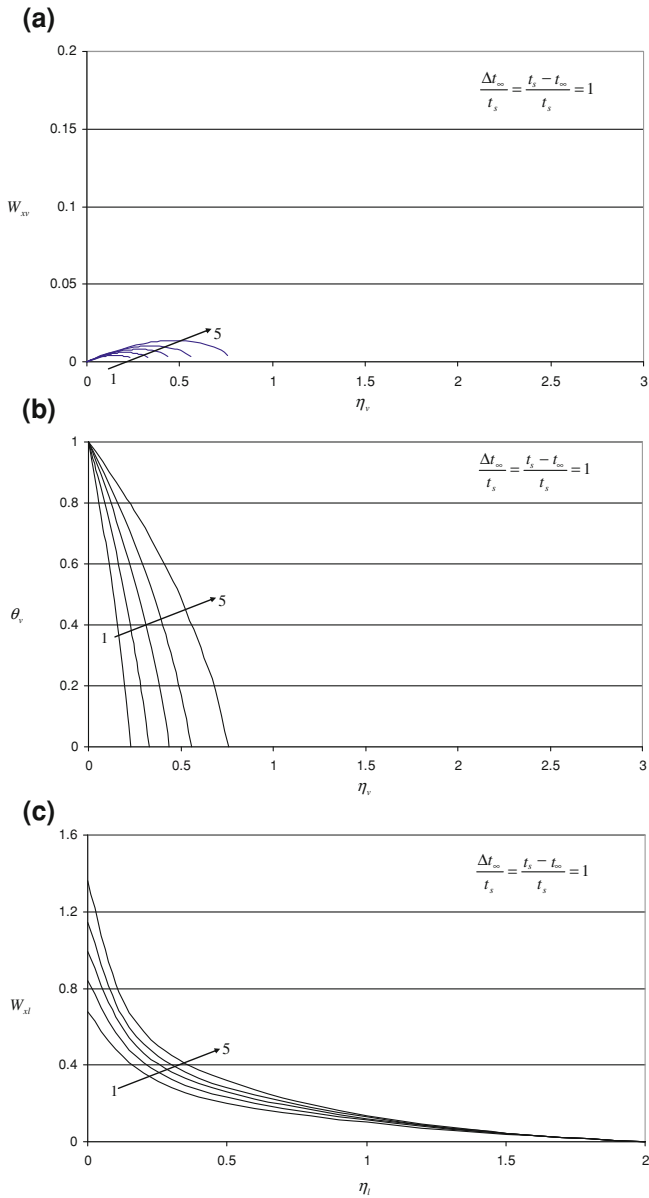


Fig. 12.4 Numerical results on **a** velocity profiles of vapor film, W_{xv} , and **b** temperature profiles of vapor film, θ_v , as well as **c** velocity profiles of liquid film, W_{xl} , for laminar film boiling of water at $\frac{\Delta t_{\infty}}{t_s} \left(= \frac{t_s - t_{\infty}}{t_s} \right) = 1$ and different $\frac{\Delta t_w}{t_s} = \frac{t_w - t_s}{t_s}$. Lines 1–5: $\frac{\Delta t_w}{t_s} = \frac{t_w - t_s}{t_s} = 2.77, 3.77, 4.77, 5.77$ and 7.27 °C, respectively

Furthermore, with increasing wall superheated grade, $\frac{\Delta t_w}{t_s} \left(= \frac{t_w - t_s}{t_s} \right)$, the effect of wall superheated grade on the velocity field of liquid film will decrease.

12.5 Remarks

In the theoretical and mathematical models of the laminar free convection film boiling of liquids, the various physical matching conditions including variable physical properties and three-point boundary values conditions of the two-phase film flow are rigorously taken into account. Then, the numerical solutions of momentum and temperature fields at different wall superheated grades $\frac{\Delta t_w}{t_s}$ and liquid bulk subcooled grades $\frac{\Delta t_\infty}{t_s}$ are theoretically reliable. On this basis, a system of rigorous numerical solutions for momentum and temperature fields of the two-phase film flows are calculated for taking the film boiling of water as the example, in which the related boiling of saturated water is only a special case.

The numerical procedure presented in Sect. 12.3 is reliable for rigorous solutions of the theoretical models with three-point boundary value problem of the laminar free convection film boiling of liquids with consideration of a system of physical conditions including variable physical properties.

The dimensionless velocity components W_x and W_y have definite physical meanings; then, the corresponding solutions of the models can be understood easily. Therefore, the new similarity analysis method has its special advantage over the traditional Falkner-Skan transformation for the theoretical and calculative models of the film boiling of liquids.

Velocity of vapor film will increase with increasing wall superheated grades $\frac{\Delta t_w}{t_s} \left(= \frac{t_w - t_s}{t_s} \right)$. With increasing the wall superheated grades $\frac{\Delta t_w}{t_s} \left(= \frac{t_w - t_s}{t_s} \right)$, the maximum of velocity field will increase and shift far away from the plate. In addition, the velocity of vapor film will decrease with increasing the liquid subcooled grade, $\frac{\Delta t_\infty}{t_s} \left(= \frac{t_s - t_\infty}{t_s} \right)$.

The temperature profiles of vapor film will increase with increasing wall superheated grade, $\frac{\Delta t_w}{t_s} \left(= \frac{t_w - t_s}{t_s} \right)$, and decrease with increasing liquid subcooled grade, $\frac{\Delta t_\infty}{t_s} \left(= \frac{t_s - t_\infty}{t_s} \right)$. Furthermore, the temperature profile level will decrease slower and slower with increasing the liquid subcooled degree $\frac{\Delta t_\infty}{t_s} \left(= \frac{t_s - t_\infty}{t_s} \right)$.

The velocity of liquid film will increase with increasing the wall superheated grade $\frac{\Delta t_w}{t_s} \left(= \frac{t_w - t_s}{t_s} \right)$, and decrease with increasing liquid subcooled grade, $\frac{\Delta t_\infty}{t_s} \left(= \frac{t_s - t_\infty}{t_s} \right)$. With increasing the liquid subcooled degree $\frac{\Delta t_\infty}{t_s} \left(= \frac{t_s - t_\infty}{t_s} \right)$, the thickness of liquid film will increase, and the velocity profile level of liquid film will decrease slower and slower. Furthermore, with increasing wall superheated grade, $\frac{\Delta t_w}{t_s} \left(= \frac{t_w - t_s}{t_s} \right)$, the effect of wall superheated grade on the velocity field of liquid film will decrease.

12.6 Exercises

1. Please give out a detailed derivation for obtaining Eqs. (12.5)–(12.8) on physical property factors of vapor film flow for laminar free convection film boiling of liquid.
2. Please give out a detailed derivation for obtaining Eqs. (12.12)–(12.14) on physical property factors of water film flow for laminar free convection film boiling of liquid.
3. Which differences are there for treatment of variable physical properties between the vapor film flow on laminar free convection film boiling of liquid and gas laminar free convection?
4. Which differences are there for treatment of variable physical properties between the liquid film flow on laminar free convection film boiling of liquid and liquid laminar free convection?
5. Do you think that the variable physical properties are rigorously considered and treated in this present system of mathematical models on laminar free convection film boiling of liquid? Why?
6. Which variations of the velocity and temperature fields of the laminar free convection film boiling of liquid happen together with the wall superheated grade, $\frac{\Delta t_w}{t_s} (= \frac{t_w - t_s}{t_s})$ and liquid subcooled degree $\frac{\Delta t_\infty}{t_s} (= \frac{t_s - t_\infty}{t_s})$? Why?

References

1. D.Y. Shang, B.X. Wang, Effect of variable thermophysical properties on laminar free convection of gas. *Int. J. Heat Mass Transf.* **33**(7), 1387–1395 (1990)
2. VDI—Wärmeatlas, *Berechnungsblätter für Wärmeübertragung*, 5, erweiterte Auflage, (VDI Verlage GmbH, Düsseldorf, 1988)

Chapter 13

Heat and Mass Transfer of Laminar Free Convection Film Boiling of Liquid

Abstract By means of the heat and mass transfer analysis based on the new similarity analysis method, it is found that only the wall temperature gradient and mass flow rate parameter are no-given variables respectively, for prediction of heat and mass transfer of the film boiling. The wall temperature gradient is proportional to heat transfer, and will decrease with increasing the wall superheated grade, and increase with increasing the bulk subcooled grade. Additionally, the wall temperature gradient is steeper with higher liquid bulk subcooled grade and with lower wall superheated grade. The curve-fit equation for evaluation of the wall temperature gradient provided in this chapter agrees very well with the related rigorous numerical solutions, and useful for a reliable prediction of heat transfer of the laminar film boiling of water. From the numerical results, it is seen that vapor film thickness will increase with increasing wall superheated grade or with decreasing the water bulk subcooled grade, and in the iterative calculation it is a key work to correctly determine the suitable value. The solutions of the governing equations are converged in very rigorous values of vapor film thickness. The interfacial velocity component will increase with increasing the wall superheated grade except the case for very low liquid bulk subcooled grade, and will decrease with increasing the liquid bulk subcooled grade. The boiling mass flow rate is proportional to the induced mass flow rate parameter. The mass flow rate parameter will increase with increasing the wall superheated grade, decrease obviously with increasing the liquid subcooled grade, and decrease slower and slower with increasing the liquid subcooled grade. The mass flow rate parameter is formulated according to the numerical solutions, and then, prediction equation for boiling mass transfer is created for reliable evaluation.

13.1 Introduction

In Chap. 12 we presented the solutions to velocity and temperature fields of laminar free convection film boiling of liquid, where the film condensation of saturated liquid is regarded as the special case. In this chapter, studies will be further carried

out on heat and mass transfer for the laminar free convection film boiling of liquid provided by Shang, Wang and Zhong [1–3]. Based on the mathematical model and numerical method presented in Chaps. 11 and 12, the calculation results on heat and mass transfer of the two-phase boundary-layer problem are further obtained with the successively iterative procedure. The laminar free convection film boiling of water is taken as an example, and the theoretical models have been rigorously solved at different wall superheated grade with different liquid subcooled grade. The numerical solutions on heat and mass transfer of the film boiling of liquid are rigorously evaluated at the different conditions, and the film boiling of saturated liquid is taken as its special case. Using heat and mass transfer analysis, the theoretical equations of heat transfer coefficient and mass flow rate are derived. With the numerical solutions the wall temperature gradient and interfacial mass flow rate parameter are formulated, and then, the prediction of heat and mass transfer of laminar free convection film boiling of liquid is realized for different wall superheated grade and different liquid subcooled grade.

13.2 Heat Transfer Analysis

Consulting the *heat transfer analysis* in Chap. 6 for heat transfer analysis on gas laminar free convection, the heat transfer theoretical equations can be expressed as follows for laminar free convection film boiling of liquid:

The *local heat transfer rate* is described as

$$q_x = \lambda_{v,w}(T_w - T_s) \left(\frac{1}{4} Gr_{xv,s} \right)^{1/4} x^{-1} \left(-\frac{d\theta_v}{d\eta_v} \right)_{\eta=0} \quad (13.1)$$

With the Newtonian cooling law, the *local heat transfer coefficient* on the surface, defined as $q_x = \alpha_x(T_w - T_s)$, will be

$$\alpha_x = \lambda_{v,w} \left(\frac{1}{4} Gr_{xv,s} \right)^{1/4} x^{-1} \left(-\frac{d\theta_v}{d\eta_v} \right)_{\eta=0} \quad (13.2)$$

The *local Nusselt number*, defined as $Nu_{xv,w} = \frac{\alpha_x x}{\lambda_{v,w}}$, is expressed by

$$Nu_{x,w} = \left(\frac{1}{4} Gr_{xv,s} \right)^{1/4} \left(-\frac{d\theta_v}{d\eta_v} \right)_{\eta=0} \quad (13.3)$$

The *total heat transfer rate* for position $x = 0$ to x with width of b on the plate is an integration $Q_x = \iint_A q_x dA = \int_0^x q_x b dx$ where $A = b \times x$, and hence

$$Q_x = \frac{4}{3} b \lambda_{v,w} (T_w - T_s) \left(\frac{1}{4} Gr_{xv,s} \right)^{1/4} \left(-\frac{d\theta_v}{d\eta_v} \right)_{\eta_v=0} \quad (13.4)$$

The *average heat transfer rate*, defined as $\bar{Q}_x = Q_x / (b \times x)$ is given by

$$\bar{Q}_x = \frac{4}{3} x^{-1} \lambda_{v,w} (T_w - T_s) \left(\frac{1}{4} Gr_{xv,s} \right)^{1/4} \left(-\frac{d\theta_v}{d\eta_v} \right)_{\eta_v=0} \quad (13.5)$$

The *average heat transfer coefficient* $\bar{\alpha}_x$ defined as $\bar{Q}_x = \bar{\alpha}_x (T_w - T_s) \times b \times x$ is expressed as

$$\bar{\alpha}_x = \frac{4}{3} \lambda_{v,w} \left(\frac{1}{4} Gr_{xv,s} \right)^{1/4} x^{-1} \left(-\frac{d\theta_v}{d\eta_v} \right)_{\eta_v=0} \quad (13.6)$$

The *average Nusselt number* is defined as $\bar{Nu}_{x,w} = \frac{\bar{\alpha}_x x}{\lambda_{v,w}}$, and hence

$$\bar{Nu}_{x,w} = \frac{4}{3} \left(\frac{1}{4} Gr_{xv,s} \right)^{1/4} \left(-\frac{d\theta_v}{d\eta_v} \right)_{\eta_v=0} \quad (13.7)$$

Therefore, we have

$$\begin{aligned} Q_x &= \frac{4}{3} b x q_x \\ \bar{\alpha}_x &= \frac{4}{3} \alpha_x \\ \bar{Nu}_{x,w} &= \frac{4}{3} Nu_{x,w} \end{aligned}$$

Obviously, the theoretical Eqs. (13.1)–(13.7) on heat transfer of laminar free convection film boiling of liquid are identical to the corresponding Eqs. (6.36)–(6.42) in Chap. 6 on laminar free convection, with only differences that the *bulk temperature* T_∞ and the local Grashof number $Gr_{x,\infty}$ of former case are, respectively, replaced by the vapor saturated temperature T_s and the local Grashof number $Gr_{xv,s}$ for the latter case.

It is seen that for practical calculation of heat transfer, only the *wall dimensionless temperature gradient* $\left(\frac{d\theta_v}{d\eta_v} \right)_{\eta_v=0}$ dependent on the solution is no-given variable.

13.3 Wall Dimensionless Temperature Gradient

From the heat transfer analysis, it is found that heat transfer for the film boiling of liquid is in direct proportion to *wall dimensionless temperature gradient* $\left(\frac{d\theta_v}{d\eta_v}\right)_{\eta_v=0}$, the only one no-given variable for prediction of heat transfer. Then, correct prediction of the temperature gradient $\left(\frac{d\theta_v}{d\eta_v}\right)_{\eta_v=0}$ is the key work for prediction of heat transfer of the film boiling of liquid.

The rigorous solutions on the dimensionless temperature gradients $\left(\frac{d\theta_v}{d\eta_v}\right)_{\eta_v=0}$ for the film boiling of water are computed, and the results are tabulated and plotted, respectively, in Table 13.1 and Fig. 13.1.

It is obviously seen from Fig. 13.1 that the temperature gradient $\left(\frac{d\theta_v}{d\eta_v}\right)_{\eta_v=0}$ will decrease slower and slower with increasing the wall superheated grade, $\frac{\Delta t_w}{t_s}$ ($= \frac{t_w - t_s}{t_s}$). In addition, the temperature gradient $\left(\frac{d\theta_v}{d\eta_v}\right)_{\eta_v=0}$ will increase with increasing the bulk water subcooled grade $\frac{\Delta t_\infty}{t_s}$.

Based on the rigorous numerical solutions $\left(\frac{d\theta_v}{d\eta_v}\right)_{\eta_v=0}$ in Table 13.1, the following correlation was obtained by means of a curve-fit method for laminar free convection film boiling of water:

$$-\left(\frac{d\theta_v}{d\eta_v}\right)_{\eta_v=0} = A \left(\frac{\Delta t_w}{t_s}\right)^B \quad \left(2.77 \leq \frac{\Delta t_w}{t_s} \leq 8.27\right) \quad (13.8)$$

$$A = 25.375 \left(\frac{\Delta t_\infty}{t_s}\right)^2 + 7.2275 \left(\frac{\Delta t_\infty}{t_s}\right) + 1.2993 \quad \left(0 \leq \frac{\Delta t_\infty}{t_s} \leq 0.3\right)$$

$$A = -6.7567 \left(\frac{\Delta t_\infty}{t_s}\right)^2 + 21.563 \left(\frac{\Delta t_\infty}{t_s}\right) - 0.1131 \quad \left(0.3 < \frac{\Delta t_\infty}{t_s} \leq 1\right)$$

$$B = 2.2117 \left(\frac{\Delta t_\infty}{t_s}\right)^2 - 2.3472 \left(\frac{\Delta t_\infty}{t_s}\right) - 0.843 \quad \left(0 \leq \frac{\Delta t_\infty}{t_s} \leq 0.3\right)$$

$$B = 0.3585 \left(\frac{\Delta t_\infty}{t_s}\right)^2 - 0.6057 \left(\frac{\Delta t_\infty}{t_s}\right) - 1.2017 \quad \left(0.3 < \frac{\Delta t_\infty}{t_s} \leq 1\right)$$

The results of $\left(-\frac{d\theta_v}{d\eta_v}\right)_{\eta_v=0}$ calculated by Eq. (13.8) are also listed in Table 13.1. It is shown that the calculated results by the correlation (13.8) coincide very well with the corresponding rigorous numerical solutions $-\left(\frac{d\theta_v}{d\eta_v}\right)_{\eta_v=0}$.

Equation (13.8) is corresponding to the laminar free film boiling of subcooled water. However, if the liquid subcooled grade tends to zero, Eq. (13.8) will be simpli-

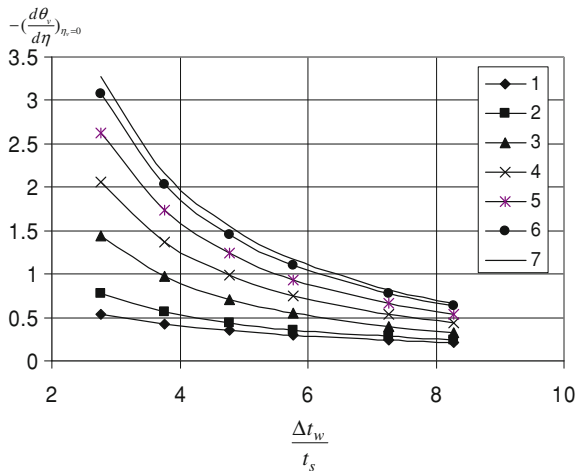
Table 13.1 Numerical results of η_{fs} , $W_{xv,s}$, $W_{yv,s}$, $\left(\frac{d\theta_v}{d\eta_v}\right)_{\eta_v=0}$, and Φ_s ($\eta_{\text{fs}} W_{xv,s} - W_{yv,s}$) for the laminar free film boiling of water (A part of the data are cited from Shang, Wang, and Zhong [3])

t_w (°C)	$\frac{\Delta t_w}{T_s}$	t_∞ (°C)	$\frac{\Delta t_\infty}{T_s}$	η_{fs}	$-W_{yv,s}$	$W_{xv,s}$	$-\left(\frac{d\theta_v}{d\eta_v}\right)_{\eta_v=0}$ (1)	$-\left(\frac{d\theta_v}{d\eta_v}\right)_{\eta_v=0}$ (2)	$\Delta\left(-\frac{d\theta_v}{d\eta_v}\right)_{\eta_v=0}$	Φ_s
377	2.77	100	0	1.437	0.05362	0.01084	0.5411	0.550426	0.017235	0.23006
477	3.77	100	0	1.728	0.06569	0.01080	0.4285	0.424477	-0.00939	0.28142
577	4.77	100	0	2.019	0.07634	0.01068	0.3531	0.348112	-0.01413	0.32692
677	5.77	100	0	2.308	0.08598	0.01057	0.2997	0.296509	-0.01065	0.36832
827	7.27	100	0	2.745	0.09868	0.01035	0.2433	0.244026	0.002984	0.42313
927	8.27	100	0	3.038	0.10625	0.01020	0.2158	0.218903	0.014379	0.45599
377	2.77	90	0.10	0.9828	0.01756	0.00855	0.7733	0.776338	0.003929	0.07865
477	3.77	90	0.10	1.2832	0.02746	0.00910	0.5621	0.560721	-0.00245	0.12153
577	4.77	90	0.10	1.5800	0.03729	0.00939	0.4387	0.437409	-0.00294	0.16399
677	5.77	90	0.10	1.8728	0.04675	0.00957	0.3587	0.357795	-0.00252	0.20491
827	7.27	90	0.10	2.3135	0.05999	0.00967	0.2802	0.280347	0.000525	0.26232
927	8.27	90	0.10	2.6084	0.06820	0.00968	0.2439	0.244688	0.003231	0.29803
377	2.77	70	0.30	0.5240	0.00271	0.00543	1.4414	1.456317	0.010349	0.01368
477	3.77	70	0.30	0.7369	0.00524	0.00616	0.9684	0.961161	-0.00748	0.02549
577	4.77	70	0.30	0.9675	0.00859	0.00672	0.7054	0.699924	-0.00776	0.04085
677	5.77	70	0.30	1.2114	0.01268	0.00717	0.5438	0.541526	-0.00418	0.05939
827	7.27	70	0.30	1.5990	0.01984	0.00769	0.3954	0.396575	0.002972	0.09166
927	8.27	70	0.30	1.8682	0.02511	0.00795	0.3313	0.333327	0.006118	0.11528
377	2.77	50	0.50	0.3652	0.00093	0.00410	2.0672	2.124042	0.027497	0.00521
477	3.77	50	0.50	0.5191	0.00183	0.00470	1.3734	1.37328	-8.7E-05	0.00975
577	4.77	50	0.50	0.6900	0.00309	0.00518	0.9872	0.984433	-0.0028	0.01593
677	5.77	50	0.50	0.8760	0.00474	0.00561	0.7496	0.752025	0.003235	0.02411
827	7.27	50	0.50	1.1827	0.00791	0.00613	0.5317	0.542291	0.019919	0.03891
927	8.27	50	0.50	1.4033	0.01048	0.00644	0.4379	0.451895	0.031959	0.05096

t_w (°C)	$\frac{\Delta t_w}{t_s}$	t_{∞} (°C)	$\frac{\Delta t_{\infty}}{t_s}$	$\eta_{v\delta}$	$-W_{v,v,s}$	$W_{x,v,s}$	$-\left(\frac{d\theta_v}{d\eta_v}\right)_{\eta_v=0}$ (1)	$-\left(\frac{d\theta_v}{d\eta_v}\right)_{\eta_v=0}$ (2)	$\Delta\left(-\frac{d\theta_v}{d\eta_v}\right)_{\eta_v=0}$	Φ_s
377	2.77	30	0.70	0.2881	0.00046	0.00335	2.6202	2.66362	0.016571	0.00281
477	3.77	30	0.70	0.4113	0.00091	0.00385	1.7328	1.703608	-0.01685	0.00522
577	4.77	30	0.70	0.5484	0.00154	0.00426	1.2416	1.211185	-0.0245	0.00849
677	5.77	30	0.70	0.6992	0.00238	0.00463	0.9384	0.919084	-0.02058	0.01275
827	7.27	30	0.70	0.9504	0.00404	0.00509	0.6607	0.657404	-0.00499	0.02101
927	8.27	30	0.70	1.1332	0.00543	0.00537	0.5412	0.545347	0.007663	0.02779
377	2.77	10	0.90	0.2450	0.00029	0.00284	3.0810	3.133876	0.017162	0.00184
477	3.77	10	0.90	0.3497	0.00056	0.00327	2.0381	2.000413	-0.01849	0.00337
577	4.77	10	0.90	0.4671	0.00094	0.00362	1.4577	1.420053	-0.02583	0.00547
677	5.77	10	0.90	0.5964	0.00146	0.00394	1.0999	1.076263	-0.02149	0.00820
827	7.27	10	0.90	0.8130	0.00250	0.00434	0.7720	0.768691	-0.00429	0.01352
927	8.27	10	0.90	0.9705	0.00336	0.00459	0.6315	0.637137	0.008926	0.01790
377	2.77	0	1.00	0.2309	0.00024	0.00262	3.2686	3.357434	0.027178	0.00157
477	3.77	0	1.00	0.3298	0.00047	0.00302	2.1609	2.148105	-0.00592	0.00287
577	4.77	0	1.00	0.4400	0.00079	0.00335	1.5472	1.527605	-0.01266	0.00462
677	5.77	0	1.00	0.5613	0.00122	0.00365	1.1686	1.159441	-0.00784	0.00691
827	7.27	0	1.00	0.7643	0.00207	0.00403	0.8211	0.829544	0.010284	0.01135
927	8.27	0	1.00	0.9163	0.00282	0.00426	0.6688	0.688244	0.029073	0.01517

Note $\left(-\frac{d\theta_v}{d\eta_v}\right)_{\eta_v=0}$ (1) denotes numerical solution; $\left(-\frac{d\theta_v}{d\eta_v}\right)_{\eta_v=0}$ (2) denotes predicted results by using Eq. (13.8); and (3) $\Delta\left(-\frac{d\theta_v}{d\eta_v}\right)_{\eta_v=0}$ denotes predicted deviation of $\left(-\frac{d\theta_v}{d\eta_v}\right)_{\eta_v=0}$ by Eq. (13.8)

Fig. 13.1 Temperature gradient $\left(\frac{d\theta_v}{d\eta_v}\right)_{\eta_v=0}$ with variation of wall superheated grade $\frac{\Delta t_w}{t_s} = \frac{t_w - t_s}{t_s}$ and bulk sub-cooled grade $\frac{\Delta t_\infty}{t_s} = \frac{t_s - t_\infty}{t_s}$ for laminar free film boiling of water. Note 1–7: $\frac{\Delta t_\infty}{t_s} = 0, 0.1, 0.3, 0.5, 0.7, 0.9,$ and 1 ($\frac{\Delta t_\infty}{t_s} = 0$ is corresponding to the film boiling of saturated water)



fied to the following equation for describing the laminar free film boiling of saturated water:

$$\left(\left(-\frac{d\theta_v}{d\eta_v}\right)_{\eta_v=0}\right)_{\Delta t_\infty=0} = 1.2993 \left(\frac{\Delta t_w}{t_s}\right)^{-0.843} \quad \left(2.77 \leq \frac{\Delta t_w}{t_s} \leq 8.27\right) \quad (13.9)$$

13.4 Practical Prediction Equations on Boiling Heat Transfer

By using Eq.(13.8), the Eqs.(13.1) and (13.3) are reliable for prediction of heat transfer of laminar free film convection boiling of water.

The local heat transfer rate is described as

$$q_x = A\lambda_{v,w}(T_w - T_s) \left(\frac{1}{4}Gr_{xv,s}\right)^{1/4} x^{-1} \left(\frac{\Delta t_w}{t_s}\right)^B \quad (13.1^*)$$

With the Newtonian cooling law, the local heat transfer coefficient on the surface, defined as $q_x = \alpha_x(T_w - T_s)$, will be

$$\alpha_x = A\lambda_{v,w} \left(\frac{1}{4}Gr_{xv,s}\right)^{1/4} x^{-1} \left(\frac{\Delta t_w}{t_s}\right)^B \quad (13.2^*)$$

The local Nusselt number, defined as $Nu_{xv,w} = \frac{\alpha_x x}{\lambda_{v,w}}$, is expressed by

$$Nu_{xv,w} = A \left(\frac{1}{4}Gr_{xv,s}\right)^{1/4} \left(\frac{\Delta t_w}{t_s}\right)^B \quad (13.3^*)$$

Total heat transfer rate for position $x = 0$ to x with width of b on the plate is expressed as

$$Q_x = \frac{4}{3}Ab\lambda_{v,w}(T_w - T_s) \left(\frac{1}{4}Gr_{xv,s}\right)^{1/4} \left(\frac{\Delta t_w}{t_s}\right)^B \quad (13.4^*)$$

The average heat transfer rate, defined as $\bar{Q}_x = Q_x/(b \times x)$ is given by

$$\bar{Q}_x = \frac{4}{3}Ax^{-1}\lambda_{v,w}(T_w - T_s) \left(\frac{1}{4}Gr_{xv,s}\right)^{1/4} \left(\frac{\Delta t_w}{t_s}\right)^B \quad (13.5^*)$$

The average heat transfer coefficient $\bar{\alpha}_x$ defined as $Q_x = \bar{\alpha}_x(T_w - T_s) \times b \times x$ is expressed as

$$\bar{\alpha}_x = \frac{4}{3}A\lambda_{v,w} \left(\frac{1}{4}Gr_{xc,s}\right)^{1/4} x^{-1} \left(\frac{\Delta t_w}{t_s}\right)^B \quad (13.6^*)$$

The average Nusselt number is defined as $\overline{Nu}_{xv,w} = \frac{\bar{\alpha}_x x}{\lambda_{v,w}}$, and hence

$$\overline{Nu}_{xv,w} = \frac{4}{3}A \left(\frac{1}{4}Gr_{xv,s}\right)^{1/4} \left(\frac{\Delta t_w}{t_s}\right)^B \quad (13.7^*)$$

where

$$2.77 \leq \frac{\Delta t_w}{t_s} \leq 8.27$$

$$A = 25.375 \left(\frac{\Delta t_\infty}{t_s}\right)^2 + 7.2275 \left(\frac{\Delta t_\infty}{t_s}\right) + 1.2993 \quad \left(0 \leq \frac{\Delta t_\infty}{t_s} \leq 0.3\right)$$

$$A = -6.7567 \left(\frac{\Delta t_\infty}{t_s}\right)^2 + 21.563 \left(\frac{\Delta t_\infty}{t_s}\right) - 0.1131 \quad \left(0.3 < \frac{\Delta t_\infty}{t_s} \leq 1\right)$$

$$B = 2.2117 \left(\frac{\Delta t_\infty}{t_s}\right)^2 - 2.3472 \left(\frac{\Delta t_\infty}{t_s}\right) - 0.843 \quad \left(0 \leq \frac{\Delta t_\infty}{t_s} \leq 0.3\right)$$

$$B = 0.3585 \left(\frac{\Delta t_\infty}{t_s}\right)^2 - 0.6057 \left(\frac{\Delta t_\infty}{t_s}\right) - 1.2017 \quad \left(0.3 < \frac{\Delta t_\infty}{t_s} \leq 1\right)$$

With the reliable equation on the dimensionless temperature gradient, Eqs. (13.1)–(13.7) become reliable equations for practical prediction of heat transfer for laminar free film boiling of water on a vertical flat plate.

13.5 Mass Transfer Analysis

Set g_x to be a *local mass flow rate* entering the vapor film at position x per unit area of the plate. According to the boundary layer theory of fluid mechanics, g_x is expressed as

$$g_x = \rho_{v,s} \left(w_{xv,s} \frac{d\delta_v}{dx} - w_{yv,s} \right)_s$$

With the corresponding dimensionless variables in (11.17) and (11.18), the above equation is changed into the following one:

$$g_x = \rho_{v,s} \left[2\sqrt{gx} \left(\frac{\rho_{l,\infty}}{\rho_{v,w}} - 1 \right)^{1/2} W_{xv,s} \left(\frac{d\delta_v}{dx} \right)_s - 2\sqrt{gx} \left(\frac{\rho_{l,\infty}}{\rho_{v,w}} - 1 \right)^{1/2} \left(\frac{1}{4} Gr_{xv,s} \right)^{-1/4} W_{yv,s} \right]$$

With definition of $Gr_{xv,s}$, we have

$$\rho_{l,\infty}/\rho_{v,w} - 1 = \frac{v_{v,s}^2}{gx^3} Gr_{xv,s}$$

Then, g_x is expressed as

$$\begin{aligned} g_x &= \rho_{v,s} \left[2\sqrt{gx} W_{xv,s} \left(\frac{d\delta_v}{dx} \right)_s - 2\sqrt{gx} \left(\frac{1}{4} Gr_{xv,s} \right)^{-1/4} W_{yv,s} \right] \left(\frac{v_{v,s}^2}{gx^3} Gr_{xv,s} \right)^{1/2} \\ &= 2\rho_{v,s} \left[2\sqrt{gx} W_{xv,s} \left(\frac{d\delta_v}{dx} \right)_s - 2\sqrt{gx} \left(\frac{1}{4} Gr_{xv,s} \right)^{-1/4} W_{yv,s} \right] \\ &\quad \times \left(\frac{v_{v,s}^2}{gx^3} \right)^{1/2} \left(\frac{1}{4} Gr_{xv,s} \right)^{1/2} \end{aligned}$$

where the boiled vapor film thickness is expressed as follows according to Eq. (11.14):

$$\delta_v = \eta_{v\delta} \left(\frac{1}{4} Gr_{xv,s} \right)^{-1/4} x \quad (13.10)$$

With the definition of the local Grashof number $Gr_{xv,s}$, Eq. (13.10) is changed into

$$\delta_v = \eta_{v\delta} \left(\frac{1}{4} \frac{g(\rho_{l,\infty}/\rho_{v,w} - 1)x^3}{v_{v,s}^2} \right)^{1/4} x$$

Hence,

$$\left(\frac{d\delta_v}{dx}\right)_s = \frac{1}{4}\eta_{v\delta} \left(\frac{1}{4}Gr_{xv,s}\right)^{-1/4} \quad (13.11)$$

Then,

$$\begin{aligned} g_x &= 2\rho_{v,s} \left[2\sqrt{gx}W_{xv,s} \frac{1}{4}\eta_{v\delta} \left(\frac{1}{4}Gr_{xv,s}\right)^{-1/4} - 2\sqrt{gx} \left(\frac{1}{4}Gr_{xv,s}\right)^{-1/4} W_{yv,s} \right] \\ &\quad \times \left(\frac{v_{v,s}^2}{gx^3}\right)^{1/2} \left(\frac{1}{4}Gr_{xv,s}\right)^{1/2} \\ &= 2\rho_{v,s} \left[2\sqrt{gx}W_{xv,s} \frac{1}{4}\eta_{v\delta} - 2\sqrt{gx}W_{yv,s} \right] \left(\frac{v_{v,s}^2}{gx^3}\right)^{1/2} \left(\frac{1}{4}Gr_{xv,s}\right)^{1/4} \end{aligned}$$

i.e.

$$g_x = \mu_{v,s}x^{-1} \left(\frac{1}{4}Gr_{xv,s}\right)^{1/4} (\eta_{v\delta}W_{xv,s} - 4W_{yv,s})$$

i.e.

$$g_x = \mu_{v,s}x^{-1} \left(\frac{1}{4}Gr_{xv,s}\right)^{1/4} \Phi_s \quad (13.12)$$

where

$$\Phi_s = (\eta_{v\delta}W_{xv,s} - 4W_{yv,s}) \quad (13.13)$$

is regarded as *mass flow rate parameter* of the film boiling of liquid.

If G_x is taken to express *total mass flow rate* entering the boundary layer for position $x = 0$ to x with width of b of the plate, it should be the following integration:

$$\begin{aligned} G_x &= \iint_A (g_x)_i dA \\ &= b \int_0^x (g_x)_i dx \end{aligned}$$

where $A = b \cdot x$ is the related area of the plate.

Then, G_x is expressed as

$$G_x = b \int_0^x \left[\mu_{v,s} x^{-1} \left(\frac{1}{4} Gr_{xv,s} \right)^{1/4} \Phi_s \right] dx$$

i.e.

$$G_x = \frac{4}{3} b \cdot \mu_{v,s} \left(\frac{1}{4} Gr_{xv,s} \right)^{1/4} \Phi_s \quad (13.14)$$

It is seen that, for practical calculation of boiling mass transfer, only Φ_s dependent on numerical solution is no-given variable.

13.6 Mass Flow Rate Parameter

From Eq. (13.13), it is seen that the *mass flow rate parameter* Φ_s , the only no-given variable for prediction of the boiling mass transfer, depends on the vapor film thickness $\eta_{v\delta}$, as well as the vapor velocity components at the vapor–liquid interface, $W_{xv,s}$, and $W_{yv,s}$. Now, it is necessary to investigate these physical variables.

13.6.1 Vapor Film Thickness

The numerical results for *vapor film thickness* $\eta_{v\delta}$ of the film boiling of subcooled water are listed in Table 13.1 and plotted in Fig. 13.2 together with wall superheated grade $\frac{\Delta t_w}{t_s}$ and water bulk subcooled grade $\frac{\Delta t_\infty}{t_s}$. It is seen that $\eta_{v\delta}$ will increase with increasing *wall superheated grade* $\frac{\Delta t_w}{t_s}$. The reason is easy to be understood that with increasing the wall superheated grade $\frac{\Delta t_w}{t_s}$, the vaporization rate will increase; thus, the vapor film thickness $\eta_{v\delta}$ will increase.

In Fig. 13.2 it is seen that with increasing the water *bulk subcooled grade* $\frac{\Delta t_\infty}{t_s}$, the vapor film thickness $\eta_{v\delta}$ will decrease. The reason is that with increasing the water bulk subcooled grade $\frac{\Delta t_\infty}{t_s}$, the vaporization of the bulk liquid will become more difficult at the liquid–vapor interface. Meanwhile, with increasing the water bulk subcooled grade $\frac{\Delta t_\infty}{t_s}$, the vapor film thickness $\eta_{v\delta}$ will decrease slower and slower.

It should be indicated that in the iterative calculation of the film boiling problem, it is a key work to correctly determine suitable value η_l . The solutions of the models are converged in very rigorous values of $\eta_{v\delta}$ as shown in Table 13.1 and Fig. 13.2; otherwise, the convergence solutions will not be obtained.

Based on the rigorous numerical solutions listed in Table 13.1, the following *curve-fit equation* is obtained for *vapor film thickness* $\eta_{v\delta}$ above the laminar free film boiling of saturated water:

Fig. 13.2 The film thickness $\eta_{v\delta}$ with wall superheated grade $\frac{\Delta t_w}{t_s}$ and water bulk subcooled grade $\frac{\Delta t_\infty}{t_s}$ for laminar free film boiling of water. Note 1–7: $\frac{\Delta t_\infty}{t_s} = 0, 0.1, 0.3, 0.5, 0.7, 0.9,$ and 1 ($\frac{\Delta t_\infty}{t_s} = 0$ is corresponding to film boiling of saturated water)

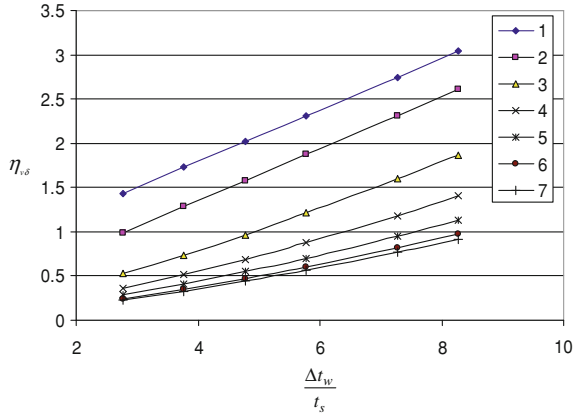
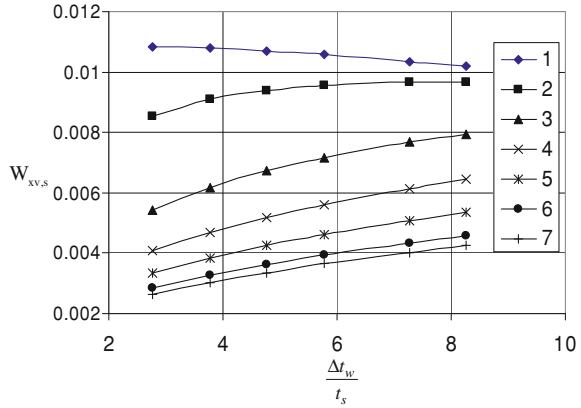


Fig. 13.3 Variation of $W_{xv,s}$ with $\frac{\Delta t_w}{t_s}$ and $\frac{\Delta t_\infty}{t_s}$ for laminar free film boiling of water. Note 1–7: $\frac{\Delta t_\infty}{t_s} = 0, 0.1, 0.3, 0.5, 0.7, 0.9,$ and 1 ($\frac{\Delta t_\infty}{t_s} = 0$ is corresponding to film boiling of saturated water)



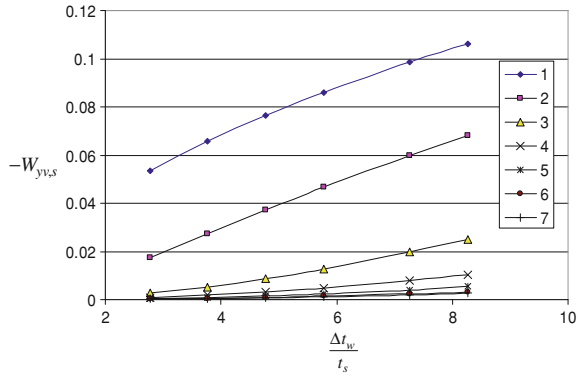
$$\eta_{v\delta} = 0.291 \frac{\Delta t_w}{t_s} + 0.631 \tag{13.15}$$

13.6.2 Interfacial Velocity Components

The rigorous numerical solutions of *interfacial velocity components* $W_{xv,s}$ and $W_{yv,s}$ for the film boiling of subcooled water are described in Table 13.1, and plotted in Figs. 13.3 and 13.4, respectively, with variations of wall superheated grade $\frac{\Delta t_w}{t_s}$ and the water bulk subcooled grade $\frac{\Delta t_\infty}{t_s}$. It is found that the variations of interfacial velocity components $W_{xv,s}$ and $W_{yv,s}$ vary as follows with *wall superheated grade* $\frac{\Delta t_w}{t_s}$ and the *water bulk subcooled degree* $\frac{\Delta t_\infty}{t_s}$:

The interfacial velocity component $W_{xv,s}$ will increase with increasing the wall superheated grade Δt_w except for very low water bulk subcooled grade $\frac{\Delta t_\infty}{t_s}$. In

Fig. 13.4 Variation of $-W_{yv,s}$ with $\frac{\Delta t_w}{t_s}$ and $\frac{\Delta t_\infty}{t_s}$ for laminar free film boiling of water. Note 1–7: $\frac{\Delta t_\infty}{t_s} = 0, 0.1, 0.3, 0.5, 0.7, 0.9,$ and 1 ($\frac{\Delta t_\infty}{t_s} = 0$ is corresponding to the film boiling of saturated water)



addition, the interfacial velocity component $W_{xv,s}$ will decrease with increasing the water bulk subcooled grade $\frac{\Delta t_\infty}{t_s}$. Meanwhile, the interfacial velocity component $W_{xv,s}$ will decrease slower and slower with increasing the water bulk subcooled grade $\frac{\Delta t_\infty}{t_s}$.

The interfacial velocity component $W_{xv,s}$ will increase with increasing the wall superheated grade Δt_w , especially in the range of lower water subcooled grade $\frac{\Delta t_\infty}{t_s}$. In addition, they will decrease with increasing the water bulk subcooled grade $\frac{\Delta t_\infty}{t_s}$, and will decrease slower and slower with increasing the water subcooled grade $\frac{\Delta t_\infty}{t_s}$. It is seen that the value of the interfacial velocity component $W_{yv,s}$ is usually much more than that of the interfacial velocity component $W_{xv,s}$. Then, it is follows that the interfacial velocity component $W_{yv,s}$ will dominate the interfacial mass flow rate in general. However, the effect of the interfacial velocity component $W_{xv,s}$ on the interfacial mass flow rate can never be ignored.

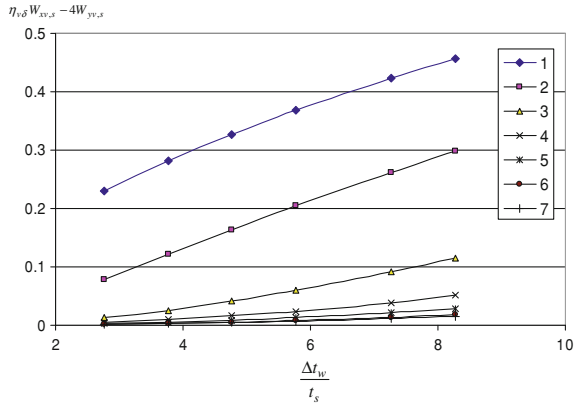
13.6.3 Mass Flow Rate Parameter

The mass flow rate parameters $\Phi_s = \eta_{v\delta} W_{xv,s} - W_{yv,s}$ for the film boiling of subcooled water are described in Table 13.1, and plotted in Fig. 13.5, respectively, with variations of wall superheated grade Δt_w and the water bulk subcooled grade $\frac{\Delta t_\infty}{t_s}$. It is found that the mass flow rate parameter $\eta_{v\delta} W_{xv,s} - W_{yv,s}$ varies as follows with wall superheated grade Δt_w and the water bulk subcooled degree $\frac{\Delta t_\infty}{t_s}$.

From Fig. 13.5 it is obviously seen that the mass flow rate parameter $\Phi_s = (\eta_{v\delta} W_{xv,s} - 4W_{yv,s})$ will increase with increasing the wall superheated grade Δt_w , especially in the range of lower water subcooled grade $\frac{\Delta t_\infty}{t_s}$. Meanwhile, it will decrease with increasing the water bulk subcooled grade. With increasing the water bulk subcooled grade, the mass flow rate parameter with decrease slower and slower.

Based on the rigorous numerical solutions, the following curve-fit equation is obtained for mass flow rate parameter Φ_s with $\frac{\Delta t_\infty}{t_s} = 0$ for the laminar film boiling

Fig. 13.5 Variation of mass flow rate parameter $\Phi_s = \eta_{v\delta} W_{xv,s} - W_{yv,s}$ with $\frac{\Delta t_w}{t_s}$ and $\frac{\Delta t_\infty}{t_s}$ for laminar free film boiling of water. Note 1–7: $\frac{\Delta t_\infty}{t_s} = 0, 0.1, 0.3, 0.5, 0.7, 0.9,$ and 1 ($\frac{\Delta t_\infty}{t_s} = 0$ is corresponding to the film boiling of saturated water)



of saturated water:

$$(\Phi_s)_{\Delta t_\infty=0} = -0.002 \left(\frac{\Delta t_w}{t_s} \right)^2 + 0.0635 \frac{\Delta t_w}{t_s} + 0.0705 \tag{13.16}$$

13.7 Practical Prediction Equation on Boiling Mass Transfer

With Eq. (13.16), Eq. (13.14) becomes

$$G_x = \frac{4}{3} b \cdot \mu_{v,s} \left(\frac{1}{4} Gr_{xv,s} \right)^{1/4} \left[-0.002 \left(\frac{\Delta t_w}{t_s} \right)^2 + 0.0635 \frac{\Delta t_w}{t_s} + 0.0705 \right] \tag{13.14*}$$

This equation can be used as *practical prediction equation on boiling mass transfer* of laminar free convection film boiling of saturated water on a vertical flat plate.

13.8 Summary

So far, governing equations and the equations for heat and mass transfer of the laminar free film boiling of liquid can be summarized in Tables 13.2 and 13.3, respectively. Meanwhile, the film boiling of saturated liquid can be regarded as its special case of the film boiling.

Table 13.2 Summary of governing equations of the laminar free film boiling of liquid

Term	Expression
<i>Partial differential equations for vapor film</i>	
Mass equation	$\frac{\partial}{\partial x}(\rho_v w_{xv}) + \frac{\partial}{\partial y}(\rho_v w_{yv}) = 0$
Momentum equation	$\rho_v \left(w_{xv} \frac{\partial w_{xv}}{\partial x} + w_{yv} \frac{\partial w_{xv}}{\partial y} \right) = \frac{\partial}{\partial y} \left(\mu_v \frac{\partial w_{xv}}{\partial y} \right) + g(\rho_{l,\infty} - \rho_v)$
Energy equation	$\rho_v c_{pv} \left(w_{xv} \frac{\partial T_v}{\partial x} + w_{yv} \frac{\partial T_v}{\partial y} \right) = \frac{\partial}{\partial y} \left(\lambda_v \frac{\partial T_v}{\partial y} \right)$
<i>Partial differential equations for subcooled liquid film</i>	
Mass equation	$\frac{\partial}{\partial y}(\rho_l w_{yl}) + \frac{\partial}{\partial x}(\rho_l w_{xl}) = 0$
Momentum equation	$\rho_l \left(w_{xl} \frac{\partial w_{xl}}{\partial x} + w_{yl} \frac{\partial w_{xl}}{\partial y} \right) = \frac{\partial}{\partial y} \left(\mu_l \frac{\partial w_{xl}}{\partial y} \right) + g(\rho_{l,\infty} - \rho_l)$
Energy equation	$\rho_l c_{pl} \left(w_{xl} \frac{\partial T_l}{\partial x} + w_{yl} \frac{\partial T_l}{\partial y} \right) = \frac{\partial}{\partial y} \left(\lambda_l \frac{\partial T_l}{\partial y} \right)$
(It is omitted for the laminar free film boiling of saturated liquid)	
<i>Boundary conditions</i>	
$y = 0$	$w_{xv} = 0, \quad w_{yv} = 0, \quad T = T_w$
$y = \delta_v$	$w_{xv,s} = w_{xl,s}$ $\rho_{v,s} \left(w_{xv} \frac{\partial \delta_{xv}}{\partial x} - w_{yv} \right)_s = \rho_{l,s} \left(w_{xl} \frac{\partial \delta_{xl}}{\partial x} - w_{yl} \right)_s$ $\mu_{v,s} \left(\frac{\partial w_{xv}}{\partial y} \right)_s = \mu_{l,s} \left(\frac{\partial w_{xl}}{\partial y} \right)_s$ $-\lambda_{v,s} \left(\frac{\partial T_v}{\partial y} \right)_{y=\delta_v} = h_{fg} \rho_{v,s} \left(w_{xv} \frac{\partial \delta_{xv}}{\partial x} - w_{yv} \right)_s - \lambda_{l,s} \left(\frac{\partial T_l}{\partial y} \right)_{y=\delta_v}$
(The heat conduction term $-\lambda_{l,s} \left(\frac{\partial T_l}{\partial y} \right)_{y=\delta_v}$ will be omitted for the laminar free film boiling of saturated liquid)	
$T = T_s$	
$w_{xl} \rightarrow 0, \quad t_l \rightarrow t_\infty$	
$y \rightarrow \infty$	

Term	Expression
<i>Similarity variables for vapor film</i>	
$Gr_{xv,s}$	$\left(\frac{1}{4}Gr_{xv,s}\right)^{1/4} \frac{y}{x}$ $\frac{g(\rho_{l,\infty}/\rho_{v,w}-1)x^3}{v_{v,s}^2}$
θ_v	$\frac{T-T_w}{T_w-T_s}$ <p>(The definition of θ_v is omitted for the film boiling of saturated liquid)</p>
W_{xv}	$\left(2\sqrt{g\bar{x}}(\rho_{l,\infty}/\rho_{v,w}-1)^{1/2}\right)^{-1} W_{xv}$
W_{yv}	$\left(2\sqrt{g\bar{x}}(\rho_{l,\infty}/\rho_{v,w}-1)^{1/2}\left(\frac{1}{4}Gr_{xv,s}\right)^{-1/4}\right)^{-1} W_{yv}$
<i>Ordinary differential equations for vapor film</i>	
Mass equation	$2W_{xv} - \eta_v \frac{dW_{xv}}{d\eta_v} + 4\frac{dW_{xv}}{d\eta_v} - \frac{1}{\rho_v} \frac{d\rho_v}{d\eta_v} (\eta_v W_{xv} - 4W_{yv}) = 0$
Momentum equation	$\frac{v_{v,s}}{v_v} \left(W_{xv} \left(2W_{xv} - \eta_v \frac{dW_{xv}}{d\eta_v} \right) + 4W_{yv} \frac{dW_{xv}}{d\eta_v} \right)$ $= \frac{d^2 W_{xv}}{d\eta_v^2} + \frac{1}{\mu_v} \frac{d\mu_v}{d\eta_v} \frac{dW_{xv}}{d\eta_v} + \frac{v_{v,s}}{v_v} \frac{\rho_{v,w}}{\rho_v} \frac{\rho_{l,\infty} - \rho_v}{\rho_v}$
Energy equation	$Pr_v \frac{v_{v,s}}{v_v} (-\eta_v W_{xv} + 4W_{yv}) \frac{d\theta_v}{d\eta_v} = \frac{d^2 \theta_v}{d\eta_v^2} + \frac{1}{\lambda_v} \frac{d\theta_v}{d\eta_v} \frac{d\theta_v}{d\eta_v}$ <p>(This energy equation should be omitted for the film boiling of saturated liquid)</p>
<i>Similarity variables for liquid film</i>	
η_l	$\left(\frac{1}{4}Gr_{xl,\infty}\right)^{1/4} \frac{y}{x}$
$Gr_{xl,\infty}$	$\frac{g(\rho_{l,\infty}/\rho_{l,s}-1)x^3}{v_{l,\infty}^2}$
θ_l	$\frac{T-T_\infty}{T_s-T_\infty}$
W_{xl}	$\left(2\sqrt{g\bar{x}}(\rho_{l,\infty}/\rho_{l,s}-1)^{1/2}\right)^{-1} W_{xl}$
W_{yl}	$\left(2\sqrt{g\bar{x}}(\rho_{l,\infty}/\rho_{l,s}-1)^{1/2}\left(\frac{1}{4}Gr_{xl,\infty}\right)^{-1/4}\right)^{-1} W_{yl}$

(continued)

Table 13.2 (continued)

Term	Expression
<i>Ordinary differential equations for liquid film</i>	
Mass equations	$2W_{x,l} - \eta_l \frac{dW_{x,l}}{d\eta_l} + 4 \frac{dW_{y,l}}{d\eta_l} - \frac{1}{\rho_l} \frac{d\rho_l}{d\eta_l} (\eta_l W_{x,l} - 4W_{y,l}) = 0$
Momentum Equation	$\frac{v_{l,\infty}}{v_l} \left[W_{x,l} \left(2W_{x,l} - \eta_l \frac{dW_{x,l}}{d\eta_l} \right) + 4W_{y,l} \frac{dW_{x,l}}{d\eta_l} \right] = \frac{d^2 W_{x,l}}{d\eta_l^2} + \frac{1}{\mu_l} \frac{dW_{x,l}}{d\eta_l} \frac{d\mu_l}{d\eta_l} + \frac{v_{l,\infty}}{v_l} \left(\frac{\rho_{l,\infty}}{\rho_{l,s}} - 1 \right)$
Energy equation	$Pr_l \frac{v_{l,\infty}}{v_l} (-\eta_l W_{x,l} + 4W_{y,l}) \frac{d\theta_l}{d\eta_l} = \frac{d^2 \theta_l}{d\eta_l^2} + \frac{1}{\lambda_l} \frac{d\lambda_l}{d\eta_l} \frac{d\theta_l}{d\eta_l}$
(It is omitted for the laminar free film boiling of saturated liquid)	
<i>Equivalent dimensionless boundary condition equations</i>	
$\eta_v = 0 :$	$W_{x,v} = 0, \quad W_{y,v} = 0, \quad \theta_v = 1$
$\eta_v = \eta_{v\delta} (\eta_l = 0) :$	$W_{x,l,s} = \left(\frac{\rho_{l,\infty}}{\rho_{v,w}} - 1 \right)^{1/2} \left(\frac{\rho_{l,\infty}}{\rho_{l,s}} - 1 \right)^{-1/2} W_{xv,s}$ $W_{y,l,s} = -0.25 \frac{\rho_{v,s}}{\rho_{l,s}} \left(\frac{v_{v,s}}{v_{l,\infty}} \right)^{1/2} \left(\frac{\rho_{l,\infty}}{\rho_{v,w}} - 1 \right)^{1/4} \left(\frac{\rho_{l,\infty}}{\rho_{l,s}} - 1 \right)^{-1/4} (W_{xv,s} \eta_{v\delta} - 4W_{yv,s})$ $\left(\frac{dW_{x,l}}{d\eta_l} \right)_{\eta_l=0} = \frac{h_{fg} \mu_{v,s}}{h_{l,s}} \left(\frac{\rho_{l,\infty}}{\rho_{v,w}} - 1 \right)^{3/4} \left(\frac{\rho_{l,\infty}}{\rho_{l,s}} - 1 \right)^{-3/4} \left(\frac{v_{l,\infty}}{v_{v,s}} \right)^{1/2} \left(\frac{dW_{x,v}}{d\eta_v} \right)_{\eta_v=\eta_{v\delta}}$ $\left(\frac{d\theta_l}{d\eta_l} \right)_{\eta_l=0} = \left(\frac{\rho_{l,\infty}}{\rho_{v,w}} - 1 \right)^{1/4} \left(\frac{\rho_{l,\infty}}{\rho_{l,s}} - 1 \right)^{-1/4} \left(\frac{v_{l,\infty}}{v_{v,s}} \right)^{-1/2} \times \left(\frac{h_{fg} \mu_{v,s} (W_{xv,s} \eta_{v\delta} - 4W_{yv,s}) + \lambda_{v,s} (T_w - T_s) \left(\frac{d\theta_v}{d\eta_v} \right)_{\eta_v=\eta_{v\delta}}}{\lambda_{l,s} (T_s - T_\infty)} \right)$
$\theta_v = 0, \quad \theta_l = 1$	
$\eta_l \rightarrow \infty :$	$W_{x,l} \rightarrow 0, \quad \theta_l \rightarrow 0$
<i>Equations on treatment of variable physical properties for vapor film</i>	
For variable physical properties	
Equations with temperature parameter method $\frac{\mu_{v,w}}{\mu_{v,s}} = \left(\frac{T_w}{T_s} \right)^{n_\mu}$	
$\frac{\lambda_{v,w}}{\lambda_{v,s}} = \left(\frac{T_w}{T_s} \right)^{n_\lambda}$	
$\frac{\rho_{v,w}}{\rho_{v,s}} = \left(\frac{T_w}{T_s} \right)^{-1}$	

Term	Expression
Equations of physical property factors	$\frac{v_{i,w}}{v_{i,\infty}} = \left(\frac{T_w}{T_s}\right)^{n_{i,w}+1}$ $\frac{1}{\rho_i} \frac{d\rho_i}{d\eta_i} = -\frac{(T_w/T_s-1)d\theta_{i,w}/d\eta_i}{(T_w/T_s-1)\theta_{i,w}+1}$ $\frac{1}{\mu_i} \frac{d\mu_i}{d\eta_i} = \frac{n_{i,w}(T_w/T_s-1)d\theta_{i,w}/d\eta_i}{(T_w/T_s-1)\theta_{i,w}+1}$ $\frac{1}{\lambda_i} \frac{d\lambda_i}{d\eta_i} = \frac{n_{i,\lambda}(T_w/T_s-1)d\theta_{i,w}/d\eta_i}{(T_w/T_s-1)\theta_{i,w}+1}$ $\frac{\mu_{i,\infty}}{\mu_i} = [(T_w/T_s - 1)\theta_{i,w} + 1]^{-n_{i,\mu}}$ $\frac{v_{i,\infty}}{v_i} = [(T_w/T_s - 1)\theta_{i,w} + 1]^{-n_{i,w}+1}$
<i>Equations on treatment of variable physical properties for liquid film</i>	<p>Equations with polynomial approach for water</p> $\rho_l = -4.48 \times 10^{-3}t_l^2 + 999.9$ $\lambda_l = -8.01 \times 10^{-6}t_l^2 + 1.94 \times 10^{-3}t_l + 0.563$ $\mu_l = \exp\left[-1.6 - \frac{1150}{T_l} + \left(\frac{690}{T_l}\right)^2\right] \times 10^{-3}$
Equations of physical property factors	<p>Equations of physical property factors for water</p> $\frac{1}{\rho_l} \frac{d\rho_l}{d\eta_l} = \frac{(-2 \times 4.48 \times 10^{-3}t_l)(6_s - t_{\infty}) \frac{d\theta_l}{d\eta_l}}{(-4.48 \times 10^{-3}t_l^2 + 999.9)}$ $\frac{1}{\mu_l} \frac{d\mu_l}{d\eta_l} = \left(\frac{1.150}{T_l^2} - 2 \times \frac{690^2}{T_l^3}\right)(t_s - t_{\infty}) \frac{d\theta_l}{d\eta_l}$ $\frac{1}{\rho_l} \frac{d\rho_l}{d\eta_l} = \frac{-2 \times 4.48 \times 10^{-3}t_l(6_s - t_{\infty}) \frac{d\theta_l}{d\eta_l}}{-4.48 \times 10^{-3}t_l^2 + 999.9}$ $\frac{1}{\mu_l} \frac{d\mu_l}{d\eta_l} = \left(\frac{1.150}{T_l^2} - 2 \times \frac{690^2}{T_l^3}\right)(t_s - t_{\infty}) \frac{d\theta_l}{d\eta_l}$ $\frac{1}{\lambda_l} \frac{d\lambda_l}{d\eta_l} = \frac{(-2 \times 8.01 \times 10^{-6}t_l + 1.94 \times 10^{-3})(6_s - t_{\infty}) \frac{d\theta_l}{d\eta_l}}{-8.01 \times 10^{-6}t_l^2 + 1.94 \times 10^{-3}t_l + 0.563}$ $\frac{v_{l,s}}{v_l} = \frac{\mu_{l,s}}{\mu_l} \frac{\rho_l}{\rho_{l,s}} = \exp\left[1.150\left(\frac{1}{T_l} - \frac{1}{T_s}\right) + 690^2\left(\frac{1}{T_s} - \frac{1}{T_l}\right)\right] \frac{-4.48 \times 10^{-3}t_l^2 + 999.9}{-4.48 \times 10^{-3}t_l^2 + 999.9}$ $\text{Pr}_{l,s} = \frac{\rho_l}{\rho_{l,s}} \frac{\lambda_{l,s}}{\lambda_l} = \text{Pr}_{l,s} \left(\frac{-4.48 \times 10^{-3}t_l^2 + 999.9}{-4.48 \times 10^{-3}t_l^2 + 999.9}\right) \left(\frac{-8.01 \times 10^{-6}t_l^2 + 1.94 \times 10^{-3}t_l + 0.563}{-8.01 \times 10^{-6}t_l^2 + 1.94 \times 10^{-3}t_l + 0.563}\right)$

Table 13.3 Summary of equations on boiling heat and mass transfer of the laminar free film boiling of liquid

Theoretical equations on boiling heat transfer

$$q_x, \text{ defined as } -\lambda_{v,w} \left(\frac{\partial T}{\partial y} \right)_{y=0}$$

$$\alpha_x, \text{ defined as } q_x = \alpha_x (t_w - t_s)$$

$$Nu_{x,w}, \text{ defined as } \frac{\alpha_x x}{\lambda_{v,w}}$$

$$Q_x, \text{ defined as } Q_x = \int_A \int q_x dA \int_0^x q_x dx$$

$$\bar{Q}_x, \text{ defined as } \bar{Q}_x = Q_x / (b \times x)$$

$$\bar{\alpha}_x, \text{ defined as } \bar{\alpha}_x = \bar{Q}_x / (t_w - t_s)$$

$$\bar{Nu}_{x,w}, \text{ defined as } \frac{\bar{\alpha}_x x}{\lambda_{v,w}}$$

Wall dimensionless temperature gradient (for the laminar film boiling of water)

Prediction equation

$$-\lambda_{v,w} (T_w - T_s) \left(\frac{1}{4} Gr_{xv,s} \right)^{1/4} x^{-1} \left(\frac{d\theta_v}{d\eta_v} \right)_{\eta_v=0}$$

$$-\lambda_{v,w} \left(\frac{1}{4} Gr_{xv,s} \right)^{1/4} x^{-1} \left(\frac{d\theta_v}{d\eta_v} \right)_{\eta_v=0}$$

$$-\left(\frac{1}{4} Gr_{xv,s} \right)^{1/4} \left(\frac{d\theta_v}{d\eta_v} \right)_{\eta_v=0}$$

$$-\frac{4}{3} \lambda_{v,w} (T_w - T_\infty) \left(\frac{1}{4} Gr_{xv,s} \right)^{1/4} \left(\frac{d\theta_v}{d\eta_v} \right)_{\eta_v=0}$$

$$-\frac{4}{3} x^{-1} \lambda_w (T_w - T_\infty) \left(\frac{1}{4} Gr_{xv,s} \right)^{1/4} \left(-\frac{d\theta}{d\eta} \right)_{\eta_v=0}$$

$$-\frac{4}{3} \lambda_{v,w} \left(\frac{1}{4} Gr_{xv,s} \right)^{1/4} x^{-1} \left(\frac{d\theta_v}{d\eta_v} \right)_{\eta_v=0}$$

$$-\frac{4}{3} \left(\frac{1}{4} Gr_{xv,s} \right)^{1/4} \left(\frac{d\theta_v}{d\eta_v} \right)_{\eta_v=0}$$

$$\left(-\frac{d\theta_v}{d\eta_v} \right)_{\eta_v=0} = A \left(\frac{\Delta t_w}{t_s} \right)^B \quad (2.77 \leq \frac{\Delta t_w}{t_s} \leq 8.27)$$

$$A = 25.375 \left(\frac{\Delta t_\infty}{t_s} \right)^2 + 7.2275 \left(\frac{\Delta t_\infty}{t_s} \right) + 1.2993 \quad (0 \leq \frac{\Delta t_\infty}{t_s} \leq 0.3)$$

$$A = -6.7567 \left(\frac{\Delta t_\infty}{t_s} \right)^2 + 21.563 \left(\frac{\Delta t_\infty}{t_s} \right) - 0.1131 \quad (0.3 < \frac{\Delta t_\infty}{t_s} \leq 1)$$

$$B = 2.2117 \left(\frac{\Delta t_\infty}{t_s} \right)^2 - 2.3472 \left(\frac{\Delta t_\infty}{t_s} \right) - 0.843 \quad (0 \leq \frac{\Delta t_\infty}{t_s} \leq 0.3)$$

$$B = 0.3585 \left(\frac{\Delta t_\infty}{t_s} \right)^2 - 0.6057 \frac{\Delta t_\infty}{t_s} - 1.2017 \quad (0.3 < \frac{\Delta t_\infty}{t_s} \leq 1)$$

While,

$$\left(-\frac{d\theta_v}{d\eta_v} \right)_{\eta_v=0} \Big|_{\Delta t=0} = 1.2993 \left(\frac{\Delta t_w}{t_s} \right)^{-0.843} \quad (2.77 \leq \frac{\Delta t_w}{t_s} \leq 8.27)$$

(continued)

Table 13.3 (continued)

Theoretical equation on boiling mass transfer

g_x defined as

$$g_x = \rho_{v,s} \left(w_{xv,s} \frac{d\delta}{dx} - w_{yv,s} \right)_s$$

G_x , defined as $G_x = \int_A (g_x) dA$

Mass flow rate parameter

Φ_s definition

$$\Phi_s = (\eta_{v\delta} W_{xv,s} - 4W_{yv,s})$$

For the laminar film boiling of saturated water $\Phi_s = -0.002 \left(\frac{\Delta t_w}{t_s} \right)^2 + 0.0635 \frac{\Delta t_w}{t_s} + 0.0705$

Practical prediction equation on boiling mass transfer (for the laminar film boiling of saturated water)

$$G_x = \frac{4}{3} b \cdot \mu_{v,s} \left(\frac{1}{4} Gr_{xv,s} \right)^{1/4} \left[-0.002 \left(\frac{\Delta t_w}{t_s} \right)^2 + 0.0635 \frac{\Delta t_w}{t_s} + 0.0705 \right]$$

Dimensionless vapor film thickness

$$\eta_{v\delta}, \text{ defined as } \left(\frac{1}{4} Gr_{xv,s} \right)^{1/4} \frac{\delta y}{x}$$

For the laminar free film boiling of saturated water $0.291 \frac{\Delta t_w}{t_s} + 0.631$

13.9 Remarks

Through the theoretical analysis of heat and mass transfer of laminar free convection film boiling of liquid, it is found that heat transfer of laminar free film boiling is proportional to wall temperature gradients $\left(\frac{d\theta_w}{d\eta_v}\right)_{\eta_v=0}$, the only one no-given variable for prediction of heat transfer of the film boiling. The wall temperature gradients $-\left(\frac{d\theta_w}{d\eta_v}\right)_{\eta_v=0}$ and heat transfer of the film boiling will decrease with increasing the wall superheated grade $\frac{\Delta t_w}{t_s}$, and increase with increasing the bulk subcooled grade $\frac{\Delta t_\infty}{t_s}$. Additionally, the wall temperature gradient $\left(\frac{d\theta_w}{d\eta_v}\right)_{\eta_v=0}$ and heat transfer of the film boiling are steeper with higher liquid bulk subcooled grade $\frac{\Delta t_\infty}{t_s}$ and with lower wall superheated grade $\frac{\Delta t_w}{t_s}$. The curve-fit equation for evaluation of the temperature gradient $\left(-\frac{d\theta_w}{d\eta_v}\right)_{\eta_v=0}$ introduced in this chapter agrees very well with the related rigorous numerical solutions, and then useful for a reliable prediction of heat transfer of the laminar film boiling of water.

The vapor film thickness $\eta_{v\delta}$ will increase with increasing wall superheated grade $\frac{\Delta t_w}{t_s}$ or with decreasing the water bulk subcooled grade $\frac{\Delta t_\infty}{t_s}$. In the iterative calculation of the film boiling problem, it is a key work to correctly determine suitable value η_l . The solutions of the governing models are converged in very rigorous values of $\eta_{v\delta}$ as shown in Table 13.1 and Fig. 13.2, otherwise the convergence solutions will not be obtained.

The interfacial velocity component $W_{xv,s}$ will increase with increasing the wall superheated grade $\frac{\Delta t_w}{t_s}$ except the case for very low liquid bulk subcooled grade $\frac{\Delta t_\infty}{t_s}$. Meanwhile, the interfacial velocity component $W_{xv,s}$ will decrease with increasing the liquid bulk subcooled grade $\frac{\Delta t_\infty}{t_s}$.

The interfacial velocity component $-W_{yv,s}$ will increase with increasing the wall superheated grade Δt_w , and will decrease obviously with increasing the liquid subcooled grade $\frac{\Delta t_\infty}{t_s}$. In addition, the interfacial velocity component $W_{yv,s}$ will decrease slower and slower with increasing the liquid subcooled grade $\frac{\Delta t_\infty}{t_s}$. The value of the interfacial velocity component $-W_{xv,s}$ is usually much larger than that of the interfacial velocity component $W_{xv,s}$ usually. Then, it follows that $-W_{yv,s}$ will dominate the interfacial mass flow rate in general. However, the effect of the interfacial velocity component $W_{xv,s}$ on the interfacial mass flow rate can never be ignored.

The boiling mass flow rate is proportional to the induced mass flow rate parameter which is the only one no-given variable for prediction of the mass flow rate. The mass flow rate parameter will increase with increasing the wall superheated grade Δt_w , decrease obviously with increasing the liquid subcooled grade $\frac{\Delta t_\infty}{t_s}$, and decrease slower and slower with increasing the liquid subcooled grade $\frac{\Delta t_\infty}{t_s}$.

The effects of the wall superheated grade $\frac{\Delta t_w}{t_s}$ and liquid bulk subcooled grade $\frac{\Delta t_\infty}{t_s}$ on the momentum, heat, and mass transfer presented here also reveal effects

of variable physical properties of both vapor and liquid film on the film boiling of liquid.

13.10 Calculation Examples

Example 1: A flat plate 0.3 m in width and 0.3 m in length is suspended vertically in water. The plate temperature $t_w = 577^\circ\text{C}$, and the water temperature is $t_\infty = t_s = 100^\circ\text{C}$. Assume that the boiling is the laminar film boiling, please calculate

- (i) boiling heat and mass transfer of the plate,
- (ii) vapor film thicknesses at $x = 0, 0.01, 0.05, 0.1, 0.15, 0.2,$ and 0.3 m

Solution:

The wall superheated grade is $\frac{\Delta t_w}{t_s} = \frac{t_w - t_s}{t_s} = \frac{577 - 100}{100} = 4.77$, and the water bulk subcooled grade is $\frac{\Delta t_\infty}{t_s} = \frac{t_s - t_\infty}{t_s} = \frac{100 - 100}{100} = 0$, which shows that it is the film boiling of saturated water. For water saturated physical properties at $t_s = 100^\circ\text{C}$ we obtain $\rho_{l,s} = 958.4 \text{ kg/m}^3$, and for saturated water vapor at 100°C , we obtain $\nu_{v,s} = 20.55 \times 10^{-6} \text{ m}^2/\text{s}$, $\rho_{v,s} = 0.5974 \text{ kg/m}^3$, and $\mu_{v,s} = 12.28 \times 10^{-6} \text{ kg/(ms)}$. In addition, for water vapor at the wall temperature $t_w = 577^\circ\text{C}$ we obtain $\rho_{v,w} = 0.2579 \text{ kg/m}^3$ and $\lambda_{v,w} = 0.0637 \text{ kg/m}^3$.

- (i) Calculate the condensate heat and mass transfer

For heat transfer

With Eq. (12.15) the local Grashof number is evaluated as

$$\begin{aligned} Gr_{xv,s} &= \frac{g(\rho_{l,\infty}/\rho_{v,w} - 1)x^3}{\nu_{v,s}^2} \\ &= \frac{9.8 \times (958.4/0.2579 - 1) \times 0.3^3}{(20.55 \times 10^{-6})^2} \\ &= 2.3278 \times 10^{12} \end{aligned}$$

With Eq. (13.9), the dimensionless temperature gradient of the film boiling of saturated liquid is evaluated as

$$\left(\left(-\frac{d\theta_v}{d\eta_v} \right)_{\eta_v=0} \right)_{\Delta t=0} = 1.2993 \left(\frac{\Delta t_w}{t_s} \right)^{-0.843} = 1.2993 \times 4.77^{-0.843} = 0.3481$$

With Eq. (13.3), the local Nusselt number is evaluated as

$$\begin{aligned}
 Nu_{xv,w} &= - \left(\frac{1}{4} Gr_{xv,s} \right)^{1/4} \left(\left(\frac{d\theta}{d\eta} \right)_{\eta=0} \right)_{\Delta t_{\infty}=0} \\
 &= \left(\frac{1}{4} \times 2.3278 \times 10^{12} \right)^{1/4} \times 0.3481 \\
 &= 304.036
 \end{aligned}$$

The mean Nusselt number is evaluated as

$$\overline{Nu}_{xv,w} = \frac{\alpha_x x}{\lambda_{v,w}} = \frac{4}{3} \times 304.036 = 405.38$$

With definition of the mean Nusselt number, the mean heat transfer coefficient is evaluated as

$$\overline{\alpha}_x = \overline{Nu}_{xv,w} = \frac{\lambda_{v,w}}{x} = 405.38 \times 0.0637/0.3 = 86.076 \text{ W/(m K)}$$

With Newtonian cooling law, the total heat transfer rate of plate at the plate temperature $t_w = 577^\circ\text{C}$ is calculated as follows:

$$\begin{aligned}
 Q_x &= \overline{\alpha}_x (t_w - t_s) A \\
 &= \overline{\alpha}_x (t_w - t_s) \times b \times x \\
 &= 86.076 \times (577 - 100) \times 0.3 \times 0.3 \\
 &= 3,695 \text{ W}
 \end{aligned}$$

For mass flow rate of the boiling

With Eq. (13.15), the mass flow rate parameter $\Phi_s (\eta_{v\delta} W_{xv,s} - 4W_{yv,s})$ of film boiling of saturated water at $t_s = 100^\circ\text{C}$ can be evaluated as

$$\begin{aligned}
 \Phi_s &= \eta_{v\delta} W_{xv,s} - 4W_{yv,s} \\
 &= -0.002 \left(\frac{\Delta t_w}{t_s} \right)^2 + 0.0635 \frac{\Delta t_w}{t_s} + 0.0705 \\
 &= -0.002 \times 4.77^2 + 0.0635 \times 4.77 + 0.0705 \\
 &= 0.327889
 \end{aligned}$$

Then, the total mass flow rate entering the boiled vapor film through the area with width of b and with length from $x = 0$ to x for the film boiling is

$$\begin{aligned}
 G_x &= \frac{4}{3} b \cdot \mu_{v,s} \left(\frac{1}{4} Gr_{xv,s} \right)^{1/4} \Phi_s \\
 &= \frac{4}{3} \times 0.3 \times 12.28 \times 10^{-6} \times \left(\frac{1}{4} \times 2.3278 \times 10^{12} \right)^{1/4} \times 0.327889 \\
 &= 0.001407 \text{ kg/s} \\
 &= 5.0652 \text{ kg/h}
 \end{aligned}$$

(ii) Calculate the vapor film thicknesses

For the laminar film boiling of saturated water, Eq. (13.14) is taken to evaluate η_{δ} as

$$\begin{aligned}
 \eta_{v\delta} &= 0.291 \frac{\Delta t_w}{t_s} + 0.631 \\
 &= 0.291 \times 4.77 + 0.631 \\
 &= 2.01907
 \end{aligned}$$

From Eq. (10.14), the condensate film thickness δ_v is expressed as

$$\begin{aligned}
 \delta_v &= \eta_{\delta_v} x \left(\frac{1}{4} Gr_{xv,s} \right)^{-1/4} \\
 &= \eta_{\delta_v} x \left(\frac{1}{4} \frac{g(\rho_{l,s}/\rho_{v,w} - 1)x^3}{\nu_{v,s}^2} \right)^{-1/4} \\
 &= \eta_{\delta_v} \left(\frac{1}{4} \frac{g(\rho_{l,s}/\rho_{v,w} - 1)}{\nu_{v,s}^2} \right)^{-1/4} x^{1/4} \\
 &= 2.01907 \times \left(\frac{1}{4} \times \frac{9.81 \times (958.4/0.2579 - 1)}{(20.55 \times 10^{-6})^2} \right)^{-1/4} \times x^{1/4} \\
 &= 0.00093707 \times x^{1/4}
 \end{aligned}$$

$$\text{For } x = 0, \quad \delta_v = 0 \text{ m}$$

$$\text{For } x = 0.01 \text{ m, } \delta_v = 0.00093707 \times 0.05^{1/4} = 0.000296 \text{ m}$$

$$\text{For } x = 0.05 \text{ m, } \delta_v = 0.00093707 \times 0.01^{1/4} = 0.000443 \text{ m}$$

$$\text{For } x = 0.1 \text{ m, } \delta_v = 0.00093707 \times 0.1^{1/4} = 0.0005268 \text{ m}$$

$$\text{For } x = 0.15 \text{ m, } \delta_v = 0.00093707 \times 0.15^{1/4} = 0.000583 \text{ m}$$

$$\text{For } x = 0.2 \text{ m, } \delta_v = 0.00093707 \times 0.2^{1/4} = 0.000627 \text{ m}$$

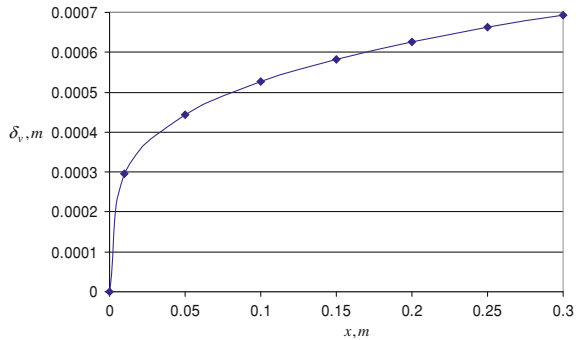
$$\text{For } x = 0.25 \text{ m, } \delta_v = 0.00093707 \times 0.25^{1/4} = 0.000663 \text{ m}$$

$$\text{For } x = 0.3 \text{ m, } \delta_v = 0.00093707 \times 0.3^{1/4} = 0.000694 \text{ m}$$

Table 13.4 The variation of condensate film thickness y with the position x

x (m)	0	0.01	0.05	0.1	0.15	0.2	0.25	0.3
δ_v (m)	0	0.000296	0.000443	0.0005268	0.000583	0.000627	0.000663	0.000694

Fig. 13.6 The variation of condensate film thickness δ_v with the position x



For clear expression, the variation of condensate film thickness y with the position x is listed and plotted as the Table 13.4 and Fig. 13.6.

Example 2: A flat plate with 0.3 m in width and 0.3 m in length is suspended vertically in water. The plate temperature is kept at $t_w = 577^\circ\text{C}$. The water bulk temperature is $t_\infty = 90^\circ\text{C}$. Assume the steady laminar film boiling occurs on the plates. Calculate the heat transfer and mass flow rate of the film boiling.

Solutions:

The wall superheated grade is $\frac{\Delta t_w}{t_s} = \frac{t_w - t_s}{t_s} = \frac{577 - 100}{100} = 4.77$, and the water bulk subcooled grade is $\frac{\Delta t_\infty}{t_s} = \frac{t_s - t_\infty}{t_s} = \frac{100 - 90}{100} = 0.1$.

The related physical properties are water saturated density $\rho_{l,s} = 958.4\text{kg/m}^3$ at $t_s = 100^\circ\text{C}$, saturated water vapor kinetic $\nu_{v,s} = 20.55 \times 10^{-6}\text{m}^2/\text{s}$, density $\rho_{v,s} = 0.5974\text{kg/m}^3$ and absolute viscosity $\mu_{v,s} = 12.28 \times 10^{-6}$ at $t_s = 100^\circ\text{C}$, water vapor density $\rho_{v,w} = 0.2579\text{kg/m}^3$ and thermal conductivity $\lambda_{v,w} = 0.0637\text{W}/(\text{m K})$ at $t_w = 577^\circ\text{C}$, and subcooled water density $\rho_{l,\infty} = 965.3\text{kg/m}^3$ at $t_\infty = 90^\circ\text{C}$.

1. For heat transfer

With Eq. (13.8) the temperature gradient of the film boiling of subcooled water vapor is evaluated as

$$-\left(\frac{d\theta_v}{d\eta_v}\right)_{\eta_v=0} = A \left(\frac{\Delta t_w}{t_s}\right)^B \quad (2.77 \leq \frac{\Delta t_w}{t_s} \leq 8.27) \quad (13.8)$$

$$A = 25.375 \left(\frac{\Delta t_{\infty}}{t_s} \right)^2 + 7.2275 \left(\frac{\Delta t_{\infty}}{t_s} \right) + 1.2993 \quad \left(0 \leq \frac{\Delta t_{\infty}}{t_s} \leq 0.3 \right)$$

$$A = -6.7567 \left(\frac{\Delta t_{\infty}}{t_s} \right)^2 + 21.563 \left(\frac{\Delta t_{\infty}}{t_s} \right) - 0.1131 \quad \left(0.3 < \frac{\Delta t_{\infty}}{t_s} \leq 1 \right)$$

$$B = 2.2117 \left(\frac{\Delta t_{\infty}}{t_s} \right)^2 - 2.3472 \left(\frac{\Delta t_{\infty}}{t_s} \right) - 0.843 \quad \left(0 \leq \frac{\Delta t_{\infty}}{t_s} \leq 0.3 \right)$$

$$B = 0.3585 \left(\frac{\Delta t_{\infty}}{t_s} \right)^2 - 0.6057 \frac{\Delta t_{\infty}}{t_s} - 1.2017 \quad \left(0.3 < \frac{\Delta t_{\infty}}{t_s} \leq 1 \right)$$

Since $\frac{\Delta t_{\infty}}{t_s} = 0.1 < 0.3$

The following formulae and calculations for the coefficients A, B, and C are available:

$$A = 25.375 \left(\frac{\Delta t_{\infty}}{t_s} \right)^2 + 7.2275 \left(\frac{\Delta t_{\infty}}{t_s} \right) + 1.2993 \quad \left(0 \leq \frac{\Delta t_{\infty}}{t_s} \leq 0.3 \right)$$

$$B = 2.2117 \left(\frac{\Delta t_{\infty}}{t_s} \right)^2 - 2.3472 \left(\frac{\Delta t_{\infty}}{t_s} \right) - 0.843 \quad \left(0 \leq \frac{\Delta t_{\infty}}{t_s} \leq 0.3 \right)$$

$$\begin{aligned} A &= 25.375 \left(\frac{\Delta t_{\infty}}{t_s} \right)^2 + 7.2275 \left(\frac{\Delta t_{\infty}}{t_s} \right) + 1.2993 \\ &= 25.375 \times (0.1)^2 + 7.2275 \times (0.1) + 1.2993 \\ &= 2.2758 \end{aligned}$$

$$\begin{aligned} B &= 2.2117 \left(\frac{\Delta t_{\infty}}{t_s} \right)^2 - 2.3472 \left(\frac{\Delta t_{\infty}}{t_s} \right) - 0.843 \\ &= 2.2117 \times (0.1)^2 - 2.3472 \times (0.1) - 0.843 \\ &= -1.0556 \end{aligned}$$

Then,

$$-\left(\frac{d\theta_v}{d\eta_v} \right)_{\eta_v=0} = A \left(\frac{\Delta t_w}{t_s} \right)^B = 2.2758 \times 4.77^{-1.0556} = 0.437411$$

With Eq.(11.15) local Grashof number $Gr_{xv,s}$ is evaluated as

$$\begin{aligned}
 Gr_{xv,s} &= \frac{g(\rho_{l,\infty}/\rho_{v,w} - 1)x^3}{\nu_{v,s}^2} \\
 &= \frac{9.8(965.3/0.2579 - 1) \times 0.3^3}{(20.55 \times 10^{-6})^2} \\
 &= 2.34456 \times 10^{12}
 \end{aligned}$$

With Eq. (13.14) the local Nusselt number is evaluated as

$$\begin{aligned}
 Nu_{xv,w} &= - \left(\frac{1}{4} Gr_{xv,s} \right)^{1/4} \left(\frac{d\theta_v}{d\eta_v} \right)_{\eta_v=0} \\
 &= \left(\frac{1}{4} \times 2.34456 \times 10^{12} \right)^{1/4} \times 0.437411 \\
 &= 382.73
 \end{aligned}$$

According to the definition of the local Nusselt number, $Nu_{xv,w} = \frac{\alpha_x x}{\lambda_{v,w}}$, then

$$\begin{aligned}
 \alpha_x &= \frac{Nu_{xv,w} \lambda_{v,w}}{x} \\
 &= \frac{382.73 \times 0.0637}{0.3} \\
 &= 81.266 \text{ W}/(\text{m}^2 \text{ K})
 \end{aligned}$$

At last, average heat transfer coefficient $\bar{\alpha}_x$ and total heat transfer rate Q_x of the film boiling on the plate are calculated

$$\begin{aligned}
 \bar{\alpha}_x &= \frac{4}{3} \alpha_x \\
 &= \frac{4}{3} \times 81.266 \\
 &= 108.35 \text{ W}/(\text{m}^2 \text{ K}) \\
 Q_x &= \bar{\alpha}_x (t_w - t_s) A \\
 &= 108.35 \times (577 - 100) \times 0.3 \times 0.3 \\
 &= 4651.47 \text{ W}
 \end{aligned}$$

2. For mass flow rate of the boiling

The total mass flow rate of the film boiling of water is expressed as

$$G_x = \frac{4}{3} b \cdot \mu_{v,s} \left(\frac{1}{4} Gr_{xv,s} \right)^{1/4} \Phi_s$$

From Table 13.1, the related mass flow rate parameter $\Phi_s = (\eta_{v\delta} W_{xv,s} - 4W_{yv,s})$ is obtained as 0.16399 for $\frac{\Delta t_w}{t_s} = 4.77$ and $\frac{\Delta t_\infty}{t_s} = 0.1$.

Then,

$$\begin{aligned} G_x &= \frac{4}{3} b \cdot \mu_{v,s} \left(\frac{1}{4} Gr_{xv,s} \right)^{1/4} \Phi_s \\ &= \frac{4}{3} \times 0.3 \times 12.28 \times 10^{-6} \times \left(\frac{1}{4} \times 2.34456 \times 10^{12} \right)^{1/4} \times 0.16399 \\ &= 0.000705 \text{ kg/s} \\ &= 2.537 \text{ kg/h} \end{aligned}$$

13.11 Exercises

1. Please give a detailed derivation for the theoretical Eqs.(13.1)–(13.7) on heat transfer analysis of laminar free convection film boiling of liquid.
2. Please tell me the effect of the wall superheated grade on the boiling heat and mass transfer of laminar free convection film boiling of liquid, and explain the reason.
3. Please tell me the effect of the bulk subcooled grade on the boiling heat and mass transfer of laminar free convection film boiling of liquid, and explain the reason.
4. Please tell me effect of which grade (wall superheated or bulk subcooled grade) is stronger on laminar free convection film boiling of liquid.
5. Please explain why Eqs. (13.1*)–(13.7*) are able to be recommended for practical prediction of heat transfer of laminar free convection film boiling of liquid on an isothermal vertical flat plate?
6. Please explain why Eq. (13.14*) is able to be recommended for practical prediction of condensate mass transfer of laminar free convection film boiling of liquid on an isothermal vertical flat plate?

References

1. D.Y. Shang, L.C. Zhong, B.X. Wang, in *Study of Film Boiling of Water with Variable Thermophysical Properties Along a Vertical Plate, Transfer Phenomena*, ed. by B.X. Wang. Science and Technology (Higher Education Press, Beijing, 1992), pp. 427–432
2. L.C. Zhong, D.Y. Shang, B.X. Wang, Effect of variable thermophysical properties on film boiling of liquid. *J. Northeast. Univ.* **15**(88), 6–11 (1994)
3. D.Y. Shang, B.X. Wang, L.C. Zhong, A study on laminar film boiling of liquid along an isothermal vertical plates in a pool with consideration of variable thermophysical properties. *Int. J. Heat Mass Transfer* **37**(5), 819–828 (1994)

Chapter 14

Complete Mathematical Model of Laminar Free Convection Film Condensation of Pure Vapour

Abstract In this chapter, the work is focused on constitution of mathematical models of the laminar free convection film condensation of superheated vapor, while, the film condensation of saturated vapor is only regarded as its special case. The new similarity analysis method is successfully applied for similarity transformation of the governing partial differential equations of laminar free convection film condensation of superheated vapor with consideration of coupled effects of variable physical properties of liquid and vapor films. In the transformed governing ordinary differential equations, the dimensionless velocity components of liquid and vapor films have definite physical meanings, and then the solutions of the governing models can be understood easily. In the analysis and similarity transformation of the mathematical models, the interfacial balance equations between the liquid and vapor films are considered in detail, such as mass flow rate balance, velocity component balance, shear force balance, temperature balance, and energy balance. Therefore, such mathematical model is serious theoretically and has its application value in practice.

14.1 Introduction

It was Nusselt [1] who first treated the laminar free convection film condensation of saturated steam on a vertical isothermal flat plate. His theory was based on the assumption that the inertia and thermal convection of condensate film, the vapor drag due to the shear force at the liquid–vapor interface, the dependence of the physical properties of the condensate medium on temperature, and the effect of the liquid–vapour interfacial wave are neglected. Bromley [2] and Rohsenow [3] first investigated the effects of thermal convection. Later on, the study of Sparrow and Gregg [4] included also the effects of thermal convection and inertia forces in the liquid film by using the boundary layer analysis, and Koh et al. [5] further solved numerically a boundary-layer model for both the condensate and vapor films. Chen

[6] has considered analytically the effect of thermal convection, the inertia, and the interfacial shear force.

On the basis of previous studies on the independent-temperature physical properties Drew [7], Labuntsov [8] made relatively simple modifications for variable thermophysical properties. Then, Poots and Miles [9] studied the effects of variable thermophysical properties on laminar free convection film condensation of saturated steam on a vertical flat plate. They simplified the governing equations of the liquid and vapor phases by neglecting the effects of surface tension at the liquid–vapor interface, and obtained solutions of the ordinary differential equations. Stinnesbeck and Herwig [10] provided an asymptotic analysis of laminar free convection film condensation on a vertical flat plate including variable property effect. Nevertheless, the results obtained do not allow heat and mass transfer prediction, probably due to the difficulty of getting a solution.

Actually, a lot of related phenomena are the film condensation of superheated vapor. Then, the study on heat and mass transfer of this problem has a strong practical background. Minkowycz and Sparrow reported their study results for film condensation heat transfer with consideration of superheated vapor [11]. Their work showed that superheated temperature brings about only a slight increase in the heat transfer during the condensation of a pure vapor. They also indicated that for a given degree of superheating, q/q_{Nu} is almost independent on Δt_w . Anyway, study of the condensation of superheated vapor is scarcely found in the literature. Then, there is lack of a theoretical development for prediction of heat transfer of the film condensation, and especially, the theoretical study of the effect of the vapor superheated temperature on the condensate mass transfer did not appear in the common literature. The reason is that it is difficult to study the two-phase boundary layer problem, because the traditional theoretical methods, such as Falkner–Skan transformation for the similarity transformation of the governing partial differential equations and for treatment of variable thermophysical properties are not suitable for the successive studies.

In this book, Chaps. 14–17 will be used to present the extensive study results of Shang, Wang, etc. [12–14] for film condensation free convection of vapor with consideration of various physical factors including variable thermophysical properties. Meanwhile, following the previous chapters, the velocity component method is further applied for a novel similarity transformation of the governing partial equations of the two-phase boundary layers, and the advanced approach presented in the previous chapters for treatment of variable thermophysical properties of the medium in condensate and vapor films is used. Then, the mathematical models are presented for description of the laminar free convection film condensation of vapor. The mathematical models with three-point boundary value problem are further solved with different wall subcooled and vapor superheated grades. According to the numerical results, the effects of wall subcooled and vapor superheated grades on velocity and temperature fields as well as heat and mass transfer of laminar free film condensation of superheated vapor is further clarified. On these bases, theoretically rigorous and practically simple formulae are obtained for prediction of heat transfer and mass flow rate of the film condensation of water.

At first, in this chapter the detailed mathematical model on extended theory of steady-state laminar free convection film condensation process of vapor on an isothermal vertical flat plate is established. Its equations provide a complete account of the physical process for consideration of various physical factors including variable thermophysical properties. It will be taken as a foundation of the study on the laminar film condensation of vapor for the following chapters.

14.2 Governing Partial Differential Equations

The analytical model and coordinating system used for the laminar free convection film condensation of superheated vapor on a vertical flat plate is shown in Fig. 14.1. An isothermal vertical flat plate is suspended in a large volume of quiescent pure superheated vapor at atmospheric pressure. The plate temperature is t_w , the saturation temperature of the vapor is t_s , and the ambient temperature is t_∞ . If the provided condition for the model is $t_w < t_s$, a steady two-dimensional film condensation will occur on the plate. We assume that laminar flow within the liquid and vapor phases is induced by gravity, and take into account the various physical factors including shear force between the condensate and vapor films, as well as variable thermophysical properties, and the inertia force and thermal convection of the medium in the condensate and vapor films. Then the conservation governing partial differential equations of mass, momentum, and energy for steady laminar condensation in two-phase boundary layer are as follows:

For condensate liquid film

$$\frac{\partial}{\partial x} (\rho_l w_{x1}) + \frac{\partial}{\partial y} (\rho_l w_{y1}) = 0 \quad (14.1)$$

$$\rho_l \left(w_{x1} \frac{\partial w_{x1}}{\partial x} + w_{y1} \frac{\partial w_{x1}}{\partial y} \right) = \frac{\partial}{\partial y} \left(\mu_l \frac{\partial w_{x1}}{\partial y} \right) + g (\rho_l - \rho_{v,\infty}) \quad (14.2)$$

$$\rho_l c_{pl} \left(w_{x1} \frac{\partial t_1}{\partial x} + w_{y1} \frac{\partial t_1}{\partial y} \right) = \frac{\partial}{\partial y} \left(\lambda_l \frac{\partial t_1}{\partial y} \right) \quad (14.3)$$

where Eqs. (14.1)–(14.3) are mass, momentum, and energy equations of liquid film.

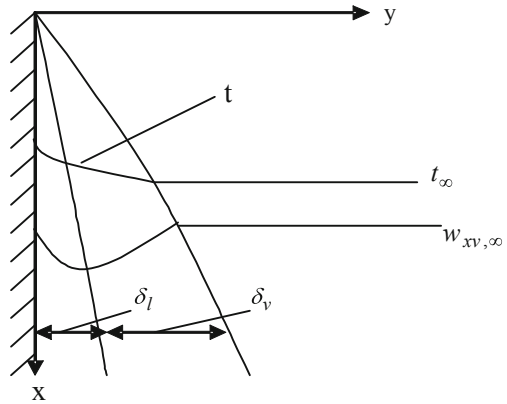
For vapor film

$$\frac{\partial}{\partial x} (\rho_v w_{xv}) + \frac{\partial}{\partial y} (\rho_v w_{yv}) = 0 \quad (14.4)$$

$$\rho_v \left(w_{xv} \frac{\partial w_{xv}}{\partial x} + w_{yv} \frac{\partial w_{xv}}{\partial y} \right) = \frac{\partial}{\partial y} \left(\mu_v \frac{\partial w_{xv}}{\partial y} \right) + g (\rho_v - \rho_{v,\infty}) \quad (14.5)$$

$$\rho_v c_{pv} \left(w_{xv} \frac{\partial T_v}{\partial x} + w_{yv} \frac{\partial T_v}{\partial y} \right) = \frac{\partial}{\partial y} \left(\lambda_v \frac{\partial T_v}{\partial y} \right) \quad (14.6)$$

Fig. 14.1 Physical model and coordinate system of laminar free convection film condensation of superheated vapor



where Eqs. (14.4)–(14.6) are mass, momentum, and energy equations of vaporid film.

The boundary conditions are

$$y = 0: w_{xl} = 0, w_{yl} = 0, t_l = t_w \tag{14.7}$$

$$y = \delta_l:$$

$$w_{xl,s} = w_{xv,s} \tag{14.8}$$

$$\rho_{l,s} \left(w_{xl} \frac{\partial \delta_{xl}}{\partial x} - w_{yl} \right)_s = \rho_{v,s} \left(w_{xv} \frac{\partial \delta_{xv}}{\partial x} - w_{yv} \right)_s \tag{14.9}$$

$$\mu_{l,s} \left(\frac{\partial w_{xl}}{\partial y} \right)_s = \mu_{v,s} \left(\frac{\partial w_{xv}}{\partial y} \right)_s \tag{14.10}$$

$$\lambda_{l,s} \left(\frac{\partial t_l}{\partial y} \right)_{y=\delta_l} = h_{fg} \rho_{v,s} \left(w_{xv} \frac{\partial \delta_v}{\partial x} - w_{yv} \right)_s + \lambda_{v,s} \left(\frac{\partial t_v}{\partial y} \right)_{y=\delta_l} \tag{14.11}$$

$$T = T_s \tag{14.12}$$

$$y \rightarrow \infty : w_{xv} = 0, T_v \rightarrow T_\infty \tag{14.13}$$

where Eqs. (14.8)–(14.12) express the physical matching conditions such as velocity, local mass flux, shear force, heat flux, and temperature balances at the *liquid–vapor interface* respectively. While, Eqs. (14.7) and (14.13) express the related conditions at the wall and bulk respectively.

In order to conveniently solve the governing equations in a suitable dimensionless form, it is necessary to transform similarly the governing partial differential equations and the boundary conditions into their dimensionless forms. We still use the new

similarity analysis method to carry out this transformation. At first, we introduce the similarity variables as follows:

14.3 Similarity Variables

Due to the two-phase boundary layer there should be two sets of the transformation variables, the transformation variables for vapor and liquid films.

For liquid film

For liquid film the dimensionless coordinate variable η_l and the local Grashof number $Gr_{x,l,s}$ are set up at first as follows:

$$\eta_l = \left(\frac{1}{4} Gr_{x,l,s} \right)^{1/4} \frac{y}{x}$$

and

$$Gr_{x,l,s} = \frac{g(\rho_{l,w} - \rho_{v,\infty})x^3}{\nu_{l,s}^2 \rho_{l,s}}. \quad (14.14)$$

Dimensionless temperature is assumed as

$$\theta_l = \frac{t_l - t_s}{t_w - t_s}. \quad (14.15)$$

The dimensionless velocity components are given as

$$W_{x,l} = \left(2\sqrt{gx} \left(\frac{\rho_{l,w} - \rho_{v,\infty}}{\rho_{l,s}} \right)^{1/2} \right)^{-1} w_{x,l} \quad (14.16)$$

$$W_{y,l} = \left(2\sqrt{gx} \left(\frac{\rho_{l,w} - \rho_{v,\infty}}{\rho_{l,s}} \right)^{1/2} \left(\frac{1}{4} Gr_{x,l,s} \right)^{-4} \right)^{-1} w_{y,l}. \quad (14.17)$$

For vapor film

For vapor film, the dimensionless coordinate variable η_v and the local Grashof number $Gr_{x,v,\infty}$ are assumed as respectively

$$\eta_v = \left(\frac{1}{4} Gr_{x,v,\infty} \right)^{1/4} \frac{y}{x} \quad (14.18)$$

$$Gr_{x,v,\infty} = \frac{g(\rho_{v,s}/\rho_{v,\infty} - 1)x^3}{\nu_{v,\infty}^2}. \quad (14.19)$$

The dimensionless temperature is defined as

$$\theta_v = \frac{T_v - T_\infty}{T_s - T_\infty}. \quad (14.20)$$

The dimensionless velocity components are assumed as

$$W_{xv} = \left(2\sqrt{gx} (\rho_{v,s}/\rho_{v,\infty} - 1)^{1/2}\right)^{-1} w_{xv} \quad (14.21)$$

$$W_{yv} = \left(2\sqrt{gx} (\rho_{v,s}/\rho_{v,\infty} - 1)^{1/2} \left(\frac{1}{4}\text{Gr}_{xv,\infty}\right)^{-1/4}\right)^{-1} w_{yv}. \quad (14.22)$$

14.4 Governing Ordinary Differential Equations

Consulting the derivations in Chap. 11 for laminar free convection film boiling of subcooled liquid and by means of the above equations of the similarity variables, the governing partial differential equations Eqs. (14.1)–(14.6) and their boundary condition equations (14.7)–(14.13) for laminar free convection film condensation of superheated vapor can be equivalent transformed into the following governing ordinary differential equations, respectively (see the transformation in Appendix A and B):

For liquid film

$$2W_{x1} - \eta_1 \frac{dW_{x1}}{d\eta_1} + 4 \frac{dW_{y1}}{d\eta_1} - \frac{1}{\rho_1} \frac{d\rho_1}{d\eta_1} (\eta_1 W_{x1} - 4W_{y1}) = 0 \quad (14.23)$$

$$\begin{aligned} & \frac{\nu_{1,s}}{\nu_1} \left(W_{x1} \left(2W_{x1} - \eta_1 \frac{dW_{x1}}{d\eta_1} \right) + 4W_{y1} \frac{dW_{x1}}{d\eta_1} \right) \\ & = \frac{d^2 W_{x1}}{d\eta_1^2} + \frac{1}{\mu_1} \frac{d\mu_1}{d\eta_1} \frac{dW_{x1}}{d\eta_1} + \frac{\mu_{1,s}}{\mu_1} \frac{\rho_1 - \rho_{v,\infty}}{\rho_{1,w} - \rho_{v,\infty}} \end{aligned} \quad (14.24)$$

$$Pr_1 \frac{\nu_{1,s}}{\nu_1} [-W_{x1}\eta_1 + 4W_{y1}] \frac{d\theta_1}{d\eta_1} = \frac{d^2 \theta_1}{d\eta_1^2} + \frac{1}{\lambda_1} \frac{d\lambda_1}{d\eta_1} \frac{d\theta_1}{d\eta_1} \quad (14.25)$$

where Eqs. (14.23)–(14.25) respectively express the mass, momentum, and energy equations of liquid film.

For vapor film

$$2W_{xv} - \eta_v \frac{dW_{xv}}{d\eta_v} + 4 \frac{dW_{yv}}{d\eta_v} - \frac{1}{\rho_v} \frac{d\rho_v}{d\eta_v} (\eta_v W_{xv} - 4W_{yv}) = 0 \quad (14.26)$$

$$\begin{aligned} & \frac{\nu_{v,\infty}}{\nu_v} \left(W_{xv} \left(2W_{xv} - \eta_v \frac{dW_{xv}}{d\eta_v} \right) + 4W_{yv} \left(\frac{dW_{xv}}{d\eta_v} \right) \right) \\ &= \frac{d^2 W_{xv}}{d\eta_v^2} + \frac{1}{\mu_v} \frac{d\mu_v}{d\eta_v} \frac{dW_{xv}}{d\eta_v} + \frac{\mu_{v,\infty}}{\mu_v} \frac{\rho_v - \rho_{v,\infty}}{\rho_{v,s} - \rho_{v,\infty}} \end{aligned} \quad (14.27)$$

$$\text{Pr}_v \frac{\nu_{v,\infty}}{\nu_v} (-\eta_v W_{xv} + 4W_{yv}) \frac{d\theta_v}{d\eta_1} = \frac{1}{\lambda_v} \frac{d\lambda_v}{d\eta} \frac{d\theta_v}{d\eta_v} + \frac{d^2 \theta_v}{d\eta_v^2} \quad (14.28)$$

where Eqs. (14.26)–(14.28) respectively express the mass, momentum, and energy equations of vapor film.

For Boundary conditions:

By means of the above equations of the similarity variables, the boundary condition equations are transformed into the following dimensionless ones respectively:

$$\eta_1 = 0 : W_{x1} = 0, W_{y1} = 0, \theta_1 = 1 \quad (14.29)$$

$$W_{xv,s} = \left(\frac{\rho_{1,w} - \rho_{v,\infty}}{\rho_{1,s}} \right)^{1/2} \left(\frac{\rho_{v,s} - \rho_{v,\infty}}{\rho_{v,\infty}} \right)^{-1/2} W_{x1,s} \quad (14.30)$$

$$\begin{aligned} w_{yv} &= -\frac{1}{4} \frac{\rho_{1,s}}{\rho_{v,s}} \left(\frac{\nu_{1,s}}{\nu_{v,\infty}} \right)^{1/2} \left(\frac{\rho_{1,w} - \rho_{v,\infty}}{\rho_{1,s}} \right)^{1/4} \\ &\times (\rho_{v,s}/\rho_{v,\infty} - 1)^{-1/4} [W_{x1}\eta_{1\delta} - 4W_{y1}] \end{aligned} \quad (14.31)$$

$$\begin{aligned} \left(\frac{dW_{xv}}{d\eta_v} \right)_{\eta_v=0} &= \frac{\mu_{1,s}}{\mu_{v,s}} \left(\frac{\nu_{v,\infty}}{\nu_{1,s}} \right)^{1/2} \left(\frac{\rho_{1,w} - \rho_{v,\infty}}{\rho_{1,s}} \right)^{3/4} \\ &\times \left(\frac{\rho_{v,s}}{\rho_{v,\infty}} - 1 \right)^{-3/4} \left(\frac{dW_{x1}}{d\eta_1} \right)_{\eta_1=\eta_{1,\delta}} \end{aligned} \quad (14.32)$$

$$\begin{aligned} & \left(\frac{d\theta_v}{d\eta_v} \right)_{\eta_v=\eta_{v\delta}} \\ &= \frac{\lambda_{1,s} (t_w - t_s) \left(\frac{\nu_{v,\infty}}{\nu_{1,s}} \right)^{1/2} \left(\frac{\rho_{1,w} - \rho_{v,\infty}}{\rho_{1,s}} \right)^{1/4} (\rho_{v,s}/\rho_{v,\infty} - 1)^{-1/4} \left(\frac{d\theta_1}{d\eta_1} \right)_{\eta_1=\eta_{1\delta}} + 4h_{fg} \rho_{v,s} \nu_{v,\infty} W_{yv,s}}{\lambda_{v,s} (T_s - T_\infty)} \end{aligned} \quad (14.33)$$

$$\theta_1 = 0, \theta_v = 1 \quad (14.34)$$

$$\eta_v \rightarrow \infty : W_{xv} \rightarrow \theta, \theta_v \rightarrow 0. \quad (14.35)$$

Equations (14.30)–(14.34) express the physical matching conditions such as velocity, local mass flux, shear force, heat flux, and temperature balances at the vapor–liquid interface respectively. While, Eqs. (14.29) and (14.35) express the related conditions at the wall and bulk respectively.

14.5 Identical Governing Equations on Laminar Free Film Condensation of Saturated or Superheated Vapor

In fact, the laminar free convection film condensation of saturated vapor with the superheated temperature $\Delta t_\infty = t_\infty - t_s = 0$ can be regarded as a special case of that of superheated vapor. Therefore, the above mathematical model of the laminar free film condensation of superheated vapor is completely suitable for that of saturated vapor, if the following simplifications are done:

- (i) The energy equation of vapour film is omitted. Then, its related dimensionless form is ignored.
- (ii) The defined dimensionless temperature variable for vapor film is omitted.
- (iii) The vapor film heat conduction in the interfacial boundary condition is ignored.

Strictly speaking, the defined similarity variable $Gr_{xv,\infty}$ in (14.19) should be zero for the film condensation of saturated vapor, since the liquid density $\rho_{l,\infty}$ at t_∞ is equal to $\rho_{l,s}$ at t_s in this case. If so, it will never be possible to do all the above similarity transformations of the governing equations. For solving this problem, the temperature t_∞ can be regarded very close to t_s , so that the value of $\rho_{v,\infty}$ is very close to the value of $\rho_{v,s}$. For example, if the temperature relative deviation $(t_\infty - t_s)/t_s$ is less than an arbitrary small number ε , the film condensation of superheated vapor will be very close to that of saturated vapor. Such arbitrary number ε can be found out by using an asymptotic approach.

The advantage of the above treatment is that the mathematical models of the laminar free film condensation of superheated and saturated vapor become identical.

14.6 Remarks

The new similarity analysis method is successfully applied for similarity transformation of the governing partial differential equations of laminar free convection film condensation of superheated vapor with consideration of coupled effects of variable physical properties of liquid and vapor films. In the transformed governing ordinary differential equations, the dimensionless velocity components of liquid and vapor films have definite physical meanings, and then the solutions of the models can be understood easily. The new similarity analysis method is appropriate for the treatment of the three-point value problem.

In the analysis and similarity transformation of the mathematical models, the interfacial balance equations between the liquid and vapor films are considered in detail, such as mass flow rate balance, velocity component balance, shear force balance, temperature balance, and energy balance. Therefore, such a mathematical model is serious theoretically and has its application value in practice.

In this chapter, our work is focused on constitution of mathematical models of the laminar free convection film condensation of superheated vapor, while, the film

condensation of saturated vapor is only regarded as its special case. Thus, the mathematical models of the laminar free convection film condensation of superheated and saturated vapors become identical.

14.7 Exercises

1. Which boundary conditions are considered at the liquid–vapor interface of laminar free convection film condensation of pure vapor?
2. Please compare the governing mathematical models between the laminar film boiling and condensation, and find out their differences.
3. Please compare the interfacial boundary condition equations between the laminar free convection film boiling and condensation, and find out their differences.
4. Please compare the dimensionless similarity variables between the laminar free convection film boiling and condensation, and point out their differences.
5. Based on the governing partial differential equations of laminar free convection film condensation of superheated vapour, please give the corresponding equations of saturated vapor.
6. Please explain the identical governing system of mathematical model laminar free convection film condensation of superheated and saturated vapor.

Appendix A: Similarity Transformation for Governing Ordinary Differential Equations

A1. For liquid film

Transformation of Eq. (14.1):

At first, Eq. (14.1) is rewritten as

$$\rho_l \left(\frac{\partial w_{x1}}{\partial x} + \frac{\partial w_{y1}}{\partial y} \right) + w_{x1} \frac{\partial \rho_l}{\partial x} + w_{y1} \frac{\partial \rho_l}{\partial y} = 0. \quad (\text{A.1})$$

With Eqs. (14.14), (14.15) and (14.16) we can obtain the following correlations:

$$\frac{\partial w_{x1}}{\partial x} = \sqrt{\frac{g}{x}} \left(\frac{\rho_{l,w} - \rho_{v,\infty}}{\rho_{l,s}} \right)^{1/2} \left(W_{x1} - \frac{1}{2} \eta_1 \frac{dW_{x1}}{d\eta_1} \right) \quad (\text{A.2})$$

$$\frac{\partial w_{y1}}{\partial y} = 2 \sqrt{\frac{g}{x}} \left(\frac{\rho_{l,w} - \rho_{v,\infty}}{\rho_{l,s}} \right)^{1/2} \frac{dW_{y1}}{d\eta_1} \quad (\text{A.3})$$

$$\frac{\partial \rho_l}{\partial x} = -\frac{1}{4} \eta_1 x^{-1} \frac{d\rho_l}{d\eta_1} \quad (\text{A.4})$$

$$\frac{\partial \rho_l}{\partial y} = \frac{d\rho_l}{d\eta_1} \left(\frac{1}{4} \text{Gr}_{x1,s} \right)^{1/4} x^{-1}. \quad (\text{A.5})$$

With Eqs. (14.16), (14.17) and (A.2)–(A.5), Eq. (A.1) is changed to

$$\begin{aligned} \rho_l \left(\sqrt{\frac{g}{x}} \left(\frac{\rho_{l,w} - \rho_{v,\infty}}{\rho_{l,s}} \right)^{1/2} \left(W_{x1} - \frac{1}{2} \eta_l \frac{dW_{x1}}{d\eta_l} \right) + 2 \sqrt{\frac{g}{x}} \left(\frac{\rho_{l,w} - \rho_{v,\infty}}{\rho_{l,s}} \right)^{1/2} \frac{dW_{y1}}{d\eta_l} \right) \\ + 2 \sqrt{gx} \left(\frac{\rho_{l,w} - \rho_{v,\infty}}{\rho_{l,s}} \right)^{1/2} W_{x1} \left(-\frac{1}{4} \eta_l x^{-1} \frac{d\rho_l}{d\eta_l} \right) \\ + 2 \sqrt{gx} \left(\frac{\rho_{l,w} - \rho_{v,\infty}}{\rho_{l,s}} \right)^{1/2} \left(\frac{1}{4} Gr_{x1,s} \right)^{-1/4} W_{y1} \frac{d\rho_l}{d\eta_l} \left(\frac{1}{4} Gr_{x1,s} \right)^{1/4} x^{-1} = 0. \end{aligned}$$

The above equation is divided by $\left(\frac{\rho_{l,w} - \rho_{v,\infty}}{\rho_{l,s}} \right)^{1/2} \sqrt{\frac{g}{x}}$ and is simplified to

$$2W_{x1} - \eta_l \frac{dW_{x1}}{d\eta_l} + 4 \frac{dW_{y1}}{d\eta_l} - \frac{1}{\rho_l} \frac{d\rho_l}{d\eta_l} (\eta_l W_{x1} - 4W_{y1}) = 0. \quad (14.23)$$

Transformation of Eq. (14.2):

Equation (14.2) is rewritten as

$$\rho_l \left(w_{x1} \frac{\partial w_{x1}}{\partial x} + w_{y1} \frac{\partial w_{x1}}{\partial y} \right) = \frac{\partial \mu_1}{\partial y} \frac{\partial w_{x1}}{\partial y} + \mu_1 \frac{\partial^2 w_{x1}}{\partial y^2} + g (\rho_l - \rho_{v,\infty}). \quad (A.6)$$

With the dimensionless transformation variables assumed in Eqs. (14.14), (14.15) and (14.16) we get

$$\frac{\partial w_{x1}}{\partial y} = 2 \sqrt{gx} \left(\frac{\rho_{l,w} - \rho_{v,\infty}}{\rho_{l,s}} \right)^{1/2} \frac{dW_{x1}}{d\eta_l} x^{-1} \left(\frac{1}{4} Gr_{x1,s} \right)^{1/4} \quad (A.7)$$

$$\begin{aligned} \frac{\partial^2 w_{x1}}{\partial y^2} &= 2 \sqrt{gx} \left(\frac{\rho_{l,w} - \rho_{v,\infty}}{\rho_{l,s}} \right)^{1/2} \frac{d^2 W_{x1}}{d\eta_l^2} x^{-1} \left(\frac{1}{4} Gr_{x1,s} \right)^{1/4} \left(\frac{1}{4} Gr_{x1,s} \right)^{1/4} x^{-1} \\ &= 2 \sqrt{gx} \left(\frac{\rho_{l,w} - \rho_{v,\infty}}{\rho_{l,s}} \right)^{1/2} \frac{d^2 W_{x1}}{d\eta_l^2} \left(\frac{1}{4} Gr_{x1,s} \right)^{1/2} x^{-2} \end{aligned} \quad (A.8)$$

$$\frac{\partial \mu_1}{\partial y} = \frac{d\mu_1}{d\eta_l} \left(\frac{1}{4} Gr_{x1,s} \right)^{1/4} x^{-1}. \quad (A.9)$$

With Eqs. (A.7)–(A.9), Eq. (A.6) is changed to

$$\begin{aligned} \rho_l \left(2 \sqrt{gx} \left(\frac{\rho_{l,w} - \rho_{v,\infty}}{\rho_{l,s}} \right)^{1/2} W_{x1} \sqrt{\frac{g}{x}} \left(\frac{\rho_{l,w} - \rho_{v,\infty}}{\rho_{l,s}} \right)^{1/2} \right. \\ \times \left(W_{x1} - \frac{1}{2} \eta_l \frac{dW_{x1}}{d\eta_l} \right) + 2 \sqrt{gx} \left(\frac{\rho_{l,w} - \rho_{v,\infty}}{\rho_{l,s}} \right)^{1/2} \left(\frac{1}{4} Gr_{x1,s} \right)^{-1/4} \\ \times W_{y1} 2 \sqrt{gx} \left(\frac{\rho_{l,w} - \rho_{v,\infty}}{\rho_{l,s}} \right)^{1/2} \frac{dW_{x1}}{d\eta_l} x^{-1} \left(\frac{1}{4} Gr_{x1,s} \right)^{1/4} \left. \right) \end{aligned}$$

$$\begin{aligned}
 &= \frac{d\mu_1}{d\eta_1} \left(\frac{1}{4}\text{Gr}_{x1,s}\right)^{1/4} x^{-1} 2\sqrt{gx} \left(\frac{\rho_{1,w} - \rho_{v,\infty}}{\rho_{1,s}}\right)^{1/2} \frac{dW_{x1}}{d\eta_1} x^{-1} \left(\frac{1}{4}\text{Gr}_{x1,s}\right)^{1/4} \\
 &\quad + \mu_1 2\sqrt{gx} \left(\frac{\rho_{1,w} - \rho_{v,\infty}}{\rho_{1,s}}\right)^{1/2} \frac{d^2W_{x1}}{d\eta_1^2} \left(\frac{1}{4}\text{Gr}_{x1,s}\right)^{1/2} x^{-2} + g(\rho_1 - \rho_{v,\infty}).
 \end{aligned}$$

The above equation is divided by $g\left(\frac{\rho_{1,w} - \rho_{v,\infty}}{\rho_{1,s}}\right)$ and further simplified to the following one by using the definition of $\text{Gr}_{xv,s}$:

$$\begin{aligned}
 \rho_1 \left(2W_{x1} \left(W_{x1} - \frac{1}{2}\eta_1 \frac{dW_{x1}}{d\eta_1} \right) + 2W_{y1} 2 \frac{dW_{x1}}{d\eta_1} \right) &= \frac{d\mu_1}{d\eta_1} \left(\frac{1}{4} \frac{1}{v_{1,s}^2} \right)^{1/2} 2 \frac{dW_{x1}}{d\eta_1} \\
 + \mu_1 2 \frac{d^2W_{x1}}{d\eta_1^2} \left(\frac{1}{4} \frac{1}{v_{1,s}^2} \right)^{1/2} &+ \rho_{1,s} \frac{\rho_1 - \rho_{v,\infty}}{\rho_{1,w} - \rho_{v,\infty}}.
 \end{aligned}$$

The above equation is multiplied by $\frac{v_{1,s}}{\mu_1}$ and simplified to

$$\begin{aligned}
 \frac{v_{1,s}}{v_1} \left(W_{x1} \left(2W_{x1} - \eta_1 \frac{dW_{x1}}{d\eta_1} \right) + 4W_{y1} \frac{dW_{x1}}{d\eta_1} \right) \\
 = \frac{d^2W_{x1}}{d\eta_1^2} + \frac{1}{\mu_1} \frac{d\mu_1}{d\eta_1} \frac{dW_{x1}}{d\eta_1} + \frac{\mu_{1,s}}{\mu_1} \frac{\rho_1 - \rho_{v,\infty}}{\rho_{1,w} - \rho_{v,\infty}}.
 \end{aligned} \tag{14.24}$$

Transformation of Eq. (14.3):

Equation (14.3) is first rewritten as

$$\rho_1 c_{p1} \left(w_{x1} \frac{\partial t_1}{\partial x} + w_{y1} \frac{\partial t_1}{\partial y} \right) = \lambda_1 \frac{\partial^2 t_1}{\partial y^2} + \frac{\partial \lambda_1}{\partial y} \frac{\partial t_1}{\partial y} \tag{A.10}$$

where

$$t_1 = (t_w - t_s) \theta_1 + t_s \tag{A.11}$$

$$\frac{\partial t_1}{\partial x} = -(t_w - t_s) \frac{d\theta_1}{d\eta_1} \left(\frac{1}{4}\right) \eta_1 x^{-1} \tag{A.12}$$

$$\frac{\partial t_1}{\partial y} = (t_w - t_s) \frac{d\theta_1}{d\eta_1} \left(\frac{1}{4}\text{Gr}_{x1,s}\right)^{1/4} x^{-1} \tag{A.13}$$

$$\frac{\partial^2 t_1}{\partial y^2} = (t_w - t_s) \frac{d^2\theta_1}{d\eta_1^2} \left(\frac{1}{4}\text{Gr}_{x1,s}\right)^{1/2} x^{-2} \tag{A.14}$$

$$\frac{\partial \lambda_1}{\partial y} = \frac{d\lambda_1}{d\eta_1} \left(\frac{1}{4}\text{Gr}_{x1,s}\right)^{1/4} x^{-1}. \tag{A.15}$$

With Eqs. (14.16), (14.17) and (A.11)–(A.14), Eq. (A.10) will become

$$\begin{aligned}
& \rho_1 c_{p1} \left(2\sqrt{gx} \left(\frac{\rho_{1,w} - \rho_{v,\infty}}{\rho_{1,s}} \right)^{1/2} W_{x1} \left(-(t_w - t_s) \frac{d\theta_1}{d\eta_1} \left(\frac{1}{4} \right) \eta_1 x^{-1} \right) \right. \\
& \quad \left. + 2\sqrt{gx} \left(\frac{\rho_{1,w} - \rho_{v,\infty}}{\rho_{1,s}} \right)^{1/2} \left(\frac{1}{4} \text{Gr}_{x1,s}^{-1/4} \right) W_{y1} (t_w - t_s) \frac{d\theta_1}{d\eta_1} \left(\frac{1}{4} \text{Gr}_{x1,s} \right)^{1/4} x^{-1} \right) \\
& = \lambda_1 (t_w - t_s) \frac{d^2\theta_1}{d\eta_1^2} \left(\frac{1}{4} \text{Gr}_{x1,s} \right)^{1/2} x^{-2} + \frac{d\lambda_1}{d\eta_1} \left(\frac{1}{4} \text{Gr}_{x1,s} \right)^{1/4} x^{-1} \\
& \quad \times (t_w - t_s) \frac{d\theta_1}{d\eta_1} \left(\frac{1}{4} \text{Gr}_{x1,s} \right)^{-1/4} x^{-1}.
\end{aligned}$$

The above equation is divided by $(t_w - t_s)$, and is expressed as follows by using the definition of local Grashof number $\text{Gr}_{x1,s}$:

$$\begin{aligned}
& \rho_1 c_{p1} \left(2\sqrt{gx} \left(\frac{\rho_{1,w} - \rho_{v,\infty}}{\rho_{1,s}} \right)^{1/2} W_{x1} \left(-\frac{d\theta_1}{d\eta_1} \left(\frac{1}{4} \right) \eta_1 x^{-1} \right) \right. \\
& \quad \left. + 2\sqrt{gx} \left(\frac{\rho_{1,w} - \rho_{v,\infty}}{\rho_{1,s}} \right)^{1/2} W_{y1} \frac{d\theta_1}{d\eta_1} x^{-1} \right) \\
& = \lambda_1 \frac{d^2\theta_1}{d\eta_1^2} \left(\frac{1}{4} \frac{g (\rho_{1,w} - \rho_{v,\infty}) x^3}{\nu_{1,s}^2 \rho_{1,s}} \right)^{1/2} x^{-2} \\
& \quad + \frac{d\lambda_1}{d\eta_1} \left(\frac{1}{4} \frac{g (\rho_{1,w} - \rho_{v,\infty}) x^3}{\nu_{1,s}^2 \rho_{1,s}} \right)^{1/2} x^{-1} \frac{d\theta_1}{d\eta_1} x^{-1}.
\end{aligned}$$

The above equation is divided by $\sqrt{\frac{g}{x} \left(\frac{\rho_{1,w} - \rho_{v,\infty}}{\rho_{1,s}} \right)^{1/2}}$, and simplified to the following one

$$\rho_1 c_{p1} \left(W_{x1} \left(-\frac{d\theta_1}{d\eta_1} \eta_1 \right) + 4W_{y1} \frac{d\theta_1}{d\eta_1} \right) = \lambda_1 \frac{d^2\theta_1}{d\eta_1^2} \left(\frac{1}{\nu_{1,s}^2} \right)^{1/2} + \frac{d\lambda_1}{d\eta_1} \left(\frac{1}{\nu_{1,s}^2} \right)^{1/2} \frac{d\theta_1}{d\eta_1}.$$

The above equation is multiplied by $\frac{\nu_{1,s}}{\lambda_1}$, and simplified to

$$\frac{\rho_1 c_{p1}}{\lambda_1} \nu_{1,s} \left(W_{x1} \left(-\frac{d\theta_1}{d\eta_1} \eta_1 \right) + 4W_{y1} \frac{d\theta_1}{d\eta_1} \right) = \frac{d^2\theta_1}{d\eta_1^2} + \frac{1}{\lambda_1} \frac{d\lambda_1}{d\eta_1} \frac{d\theta_1}{d\eta_1}$$

i.e.

$$\text{Pr}_1 \frac{\nu_{1,s}}{\nu_1} [-W_{x1}\eta_1 + 4W_{y1}] \frac{d\theta_1}{d\eta_1} = \frac{d^2\theta_1}{d\eta_1^2} + \frac{1}{\lambda_1} \frac{d\lambda_1}{d\eta_1} \frac{d\theta_1}{d\eta_1}. \quad (14.25)$$

In addition, from the analysis in Chap. 6, it is known that the physical factor $\text{Pr}_1 \frac{\nu_{1,s}}{\nu_1}$ in

A2. For vapor film

Transformation of Eq. (14.4):

Equation (14.4) is rewritten as

$$\rho_v \left(\frac{\partial w_{xv}}{\partial x} + \frac{\partial w_{yv}}{\partial y} \right) + w_{xv} \frac{\partial \rho_v}{\partial x} + w_{yv} \frac{\partial \rho_v}{\partial y} = 0. \quad (\text{A.16})$$

With the similarity variables assumed in Eqs. (14.18), (14.19), (14.21) and (14.22) we can obtain the following correlations:

$$\frac{\partial w_{xv}}{\partial x} = \sqrt{\frac{g}{x}} (\rho_{v,s}/\rho_{v,\infty} - 1)^{1/2} \left(W_{xv} - \frac{1}{2} \eta_v \frac{dW_{xv}}{d\eta} \right) \quad (\text{A.17})$$

$$\frac{\partial w_{yv}}{\partial y} = 2 \sqrt{\frac{g}{x}} (\rho_{v,s}/\rho_{v,\infty} - 1)^{1/2} \frac{dW_{yv}}{d\eta_v} \quad (\text{A.18})$$

$$\frac{\partial \rho_v}{\partial x} = -\frac{1}{4} \eta_v x^{-1} \frac{d\rho_v}{d\eta_v} \quad (\text{A.19})$$

$$\frac{\partial \rho_v}{\partial y} = \frac{d\rho_v}{d\eta_v} \left(\frac{1}{4} \text{Gr}_{xv,s} \right)^{1/4} x^{-1}. \quad (\text{A.20})$$

With equations (A.17)–(A.20), (A.16) can be changed into

$$\begin{aligned} & \rho_v \left(\sqrt{\frac{g}{x}} (\rho_{v,s}/\rho_{v,\infty} - 1)^{1/2} \left(W_{xv} - \frac{1}{2} \eta_v \frac{dW_{xv}}{d\eta} \right) \right. \\ & \quad \left. + 2 \sqrt{\frac{g}{x}} (\rho_{v,s}/\rho_{v,\infty} - 1)^{1/2} \left(\frac{dW_{yv}}{d\eta_v} \right) \right) \\ & \quad + 2 \sqrt{gx} (\rho_{v,s}/\rho_{v,\infty} - 1)^{1/2} w_{xv} \left(-\frac{1}{4} \eta_v x^{-1} \frac{d\rho_v}{d\eta_v} \right) \\ & \quad + 2 \sqrt{gx} (\rho_{v,s}/\rho_{v,\infty} - 1)^{1/2} \left(\frac{1}{4} \text{Gr}_{xv,s} \right)^{-1/4} \\ & \quad \times w_{yv} \frac{d\rho_v}{d\eta_v} \left(\frac{1}{4} \text{Gr}_{xv,s} \right)^{1/4} x^{-1} = 0. \end{aligned}$$

The above equation is divided by $\sqrt{\frac{g}{x}} (\rho_{v,s}/\rho_{v,\infty} - 1)^{1/2}$ and is further simplified to

$$2W_{xv} - \eta_v \frac{dW_{xv}}{d\eta} + 4 \frac{dW_{yv}}{d\eta_v} - \frac{1}{\rho_v} \frac{d\rho_v}{d\eta_v} (\eta_v w_{xv} - 4w_{yv}) = 0. \quad (\text{14.26})$$

Transformation of Eq. (14.5):

Equation (14.5) is rewritten as

$$\rho_v \left(w_{xv} \frac{\partial w_{xv}}{\partial x} + w_{yv} \frac{\partial w_{xv}}{\partial y} \right) = \mu_v \frac{\partial^2 w_{xv}}{\partial y^2} + \frac{\partial w_{xv}}{\partial y} \frac{\partial \mu_v}{\partial y} + g (\rho_v - \rho_{v,\infty}). \quad (\text{A.21})$$

With the similarity variables assumed in Eqs. (14.18), (14.19), (14.21) and (14.22) we can obtain the following correlations:

$$\frac{\partial w_{xv}}{\partial y} = 2\sqrt{gx} (\rho_{v,s}/\rho_{v,\infty} - 1)^{1/2} \frac{dW_{xv}}{d\eta_v} x^{-1} \left(\frac{1}{4} \text{Gr}_{xv,\infty} \right)^{1/4} \quad (\text{A.22})$$

$$\begin{aligned} \frac{\partial^2 w_{xv}}{\partial y^2} &= 2\sqrt{gx} (\rho_{v,s}/\rho_{v,\infty} - 1)^{1/2} \frac{d^2 W_{xv}}{d\eta_v^2} x^{-1} \left(\frac{1}{4} \text{Gr}_{xv,\infty} \right)^{1/4} \left(\frac{1}{4} \text{Gr}_{xv,\infty} \right)^{1/4} x^{-1} \\ &= 2\sqrt{gx} (\rho_{v,s}/\rho_{v,\infty} - 1)^{1/2} \frac{d^2 W_{xv}}{d\eta_v^2} \left(\frac{1}{4} \text{Gr}_{xv,\infty} \right)_{1/2} x^{-2} \end{aligned} \quad (\text{A.23})$$

$$\frac{\partial \mu_v}{\partial y} = \frac{d\mu_v}{d\eta_v} \left(\frac{1}{4} \text{Gr}_{xv,\infty} \right)^{1/4} x^{-1}. \quad (\text{A.24})$$

With Eqs. (A.22)–(A.24), (14.18), (14.19), (14.21) and (14.22), Eq. (A.21) becomes

$$\begin{aligned} &\rho_v \left(2\sqrt{gx} (\rho_{v,s}/\rho_{v,\infty} - 1)^{1/2} W_{xv} \sqrt{\frac{g}{x}} (\rho_{v,s}/\rho_{v,\infty} - 1)^{1/2} \left(W_{xv} - \frac{1}{2} \eta_v \frac{dW_{xv}}{d\eta} \right) \right. \\ &\quad \left. + 2\sqrt{gx} (\rho_{v,s}/\rho_{v,\infty} - 1)^{1/2} \left(\frac{1}{4} \text{Gr}_{xv,\infty} \right)^{-1/4} W_{yv} 2\sqrt{gx} (\rho_{v,s}/\rho_{v,\infty} - 1)^{1/2} \right. \\ &\quad \left. \times \frac{dW_{xv}}{d\eta_v} x^{-1} \left(\frac{1}{4} \text{Gr}_{xv,\infty} \right)^{1/4} \right) \\ &= \mu_v 2\sqrt{gx} (\rho_{v,s}/\rho_{v,\infty} - 1)^{1/2} \frac{d^2 W_{xv}}{d\eta_v^2} \left(\frac{1}{4} \text{Gr}_{xv,\infty} \right)_{1/2} x^{-2} \\ &\quad + 2\sqrt{gx} (\rho_{v,s}/\rho_{v,\infty} - 1)^{1/2} \frac{dW_{xv}}{d\eta_v} x^{-1} \left(\frac{1}{4} \text{Gr}_{xv,\infty} \right)^{1/4} \\ &\quad \times \frac{d\mu_v}{d\eta_v} \left(\frac{1}{4} \text{Gr}_{xv,\infty} \right)^{1/4} x^{-1} + g (\rho_v - \rho_{v,\infty}). \end{aligned}$$

The above equation is divided by $(\rho_{v,s}/\rho_{v,\infty} - 1)^{1/2}$, and simplified to the following one by using the definition of $\text{Gr}_{xv,\infty}$:

$$\begin{aligned} \rho_v \left(W_{xv} \left(2W_{xv} - \eta_v \frac{dW_{xv}}{d\eta} \right) + 4W_{yv} \frac{dW_{xv}}{d\eta_v} \right) &= \mu_v \frac{d^2 W_{xv}}{d\eta_v^2} \left(\frac{1}{v_{v,\infty}^2} \right)^{1/2} \\ &+ \frac{dW_{xv}}{d\eta_v} \left(\frac{1}{v_{v,\infty}^2} \right)^{1/2} \frac{d\mu_v}{d\eta_v} + \rho_{v,\infty} \frac{\rho_v - \rho_{v,\infty}}{\rho_{v,s} - \rho_{v,\infty}}. \end{aligned}$$

The above equation is multiplied by $\frac{v_{v,\infty}}{v_v} \frac{1}{\rho_v}$, and simplified to

$$\begin{aligned} \frac{v_{v,\infty}}{v_v} \left(W_{xv} \left(2W_{xv} - \eta_v \frac{dW_{xv}}{d\eta_v} \right) + 4W_{yv} \left(\frac{dW_{xv}}{d\eta_v} \right) \right) \\ = \frac{d^2 W_{xv}}{d\eta_v^2} + \frac{1}{\mu_v} \frac{d\mu_v}{d\eta_v} \frac{dW_{xv}}{d\eta_v} + \frac{\mu_{v,\infty}}{\mu_v} \frac{\rho_v - \rho_{v,\infty}}{\rho_{v,s} - \rho_{v,\infty}}. \end{aligned} \quad (14.27)$$

Transformation of Eq. (14.6):

Equation (14.6) is rewritten as

$$\rho_v c_{pv} \left(w_{xv} \frac{\partial T_v}{\partial x} + w_{yv} \frac{\partial T_v}{\partial y} \right) = \frac{\partial \lambda_v}{\partial y} \frac{\partial T_v}{\partial y} + \lambda_v \frac{\partial^2 T_v}{\partial y^2}. \quad (A.25)$$

With the similarity variables assumed in Eqs. (14.18)–(14.22) the following correlations are produced:

$$T_v = (T_s - T_\infty) \theta_1 + T_\infty \quad (A.26)$$

$$\frac{\partial T_v}{\partial x} = -(T_s - T_\infty) \frac{d\theta_v}{d\eta_v} \left(\frac{1}{4} \right) \eta_v x^{-1} \quad (A.27)$$

$$\frac{\partial T_v}{\partial y} = (T_s - T_\infty) \frac{d\theta_v}{d\eta_v} \left(\frac{1}{4} \text{Gr}_{xv,\infty} \right)^{1/4} x^{-1} \quad (A.28)$$

$$\frac{\partial^2 T_v}{\partial y^2} = (T_s - T_\infty) \frac{d^2 \theta_v}{d\eta_v^2} \left(\frac{1}{4} \text{Gr}_{xv,\infty} \right)^{1/2} x^{-2} \quad (A.29)$$

$$\frac{\partial \lambda_v}{\partial y} = \frac{d\lambda_v}{d\eta} \left(\frac{1}{4} \text{Gr}_{xv,\infty} \right)^{1/4} x^{-1}. \quad (A.30)$$

With Eqs. (14.21), (14.22), (A.26)–(A.30), Eq. (A.25) is transformed into

$$\begin{aligned} \rho_v c_{pv} \left[\left(2\sqrt{gx} (\rho_{v,s}/\rho_{v,\infty} - 1)^{1/2} \right) w_{xv} \left(-(T_s - T_\infty) \frac{d\theta_v}{d\eta_v} \left(\frac{1}{4} \right) \eta_v x^{-1} \right) \right. \\ \left. + \left(2\sqrt{gx} (\rho_{v,s}/\rho_{v,\infty} - 1)^{1/2} \left(\frac{1}{4} \text{Gr}_{xv,\infty} \right)^{-1/4} \right) w_{yv} \right] \end{aligned}$$

$$\begin{aligned}
& \times (T_s - T_\infty) \frac{d\theta_v}{d\eta_v} \left(\frac{1}{4} \text{Gr}_{xv,\infty} \right)^{-1/4} x^{-1} \Big] \\
& = \frac{d\lambda_v}{d\eta} \left(\frac{1}{4} \text{Gr}_{xv,\infty} \right)^{1/4} x^{-1} (T_s - T_\infty) \frac{d\theta_v}{d\eta_v} \left(\frac{1}{4} \text{Gr}_{xv,\infty} \right)^{1/4} x^{-1} \\
& \quad + \lambda_v (T_s - T_\infty) \frac{d^2\theta_v}{d\eta_v^2} \left(\frac{1}{4} \text{Gr}_{xv,\infty} \right)^{1/2} x^{-2}.
\end{aligned}$$

The above equation is divided by $T_s - T_\infty$, and simplified to the following one by means of definition of local Grashof number $\text{Gr}_{xv,\infty}$:

$$\begin{aligned}
& \rho_v c_{pv} \left[\left(2\sqrt{gx} \left(\rho_{v,s}/\rho_{v,\infty}^{-1} \right)^{1/2} \right) w_{xv} \left(-\frac{d\theta_v}{d\eta_v} \left(\frac{1}{4} \right) \eta_v x^{-1} \right) \right. \\
& \quad \left. + \left(2\sqrt{gx} \left(\rho_{v,s}/\rho_{v,\infty} - 1 \right)^{1/2} w_{yv} \frac{d\theta_v}{d\eta_v} x^{-1} \right) \right] \\
& = \frac{d\lambda_v}{d\eta} x^{-1} \frac{d\theta_v}{d\eta_v} \left(\frac{1}{4} \frac{g \left(\rho_{v,s}/\rho_{v,\infty} - 1 \right) x^3}{\nu_{v,\infty}^2} \right)^{1/2} x^{-1} \\
& \quad + \lambda_v \frac{d^2\theta_v}{d\eta_v^2} \left(\frac{1}{4} \frac{g \left(\rho_{v,s}/\rho_{v,\infty} - 1 \right) x^3}{\nu_{v,\infty}^2} \right)^{1/2} x^{-2}.
\end{aligned}$$

The above equation is divided by $\sqrt{\frac{g}{x}} \left(\rho_{v,s}/\rho_{v,\infty} - 1 \right)^{1/2}$, and simplified to

$$\begin{aligned}
& \rho_v c_{pv} \left[(2)w_{xv} \left(-\frac{d\theta_v}{d\eta_v} \left(\frac{1}{4} \right) \eta_v \right) + 2W_{yv} \frac{d\theta_v}{d\eta_v} \right] \\
& = \frac{d\lambda_v}{d\eta} \frac{d\theta_v}{d\eta_v} \left(\frac{1}{4} \frac{1}{\nu_{v,\infty}^2} \right)^{1/2} + \lambda_v \frac{d^2\theta_v}{d\eta_v^2} \left(\frac{1}{4} \frac{1}{\nu_{v,\infty}^2} \right)^{1/2}.
\end{aligned}$$

The above equation is multiplied by $\frac{2\nu_{v,\infty}}{\lambda_v}$, and simplified to

$$Pr_v \frac{\nu_{v,\infty}}{\nu_v} \left(-\eta_v W_{xv} + 4W_{yv} \right) \frac{d\theta_v}{d\eta_v} = \frac{1}{\lambda_v} \frac{d\lambda_v}{d\eta} \frac{d\theta_v}{d\eta_v} + \frac{d^2\theta_v}{d\eta_v^2}. \quad (14.28)$$

Appendix B: Similarity Transformation for Boundary Condition Equations

1. Derivation of Eq. (14.7)

With the related defined variables in Eqs. (14.15) to (14.17), Eq. (14.7) can be easily derived to

$$\eta_l = 0: \quad W_{xl} = 0, \quad W_{yl} = 0, \quad \theta_l = 1. \quad (14.29)$$

By the way, the equation $y = \delta_l$ can be changed to $\eta_l = \eta_{l\delta} (\eta_v = 0)$:

2. Derivation of Eq. (14.8)

With Eqs. (14.16), (14.17) and (14.14), Eq. (14.8) can be easily changed to

$$W_{xv,s} = \left(\frac{\rho_{l,w} - \rho_{v,\infty}}{\rho_{l,s}} \right)^{1/2} \left(\frac{\rho_{v,s} - \rho_{v,\infty}}{\rho_{v,\infty}} \right)^{-1/2} W_{xl,s}. \quad (14.30)$$

3. Derivation of Eq. (14.9)

With Eq. (14.14) we have

$$\eta_{l\delta} = \left(\frac{1}{4} \text{Gr}_{xl,s} \right)^{1/4} \frac{\delta}{x} \quad (B.1)$$

for liquid film.

i.e.

$$\delta_l = \eta_{l\delta} \left(\frac{1}{4} \frac{g (\rho_l w - \rho_v, s) x^3}{v_{l,s}^2 \rho_{l,s}} \right)^{-1/4} x.$$

With definition of $\text{Gr}_{xl,s}$, we have

$$\frac{d\delta_l}{dx} = \frac{1}{4} \eta_{l\delta} \left(\frac{1}{4} \text{Gr}_{xl,s} \right)^{-1/4}. \quad (B.2)$$

Similarly, we obtain

$$\frac{d\delta_v}{dx} = \frac{1}{4} \eta_{v\delta} \left(\frac{1}{4} \text{Gr}_{xv,s} \right)^{-1/4} \quad (B.3)$$

for vapor film.

With Eqs. (B.1)–(B.3), (14.14), (14.16), (14.17), (14.19), (14.21) and (14.22), Eq. (14.9) is changed to

$$\begin{aligned} & \rho_{l,s} \left[2\sqrt{gx} \left(\frac{\rho_{l,w} - \rho_{v,\infty}}{\rho_{l,s}} \right)^{1/2} W_{xl} \frac{1}{4} \eta_{l\delta} \left(\frac{1}{4} \text{Gr}_{xl,s} \right)^{-1/4} \right. \\ & \quad \left. - 2\sqrt{gx} \left(\frac{\rho_{l,w} - \rho_{v,\infty}}{\rho_{l,s}} \right)^{1/2} \left(\frac{1}{4} \text{Gr}_{xl,s} \right)^{-1/4} W_{yl} \right]_s \\ & = \rho_{v,s} \left[2\sqrt{gx} (\rho_{v,s}/\rho_{v,\infty} - 1)^{1/2} W_{xv} \frac{1}{4} \eta_{v\delta} \left(\frac{1}{4} \text{Gr}_{vl,\infty} \right)^{-1/4} \right] \end{aligned}$$

$$-\left(2\sqrt{gx}(\rho_{v,s}/\rho_{v,\infty}-1)^{1/2}\left(\frac{1}{4}\text{Gr}_{xv,\infty}\right)^{-1/4}\right)^{-1} w_{yv} \Big]_s$$

i.e.

$$\begin{aligned} & \rho_{l,s} \left[2 \left(\frac{\rho_{l,w} - \rho_{v,\infty}}{\rho_{l,s}} \right)^{1/2} W_{x1} \frac{1}{4} \eta_{l\delta} \left(\frac{1}{4} \text{Gr}_{x1,s} \right)^{-1/4} \right. \\ & \quad \left. - 2 \left(\frac{\rho_{l,w} - \rho_{v,\infty}}{\rho_{l,s}} \right)^{1/2} \left(\frac{1}{4} \text{Gr}_{x1,s} \right)^{-1/4} W_{y1} \right]_s \\ & = \rho_{v,s} \left[2 (\rho_{v,s}/\rho_{v,\infty} - 1)^{1/2} W_{xv} \frac{1}{4} \eta_{v\delta} \left(\frac{1}{4} \text{Gr}_{v1,\infty} \right)^{-1/4} \right. \\ & \quad \left. - \left(2 (\rho_{v,s}/\rho_{v,\infty} - 1)^{1/2} \left(\frac{1}{4} \text{Gr}_{xv,\infty} \right)^{-1/4} \right)^{-1} w_{yv} \right]_s. \end{aligned}$$

With the definitions of $\text{Gr}_{x1,s}$ and $\text{Gr}_{xv,\infty}$, the above equation is simplified to

$$\begin{aligned} & \rho_{l,s} [W_{x1}\eta_{l\delta} - 4W_{y1}]_s \left(\frac{\rho_{l,w} - \rho_{v,\infty}}{\rho_{l,s}} \right)^{1/2} \left(\frac{1}{4} \frac{g(\rho_{l,w} - \rho_{v,\infty})x^3}{v_{l,s}^2 \rho_{l,s}} \right)^{-1/4} \\ & = \rho_{v,s} [W_{xv}\eta_{v\delta} - (4w_{yv})]_s (\rho_{v,s}/\rho_{v,\infty} - 1)^{1/2} \left(\frac{1}{4} \frac{g(\rho_{v,s}/\rho_{v,\infty} - 1)x^3}{v_{v,\infty}^2} \right)^{-1/4} \end{aligned}$$

i.e.

$$\begin{aligned} & \rho_{l,s} [W_{x1}\eta_{l\delta} - 4W_{y1}]_s \left(\frac{\rho_{l,w} - \rho_{v,\infty}}{\rho_{l,s}} \right)^{1/4} \left(\frac{1}{v_{l,s}^2} \right)^{-1/4} \\ & = \rho_{v,s} [W_{xv}\eta_{v\delta} - (4w_{yv})]_s (\rho_{v,s}/\rho_{v,\infty} - 1)^{1/4} \left(\frac{1}{v_{v,\infty}^2} \right)^{-1/4}. \end{aligned}$$

Since $\eta_{v\delta} = 0$ at the liquid–vapor interface, the above equation can be further simplified to

$$\rho_{l,s} [W_{x1}\eta_{l\delta} - 4W_{y1}]_s \left(\frac{\rho_{l,w} - \rho_{v,\infty}}{\rho_{l,s}} \right)^{1/4} (\rho_{v,s}/\rho_{v,\infty} - 1)^{-1/4} \left(\frac{v_{l,s}}{v_{v,\infty}} \right)^{1/2} = -\rho_{v,s} 4w_{yv}.$$

Then,

$$w_{yv,s} = -\frac{1}{4} \frac{\rho_{l,s}}{\rho_{v,s}} \left(\frac{v_{l,s}}{v_{v,\infty}} \right)^{1/2} \left(\frac{\rho_{l,w} - \rho_{v,\infty}}{\rho_{l,s}} \right)^{1/4} (\rho_{v,s}/\rho_{v,\infty} - 1)^{-1/4} [W_{x1}\eta_{l\delta} - 4W_{y1}]_s. \quad (14.31)$$

4. Derivation of Eq. (14.10)

With Eqs. (14.15) and (14.20), Eq. (14.10) is changed to

$$\begin{aligned} & \mu_{l,s} 2\sqrt{g\bar{x}} \left(\frac{\rho_{l,w} - \rho_{v,\infty}}{\rho_{l,s}} \right)^{1/2} \left(\frac{dW_{x1}}{d\eta_l} \right)_s x^{-1} \left(\frac{1}{4} \text{Gr}_{x1,s} \right)^{1/4} \\ & = \mu_{v,s} 2\sqrt{g\bar{x}} (\rho_{v,s}/\rho_{v,\infty} - 1)^{1/2} \left(\frac{dW_{xv}}{d\eta_v} \right)_s x^{-1} \left(\frac{1}{4} \text{Gr}_{xv,s} \right)^{1/4}. \end{aligned}$$

With the definitions of $\text{Gr}_{x1,s}$ and $\text{Gr}_{xv,\infty}$, the above equation is simplified to

$$\begin{aligned} \left(\frac{dW_{xv}}{d\eta_v} \right)_{\eta_v=0} & = \frac{\mu_{l,s}}{\mu_{v,s}} \left(\frac{v_{v,\infty}}{v_{l,s}} \right)^{1/2} \left(\frac{\rho_{l,w} - \rho_{v,\infty}}{\rho_{l,s}} \right)^{3/4} \\ & \times \left(\frac{\rho_{v,s}}{\rho_{v,\infty}} - 1 \right)^{-3/4} \left(\frac{dW_{x,l}}{d\eta_l} \right)_{\eta_l=\eta_{l,\delta}}. \end{aligned} \quad (14.32)$$

5. Derivation of Eq. (14.11)

With Eqs. (14.14), (14.15), (14.18) and (14.20) Eq. (14.11) is changed to

$$\begin{aligned} & \lambda_{v,s} (T_s - T_\infty) \left(\frac{d\theta_v}{d\eta_l} \right)_{\eta_v=\eta_{v,\delta}} \left(\frac{1}{4} \text{Gr}_{xv,\infty} \right)^{1/4} x^{-1} \\ & = \lambda_{l,s} (t_w - t_s) \left(\frac{d\theta_l}{d\eta_l} \right)_{\eta_l=\eta_{l,\delta}} \left(\frac{1}{4} \text{Gr}_{x1,s} \right)^{1/4} x^{-1} \\ & - h_{fg} \rho_{v,s} \left[2\sqrt{g\bar{x}} (\rho_{v,s}/\rho_{v,\infty} - 1)^{1/2} W_{xv,s} \frac{1}{4} \eta_{vs} \left(\frac{1}{4} \text{Gr}_{xv,\infty} \right)^{-1/4} \right. \\ & \left. - 2\sqrt{g\bar{x}} (\rho_{v,s}/\rho_{v,\infty} - 1)^{1/2} \left(\frac{1}{4} \text{Gr}_{xv,\infty} \right)^{-1/4} W_{yv,s} \right] \end{aligned}$$

i.e.

$$\begin{aligned} & \lambda_{v,s} (T_s - T_\infty) \left(\frac{d\theta_v}{d\eta_l} \right)_{\eta_v=\eta_{v,\delta}} \left(\frac{1}{4} \text{Gr}_{xv,\infty} \right)^{1/4} x^{-1} \\ & = \lambda_{l,s} (t_w - t_s) \left(\frac{d\theta_l}{d\eta_l} \right)_{\eta_l=\eta_{l,\delta}} \left(\frac{1}{4} \text{Gr}_{x1,s} \right)^{1/4} x^{-1} \end{aligned}$$

$$\begin{aligned}
& - h_{fg} \rho_{v,s} \left[2W_{xv,s} \frac{1}{4} \eta_{v\delta} - 2W_{yv,s} \right] \left(\frac{1}{4} \text{Gr}_{xv,\infty} \right)^{-1/4} \\
& \quad \times \sqrt{gx} (\rho_{v,s} / \rho_{v,\infty} - 1)^{1/2}.
\end{aligned} \tag{B.4}$$

With the definition of $\text{Gr}_{xv,\infty}$, we have

$$\rho_{v,s} / \rho_{v,\infty} - 1 = \frac{v_{v,\infty}^2}{gx^3} \text{Gr}_{xv,\infty} \tag{B.5}$$

With Eq. (B.5), (B.4) is changed to

$$\begin{aligned}
& \lambda_{v,s} (T_s - T_\infty) \left(\frac{d\theta_v}{d\eta_1} \right)_{\eta_v = \eta_{v\delta}} \left(\frac{1}{4} \text{Gr}_{xv,\infty} \right)^{1/4} x^{-1} \\
& = \lambda_{1,s} (t_w - t_s) \left(\frac{d\theta_1}{d\eta_1} \right)_{\eta_1 = \eta_{1\delta}} \left(\frac{1}{4} \text{Gr}_{x1,s} \right)^{1/4} x^{-1} \\
& - h_{fg} \rho_{v,s} \left[2W_{xv,s} \frac{1}{4} \eta_{v\delta} - 2W_{yv,s} \right] \left(\frac{1}{4} \text{Gr}_{xv,\infty} \right)^{-1/4} \\
& \quad \times \sqrt{gx} \left(\frac{v_{v,\infty}^2}{gx^3} \text{Gr}_{xv,\infty} \right)^{1/2}.
\end{aligned}$$

The above equation is simplified to

$$\begin{aligned}
& \lambda_{v,s} (T_s - T_\infty) \left(\frac{d\theta_v}{d\eta_1} \right)_{\eta_v = \eta_{v\delta}} \left(\frac{1}{4} \text{Gr}_{xv,\infty} \right)^{1/4} x^{-1} \\
& = \lambda_{1,s} (t_w - t_s) \left(\frac{d\theta_1}{d\eta_1} \right)_{\eta_1 = \eta_{1\delta}} \left(\frac{1}{4} \text{Gr}_{x1,s} \right)^{1/4} x^{-1} \\
& - h_{fg} \rho_{v,s} \left[2W_{xv,s} \frac{1}{4} \eta_{v\delta} - 2W_{yv,s} \right] \left(\frac{1}{4} \text{Gr}_{xv,\infty} \right)^{-1/4} \\
& \quad \times \sqrt{gx} \left(\frac{v_{v,\infty}^2}{gx^3} \right)^{1/2} 2 \left(\frac{1}{4} \text{Gr}_{xv,\infty} \right)^{1/2}
\end{aligned}$$

i.e.

$$\lambda_{v,s} (T_s - T_\infty) \left(\frac{d\theta_v}{d\eta_1} \right)_{\eta_v = \eta_{v\delta}} \left(\frac{1}{4} \text{Gr}_{xv,\infty} \right)^{1/4} x^{-1}$$

$$\begin{aligned}
&= \lambda_{1,s} (t_w - t_s) \left(\frac{d\theta_1}{d\eta_1} \right)_{\eta_1=\eta_{v\delta}} \left(\frac{1}{4} \text{Gr}_{x1,s} \right)^{1/4} x^{-1} \\
&\quad - h_{fg} \rho_{v,s} [\eta_{v\delta} W_{xv,s} - 4W_{yv,s}] \left(\frac{1}{4} \text{Gr}_{xv,\infty} \right)^{1/4} x^{-1} \nu_{v,\infty}.
\end{aligned}$$

With the definitions of $\text{Gr}_{x1,s}$ and $\text{Gr}_{xv,\infty}$, the above equation is changed to

$$\begin{aligned}
&\lambda_{v,s} (T_s - T_\infty) \left(\frac{d\theta_v}{d\eta_1} \right)_{\eta_v=\eta_{v\delta}} \left(\frac{1}{4} \frac{g (\rho_{v,s}/\rho_{v,\infty} - 1) x^3}{\nu_{v,\infty}^2} \right)^{1/4} x^{-1} \\
&= \lambda_{1,s} (t_w - t_s) \left(\frac{d\theta_1}{d\eta_1} \right)_{\eta_1=\eta_{1\delta}} \left(\frac{1}{4} \frac{g (\rho_{1,w} - \rho_{v,\infty}) x^3}{\nu_{1,s}^2 \rho_{1,s}} \right)^{1/4} x^{-1} \\
&\quad - h_{fg} \rho_{v,s} [\eta_{v\delta} W_{xv,s} - 4W_{yv,s}] \left(\frac{1}{4} \frac{g (\rho_{v,s}/\rho_{v,\infty} - 1) x^3}{\nu_{v,\infty}^2} \right)^{1/4} x^{-1} \nu_{v,\infty}
\end{aligned}$$

i.e.

$$\begin{aligned}
&\lambda_{v,s} (T_s - T_\infty) \left(\frac{d\theta_v}{d\eta_1} \right)_{\eta_v=\eta_{v\delta}} \left(\frac{\rho_{v,s}/\rho_{v,\infty} - 1}{\nu_{v,\infty}^2} \right)^{1/4} \\
&= \lambda_{1,s} (t_w - t_s) \left(\frac{d\theta_1}{d\eta_1} \right)_{\eta_1=\eta_{1\delta}} \left(\frac{\rho_{1,w} - \rho_{v,\infty}}{\nu_{1,s}^2 \rho_{1,s}} \right)^{1/4} \\
&\quad - h_{fg} \rho_{v,s} [\eta_{v\delta} W_{xv,s} - 4W_{yv,s}] \left(\frac{\rho_{v,s}/\rho_{v,\infty} - 1}{\nu_{v,\infty}^2} \right)^{1/4} \nu_{v,\infty}.
\end{aligned}$$

The above equation is further simplified to

$$\frac{\left(\frac{d\theta_v}{d\eta_1} \right)_{\eta_v=\eta_{v\delta}}}{\lambda_{v,s} (T_s - T_\infty)} = \frac{\lambda_{1,s} (t_w - t_s) \left(\frac{\nu_{v,\infty}}{\nu_{1,s}} \right)^{1/2} \left(\frac{\rho_{1,w} - \rho_{v,\infty}}{\rho_{1,s}} \right)^{1/4} (\rho_{v,s}/\rho_{v,\infty} - 1)^{-1/4} \left(\frac{d\theta_1}{d\eta_1} \right)_{\eta_1=\eta_{1\delta}} - h_{fg} \rho_{v,s} \nu_{v,\infty} [\eta_{v\delta} W_{xv,s} - 4W_{yv,s}]}{\lambda_{v,s} (T_s - T_\infty)}.$$

Since $\eta_{v\delta} = 0$ at the liquid–vapor interface, the above equation is simplified to

$$\begin{aligned}
&\left(\frac{d\theta_v}{d\eta_1} \right)_{\eta_v=\eta_{v\delta}} = \frac{\lambda_{1,s} (t_w - t_s) \left(\frac{\nu_{v,\infty}}{\nu_{1,s}} \right)^{1/2} \left(\frac{\rho_{1,w} - \rho_{v,\infty}}{\rho_{1,s}} \right)^{1/4} (\rho_{v,s}/\rho_{v,\infty} - 1)^{-1/4} \left(\frac{d\theta_1}{d\eta_1} \right)_{\eta_1=\eta_{1\delta}} + 4h_{fg} \rho_{v,s} \nu_{v,\infty} W_{yv,s}}{\lambda_{v,s} (T_s - T_\infty)}. \tag{14.33}
\end{aligned}$$

In addition, Eqs. (14.12) and (14.13) can be easily changed to

$$\theta_1 = 0, \theta_v = 1 \quad (14.34)$$

$$\eta_v \rightarrow \infty: W_{xv} \rightarrow 0, \theta_v \rightarrow 0. \quad (14.35)$$

References

1. W. Nusselt, Die Oberflächenkondensation des Wasserdampfes. Z. Ver. D. Ing. **60**, 541–569 (1916)
2. L.A. Bromley, Effect of heat capacity of condensate in condensing. Ind. Eng. Chem. **44**, 2966–2969 (1952)
3. W.M. Rohsenow, Heat transfer and temperature distribution in laminar film condensation. Trans. Am. Soc. Mech. Eng. **78**, 1645–1648 (1956)
4. E.M. Sparrow, J.L. Gregg, A boundary-layer treatment of laminar film condensation. J. Heat Transf. **81**, 13–18 (1959)
5. J.C. Koh, E.M. Sparrow, J.P. Hartnett, The two phase boundary layer in laminar film condensation. Int. J. Heat Mass Transf. **2**, 69–88 (1961)
6. M.M. Chen, An analytical study of laminar film condensation: part 1—flat plate. J. Heat Transf. **81**, 48–54 (1961)
7. W.H. McAdams, *Heat Transmission*, 3rd edn. (McGraw-Hill, New York, 1954), pp. 331–332
8. D.A. Labuntsov, Effect of temperature dependence of physical parameters of condensate on heat transfer in film condensation of steam. Teploenergetika **4**(2), 49–51 (1957)
9. G. Poots, R.G. Miles, Effects of variable physical properties on laminar film condensation of saturated steam on a vertical flat plate. Int. J. Heat Mass Transf. **10**, 1677–1692 (1967)
10. J. Stinnesbeck, H. Heawig, An asymptotic analysis of laminar film condensation on a vertical flat plate including variable property effects. in *Proceedings of the Ninth International Heat Transfer Conference Jerusalem*, vol. 6, 1990
11. W.J. Minkowcs, E.M. Sparrow, Condensation heat transfer in the presence of noncondensable, interface resistance, superheating, variable properties, and diffusion. Int. J. Heat Mass Transf. **9**, 1125–1144 (1966)
12. D.Y. Shang, T. Adamek, in *Study of Laminar Film Condensation of Saturated Steam for Consideration of Variable Thermophysical Properties, Transport Phenomena, Science and Technology*, ed. by B.X. Wang (Higher Education press, Beijing, 1992), pp. 470–475
13. D.Y. Shang, T. Adamek, Study on laminar film condensation of saturated steam on a vertical flat plate for consideration of various physical factors including variable thermophysical properties. Wärme- und Stoffübertragung **30**, 89–100 (1994)
14. D.Y. Shang, B.X. Wang, An extended study on steady-state laminar film condensation of a superheated vapor on an isothermal vertical plate. Int. J. Heat Mass Transf. **40**(4), 931–941 (1997)

Chapter 15

Velocity and Temperature Fields of Laminar Free Convection Film Condensation of Pure Vapour

Abstract The work is dealt with for solutions of velocity and temperature fields on laminar free film condensation of superheated vapor on a vertical flat plate at atmospheric pressure with consideration of various factors including variable physical properties. The film condensation of saturated vapor is only its special case. The system of ordinary differential equations is computed by a successively iterative procedure and an iterative method is adopted for the numerical solutions of the three-point boundary value problem. With increasing the wall subcooled grades, the maximum of velocity field of liquid film will increase and shift far away from the plate. In addition, the velocity of liquid film will decrease with increasing the vapor superheated grade. Compared with the effect of wall subcooled grades on the velocity of liquid film, the related effect of the vapor superheated grade is obviously weak. With increasing the wall subcooled grades, the thickness of liquid film will increase. With increasing the vapor superheated grade, the thickness of liquid film will decrease. The temperature grade of liquid film on the wall will decrease with increase in wall subcooled grade, and increase with increasing vapor superheated grade. Compared with the effect of wall subcooled grades on the temperature of liquid film, the related effect of the vapor superheated grade is obviously weak. The velocity of vapor film will increase with increasing the wall superheated grades, and decrease with increasing vapor superheated grade. With increasing wall subcooled grade, the velocity of vapor film will decrease slightly. With increasing the vapor superheated grade, the velocity of vapor film will decrease obviously.

15.1 Introduction

In Chap. 14, the complete mathematical model was derived for laminar free film condensation of vapor, where the model of the film condensation of saturated vapor is regarded as its special case. On the basis of Chap. 14, in this chapter, the mathematical model with the governing ordinary differential equations and the complete

boundary conditions are solved by a successively iterative procedure at different wall subcooled degrees and different vapor superheated degrees. Meanwhile, the temperature parameter method and polynomial formulae are used for treatment of the variable physical properties of the vapor and liquid films respectively. The distributions of velocity and temperature fields of the laminar free film condensation of liquid are rigorously determined.

15.2 Treatment of Variable Physical Properties

The treatment of variable physical properties for the medium of the liquid and vapor films must be done for solving the ordinary differential equations with the boundary condition equations. The approaches for the treatment of variable physical properties are presented as follows:

15.2.1 For Liquid Film

Treatment of variable physical properties of liquid will be done according to the polynomial method. For example, for water the temperature-dependent expressions of density, thermal conductivity, and absolute viscosity can be expressed as follows:

$$\rho_l = -4.48 \times 10^{-3} t^2 + 999.9 \quad (15.1)$$

$$\lambda_l = -8.01 \times 10^{-6} t^2 + 1.94 \times 10^{-3} t + 0.563 \quad (15.2)$$

$$\mu_l = \exp \left[-1.6 - \frac{1150}{T} + \left(\frac{690}{T} \right)^2 \right] \times 10^{-3} \quad (15.3)$$

According to Eqs. (5.24) to (5.26), the *physical property factors* $\frac{1}{\rho_l} \frac{d\rho_l}{d\eta_l}$, $\frac{1}{\mu_l} \frac{d\mu_l}{d\eta_l}$ and $\frac{1}{\lambda_l} \frac{d\lambda_l}{d\eta_l}$ in governing Eqs. (14.23) to (14.25) for water film become the following equations at atmospheric pressure:

$$\frac{1}{\rho_l} \frac{d\rho_l}{d\eta_l} = \frac{-2 \times 4.48 \times 10^{-3} t (t_w - t_s)}{-4.48 \times 10^{-3} t^2 + 999.9} \frac{d\theta_l}{d\eta_l} \quad (15.4)$$

$$\frac{1}{\mu_l} \frac{d\mu_l}{d\eta_l} = \left(\frac{1150}{T^2} - 2 \times \frac{690^2}{T^3} \right) (t_w - t_s) \frac{d\theta_l}{d\eta_l} \quad (15.5)$$

$$\frac{1}{\lambda_l} \frac{d\lambda_l}{d\eta_l} = \frac{(-2 \times 8.01 \times 10^{-6}t + 1.94 \times 10^{-3})(t_w - t_s) \frac{d\theta_l}{d\eta_l}}{-8.01 \times 10^{-6}t^2 + 1.94 \times 10^{-3}t + 0.563} \quad (15.6)$$

15.2.2 For Vapor Film

The temperature parameter method introduced in Chap. 5 [1] will be used for the treatment of variable physical properties of the vapor medium. For the situation here, the boundary temperature T_∞ is taken, and the simple power-law equations will be

$$\frac{\mu_v}{\mu_{v,\infty}} = \left(\frac{T}{T_\infty} \right)^{n_\mu} \quad (15.7)$$

$$\frac{\lambda_v}{\lambda_{v,\infty}} = \left(\frac{T}{T_\infty} \right)^{n_\lambda} \quad (15.8)$$

$$\frac{\rho_v}{\rho_{v,\infty}} = \left(\frac{T}{T_\infty} \right)^{-1} \quad (15.9)$$

Here we omit the equation for specific heat. With Eqs. (15.7) and (15.9), we have

$$\frac{\nu_v}{\nu_{v,\infty}} = \left(\frac{T}{T_\infty} \right)^{n_\mu+1} \quad (15.10)$$

In addition, according to Chap. 5, we have the following equations for description of the physical property factors $\frac{1}{\rho_v} \frac{d\rho_v}{d\eta_v}$, $\frac{1}{\mu_v} \frac{d\mu_v}{d\eta_v}$, $\frac{1}{\lambda_v} \frac{d\lambda_v}{d\eta_v}$ and $\frac{\nu_{v,\infty}}{\nu_v}$:

$$\frac{1}{\rho_v} \frac{d\rho_v}{d\eta_v} = - \frac{(T_s/T_\infty - 1)d\theta_v/d\eta_v}{(T_s/T_\infty - 1)\theta_v + 1} \quad (15.11)$$

$$\frac{1}{\mu_v} \frac{d\mu_v}{d\eta_v} = \frac{n_\mu(T_s/T_\infty - 1)d\theta_v/d\eta_v}{(T_s/T_\infty - 1)\theta_v + 1} \quad (15.12)$$

$$\frac{1}{\lambda_v} \frac{d\lambda_v}{d\eta_v} = \frac{n_\lambda(T_s/T_\infty - 1)d\theta_v/d\eta_v}{(T_s/T_\infty - 1)\theta_v + 1} \quad (15.13)$$

$$\frac{\nu_{v,\infty}}{\nu_v} = [(T_s/T_\infty - 1)\theta_v + 1]^{-(n_\mu+1)} \quad (15.14)$$

15.3 Numerical Solutions

15.3.1 Calculation Procedure

The calculation procedure of the equations of the two-phase boundary layer of the film condensation of vapor belongs to *three-point boundary value problem*, and is carried out numerically by two steps. In the first step, the solutions of Eqs. (14.23) to (14.25) of the liquid film of Chap. 14 are assumed to be without shear force of vapor at the liquid–vapor interface. For this case, the boundary condition (14.23) must be changed into

$$\left(\frac{dW_{xl}}{d\eta_l} \right)_{\eta_l=\eta_{l,\delta}} = 0 \quad (15.15)$$

In this case, Eqs. (14.29) and (14.34) are taken as the boundary conditions of the two-point boundary value problem of Eqs. (14.23) to (14.25) for liquid film, and are solved by the shooting method. Furthermore, the second step for carrying out calculation of three-point boundary value problem for coupling equations of liquid film with equations for vapor films is started. In this step, first the boundary values $W_{xv,s}$ and $W_{yv,s}$ are found out by Eqs. (14.30) and (14.31) respectively. Then, Eqs. (14.26) to (14.28) for the vapor film are calculated with the boundary conditions (14.34) and (14.35) and the above values of $W_{xv,s}$ and $W_{yv,s}$. On this basis, judgment Eqs. (14.32) and (14.33) are used for checking convergence of the solutions. By means of the judgment equations the calculation is iterated with appropriate change of the values $W_{xl,s}$ and $\eta_{l,\delta}$. In each iteration, the calculations of Eqs. (14.23) to (14.25) for liquid film and Eqs. (14.26) to (14.28) for vapor film are made successively by the shooting method.

15.3.2 Numerical Solution

From the governing ordinary equations and their boundary conditions, it will be expected that for consideration of variable thermophysical properties of the liquid and vapor medium, the dimensionless velocity and temperature fields for the film condensation of vapor will depend on the temperature-dependent properties of the liquid and vapor medium, and finally on the temperature conditions t_w , t_s and t_∞ .

All physical properties for water and water vapor at saturated temperature used in the calculation come from Ref. [2–4]. For convenience some special values of the physical properties are listed in Tables 15.1 and 15.2.

As an example of application for solving the theoretical and mathematical mode of laminar film condensation of water vapor on an isothermal vertical plate, the numerical calculation was carried out, while the film boiling of saturated water is taken as its special case. From Chap. 5 we know that the temperature parameters

Table 15.1 The physical property values for water and water vapor at saturated temperature

Term	value	
	For water	For water vapour
t_s (°C)	100	100
c_p (J/(kg/K))	4216	–
h_{fg} (kJ/kg)	–	2257.3
Pr	1.76	1
ρ (kg/m ³)	958.1	0.5974
μ (kg/(m/s))	282.2×10^{-6}	12.28×10^{-6}
ν (m ² /s)	0.294×10^{-6}	20.55×10^{-6}
λ (W/(m/K))	0.677	0.02478

Table 15.2 The values of water density at different temperatures

t (°C)	0	20	40	60	80	95	99.9
ρ (kg/m ³)	999.8	998.3	992.3	983.2	971.4	961.7	958.1

n_μ, n_λ and n_{c_p} of water vapor are 1.04, 1.185, and 0.003. Such low value of n_{c_p} make it possible to actually treat n_{c_p} of water vapor as zero, i.e., c_p is taken as constant.

For laminar free film condensation of water vapor for *vapor superheated grade* $\frac{\Delta t_\infty}{t_s} (= \frac{t_\infty - t_s}{t_s}) = 0$, the numerical calculations have been carried out and some typical calculated results for velocity fields W_{xl} and temperature fields θ_l of liquid film, and velocity field W_{xv} of vapor film are plotted in Figs. 15.1–15.4 with different *wall subcooled grades* $\frac{\Delta t_w}{t_s} = \frac{t_s - t_w}{t_s}$ and *vapor superheated grades* $\frac{\Delta t_\infty}{t_s} = \frac{t_s - t_\infty}{t_s}$.

15.4 Variations of Velocity and Temperature Fields

From these numerical results, the following variations of velocity and temperature fields are found together with wall subcooled grades and vapor superheated grade:

15.4.1 For Velocity Fields of Liquid Film

From Figs. 15.1–15.4, it is seen that the velocity of liquid film will increase with increase in *wall subcooled grades* $\frac{\Delta t_w}{t_s} = \frac{t_s - t_w}{t_s}$. Increasing the wall subcooled grades $\frac{\Delta t_w}{t_s} = \frac{t_s - t_w}{t_s}$, the maximum of velocity field of liquid film will increase and shift far away from the plate. In addition, the velocity of liquid film will decrease with increase in the *water vapor superheated grade*, $\frac{\Delta t_\infty}{t_s} = \frac{t_\infty - t_s}{t_s}$. However, compared with the effect of wall subcooled grades on the velocity of liquid film, the related effect of the water vapor superheated grade is obviously weak.

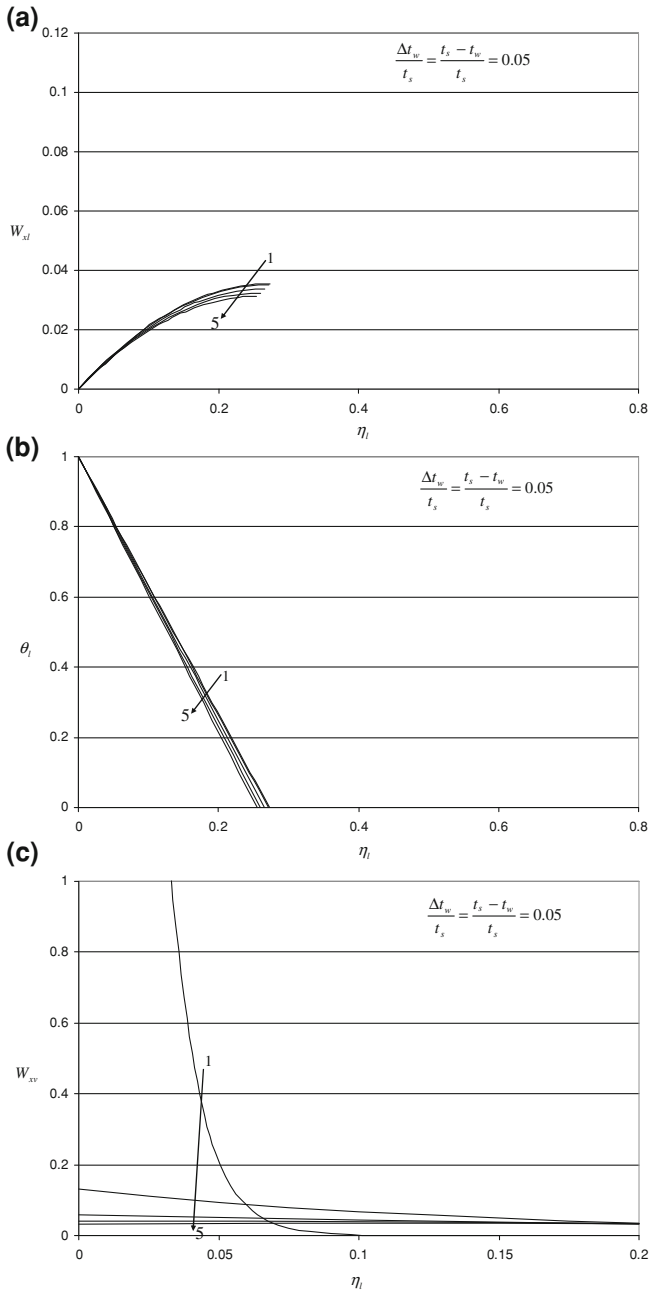


Fig. 15.1 Numerical results on **a** velocity profiles of liquid film, w_{xl} , and **b** temperature profiles of liquid film, θ_l , and **c** velocity profiles of vapor film, w_{xv} , for laminar free film condensation of subcooled water vapor with wall subcooled grade $\frac{\Delta t_w}{t_s} = 0.05$ (Lines 1–5: vapor superheated grade $\frac{\Delta t_{\infty}}{t_s} = 0, 1.27, 2.27, 3.27, \text{ and } 4.27$)

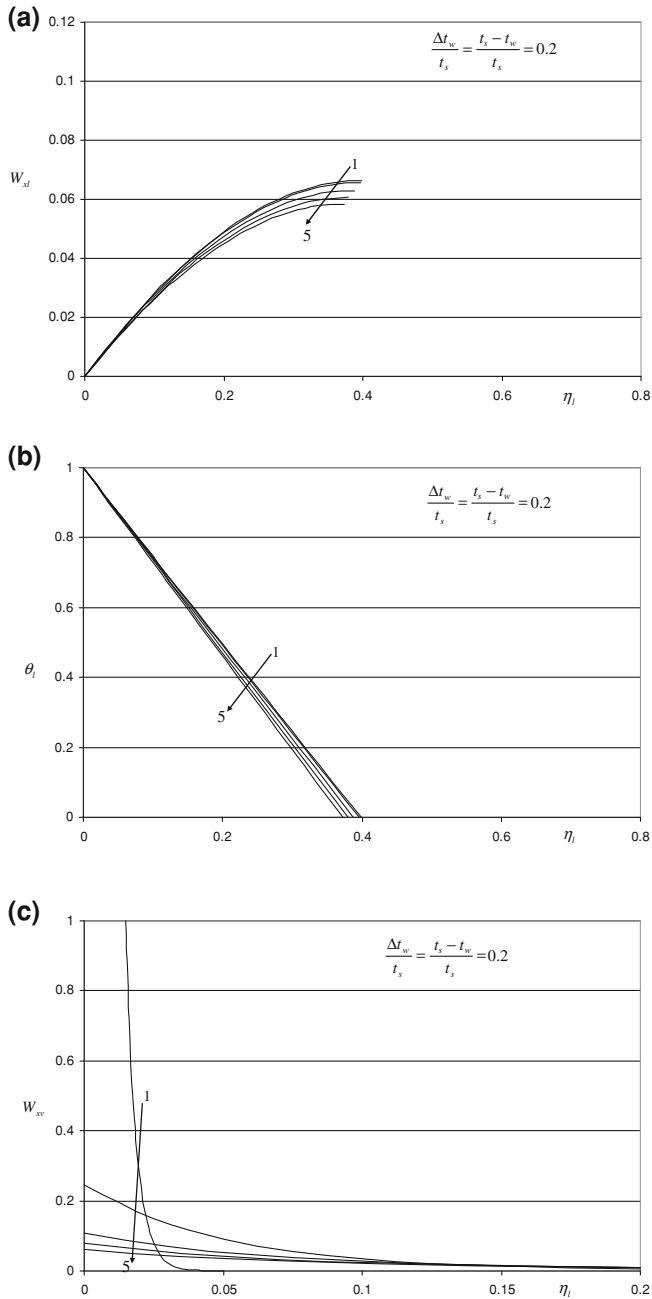


Fig. 15.2 Numerical results on **a** velocity profiles of liquid film, w_{xl} , and **b** temperature profiles of liquid film, θ_l , and **c** velocity profiles of vapor film, w_{xv} , for laminar free film condensation of subcooled water vapor with wall subcooled grade $\frac{\Delta t_w}{t_s} = 0.2$ (Lines 1–5: vapor superheated grade $\frac{\Delta t_\infty}{t_s} = 0, 1.27, 2.27, 3.27, \text{ and } 4.27$)

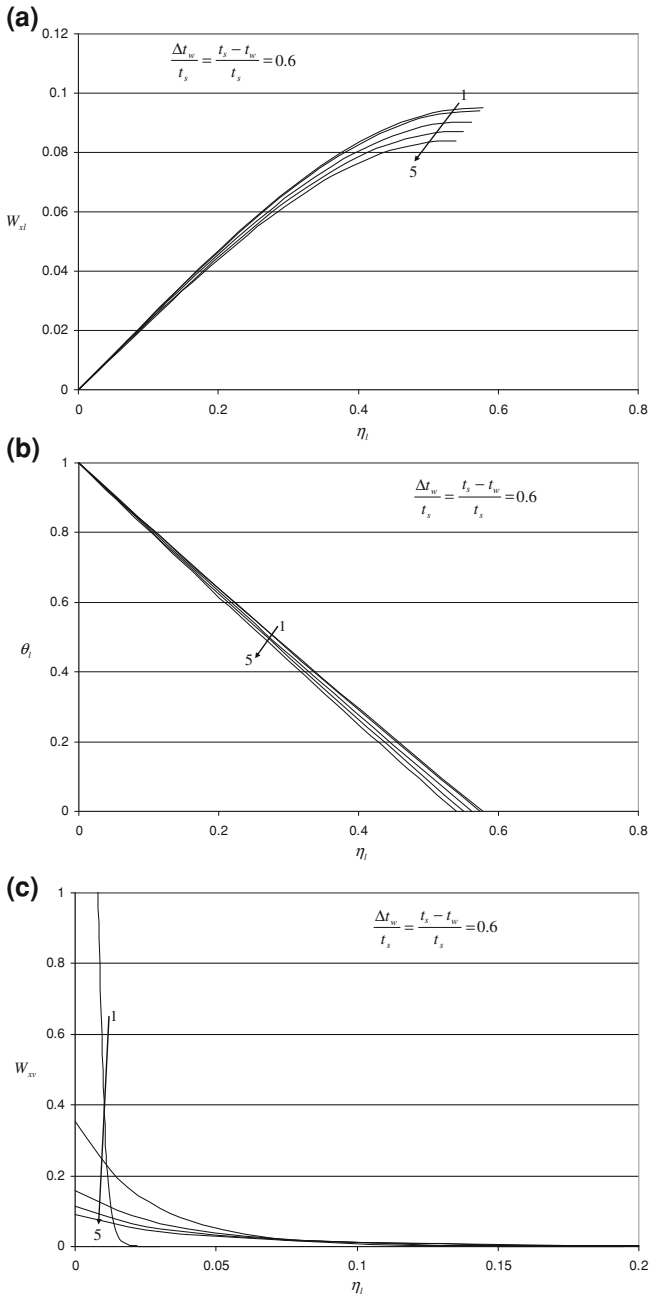


Fig. 15.3 Numerical results on **a** velocity profiles of liquid film, w_{xl} , and **b** temperature profiles of liquid film, θ_l , and **c** velocity profiles of vapor film, w_{xv} , for laminar free film condensation of subcooled water vapor with wall subcooled grade $\frac{\Delta t_w}{t_s} = 0.6$ (Lines 1–5: vapor superheated grade $\frac{\Delta t_\infty}{t_s} = 0, 1.27, 2.27, 3.27, \text{ and } 4.27$)

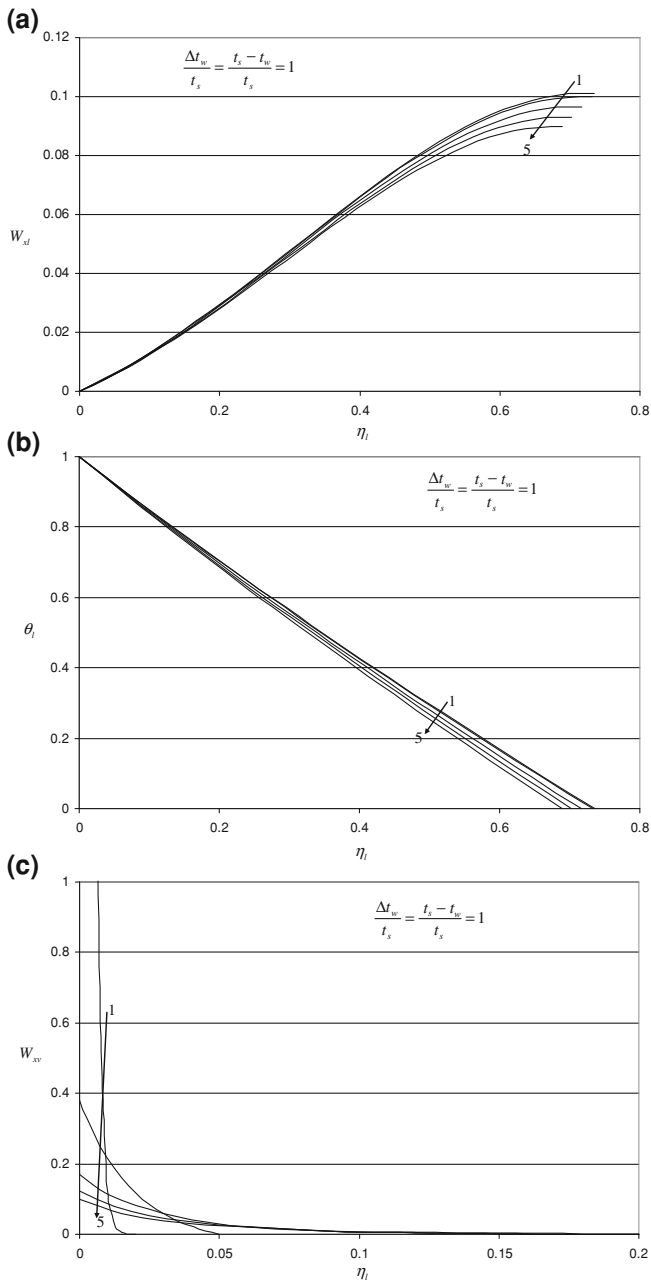


Fig. 15.4 Numerical results on **a** velocity profiles of liquid film, w_{xl} , and **b** temperature profiles of liquid film, θ_l , and **c** velocity profiles of vapor film, w_{xv} , for laminar free film condensation of subcooled water vapor with wall subcooled grade $\frac{\Delta t_w}{t_s} = 1$ (Lines 1–5: vapor superheated grade $\frac{\Delta t_\infty}{t_s} = 0, 1.27, 2.27, 3.27, \text{ and } 4.27$)

Furthermore, with increase in the wall subcooled grades $\frac{\Delta t_w}{t_s} = \frac{t_s - t_w}{t_s}$, the thickness of liquid film will increase. With increase in the water vapor superheated grade, $\frac{\Delta t_\infty}{t_s} = \frac{t_\infty - t_s}{t_s}$, the thickness of liquid film will decrease.

15.4.2 For Temperature Fields of Liquid Film

From Figs. 15.1–15.4, it is seen that the temperature field of liquid film on the wall will decrease with increase in wall subcooled grade $\frac{\Delta t_w}{t_s} = \frac{t_s - t_w}{t_s}$, and increase with increase in water vapor superheated grade $\frac{\Delta t_\infty}{t_s} = \frac{t_\infty - t_s}{t_s}$. However, compared with the effect of wall subcooled grades on the temperature of liquid film, the related effect of the water vapor superheated grade is obviously weak.

15.4.3 For Velocity Fields of Vapor Film

From Figs. 15.1–15.4, it is seen that the velocity of vapor film will increase with increase in the wall subcooled grades $\frac{\Delta t_w}{t_s} = \frac{t_s - t_w}{t_s}$, and decrease with increase in vapor superheated grade $\frac{\Delta t_\infty}{t_s} = \frac{t_\infty - t_s}{t_s}$. Furthermore, by increasing wall subcooled grade $\frac{\Delta t_w}{t_s} = \frac{t_s - t_w}{t_s}$, the velocity of vapor film will decrease slightly. By increasing the vapor superheated grade $\frac{\Delta t_\infty}{t_s} = \frac{t_\infty - t_s}{t_s}$, the velocity of vapor film will decrease obviously.

15.5 Remarks

In this chapter we deal with the solutions of velocity and temperature fields on laminar free film condensation of vapor on a vertical flat plate at atmospheric pressure with consideration of various physical property factors including variable physical properties. The film condensation of saturated vapor is only its special case.

The system of ordinary differential equations and its related boundary conditions is computed by a successively iterative procedure and an iterative method is adopted for the numerical solutions of the three-point boundary value problem. On the basis of the rigorous numerical solutions, the following points are included for the velocity and temperature fields of laminar free convection film condensation of vapor:

With increase in the wall subcooled grades $\frac{\Delta t_w}{t_s} = \frac{t_s - t_w}{t_s}$, the maximum of velocity field of liquid film will increase and shift far away from the plate. In addition, the velocity of liquid film will slightly decrease with increase in the vapor superheated grade $\frac{\Delta t_\infty}{t_s} = \frac{t_\infty - t_s}{t_s}$. Compared with the effect of wall subcooled grades on the

velocity of liquid film, the related effect of the vapor superheated grade is obviously weak.

With increase in the wall subcooled grades $\frac{\Delta t_w}{t_s} = \frac{t_s - t_w}{t_s}$, the thickness of liquid film will increase. With increase in the vapor superheated grade, $\frac{\Delta t_\infty}{t_s} = \frac{t_\infty - t_s}{t_s}$, the thickness of liquid film will decrease.

The temperature grade of liquid film on the wall will decrease with increase in the wall subcooled grade $\frac{\Delta t_w}{t_s} = \frac{t_s - t_w}{t_s}$, and increase slightly with increasing vapor superheated grade $\frac{\Delta t_\infty}{t_s} = \frac{t_\infty - t_s}{t_s}$. Compared with the effect of wall subcooled grades on the temperature of liquid film, the related effect of the vapor superheated grade is obviously weak.

The velocity of vapor film will increase with increase in the wall superheated grades $\frac{\Delta t_w}{t_s} = \frac{t_s - t_w}{t_s}$, and decrease slightly with increase in vapor superheated grade $\frac{\Delta t_\infty}{t_s} = \frac{t_\infty - t_s}{t_s}$. With increasing wall subcooled grade $\frac{\Delta t_w}{t_s} = \frac{t_s - t_w}{t_s}$, the velocity of vapor film will decrease slightly. With increasing vapor superheated grade $\frac{\Delta t_\infty}{t_s} = \frac{t_\infty - t_s}{t_s}$, the velocity of vapor film will decrease obviously.

15.6 Exercises

1. Please give out a detailed derivation for obtaining Eqs. (15.4–15.6) on physical property factors for water condensate film flow of laminar free convection film condensation of pure vapor.
2. Please give out a detailed derivation for obtaining Eqs. (15.11–15.14) on physical property factors for vapor film flow of laminar free convection film condensation of pure vapor.
3. Do you think that the variable physical properties are rigorously considered and treated in this present system of mathematical models on the laminar free convection film condensation of vapor? Why?
4. Please describe the variations of the velocity and temperature fields of the laminar free convection film condensation of vapor caused by the wall superheated grade, $\frac{\Delta t_w}{t_s} \left(= \frac{t_s - t_w}{t_s} \right)$ and liquid subcooled degree $\frac{\Delta t_\infty}{t_s} \left(= \frac{t_s - t_\infty}{t_s} \right)$?
5. Compare the variation regulation of the velocity and temperature fields on the laminar free film condensation of vapor to that on laminar free convection film boiling of liquid.
6. Please find out the difference in the variation regulation of the velocity and temperature fields on the laminar free convection film condensation of vapor from that on laminar free film boiling of liquid, and explain the reason.

References

1. VDI-Warmeatlas, Berechnungsblltter fur die Wärmeübertragu, 5, ereiterte Auflage, VDI Verlage GmbH, Dusseldorf, 1988
2. D.Y. Shang, T. Adamek, Study of laminar film condensation of saturated steam for consideration of variable thermophysical properties, in *Transport Phenomena, Science and Technology*, ed. by B.X. Wang (Higher Education press, Beijing, 1992), pp. 470–475
3. D.Y. Shang, T. Adamek, Study on laminar film condensation of saturated steam on a vertical flat plate for consideration of various physical factors including variable thermophysical properties. *Wärme- und Stoffübertragung* **30**, 89–100 (1994)
4. D.Y. Shang, B.X. Wang, An extended study on steady-state laminar film condensation of a superheated vapor on an isothermal vertical plate. *Int. J. Heat Mass Transf.* **40**(4), 931–941 (1997)

Chapter 16

Heat and Mass Transfer of Laminar Free Convection Film Condensation of Pure Vapor

Abstract With heat and mass transfer analysis, the theoretical equations for Nusselt number and mass flow rate are provided for the laminar free convection film condensation of vapor where only the wall temperature gradient and condensate mass flow rates are unknown variables, respectively. With increase of the wall subcooled grade, the wall temperature gradient will decrease, especially for lower wall subcooled grade. While, with increase of the vapor bulk superheated grade, the wall temperature gradient will increase. However, the effect of the wall subcooled grade on the wall temperature gradient is more obvious than that of the vapor bulk superheated grade. With increase of the wall subcooled grade, the condensate film thickness will increase, especially for lower wall subcooled grade, while with increase of the superheated grade, the condensate film thickness will decrease. However, the effect of the wall subcooled grade on the condensate film thickness is more obvious than that of the vapor bulk superheated grade. With increase of the wall subcooled grade, the velocity components will increase, especially for the small value of the wall subcooled grade. While with increase of the vapor bulk superheated grade, the velocity components will decrease. As per the results, with increase of the wall subcooled grade, the condensate mass flow rate parameter will increase, especially due to the function of condensate film thickness. While with increase of the vapor bulk superheated grade, the mass flow rate parameter will decrease. However, the effect of the wall subcooled grade on the condensate mass flow rate parameter is more obvious than that of the vapor bulk superheated grade. On the basis of the rigorous numerical solutions, the wall temperature gradient and then mass flow rate parameter are formulated, and then the formulated equations for reliable predictions of heat and mass transfer are created for heat and mass transfer application of the laminar free convection film condensation of water vapor.

16.1 Introduction

In Chap. 14, the complete mathematical model was provided for laminar free convection film condensation of vapor, where the model of film condensation of saturated vapor is regarded as its special case [1–3]. In Chap. 15, the mathematical model with the governing ordinary differential equations and the complete boundary conditions were solved by a successively iterative procedure at different wall subcooled degrees and different vapor superheated degrees. Meanwhile, the temperature parameter method and polynomial formulae reported in Chap. 5 are used for treatment of the variable thermophysical properties of the vapor and liquid films, respectively. The distributions of velocity and temperature fields of the laminar free film condensation of vapor were rigorously calculated.

In this chapter, the effect of wall subcooled grade and vapor superheated grade on heat and mass transfer of laminar free convection film condensation of vapor is further clarified. On this basis, the theoretically rigorous and practically simple formulae will be obtained for prediction of heat transfer and mass flow rate of the film condensation of vapor.

16.2 Heat Transfer Analysis

Consulting the *heat transfer analysis* in Chap. 8 for heat transfer analysis on liquid laminar free convection, the heat transfer theoretical equations can be expressed as follows for laminar free convection film condensation of liquid:

The local heat transfer rate is described as

$$q_x = \lambda_{l,w}(t_w - t_s) \left(\frac{1}{4} \text{Gr}_{x,l,s} \right)^{1/4} x^{-1} \left(-\frac{d\theta_l}{d\eta_l} \right)_{\eta_l=0} \quad (16.1)$$

With the Newtonian cooling law, the *local heat transfer coefficient* on the surface, defined as $q_x = \alpha_x(T_w - T_s)$, will be

$$\alpha_x = \lambda_{l,w} \left(\frac{1}{4} \text{Gr}_{x,l,s} \right)^{1/4} x^{-1} \left(-\frac{d\theta_l}{d\eta_l} \right)_{\eta_l=0}. \quad (16.2)$$

The *local Nusselt number*, defined as $\text{Nu}_{x,l,w} = \frac{\alpha_x x}{\lambda_{l,w}}$, is expressed by

$$\text{Nu}_{x,w} = \left(\frac{1}{4} \text{Gr}_{x,l,s} \right)^{1/4} \left(-\frac{d\theta_l}{d\eta_l} \right)_{\eta_l=0}. \quad (16.3)$$

The *total heat transfer rate* for position $x = 0$ to x with width of b on the plate is an integration

$$Q_x = \iint_A q_x dA = \int_0^x q_x b dx$$

where $A = b \times x$, and hence

$$Q_x = \frac{4}{3} b \lambda_{l,w} (t_w - t_s) \left(\frac{1}{4} \text{Gr}_{x,l,s} \right)^{1/4} \left(-\frac{d\theta_l}{d\eta_l} \right)_{\eta_l=0}. \quad (16.4)$$

The *average heat transfer rate*, defined as $\bar{Q}_x = Q_x / (b \times x)$ is given by

$$\bar{Q}_x = \frac{4}{3} x^{-1} \lambda_w (t_w - t_s) \left(\frac{1}{4} \text{Gr}_{x,l,s} \right)^{1/4} \left(-\frac{d\theta}{d\eta} \right)_{\eta_v=0}. \quad (16.5)$$

The *average heat transfer coefficient* \bar{Q}_x defined as $\bar{Q}_x = \bar{\alpha}_x (t_w - t_s) A$ is expressed as

$$\bar{\alpha}_x = \frac{4}{3} \lambda_{l,w} \left(\frac{1}{4} \text{Gr}_{x,l,s} \right)^{1/4} x^{-1} \left(-\frac{d\theta_l}{d\eta_l} \right)_{\eta_l=0}. \quad (16.6)$$

The *average Nusselt number* defined as $\bar{\text{Nu}}_{x,l,w} = \frac{\bar{\alpha}_x x}{\lambda_{l,w}}$ will be

$$\bar{\text{Nu}}_{x,l,w} = \frac{4}{3} \left(\frac{1}{4} \text{Gr}_{x,l,s} \right)^{1/4} \left(-\frac{d\theta_l}{d\eta_l} \right)_{\eta_l=0}. \quad (16.7)$$

Therefore, we have

$$\begin{aligned} Q_x &= \frac{4}{3} b x q_x \\ \bar{\alpha}_x &= \frac{4}{3} \alpha_x \\ \bar{\text{Nu}}_{x,w} &= \frac{4}{3} \text{Nu}_{x,w}. \end{aligned}$$

Obviously, the theoretical Eqs. (16.1)–(16.7) on heat transfer of laminar free condensation of liquid are identical to the corresponding equations in Chap. 8 on liquid laminar free convection, with only differences that the bulk temperature T_∞ and the *local Grashof number* $\text{Gr}_{x,\infty}$ of latter case are, respectively, replaced by the saturated temperature T_s and the local Grashof number $\text{Gr}_{x,l,s}$.

It is seen that, for practical calculation of heat transfer, only $\left(\frac{d\theta_l}{d\eta_l} \right)_{\eta_l=0}$ dependent on the solutions is no-given variable.

16.3 Wall Dimensionless Temperature Gradient

From the heat transfer analysis, it is found that heat transfer for the film condensation of vapor is in direct proportion to wall dimensionless temperature gradient $\left(\frac{d\theta_l}{d\eta_l} \right)_{\eta_l=0}$

the only one no-given variable for prediction of heat transfer. Then, correct prediction of the temperature gradient $\left(\frac{d\theta_l}{d\eta_l}\right)_{\eta_l=0}$ is the key work for prediction of heat transfer of the film condensation of vapor.

The numerical solutions for dimensionless temperature gradient $\left(\frac{d\theta_l}{d\eta_l}\right)_{\eta_l=0}$ for the film condensation of water vapor at the different wall subcooled grades $\frac{\Delta t_w}{t_s} = \frac{t_s - t_w}{t_s}$ and vapor superheated grades $\frac{\Delta t_\infty}{t_s} = \frac{t_\infty - t_s}{t_s}$ are obtained and described in Table 16.1, and plotted in Fig. 16.1.

It is seen that with increasing the wall subcooled grade $\frac{\Delta t_w}{t_s} = \frac{t_s - t_w}{t_s}$, the temperature gradient $\left(\frac{d\theta_l}{d\eta_l}\right)_{\eta_l=0}$ will decrease slower and slower. With increase of the vapor bulk superheated grade $\frac{\Delta t_\infty}{t_s} = \frac{t_\infty - t_s}{t_s}$, the temperature gradient $\left(\frac{d\theta_l}{d\eta_l}\right)_{\eta_l=0}$ will increase. However, the effect of the wall subcooled grade $\frac{\Delta t_w}{t_s} = \frac{t_s - t_w}{t_s}$ on the temperature gradient $\left(\frac{d\theta_l}{d\eta_l}\right)_{\eta_l=0}$ is more obvious than that of the vapor bulk superheated grade $\frac{\Delta t_\infty}{t_s} = \frac{t_\infty - t_s}{t_s}$.

Based on the numerical solutions, the wall dimensionless temperature gradient $\left(-\left(\frac{d\theta_l}{d\eta_l}\right)_{\eta_l=0}\right)_{\Delta t_\infty=0}$ for the film condensation of saturated water vapor is formulated by using a curve-fitting method. Then, the *formulation equation of the wall dimensionless temperature gradient* is shown as follows for the film condensation of saturated water vapor:

$$\left(-\left(\frac{d\theta_l}{d\eta_l}\right)_{\eta_l=0}\right)_{\Delta t_\infty=0} = \frac{1.74 - 0.19 \frac{\Delta t_w}{t_s}}{\left(\frac{\Delta t_w}{t_s}\right)^{1/4}} \quad \left(0.001 \leq \frac{\Delta t_w}{t_s} \leq 1\right) \quad (16.8)$$

The results predicted the numerical solutions, the wall dimensionless temperature gradient $\left(-\left(\frac{d\theta_l}{d\eta_l}\right)_{\eta_l=0}\right)_{\Delta t_\infty=0}$ for the film condensation of saturated water vapor by using Eq. (16.8) are listed in Table 16.1 compared with the related numerical solutions. It is seen that their agreement is very good.

Based on these numerical solutions, the following formulae are obtain by using a *curve matching method for practical prediction equation of wall dimensionless temperature gradient* $\left(\frac{d\theta_l}{d\eta_l}\right)_{\eta_l=0}$ for the laminar free convection film condensation of water vapor (saturated and superheated):

$$\begin{aligned} -\left(\frac{d\theta_l}{d\eta_l}\right)_{\eta_l=0} &= \left(-\left(\frac{d\theta_l}{d\eta_l}\right)_{\eta_l=0}\right)_{\Delta t_\infty=0} + a \cdot \frac{\Delta t_\infty}{t_s} \\ &\quad \left(0.05 \leq \frac{\Delta t_w}{t_s} \leq 1\right) \text{ and } \left(0 \leq \frac{\Delta t_\infty}{t_s} \leq 4.27\right) \end{aligned} \quad (16.9)$$

Table 16.1 Numerical and predicted results on wall dimensionless temperature gradient $\left(-\frac{d\theta}{d\eta}\right)_{\eta=0}$ for film condensation of water vapor (saturated and superheated) on a vertical flat plate

$\frac{\Delta t_{\text{sat}}}{t_s} (= \frac{t_{\infty} - t_s}{t_s})$	t_s °C							
	99.9	95	90	80	60	40	20	0
$\frac{\Delta t_{\text{sat}}}{t_s} (= \frac{t_s - t_w}{t_s} (t_s = 100^\circ\text{C}))$								
0.001	0.05	0.10	0.20	0.40	0.60	0.80	1.00	
$\left(-\frac{d\theta}{d\eta}\right)_{\eta=0}$								
0	9.8338	3.67507	3.06412	2.53975	2.07889	1.83238	1.6679	1.55107
	9.78367061	3.659561	3.060418	2.545083	2.092369	1.847492	1.679105	1.55
0.27	9.983	3.6966	3.0847	2.556	2.0912	1.8429	1.6772	1.5601
	10.6828	3.681212	3.077859	2.559133	2.10368	1.857466	1.688223	1.558505
1.27		3.7787	3.1518	2.6111	2.1355	1.8817	1.7126	1.5895
		3.761398	3.142456	2.611171	2.145608	1.894407	1.721994	1.590005
2.27	11.5745	3.8579	3.2165	2.6646	2.1783	1.9187	1.7454	1.6204
		3.841585	3.207053	2.663209	2.187529	1.931348	1.755764	1.621505
3.27	12.6908	3.9339	3.2819	2.716	2.2211	1.9556	1.7783	1.6503
		3.921772	3.271650	2.715247	2.229449	1.96828	1.789534	1.653005
4.27	14.0355	4.0099	3.3398	2.7665	2.2617	1.9911	1.8096	1.6793
		4.001958	3.336246	2.767285	2.271370	2.00522	1.8233053	1.684505

Note (1) denotes numerical solutions, and (2) denotes the results predicted by Eqs. (16.8)–(16.10)

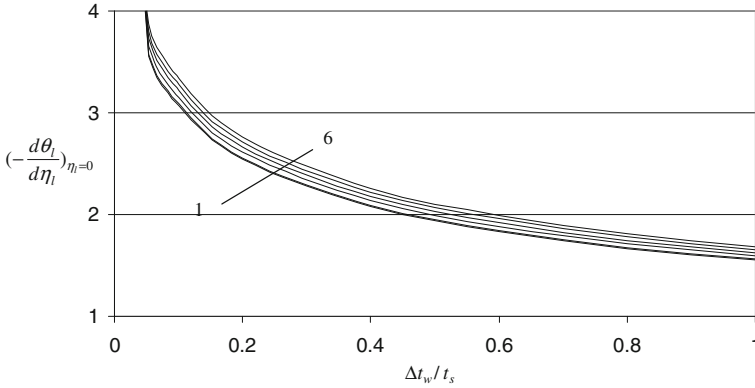


Fig. 16.1 Numerical solution of $-\left(\frac{d\theta_l}{d\eta_l}\right)_{\eta=0}$ for laminar free convection film condensation of water vapor lines 1 to 6: $\frac{\Delta t_\infty}{t_s} = \frac{t_\infty - t_s}{t_s} = 0, 0.27, 1.27, 2.27, 3.27,$ and $4.27,$ respectively

$$a = 0.0315 \times \left(\frac{\Delta t_w}{t_s}\right)^{-0.3119} \tag{16.10}$$

The results predicted by using Eqs. (16.8)–(16.10) on the wall dimensionless temperature gradient $-\left(\frac{d\theta_l}{d\eta_l}\right)_{\eta=0}$ for the film condensation of water vapor on a flat plate are listed in Table 16.1 compared with the related numerical solutions. It is seen that their agreement is pretty good.

16.4 Practical Prediction Equations on Condensation Heat Transfer

Combined with Eqs. (16.8)–(16.10), Eqs. (16.1)–(16.6) will become the following equations, respectively, for prediction on the heat transfer of laminar free convection film condensation of water vapor on a veridical flat plate:

Local heat transfer rate at position x per unit area on the plate can be predicted by

$$q_x = \lambda_{l,w}(t_w - t_s) \left(\frac{1}{4}\text{Gr}_{xl,s}\right)^{1/4} x^{-1} \left[\left(-\left(\frac{d\theta_l}{d\eta_l}\right)_{\eta=0}\right)_{\Delta t_\infty=0} + a \cdot \frac{\Delta t_\infty}{t_s} \right] \tag{16.1*}$$

The *local Nusselt number* can be predicted by

$$\text{Nu}_{xl,w} = \left(\frac{1}{4}\text{Gr}_{xl,s}\right)^{1/4} \left[\left(\left(\frac{d\theta_l}{d\eta_l}\right)_{\eta=0}\right)_{\Delta t_\infty=0} + a \cdot \frac{\Delta t_\infty}{t_s} \right] \tag{16.3*}$$

The *total heat transfer rate* for position $x = 0$ to x with width of b on the plate can be predicted by

$$Q_x = \frac{4}{3} b \lambda_{l,w} (t_w - t_s) \left(\frac{1}{4} \text{Gr}_{xl,s} \right)^{1/4} \left[\left(- \left(\frac{d\theta_l}{d\eta} \right)_{\eta=0} \right)_{\Delta t_\infty=0} + a \cdot \frac{\Delta t_\infty}{t_s} \right] \quad (16.4^*)$$

Here, the dimensionless temperature gradient on the wall for the film condensation of superheated water vapor, $\left(- \left(\frac{d\theta_l}{d\eta} \right)_{\eta=0} \right)_{\Delta t_\infty=0}$, and the coefficient a are calculated by Eqs. (16.8) to (16.10) respectively.

16.5 Mass Transfer Analysis

The *condensate mass transfer analysis* expressions for film condensation of vapor can be given below:

Set g_x to be a *local mass flow rate* entering the liquid film at position x per unit area of the plate. According to the boundary layer theory of fluid mechanics, g_x is expressed as

$$g_x = \rho_{l,s} \left(w_{xl,s} \frac{d\delta_l}{dx} - w_{yl,s} \right)_s$$

With Eqs. (14.16) and (14.17), the above equation is finally changed as

$$g_x = \rho_{l,s} \left[2\sqrt{gx} \left(\frac{\rho_{l,w} - \rho_{v,\infty}}{\rho_{l,s}} \right)^{1/2} W_{xl,s} \frac{1}{4} \eta_{l\delta} \left(\frac{1}{4} \text{Gr}_{xl,s} \right)^{-1/4} - 2\sqrt{gx} \left(\frac{\rho_{l,w} - \rho_{v,\infty}}{\rho_{l,s}} \right)^{1/2} \left(\frac{1}{4} \text{Gr}_{xl,s} \right)^{-4} W_{yl,s} \right]$$

The above equation is simplified to

$$g_x = 2\rho_{l,s} \left[W_{xl,s} \frac{1}{4} \eta_{l\delta} - W_{yl,s} \right] \sqrt{gx} \left(\frac{\rho_{l,w} - \rho_{v,\infty}}{\rho_{l,s}} \right)^{1/2} \left(\frac{1}{4} \text{Gr}_{xl,s} \right)^{-1/4} \quad (16.11)$$

With Eq. (14.14) for definition of $\text{Gr}_{xl,s}$, we have

$$\frac{\rho_{l,w} - \rho_{v,\infty}}{\rho_{l,s}} = \frac{v_{l,s}^2}{gx^3} \text{Gr}_{xl,s} \quad (16.12)$$

With Eqs. (16.12), Eq. (16.11) is changed to

$$g_x = 2\rho_{l,s} \left[W_{xl,s} \frac{1}{4}\eta l\delta - \sqrt{g_x} W_{yl,s} \right] \left(\frac{v_{l,s}^2}{g x^3} \text{Gr}_{xl,s} \right)^{1/2} \left(\frac{1}{4} \text{Gr}_{xl,s} \right)^{-1/4}$$

i.e.,

$$g_x = 4\rho_{l,s} \left[W_{xl,s} \frac{1}{4}\eta l\delta - W_{yl,s} \right] \sqrt{g_x} \left(\frac{v_{l,s}^2}{g^3} \right)^{1/2} \left(\frac{1}{4} \text{Gr}_{xl,s} \right)^{1/2} \left(\frac{1}{4} \text{Gr}_{xl,s} \right)^{-1/4}$$

The above equation is further simplified to

$$g_x = \mu_{l,s} x^{-1} \left(\frac{1}{4} \text{Gr}_{xl,s} \right)^{1/4} [\eta l\delta W_{xl,s} - 4W_{yl,s}]$$

i.e.,

$$g_x = \mu_{l,s} x^{-1} \left(\frac{1}{4} \text{Gr}_{xl,s} \right)^{1/4} \Phi_s \quad (16.13)$$

where

$$\Phi_s = \eta l\delta W_{xl,s} - 4W_{yl,s} \quad (16.14)$$

is defined as the *mass flow rate parameter* of the film condensation.

Take G_x to express *total mass flow rate* entering the boundary layer for position $x = 0$ to x with width of b of the plate, it should be the following integration:

$$\begin{aligned} G_x &= \iint_A g_x dA \\ &= b \int_0^x g_x dx \end{aligned}$$

where $A = b \cdot x$ is related area of the plate, and b is the related width of the plate.

Then, we obtain

$$G_x = b \int_0^x \mu_{l,s} x^{-1} \left(\frac{1}{4} \text{Gr}_{xl,s} \right)^{1/4} (\eta l\delta W_{xl,s} - 4W_{yl,s}) dx$$

With Eq. (13.15) for definition of $\text{Gr}_{xl,s}$, we obtain

$$G_x = \frac{4}{3} b \cdot \mu_{l,s} \left(\frac{1}{4} \text{Gr}_{xl,s} \right)^{1/4} (\eta l\delta W_{xl,s} - 4W_{yl,s})$$

or

$$G_x = \frac{4}{3} b \cdot \mu_{l,s} \left(\frac{1}{4} \text{Gr}_{x,l,s} \right)^{1/4} \Phi_s \quad (16.15)$$

16.6 Mass Flow Rate Parameter

From Eqs. (16.13) to (16.15), it follows that the mass flow rates of the condensate, g_x and G_x , depend on the defined local Grashof number $\text{Gr}_{x,l,s}$, absolute viscosity $\mu_{l,s}$ and mass flow rate parameter Φ_s of the film condensation. Obviously, for practical evaluation of the mass flow rate of the film condensation, only mass flow rate parameter Φ_s dependent on the numerical solutions is unknown variable. From Eq. (16.14), it is known that mass flow rate parameter Φ_s depends on the dimensionless condensate film thickness $\eta_{l\delta}$, as well as the dimensionless condensate velocity components at the liquid–vapor interface, $W_{x,l,s}$ and $W_{y,l,s}$.

16.6.1 Condensate Film Thickness and Velocity Components at the Interface

The numerical solutions on *dimensionless condensate film thickness* $\eta_{l\delta}$ for the film condensation of water vapor (saturated and superheated) with variation of Variation of the wall subcooled grade $\frac{\Delta t_w}{t_s} = \frac{t_s - t_w}{t_s}$ and vapor bulk superheated grade $\frac{\Delta t_\infty}{t_s} \left(= \frac{t_\infty - t_s}{t_s} \right)$ are listed in Table 16.2, and plotted in Fig. 16.2, respectively. Then, we can understand the following effects of wall subcooled Grade $\frac{\Delta t_w}{t_s} = \frac{t_s - t_w}{t_s}$ and vapor bulk superheated temperature $\frac{\Delta t_\infty}{t_s} \left(= \frac{t_\infty - t_s}{t_s} \right)$ on $\eta_{l\delta}$.

From Fig. 16.2, it is seen that with increasing the wall subcooled grade $\frac{\Delta t_w}{t_s} = \frac{t_s - t_w}{t_s}$, the condensate film thickness η_{δ_l} will increase, while with increasing vapor bulk superheated grade $\frac{\Delta t_\infty}{t_s} \left(= \frac{t_\infty - t_s}{t_s} \right)$, the condensate film thickness η_{δ_l} will decrease.

Furthermore, the effect of the wall subcooled grade $\frac{\Delta t_w}{t_s} = \frac{t_s - t_w}{t_s}$ on the condensate film thickness η_{δ_l} is more obvious than that of vapor bulk superheated grade $\frac{\Delta t_\infty}{t_s} \left(= \frac{t_\infty - t_s}{t_s} \right)$.

Meanwhile, the rigorous numerical solutions of the condensate liquid film thickness $(\eta_{l\delta})_{\Delta t_\infty=0}$ for the film condensation of saturated water vapor on a flat plate are formulated as follows by using a curve-fitting method:

$$(\eta_{l\delta})_{\Delta t_\infty=0} = 0.5934 \left(\frac{\Delta t_w}{t_s} \right)^{0.2562} \left(0.001 \leq \frac{\Delta t_w}{t_s} \leq 0.2 \right) \quad (16.16)$$

Table 16.2 Numerical solution of condensate film thickness η_{δ_f} with variation of $\frac{\Delta t_w}{t_s} = \frac{t_s - t_w}{t_s}$ and $\frac{\Delta t_{\infty}}{t_s} = \frac{t_s - t_{\infty}}{t_s}$ for laminar film condensation of superheated water vapor on a vertical flat plate

$\frac{\Delta t_{\infty}}{t_s} \left(= \frac{t_{\infty} - t_s}{t_s} \right)$	t_w , °C							
	99.9	95	90	80	60	40	20	0
$\frac{\Delta t_w}{t_s} = \frac{t_s - t_w}{t_s}$	0.001	0.05	0.10	0.20	0.40	0.60	0.80	1.00
η_{δ_f}								
0	(1) 0.10159	0.27283	0.32783	0.39827	0.49577	0.57703	0.65534	0.73559
	(2) 0.10109915	0.275437874	0.3289633	0.4059	0.4893	0.5727	0.6561	0.7395
0.27	(1) 0.10018	0.27116	0.32584	0.39587	0.4928	0.57355	0.6516	0.7311
	(2) 0.273912711	0.273912711	0.3272691	0.4038858	0.4867188	0.569649	0.6526764	0.735801
1.27	(1) 0.09361	0.26525	0.31885	0.3874	0.4823	0.5613	0.6375	0.71685
	(2) 0.268263961	0.268263961	0.3209941	0.3964258	0.4771588	0.558349	0.6399964	0.722101
2.27	(1) 0.0864	0.25978	0.3124	0.37953	0.4726	0.5501	0.625	0.70247
	(2) 0.262615211	0.262615211	0.3147191	0.3889658	0.4675988	0.547049	0.6273164	0.708401
3.27	(1) 0.0788	0.25475	0.30614	0.37227	0.4633	0.5394	0.613	0.68915
	(2) 0.256966461	0.256966461	0.3084441	0.3815058	0.4580388	0.535749	0.6146364	0.694701
4.27	(1) 0.07125	0.24991	0.3008	0.3654	0.4548	0.5295	0.602	0.67675
	(2) 0.251317711	0.251317711	0.3021691	0.3740458	0.4484788	0.524449	0.6019564	0.681001

Note: (1) denotes the numerical solutions, and (2) demonstrates the prediction values

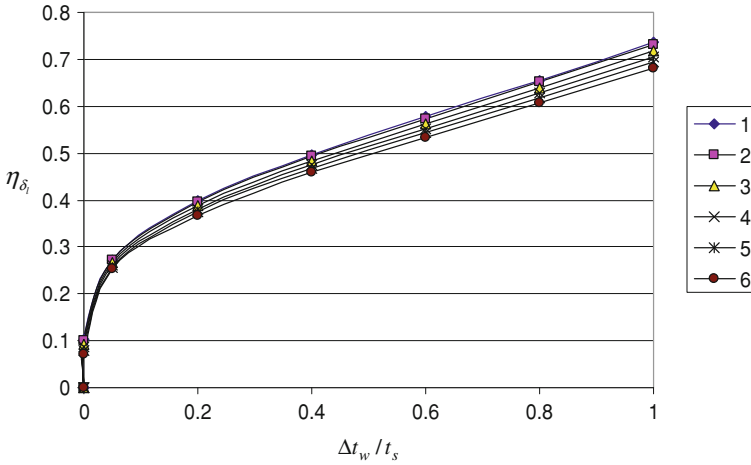


Fig. 16.2 Numerical solution of η_{δ_l} with $\frac{\Delta t_w}{t_s} = \frac{t_s - t_w}{t_s}$ and $\frac{\Delta t_\infty}{t_s} (= \frac{t_\infty - t_s}{t_s})$ for laminar film condensation of water vapor (saturated and superheated) lines 1-6: $\frac{\Delta t_\infty}{t_s} (= \frac{t_\infty - t_s}{t_s}) = 0, 0.27, 1.27, 2.27, 3.27,$ and $4.27,$ respectively

$$(\eta_{\delta})_{\Delta t_\infty=0} = 0.417 \frac{\Delta t_w}{t_s} + 0.3223 \quad \left(0.2 < \frac{\Delta t_w}{t_s} \leq 1 \right) \tag{16.17}$$

The results of the condensate liquid film thickness $(\eta_{l\delta})_{\Delta t_\infty=0}$ of the film condensation of saturated water vapor on a flat plate predicted by Eqs. (16.16) and (16.17) are listed in Table 16.2 compared with the related numerical solutions. It is seen that Eqs. (16.16) and (16.17) are coincident very well to the numerical solutions.

The rigorous numerical solutions of the condensate liquid film thickness $\eta_{l\delta}$ of the film condensation of water vapor (saturated and superheated) on a flat plate are formulated as following by using the curve-fitting method:

$$\eta_{l\delta} = (\eta_{l\delta})_{\Delta t_\infty=0} + a \frac{\Delta t_\infty}{t_s} \quad \left(0 \leq \frac{\Delta t_\infty}{t_s} \leq 4.27 \right) \tag{16.18}$$

where

$$a = 0.0045 \left(\frac{\Delta t_w}{t_s} \right)^2 - 0.0132 \left(\frac{\Delta t_w}{t_s} \right) - 0.005 \quad \left(0.05 \leq \frac{\Delta t_w}{t_s} \leq 1 \right) \tag{16.19}$$

The results on the condensate liquid film thickness $\eta_{l\delta}$ of the film condensation of superheated water vapor on a flat plate predicted by using Eqs. (16.18) and (16.19) are listed in Table 16.2 with the variation of wall subcooled grade $\frac{\Delta t_w}{t_s}$ and vapor superheated grade $\frac{\Delta t_\infty}{t_s}$, and compared with the related numerical results. It is found that such predicted results are very well coincident to the numerical solutions.

Table 16.3 Numerical solutions of $W_{xl,\delta}$ with $\frac{\Delta t_w}{t_s} = \frac{t_s - t_w}{t_s}$ and $\frac{\Delta t_\infty}{t_s} (= \frac{t_\infty - t_s}{t_s})$ for laminar free convection film condensation of water vapor (saturated and superheated)

$\frac{\Delta t_\infty}{t_s} (= \frac{t_\infty - t_s}{t_s})$	t_w °C							
	99.9	95	90	80	60	40	20	0
	$\frac{\Delta t_w}{t_s} = \frac{t_s - t_w}{t_s}$							
	0.001	0.05	0.10	0.20	0.40	0.60	0.80	1.00
$W_{xl,\delta}$								
0	0.005124	0.03542	0.04895	0.06609	0.08501	0.09455	0.09920	0.10100
0.27	0.005025	0.035019	0.04840	0.06534	0.08407	0.09353	0.09811	0.10003
1.27	0.00446	0.03360	0.04644	0.06272	0.08079	0.08995	0.09435	0.09657
2.27	0.003844	0.03230	0.04466	0.06032	0.07779	0.08667	0.09100	0.09308
3.27	0.00323	0.03112	0.04295	0.05814	0.07496	0.08360	0.08780	0.08987
4.37	0.00267	0.03000	0.04152	0.05611	0.07240	0.08078	0.08495	0.08692

Table 16.4 Numerical solutions of $-W_{yl,\delta}$ with $\frac{\Delta t_w}{t_s} = \frac{t_s - t_w}{t_s}$ and $\frac{\Delta t_\infty}{t_s} (= \frac{t_\infty - t_s}{t_s})$ for laminar film condensation of water vapor (saturated and superheated)

$\frac{\Delta t_\infty}{t_s} (= \frac{t_\infty - t_s}{t_s})$	t_w							
	99.9	95	90	80	60	40	20	1
	$\frac{\Delta t_w}{t_s} = \frac{t_s - t_w}{t_s}$							
	0.001	0.05	0.10	0.20	0.40	0.60	0.80	1.00
$-W_{yl,\delta}$								
0	0.00013	0.00241	0.00399	0.00648	0.01004	0.01230	0.01346	0.01362
0.27	0.000125	0.002367	0.003918	0.00636	0.0099	0.01209	0.01324	0.01339
1.27	0.000103	0.002219	0.003675	0.00597	0.00934	0.01135	0.01241	0.0121263
2.27	0.000082	0.002087	0.00346	0.00562	0.00873	0.01070	0.01171	0.01189
3.27	0.000062	0.001969	0.003258	0.00531	0.00823	0.01010	0.01106	0.01124
4.27	0.000046	0.001861	0.003093	0.00503	0.00780	0.0096	0.01048	0.01064

16.6.2 Interfacial Velocity Components

Furthermore, the numerical solutions on the *dimensionless condensate velocity components* at the liquid–vapor interface, $W_{xl,s}$ and $W_{yl,s}$, for the film condensation of water vapor (saturated and superheated) with variation of the *wall subcooled grade* $\frac{\Delta t_w}{t_s} = \frac{t_s - t_w}{t_s}$ and vapor bulk superheated grade $\frac{\Delta t_\infty}{t_s} (= \frac{t_\infty - t_s}{t_s})$ are listed in Tables 16.3 and 16.4, and plotted in Figs. 16.3 and 16.4 respectively. Then, we can understand the effects of wall subcooled Grade $\frac{\Delta t_w}{t_s} = \frac{t_s - t_w}{t_s}$ and *vapor bulk superheated temperature* $\frac{\Delta t_\infty}{t_s} (= \frac{t_\infty - t_s}{t_s})$ on $W_{xl,s}$ and $W_{yl,s}$.

It is seen from Figs. 16.3 and 16.4 that with increasing the wall subcooled grade $\frac{\Delta t_w}{t_s} = \frac{t_s - t_w}{t_s}$, the velocity components $W_{xl,s}$ and $-W_{yl,s}$ will increase, especially

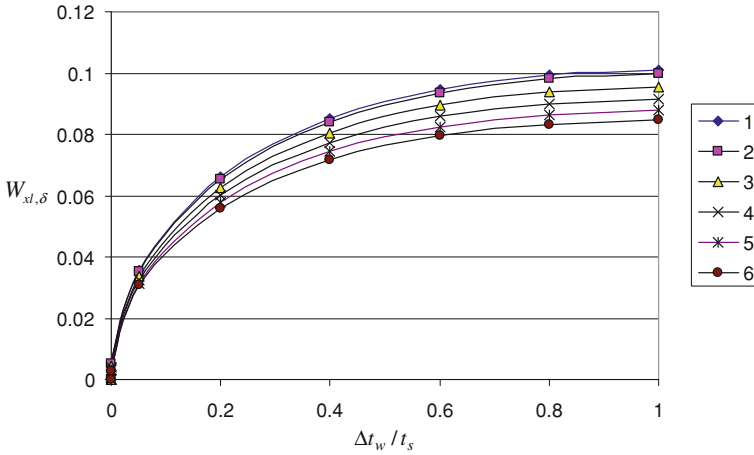


Fig. 16.3 Numerical solution of $W_{xl,\delta}$ with $\frac{\Delta t_w}{t_s} = \frac{t_s - t_w}{t_s}$ and $\frac{\Delta t_\infty}{t_s} (= \frac{t_\infty - t_s}{t_s})$ for laminar film condensation of water vapor (saturated and superheated) lines 1–6: $\frac{\delta t_\infty}{t_s} (= \frac{t_\infty - t_s}{t_s}) = 0, 0.27, 1.27, 2.27, 3.27,$ and 4.27 , respectively

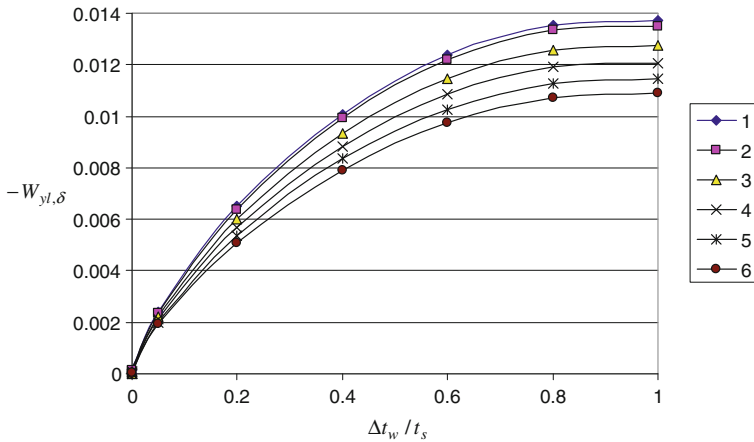


Fig. 16.4 Numerical solution of $-W_{yl,\delta}$ with $\frac{\Delta t_w}{t_s} = \frac{t_s - t_w}{t_s}$ and $\frac{\Delta t_\infty}{t_s} (= \frac{t_\infty - t_s}{t_s})$ for laminar free convection film condensation of water vapor (saturated and superheated) lines 1–6: $\frac{\Delta t_\infty}{t_s} (= \frac{t_\infty - t_s}{t_s}) = 0, 0.27, 1.27, 2.27, 3.27,$ and 4.27 , respectively

for smaller wall subcooled grade $\frac{\Delta t_w}{t_s} = \frac{t_s - t_w}{t_s}$. While with increasing the bulk superheated grade $\frac{\Delta t_\infty}{t_s} (= \frac{t_\infty - t_s}{t_s})$, the velocity components $W_{xl,s}$ and $-W_{yl,s}$ will decrease.

16.6.3 Condensate Mass Flow Rate Parameter

Based on the numerical solutions listed in Table 16.2 to Fig. 16.4 on the dimensionless condensate film thickness $\eta_{l\delta}$, and dimensionless condensate film velocity components at the liquid–vapor interface, $W_{xl,s}$ and $-W_{yl,s}$, the numerical solutions on Φ_s for the film condensation of water vapor (saturated and superheated) on a flat plate, with variation of the wall subcooled grade $\frac{\Delta t_w}{t_s} = \frac{t_s - t_w}{t_s}$ and vapor bulk superheated grade $\frac{\Delta t_\infty}{t_s} (= \frac{t_\infty - t_s}{t_s})$ are evaluated by using Eq. (16.14), listed in Table 16.5, and plotted in Fig. 16.5.

It is seen from Fig. 16.5 that with increase of the wall subcooled grade $\frac{\Delta t_w}{t_s} = \frac{t_s - t_w}{t_s}$, the mass flow rate parameter Φ_s will increase, especially for the smaller wall subcooled grade $\frac{\Delta t_w}{t_s} = \frac{t_s - t_w}{t_s}$. While with increase of the vapor bulk superheated grade $\frac{\Delta t_\infty}{t_s} (= \frac{t_\infty - t_s}{t_s})$, the mass flow rate parameter Φ_s will decrease. On the other hand, effect of the wall subcooled grade $\frac{\Delta t_w}{t_s} = \frac{t_s - t_w}{t_s}$ on the mass flow rate parameter Φ_s is more obvious than that of the vapor bulk superheated grade $\frac{\Delta t_\infty}{t_s} (= \frac{t_\infty - t_s}{t_s})$.

According to the corresponding numerical solutions, the expressions for the condensate mass flow rate parameter $(\Phi_s)_{\Delta t_\infty=0}$ of the film condensation of saturated water vapor are obtained as follows by means of a curve-matching method:

$$(\Phi_s)_{\Delta t_\infty=0} = \left(0.186 - 0.057 \frac{\Delta t_w}{t_s}\right) \left(\frac{\Delta t_w}{t_s}\right)^{3/4} \left(0.001 \leq \frac{\Delta t_w}{t_s} \leq 1\right) \quad (16.20)$$

The predicted values on $(\Phi_s)_{\Delta t_\infty=0}$ by using Eq. (16.20) are listed in Table 16.5 compared with the related numerical solutions, and it is seen that the agreement is pretty good.

According to the corresponding numerical solutions, the expressions for the condensate mass flow rate parameter Φ_s of the film condensation of water vapor (both of saturated vapor and superheated vapor) are obtained as follows by means of a curve-matching method:

$$\text{For } 0 \leq \frac{\Delta t_\infty}{t_s} \leq 4.27$$

$$\Phi_s = (\Phi_s)_{\Delta t_\infty=0} - B \frac{\Delta t_\infty}{t_s} \left(0.05 \leq \frac{\Delta t_w}{t_s} \leq 1\right) \quad (16.21)$$

where

$$B = 10^{-4} \times \left[2.756 + 121.4 \frac{\Delta t_w}{t_s} - 60 \left(\frac{\Delta t_w}{t_s}\right)^2\right] \left(0.05 \leq \frac{\Delta t_w}{t_s} \leq 1\right) \quad (16.22)$$

Table 16.5 Numerical solutions and predicted results on Φ_s with $\frac{\Delta t_w}{t_s} = \frac{t_s - t_w}{t_s}$ and $\frac{\Delta t_o}{t_s} = \left(\frac{t_o - t_s}{t_s} \right)$ for laminar free convection film condensation of water vapor (saturated and superheated)

$\frac{\Delta t_o}{t_s} \left(= \frac{t_o - t_s}{t_s} \right)$	t_w °C									
	99.9	95	90	80	60	40	20	0		
$\frac{\Delta t_w}{t_s} = \frac{t_s - t_w}{t_s}$										
0.001	0.05	0.1	0.20	0.40	0.60	0.80	1.00			
Φ_s										
0	(1) 0.001041	0.019304	0.032007	0.052242	0.082305	0.103758	0.11885	0.128775		
	(2)	0.0193657	0.0320623	0.0522175	0.0820852	0.1034868	0.1187639	0.129		
0.27	(1) 0.001003	0.018965	0.031443	0.051306	0.08103	0.102004	0.116888	0.126692		
	(2)	0.0191315	0.0316763	0.0515524	0.0809589	0.1020289	0.1171040	0.1272677		
1.27	(1) 0.00083	0.017788	0.029507	0.048178	0.076325	0.095889	0.109788	0.119746		
	(2)	0.0182639	0.0302467	0.0490888	0.0767873	0.0966293	0.1109564	0.1208521		
2.27	(1) 0.00066	0.016739	0.027792	0.045373	0.071684	0.090477	0.103715	0.112946		
	(2)	0.0173963	0.0288171	0.0466252	0.0726157	0.0912297	0.1048088	0.1144365		
3.27	(1) 0.000503	0.015804	0.026181	0.042884	0.067649	0.085494	0.098061	0.106893		
	(2)	0.0165287	0.0273875	0.0441616	0.0684441	0.0858301	0.0986612	0.1080209		
4.27	(1) 0.0003742	0.014943	0.0248612	0.0406225	0.0641275	0.0811730	0.0930599	0.1013831		
	(2)	0.0156611	0.0259579	0.0416980	0.0642725	0.0804305	0.0925136	0.1016053		

(1) Numerical solutions and (2) predicted results

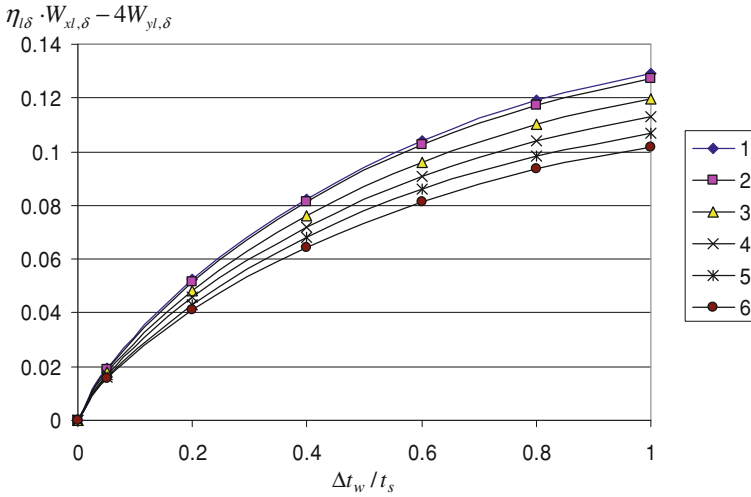


Fig. 16.5 Numerical results of $\Phi_s = \eta_{l\delta} W_{xl,s} - 4W_{yl,s}$ with $\frac{\Delta t_w}{t_s} \left(= \frac{t_s - t_w}{t_s} \right)$ and $\frac{\Delta t_\infty}{t_s} \left(= \frac{t_\infty - t_s}{t_s} \right)$ for laminar free convection film condensation of water vapor (saturated and superheated) Lines 1 to 6: $\frac{\Delta t_\infty}{t_s} \left(= \frac{t_\infty - t_s}{t_s} \right) = 0, 0.27, 1.27, 2.27, 3.27$ and 4.27 , respectively

The results on the condensate mass flow rate parameter Φ_s evaluated by using Eqs. (16.20)–(16.22) are listed in Table 16.5 compared with the related numerical solutions. It is seen that their agreement is pretty good.

16.7 Practical Prediction Equations on Condensation Mass Transfer

With Eqs. (16.20) to (16.22), Eq. (16.15) becomes

for $(0 \leq \frac{\Delta t_\infty}{t_s} \leq 4.27$ and $0.05 \leq \frac{\Delta t_w}{t_s} \leq 1)$

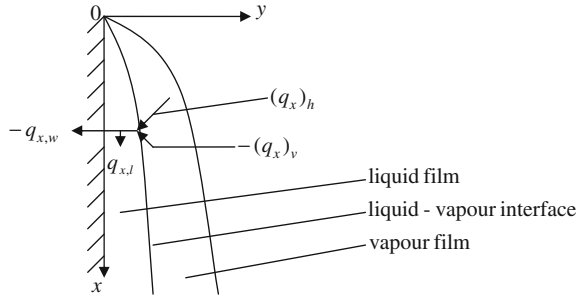
$$G_x = \frac{4}{3} b \cdot \mu_{l,s} \left(\frac{1}{4} Gr_{xl,s} \right)^{1/4} \left[\left(0.186 - 0.057 \frac{\Delta t_w}{t_s} \right) \left(\frac{\Delta t_w}{t_s} \right)^{3/4} - B \frac{\Delta t_\infty}{t_s} \right] \tag{16.15*}$$

where

$$B = 10^{-4} \times \left[2.756 + 121.4 \frac{\Delta t_w}{t_s} - 60 \left(\frac{\Delta t_w}{t_s} \right)^2 \right] \tag{16.22}$$

Equation (16.15*) with Eq. (16.23). This equation can be used to practically predict mass transfer of laminar free convection film condensation of water vapor on a vertical flat plate.

Fig. 16.6 Diagram of equivalent heat and transfer with the two-phase free convection film condensation



16.8 Condensate Mass–Energy Transformation Equation

16.8.1 Theoretical Analysis on Condensate Mass–Energy Transformation

The diagram of heat transfer balance with the two-phase flow free convection film condensation is expressed in Fig. 16.6. At the liquid–vapor interface, the liquid heat conduction $(q_x)_l$ is balanced by the latent heat of vapor condensation, $(q_h)_h = h_{fg}g_x$, and the vapor heat conduction $(q_x)_v$, i.e.,

$$(q_x)_l = h_{fg}g_x - (q_x)_v \tag{16.23}$$

It is indicated that the negative signs of the heat transfer rate express that the direction of the related heat fluxes are negative to the coordinative direction.

Additionally, the interfacial liquid heat conductivity rate $(q_x)_l$ is divided to two parts, and shown as below:

$$(q_x)_l = -q_{x,w} + q_{x,l} \tag{16.24}$$

where $q_{x,w}$ is the defined condensation heat transfer rate on the wall, and $q_{x,l}$ is the heat transfer rate brought out by the liquid film flow.

With Eq. (16.24), Eq. (16.23) becomes

$$h_{fg}g_x - (q_x)_v \equiv -q_{x,w} + q_{x,l} \tag{16.25}$$

If we focus on the film condensation of saturated vapor, the vapor heat conduction can be regarded as $(q_x)_v = 0$. Then, Eq. (16.25) is described as

$$h_{fg}g_x = -q_{x,w} + q_{x,l} \tag{16.26}$$

By ignoring $q_{x,l}$ on the defined condensation heat transfer rate on the wall, Eq. (16.26) becomes

$$h_{fg}g_x = -q_{x,w} \tag{16.27}$$

With Eqs. (16.1) and (16.15), Eq. (16.27) becomes

$$h_{fg}\mu_{l,s}x^{-1}\left(\frac{1}{4}\text{Gr}_{xl,s}\right)^{1/4}\Phi_s = -\lambda_{l,w}(t_w - t_s)\left(\frac{1}{4}\text{Gr}_{xl,s}\right)^{1/4}x^{-1}\left(-\frac{d\theta_l}{d\eta_l}\right)_{\eta_l=0}$$

With definitions of $\text{Gr}_{xv,\infty}$ and $\text{Gr}_{xl,s}$, the above equation becomes

$$\left(-\frac{d\theta_l}{d\eta_l}\right)_{\eta_l=0} = C_{mh}\Phi_s \quad (16.28)$$

where

$$C_{mh} = \frac{\mu_{l,s}h_{fg}}{\lambda_{l,w}(t_s - t_w)} \quad (16.29)$$

Here, Eq. (16.28) with Eq. (16.29) is regarded as the *condensate mass–energy transformation equation* for laminar free convection film condensation of saturated vapor. C_{mh} is the related condensate mass–energy transformation coefficients dependent on the wall subcooled temperature and the some special physical properties. It is interesting that Eqs. (16.28) and (16.29) for laminar free convection film condensation are identical to those in [4] (see its Chap. 11) for laminar forced convection film condensation. Obviously, the condensate mass–energy transformation Eq. (16.28) with Eq. (16.29) is universally suitable for laminar free or forced film condensation.

16.8.2 Condensate Mass–Energy Transformation Coefficient

From Eqs. (16.28) and (16.29) it is found that there are two approaches for determination of the condensate mass–energy transformation coefficients. They are numerical solution and prediction value.

Numerical solution

From Eq. (16.28) we can obtain the numerical solution on the condensate mass–energy transformation coefficient of the laminar free convection film condensation of vapor as follows:

$$C_{mh} = \frac{\left(-\frac{d\theta_l(\eta_l)}{d\eta_l}\right)_{\eta_l=0}}{\Phi_s} \quad (16.30)$$

By using Eq. (16.30) and numerical solutions of the wall dimensionless temperature gradient $\left(-\frac{d\theta_l(\eta_l)}{d\eta_l}\right)_{\eta_l=0}$ and condensate mass flow rate parameter Φ_s , the numerical solutions of densate mass–energy transformation coefficient on the laminar free convection film condensation of saturated water vapor are obtained, listed in Table 16.6, and plotted in Fig. 16.7.

Table 16.6 Evaluated results on C_{mh} based on Eq. (16.26), and Eq. (16.27) with numerical solutions Φ_s and $\left(-\frac{d\theta_s(\eta)}{d\eta}\right)_{\eta=0}$ for laminar free convection film condensation of water vapor on a horizontal flat plate

$\frac{\Delta t_w}{f_s}$	0.05	0.1	0.2	0.4	0.6	0.8	1
$t_s - t_w$ °C	5	10	20	40	60	80	100
t_w °C	95	90	80	60	40	20	0
$\lambda_{l,w} W / (\text{m K})$	0.6750	0.6727	0.6669	0.6506	0.6278	0.5986	0.563
$\left(-\frac{d\theta_s(\eta)}{d\eta}\right)_{\eta=0}$ (numerical solutions)	3.674	3.066	2.5408	2.079	1.8322	1.6681	1.5504
Φ_s (numerical solutions)	0.019304	0.032007	0.052242	0.082305	0.103758	0.11885	0.128775
$C_{\text{mh}}^* = \frac{\left(-\frac{d\theta_s(\eta)}{d\eta}\right)_{\eta=0}}{\Phi_s}$ (numerical solution)	190.326812	95.7907121	48.6355103	25.2595796	17.6583657	14.0353708	12.0396423
$C_{\text{mh}}^{**} = \frac{\mu_{l,s} h_{\text{fg}}}{\lambda_{l,w} (t_s - t_w)}$ (prediction)	188.92763	94.786792	47.8055743	24.5016427	16.9276508	13.3150424	11.3255906
$\frac{C_{\text{mh}}^{**} - C_{\text{mh}}^*}{C_{\text{mh}}^*}$	-0.007406	-0.010591	-0.017361	-0.030934	-0.043167	-0.054099	-0.063048

Note the present values of physical properties $\lambda_{l,w}$, $\mu_{l,s}$ and h_{fg} are corresponding to the numerical program. ($\mu_{l,s} = 282.5 \times 10^{-6} \text{ Kg}/(\text{m s})$, $h_{\text{fg}} = 2257.1 \text{ kJ}/\text{kg}$)

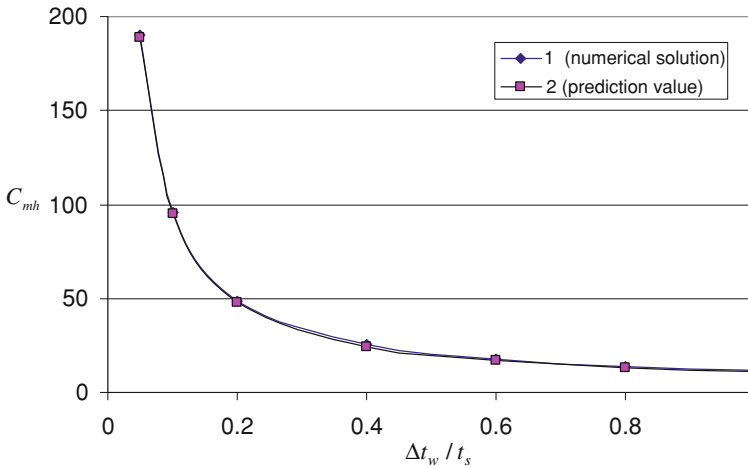


Fig. 16.7 Numerical solutions and prediction values C_{mh} for laminar free convection film condensation of saturated water vapor

Prediction value

Equation (16.29) expresses the prediction value on the condensate mass–energy transformation coefficient for the laminar free convection film condensation of vapor. With Eq. (16.29), the value on the condensate mass–energy transformation coefficient of laminar free convection film condensation of vapor only depend on physical conditions. Now, the prediction value on the condensate mass–energy transformation coefficient of laminar free film condensation of saturated water vapor are evaluated by using Eq. (16.29), listed in Table 16.6, and plotted in Fig. 16.7.

It is seen that the values of mass–energy transformation coefficient C_{mh} obtained by the different approaches are well coincident. However, their deviation is caused by omitting the film condensation of saturated vapor, the vapor heat conduction $(q_x)_v$.

It should be indicated that, according to the derivation, the condensate mass–energy transformation Eq. (16.28) with (16.29) is universally suitable for any laminar forced film condensation.

16.9 Summary

So far, we have presented the recent developments on laminar free convection film condensation of vapor (both saturated and superheated vapor). On this basis, governing equations, heat and mass transfer with the related equations of the laminar free convection film condensation of vapor (saturated and superheated) can be summarized in Tables 16.7 and 16.8, respectively.

Table 16.7 Summary of governing equations of laminar free convection film condensation of vapor

Term	Equations
<i>Partial differential equations for condensate liquid film</i>	
Mass equation	$\frac{\partial}{\partial x} (\rho_l w_{x,l}) + \frac{\partial}{\partial y} (\rho_l w_{y,l}) = 0$
Momentum equation	$\rho_l \left(w_{x,l} \frac{\partial w_{x,l}}{\partial x} + w_{y,l} \frac{\partial w_{x,l}}{\partial y} \right) = \frac{\partial}{\partial y} \left(\mu_l \frac{\partial w_{x,l}}{\partial y} \right) + g(\rho_l - \rho_{v,\infty})$
Energy equation	$\rho_l c_{p,l} \left(w_{x,l} \frac{\partial t_l}{\partial x} + w_{y,l} \frac{\partial t_l}{\partial y} \right) = \frac{\partial}{\partial y} \left(\lambda_l \frac{\partial t_l}{\partial y} \right)$
<i>Partial differential equations for vapor film</i>	
Mass equation	$\frac{\partial}{\partial x} (\rho_v w_{x,v}) + \frac{\partial}{\partial y} (\rho_v w_{y,v}) = 0$
Momentum equation	$\rho_v \left(w_{x,v} \frac{\partial w_{x,v}}{\partial x} + w_{y,v} \frac{\partial w_{x,v}}{\partial y} \right) = \frac{\partial}{\partial y} \left(\mu_v \frac{\partial w_{x,v}}{\partial y} \right) + g(\rho_v - \rho_{v,\infty})$
Energy equation	$\rho_v c_{p,v} \left(w_{x,v} \frac{\partial T_v}{\partial x} + w_{y,v} \frac{\partial T_v}{\partial y} \right) = \frac{\partial}{\partial y} \left(\lambda_v \frac{\partial T_v}{\partial y} \right)$
<i>Boundary conditions</i>	
$y = 0$	$w_{x,l} = 0, w_{y,l} = 0, t_l = t_w$
$y = \delta_l$	$w_{x,l,s} = w_{x,v,s}$
	$\rho_{l,s} \left(w_{x,l} \frac{\partial \delta_l}{\partial x} - w_{y,l} \right)_s = \rho_{v,s} \left(w_{x,v} \frac{\partial \delta_v}{\partial x} - w_{y,v} \right)_s$
	$\mu_{l,s} \left(\frac{\partial w_{x,l}}{\partial y} \right)_s = \mu_{v,s} \left(\frac{\partial w_{x,v}}{\partial y} \right)_s$
	$-\lambda_{l,s} \left(\frac{\partial t_l}{\partial y} \right)_{y=\delta_l} = h_{fg} \rho_{l,s} \left(w_{x,l} \frac{\partial \delta_l}{\partial x} - w_{y,l} \right)_s - \lambda_{v,s} \left(\frac{\partial t_v}{\partial y} \right)_{y=\delta_l}$
	$T = T_s$
$y \rightarrow \infty$	$w_{x,v} \rightarrow 0, T_v \rightarrow T_\infty$
<i>Assumed similarity variables based on the new similarity analysis method for condensate liquid film</i>	
η_l	$\left(\frac{1}{4} \text{Gr}_{x,l,s} \right)^{1/4} \frac{y}{x}$
$\text{Gr}_{x,l,s}$	$\frac{g(\rho_l w - \rho_{v,\infty}) x^3}{\nu_{l,s}^2 \rho_{l,s}}$
θ_l	$\frac{t_l - t_s}{t_w - t_s}$

(continued)

Table 16.7 (continued)

Term	Equations
w_{xI}	$\left(2\sqrt{g\bar{x}} \left(\frac{\rho_{l,w} - \rho_{v,\infty}}{\rho_{l,s}} \right)^{1/2} \right)^{-1} w_{xI}$
w_{yI}	$\left(2\sqrt{g\bar{x}} \left(\frac{\rho_{l,w} - \rho_{v,\infty}}{\rho_{l,s}} \right)^{1/2} \left(\frac{1}{4} Gr_{xI, s} \right)^{-1/4} \right)^{-1} w_{yI}$
<i>Ordinary differential equations for condensate liquid film</i>	
Mass equation	$2w_{xI} - \eta_l \frac{dw_{xI}}{d\eta_l} + 4 \frac{dw_{xI}}{d\eta_l} + \frac{1}{\rho_l} \frac{d\rho_l}{d\eta_l} (-\eta_l W_{xI} + 4W_{yI}) = 0$
Momentum equation	$\frac{\nu_{l,s}}{\nu_l} \left(W_{xI} \left(2W_{xI} - \eta_l \frac{dw_{xI}}{d\eta_l} \right) + 4W_{yI} \frac{dw_{xI}}{d\eta_l} \right) = \frac{d^2 w_{xI}}{d\eta_l^2} + \frac{1}{\mu_l} \frac{d\mu_l}{d\eta_l} \frac{dw_{xI}}{d\eta_l} + \frac{\mu_{l,s}}{\mu_l} \frac{\rho_{l,s}}{\rho_{l,w} - \rho_{v,\infty}}$
Energy equation	$Pr_l \frac{\rho_l}{\rho_{l,s}} \frac{\mu_{l,s}}{\mu_l} (-\eta_l W_{xI} + 4W_{yI}) \frac{d\theta_l}{d\eta_l} = \frac{d^2 \theta_l}{d\eta_l^2} + \frac{1}{\lambda_l} \frac{d\lambda_l}{d\eta_l} \frac{d\theta_l}{d\eta_l}$
<i>Assumed similarity variables based on the new similarity analysis method for vapor film</i>	
η_v	$\eta_v = \left(\frac{1}{4} Gr_{xv,\infty} \right)^{1/4} \frac{y}{x}$
$Gr_{xv,\infty}$	$\frac{g(\rho_{v,s}/\rho_{v,\infty} - 1)x^3}{\nu_{v,\infty}^2}$
θ_v	$\frac{T_v - T_\infty}{T_s - T_\infty}$
W_{xv}	$\left(2\sqrt{g\bar{x}} (\rho_{v,s}/\rho_{v,\infty} - 1)^{1/2} \right)^{-1} w_{xv}$
W_{yv}	$\left(2\sqrt{g\bar{x}} (\rho_{v,s}/\rho_{v,\infty} - 1)^{1/2} \left(\frac{1}{4} Gr_{xv,\infty} \right)^{-1/4} \right)^{-1} w_{yv}$
<i>Ordinary differential equations for vapor film</i>	
Mass equations	$2W_{xv} - \eta_v \frac{dW_{xv}}{d\eta_v} + 4 \frac{dW_{xv}}{d\eta_v} + \frac{1}{\rho_v} \frac{d\rho_v}{d\eta_v} (-\eta_v W_{xv} + 4W_{yv}) = 0$
Momentum Equation	$\frac{\nu_{v,\infty}}{\nu_v} \left(W_{xv} \left(2W_{xv} - \eta_v \frac{dW_{xv}}{d\eta_v} \right) + 4W_{yv} \left(\frac{dW_{xv}}{d\eta_v} \right) \right) = \frac{d^2 W_{xv}}{d\eta_v^2} + \frac{1}{\mu_v} \frac{d\mu_v}{d\eta_v} \frac{dW_{xv}}{d\eta_v} + \frac{\mu_{v,\infty}}{\mu_v} \frac{\rho_{v,\infty}}{\rho_{v,s} - \rho_{v,\infty}}$
Energy equation	$Pr_v \frac{\nu_{v,\infty}}{\nu_v} (-\eta_v W_{xv} + 4W_{yv}) \frac{d\theta_v}{d\eta_v} = \frac{d^2 \theta_v}{d\eta_v^2} + \frac{1}{\lambda_v} \frac{d\lambda_v}{d\eta_v} \frac{d\theta_v}{d\eta_v}$

Table 16.7 (continued)

Term	Equations
<i>Dimensionless boundary conditions</i>	
$\eta_l = 0$	$w_{xl} = 0, w_{yl} = 0, \theta_l = 1$
$\eta_l = \eta_{l\delta} (\eta_v = 0)$	$W_{xv,s} = \left(\frac{\rho_{l,w} - \rho_{v,\infty}}{\rho_{l,s}} \right)^{1/2} \left(\frac{\rho_{v,s} - \rho_{v,\infty}}{\rho_{v,\infty}} \right)^{-1/2} W_{x,l,s}$ $w_{y,v,s} = -0.25 \frac{\rho_{l,s}}{\rho_{v,s}} \left(\frac{v_{l,s}}{v_{v,\infty}} \right)^{1/2} \left(\frac{\rho_{l,w} - \rho_{v,\infty}}{\rho_{l,s}} \right)^{1/4} \left(\frac{\rho_{v,s} - \rho_{v,\infty}}{\rho_{v,\infty}} \right)^{-1/4} (\eta_{l,\lambda} W_{x,l,s} - 4W_{y,l,s})$ $\left(\frac{dW_{xv}}{d\eta_v} \right)_{\eta_v} = 0 = \frac{\mu_{l,s}}{\mu_{v,s}} \left(\frac{v_{l,s}}{v_{v,s}} \right)^{1/2} \left(\frac{\rho_{l,w} - \rho_{v,\infty}}{\rho_{l,s}} \right)^{3/4} \left(\frac{\rho_{v,s} - \rho_{v,\infty}}{\rho_{v,\infty}} - 1 \right)^{-3/4} \left(\frac{dW_{x,l}}{d\eta_l} \right) \eta_l = \eta_{l,\delta}$ $\left(\frac{d\theta_v}{d\eta_l} \right)_{\eta_v} = \eta_{v,\delta}$ $= \frac{\lambda_{l,s} (w - t_s) \left(\frac{v_{v,\infty}}{v_{l,s}} \right)^{1/2} \left(\frac{\rho_{l,w} - \rho_{v,\infty}}{\rho_{l,s}} \right)^{1/4} (\rho_{v,s} / \rho_{v,\infty} - 1)^{1/4} \left(\frac{d\theta_l}{d\eta_l} \right) \eta_l = \eta_{l,\delta} + 4H_{fg} \rho_{v,s} v_{v,\infty} W_{y,v,s}}{\lambda_{v,s} (T_s - T_\infty)}$
$\eta_v \rightarrow \infty$	$\theta_l = 0, \theta_y = 1$
<i>Equations on treatment of variable physical properties</i>	$W_{xv} = 0, \theta_v = 0$
For medium of liquid film	Equations with polynomial approach
(Take the film condensation of water vapor as example)	$\rho_l = -4.48 \times 10^{-3} T_l^2 + 999.9$
	$\lambda_l = -8.01 \times 10^{-6} T_l^2 + 1.94 \times 10^{-3} T_l + 0.563$
	$\mu_l = \exp \left[-1.6 - \frac{1150}{T_l} + \left(\frac{690}{T_l} \right)^2 \right] \times 10^{-3}$
	Equations of physical property factors
	$\frac{1}{\rho_l} \frac{d\rho_l}{d\eta_l} = \frac{[-(-2 \times 4.48 \times 10^{-3} T_l)(w - t_s) \frac{d\theta_l}{d\eta_l}]}{(-4.48 \times 10^{-3} T_l^2 + 999.9)}$
	$\frac{1}{\mu_l} \frac{d\mu_l}{d\eta_l} = \left(\frac{1150}{T_l^2} - 2 \times \frac{690}{T_l^3} \right) (t_w - t_s) \frac{d\theta_l}{d\eta_l}$

(continued)

Table 16.7 (continued)

Term	Equations
	$\frac{1}{\lambda_l} \frac{d\lambda_l}{dt} = \frac{[-2 \times 8.01 \times 10^{-6} t_f + 1.94 \times 10^{-3}] (t_w - t_s) \frac{dt_f}{dt}}{-8.01 \times 10^{-6} t_f^2 + 1.94 \times 10^{-3} t_f + 0.563}$
	$\frac{\mu_{l,s}}{\mu_l} = \exp \left(1150 \left(\frac{1}{T_l} - \frac{1}{T_s} \right) + 690^2 \left(\frac{1}{T_s} - \frac{1}{T_l} \right) \right)$
	$\frac{\nu_{l,s}}{\nu_l} = \frac{\mu_{l,s}}{\mu_l} \frac{\rho_l}{\rho_{l,s}} = \exp \left(1150 \left(\frac{1}{T_l} - \frac{1}{T_s} \right) + 690^2 \left(\frac{1}{T_s} - \frac{1}{T_l} \right) \right) \frac{-4.48 \times 10^{-3} t_f^2 + 999.9}{-4.48 \times 10^{-3} t_f^2 + 999.9}$
	$\text{Pr}_{l,s} \frac{\rho_l}{\rho_{l,s}} \frac{\lambda_{l,s}}{\lambda_l} = \text{Pr}_{l,s} \left(\frac{-4.48 \times 10^{-3} t_f^2 + 999.9}{-4.48 \times 10^{-3} t_f^2 + 999.9} \right) \left(\frac{-8.01 \times 10_6 t_f^2 + 1.94 \times 10^{-3} t_f + 0.0563}{-8.01 \times 10_6 t_f^2 + 1.94 \times 10^{-3} t_f + 0.0563} \right)$
For medium of vapor film	Equations with temperature parameter method based on simple power-law of gas
	$\frac{\mu_{v,\infty}}{\mu_{v,0}} = \left(\frac{T_{v,\infty}}{T_{v,0}} \right)^{n_\mu}$
	$\frac{\lambda_{v,\infty}}{\lambda_{v,0}} = \left(\frac{T_{v,\infty}}{T_{v,0}} \right)^{n_\lambda}$
	$\frac{\rho_{v,\infty}}{\rho_{v,0}} = \left(\frac{T_{v,\infty}}{T_{v,0}} \right)^{-1}$
	$\frac{\nu_{v,\infty}}{\nu_{v,0}} = \left(\frac{T_{v,\infty}}{T_{v,0}} \right)^{n_\mu + 1}$
	Equations of physical property factors
	$\frac{1}{\rho_v} \frac{d\rho_v}{dT_v} = - \frac{(T_s/T_\infty - 1) d\theta_v/dT_v}{(T_s/T_\infty - 1)\theta_v + 1}$
	$\frac{1}{\mu_v} \frac{d\mu_v}{dT_v} = \frac{n_\mu (T_s/T_\infty - 1) d\theta_v/dT_v}{(T_s/T_\infty - 1)\theta_v + 1}$
	$\frac{1}{\lambda_v} \frac{d\lambda_v}{dT_v} = \frac{n_\lambda (T_s/T_\infty - 1) d\theta_v/dT_v}{(T_s/T_\infty - 1)\theta_v + 1}$
	$\frac{\mu_{v,\infty}}{\mu_{v,0}} = [(T_s/T_\infty - 1)\theta_v + 1]^{-n_\mu}$
	$\frac{\nu_{v,\infty}}{\nu_{v,0}} = [(T_s/T_\infty - 1)\theta_v + 1]^{-(n_\mu + 1)}$

Table 16.8 Summary of equations for condensate heat and mass transfer of the laminar film condensation of vapor (saturated and superheated)

Term	Equations
<i>Heat transfer equations</i>	
q_x (defined as $-\lambda_{v,w} \left(\frac{\partial t}{\partial y} \right)_{y=0}$)	$\lambda_{l,w} (t_w - t_s)^{1/4} \left(\frac{1}{4} \text{Gr}_{x,l,s} \right)^{1/4} x^{-1} \left(-\frac{d\theta_l}{d\eta} \right)_{\eta=0}$
α_x (defined as $\frac{q_x}{T_w - T_x}$)	$\lambda_{l,w} \left(\frac{1}{4} \text{Gr}_{x,l,s} \right)^{1/4} x^{-1} \left(-\frac{d\theta_l}{d\eta} \right)_{\eta=0}$
$\text{Nu}_{x,w}$ defined as $\text{Nu}_{x,l,w} = \frac{\alpha_x x}{\lambda_{l,w}}$ is	$\text{Nu}_{x,l,w} = \left(\frac{1}{4} \text{Gr}_{x,l,s} \right)^{1/4} \left(-\frac{d\theta_l}{d\eta} \right)_{\eta=0}$
Q_x defined as $Q_x = \iint_A q_x dA$	$Q_x = \frac{4}{3} b \lambda_{l,w} (t_w - t_s)^{1/4} \left(\frac{1}{4} \text{Gr}_{x,l,s} \right)^{1/4} \left(-\frac{d\theta_l}{d\eta} \right)_{\eta=0}$
\bar{Q}_x defined as $\bar{Q}_x = Q_x / (b \times x)$	$\bar{Q}_x = \frac{4}{3} x^{-1} \lambda_{l,w} (t_w - t_s)^{1/4} \left(\frac{1}{4} \text{Gr}_{x,l,s} \right)^{1/4} \left(-\frac{d\theta_l}{d\eta} \right)_{\eta=0} = 0$
$\bar{\alpha}_x$ (defined as $\bar{\alpha}_x = \frac{\bar{Q}_x x}{\lambda_{l,w}}$)	$\frac{4}{3} \lambda_{l,w} \left(\frac{1}{4} \text{Gr}_{x,l,s} \right)^{1/4} x^{-1} \left(-\frac{d\theta_l}{d\eta} \right)_{\eta=0}$
$\bar{\text{Nu}}_{x,w}$ (defined as $= \frac{\bar{Q}_x x}{\lambda_{l,w}}$)	$\frac{4}{3} \left(\frac{1}{4} \text{Gr}_{x,l,s} \right)^{1/4} \left(-\frac{d\theta_l}{d\eta} \right)_{\eta=0}$
<i>Prediction equations on wall dimensionless temperature gradient</i> $\left(-\frac{d\theta_l}{d\eta} \right)_{\eta=0}$ (the only no-given variable	
in the above heat transfer equations)	
$\left(-\frac{d\theta_l}{d\eta} \right)_{\eta=0}$	for film condensation of water vapor (saturated and superheated) $\left(-\frac{d\theta_l}{d\eta} \right)_{\eta=0} = \left(\left(-\frac{d\theta_l}{d\eta} \right)_{\eta=0} \right)_{\Delta t_{\infty}=0} + a \cdot \frac{\Delta t_{\infty}}{t_s} \left(0 \leq \frac{\Delta t_{\infty}}{t_s} \leq 4.27 \right)$
$\left(\left(-\frac{d\theta_l}{d\eta} \right)_{\eta=0} \right)_{\Delta t_{\infty}=0}$	$a = 0.0315 \times \left(\frac{\Delta t_w}{t_s} \right)^{-0.3119} \left(0.05 \leq \frac{\Delta t_w}{t+s} \leq 1 \right)$
	for film condensation of saturated water vapor
	$1.74 - 0.19 \frac{\Delta t_w}{t_s} \left(\frac{\Delta t_w}{t_s} \right)^{1/4} \left(0.001 \leq \frac{\Delta t_w}{t_s} \leq 1 \right)$

(continued)

Table 16.8 (continued)

Term	Equations
<i>Equations for practical prediction of heat transfer on laminar free film condensation of water vapor</i>	
q_x , defined as $-\lambda_{l,w} \left(\frac{\partial T}{\partial y} \right)_{y=0}$	$q_x = -\lambda_{l,w} (t_w - t_s) \left(\frac{1}{4} \text{Gr}_{x,l,s} \right)^{1/4} x^{-1} \left[\left(- \left(\frac{d\theta_l}{d\eta} \right)_{\eta=0} \right)_{\Delta t_{\infty}=0} + a \cdot \frac{\Delta t_{\infty}}{t_s} \right]$
α_x defined as $q_x = \alpha_x (t_w - t_s)$	$q_x = -\lambda_{l,w} \left(\frac{1}{4} \text{Gr}_{x,l,s} \right)^{1/4} x^{-1} \left(- \frac{d\theta_l}{d\eta} \right)_{\eta=0}$
$\text{Nu}_{x,l,w}$ defined as $\frac{\alpha_x x}{\lambda_{l,w}}$	$\text{Nu}_{x,l,w} = \left(\frac{1}{4} \text{Gr}_{x,l,s} \right)^{1/4} \left[\left(\left(\frac{d\theta_l}{d\eta} \right)_{\eta=0} \right)_{\Delta t_{\infty}=0} + a \cdot \frac{\Delta t_{\infty}}{t_s} \right]$
Q_x , defined as $Q_x = \int_A q_x dA = \int_0^x q_x b dx$	$Q_x = \frac{4}{3} b \lambda_{l,w} (t_w - t_s) \left(\frac{1}{4} \text{Gr}_{x,l,s} \right)^{1/4} \left[\left(- \left(\frac{d\theta_l}{d\eta} \right)_{\eta=0} \right)_{\Delta t_{\infty}=0} + a \cdot \frac{\Delta t_{\infty}}{t_s} \right]$
\bar{Q}_x , defined as $\bar{Q}_x / (b \times x)$	$Q_x = \frac{4}{3} x^{-1} \lambda_{l,w} (t_w - t_s) \left(\frac{1}{4} \text{Gr}_{x,l,s} \right)^{1/4} \left[\left(- \left(\frac{d\theta_l}{d\eta} \right)_{\eta=0} \right)_{\Delta t_{\infty}=0} + a \cdot \frac{\Delta t_{\infty}}{t_s} \right]$
$\bar{\alpha}_x$, defined as $\bar{Q}_x = \bar{\alpha}_x (t_w - t_s)$	$\bar{\alpha}_x = \frac{4}{3} \lambda_{l,w} \left(\frac{1}{4} \text{Gr}_{x,l,s} \right)^{1/4} x^{-1} \left[\left(- \left(\frac{d\theta_l}{d\eta} \right)_{\eta=0} \right)_{\Delta t_{\infty}=0} + a \cdot \frac{\Delta t_{\infty}}{t_s} \right]$
$\bar{\text{Nu}}_{x,w}$, defined as $\frac{\bar{\alpha}_x x}{\lambda_{l,w}}$	$\bar{\text{Nu}}_{x,w} = \frac{4}{3} \left(\frac{1}{4} \text{Gr}_{x,l,s} \right)^{1/4} \left[\left(- \left(\frac{d\theta_l}{d\eta} \right)_{\eta=0} \right)_{\Delta t_{\infty}=0} + a \cdot \frac{\Delta t_{\infty}}{t_s} \right]$
<i>Condensate mass transfer equations</i>	
Condensate liquid film thickness δ_l	$\eta_{l,\delta} \left(\frac{1}{4} \text{Gr}_{x,l,s} \right)^{1/4} x$
Local Grashof number of liquid film $\text{Gr}_{x,l,s}$	$\frac{g(\rho_l - \rho_{v,\infty})x^3}{\nu_{l,s}^2 \rho_{l,s}}$
Local mass flow rate g_x	$\mu_{l,s} x^{-1} \left(\frac{1}{4} \text{Gr}_{x,l,s} \right)^{1/4} \Phi_s$
Total mass flow rate G_x	$\frac{4}{3} b \cdot \mu_{l,s} \left(\frac{1}{4} \text{Gr}_{x,l,s} \right)^{1/4} \Phi_s$
<i>Prediction equations on condensate mass flow rate parameter Φ_s (the only no-given variable in the above condensate mass transfer equations)</i>	

Term	Equations
Φ_s (defined as $\eta_{l\delta} W_{x,l,s} - 4W_{y,l,s}$)	For film condensation of water vapor (saturated and superheated) $\Phi_s = (\Phi_s)_{\Delta T_{\infty}=0} - B \frac{\Delta T_{\infty}}{t_s}$
$(\Phi_s)_{\Delta T_{\infty}=0}$ defined as $(\eta_{l\delta} W_{x,l,s} - 4W_{y,l,s})_{\Delta T_{\infty}=0}$	$(0.005 \leq \frac{\Delta T_w}{t_s} \leq 1) \text{ and } (0 \leq \frac{\Delta T_{\infty}}{t_s} \leq 4.27)$ $B = 10^{-4} \times \left[2.756 + 121.4 \frac{\Delta T_w}{t_s} - 60 \left(\frac{\Delta T_w}{t_s} \right)^2 \right]$
<i>Equations for practical prediction of condensate mass transfer on laminar free film condensation of water vapor</i>	For film condensation of saturated water vapor
Total mass flow rate on the plate	for $(0 \leq \frac{\Delta T_{\infty}}{t_s} \leq 4.27$ and $0.05 \leq \frac{\Delta T_w}{t_s} \leq 1)$
<i>Prediction equations on condensate liquid film thickness $\eta_{l\delta}$</i>	$G_x = \frac{4}{3} b \cdot \mu_{l,s} \left(\frac{1}{4} Gr_{x,l,s} \right)^{1/4} \left[\left(0.186 - 0.057 \frac{\Delta T_w}{t_s} \right)^{3/4} \left(\frac{\Delta T_w}{t_s} \right) - B \frac{\Delta T_{\infty}}{t_s} \right]$
Dimensionless liquid film thickness $\eta_{l\delta}$	where
Dimensionless liquid film thickness $\eta_{l\delta}$	$B = 10^{-4} \times \left[2.756 + 121.4 \frac{\Delta T_w}{t_s} - 60 \left(\frac{\Delta T_w}{t_s} \right)^2 \right]$
Dimensionless liquid film thickness $\eta_{l\delta}$	For film condensation of water vapor (saturated and superheated)
$(\eta_{l\delta})_{\Delta T_{\infty}=0}$	$(\eta_{l\delta})_{\Delta T_{\infty}=0} = 0.5934 \left(\frac{\Delta T_w}{t_s} \right)^{0.2562} \left(0.001 \leq \frac{\Delta T_w}{t_s} \leq 0.2 \right)$
$(\eta_{l\delta})_{\Delta T_{\infty}=0}$	$(\eta_{l\delta})_{\Delta T_{\infty}=0} = 0.417 \left(\frac{\Delta T_w}{t_s} \right) + 0.3223 \left(0.2 \leq \frac{\Delta T_w}{t_s} \leq 1 \right)$

16.10 Remarks

In this chapter, we deal with heat and mass transfer of laminar free convection film condensation of vapor with consideration of various physical factors including variable physical properties. The film condensation of saturated vapor is taken as its special case only with the vapor bulk superheated grade $\frac{\Delta t_\infty}{t_s} = \frac{t_\infty - t_s}{t_s} = 0$. The present presentation here on heat and mass transfer is an extension of former studies and the following points are concluded:

With heat and mass transfer analysis, the theoretical equations for Nusselt number and mass flow rate are derived for the laminar free convection film condensation of vapor. For practical prediction of heat transfer, only the temperature gradient $\left(\frac{d\theta_l}{d\eta_l}\right)_{\eta_l=0}$ dependent on the numerical solutions of the governing equations is unknown variable. While, for practical prediction of condensate mass flow rate, only the condensate mass flow rate parameter Φ_s dependent on the numerical solutions of the governing equations is unknown variable.

With increase of the wall subcooled grade $\frac{\Delta t_w}{t_s} = \frac{t_s - t_w}{t_s}$, the temperature gradient $\left(-\frac{d\theta_l}{d\eta_l}\right)_{\eta_l=0}$ will decrease, especially for lower wall subcooled grade $\frac{\Delta t_w}{t_s} = \frac{t_s - t_w}{t_s}$. While, with increasing the vapor bulk superheated grade $\frac{\Delta t_\infty}{t_s} = \frac{t_\infty - t_s}{t_s}$, the temperature gradient $\left(-\frac{d\theta_l}{d\eta_l}\right)_{\eta_l=0}$ will increase. However, the effect of the wall subcooled grade $\frac{\Delta t_w}{t_s} = \frac{t_s - t_w}{t_s}$ on the temperature gradient $\left(-\frac{d\theta_l}{d\eta_l}\right)_{\eta_l=0}$ is more obvious than that of the vapor bulk superheated grade $\frac{\Delta t_\infty}{t_s} = \frac{t_\infty - t_s}{t_s} = 0$.

With increasing the wall subcooled grade $\frac{\Delta t_w}{t_s} = \frac{t_s - t_w}{t_s}$, the condensate film thickness η_{δ_l} will increase, especially for lower wall subcooled grade $\frac{\Delta t_w}{t_s} = \frac{t_s - t_w}{t_s}$, while with increasing the superheated grade $\frac{\Delta t_\infty}{t_s} = \frac{t_\infty - t_s}{t_s}$, the condensate film thickness η_{δ_l} will decrease. However, the effect of the wall subcooled grade $\frac{\Delta t_w}{t_s} = \frac{t_s - t_w}{t_s}$ on the condensate film thickness η_{δ_l} is more obvious than that of the vapor bulk superheated grade $\frac{\Delta t_\infty}{t_s} = \frac{t_\infty - t_s}{t_s}$.

With increase of the wall subcooled grade $\frac{\Delta t_w}{t_s} = \frac{t_s - t_w}{t_s}$, the velocity components and $-W_{y_l,s}$ will increase, especially for the small value of $\frac{\Delta t_w}{t_s} = \frac{t_s - t_w}{t_s}$. While with increasing the superheated grade $\frac{\Delta t_\infty}{t_s} = \frac{t_\infty - t_s}{t_s} = 0$, the velocity components $W_{x_l,s}$ and $-W_{y_l,s}$ will decrease.

As per the results, with increase of the wall subcooled grade $\frac{\Delta t_w}{t_s} = \frac{t_s - t_w}{t_s}$, the condensate mass flow rate parameter $\Phi_s = \eta_{\delta_l} W_{x_l,s} - W_{y_l,s}$ will increase, especially due to the function of condensate film thickness η_{δ_l} . While with increasing the superheated grade $\frac{\Delta t_\infty}{t_s} = \frac{t_\infty - t_s}{t_s}$, the mass flow rate parameter Φ_s will decrease. However, the effect of the wall subcooled grade $\frac{\Delta t_w}{t_s} = \frac{t_s - t_w}{t_s}$ on the condensate mass flow rate parameter is more obvious than that of the superheated grade $\frac{\Delta t_\infty}{t_s} = \frac{t_\infty - t_s}{t_s}$.

On the basis of the rigorous numerical solutions, the temperature gradient $\left(\frac{d\theta_l}{d\eta_l}\right)_{\eta_l=0}$ and then mass flow rate parameter Φ_s are formulated, and then, the equations for reliable predictions of heat and mass transfer are created for the laminar free convection film condensation of water vapor.

16.11 Calculation Example

Example 1 A flat plate with 0.3 m in width and 0.3 m in length is suspended vertically in the superheated water vapor. The wall temperature of the plate is $t_w = 98^\circ\text{C}$, and the vapor bulk temperature is $t_\infty = t_s = 100^\circ\text{C}$. Suppose the condensate film is laminar, please calculate the free convection condensation heat and mass transfer on the plate.

Calculation:

The vapor superheated grade is $\frac{\Delta t_\infty}{t_s} = \frac{t_\infty - t_s}{t_s} = 0$, then, the water vapor bulk is at the saturated state with $\rho_v = 0.5974 \text{ kg/m}^3$.

The wall subcooled grade is $\frac{\Delta t_w}{t_s} = \frac{t_s - t_w}{t_s} = \frac{100 - 98}{100} = 0.02$, and $\rho_{l,w} = 961.6 \text{ kg/m}^3$, and $\lambda_l = 0.6824 \text{ W/(m}^\circ\text{C)}$ at $t_w = 98^\circ\text{C}$.

Additionally, for saturated condition of water at 100°C , there should be the following property data, i.e., $\rho_{l,s} = 958.1 \text{ kg/m}^3$, $\nu_{l,s} = 0.294 \times 10^{-6} \text{ m}^2/\text{s}$, $\mu_{l,s} = 281.7 \times 10^{-6} \text{ kg/(m}\cdot\text{s)}$.

1. For heat transfer

From section 16.2 the average heat transfer coefficient of the laminar free convection film condensation of saturated vapor is evaluated as

$$\bar{\alpha}_x = -\frac{4}{3}\lambda_{l,w} \left(\frac{1}{4}\text{Gr}_{x,l,s}\right)^{1/4} x^{-1} \left(-\left(\frac{d\theta_l}{d\eta_l}\right)_{\eta_l=0}\right)_{\Delta t_\infty=0}$$

From Eq.(14.14) the local Grashof number of the film condensation is evaluated as

$$\begin{aligned} \text{Gr}_{x,l,s} &= \frac{g(\rho_{l,w} - \rho_{v,s})x^3}{\nu_{l,s}^2 \rho_{l,s}} \\ &= \frac{9.8 \times (961.6 - 0.5974) \times 0.3^3}{(0.294 \times 10^{-6})^2 \times 958.1} \\ &= 3.0705 \times 10^{12} \end{aligned}$$

From Eq. (16.8), the temperature gradient $\left(\left(\frac{d\theta_l}{d\eta_l}\right)_{\eta_l=0}\right)_{\Delta t_\infty=0}$ for the laminar free convection film condensation of saturated water vapor is calculated as

$$\begin{aligned} \left(-\left(\frac{d\theta_l}{d\eta_l}\right)_{\eta_l=0}\right)_{\Delta t_\infty=0} &= \frac{1.74 - 0.19 \frac{\Delta t_w}{t_s}}{\left(\frac{\Delta t_w}{t_s}\right)^{1/4}} \\ &= \frac{1.74 - 0.19 \times 0.02}{0.02^{1/4}} \\ &= 4.6168 \end{aligned}$$

Then, the local heat transfer coefficient is evaluated as

$$\begin{aligned} \bar{\alpha}_x &= \frac{4}{3} \lambda_{l,w} \left(\frac{1}{4} \text{Gr}_{x,l,s}\right)^{1/4} x^{-1} \left(-\left(\frac{d\theta_l}{d\eta_l}\right)_{\eta_l=0}\right)_{\Delta t_\infty=0} \\ &= \frac{4}{3} \times 0.6824 \times \left(\frac{1}{4} \times 3.0705 \times 10^{12}\right)^{1/4} \times 0.3^{-1} \times 4.6168 \\ &= 13106.44 \text{ W}/(\text{m}^2\text{C}) \end{aligned}$$

The total heat transfer of laminar free convection film condensation of the superheated water vapor on the vertical plate is calculated

$$\begin{aligned} Q_x &= \bar{\alpha}_x (t_w - t_s) A \\ &= 13106.44 \times (98 - 100) \times 0.3 \times 0.3 \\ &= -2359.16 \text{ W} \end{aligned}$$

The negative means that the heat transfer direction is to the plate from the condensate film.

2. For mass flow rate of the condensation

From Eqs. (16.15) the total mass flow rate G_x of the laminar film condensate of saturated vapor for position $x = 0$ to x with width of b of the plate is evaluated as

$$G_x = \frac{4}{3} b \cdot \mu_{l,s} \left(\frac{1}{4} \text{Gr}_{x,l,s}\right)^{1/4} (\Phi_s)_{\Delta t_\infty=0}$$

From Eq. (16.20), the mass flow rate parameter $(\Phi_s)_{\Delta t_\infty=0}$ is calculated as

$$\begin{aligned} (\Phi_s)_{\Delta t_\infty=0} &= \left(0.186 - 0.057 \frac{\Delta t_w}{t_s}\right) \left(\frac{\Delta t_w}{t_s}\right)^{3/4} \\ &= (0.186 - 0.057 \times 0.02)(0.02)^{3/4} \\ &= 0.0098314 \end{aligned}$$

Then, the total mass flow rate G_x of the laminar free convection film condensation of saturated water vapor is calculated as

$$\begin{aligned} G_x &= \frac{4}{3} b \cdot \mu_{l,s} \left(\frac{1}{4} \text{Gr}_{x,l,s} \right)^{1/4} (\Phi_s)_{\Delta t_\infty=0} \\ &= \frac{4}{3} \times 0.3 \times 281.7 \times 10^{-6} \times \left(\frac{1}{4} \times 3.0705 \times 10^{12} \right)^{1/4} \times 0.0098314 \\ &= 0.001037 \text{ kg/s} \\ &= 3.7329 \text{ kg/h} \end{aligned}$$

Example 2 A flat plate with 0.3 m in width and 0.3 m in height is suspended vertically in the saturated water vapor, i.e., $\Delta t_\infty = t_\infty - t_S = 0^\circ\text{C}$. The wall temperature is $t_w = 90^\circ\text{C}$ and then the wall subcooled grade is $\frac{\Delta t_w}{t_s} = \frac{t_s - t_w}{t_s} = \frac{100 - 90}{100} = 0.1$. Assume laminar free convection film condensation occurs on the plate, please calculate:

- (i) heat transfer and mass flow rate of the film boiling of saturated water vapor on the plate
- (ii) condensate film thickness at $x = 0, 0.01, 0.05, 0.1, 0.15, 0.2, 0.25,$ and 0.3 m from the top ($x = 0$) of the plate

Calculation:

At first, the related physical properties are given as follows: $\rho_{v,s} = 0.5974 \text{ g/m}^3$ for saturated water vapor at $t_S = 100^\circ\text{C}$, $\rho_{l,s} = 958.1 \text{ kg/m}^3$, $\nu_{l,s} = 0.294 \times 10^{-6} \text{ m}^2/\text{s}$, and $\mu_{l,s} = 281.7 \times 10^{-6} \text{ kg}/(\text{m s})$ for saturated water at $t_S = 100^\circ\text{C}$, and $\rho_{l,w} = 965.3 \text{ kg/m}^3$ and $\lambda_l = 0.68$ for water at $t_w = 90^\circ\text{C}$.

- (i) heat transfer and mass flow rate of the laminar free convection film condensation of saturated water steam on two sides of the plate

For heat transfer

With Eq. (14.14), the local Grashof number $\text{Gr}_{x,l,s}$ is evaluated as

$$\begin{aligned} \text{Gr}_{x,l,s} &= \frac{g(\rho_{l,w} - \rho_v)x^3}{\nu_{l,s}^2 \rho_{l,s}} \\ &= \frac{9.8 \times (965.3 - 0.5974) \times 0.3^3}{(0.294 \times 10^{-6})^2 \times 958.1} \\ &= 3.08232 \times 10^{12} \end{aligned}$$

Additionally with Eq. (16.8) the temperature gradient of the laminar free convection film condensation of the saturated water vapor is calculated as

$$\left(- \left(\frac{d\theta_l}{d\eta_l} \right)_{\eta_l=0} \right)_{\Delta t_\infty=0} = \frac{1.74 - 0.19 \frac{\Delta t_w}{t_s}}{\left(\frac{\Delta t_w}{t_s} \right)}$$

$$\begin{aligned}
 &= \frac{1.74 - 0.19 \times \frac{10}{100}}{\left(\frac{10}{100}\right)^{1/4}} \\
 &= 3.060
 \end{aligned}$$

Then from Eqs. (16.6) the average heat transfer coefficient is evaluated as

$$\begin{aligned}
 \bar{\alpha}_x &= \frac{4}{3} \lambda_{l,w} \left(\frac{1}{4} \text{Gr}_{x,l,s}\right)^{1/4} x^{-1} \left(\left(-\frac{d\theta_l}{d\eta_l}\right)_{\eta=0}\right)_{\Delta t_\infty=0} \\
 &= \frac{4}{3} \times 0.68 \times \left(\frac{1}{4} \times 3.08232 \times 10^{12}\right)^{1/4} \times (0.3)^{-1} \times 3.060 \\
 &= 8664.67 \text{ W}/(\text{m}^2\text{°C})
 \end{aligned}$$

The heat transfer of laminar free convection film condensation of the saturated water vapor on the vertical plate is calculated

$$\begin{aligned}
 Q_x &= \bar{\alpha}_x (t_w - t_s) A \\
 &= 8664.67 \times (90 - 100) \times 0.3 \times 0.3 \\
 &= -7798.2 \text{ W}
 \end{aligned}$$

The negative sign means that the heat flux is to the plate from the condensate film.

For mass flow rate of the condensation

The mass flow rate parameter of the laminar free convection film condensation of saturated water vapor is evaluated as

$$\begin{aligned}
 (\Phi_s)_{\Delta t_\infty=0} &= (\eta l \delta \cdot W_{x,l,\delta} - 4W_{y,l,\delta})_{\Delta t_\infty=0} \\
 &= \left(0.186 - 0.057 \frac{\Delta t_w}{t_s}\right) \left(\frac{\Delta t_w}{t_s}\right)^{3/4} \\
 &= \left(0.186 - 0.057 \times \frac{10}{100}\right) \left(\frac{10}{100}\right)^{3/4} \\
 &= 0.032062
 \end{aligned}$$

The total mass flow rate of the film condensation of saturated water vapor is

$$\begin{aligned}
 G_x &= \frac{4}{3} b \cdot \mu_{l,s} \left(\frac{1}{4} \text{Gr}_{x,l,s}\right)^{1/4} (\Phi_s)_{\Delta t_\infty=0} \\
 &= \frac{4}{3} \times 0.3 \times 281.7 \times 10^{-6} \times \left(\frac{1}{4} \times 3.08232 \times 10^{12}\right)^{1/4} \times 0.032062 \\
 &= 0.0033849 \text{ kg/s} \\
 &= 12.186 \text{ kg/h}
 \end{aligned}$$

(ii) condensate film thickness

The wall subcooled grade is 0.1, then, Eq. (16.16) is taken to evaluate $\eta_{l\delta}$ as

$$\begin{aligned}\eta_{l\delta} &= 0.5934 \left(\frac{\Delta t_w}{t_s} \right)^{0.2562} \\ &= 0.5934 \times (0.1)^{0.2562} \\ &= 0.32896\end{aligned}$$

From the definition of local Grashof number $Gr_{x,l,s}$, the condensate film thickness δ_l is expressed as

$$\begin{aligned}\delta_l &= \eta_l x \left(\frac{1}{4} Gr_{x,l,s} \right)^{-1/4} \\ &= \eta_l x \left(\frac{1}{4} \frac{g(\rho_{l,w} - \rho_{v,s})x^3}{v_{l,s}^2 \rho_{l,s}} \right)^{-1/4} \\ &= \eta_l \left(\frac{1}{4} \frac{g(\rho_{l,w} - \rho_{v,s})}{v_{l,s}^2 \rho_{l,s}} \right)^{-1/4} x^{1/4} \\ &= 0.32896 \times \left(\frac{1}{4} \times \frac{9.8 \times (965.3 - 0.5974)}{(0.294 \times 10^{-6})^2 \times 958.1} \right)^{-1/4} \times x^{1/4} \\ &= 0.000142324 \times x^{1/4}\end{aligned}$$

$$\text{For } x = 0, \quad \delta_l = 0$$

$$\text{For } x = 0.01 \text{ m, } \delta_l = 0.000142324 \times 0.01^{1/4} = 4.5 \times 10^{-5} \text{ m}$$

$$\text{For } x = 0.05 \text{ m, } \delta_l = 0.000142324 \times 0.05^{1/4} = 6.73 \times 10^{-5} \text{ m}$$

$$\text{For } x = 0.1 \text{ m, } \delta_l = 0.000142324 \times 0.1^{1/4} = 8 \times 10^{-5} \text{ m}$$

$$\text{For } x = 0.15 \text{ m, } \delta_l = 0.000142324 \times 0.15^{1/4} = 8.86 \times 10^{-5} \text{ m}$$

$$\text{For } x = 0.2 \text{ m, } \delta_l = 0.000142324 \times 0.2^{1/4} = 9.52 \times 10^{-5} \text{ m}$$

$$\text{For } x = 0.25 \text{ m, } \delta_l = 0.000142324 \times 0.25^{1/4} = 0.000101 \text{ m}$$

$$\text{For } x = 0.3 \text{ m, } \delta_l = 0.000142324 \times 0.3^{1/4} = 0.000105 \text{ m}$$

For clear expression, the condensate film thickness δ_l with the position x is listed and plotted as Table 16.10 and Fig. 16.8 respectively.

Example 3 A flat plate with 0.3 m width and 0.3 m length is suspended vertically in the superheated water vapor with $t_\infty = 227^\circ\text{C}$. The wall temperature is $t_w = 90^\circ\text{C}$. Suppose the film condensation is laminar, please calculate the condensate heat and mass transfer on the plate.

Table 16.10 The condensate film thickness y with the position x

x m	0	0.01	0.05	0.1	0.15	0.2	0.25	0.3
δ_l m	0	4.5×10^{-5}	6.73×10^{-5}	8×10^{-5}	8.86×10^{-5}	9.52×10^{-5}	0.000101	0.000105

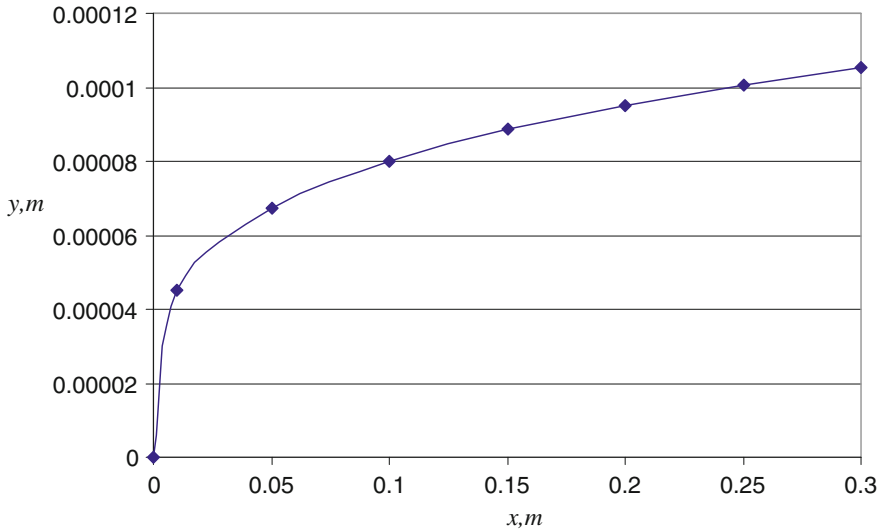


Fig. 16.8 The condensate film thickness δ_l with the position x

Solution:

The wall subcooled temperatures of the plate is $\Delta t_w = t_s - t_w = 100 - 90 = 10^\circ\text{C}$, and then, the wall subcooled grade is $\frac{\Delta t_w}{t_s} = \frac{10}{100} = 0.1$. We have $\rho_{l,w} = 965.32 \text{ kg/m}^3$, and $\lambda_l = 0.68 \text{ W}/(\text{m}^\circ\text{C})$ for water at $t_w = 90^\circ\text{C}$.

The vapor superheated temperature is $\Delta t_\infty = t_\infty - t_s = 0227 - 100 = 127^\circ\text{C}$, then, the vapor superheated grade is $\frac{\Delta t_\infty}{t_s} = \frac{t_\infty - t_s}{t_s} = \frac{127}{100} = 1.27$. We have $\rho_{v,\infty} = 0.4405 \text{ kg/m}^3$ for water vapor at $t_\infty = 227^\circ\text{C}$.

Additionally, we have $\rho_{l,s} = 958.1 \text{ kg/m}^3$, $\nu_{l,s} = 0.294 \times 10^{-6} \text{ m}^2/\text{s}$, $\mu_{l,s} = 281.7 \times 10^{-6} \text{ kg}/(\text{m s})$ for saturated water at 100°C .

1. *For heat transfer*

From Eqs. (16.6) the average heat transfer coefficient is evaluated as

$$\bar{\alpha}_x = \frac{4}{3} \lambda_{l,w} \left(\frac{1}{4} \text{Gr}_{x,l,s} \right)^{1/4} x^{-1} \left(\frac{d\theta_l}{d\eta_l} \right)_{\eta_l=0}$$

From Eq. (14.14) the local Grashof number $\text{Gr}_{x,l,s}$ of the film condensation should be evaluated as

$$\begin{aligned}
 Gr_{x,l,s} &= \frac{g(\rho_{l,w} - \rho_{v,\infty})x^3}{\nu_{l,s}^2 \rho_{l,s}} \\
 &= \frac{9.8 \times (965.32 - 0.4405) \times 0.3^3}{(0.294 \times 10^{-6})^2 \times 958.1} \\
 &= 3.08289 \times 10^{12}
 \end{aligned}$$

From Eq. (16.9) the temperature gradient of the laminar free convection film condensation of the superheated water vapor is calculated as

$$-\left(\frac{d\theta_l}{d\eta_l}\right)_{\eta_l=0} = \left(-\left(\frac{d\theta_l}{d\eta_l}\right)_{\eta_l=0}\right)_{\Delta t_\infty=0} + a \cdot \frac{\Delta t_\infty}{t_s}$$

From Eq. (16.8) the dimensionless temperature gradient $\left(-\left(\frac{d\theta_l}{d\eta_l}\right)_{\eta_l=0}\right)_{\Delta t_\infty=0}$ for the film condensation of saturated water vapor is evaluated as

$$\begin{aligned}
 \left(-\left(\frac{d\theta_l}{d\eta_l}\right)_{\eta_l=0}\right)_{\Delta t_\infty=0} &= \frac{1.74 - 0.19 \frac{\Delta t_w}{t_s}}{\left(\frac{\Delta t_w}{t_s}\right)^{1/4}} \\
 &= \frac{1.74 - 0.19 \times 0.1}{0.1^{1/4}} \\
 &= 3.060419
 \end{aligned}$$

From Eq. (16.10), the coefficient a is calculated as

$$\begin{aligned}
 a &= 0.0315 \times \left(\frac{\Delta t_w}{t_s}\right)^{-0.3119} \\
 &= 0.0315 \times (0.1)^{-0.3119} \\
 &= 0.064597
 \end{aligned}$$

Then, the temperature gradient of the laminar free convection film condensation of the superheated water vapor is calculated as

$$\begin{aligned}
 -\left(\frac{d\theta}{d\eta_l}\right)_{\eta_l=0} &= \left(-\left(\frac{d\theta_l}{d\eta_l}\right)_{\eta_l=0}\right)_{\Delta t_\infty=0} + a \cdot \frac{\Delta t_\infty}{t_s} \\
 &= 3.060419 + 0.064597 \times 1.27 \\
 &= 3.142457
 \end{aligned}$$

Then, the average heat transfer coefficient is evaluated as

$$\begin{aligned}
 \bar{\alpha}_x &= -\frac{4}{3}\lambda_{l,w} \left(\frac{1}{4}\text{Gr}_{x,l,s}\right)^{1/4} x^{-1} \left(\frac{d\theta_l}{d\eta_l}\right)_{\eta_l=0} \\
 &= \frac{4}{3} \times 0.68 \times \left(\frac{1}{4} \times 3.08289 \times 10^{12}\right)^{1/4} \times (0.3)^{-1} \times 3.142457 \\
 &= 8898.57 \text{ W}/(\text{m}^2\text{C})
 \end{aligned}$$

The total heat transfer rate of laminar free convection film condensation of the superheated water vapor on the vertical plate is calculated

$$\begin{aligned}
 Q_x &= \bar{\alpha}_x(t_w - t_s)A \\
 &= 8898.57 \times (90 - 100) \times 0.3 \times 0.3 \\
 &= -8008.72 \text{ W}
 \end{aligned}$$

The negative means that the heat transfer direction is to the plate from the condensate film.

2. For mass flow rate of the condensation

From Eq. (16.15), the total mass flow rate entering the liquid film for position $x = 0$ to x with width of b of the plate is evaluated as

$$G_x = \frac{4}{3}b \cdot \mu_{l,s} \left(\frac{1}{4}\text{Gr}_{x,l,s}\right)^{1/4} (\Phi_s)$$

Here from Eq. (16.21), the mass flow rate parameter film condensation of superheated vapor is evaluated as

$$(\Phi_s) = (\Phi_s)_{\Delta t_\infty=0} - b \frac{\Delta t_\infty}{t_s}$$

where the mass flow rate parameter of the laminar free convection film condensation of saturated water vapor is calculated as

$$\begin{aligned}
 (\Phi_s)_{\Delta t_\infty=0} &= \left(0.186 - 0.057 \frac{\Delta t_w}{t_s}\right) \left(\frac{\Delta t_w}{t_s}\right)^{3/4} \\
 &= (0.186 - 0.057 \times 0.1)(0.1)^{3/4} \\
 &= 0.032062378
 \end{aligned}$$

Additionally, the coefficient b is evaluated as

$$\begin{aligned}
 b &= 10^{-4} \times \left[2.756 + 121.4 \frac{\Delta t_w}{t_s} - 60 \left(\frac{\Delta t_w}{t_s}\right)^2\right] \\
 &= 10^{-4} \times [2.756 + 121.4 \times 0.1 - 60 \times (0.1)^2] \\
 &= 0.00143
 \end{aligned}$$

The mass flow rate parameter of the laminar free convection film condensation of superheated water steam is calculated as

$$\begin{aligned}\Phi_s &= (\Phi_s)_{\Delta t_\infty=0} - b \frac{\Delta t_\infty}{t_s} \\ &= 0.032062378 - 0.00143 \times 1.27 \\ &= 0.030246\end{aligned}$$

The mass flow rate G_x of the laminar free convection film condensation of superheated water vapor is calculated as

$$\begin{aligned}G_x &= \frac{4}{3} b \cdot \mu_{l,s} \left(\frac{1}{4} \text{Gr}_{x,l,s} \right)^{1/4} (\Phi_s) \\ &= \frac{4}{3} \times 0.3 \times 281.7 \times 10^{-6} \times \left(\frac{1}{4} \times 3.08289 \times 10^{12} \right)^{1/4} \times 0.030246 \\ &= 0.0031933 \text{ kg/s} \\ &= 11.496 \text{ kg/h}\end{aligned}$$

16.12 Exercises

1. Please describe the effect of wall subcooled grade and bulk superheated grade on heat and mass transfer of laminar free convection film condensation of vapour, respectively.
2. Please give a detailed derivation for the theoretical Eqs. (13.1)–(13.7) on heat transfer analysis of laminar free convection film condensation of vapour.
3. Can you point out the difference of variations of velocity and temperature fields on laminar free convection film condensation from those on laminar free convection film boiling?
4. Please explain why Eqs. (16.1*)–(16.7*) can be recommended for practical prediction of heat transfer of laminar free convection film condensation of water vapor on a vertical flat plate?
5. Please explain why Eq. (16.15*) can be recommended for practical prediction of condensate mass transfer of laminar free convection film condensation of vapor on a vertical flat plate?
6. Compare the variation regulation of the heat and mass transfer on the laminar free convection film condensation of vapor to that on laminar free convection film boiling of liquid.
7. Please find out the difference of the variation regulation of the heat and mass transfer on the laminar free convection film condensation of vapor from that on laminar free convection film boiling of liquid, and explain their differences.

8. Please tell me which applications the condensate mass–energy transformation equation has?
9. Which significance that the equation of the condensate mass-energy transformation has for laminar free convection film condensation?

References

1. D.Y. Shang, T. Adamek, Study of laminar film condensation of saturated steam for consideration of variable thermophysical properties. in *Transport phenomena, Science and Technology*, ed. by B.X. Wang (Higher Education press, Beijing, 1992), pp. 470–475
2. D.Y. Shang, T. Adamek, Study on laminar film condensation of saturated steam on a Wvertical flat plate for consideration of various physical factors including ariable thermophysical properties. in *Warme- und Stoffubertragung 30* (Springer, New York, 1994), pp. 89–100
3. D.Y. Shang, B.X. Wang, An extended study on steady-state laminar film condensation of a superheated vapor on an isothermal vertical plate. *Int. J. Heat Mass Transf.* **40**(4), 931–941 (1997)
4. D.Y. Shang, *Theory of Heat Transfer with Forced Convection Film Flows*, Springer Heidelberg, Dordrecht London, New York, 2011.

Chapter 17

Effects of Various Physical Conditions on Heat Transfer of the Free Convection Film Condensation

Abstract In this chapter, the film condensation of saturated water vapor is taken as an example for analyzing the effects of various physical conditions on heat transfer. The effects of four physical conditions including Boussinesq approximation (i.e. ignoring variable physical properties), shear force at the liquid–vapor interface, inertia force of the condensate film, and the thermal convection of the condensate film on the heat transfer coefficient of the film condensation are deeply investigated. It is found that the variable physical properties and thermal convection cause larger effect on heat transfer of laminar free convection film condensation, meanwhile, the effect of the variable physical properties is even larger than that of the thermal convection. It follows that it is necessary to consider variable physical properties for investigation on heat transfer of free film condensation. Compared with the variable physical properties and thermal convection, the effect of the Interfacial shear force and inertia force will be much smaller on heat transfer of laminar free convection film condensation, meanwhile, the effect of the inertia force is little bit smaller than that of the interfacial shear force.

17.1 Introduction

In Chap. 14, the extended theory of steady state laminar free convection film condensation process of pure vapor at atmospheric pressure on an isothermal vertical flat plate is established. Its equations provide a complete account of the analyses and calculation of its physical process for consideration of various physical factors including variable thermophysical properties.

In this chapter, effects of various physical conditions on heat and mass transfer of the film condensation of saturated vapor will be further presented [1, 2]. To this end, the film condensation of saturated water vapor is taken as an example, and, four different assumptions, such as Boussinesq approximation of condensate film, ignoring shear force at the liquid–vapor interface, ignoring condensate film inertia force,

and ignoring condensate film thermal convection are considered for investigation of their effects on the condensate heat transfer coefficient, condensate film thickness, and mass flow rate of the film condensation. Quantitative comparisons from these results indicate the following points:

Effect of the Physical Conditions on Heat Transfer Coefficient

The Boussinesq approximation of the condensate film will greatly decrease the heat transfer coefficient of the condensation and cause the largest effect on the heat transfer coefficient compared with those caused by other physical conditions. The thermal convection of condensate film will increase the heat transfer coefficient of the condensation, and its effect on the heat transfer coefficient is larger than those caused by the liquid–vapor interfacial shear force and the inertia force of condensate film. The liquid–vapor interfacial shear force and the inertia force of the condensate film will decrease the heat transfer coefficient very slightly.

Effect of the Physical Conditions on Condensate Film Thickness

The Boussinesq approximation of the condensate film will greatly decrease the condensate film thickness and cause the largest effect on the condensate film thickness compared to those caused by other physical conditions. The thermal convection of condensate film will decrease the condensate film thickness, and its effect on the condensate film thickness is larger than those caused by the liquid–vapor interfacial shear force and the inertia force of condensate film. The liquid–vapor interfacial shear force and the inertia force of the condensate film will increase the condensate film thickness very slightly.

Effect of the Physical Conditions on Condensate Mass Flow Rate

The condensate film thermal convection will greatly decrease the mass flow rate of the film condensation, and will cause the largest effect on the condensate mass flow rate compared with those caused by other physical conditions. The other physical conditions, such as Boussinesq approximation, the liquid–vapor interfacial shear force, and the condensate film inertia force will decrease the condensate mass flow rate very slightly. While, the condensate film inertia force has the smallest effect on the condensate mass flow rate compared with the other physical conditions.

17.2 Review of Governing Equations for Film Condensation of Saturated Vapor

In Chap. 14, the governing equations for laminar free convection film condensation of saturated vapor were presented. In this chapter, it is necessary to have a brief review of those equations for a further analysis.

17.2.1 Partial Differential Equations

The analytical model and coordinate system used for the laminar free convection film condensation of the saturated vapor on an isothermal vertical flat plate is shown in Fig. 14.1, which is a special case of that of the general vapor with the zero superheated grade. The conservation partial differential equations of mass, momentum, and energy for steady laminar saturated condensation in two-phase boundary layer are as follows:

For Condensate Liquid Film

$$\frac{\partial}{\partial x}(\rho_l w_{xl}) + \frac{\partial}{\partial y}(\rho_l w_{yl}) = 0 \quad (17.1)$$

$$\rho_l \left(w_{xl} \frac{\partial w_{xl}}{\partial x} + w_{yl} \frac{\partial w_{xl}}{\partial y} \right) = \frac{\partial}{\partial y} \left(\mu_l \frac{\partial w_{xl}}{\partial y} \right) + g(\rho_l - \rho_v) \quad (17.2)$$

$$\rho_l c_{pl} \left(w_{xl} \frac{\partial t}{\partial x} + w_{yl} \frac{\partial t}{\partial y} \right) = \frac{\partial}{\partial y} \left(\lambda_l \frac{\partial t}{\partial y} \right) \quad (17.3)$$

For Vapor Film

$$\frac{\partial}{\partial x}(w_{xv}) + \frac{\partial}{\partial y}(w_{yv}) = 0 \quad (17.4)$$

$$w_{xv} \frac{\partial w_{xv}}{\partial x} + w_{yv} \frac{\partial w_{xv}}{\partial y} = \nu_v \frac{\partial^2 w_{xv}}{\partial y^2} \quad (17.5)$$

For Boundary Conditions

$y = 0$:

$$w_{xl} = 0, \quad w_{yl} = 0, \quad t_l = t_w \quad (17.6)$$

$y = \delta_v$

$$w_{xl,s} = w_{xv,s} \quad (17.7)$$

$$\rho_{l,s} \left(w_{xl} \frac{\partial \delta_l}{\partial x} - w_{yl} \right)_s = \rho_v \left(w_{xv} \frac{\partial \delta_v}{\partial x} - w_{yv} \right)_s \quad (17.8)$$

$$\mu_{l,s} \left(\frac{\partial w_{xl}}{\partial y} \right)_s = \mu_v \left(\frac{\partial w_{xv}}{\partial y} \right)_s \quad (17.9)$$

$$\lambda_{l,s} \left(\frac{\partial t_l}{\partial y} \right)_{y=\delta_l} = h_{fg} \rho_{l,s} \left(w_{xl} \frac{\partial \delta_l}{\partial x} - w_{yl} \right)_s \quad (17.10)$$

$$t_l = t_s \quad (17.11)$$

$y \rightarrow \infty$:

$$w_{xv} \rightarrow 0, \quad (17.12)$$

17.2.2 Similarity Variables

Same as those in Chap. 14, the following dimensionless variables are assumed for the similarity transformation of the governing partial differential equations of the film condensation of saturated vapor:

For Liquid Film

For liquid film the similarity transformation variables are assumed as follows:

At first, the dimensionless coordinate variable η_l is set up as

$$\eta_l = \left(\frac{1}{4} \text{Gr}_{xl,s} \right)^{1/4} \frac{y}{x} \quad (17.13)$$

where the local Grashof number $\text{Gr}_{xl,s}$ is assumed as

$$\text{Gr}_{xl,s} = \frac{g(\rho_{l,w} - \rho_{v,s})x^3}{\nu_{l,s}^2 \rho_{l,s}} \quad (17.14)$$

The dimensionless temperature is given as

$$\theta_l = \frac{t_l - t_s}{t_w - t_s} \quad (17.15)$$

The dimensionless velocity components are assumed as

$$W_{xl} = \left(2\sqrt{gx} \left(\frac{\rho_{l,w} - \rho_{v,s}}{\rho_{l,s}} \right)^{1/2} \right)^{-1} w_{xl} \quad (17.16)$$

$$W_{yl} = \left(2\sqrt{gx} \left(\frac{\rho_{l,w} - \rho_{v,s}}{\rho_{l,s}} \right)^{1/2} \left(\frac{1}{4} \text{Gr}_{xl,s} \right)^{-1/4} \right)^{-1} w_{yl} \quad (17.17)$$

For Vapor Film

The vapor film dimensionless coordinate variable η_v and the local Grashof number $\text{Gr}_{xv,s}$ are assumed as respectively

$$\eta_v = \left(\frac{1}{4} \text{Gr}_{xv} \right)^{1/4} \frac{y}{x}, \quad \text{Gr}_{xv} = \frac{gx^3}{\nu_{v,s}^2} \quad (17.18)$$

The dimensionless velocity components are assumed as

$$W_{xv} = (2\sqrt{gx})^{-1} W_{xv} \quad (17.19)$$

$$W_{yv} = \left(2\sqrt{gx} \left(\frac{1}{4} \text{Gr}_{xv} \right)^{-1/4} \right)^{-1} w_{yv} \quad (17.20)$$

17.2.3 Transformed Dimensionless Differential Equations

The governing partial differential equations and the boundary conditions for the free film convection film condensation of saturated vapor are transformed to the following forms:

For Liquid Film

$$2W_{x1} - \eta_1 \frac{dW_{x1}}{d\eta_1} + 4 \frac{dW_{y1}}{d\eta_1} - \frac{1}{\rho_l} \frac{d\rho_l}{d\eta_1} (-\eta_1 W_{x1} + 4W_{y1}) = 0 \quad (17.21)$$

$$\frac{\nu_{l,s}}{\nu_l} \left(W_{xl} \left(2W_{xl} - \eta_l \frac{dW_{xl}}{d\eta_l} \right) + 4W_{yl} \frac{dW_{xl}}{d\eta_l} \right) = \frac{d^2 W_{xl}}{d\eta_l^2} + \frac{1}{\mu_l} \frac{d\mu_l}{d\eta_l} \frac{dW_{xl}}{d\eta_l} + \frac{\mu_{l,s}}{\mu_l} \frac{\rho_l - \rho_{v,s}}{\rho_{l,w} - \rho_{v,s}} \quad (17.22)$$

$$\text{Pr}_l \frac{\mu_{l,s}}{\mu_l} \frac{\rho_l}{\rho_{l,s}} [-\eta_l W_{xl} + 4W_{yl}] \frac{d\theta_l}{d\eta_l} = \frac{d^2 \theta_l}{d\eta_l^2} + \frac{1}{\lambda_l} \frac{d\lambda_l}{d\eta_l} \frac{d\theta_l}{d\eta_l} \quad (17.23)$$

For Vapor Film

$$2W_{xv} - \eta_v \frac{dW_{xv}}{d\eta_v} + 4 \frac{dW_{yv}}{d\eta_v} = 0 \quad (17.24)$$

$$W_{xv} \left(2W_{xv} - \eta_v \frac{dW_{xv}}{d\eta_v} \right) + 4W_{yv} \frac{dW_{xv}}{d\eta_v} = \frac{d^2 W_{xv}}{d\eta_v^2} \quad (17.25)$$

For Boundary Conditions

$\eta_l = 0$:

$$W_{xl} = 0, \quad W_{yl} = 0, \quad \theta_l = 1 \quad (17.26)$$

$$\eta_v = \eta_{l\delta} (\eta_v = 0):$$

$$W_{xv,s} = \left(\frac{\rho_{l,w} - \rho_{v,s}}{\rho_{l,s}} \right)^{1/2} W_{xl,s} \tag{17.27}$$

$$\rho_{l,s} \left(w_{xl} \frac{\partial \delta_l}{\partial x} - w_{yl} \right)_s = \rho_v \left(w_{xv} \frac{\partial \delta_v}{\partial x} - w_{yv} \right)_s$$

$$W_{yv,s} = -0.25 \frac{\rho_{l,s}}{\rho_v} \left(\frac{v_{v,s}}{v_v} \right)^{1/2} \left(\frac{\rho_{l,w} - \rho_{v,s}}{\rho_{l,s}} \right)^{1/4} (W_{xl,s} \eta_{l\delta} - 4W_{yl,s}) \tag{17.28}$$

$$\left(\frac{dW_{xv}}{d\eta_v} \right)_{\eta_v=0} = \frac{\mu_{l,s}}{\mu_v} \left(\frac{\rho_{l,w} - \rho_{v,s}}{\rho_{l,s}} \right)^{3/4} \left(\frac{v_{v,s}}{v_{l,s}} \right)^{1/2} \left(\frac{dW_{xl}}{d\eta_l} \right)_{\eta_l=\eta_{l\delta}} \tag{17.29}$$

$$h_{fg} \text{Pr}_{l,s} (W_{xl,s} \eta_{l\delta} - 4W_{yl,s}) + \lambda_{l,s} (t_w - t_s) \left(\frac{d\theta_l}{d\eta_l} \right)_{\eta_l=\eta_{l\delta}} = 0 \tag{17.30}$$

$$\theta_l = 0 \tag{17.31}$$

$\eta_v \rightarrow \infty$:

$$W_{xv} \rightarrow 0, \tag{17.32}$$

In the governing equations here various physical conditions, such as all variable thermophysical properties (except for that of specific heat), shear force at liquid–vapor interface, and condensate film inertia force and condensate film thermal convection are considered. The above physical conditions are overall named more complete condition for further investigations.

17.3 Different Physical Assumptions

17.3.1 Assumption a (with Boussinesq Approximation of Condensate Film)

The assumption a is defined that on the basis of the more complete condition the Boussinesq approximation is further considered in the governing differential equations of the condensate film. With assumption a, associated partial differential equations of the condensate film become

$$\frac{\partial w_{xl}}{\partial x} + \frac{\partial w_{yl}}{\partial y} = 0 \quad (17.33)$$

$$w_{xl} \frac{\partial w_{xl}}{\partial x} + w_{yl} \frac{\partial w_{xl}}{\partial y} = \nu_l^* \frac{\partial^2 w_{xl}}{\partial y_l^2} + \frac{g(\rho_l - \rho_{v,s})}{\rho_l^*} \quad (17.34)$$

$$\frac{\rho_l^* c_{pl}^*}{\lambda_l^*} \left(w_{xl} \frac{\partial t}{\partial x} + w_{yl} \frac{\partial t}{\partial y} \right) = \frac{\partial^2 t}{\partial y^2} \quad (17.35)$$

where the superscript * implies the value at reference temperature t^* that is described by mean temperature $(t_w + t_s)/2$.

Strictly speaking, for the boundary conditions under the Boussinesq approximation, the variable physical properties need not be considered. However, for examining the effect of the variable physical properties we still take the boundary conditions (17.6–17.12) with the temperature-dependent physical properties as the associated boundary conditions.

With the expressions (17.13–17.17) for the defined variables of the condensate film, the following governing ordinary differential equations can be derived from Eqs. (17.33–17.35) as:

$$2W_{xl} - \eta_l \frac{dW_{xl}}{d\eta_l} + 4 \frac{dW_{yl}}{d\eta_l} = 0 \quad (17.36)$$

$$\frac{\nu_{l,s}}{\nu_l^*} \left(W_{xl} \left(2W_{xl} - \eta_l \frac{dW_{xl}}{d\eta_l} \right) + 4W_{yl} \frac{dW_{xl}}{d\eta_l} \right) = \frac{d^2 W_{xl}}{d\eta_l^2} + \frac{\mu_{l,s}}{\mu_l} \frac{\rho_l - \rho_v}{\rho_{l,w} - \rho_v} \quad (17.37)$$

$$\text{Pr}_l^* \frac{\rho_l^*}{\rho_{l,s}} \frac{\mu_{l,s}}{\mu_l^*} (-\eta_l W_{lv} + 4W_{yl}) \frac{d\theta_l}{d\eta_l} = \frac{d^2 \theta_l}{d\eta_l^2} \quad (17.38)$$

From the analysis of Chap. 7, it is possible to regard the specific heat $c_{pl,s}^*$ in Pr_l^* as constant for water for a lot of liquids in the special temperature range for engineering application. In this case, the property factors $\text{Pr}_l^* \frac{\rho_l^*}{\rho_{l,s}} \frac{\mu_{l,s}}{\mu_l^*}$ in Eq. (17.38) can be substituted by $\text{Pr}_{l,s} \frac{\rho_l^*}{\rho_{l,s}} \frac{\lambda_{l,s}}{\lambda_l^*}$.

The governing ordinary differential equations of the vapor film are also Eqs. (17.24) and (17.25). Of course, the transformed dimensionless boundary conditions are also Eqs. (17.26–17.32).

17.3.2 Assumption b (Ignoring Shear Force at Liquid–Vapor Interface)

In assumption b, the shear force at the liquid–vapor interface is neglected on the basis of the more complete conditions. The governing partial differential equations for this assumption are only Eqs. (17.1–17.3), and the governing equations of vapor film should be omitted. Consequently, the boundary conditions Eqs. (17.7), (17.8) and (17.12) are omitted, and Eqs. (17.6), (17.10), and (17.11) remain. Since the shear force at the liquid–vapor interface is neglected, the boundary condition Eqs. (17.9) is simplified to

$$y = \delta_l: \left(\frac{\partial w_{xl}}{\partial y} \right)_s = 0 \quad (17.39)$$

With Eqs. (17.13) and (17.16) for the defined similarity variables, Eq. (17.39) is changed into

$$\eta_l = \eta_{l\delta}: \left(\frac{dW_{xl}}{d\eta_l} \right)_{\eta_l = \eta_{l\delta}} = 0 \quad (17.40)$$

Thus, with the similarity transformation the governing partial equations (17.1–17.3) are transformed to Eqs. (17.21–17.23) respectively, and their boundary conditions are (17.26), (17.30), (17.31) and (17.40).

17.3.3 Assumption c (Ignoring Inertia Force of the Condensate Film)

The assumption c is defined that the inertia force of the condensate film is further omitted on the basis of the assumption b. The governing partial differential equations in this assumption are Eqs. (17.1) and (17.3), as well as the following momentum equation

$$\frac{\partial}{\partial y} \left(\mu_l \frac{\partial w_{xl}}{\partial y} \right) + g(\rho_l - \rho_{v,s}) = 0 \quad (17.41)$$

Then, by virtue of the expressions for defined similarity variables, Eqs. (17.13–17.17), the associated governing ordinary differential equations will be Eqs. (17.21) and (17.23), as well as the following equation

$$\frac{d^2 W_{xl}}{d\eta_l^2} + \frac{1}{\mu_l} \frac{d\mu_l}{d\eta_l} \frac{dW_{xl}}{d\eta_l} + \frac{\mu_{l,s}}{\mu_l} \frac{\rho_l - \rho_{v,s}}{\rho_{l,w} - \rho_{v,s}} = 0 \quad (17.42)$$

The boundary conditions for the assumption c are same as those for assumption b.

17.3.4 Assumption d (Ignoring Thermal Convection of the Condensate Film)

Assumption d is that the thermal convection of the condensate film is further omitted on the basis of the assumption c. For this further assumption, the energy Eq. (17.3) is simplified to

$$\frac{\partial}{\partial y} \left(\lambda_l \frac{\partial t}{\partial y} \right) = 0 \quad (17.43)$$

Therefore, the governing partial differential equations of this assumption should then be Eqs. (17.1), (17.41), (17.43) and the associated ordinary differential equations are Eqs. (17.21) and (17.42), as well as the following energy equation:

$$\frac{d^2 \theta_l}{d\eta_l^2} = - \frac{1}{\lambda_l} \frac{d\lambda_l}{d\eta_l} \frac{d\theta_l}{d\eta_l} \quad (17.44)$$

The associated boundary conditions for the assumption d are also the same as those for the assumption b.

17.4 Effects of Various Physical Conditions on Velocity and Temperature Fields

The numerical calculations in each assumed physical condition are carried out for different wall subcooled grade, such as $\frac{\Delta t_w}{t_s} (= \frac{t_s - t_w}{t_s}) = 0.001, 0.025, 0.05, 0.1, 0.2, 0.4, 0.6, 0.8, 1$ for film condensation of saturated water vapor. Some calculated results of the dimensionless velocity component $W_{x,l}$ and temperature fields are plotted in Figs. 17.1 and 17.2, respectively. It is seen that the physical conditions have corresponding influences both on the condensate film velocity and temperature fields, and with increasing the wall subcooled grade $\frac{\Delta t_w}{t_s}$, these influences will increase. Additionally, the effects of Boussinesq approximation on the condensate film velocity and temperature fields are much larger than those of other physical conditions. While, the effects of the condensate film thermal convection on the condensate film velocity and temperature fields are larger than those of liquid–vapor interfacial shear force and the condensate film inertia force.

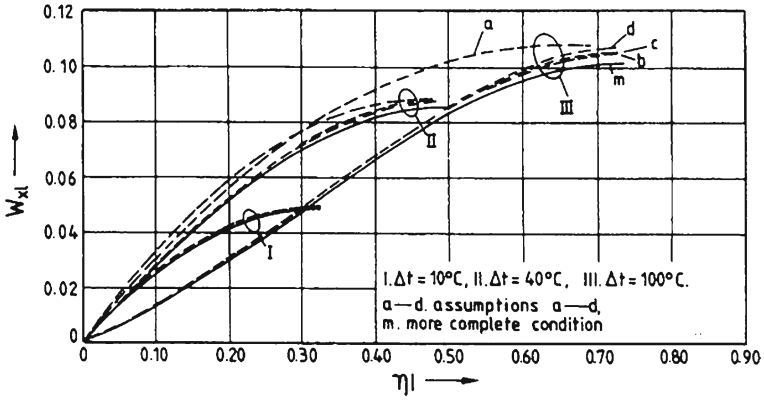


Fig. 17.1 Velocity profiles of film condensation of saturated water vapor in different Conditions, cited from Shang and Adamek [1] I $\frac{\Delta t_w}{t_s} = 0.1$, II $\frac{\Delta t_w}{t_s} = 0.4$, III $\frac{\Delta t_w}{t_s} = 1$ Line *m* for more complete condition Lines *a* to *d* for assumptions *a* to *d* respectively

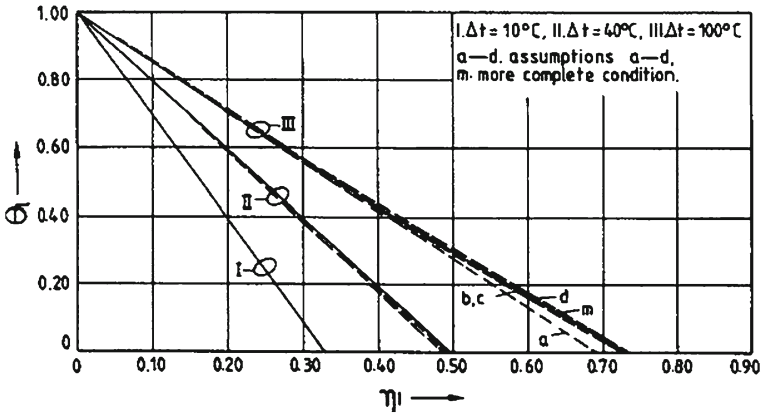


Fig. 17.2 Temperature profiles of film condensation of saturated water steam in different Conditions, cited from Shang and Adamek [1] I $\frac{\Delta t_w}{t_s} = 0.1$, II $\frac{\Delta t_w}{t_s} = 0.4$, III $\frac{\Delta t_w}{t_s} = 1$ Line *m* for more complete condition Lines *a* to *d* for assumptions *a* to *d* respectively

17.5 Effects of Various Physical Conditions on Heat Transfer

According to Eq. (16.2), the local heat transfer coefficient on the surface for the film condensation of saturated vapor is

$$\alpha_x = -\lambda_{l,w} \left(\frac{1}{4} Gr_{x,l,s} \right)^{1/4} x^{-1} \left(\left(\frac{d\theta_l}{d\eta_l} \right)_{\eta_l=0} \right)_{\Delta t_\infty=0} \tag{17.45}$$

If we define the same Grashof number $Gr_{xl,s}$ for that with the different assumed conditions, the deviations of the heat transfer coefficient caused by the related assumed conditions can be expressed as follows respectively:

Effect of Boussinesq approximation for the condensate film of saturated vapor on heat transfer coefficient can be expressed as

$$\Delta(\alpha_x)_a = \frac{(\alpha_x)_a - (\alpha_x)_m}{(\alpha_x)_m} = \frac{\left(\left(\left(-\frac{d\theta_l}{d\eta_l} \right)_{\eta_l=0} \right)_{\Delta t_\infty=0} \right)_a - \left(\left(\left(-\frac{d\theta_l}{d\eta_l} \right)_{\eta_l=0} \right)_{\Delta t_\infty=0} \right)_m}{\left(\left(\left(-\frac{d\theta_l}{d\eta_l} \right)_{\eta_l=0} \right)_{\Delta t_\infty=0} \right)_m} \quad (17.46)$$

Effect of ignoring shear force at the liquid–vapor interface on heat transfer coefficient can be expressed as

$$\Delta(\alpha_x)_b = \frac{(\alpha_x)_b - (\alpha_x)_m}{(\alpha_x)_m} = \frac{\left(\left(\left(-\frac{d\theta_l}{d\eta_l} \right)_{\eta_l=0} \right)_{\Delta t_\infty=0} \right)_b - \left(\left(\left(-\frac{d\theta_l}{d\eta_l} \right)_{\eta_l=0} \right)_{\Delta t_\infty=0} \right)_m}{\left(\left(\left(-\frac{d\theta_l}{d\eta_l} \right)_{\eta_l=0} \right)_{\Delta t_\infty=0} \right)_m} \quad (17.47)$$

Effect of ignoring inertia force of the condensate film on heat transfer coefficient can be expressed as

$$\Delta(\alpha_x)_c = \frac{(\alpha_x)_c - (\alpha_x)_b}{(\alpha_x)_b} = \frac{\left(\left(\left(-\frac{d\theta_l}{d\eta_l} \right)_{\eta_l=0} \right)_{\Delta t_\infty=0} \right)_c - \left(\left(\left(-\frac{d\theta_l}{d\eta_l} \right)_{\eta_l=0} \right)_{\Delta t_\infty=0} \right)_b}{\left(\left(\left(-\frac{d\theta_l}{d\eta_l} \right)_{\eta_l=0} \right)_{\Delta t_\infty=0} \right)_b} \quad (17.48)$$

Effect of ignoring thermal convection of the condensate film on heat transfer coefficient can be expressed as

$$\Delta(\alpha_x)_d = \frac{(\alpha_x)_d - (\alpha_x)_c}{(\alpha_x)_c} = \frac{\left(\left(\left(-\frac{d\theta_l}{d\eta_l} \right)_{\eta_l=0} \right)_{\Delta t_\infty=0} \right)_d - \left(\left(\left(-\frac{d\theta_l}{d\eta_l} \right)_{\eta_l=0} \right)_{\Delta t_\infty=0} \right)_c}{\left(\left(\left(-\frac{d\theta_l}{d\eta_l} \right)_{\eta_l=0} \right)_{\Delta t_\infty=0} \right)_c} \quad (17.49)$$

Briefly, the effect of the variable physical properties, interfacial shear force, inertia force, and thermal convection are expressed by $\Delta(\alpha_x)_a$, $\Delta(\alpha_x)_b$, $\Delta(\alpha_x)_c$, and $\Delta(\alpha_x)_d$.

The numerical solutions of temperature gradient $\left(\left(-\frac{d\theta}{d\eta} \right)_{\eta=0} \right)_{\Delta T_\infty=0}$ in the various assumptions are obtained numerically for the film boiling of saturated water vapor, and shown in Table 17.1 and Fig. 17.3, respectively. According to Eqs. (17.46–17.49), the deviation of the heat transfer coefficient related to different assumed conditions are evaluated, shown in Table 17.1, and plotted in Fig. 17.4, respectively.

It is seen that, with increasing the wall suncooled grade $\frac{\Delta T_w}{T_s}$, ignoring both of the variable physical properties and thermal convection of condensate liquid film will decrease the heat transfer coefficient at an accelerative pace, meanwhile, will cause increase heat transfer coefficient slowly on laminar free film condensation.

It is also seen that, among these assumptions, ignoring the variable physical properties (i.e. Boussinesq approximation) will cause a largest deviation of heat transfer for the film condensation. Ignoring the thermal convection of condensate liquid film will cause a large deviation of heat transfer, only less than the deviation caused by ignoring the variable physical properties. Ignoring the inertia force of the condensate liquid film will cause minimum deviation of heat transfer. While, ignoring the interfacial shear force will cause a deviation of heat transfer, only little bit larger than that caused by the inertia force of the condensate liquid film.

Briefly, the variable physical properties and thermal convection cause larger effect on heat transfer of laminar free film condensation, meanwhile, the effect of the variable physical properties is even larger than that of the thermal convection. Compared with the variable physical properties and thermal convection, the effect of the Interfacial shear force and inertia force will be much smaller on heat transfer of laminar free film condensation, meanwhile, the effect of the inertia force is little bit smaller than that of the interfacial shear force.

17.6 Remarks

In this chapter, the film condensation of saturated water vapor is taken as an example for analyzing the effects of various physical conditions on the heat transfer coefficient. The effects of the four physical conditions are considered including Boussinesq approximation (i.e. ignoring variable physical properties), shear force at the liquid–vapor interface, and inertia force and the thermal convection of the condensate film. It is found that the variable physical properties and thermal convection cause larger effect on heat transfer of laminar free film condensation, meanwhile, the effect of the variable physical properties is even larger than that of the thermal convection. It follows that it is necessary to consider variable physical properties for investigation on heat transfer of free film condensation. Compared with the variable physical properties and thermal convection, the effect of the Interfacial shear force and inertia force will be much smaller on heat transfer of laminar free film condensation, mean-

Table 17.1 Temperature gradient $\left(-\frac{dh}{d\eta}\right)_{\eta=0}$ of film condensation of saturated water vapor for different assumptions and the deviations of heat transfer coefficient caused by the related assumed conditions, cited from Shang and Adamek [1] Line m for more complete condition Lines a to d for assumptions a to d respectively

$\Delta t_w (= t_s - t_w) ^\circ\text{C}$	0.1	2.5	5	10	20	40	60	80	100
$\Delta t_w / t_s$	0.001	0.025	0.05	0.1	0.2	0.4	0.6	0.8	1
at different assumed conditions									
$\left(-\frac{dh}{d\eta}\right)_{\eta=0}$	$\Delta_{f\infty=0}$								
$\left(\left(-\frac{dh}{d\eta}\right)_{\eta=0}\right)_{\Delta_{f\infty=0}}$	9.8338	4.38135	3.67507	3.06412	2.53975	2.07889	1.83238	1.6679	1.55107
$\left(\left(\left(-\frac{dh}{d\eta}\right)_{\eta=0}\right)_{\Delta_{f\infty=0}}\right)_m$	9.83484	4.3838	3.67408	3.06138	2.52947	2.05258	1.78498	1.59648	1.44567
$\left(\left(\left(-\frac{dh}{d\eta}\right)_{\eta=0}\right)_{\Delta_{f\infty=0}}\right)_a$	9.83424	4.38346	3.677	3.06945	2.5483	2.09063	1.8454	1.68121	1.56388
$\left(\left(\left(-\frac{dh}{d\eta}\right)_{\eta=0}\right)_{\Delta_{f\infty=0}}\right)_b$	9.83424	4.38442	3.67808	3.07104	2.55086	2.09381	1.84874	1.68455	1.56665
$\left(\left(\left(-\frac{dh}{d\eta}\right)_{\eta=0}\right)_{\Delta_{f\infty=0}}\right)_c$	9.83259	4.38085	3.6739	3.062	2.53525	2.06877	1.81672	1.64711	1.52566
$\left(\left(\left(-\frac{dh}{d\eta}\right)_{\eta=0}\right)_{\Delta_{f\infty=0}}\right)_d$	9.83259	4.38085	3.6739	3.062	2.53525	2.06877	1.81672	1.64711	1.52566
deviations of heat transfer coefficient caused by the related assumed conditions [effect of the variable physical properties, interfacial shear force, inertia force, and thermal convection are expressed respectively by $\Delta(\alpha_x)_a$, $\Delta(\alpha_x)_b$, $\Delta(\alpha_x)_c$, and $\Delta(\alpha_x)_d$]									
$\Delta(\alpha_x)_a$	0.000106	0.000559	-0.000269	-0.00089	-0.00405	-0.01266	-0.02587	-0.04282	-0.06795
$\Delta(\alpha_x)_b$	0.000045	0.000482	0.000525	0.001739	0.003366	0.005647	0.007106	0.00798	0.008259
$\Delta(\alpha_x)_c$	0	0.000219	0.000294	0.000518	0.001005	0.001521	0.00181	0.001987	0.001771
$\Delta(\alpha_x)_d$	-0.000168	-0.000814	-0.001136	-0.00294	-0.00612	-0.01196	-0.01732	-0.02223	-0.02616

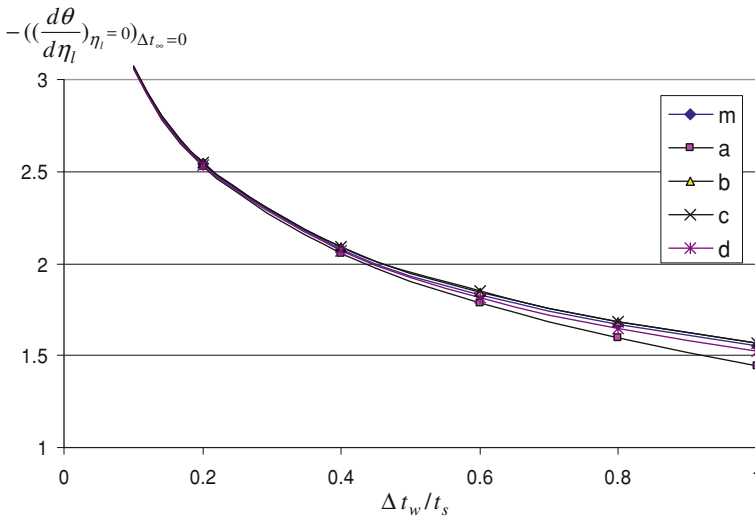


Fig. 17.3 The distributions of $\left(\left(-\frac{d\theta}{d\eta_l}\right)_{\eta_l=0}\right)_{\Delta t_{\infty}=0}$ of film condensation of saturated water vapor with different assumptions Line *m* for more complete condition Lines *a* to *d* for assumptions *a* to *d* respectively

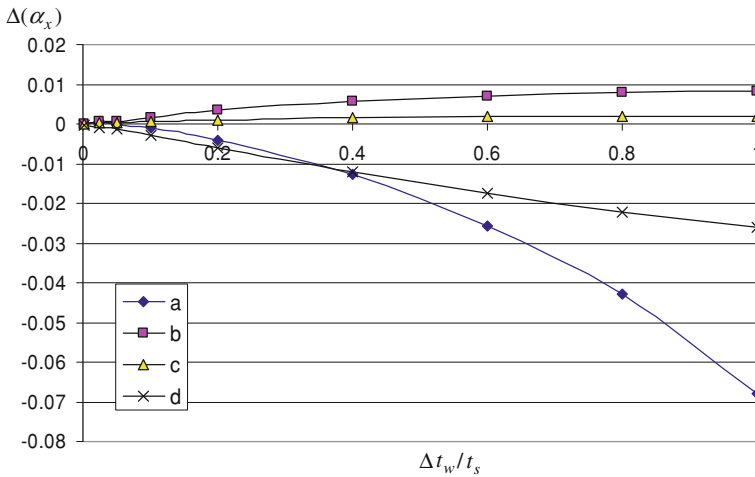


Fig. 17.4 The deviation of α_x for film condensation of saturated water vapor for different assumed conditions Lines *a*–*d* for $\Delta(\alpha_x)_a$, $\Delta(\alpha_x)_b$, $\Delta(\alpha_x)_c$ and $\Delta(\alpha_x)_d$, respectively

while, the effect of the inertia force is little bit smaller than that of the interfacial shear force.

17.7 Exercises

1. Compare the four physical conditions, i.e., variable physical properties, interfacial shear force, inertia force, and thermal convection, and find out
 - (i) which two conditions have larger effect, and which two conditions have smaller effect on heat transfer of free film condensation?
 - (ii) Which condition has the largest effect on heat transfer of free film condensation?
 - (iii) which condition has the smallest effect on heat transfer of free film condensation?
2. According to the analysis results in this chapter, please explain the importance for consideration of variable physical properties.

References

1. D.Y. Shang, T. Adamek, Study on laminar film condensation of saturated steam on a vertical flat plate for consideration of various physical factors including variable thermophysical properties. *Wärme- und Stoffübertragung* **30**, 89–100 (1994)
2. D.Y. Shang, T. Adamek, in Study of laminar film condensation of saturated steam for consideration of variable thermophysical properties, *Transport phenomena, Science and Technology*, ed. by B.X. Wang (Higher Education press, Beijing, 1992), pp. 470–475

Chapter 18

Complete Similarity Mathematical Models on Laminar Free Convection Film Condensation from Vapor–Gas Mixture

Abstract By means of the new similarity analysis method, the governing partial differential equations of laminar free convection film condensation of vapor–gas mixture are transformed into the complete dimensionless mathematical models. The transformed complete governing mathematical models are equivalent to the system of dimensionless governing equations, which involve (1) the continuity, momentum, and energy equations for both liquid and vapor–gas mixture films, as well as species conservation equation with mass diffusion in the vapor–gas mixture film, (2) a set of interfacial physical matching conditions, such as those for two-dimensional velocity component balances, shear force balance, mass flow rate balance, temperature balance, heat transfer balance, concentration condition, as well as the balance between the condensate mass flow and vapor mass diffusion. On the other hand, the transformed complete similarity mathematical models of the film condensation of vapor–gas mixture are very well coupled with a series of physical property factors, such as the density factor, absolute viscosity factor, thermal conductivity factor, of the medium of liquid film and the vapor–gas mixture film. Thus, the transformed complete similarity mathematical models are advanced ones for consideration of variable physical properties.

18.1 Introduction

Since the important role played by film condensation in many industrial applications, numerous efforts have been made for investigation of its physical phenomena. For laminar free convection film condensation of pure vapor, some detailed reviews can be found in Refs. [1–5], and meanwhile, our detailed theoretical analysis and mathematical models on laminar free convection film condensation from pure vapor [6, 7] were reported, where calculations of condensate heat and mass transfer were presented with comprehensive consideration and treatment on interfacial physical matching conditions and temperature-dependent physical properties of the two-phase film flows.

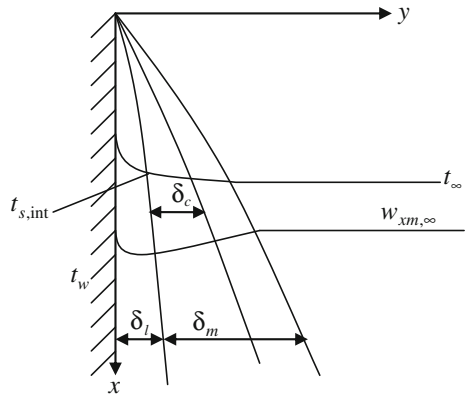
For laminar free convection film condensation from vapor in presence of non-condensable gas, Minkowycz and Sparrow [8] presented their earlier investigation. Then, numerous theoretical and experimental studies have been conducted for its successive investigations, such as those in Refs. [9–19]. Their studies demonstrated that the bulk concentration of the non-condensable gas could cause great reductions in its condensation heat transfer. This is because of the fact that the presence of non-condensable gas lowers the partial pressure of the vapor, and then reduces the vapor condensate saturation temperature at liquid–vapor interface.

In fact, the work is still a challenge for theoretical study of film condensation from vapor–gas mixture, due to its additional concentration boundary layer, temperature- and concentration-dependent physical properties, interfacial mass diffusion balance conditions, and the dropped condensate saturated temperature together with increasing the mass fraction of non-condensable gas. For resolving these issues, Ref. [20] presented a challenging work on a theoretical study of laminar free convection film condensation from vapor–gas mixture. Here, I will first present the theoretical and mathematical models for the laminar free convection film consideration of vapor–gas mixture. Meanwhile, the new similarity analysis method is used for equivalent transformation of the system of governing partial differential equations. Particularly, the following efforts will be emphasized: (1) comprehensive consideration and treatment of temperature-dependent physical properties of the condensate liquid film; (2) comprehensive consideration and treatment of the temperature and concentration-dependent physical properties of the vapor–gas mixture film; (3) seriously satisfying whole sets of the interfacial matching conditions in calculation; and (4) rigorous evaluation of the interfacial vapor condensate saturated temperature, the key prerequisite of correct calculation of the film condensation from vapor–gas mixture. On these bases, the reliable analysis, calculation, and clarification of temperature, velocity, and concentration fields, as well as condensate heat and mass transfer are further presented on the laminar free convection film condensation of vapor–gas mixture.

18.2 Governing Partial Differential Equations

The analytical model and coordinate system used for laminar free film condensation of vapor–gas mixture on an isothermal vertical flat plate is shown in Fig. 18.1. An isothermal vertical flat plate is suspended in a large volume of quiescent vapor–gas mixture at atmospheric pressure. The plate temperature is T_w , the temperature of the vapor–gas mixture bulk is T_∞ , and the saturation temperature of pure vapor at atmospheric pressure is T_s , while the interfacial vapor saturated temperature is $T_{s,int}$. If the given condition for the model is $T_w < T_{s,int}$, a steady film condensation will occur on the plate. We assume that the laminar flow within the liquid film is induced by gravity, and the vapor–gas mixture film flow is caused by the shear force at the liquid–vapor interface. We further assume that the mass flow rate of vapor is balanced to the vapor mass diffusion at the liquid–vapor interface in the steady state of the laminar free film condensation. Then, there is never an

Fig. 18.1 Physical model and coordinate system of the laminar free convection film condensation from vapor–gas mixture. Note δ_l : condensate liquid film thickness; δ_m : thicknesses of momentum or temperature boundary layer of vapor–gas mixture; δ_c : concentration boundary layer of vapor–gas mixture



additional gas boundary layer near the interface except the induced concentration boundary layer of the vapor–gas mixture. In addition, we take into account the temperature-dependent physical properties of the condensate liquid film and the temperature- and concentration-dependent physical properties of the induced vapor–gas mixture film. Then, the steady laminar governing equations for mass, momentum, energy, and concentration conservations in the two-phase boundary layer are as follows:

The governing partial differential equations for condensate liquid film are

$$\frac{\partial}{\partial x}(\rho_l w_{xl}) + \frac{\partial}{\partial y}(\rho_l w_{yl}) = 0 \tag{18.1}$$

$$\rho_l \left(w_{xl} \frac{\partial w_{xl}}{\partial x} + w_{yl} \frac{\partial w_{xl}}{\partial y} \right) = \frac{\partial}{\partial y} \left(\mu_l \frac{\partial w_{xl}}{\partial y} \right) + g(\rho_l - \rho_{m,\infty}) \tag{18.2}$$

$$\rho_l \left[w_x \frac{\partial (c_{pl} t)}{\partial x} + w_y \frac{\partial (c_{pl} t)}{\partial y} \right] = \frac{\partial}{\partial y} \left(\lambda_l \frac{\partial t}{\partial y} \right) \tag{18.3}$$

where Eqs. (18.1)–(18.3) are continuity, momentum, and energy conservation equations respectively.

The governing partial differential equations for vapor–gas mixture film are

$$\frac{\partial}{\partial x}(\rho_m w_{xm}) + \frac{\partial}{\partial y}(\rho_m w_{ym}) = 0 \tag{18.4}$$

$$\rho_m \left(w_{xm} \frac{\partial w_{xm}}{\partial x} + w_{ym} \frac{\partial w_{xm}}{\partial y} \right) = \frac{\partial}{\partial y} \left(\mu_m \frac{\partial w_{xm}}{\partial y} \right) + g(\rho_m - \rho_{m,\infty}) \tag{18.5}$$

$$\rho_m c_{pm} \left(w_{xm} \frac{\partial t_m}{\partial x} + w_{ym} \frac{\partial t_m}{\partial y} \right) = \frac{\partial}{\partial y} \left(\lambda_m \frac{\partial t_m}{\partial y} \right) + \frac{\partial}{\partial y} \left[\rho_m D_v (c_{pv} - c_{pg}) \frac{\partial C_{mv}}{\partial y} t_m \right] \tag{18.6}$$

$$\frac{\partial(w_{xm}\rho_m C_{mv})}{\partial x} + \frac{\partial(w_{ym}\rho_m C_{mv})}{\partial y} = \frac{\partial}{\partial y} \left(D_v \rho_m \frac{\partial C_{mv}}{\partial y} \right) \quad (18.7)$$

where Eqs. (18.4)–(18.6) are continuity, momentum, and energy conservation equations, while Eq. (18.7) is the species conservation equation with mass diffusion. Here, C_{mv} is vapor mass fraction in vapor–gas mixture, ρ_m , μ_m , λ_m , and Cp_m are density, absolute viscosity, thermal conductivity, and specific heat of the vapor–gas mixture, respectively, and D_v denotes vapor mass diffusion coefficient in the non-condensable gas.

The boundary conditions are

$$y = 0: \quad w_{xl} = 0, \quad w_{yl} = 0, \quad t_l = t_w \quad (18.8)$$

$$y = \delta_l: \quad w_{xl,s} = w_{xv,s} \quad (18.9)$$

$$\rho_{l,s} \left(w_{xl} \frac{\partial \delta_l}{\partial x} - w_{yl} \right)_s = \rho_{m,s} C_{mv,s} \left(w_{xm} \frac{\partial \delta_m}{\partial x} - w_{ym} \right)_s = g_x \quad (18.10)$$

$$\mu_{l,s} \left(\frac{\partial w_{xl}}{\partial y} \right)_s = \mu_{m,s} \left(\frac{\partial w_{xm}}{\partial y} \right)_s \quad (18.11)$$

$$\lambda_{l,s} \left(\frac{\partial t}{\partial y} \right)_{l,s} = \lambda_{m,s} \left(\frac{\partial t}{\partial y} \right)_{m,s} + h_{fg} \rho_{m,s} C_{mv,s} \left(w_{xm} \frac{\partial \delta_m}{\partial x} - w_{ym} \right)_{m,s} \quad (18.12)$$

$$t = t_{s,int} \quad (18.13)$$

$$C_{mv} = C_{mv,s} \quad (18.14)$$

$$\rho_{m,s} C_{m,s} \left(w_x \frac{\partial \delta}{\partial x} - w_y \right)_{m,s} = D_v \rho_{m,s} \left(\frac{\partial C_{mv}}{\partial y} \right)_{m,s} \quad (18.15)$$

$$y \rightarrow \infty: \quad w_{xm} = 0, \quad t_m = t_\infty, \quad C_{mv} = C_{mv,\infty} \quad (18.16)$$

where Eq. (18.8) expresses the physical conditions on the plate. Equations (18.9)–(18.15) express the physical matching conditions at the liquid–vapor interface, in which Eq. (18.9) expresses the velocity component continuity, Eq. (18.10) expresses the mass flow rate continuity, Eq. (18.11) expresses the balance of the shear force, Eq. (18.12) expresses the energy balance, Eq. (18.13) expresses the temperature, Eq. (18.14) expresses the concentration, and Eq. (18.15) expresses the vapor mass flow rate is balanced to the mass flow rate caused by the vapor mass diffusion. Additionally, Eq. (18.16) expresses the physical conditions in the vapor–gas mixture bulk. In addition, $\rho_{l,s}$ and $\rho_{m,s}$ are liquid and vapor–gas mixture densities at the liquid–vapor interface, respectively, $t_{s,int}$ denotes the interfacial temperature dependent on interfacial vapor mass fraction, i.e., vapor partial pressure, t_∞ denotes the temperature in the vapor–gas mixture bulk, and $C_{mv,s}$ and $C_{mv,\infty}$ denote the *vapor mass fraction* at the liquid–vapor interface and in the vapor–gas mixture bulk respectively.

It is necessary to explain Eq. (18.15) for the condition of interfacial mass diffusion balance. Originally, it should be

$$\left[\rho_l \left(w_x \frac{\partial \delta_l}{\partial x} - w_y \right) \right]_{l,s} = \left[\rho_{m,s} C_{m,s} \left(w_x \frac{\partial \delta}{\partial x} - w_y \right) \right]_{m,s} \equiv D_v \rho_{m,s} \left(\frac{\partial C_{mv}}{\partial y} \right)_{m,s} \quad (18.15 \text{ orig.})$$

18.3 Similarity Variables

With the present new similarity analysis method, the following dimensionless variables are assumed for similarity transformation of the governing partial differential equations of the laminar free convection film condensation of vapor in presence of non-condensable gas:

18.3.1 For Liquid Film

For liquid film the *dimensionless coordinate variables* η_l and the *local Grashof number* $Gr_{x1,s}$ are set up as follows respectively:

$$\eta_l = \left(\frac{1}{4} Gr_{x1,s} \right)^{1/4} \frac{y}{x} \quad (18.17)$$

$$Gr_{x1,s} = \frac{g(\rho_{l,w} - \rho_{m,\infty})x^3}{\nu_{l,s}^2 \rho_{l,s}} \quad (18.18)$$

Dimensionless temperature is assumed as

$$\theta_l = \frac{t_l - t_{s,int}}{t_w - t_{s,int}} \quad (18.19)$$

The *dimensionless velocity components* are given as respectively in x - and y -directions

$$W_{x1} = \left(2\sqrt{g_x} \left(\frac{\rho_{l,w} - \rho_{m,\infty}}{\rho_{l,s}} \right)^{1/2} \right)^{-1} W_{x1} \quad (18.20)$$

$$W_{y1} = \left(2\sqrt{g_x} \left(\frac{\rho_{l,w} - \rho_{m,\infty}}{\rho_{l,s}} \right)^{1/2} \left(\frac{1}{4} Gr_{x1,s} \right)^{-4} \right)^{-1} W_{y1} \quad (18.21)$$

Here, $\rho_{l,w}$ is condensate liquid density on the wall, $\nu_{l,s}$ is condensate liquid kinetic viscosity at the liquid–vapor interface, while, $\rho_{m,\infty}$ is density of vapor–gas mixture in the bulk.

18.3.2 For Vapor–Gas Mixture Film

For vapor–gas mixture film, the dimensionless coordinate variables η_m and the local Grashof number $\text{Gr}_{x_m, \infty}$ are assumed as respectively

$$\eta_m = \left(\frac{1}{4} \text{Gr}_{x_m, \infty} \right)^{1/4} \frac{y}{x} \quad (18.22)$$

$$\text{Gr}_{x_m, \infty} = \frac{g(\rho_{m,s}/\rho_{m,\infty} - 1)x^3}{\nu_{m,\infty}^2} \quad (18.23)$$

The dimensionless temperature is defined as

$$\theta_m = \frac{t_m - t_\infty}{t_{s,\text{int}} - t_\infty} \quad (18.24)$$

The dimensionless velocity components are assumed as respectively in x - and y -directions

$$W_{x_m} = (2\sqrt{gx}(\rho_{m,s}/\rho_{m,\infty} - 1)^{1/2})^{-1} w_{x_m} \quad (18.25)$$

$$W_{y_m} = \left(2\sqrt{gx}(\rho_{m,s}/\rho_{m,\infty} - 1)^{1/2} \left(\frac{1}{4} \text{Gr}_{x_m, \infty} \right)^{-1/4} \right)^{-1} w_{y_m} \quad (18.26)$$

The *vapor relative mass fraction* is defined as

$$\Gamma_{mv} = \frac{C_{mv} - C_{mv,\infty}}{C_{mv,s} - C_{mv,\infty}} \quad (18.27)$$

18.4 Governing Ordinary Differential Equations

With Eqs.(18.17)–(18.27), the governing partial differential equations are transformed equivalently into the following dimensionless governing equations respectively:

18.4.1 For Liquid Film Flow

$$2W_{x1} - \eta_1 \frac{dW_{x1}}{d\eta_1} + 4 \frac{dW_{y1}}{d\eta_1} - \frac{1}{\rho_1} \frac{d\rho_1}{d\eta_1} (\eta_1 W_{x1} - 4W_{y1}) = 0 \quad (18.28)$$

$$\begin{aligned} \frac{\nu_{1,s}}{\nu_1} \left[W_{x1} \left(2W_{x1} - \eta_1 \frac{dW_{x1}}{d\eta_1} \right) + 4W_{y1} \frac{dW_{x1}}{d\eta_1} \right] \\ = \frac{d^2 W_{x1}}{d\eta_1^2} + \frac{1}{\mu_1} \frac{d\mu_1}{d\eta_1} \frac{dW_{x1}}{d\eta_1} + \frac{\mu_{1,s}}{\mu_1} \frac{(\rho_1 - \rho_{m,\infty})}{\rho_{1,w} - \rho_{m,\infty}} \end{aligned} \quad (18.29)$$

$$\text{Pr}_1 \frac{\nu_{1,s}}{\nu_1} (-\eta_1 W_{x1} + 4W_{y1}) \frac{d\theta_1}{d\eta_1} = \frac{d^2 \theta_1}{d\eta_1^2} + \frac{1}{\lambda_1} \frac{d\lambda_1}{d\eta_1} \frac{d\theta_1}{d\eta_1} \quad (18.30)$$

where Eqs. (18.28)–(18.30) are continuity, momentum, and energy conservation equations respectively.

18.4.2 For Vapor–Gas Mixture Film Flow

$$2W_{xm} - \eta_m \frac{dW_{xm}}{d\eta_m} + 4 \frac{dW_{ym}}{d\eta_m} - \frac{1}{\rho_m} \frac{d\rho_m}{d\eta_m} (\eta_m W_{xm} - 4W_{ym}) = 0 \quad (18.31)$$

$$\begin{aligned} \frac{\nu_{m,\infty}}{\nu_m} \left[W_{xm} \left(2W_{xm} - \eta_m \frac{dW_{xm}}{d\eta_m} \right) + 4W_{ym} \frac{dW_{xm}}{d\eta_m} \right] \\ = \frac{d^2 W_{xm}}{d\eta_m^2} + \frac{1}{\mu_m} \frac{d\mu_m}{d\eta_m} \frac{dW_{xm}}{d\eta_m} + \frac{\mu_{m,\infty}}{\mu_m} \cdot \frac{\rho_m - \rho_{m,\infty}}{\rho_{m,s} - \rho_{m,\infty}} \end{aligned} \quad (18.32)$$

$$\begin{aligned} \frac{\nu_{m,\infty}}{\nu_m} [-\eta_m W_{xm} + 4W_{ym}] \frac{d\theta_m}{d\eta_m} \\ = \frac{1}{\text{Pr}_m} \left(\frac{d^2 \theta_m}{d\eta_m^2} + \frac{1}{\lambda_m} \frac{d\lambda_m}{d\eta_m} \cdot \frac{d\theta_m}{d\eta_m} \right) \\ - \frac{1}{\text{Sc}_{m,\infty}} \frac{\nu_{m,\infty}}{\nu_m} (C_{mv,s} - C_{mv,\infty}) \frac{c_{p_v} - c_{p_g}}{c_{p_m}} \left[\frac{d\theta_m}{d\eta_m} \frac{d\Gamma_{mv}}{d\eta_m} + \left(\theta_m \right. \right. \\ \left. \left. + \frac{t_\infty}{t_{s,\text{int}} - t_\infty} \right) \frac{d^2 \Gamma_{mv}}{d\eta_v^2} + \left(\theta_m + \frac{t_\infty}{t_{s,\text{int}} - t_\infty} \right) \frac{1}{\rho_m} \frac{d\rho_m}{d\eta_m} \frac{d\Gamma_{mv}}{d\eta_m} \right] \end{aligned} \quad (18.33)$$

$$(-\eta_m W_{xm} + 4W_{ym}) \frac{d\Gamma_{mv}}{d\eta_m} = \frac{1}{\text{Sc}_{m,\infty}} \left(\frac{d^2 \Gamma_{mv}}{d\eta_m^2} + \frac{1}{\rho_m} \frac{d\rho_m}{d\eta_m} \frac{d\Gamma_{mv}}{d\eta_m} \right) \quad (18.34)$$

where Eqs. (18.31)–(18.33) are continuity, momentum, and energy conservation equations, while Eq. (18.34) is the species conservation equation with mass diffusion. Here, $\text{Sc}_{m,\infty} = \frac{\nu_{m,\infty}}{D_v}$ is defined as local Schmidt number, and μ_m , λ_m , and C_{p_m} are absolute viscosity, thermal conductivity, and specific heat of the vapor–gas mixture, respectively.

18.4.3 For Boundary Conditions

The boundary equations (18.8)–(18.16) are respectively transformed equivalently to

$$\eta_l = 0: \quad W_{x1} = 0, \quad W_{y1} = 0, \quad \theta_l = 1 \quad (18.35)$$

$$\eta_l = \eta_{l\delta} (\eta_m = 0):$$

$$W_{xm,s} = \left(\frac{\rho_{l,w} - \rho_{m,\infty}}{\rho_{l,s}} \right)^{1/2} (\rho_{m,s}/\rho_{m,\infty} - 1)^{-1/2} W_{x1,s} \quad (18.36)$$

$$W_{ym,s} = -\frac{1}{C_{mv,s}} \frac{\rho_{l,s}}{\rho_{m,s}} \left(\frac{v_{l,s}}{v_{m,\infty}} \right)^{1/2} \left(\frac{\rho_{l,m} - \rho_{m,\infty}}{\rho_{l,s}} \right)^{1/4} (\rho_{m,s}/\rho_{m,\infty} - 1)^{-1/4} \\ \times \left(\frac{1}{4} \eta_{l\delta} W_{x1,s} - W_{y1,s} \right) \quad (18.37)$$

$$\left(\frac{dW_{xm}}{d\eta_m} \right)_s = \frac{\mu_{l,s}}{\mu_{m,s}} \left(\frac{v_{m,\infty}}{v_{l,s}} \right)^{1/2} \left(\frac{\rho_{l,w} - \rho_{m,\infty}}{\rho_{l,s}} \right)^{3/4} (\rho_{m,s}/\rho_{m,\infty} - 1)^{-3/4} \\ \times \left(\frac{dW_{x1}}{d\eta_l} \right)_s \quad (18.38)$$

$$\left(\frac{d\theta_m}{d\eta_m} \right)_s \\ = \frac{\lambda_{l,s}(t_w - t_{s,int}) \left(\frac{v_{m,\infty}}{v_{l,s}} \right)^{1/2} \left(\frac{\rho_{l,w} - \rho_{m,\infty}}{\rho_{l,s}} \right)^{1/4} (\rho_{m,s}/\rho_{m,\infty} - 1)^{-1/4} \left(\frac{d\theta_l}{d\eta_l} \right)_s + 4h_{fg}\rho_{m,s}C_{mv,s}v_{m,\infty}W_{ym,s}}{\lambda_{m,s}(t_{s,int} - t_\infty)} \quad (18.39)$$

$$\theta_l = 0 :$$

$$\theta_m = 1 \quad (18.40)$$

$$\Gamma_{mv} = 1 \quad (18.41)$$

$$\left(\frac{d\Gamma_{mv}}{d\eta_m} \right)_s = -4Sc_{m,\infty} \frac{C_{mv,s}}{(C_{mv,s} - C_{mv,\infty})} W_{ym,s} \quad (18.42)$$

$$\eta_m \rightarrow \infty: \quad W_{xm,\infty} = 0, \quad \theta_m = 0, \quad \Gamma_{mv,\infty} = 0 \quad (18.43)$$

where Eq. (18.35) expresses the physical conditions on the plate. Equations (18.36)–(18.42) express the physical matching conditions at the liquid–vapor interface, in which Eq. (18.36) expresses the velocity component continuity, Eq. (18.37) is based on the mass flow rate continuity, Eq. (18.38) is based on the balance of the shear force, Eq. (18.39) is based on the energy balance, Eq. (18.40) expresses the temperature continuity, Eq. (18.41) expresses the concentration condition, and Eq. (18.42) is based on the balance between the vapor mass flow rate and the mass flow rate caused by the vapor mass diffusion. Additionally, Eq. (18.43) expresses the physical conditions in the vapor–gas mixture bulk.

18.5 Remarks

The theoretical models of laminar free convection film condensation from vapor–gas mixture involves (1) the continuity, momentum, and energy equations for both liquid and vapor–gas mixture films, as well as species conservation equation with mass diffusion in the vapor–gas mixture film, (2) a set of interfacial physical matching conditions, such as those for two-dimensional velocity component balances, shear force balance, mass flow rate balance, temperature balance, heat transfer balance, concentration condition, as well as the balance between the condensate mass flow and vapor mass diffusion, and (3) transformed equivalent system of dimensionless governing equations based on the new similarity analysis method. With the new similarity analysis method, the similarity analysis and transformation of the governing partial differential equations with the two-phase boundary layer issues become more convenient than that by using the traditional Falkner–Skan type transformation, particularly for consideration of variable physical properties. On the other hand, by means of the new similarity analysis method, the transformed complete similarity mathematical models of the film condensation of vapor–gas mixture are well coupled with a series of physical property factors. Thus, the transformed complete similarity mathematical models are advanced ones for consideration of variable physical properties.

18.6 Exercises

1. Compare the dimensionless similarity variables between the similarity mathematical models of laminar free convection film condensation of pure vapor, and laminar free convection film condensation of vapor–gas mixture, and find out their differences.
2. Compare the similarity mathematical models of laminar free convection film condensation of pure vapor with those of the laminar free convection film condensation of vapor–gas mixture, and find out their differences.
3. According to the present complete mathematical models on laminar free convection film condensation of vapor–gas mixture, describe the advantages of the present new similarity analysis method for consideration of variable physical properties.
4. In the present complete mathematical models on laminar free convection film condensation of vapor–gas mixture, point out the physical property factors, and explain their physical significance, respectively.
5. Point out the definition of the local Schmidt number $Sc_{m,\infty}$, as well as the difference from the common Schmidt number in their physical significance.
6. Which boundary conditions are considered at the vapor–liquid interface of laminar free convection film condensation of vapor–gas mixture?

7. Further, compare the dimensionless similarity variables among the similarity mathematical models of laminar free convection, laminar free convection film boiling, laminar free convection film condensation of pure vapor, and laminar free convection film condensation of vapor–gas mixture, and find out their common grounds and differences.
8. Further, compare the similarity mathematical models of laminar free convection, laminar free convection film boiling, laminar free convection film condensation of pure vapor, and laminar free convection film condensation of vapor–gas mixture, and find out their common grounds and differences.

Appendix A: Similarity Transformation of the Governing Partial Differential Equations (18.1)–(18.7) and Their Boundary Condition Equations (18.8)–(18.16)

A.1 For Liquid Film

With the assumed transformation variables for the liquid film shown in Eqs. (18.17)–(18.21), the governing partial differential equations (18.1)–(18.3) of the liquid film are transformed into dimensionless ordinary ones as follows, respectively:

A.1.1 Similarity Transformation of Eq. (18.1)

Equation (18.1) is changed to

$$W_{x1} \frac{\partial \rho_l}{\partial x} + w_{y1} \frac{\partial \rho_l}{\partial y} + \rho_l \left(\frac{\partial w_{x1}}{\partial x} + \frac{\partial w_{y1}}{\partial y} \right) = 0 \quad (\text{A1})$$

With Eq. (18.20) we have

$$\frac{\partial w_{x1}}{\partial x} = \sqrt{\frac{g}{x}} \left(\frac{\rho_{l,w} - \rho_{m,\infty}}{\rho_{l,s}} \right)^{1/2} W_{x1} + 2\sqrt{gx} \left(\frac{\rho_{l,w} - \rho_{m,\infty}}{\rho_{l,s}} \right)^{1/2} \frac{dW_{x1}}{d\eta_1} \frac{\partial \eta_1}{\partial x}$$

With Eqs. (18.17) and (18.18) we have

$$\begin{aligned} \frac{\partial \eta_1}{\partial x} &= \frac{\partial}{\partial x} \left[\left(\frac{1}{4} \frac{g(\rho_{l,w} - \rho_{m,\infty})}{\nu_{l,s}^2 \rho_{l,s}} \right)^{1/4} \frac{y}{x^{1/4}} \right] \\ &= -\frac{1}{4} \left(\frac{1}{4} \text{Gr}_{x1,s} \right)^{1/4} \frac{y}{x^2} \end{aligned}$$

$$= -\frac{1}{4}x^{-1}\eta_1 \quad (\text{A2})$$

Then,

$$\begin{aligned} \frac{\partial w_{x1}}{\partial x} &= \sqrt{\frac{g}{x}} \left(\frac{\rho_{1,w} - \rho_{m,\infty}}{\rho_{1,s}} \right)^{1/2} W_{x1} + 2\sqrt{gx} \left(\frac{\rho_{1,w} - \rho_{m,\infty}}{\rho_{1,s}} \right)^{1/2} \frac{dW_{x1}}{d\eta} \frac{1}{4}x^{-1}\eta_1 \\ &= \sqrt{\frac{g}{x}} \left(\frac{\rho_{1,w} - \rho_{m,\infty}}{\rho_{1,s}} \right)^{1/2} \left(W_{x1} - \frac{1}{2}\eta_1 \frac{dW_{x1}}{d\eta_1} \right) \end{aligned} \quad (\text{A3})$$

With Eqs. (18.17) and (18.21) we have

$$\frac{\partial w_{y1}}{\partial y} = 2\sqrt{\frac{g}{x}} \left(\frac{\rho_{1,w} - \rho_{m,\infty}}{\rho_{1,s}} \right)^{1/2} \frac{dW_{y1}}{d\eta_1} \quad (\text{A4})$$

With Eq. (18.17) we have

$$\frac{\partial \rho_1}{\partial x} = \frac{d\rho}{d\eta_1} \frac{d\eta_1}{dx}$$

With Eq. (A2), we have

$$\frac{\partial \rho_1}{\partial x} = -\frac{1}{4}\eta_1 x^{-1} \frac{d\rho_1}{d\eta_1} \quad (\text{A5})$$

In addition, with Eq. (18.17), we have

$$\frac{\partial \rho_1}{\partial y} = \frac{d\rho}{d\eta_1} \frac{d\eta_1}{dy} = \frac{d\rho_1}{d\eta_1} \left(\frac{1}{4}\text{Gr}_{x1,ms} \right)^{1/4} x^{-1} \quad (\text{A6})$$

With Eqs. (A3)–(A6), Eq. (A1) is changed to

$$\begin{aligned} &2\sqrt{gx} \left(\frac{\rho_{1,w} - \rho_{m,\infty}}{\rho_{1,s}} \right)^{1/2} W_{x1} \left(-\frac{1}{4}\eta_1 x^{-1} \frac{d\rho_1}{d\eta_1} \right) \\ &+ 2\sqrt{gx} \left(\frac{\rho_{1,w} - \rho_{m,\infty}}{\rho_{1,s}} \right)^{1/2} \left(\frac{1}{4}\text{Gr}_{x1,\infty} \right)^{-1/4} W_{yv} \frac{d\rho_1}{d\eta_1} \left(\frac{1}{4}\text{Gr}_{x1,s} \right)^{1/4} x^{-1} \\ &+ \rho_1 \left[\sqrt{\frac{g}{x}} \left(\frac{\rho_{1,w} - \rho_{m,\infty}}{\rho_{1,s}} \right)^{1/2} \left(W_{x1} - \frac{1}{2}\eta_1 \frac{dW_{x1}}{d\eta_1} \right) \right. \\ &\left. + 2\sqrt{\frac{g}{x}} \left(\frac{\rho_{1,w} - \rho_{m,\infty}}{\rho_{1,s}} \right)^{1/2} \frac{dW_{y1}}{d\eta_1} \right] = 0 \end{aligned}$$

The above equation is simplified to

$$2\sqrt{g\bar{x}}W_{x1} \left(-\frac{1}{4}\eta_1 x^{-1} \frac{d\rho_1}{d\eta_1} \right) + 2\sqrt{g\bar{x}}W_{y1} \frac{d\rho_1}{d\eta_1} x^{-1} + \rho_1 \left[\sqrt{\frac{g}{x}} \left(W_{x1} - \frac{1}{2}\eta_1 \frac{dW_{x1}}{d\eta_1} \right) + 2\sqrt{\frac{g}{x}} \frac{dW_{y1}}{d\eta_1} \right] = 0$$

The above equation is divided by $\sqrt{\frac{g}{x}}$, and simplified to

$$2W_{x1} - \eta_1 \frac{dW_{x1}}{d\eta_1} + 4 \frac{dW_{y1}}{d\eta_1} - \frac{1}{\rho_1} \frac{d\rho_1}{d\eta_1} (\eta_1 W_{x1} - 4W_{y1}) = 0 \tag{18.28}$$

A.1.2 Similarity Transformation of Eq. (18.2)

Equation (18.2) can be rewritten as

$$\rho_1 \left(w_{x1} \frac{\partial w_{x1}}{\partial x} + w_{y1} \frac{\partial w_{x1}}{\partial y} \right) = \mu_1 \frac{\partial^2 w_{x1}}{\partial y^2} + \frac{\partial \mu_1}{\partial y} \frac{\partial w_{x1}}{\partial y} + g(\rho_1 - \rho_{m,\infty}) \tag{A7}$$

With Eqs. (18.17), (18.18), and (18.21) we have

$$\begin{aligned} \frac{\partial w_{x1}}{\partial y} &= 2\sqrt{g\bar{x}} \left(\frac{\rho_{1,w} - \rho_{m,\infty}}{\rho_{1,s}} \right)^{1/2} \frac{dW_{x1}}{d\eta} \frac{\partial \eta}{\partial y} \\ &= 2\sqrt{g\bar{x}} \left(\frac{\rho_{1,w} - \rho_{m,\infty}}{\rho_{1,s}} \right)^{1/2} \frac{dW_{y1}}{d\eta} x^{-1} \left(\frac{1}{4} Gr_{x1,s} \right)^{1/4} \end{aligned} \tag{A8}$$

Then,

$$\frac{\partial^2 w_{x1}}{\partial y^2} = 2\sqrt{g\bar{x}} \left(\frac{\rho_{1,w} - \rho_{m,\infty}}{\rho_{1,s}} \right)^{1/2} \frac{d^2 W_{x1}}{d\eta^2} x^{-2} \left(\frac{1}{4} Gr_{x1,s} \right)^{1/2} \tag{A9}$$

In addition,

$$\frac{\partial \mu_1}{\partial y} = \frac{d\mu_1}{d\eta} \left(\frac{1}{4} Gr_{x1,s} \right)^{1/4} x^{-1} \tag{A10}$$

With (A3), (A8), (A9), (18.36), and (A10), Eq. (A7) is changed to

$$\begin{aligned} \rho_1 \left[2\sqrt{g\bar{x}} \left(\frac{\rho_{1,w} - \rho_{m,\infty}}{\rho_{1,s}} \right)^{1/2} W_{x1} \sqrt{\frac{g}{x}} \left(\frac{\rho_{1,w} - \rho_{m,\infty}}{\rho_{1,s}} \right)^{1/2} \left(W_{x1} - \frac{1}{2}\eta_1 \frac{dW_{x1}}{d\eta_1} \right) \right. \\ \left. + 2\sqrt{g\bar{x}} \left(\frac{\rho_{1,w} - \rho_{m,\infty}}{\rho_{1,s}} \right)^{1/2} \left(\frac{1}{4} Gr_{x1,s} \right)^{-1/4} W_{y1} 2\sqrt{g\bar{x}} \left(\frac{\rho_{1,w} - \rho_{m,\infty}}{\rho_{1,s}} \right)^{1/2} \right] \end{aligned}$$

$$\begin{aligned}
& \times \left. \frac{dW_{x1}}{d\eta_1} x^{-1} \left(\frac{1}{4} \text{Gr}'_{x1,s} \right)^{-1/4} \right] \\
& = \mu_1 2\sqrt{gx} \left(\frac{\rho_{1,w} - \rho_{v,m\infty}}{\rho_{1,s}} \right)^{1/2} \frac{d^2 W_{x1}}{d\eta_1^2} \left(\frac{1}{4} \text{Gr}'_{x1,s} \right)^{1/2} x^{-2} \\
& + \frac{d\mu_1}{d\eta_1} \left(\frac{1}{4} \text{Gr}'_{xv}, \text{ms} \right)^{1/4} x^{-1} 2\sqrt{gx} \left(\frac{\rho_{1,w} - \rho_{m,\infty}}{\rho_{1,s}} \right)^{1/2} \frac{dW_{x1}}{d\eta_1} x^{-1} \left(\frac{1}{4} \text{Gr}'_{x1,s} \right)^{-1/4} \\
& + g (\rho_1 - \rho_{m,\infty})
\end{aligned}$$

The above equation is divided by $g \frac{\rho_{1,w} - \rho_{m,\infty}}{\rho_{1,s}}$, and simplified to

$$\begin{aligned}
& \rho_1 \left[2W_{x1} \left(W_{x1} - \frac{1}{2} \eta_1 \frac{dW_{x1}}{d\eta_1} \right) + 2W_{y1} 2 \frac{dW_{x1}}{d\eta_1} \right] \\
& = \mu_1 2 \frac{d^2 W_{x1}}{d\eta_1^2} \left(\frac{1}{4} \frac{1}{v_{1,s}^2} \right)^{1/2} + \frac{d\mu_{v,w}}{d\eta_m} 2 \frac{dW_{x1}}{d\eta_1} \left(\frac{1}{4} \frac{1}{v_{1,s}^2} \right)^{1/2} + \frac{(\rho_1 - \rho_{m,\infty})}{\frac{\rho_{1,w} - \rho_{m,\infty}}{\rho_{1,s}}}
\end{aligned}$$

The above equation is divided by $\frac{v_{1,s}}{\mu_1}$, and further simplified to

$$\begin{aligned}
& \frac{v_{1,s}}{v_1} \left[W_{x1} \left(2W_{x1} - \eta_1 \frac{dW_{x1}}{d\eta_1} \right) + 4W_{y1} \frac{dW_{x1}}{d\eta_1} \right] \\
& = \frac{d^2 W_{x1}}{d\eta_1^2} + \frac{1}{\mu_1} \frac{d\mu_1}{d\eta_1} \frac{dW_{x1}}{d\eta_1} + \frac{\mu_{1,s} (\rho_1 - \rho_{m,\infty})}{\mu_1 (\rho_{1,w} - \rho_{m,\infty})}
\end{aligned} \tag{18.29}$$

A.1.3 Similarity Transformation of Eq. (18.3)

Equation (18.3) can be rewritten as

$$\rho_1 c_{p1} \left(w_{x1} \frac{\partial t_1}{\partial x} + w_{y1} \frac{\partial t_1}{\partial x} \right) = \lambda_1 \frac{\partial^2 t_1}{\partial y^2} + \frac{\partial \lambda_1}{\partial y} \frac{\partial t_1}{\partial y} \tag{A11}$$

where

$$\frac{\partial t_1}{\partial x} = (t_w - t_{s,\text{int}}) \frac{d\theta_1}{d\eta_1} \frac{\partial \eta_1}{\partial x}$$

With Eq. (A2) the above equation becomes

$$\frac{\partial t_1}{\partial x} = -\frac{1}{4} \eta_1 x^{-1} (t_w - t_{s,\text{int}}) \frac{d\theta_1}{d\eta_1} \tag{A12}$$

In addition

$$\frac{\partial t_1}{\partial y} = -(t_w - t_{s,int}) \frac{d\theta_1}{d\eta_1} \left(\frac{1}{4} Gr'_{x1,s} \right)^{1/4} x^{-2} \quad (A13)$$

$$\frac{\partial^2 t_1}{\partial y^2} = (t_w - t_{s,int}) \frac{d^2\theta_1}{d\eta_1^2} \left(\frac{1}{4} Gr'_{x1,s} \right)^{1/2} x^{-2} \quad (A14)$$

$$\frac{\partial \lambda_1}{\partial y} = -\frac{d\lambda_1}{d\eta_1} \left(\frac{1}{4} Gr'_{x1,s} \right)^{1/4} x^{-1} \quad (A15)$$

With (A12)–(A15), and (18.20) and (18.21), Eq. (A11) is changed to

$$\begin{aligned} & \rho_1 c_{p1} \left[-2\sqrt{gx} \left(\frac{\rho_{1,w} - \rho_{v,m\infty}}{\rho_{1,s}} \right)^{1/2} W_{x1}(t_w - t_{s,int}) \frac{d\theta_1}{d\eta_1} \left(\frac{1}{4} \right) \eta_1 x^{-1} \right. \\ & \quad \left. + 2\sqrt{gx} \left(\frac{\rho_{1,w} - \rho_{v,m\infty}}{\rho_{1,s}} \right)^{1/2} \left(\frac{1}{4} Gr_{x1,m\infty} \right)^{-1/4} W_{y,1}(t_w - t_{s,int}) \frac{d\theta_1}{d\eta_1} \right. \\ & \quad \left. \left(\frac{1}{4} Gr_{x1,s} \right)^{1/4} x^{-1} \right] \\ & = \lambda_1 (t_w - t_{s,int}) \frac{d^2\theta_1}{d\eta_1^2} \left(\frac{1}{4} Gr_{x1,s} \right)^{1/2} x^{-2} + \frac{d\lambda_1}{d\eta_1} \left(\frac{1}{4} Gr_{x1,s} \right)^{1/4} x^{-1} (t_w - t_{s,int}) \\ & \quad \times \frac{d\theta_1}{d\eta_1} \left(\frac{1}{4} Gr_{x1,s} \right)^{1/4} x^{-1} \end{aligned}$$

The above equation is divided by $(T_w - T_s)$, and simplified to

$$\begin{aligned} & \rho_1 c_{p1} \left[-2\sqrt{gx} \left(\frac{\rho_{1,w} - \rho_{m,\infty}}{\rho_{1,s}} \right)^{1/2} W_{x1} \frac{d\theta_1}{d\eta_1} \left(\frac{1}{4} \right) \eta_1 x^{-1} \right. \\ & \quad \left. + 2\sqrt{gx} \left(\frac{\rho_{1,w} - \rho_{m,\infty}}{\rho_{1,s}} \right)^{1/2} W_{y,1} \frac{d\theta_1}{d\eta_1} x^{-1} \right] \\ & = \lambda_1 \frac{d^2\theta_1}{d\eta_1^2} \left(\frac{1}{4} Gr_{x1,s} \right)^{1/2} x^{-2} + \frac{d\lambda_1}{d\eta_1} \left(\frac{1}{4} Gr_{x1,s} \right)^{1/4} x^{-1} \frac{d\theta_1}{d\eta_1} \left(\frac{1}{4} Gr_{x1,s} \right)^{1/4} x^{-1} \end{aligned}$$

With definition of $Gr_{x1,s}$, the above equation is further simplified to

$$\begin{aligned} & \rho_1 c_{p1} \left[-2\sqrt{gx} \left(\frac{\rho_{1,w} - \rho_{m,\infty}}{\rho_{1,s}} \right)^{1/2} W_{x1} \frac{d\theta_1}{d\eta_1} \left(\frac{1}{4} \right) \eta_1 x^{-1} \right. \\ & \quad \left. + 2\sqrt{gx} \left(\frac{\rho_{1,w} - \rho_{m,\infty}}{\rho_{1,s}} \right)^{1/2} W_{y,1} \frac{d\theta_1}{d\eta_1} x^{-1} \right] \end{aligned}$$

$$\begin{aligned}
&= \lambda_1 \frac{d^2\theta_1}{d\eta_1^2} \left(\frac{1}{4} \frac{g(\rho_{1,w} - \rho_{m,\infty}) x^3}{\nu_{1,s}^2 \rho_{1,s}} \right)^{1/2} x^{-2} \\
&\quad + \frac{d\lambda_1}{d\eta_1} x^{-1} \frac{d\theta_1}{d\eta_1} \left(\frac{1}{4} \frac{g(\rho_{1,w} - \rho_{m,\infty}) x^3}{\nu_{1,s}^2 \rho_{1,s}} \right)^{1/2} x^{-1}
\end{aligned}$$

The above equation is divided by $[\frac{g(\rho_{1,w} - \rho_{m,\infty})}{x\rho_{1,s}}]^{1/2}$, and is further simplified to

$$\rho_1 c_{p1} \left[-2W_{x1} \frac{d\theta_1}{d\eta_1} \left(\frac{1}{4} \right) \eta_1 + 2W_{y,1} \frac{d\theta_1}{d\eta_1} \right] = \lambda_1 \frac{d^2\theta_1}{d\eta_1^2} \left(\frac{1}{4} \frac{1}{\nu_{1,s}^2} \right)^{1/2} + \frac{d\lambda_1}{d\eta_1} \frac{d\theta_1}{d\eta_1} \left(\frac{1}{4} \frac{1}{\nu_{1,s}^2} \right)^{1/2}$$

The above equation is divided by $2 \frac{\nu_{1,s}}{\lambda_1}$, and is further simplified to

$$\frac{\rho_1 c_{p1} \nu_{1,s}}{\lambda_1} \left[-W_{x1} \frac{d\theta_1}{d\eta_1} \eta_1 + 4W_{y1} \frac{d\theta_1}{d\eta_1} \right] = \frac{d^2\theta_1}{d\eta_1^2} + \frac{1}{\lambda_1} \frac{d\lambda_1}{d\eta_1} \frac{d\theta_1}{d\eta_1}$$

i.e.,

$$Pr_1 \frac{\nu_{1,s}}{\nu_1} (-\eta_1 W_{x1} + 4W_{y1}) \frac{d\theta_1}{d\eta_1} = \frac{d^2\theta_1}{d\eta_1^2} + \frac{1}{\lambda_1} \frac{d\lambda_1}{d\eta_1} \frac{d\theta_1}{d\eta_1} \quad (18.30)$$

A.2 For Vapor–Gas Mixture Film

With the assumed similarity transformation variables for vapor–gas mixture film shown in Eqs. (18.22)–(18.27), the governing partial differential equations (18.4)–(18.7) for vapor–gas mixture film are transformed equivalently into the following ones, respectively:

A.2.1 Similarity Transformation of Eq. (18.4)

Equation (18.4) is rewritten as

$$W_{xm} \frac{\partial \rho_m}{\partial x} + W_{ym} \frac{\partial \rho_m}{\partial y} + \rho_m \left[\frac{\partial W_{xm}}{\partial x} + \frac{\partial W_{ym}}{\partial y} \right] = 0 \quad (A16)$$

With Eq. (18.25) we have

$$\frac{\partial W_{xm}}{\partial x} = \sqrt{\frac{g}{x}} (\rho_{m,s}/\rho_{m,\infty} - 1)^{1/2} W_{xm} + 2\sqrt{gx} (\rho_{m,s}/\rho_{m,\infty} - 1)^{1/2} \frac{dW_{xm}}{d\eta_m} \frac{\partial \eta_m}{\partial x}$$

Similar to the derivation for Eq. (A2), we have

$$\frac{\partial \eta_m}{\partial x} = -\frac{1}{4}x^{-1}\eta_m \quad (\text{A17})$$

Then,

$$\frac{\partial w_{xm}}{\partial x} = \sqrt{\frac{g}{x}} (\rho_{m,s}/\rho_{m,\infty} - 1)^{1/2} \left(W_{xm} - \frac{1}{2}\eta_m \frac{dW_{xm}}{d\eta_m} \right) \quad (\text{A18})$$

With Eq. (18.26) we have

$$\begin{aligned} \frac{\partial w_{ym}}{\partial y} &= 2\sqrt{gx}(\rho_{m,s}/\rho_{m,\infty} - 1)^{1/2} \left(\frac{1}{4}\text{Gr}_{xm,\infty} \right)^{-1/4} \frac{dW_{ym}}{d\eta_m} \frac{\partial \eta_m}{\partial y} \\ &= 2\sqrt{gx}(\rho_{m,s}/\rho_{m,\infty} - 1)^{1/2} \left(\frac{1}{4}\text{Gr}_{xm,\infty} \right)^{-1/4} \frac{dW_{ym}}{d\eta_m} x^{-1} \left(\frac{1}{4}\text{Gr}_{xm,\infty} \right)^{1/4} \\ &= 2\sqrt{\frac{g}{x}} (\rho_{m,s}/\rho_{m,\infty} - 1)^{1/2} \frac{dW_{ym}}{d\eta_m} \end{aligned} \quad (\text{A19})$$

In addition

$$\frac{\partial \rho_m}{\partial x} = \frac{d\rho_m}{d\eta_m} \frac{\partial \eta_m}{\partial x}$$

With Eq. (A17), the above equation becomes

$$\frac{\partial \rho_m}{\partial x} = -\frac{1}{4}x^{-1}\eta_m \frac{d\rho_m}{d\eta_m} \quad (\text{A20})$$

While,

$$\begin{aligned} \frac{\partial \rho_m}{\partial y} &= \frac{d\rho_m}{d\eta_m} \frac{\partial \eta_m}{\partial y} \\ &= \frac{d\rho_m}{d\eta_m} \left(\frac{1}{4}\text{Gr}_{xm,\infty} \right)^{1/4} x^{-1} \end{aligned} \quad (\text{A21})$$

With Eqs. (A18)–(A21), and (18.25) and (18.26), Eq. (A16) is changed to

$$\begin{aligned} &-2\sqrt{gx}(\rho_{m,s}/\rho_{m,\infty} - 1)^{1/2} W_{xm} \frac{1}{4}x^{-1}\eta_m \frac{d\rho_m}{d\eta_m} \\ &+ 2\sqrt{gx}(\rho_{m,s}/\rho_{m,\infty} - 1)^{1/2} \left(\frac{1}{4}\text{Gr}_{xm,\infty} \right)^{-1/4} W_{ym} \frac{d\rho_{v,m}}{d\eta_m} \left(\frac{1}{4}\text{Gr}_{xm,s} \right)^{1/4} x^{-1} \\ &+ \rho_m \left[\sqrt{\frac{g}{x}} (\rho_{m,s}/\rho_{m,\infty} - 1)^{1/2} \left(W_{xm} - \frac{1}{2}\eta_m \frac{dW_{x,m}}{d\eta_m} \right) \right. \end{aligned}$$

$$+ 2 \sqrt{\frac{g}{x}} (\rho_{m,s}/\rho_{m,\infty} - 1)^{1/2} \frac{dW_{ym}}{d\eta_m} \Big] = 0$$

The above equation is divided by $\rho_m \sqrt{\frac{g}{x}} (\rho_{m,s}/\rho_{m,\infty} - 1)^{1/2}$, and simplified to

$$W_{xm} - \frac{1}{2} \eta_m \frac{dW_{xm}}{d\eta_m} + \frac{dW_{ym}}{d\eta_m} - \frac{1}{\rho_m} \frac{d\rho_m}{d\eta_m} \left(\frac{1}{2} \eta_m W_{xm} - 2W_{ym} \right) = 0$$

i.e.,

$$2W_{xm} - \eta_m \frac{dW_{xm}}{d\eta_m} + 4 \frac{dW_{ym}}{d\eta_m} - \frac{1}{\rho_m} \frac{d\rho_m}{d\eta_m} (\eta_m W_{xm} - 4W_{ym}) = 0 \quad (18.31)$$

A.2.2 Similarity Transformation of Eq. (18.5)

Equation (18.5) is changed to

$$\rho_m \left(w_{xm} \frac{\partial w_{xm}}{\partial x} + w_{ym} \frac{\partial w_{xm}}{\partial y} \right) = \mu_m \frac{\partial^2 w_{xm}}{\partial y^2} + \frac{\partial \mu_m}{\partial y} \frac{\partial w_{xm}}{\partial y} + g(\rho_m - \rho_{m,\infty}) \quad (A22)$$

With Eqs. (18.22) and (18.25), we have

$$\frac{\partial w_{xm}}{\partial y} = 2\sqrt{gx} (\rho_{m,s}/\rho_{m,\infty} - 1)^{1/2} \frac{dW_{xm}}{d\eta_m} \left(\frac{1}{4} \text{Gr}_{xm,\infty} \right)^{1/4} x^{-1} \quad (A23)$$

$$\frac{\partial^2 w_{xm}}{\partial y^2} = 2\sqrt{gx} (\rho_{m,s}/\rho_{m,\infty} - 1)^{1/2} \frac{d^2 W_{xm}}{d\eta_m^2} \left(\frac{1}{4} \text{Gr}_{xm,\infty} \right)^{1/2} x^{-2} \quad (A24)$$

Additionally,

$$\frac{\partial \mu_m}{\partial y} = \frac{d\mu_m}{d\eta_m} \left(\frac{1}{4} \text{Gr}_{xm,\infty} \right)^{1/4} x^{-1} \quad (A25)$$

With Eqs. (A18), (A23)–(A25), and (18.25) and (18.26), Eq. (A22) is changed to

$$\begin{aligned} \rho_m \Big[& 2\sqrt{gx} (\rho_{m,s}/\rho_{m,\infty} - 1)^{1/2} W_{xm} \sqrt{\frac{g}{x}} (\rho_{m,s}/\rho_{m,\infty} - 1)^{1/2} \\ & \times \left(W_{xm} - \frac{1}{2} \eta_m \frac{dW_{xm}}{d\eta} \right) + 2\sqrt{gx} (\rho_{m,s}/\rho_{m,\infty} - 1)^{1/2} \left(\frac{1}{4} \text{Gr}_{xm,\infty} \right)^{-1/4} \end{aligned}$$

$$\begin{aligned}
 & \times W_{ym} 2\sqrt{gx} (\rho_{m,s}/\rho_{m,\infty} - 1)^{1/2} \frac{dW_{xm}}{d\eta_m} x^{-1} \left(\frac{1}{4} Gr_{xm,\infty} \right)^{1/4} \Big] \\
 = & \mu_m 2\sqrt{gx} (\rho_{m,s}/\rho_{m,\infty} - 1)^{1/2} \frac{d^2 W_{xm}}{d\eta_m^2} \left(\frac{1}{4} Gr'_{xm,\infty} \right)^{1/2} x^{-2} \\
 & + \frac{d\mu_m}{d\eta_m} \left(\frac{1}{4} Gr_{xm,\infty} \right)^{1/4} x^{-1} 2\sqrt{gx} (\rho_{m,s}/\rho_{m,\infty} - 1)^{1/2} \\
 & \times \frac{dW_{xm}}{d\eta_m} x^{-1} \left(\frac{1}{4} Gr_{xm,\infty} \right)^{1/4} + g(\rho_m - \rho_{m,\infty})
 \end{aligned}$$

With the definition of $Gr_{xm,\infty}$, the above equation is changed to

$$\begin{aligned}
 & \rho_m \left[2\sqrt{gx} (\rho_{m,s}/\rho_{m,\infty} - 1) W_{xm} \sqrt{\frac{g}{x}} \left(W_{xm} - \frac{1}{2} \eta_m \frac{dW_{xm}}{d\eta} \right) \right. \\
 & \quad \left. + 2\sqrt{gx} (\rho_{m,s}/\rho_{m,\infty} - 1) W_{ym} 2\sqrt{gx} \frac{dW_{xm}}{d\eta_m} x^{-1} \right] \\
 = & \mu_m 2\sqrt{gx} (\rho_{m,s}/\rho_{m,\infty} - 1)^{1/2} \frac{d^2 W_{xm}}{d\eta_m^2} \left(\frac{1}{4} \frac{g(\rho_{m,s}/\rho_{m,\infty} - 1)x^3}{\nu_{m,\infty}^2} \right)^{1/2} x^{-2} \\
 & + \frac{d\mu_m}{d\eta_m} \left(\frac{1}{4} \frac{g(\rho_{m,s}/\rho_{m,\infty} - 1)x^3}{\nu_{m,\infty}^2} \right)^{1/2} x^{-1} 2\sqrt{gx} (\rho_{m,s}/\rho_{m,\infty} - 1)^{1/2} \\
 & \times \frac{dW_{xm}}{d\eta_m} x^{-1} + g(\rho_m - \rho_{m,\infty})
 \end{aligned}$$

The above equation is divided by $\frac{\mu_m}{\nu_{m,\infty}} (\rho_{m,s}/\rho_{m,\infty} - 1)$, and simplified to

$$\begin{aligned}
 & \frac{\nu_{m,\infty} \rho_m}{\mu_m} \left[W_{xm} \left(2W_{xm} - \eta_m \frac{dW_{xm}}{d\eta} \right) + 4W_{ym} \frac{dW_{xm}}{d\eta_v} \right] \\
 = & \frac{d^2 W_{xm}}{d\eta_m^2} + \frac{1}{\mu_m} \frac{d\mu_m}{d\eta_m} \frac{dW_{xm}}{d\eta_m} + \frac{\nu_{m,\infty} \rho_{m,\infty}}{\mu_m} \frac{\rho_m - \rho_{m,\infty}}{\rho_{m,s} - \rho_{m,\infty}}
 \end{aligned}$$

i.e.,

$$\begin{aligned}
 & \frac{\nu_{m,\infty}}{\nu_m} \left[W_{xm} \left(2W_{xm} - \eta_m \frac{dW_{xm}}{d\eta_m} \right) + 4W_{ym} \frac{dW_{xm}}{d\eta_m} \right] \\
 = & \frac{d^2 W_{xm}}{d\eta_m^2} + \frac{1}{\mu_m} \frac{d\mu_m}{d\eta_m} \frac{dW_{xm}}{d\eta_m} + \frac{\mu_{m,\infty}}{\mu_m} \cdot \frac{\rho_m - \rho_{m,\infty}}{\rho_{m,s} - \rho_{m,\infty}}
 \end{aligned} \tag{18.32}$$

A.2.3 Similarity Transformation of Eq. (18.6)

Equation (18.6) is changed to

$$\begin{aligned} \rho_m C p_m \left(w_{xm} \frac{\partial t}{\partial x} + w_{ym} \frac{\partial t}{\partial y} \right) &= \lambda_m \frac{\partial^2 t}{\partial y^2} + \frac{\partial \lambda_m}{\partial y} \cdot \frac{\partial t}{\partial y} - D_v (c_{p_v} - c_{p_g}) \quad (\text{A26}) \\ &\times \left[\rho_m \frac{\partial C_{mv}}{\partial y} \frac{\partial t}{\partial y} + t \rho_m \frac{\partial^2 C_{mv}}{\partial y^2} + t \frac{\partial C_{mv}}{\partial y} \frac{\partial \rho_m}{\partial y} \right] \end{aligned}$$

With Eq. (18.24) we have

$$\frac{\partial t}{\partial x} = (t_{s,\text{int}} - t_\infty) \frac{d\theta_m}{d\eta_m} \frac{\partial \eta_m}{\partial x}$$

With Eq. (A17), the above equation becomes

$$\frac{\partial t}{\partial x} = -\frac{1}{4} \eta_m x^{-1} (t_{s,\text{int}} - t_\infty) \frac{d\theta_m}{d\eta_1} \quad (\text{A27})$$

With Eqs. (18.22) and (18.24) we have

$$\frac{\partial t}{\partial y} = (t_{s,\text{int}} - t_\infty) \frac{d\theta_m}{d\eta_m} \left(\frac{1}{4} \text{Gr}_{xm,\infty} \right)^{1/4} x^{-1} \quad (\text{A28})$$

$$\frac{\partial^2 t}{\partial y^2} = (t_{s,\text{int}} - t_\infty) \frac{d^2 \theta_m}{d\eta_m^2} \left(\frac{1}{4} \text{Gr}_{xm,\infty} \right)^{1/2} x^{-2} \quad (\text{A29})$$

With Eqs. (18.22) and (18.24) we have

$$\frac{\partial \lambda_m}{\partial y} = \frac{d\lambda_m}{d\eta_m} \left(\frac{1}{4} \text{Gr}_{xm,\infty} \right)^{1/4} x^{-1} \quad (\text{A30})$$

$$\frac{\partial \rho_m}{\partial y} = \frac{d\rho_m}{d\eta_m} \left(\frac{1}{4} \text{Gr}_{xm,\infty} \right)^{1/4} x^{-1} \quad (\text{A31})$$

$$\frac{\partial C_{mv}}{\partial y} = \frac{dC_{mv}}{d\eta_m} \left(\frac{1}{4} \text{Gr}_{xm,\infty} \right)^{1/4} x^{-1} \quad (\text{A32})$$

$$\frac{\partial^2 C_{mv}}{\partial y^2} = \frac{d^2 C_{mv}}{d\eta_m^2} \left(\frac{1}{4} \text{Gr}_{xm,\infty} \right)^{1/2} x^{-2} \quad (\text{A33})$$

With Eqs. (A27)–(A31), Eq. (A26) is changed to

$$\begin{aligned}
& \rho_m c_{p_m} \left[-2\sqrt{g_x} (\rho_{m,s}/\rho_{m,\infty} - 1)^{1/2} W_{x_m}(t_{s,int} - t_\infty) \frac{d\theta_m}{d\eta_m} \left(\frac{1}{4}\right) \eta_m x^{-1} \right. \\
& \quad + 2\sqrt{g_x} (\rho_{m,s}/\rho_{m,\infty} - 1)^{1/2} \left(\frac{1}{4} Gr'_{x_m,\infty}\right)^{-1/4} \\
& \quad \left. \times W_{y_m}(t_{s,int} - t_\infty) \frac{d\theta_m}{d\eta_m} \left(\frac{1}{4} Gr_{x_m,\infty}\right)^{1/4} x^{-1} \right] \\
& = \lambda_m(t_{s,int} - t_\infty) \frac{d^2\theta_m}{d\eta_m^2} \left(\frac{1}{4} Gr_{x_m,\infty}\right)^{1/2} x^{-2} + \frac{d\lambda_m}{d\eta_m} \left(\frac{1}{4} Gr_{x_m,\infty}\right)^{1/4} x^{-1} \\
& \quad \cdot (t_{s,int} - t_\infty) \frac{d\theta_m}{d\eta_m} \left(\frac{1}{4} Gr_{x_m,\infty}\right)^{1/4} x^{-1} - D_v(c_{p_v} - c_{p_g}) \\
& \quad \times \left[\rho_m \frac{dC_{mv}}{d\eta_m} \left(\frac{1}{4} Gr_{x_m,\infty}\right)^{1/4} x^{-1} (t_{s,int} - t_\infty) \frac{d\theta_m}{d\eta_m} \left(\frac{1}{4} Gr_{x_m,\infty}\right)^{1/4} x^{-1} \right. \\
& \quad + t\rho_m \frac{d^2C_{mv}}{d\eta_m^2} \left(\frac{1}{4} Gr_{x_m,\infty}\right)^{1/2} x^{-2} + t \frac{dC_{m,v}}{d\eta_m} \left(\frac{1}{4} Gr_{x_m,\infty}\right)^{1/4} x^{-1} \\
& \quad \left. \times \frac{d\rho_m}{d\eta_m} \left(\frac{1}{4} Gr_{x_m,\infty}\right)^{1/4} x^{-1} \right]
\end{aligned}$$

With definition of $Gr_{x_m,\infty}$, the above equation is changed to

$$\begin{aligned}
& \rho_m c_{p_m} \left[-2\sqrt{g_x} (\rho_{m,s}/\rho_{m,\infty} - 1)^{1/2} W_{x_m}(t_{s,int} - T_\infty) \frac{d\theta_m}{d\eta_m} \left(\frac{1}{4}\right) \eta_m x^{-1} \right. \\
& \quad \left. + 2\sqrt{g_x} (\rho_{m,s}/\rho_{m,\infty} - 1)^{1/2} W_{y_m}(t_{s,int} - t_\infty) \frac{d\theta_m}{d\eta_m} x^{-1} \right] \\
& = \lambda_m(t_{s,int} - t_\infty) \frac{d^2\theta_m}{d\eta_m^2} \left(\frac{1}{4} \frac{g (\rho_{m,s}/\rho_{m,\infty} - 1) x^3}{v_{m,\infty}^2}\right)^{1/2} x^{-2} \\
& \quad + \frac{d\lambda_m}{d\eta_v} \left(\frac{1}{4} \frac{g (\rho_{m,s}/\rho_{m,\infty} - 1) x^3}{v_{m,\infty}^2}\right)^{1/2} x^{-1} \\
& \quad \cdot (t_{s,int} - t_\infty) \frac{d\theta_m}{d\eta_m} x^{-1} - D_v(c_{p_v} - c_{p_g}) \\
& \quad \times \left[\rho_{v,m} \frac{dC_{mv}}{d\eta_v} \left(\frac{1}{4} \frac{g (\rho_{m,s}/\rho_{m,\infty} - 1) x^3}{v_{m,\infty}^2}\right)^{1/2} x^{-1} (t_{s,int} - t_\infty) \frac{d\theta_m}{d\eta_m} x^{-1} \right. \\
& \quad \left. + t\rho_m \frac{d^2C_{mv}}{d\eta_m^2} \left(\frac{1}{4} \frac{g (\rho_{m,s}/\rho_{m,\infty} - 1) x^3}{v_{m,\infty}^2}\right)^{1/2} x^{-2} \right]
\end{aligned}$$

$$+t \frac{dC_{mv}}{d\eta_v} \left[\frac{1}{4} \frac{g (\rho_{m,s}/\rho_{m,\infty} - 1) x^3}{v_{m,\infty}^2} \right]^{1/2} x^{-1} \frac{d\rho_m}{d\eta_m} x^{-1} \Bigg]$$

The above equation is divided by $\sqrt{\frac{g}{x}} (\rho_{m,s}/\rho_{m,\infty} - 1)^{1/2}$, and simplified to

$$\begin{aligned} & \rho_m c_{p_m} \left[-2W_{xv}(t_{s,int} - t_\infty) \frac{d\theta_m}{d\eta_m} \left(\frac{1}{4} \right) \eta_m + 2W_{ym}(t_{s,int} - t_\infty) \frac{d\theta_m}{d\eta_m} \right] \\ &= \lambda_m (t_{s,int} - t_\infty) \frac{d^2\theta_m}{d\eta_m^2} \left(\frac{1}{4} \frac{1}{v_{m,\infty}^2} \right)^{1/2} + \frac{d\lambda_m}{d\eta_m} \left(\frac{1}{4} \frac{1}{v_{m,\infty}^2} \right)^{1/2} \\ & \quad \cdot (t_{s,int} - t_\infty) \frac{d\theta_m}{d\eta_m} - D_v (c_{p_v} - c_{p_g}) \\ & \quad \times \left[\rho_m \frac{dC_{mv}}{d\eta_m} \left(\frac{1}{4} \frac{1}{v_{m,\infty}^2} \right)^{1/2} (t_{s,int} - t_\infty) \frac{d\theta_m}{d\eta_m} + t \rho_m \frac{d^2C_{mv}}{d\eta_m^2} \left(\frac{1}{4} \frac{1}{v_{m,\infty}^2} \right)^{1/2} \right. \\ & \quad \left. + t \frac{dC_{v,w}}{d\eta_m} \left(\frac{1}{4} \frac{1}{v_{m,\infty}^2} \right)^{1/2} \frac{d\rho_m}{d\eta_m} \right] \end{aligned}$$

The above equation is multiplied by $2 \frac{v_{m,\infty}}{\lambda_m (t_{s,int} - t_\infty)}$, and simplified to

$$\begin{aligned} & \frac{v_{m,\infty} \rho_m \mu_m C_{p_m}}{\lambda_m \mu_m} [-\eta_m W_{xm} + 4W_{ym}] \frac{d\theta_m}{d\eta_m} \\ &= \frac{d^2\theta_m}{d\eta_m^2} + \frac{1}{\lambda_m} \frac{d\lambda_m}{d\eta_m} \frac{d\theta_m}{d\eta_m} - \frac{D_v \rho_m}{\lambda_m} (c_{p_v} - c_{p_g}) \\ & \quad \times \left[\frac{dC_{mv}}{d\eta_m} \frac{d\theta_m}{d\eta_m} + \frac{t}{t_{s,int} - t_\infty} \frac{d^2C_{mv}}{d\eta_m^2} + \frac{1}{\rho_m} \frac{d\rho_m}{d\eta_m} \frac{t}{t_{s,int} - t_\infty} \frac{dC_{mv}}{d\eta_m} \right] \end{aligned}$$

The above equation is changed to

$$\begin{aligned} & \frac{v_{m,\infty} \rho_m \mu_m C_{p_m}}{\lambda_m \mu_m} [-\eta_v W_{xm} + 4W_{ym}] \frac{d\theta_m}{d\eta_m} \tag{A34} \\ &= \frac{d^2\theta_m}{d\eta_m^2} + \frac{1}{\lambda_m} \frac{d\lambda_m}{d\eta_m} \frac{d\theta_m}{d\eta_m} - \frac{D_v \rho_m}{\lambda_m} (c_{p_v} - c_{p_g}) \\ & \quad \times \left[\frac{dC_{mv}}{d\eta_m} \frac{d\theta_m}{d\eta_m} + \left(\theta_m + \frac{t_\infty}{t_{s,int} - t_\infty} \right) \frac{d^2C_{mv}}{d\eta_m^2} \right. \\ & \quad \left. + \frac{1}{\rho_m} \frac{d\rho_m}{d\eta_m} \left(\theta_v + \frac{t_\infty}{t_{s,int} - t_\infty} \right) \frac{dC_{mv}}{d\eta_m} \right] \end{aligned}$$

With (18.27) we have

$$\frac{dC_{mv}}{d\eta_v} = (C_{mv,s} - C_{mv,\infty}) \frac{d\Gamma_{mv}}{d\eta_v} \quad (\text{A35})$$

$$\frac{d^2C_{mv}}{d\eta_v^2} = (C_{mv,s} - C_{mv,\infty}) \frac{d^2\Gamma_{mv}}{d\eta_v^2} \quad (\text{A36})$$

Then, Eq. (A34) becomes

$$\begin{aligned} & \frac{v_{m,\infty} \text{Pr}_m}{v_m} [-\eta_m W_{xm} + 4W_{ym}] \frac{d\theta_m}{d\eta_m} \\ &= \frac{d^2\theta_m}{d\eta_m^2} + \frac{1}{\lambda_m} \frac{d\lambda_m}{d\eta_m} \frac{d\theta_m}{d\eta_m} - \frac{D_v \rho_m}{\lambda_m} (C_{mv,s} - C_{mv,\infty}) (c_{p_v} - c_{p_g}) \\ & \quad \times \left[\frac{d\Gamma_{mv}}{d\eta_m} \frac{d\theta_m}{d\eta_m} + \left(\theta_m + \frac{t_\infty}{t_{s,int} - t_\infty} \right) \frac{d^2\Gamma_{mv}}{d\eta_m^2} \right. \\ & \quad \left. + \frac{1}{\rho_m} \frac{d\rho_m}{d\eta_m} \left(\theta_m + \frac{t_\infty}{t_{s,int} - t_\infty} \right) \frac{d\Gamma_{mv}}{d\eta_m} \right] \end{aligned} \quad (\text{18.33})$$

A.2.4 Similarity Transformation of Eq. (18.7)

The left-hand side of Eq. (18.7) is

$$\begin{aligned} & \frac{\partial(w_{xm}\rho_m C_{mv})}{\partial x} + \frac{\partial(w_{ym}\rho_m C_{mv})}{\partial y} \\ &= w_{xm} \left[\frac{\partial(\rho_m C_{mv})}{\partial x} \right] + \rho_m C_{mv} \frac{\partial w_{xm}}{\partial x} + w_{ym} \left[\frac{\partial(\rho_m C_{mv})}{\partial y} \right] + \rho_m C_{mv} \frac{\partial w_{ym}}{\partial y} \\ &= w_{xm} \rho_m \frac{\partial(C_{mv})}{\partial x} + w_{xm} C_{mv} \frac{\partial \rho_m}{\partial x} + \rho_m C_{mv} \frac{\partial w_{xm}}{\partial x} \\ & \quad + w_{ym} \rho_m \frac{\partial(C_{mv})}{\partial y} + w_{ym} C_{mv} \frac{\partial \rho_m}{\partial y} + \rho_m C_{mv} \frac{\partial w_{ym}}{\partial y} \\ &= w_{xm} \rho_m \frac{\partial(C_{mv})}{\partial x} + w_{ym} \rho_m \frac{\partial(C_{mv})}{\partial y} \\ & \quad + C_{m,v} \left(w_{xm} \frac{\partial \rho_m}{\partial x} + \rho_m \frac{\partial w_{xm}}{\partial x} + w_{ym} \frac{\partial \rho_m}{\partial y} + \rho_m \frac{\partial w_{ym}}{\partial y} \right) \end{aligned}$$

With Eq. (18.4) (the continuity equation of vapor-gas mixture film), the above equation is changed to

$$\frac{\partial(w_{xm}\rho_m C_{mv})}{\partial x} + \frac{\partial(w_{ym}\rho_m C_{mv})}{\partial y} = w_{xm}\rho_m \frac{\partial(C_{mv})}{\partial x} + w_{ym}\rho_m \frac{\partial(C_{mv})}{\partial y} \quad (\text{A37})$$

Then, Eq. (18.7) becomes

$$w_{xm} \frac{\partial C_{mv}}{\partial x} + w_{ym} \frac{\partial C_{mv}}{\partial y} = D_v \left(\frac{\partial^2 C_{mv}}{\partial y^2} + \frac{1}{\rho_m} \frac{\partial \rho_m}{\partial y} \frac{\partial C_{mv}}{\partial y} \right) \quad (\text{A38})$$

where D_v is regarded as constant variable.

With Eq. (18.22) we have

$$\frac{\partial C_{mv}}{\partial x} = \frac{dC_{mv}}{d\eta_m} \frac{\partial \eta_m}{\partial x} = -\frac{1}{4} \eta_m x^{-1} \frac{dC_{mv}}{d\eta_m} \quad (\text{A39})$$

$$\frac{\partial C_{mv}}{\partial x} = \frac{dC_{mv}}{d\eta_m} \frac{\partial \eta_m}{\partial x} = \frac{dC_{mv}}{d\eta_m} \left(\frac{1}{4} \text{Gr}_{xm,\infty} \right)^{1/4} x^{-1} \quad (\text{A40})$$

$$\begin{aligned} \frac{\partial^2 C_{mv}}{\partial y^2} &= \frac{\partial}{\partial y} \left(\frac{\partial C_{mv}}{\partial y} \right) \\ &= \frac{d^2 C_{mv}}{d\eta_m^2} \left(\frac{1}{4} \text{Gr}_{xm,\infty} \right)^{1/2} x^{-2} \end{aligned} \quad (\text{A41})$$

With Eqs. (A31), (A39)–(A41), Eq. (A38) is changed to

$$\begin{aligned} &- 2\sqrt{gx}(\rho_{m,s}/\rho_{m,\infty} - 1)^{1/2} W_{xm} \frac{1}{4} \eta_m x^{-1} \frac{dC_{mv}}{d\eta_m} + 2\sqrt{gx}(\rho_{m,s}/\rho_{m,\infty} - 1)^{1/2} \\ &\times \left(\frac{1}{4} \text{Gr}_{xm,\infty} \right)^{-1/4} W_{ym} \frac{dC_{mv}}{d\eta_m} \left(\frac{1}{4} \text{Gr}_{xm,\infty} \right)^{1/4} x^{-1} \\ &= D_{v,w} \left[\frac{d^2 C_{mv}}{d\eta_m^2} \left(\frac{1}{4} \text{Gr}_{xm,\infty} \right)^{1/2} x^{-2} + \frac{1}{\rho_m} \frac{d\rho_m}{d\eta_m} \left(\frac{1}{4} \text{Gr}_{xm,\infty} \right)^{1/4} x^{-1} \right. \\ &\quad \left. \times \frac{dC_{mv}}{d\eta_m} \left(\frac{1}{4} \text{Gr}_{xm,\infty} \right)^{1/4} x^{-1} \right] \end{aligned}$$

With the definition of $\text{Gr}_{xm,\infty}$, the above equation is further changed to

$$\begin{aligned} &- 2\sqrt{gx}(\rho_{m,s}/\rho_{m,\infty} - 1)^{1/2} W_{xm} \frac{1}{4} \eta_m x^{-1} \frac{dC_{mv}}{d\eta_m} \\ &+ 2\sqrt{gx}(\rho_{m,s}/\rho_{m,\infty} - 1)^{1/2} W_{ym} \frac{dC_{mv}}{d\eta_m} x^{-1} \\ &= D_v \left[\frac{d^2 C_{mv}}{d\eta_m^2} \left(\frac{1}{4} \frac{g(\rho_{m,s}/\rho_{m,\infty} - 1)x^3}{\nu_{m,\infty}^2} \right)^{1/2} x^{-2} \right. \\ &\quad \left. + \frac{1}{\rho_m} \frac{d\rho_m}{d\eta_m} x^{-1} \frac{dC_{mv}}{d\eta_m} \left(\frac{1}{4} \frac{g(\rho_{m,s}/\rho_{m,\infty} - 1)x^3}{\nu_{m,\infty}^2} \right)^{1/2} x^{-1} \right] \end{aligned}$$

The above equation is divided by $\sqrt{\frac{g}{x}}(\rho_{m,s}/\rho_{m,\infty} - 1)^{1/2}$, and simplified to

$$\begin{aligned} & -2W_{xm} \frac{1}{4} \eta_m \frac{dC_{mv}}{d\eta_m} + 2W_{ym} \frac{dC_{mv}}{d\eta_m} \\ & = D_v \left[\frac{d^2 C_{mv}}{d\eta_m^2} \left(\frac{1}{4} \frac{1}{v_{m,\infty}^2} \right)^{1/2} + \frac{1}{\rho_m} \frac{d\rho_m}{d\eta_m} \left(\frac{1}{4} \frac{1}{v_{m,\infty}^2} \right)^{1/2} \frac{dC_{mv}}{d\eta_m} \right] \end{aligned}$$

The above equation is multiplied by $\frac{2v_{m,\infty}}{D_v}$, and further simplified to

$$\frac{v_{m,\infty}}{D_v} (-W_{xm} \eta_m + 4W_{ym}) \frac{dC_{mv}}{d\eta_m} = \frac{d^2 C_{mv}}{d\eta_m^2} + \frac{1}{\rho_m} \frac{d\rho_m}{d\eta_m} \frac{dC_{mv}}{d\eta_m} \quad (\text{A42})$$

With Eqs. (A35) and (A36), Eq. (A42) becomes

$$(-\eta_m W_{xm} + 4W_{ym}) \frac{d\Gamma_{mv}}{d\eta_m} = \frac{1}{Sc_{m,\infty}} \left(\frac{d^2 \Gamma_{mv}}{d\eta_m^2} + \frac{1}{\rho_m} \frac{d\rho_m}{d\eta_m} \frac{d\Gamma_{mv}}{d\eta_m} \right) \quad (\text{18.34})$$

where the local Schmidt number $Sc_{m,\infty}$ is defined as

$$Sc_{m,\infty} = \frac{v_{m,\infty}}{D_v} \quad (\text{A43})$$

A.3 For Boundary Condition Equations

A.3.1 Similarity Transformation of Eq. (18.8)

With Eqs. (18.20) and (18.21), Eq. (18.8) can be easily transformed into the following dimensionless form:

$$\eta_l = 0: \quad W_{x1} = 0, \quad W_{y1} = 0, \quad \theta_1 = 1 \quad (\text{18.35})$$

A.3.2 Similarity Transformation of Eq. (18.9)

With Eqs. (8.20) and (18.25), Eq. (18.9) is easily transformed as

$$W_{xm,s} = \left(\frac{\rho_{l,w} - \rho_{m,\infty}}{\rho_{l,s}} \right)^{1/2} (\rho_{m,s}/\rho_{m,\infty} - 1)^{-1/2} W_{x1,s} \quad (\text{18.36})$$

A.3.3 Similarity Transformation of Eq. (18.10)

With Eqs. (18.17) and (18.18) we have

$$\delta_l = \eta_{l\delta} \left(\frac{1}{4} \frac{g (\rho_{l,w} - \rho_{m,\infty}) x^3}{\nu_{l,s}^2 \rho_{l,s}} \right)^{1/4} x$$

Then,

$$\left(\frac{\partial \delta_l}{\partial x} \right) = \frac{1}{4} \eta_{l\delta} \left(\frac{1}{4} \text{Gr}_{x1,s} \right)^{-1/4} \quad (\text{A44})$$

Similarly,

$$\left(\frac{\partial \delta_m}{\partial x} \right) = \frac{1}{4} \eta_{m\delta} \left(\frac{1}{4} \text{Gr}_{xm,\infty} \right)^{-1/4} \quad (\text{A45})$$

With Eqs. (18.20), (18.21), (18.25), (18.26), (A44), and (A45), Eq. (18.10) is changed to

$$\begin{aligned} & \rho_{l,s} \left[2\sqrt{g\bar{x}} \left(\frac{\rho_{l,m} - \rho_{m,\infty}}{\rho_{l,s}} \right)^{1/2} W_{x1,s} \frac{1}{4} \eta_{l\delta} \left(\frac{1}{4} \text{Gr}_{x1,s} \right)^{-1/4} \right. \\ & \quad \left. - 2\sqrt{g\bar{x}} \left(\frac{\rho_{l,m} - \rho_{m,\infty}}{\rho_{l,s}} \right)^{1/2} \left(\frac{1}{4} \text{Gr}_{x1,s} \right)^{-1/4} W_{y1,s} \right] \\ & = \rho_{m,s} C_{mv,s} \left[2\sqrt{g\bar{x}} (\rho_{m,s}/\rho_{m,\infty} - 1)^{1/2} W_{xm,s} \frac{1}{4} \eta_{m\delta} \left(\frac{1}{4} \text{Gr}_{xm,\infty} \right)^{-1/4} \right. \\ & \quad \left. - 2\sqrt{g\bar{x}} (\rho_{m,s}/\rho_{m,\infty} - 1)^{1/2} \left(\frac{1}{4} \text{Gr}_{xm,\infty} \right)^{-1/4} W_{ym,s} \right] \end{aligned}$$

Since $\eta_{m\delta} = 0$ at the liquid–vapor mixture interface, the above equation becomes

$$\begin{aligned} & \rho_{l,s} \left[2\sqrt{g\bar{x}} \left(\frac{\rho_{l,m} - \rho_{m,\infty}}{\rho_{l,s}} \right)^{1/2} W_{x1,s} \frac{1}{4} \eta_{l\delta} \left(\frac{1}{4} \text{Gr}_{x1,s} \right)^{-1/4} \right. \\ & \quad \left. - 2\sqrt{g\bar{x}} \left(\frac{\rho_{l,m} - \rho_{m,\infty}}{\rho_{l,s}} \right)^{1/2} \left(\frac{1}{4} \text{Gr}_{x1,s} \right)^{-1/4} W_{y1,s} \right] \\ & = -2\rho_{m,s} C_{m,vs} \sqrt{g\bar{x}} (\rho_{m,s}/\rho_{m,\infty} - 1)^{1/2} \left(\frac{1}{4} \text{Gr}_{xm,\infty} \right)^{-1/4} W_{ym,s} \end{aligned}$$

With definitions of $\text{Gr}_{x1,s}$ and $\text{Gr}_{xm,\infty}$, the above equation is changed to

$$\begin{aligned} & \rho_{l,s} \left[2\sqrt{gx} \left(\frac{\rho_{l,m} - \rho_{m,\infty}}{\rho_{l,s}} \right)^{1/2} W_{x1,s} \frac{1}{4} \eta_{l\delta} \left(\frac{1}{4} \frac{g(\rho_{l,w} - \rho_{m,\infty})x^3}{v_{l,s}^2 \rho_{l,s}} \right)^{-1/4} \right. \\ & \quad \left. - 2\sqrt{gx} \left(\frac{\rho_{l,m} - \rho_{m,\infty}}{\rho_{l,s}} \right)^{1/2} \left(\frac{1}{4} \frac{g(\rho_{l,w} - \rho_{m,\infty})x^3}{v_{l,s}^2 \rho_{l,s}} \right)^{-1/4} W_{y1,s} \right] \\ & = -2\rho_{m,s} C_{m,vs} \sqrt{gx} (\rho_{m,s}/\rho_{m,\infty} - 1)^{1/2} \left(\frac{1}{4} \frac{g(\rho_{m,s}/\rho_{m,\infty} - 1)x^3}{v_{m,\infty}^2} \right)^{-1/4} W_{ym,s} \end{aligned}$$

The above equation is further simplified to

$$\begin{aligned} & \rho_{l,s} \left[2\sqrt{gx} \left(\frac{\rho_{l,m} - \rho_{m,\infty}}{\rho_{l,s}} \right)^{1/4} W_{x1,s} \frac{1}{4} \eta_{l\delta} \left(\frac{1}{4} \frac{gx^3}{v_{l,s}^2} \right)^{-1/4} \right. \\ & \quad \left. - 2\sqrt{gx} \left(\frac{\rho_{l,m} - \rho_{m,\infty}}{\rho_{l,s}} \right)^{1/4} \left(\frac{1}{4} \frac{gx^3}{v_{l,s}^2} \right)^{-1/4} W_{y1,s} \right] \\ & = -2\rho_{m,s} C_{m,vs} \sqrt{gx} (\rho_{m,s}/\rho_{m,\infty} - 1)^{1/4} \left(\frac{1}{4} \frac{gx^3}{v_{m,\infty}^2} \right)^{-1/4} W_{ym,s} \end{aligned}$$

The above equation is multiplied by $x^{1/4}g^{-1/4}$, and simplified to

$$\begin{aligned} & \rho_{l,s} \left[2 \left(\frac{\rho_{l,m} - \rho_{m,\infty}}{\rho_{l,s}} \right)^{1/4} W_{x1,s} \frac{1}{4} \eta_{l\delta} \left(\frac{1}{4} \frac{1}{v_{l,s}^2} \right)^{-1/4} \right. \\ & \quad \left. - 2 \left(\frac{\rho_{l,m} - \rho_{m,\infty}}{\rho_{l,s}} \right)^{1/4} \left(\frac{1}{4} \frac{1}{v_{l,s}^2} \right)^{-1/4} W_{y1,s} \right] \\ & = -2\rho_{m,s} C_{mv,s} (\rho_{m,s}/\rho_{m,\infty} - 1)^{1/4} \left(\frac{1}{4} \frac{1}{v_{m,\infty}^2} \right)^{-1/4} W_{ym,s} \end{aligned}$$

i.e.,

$$\begin{aligned} & \rho_{l,s} \left[\frac{1}{4} \left(\frac{\rho_{l,m} - \rho_{m,\infty}}{\rho_{l,s}} \right)^{1/4} W_{x1,s} \eta_{l\delta} v_{l,s}^{1/2} - \left(\frac{\rho_{l,m} - \rho_{m,\infty}}{\rho_{l,s}} \right)^{1/4} v_{l,s}^{1/2} W_{y1,s} \right] \\ & = -\rho_{m,s} C_{mv,s} (\rho_{m,s}/\rho_{m,\infty} - 1)^{1/4} v_{m,\infty}^{1/2} W_{ym,s} \end{aligned}$$

Then,

$$\begin{aligned} W_{ym,s} = & -\frac{1}{C_{mv,s}} \frac{\rho_{l,s}}{\rho_{m,s}} \left(\frac{v_{l,s}}{v_{m,\infty}} \right)^{1/2} \left(\frac{\rho_{l,m} - \rho_{m,\infty}}{\rho_{l,s}} \right)^{1/4} \\ & \times (\rho_{m,s}/\rho_{m,\infty} - 1)^{-1/4} \left(\frac{1}{4} \eta_{l\delta} W_{x1,s} - W_{y1,s} \right) \end{aligned} \tag{18.37}$$

A.3.4 Similarity Transformation of Eq. (18.11)

With Eqs. (A8) and (A19), Eq. (18.11) is changed to

$$\begin{aligned} & \mu_{1,s} 2\sqrt{g\bar{x}} \left(\frac{\rho_{1,w} - \rho_{m,\infty}}{\rho_{1,s}} \right)^{1/2} \left(\frac{dW_{x1}}{d\eta_1} \right)_s x^{-1} \left(\frac{1}{4} \text{Gr}_{x1,s} \right)^{1/4} \\ &= \mu_{m,s} 2\sqrt{g\bar{x}} (\rho_{m,s}/\rho_{m,\infty} - 1)^{1/2} \left(\frac{dW_{xm}}{d\eta_v} \right)_s x^{-1} \left(\frac{1}{4} \text{Gr}_{xm,\infty} \right)^{1/4} \end{aligned}$$

With the definitions of $\text{Gr}_{x1,s}$ and $\text{Gr}_{xm,\infty}$, the above equation becomes

$$\begin{aligned} & \mu_{1,s} \left(\frac{\rho_{1,w} - \rho_{m,\infty}}{\rho_{1,s}} \right)^{1/2} \left(\frac{dW_{x1}}{d\eta_1} \right)_s x^{-1} \left(\frac{1}{4} \frac{g(\rho_{1,w} - \rho_{m,\infty})x^3}{\nu_{1,s}^2 \rho_{1,s}} \right)^{1/4} \\ &= \mu_{m,s} (\rho_{m,s}/\rho_{m,\infty} - 1)^{1/2} \left(\frac{dW_{xm}}{d\eta_m} \right)_s x^{-1} \left(\frac{1}{4} \frac{g(\rho_{m,s}/\rho_{m,\infty} - 1)x^3}{\nu_{m,\infty}^2} \right)^{1/4} \end{aligned}$$

Therefore,

$$\begin{aligned} \left(\frac{dW_{xm}}{d\eta_m} \right)_s &= \frac{\mu_{1,s}}{\mu_{m,s}} \left(\frac{\nu_{m,\infty}}{\nu_{1,s}} \right)^{1/2} \left(\frac{\rho_{1,w} - \rho_{m,\infty}}{\rho_{1,s}} \right)^{3/4} \\ &\quad \times (\rho_{m,s}/\rho_{m,\infty} - 1)^{-3/4} \left(\frac{dW_{x1}}{d\eta_1} \right)_s \end{aligned} \quad (18.38)$$

A.3.5 Similarity Transformation of Eq. (18.12)

With Eqs. (A13), (A25), (A28), (A45), and (18.26), Eq. (18.12) is changed to

$$\begin{aligned} & \lambda_{1,s} (t_w - t_{s,\text{int}}) \left(\frac{d\theta_1}{d\eta_1} \right)_s \left(\frac{1}{4} \text{Gr}_{x1,s} \right)^{1/4} x^{-1} \\ &= \lambda_{m,s} (t_{s,\text{int}} - t_\infty) \left(\frac{d\theta_\infty}{d\eta_\infty} \right)_s \left(\frac{1}{4} \text{Gr}_{xm,\infty} \right)^{1/4} x^{-1} + h_{fg} \rho_{m,s} C_{mv,s} \\ &\quad \left[2\sqrt{g\bar{x}} (\rho_{m,s}/\rho_{m,\infty} - 1)^{1/2} W_{xm} \frac{1}{4} \eta_m \delta \left(\frac{1}{4} \text{Gr}_{xm,s} \right)^{-1/4} \right. \\ &\quad \left. - 2\sqrt{g\bar{x}} (\rho_{m,s}/\rho_{m,\infty} - 1)^{1/2} \left(\frac{1}{4} \text{Gr}_{xm,\infty} \right)^{-1/4} W_{ym,s} \right]_s \end{aligned}$$

With the definitions of $\text{Gr}_{x1,s}$ and $\text{Gr}_{xm,\infty}$, the above equation is changed to

$$\lambda_{1,s} (t_w - t_{s,\text{int}}) \left(\frac{d\theta_1}{d\eta_1} \right)_s \left(\frac{1}{4} \frac{g(\rho_{1,w} - \rho_{m,\infty})x^3}{\nu_{1,s}^2 \rho_{1,s}} \right)^{1/4} x^{-1}$$

$$\begin{aligned}
&= \lambda_{v,ms}(t_{s,int} - t_{\infty}) \left(\frac{d\theta_m}{d\eta_m} \right)_s \left(\frac{1}{4} \frac{g(\rho_{m,s}/\rho_{m,\infty} - 1)x^3}{\nu_{m,\infty}^2} \right)^{1/4} x^{-1} + h_{fg}\rho_{m,s}C_{mv,s} \\
&\quad \times \left[2\sqrt{gx}(\rho_{m,s}/\rho_{m,\infty} - 1)^{1/2} W_{xm} \frac{1}{4} \eta_{m\delta} \left(\frac{1}{4} \frac{g(\rho_{m,s}/\rho_{m,\infty} - 1)x^3}{\nu_{m,\infty}^2} \right)^{1/4} \right. \\
&\quad \left. - 2\sqrt{gx}(\rho_{m,s}/\rho_{m,\infty} - 1)^{1/2} \left(\frac{1}{4} \frac{g(\rho_{m,s}/\rho_{m,\infty} - 1)x^3}{\nu_{m,\infty}^2} \right)^{-1/4} W_{ym} \right]_s
\end{aligned}$$

Since $\eta_{m\delta} = 0$ at the liquid–vapor mixture interface, the above equations becomes

$$\begin{aligned}
&\lambda_{l,s}(t_w - t_{s,int}) \left(\frac{d\theta_l}{d\eta_l} \right)_s \left(\frac{1}{4} \frac{g(\rho_{l,w} - \rho_{m,\infty})x^3}{\nu_{l,s}^2 \rho_{l,s}} \right)^{1/4} x^{-1} \\
&= \lambda_{m,s}(t_{s,int} - t_{\infty}) \left(\frac{d\theta_m}{d\eta_m} \right)_s \left(\frac{1}{4} \frac{g(\rho_{m,s}/\rho_{m,\infty} - 1)x^3}{\nu_{m,\infty}^2} \right)^{1/4} x^{-1} \\
&\quad - 2h_{fg}\rho_{m,s}C_{m,vs}\sqrt{gx}(\rho_{m,s}/\rho_{m,\infty} - 1)^{1/2} \left(\frac{1}{4} \frac{g(\rho_{m,s}/\rho_{m,\infty} - 1)x^3}{\nu_{m,\infty}^2} \right)^{1/4} W_{ym,s}
\end{aligned}$$

The above equation is divided by $(\frac{g}{4x})^{1/4}$, and simplified to

$$\begin{aligned}
&\lambda_{l,s}(t_w - t_{s,int}) \left(\frac{d\theta_l}{d\eta_l} \right)_s \left(\frac{\rho_{l,w} - \rho_{m,\infty}}{\nu_{l,s}^2 \rho_{l,s}} \right)^{1/4} \\
&= \lambda_{m,s}(t_{s,int} - t_{\infty}) \left(\frac{d\theta_m}{d\eta_m} \right)_s \left(\frac{\rho_{m,s}/\rho_{m,\infty} - 1}{\nu_{m,\infty}^2} \right)^{1/4} \\
&\quad - 4h_{fg}\rho_{m,s}C_{mv,s}(\rho_{m,s}/\rho_{m,\infty} - 1)^{1/4} \left(\frac{1}{\nu_{m,\infty}^2} \right)^{-1/4} W_{ym,s}
\end{aligned}$$

i.e.,

$$\begin{aligned}
&\lambda_{vm,s}(t_{s,int} - t_{\infty}) \left(\frac{d\theta_m}{d\eta_m} \right)_s \left(\frac{\rho_{m,s}/\rho_{m,\infty} - 1}{\nu_{m,\infty}^2} \right)^{1/4} \\
&= \lambda_{l,s}(t_w - t_{s,int}) \left(\frac{d\theta_l}{d\eta_l} \right)_s \left(\frac{\rho_{l,w} - \rho_{m,\infty}}{\nu_{l,s}^2 \rho_{l,s}} \right)^{1/4} \\
&\quad + 4h_{fg}\rho_{m,s}C_{vw,s}(\rho_{m,s}/\rho_{m,\infty} - 1)^{1/4} \left(\frac{1}{\nu_{m,\infty}^2} \right)^{-1/4} W_{ym,s}
\end{aligned}$$

Therefore,

$$\begin{aligned} & \left(\frac{d\theta_m}{d\eta_m} \right)_s \\ &= \frac{\lambda_{l,s}(t_w - t_{s,int}) \left(\frac{\nu_{m,\infty}}{\nu_{l,s}} \right)^{1/2} \left(\frac{\rho_{l,w} - \rho_{m,\infty}}{\rho_{l,s}} \right)^{1/4} (\rho_{m,s} / \rho_{m,\infty} - 1)^{-1/4} \left(\frac{d\theta_l}{d\eta_l} \right)_s + 4h_{fg}\rho_{m,s}C_{mv,s}\nu_{m,\infty}W_{ym,s}}{\lambda_{m,s}(t_{s,int} - t_\infty)} \end{aligned} \quad (18.39)$$

A.3.6 Similarity Transformation of Eq. (18.13)

With Eqs. (18.19) and (18.24), Eq. (18.13) can easily be changed to

$$\theta_l = 0, \quad \theta_v = 1 \quad (18.40)$$

A.3.7 Similarity Transformation of Eq. (18.14)

With Eq. (18.27), Eq. (18.14) is easily transformed into

$$\Gamma_{mv} = 1 \quad (18.41)$$

A.3.8 Similarity Transformation of Eq. (18.15)

With Eqs. (18.20), (18.21), (A40), and (A44), Eq. (18.15) is changed to

$$\begin{aligned} & \rho_{m,s}C_{mv,s} \left(\frac{1}{4}\text{Gr}_{xm,\infty} \right)^{1/2} \cdot 2 \cdot x^{-1}\nu_{m,\infty} 2 \left(\frac{1}{4}\text{Gr}_{xm,\infty} \right)^{-1/4} \left(\frac{1}{4}\eta_{m\delta}W_{xm,s} - W_{ym,s} \right) \\ &= D_v\rho_{m,s} \left(\frac{dC_{mv}}{d\eta_m} \right)_s \left(\frac{1}{4}\text{Gr}_{xm,\infty} \right)^{1/4} x^{-1} \end{aligned}$$

i.e.,

$$\rho_{m,s}C_{mv,s}\nu_{m,\infty}(\eta_{m\delta}W_{xm,s} - 4W_{ym,s}) = D_v\rho_{m,s} \left(\frac{dC_{mv}}{d\eta_m} \right)_s$$

Since $\eta_{m\delta} = 0$ at the liquid–vapor mixture interface, we have

$$\left(\frac{dC_{mv}}{d\eta_m} \right)_s = -4 \frac{C_{mv,s}\nu_{m,\infty}}{D_v} W_{ym,s}$$

With Eq. (18.27), the above equation becomes

$$\left(\frac{d\Gamma_{mv}}{d\eta_m}\right)_s = -4 \frac{C_{mv,s}}{(C_{mv,s} - C_{mv,\infty})} \frac{\nu_{m,\infty}}{D_v} W_{ym,s} \quad (18.42)$$

A.3.9 Similarity Transformation of Eq. (18.16)

At $y \rightarrow \infty$, with Eqs. (18.24), (18.25), and (18.27), Eq. (18.16) is easily transformed into

$$\eta_m \rightarrow \infty : W_{xm} = 0, \quad \theta_m = 0, \quad \Gamma_{mv,\infty} = 0 \quad (18.43)$$

References

1. W. Nusselt, The condensation of steam on cooled surface, *Z. d. Ver. Deut. Ing.* **60**, 541–546, 569–575 (1916) (Translated into English by D. Fullarton, *Chem. Engr. Funds.* **1**(2), 6–19 (1982)).
2. D. Butterworth, R.G. Sardesai, P. Griffith, A.E. Bergles, *Condensation, in: Heat Exchanger Design Handbook* (Hemisphere , Washington, DC, 1983)
3. P.J. Marto, Fundamentals of condensation, in *Two-Phase Flow Heat Exchangers: Thermal-Hydraulic Fundamentals and Design*, ed. by S. Kakac, A.E. Bergles, E.Q. Fernandes (Kluwer Academic, Dordrecht, 1988), pp. 221–291
4. J.G. Collier, J.R. Thome, *Convective Boiling and Condensation*, 3rd edn. (Oxford University Press, New York, 1996), pp. 430–487
5. J.W. Rose, Condensation heat transfer. *Int. J. Heat Mass Transf.* **35**, 479–485 (1999)
6. D.Y. Shang, T. Adamek, Study on laminar film condensation of saturated steam on a vertical flat plate for consideration of various physical factors including variable thermophysical properties. *Wärme- und Stoffübertragung* **30**, 89–100 (1994)
7. D.Y. Shang, B.X. Wang, An extended study on steady-state laminar film condensation of a superheated vapor on an isothermal vertical plate. *Int. J. Heat Mass Transf.* **40**(4), 931–941 (1997)
8. W.J. Minkowycz, E.M. Sparrow, Condensation heat Transfer in the presence of noncondensables, interfacial resistance, superheating, variable properties, and diffusion. *Int. J. Heat Mass Transf.* **9**, 1125–1144 (1966)
9. L. Slegers, R.A. Seban, Laminar film condensation of steam containing small concentration of air. *Int. J. Heat Mass Transf.* **13**, 1941–1947 (1970)
10. H.K. Al-Diwany, J.W. Rose, Free convection film condensation of steam in the presence of non-condensing gases. *Int. J. Heat Mass Transf.* **16**, 1359–1369 (1972)
11. R.K. Oran, C.J. Chen, Effect of lighter noncond-Nsa31 -Gas on laminar film condensation over a vertical plate. *Int. J. Heat Mass Transf.* **18**, 993–996 (1975)
12. V.M. Borishanskiy, O.P. Volkov, Effect of uncondensable gases content on heat transfer in steam condensation in a vertical tube. *Heat Transf. Sov. Res.* **9**, 35–41 (1977)
13. C.D. Morgan, C.G. Rush, Experimental measurements of condensation heat transfer with non-condensable gases present, in 21st National Heat Transfer Conference, vol. 27, Seattle, Washington, ASME, HTD, July 1983, pp. 24–28 (1983).
14. P.J. Vernier, P. Solignac, A test of some condensation models in the presence of a noncondensable gas against the eotra experiment. *Nucl. Technol.* **77**(1), 82–91 (1987)
15. S.M. Chiaasaan, B.K. Kamboj, S.I. Abdel-Khalik, Two-fluid modeling of condensation in the presence of noncondensables in two-phase channel flows. *Nucl. Sci. Eng.* **119**, 1–17 (1995)

16. Y.S. Chin, S.J. Ormiston, H.M. Soliman, A two-phase boundary-layer model for laminar mixed-convection condensation with a noncondensable gas on inclined plates. *Heat Mass Transf.* **34**, 271–277 (1998)
17. S.T. Revankar, D. Pollock, Laminar film condensation in a vertical tube in the presence of noncondensable gas. *Appl. Math. Model.* **29**(4), 341–359 (2005)
18. J.M. Martin-Valdepenas, M.A. Jimenez, F. Martin-Fuertes, J.A. Fernandez-Benitez, Comparison of film condensation models in presence of non-condensable gases implemented in a CFD Code. *Heat and Mass Transf.* **41**(11), 961–976 (2005)
19. S. Oh, S.T. Revankar, Experimental and theoretical investigation of film condensation with noncondensable gas. *Int. J. Heat Mass Transf.* **49**(15–16), 2523–2534 (2006)
20. D.Y. Shang, L.C. Zhong, Extensive study on laminar free film condensation from vapor-gas mixture. *Int. J. Heat Mass Transf.* **51**, 4300–4314 (2008)

Chapter 19

Velocity, Temperature, and Concentration Fields on Laminar Free Convection Film Condensation of Vapor–Gas Mixture

Abstract A set of physical matching conditions at the liquid–vapor interface are considered and rigorously satisfied for getting reliable solutions related to the three-point boundary value problem on the laminar free convection film condensation of vapor–gas mixture. With the example on the laminar free convection film condensation of water vapor–air mixture, a system of the interfacial vapor saturation temperature $T_{s,int}$ is found out, which only depends on the bulk vapor mass fraction for a special bulk temperature. The numerical solutions of the interfacial vapor saturation temperature $T_{s,int}$ are further formulated into an equation for its reliable prediction. A system of rigorous numerical results is successfully obtained, including velocity and temperature fields of the condensate liquid film, as well as the velocity, temperature, and concentration fields of the vapor–gas mixture film. With increasing the vapor mass fraction (or decreasing the gas mass fraction) in the bulk, the condensate liquid film thickness, the condensate liquid velocity, and vapor–gas mixture velocity at the liquid–vapor interface will increase at an accelerative pace. It proved that the noncondensable gas in the vapor–gas mixture has a decisive effect on the laminar free convection film condensation from vapor–gas mixture. The wall temperature has also a decisive effect on the laminar free convection film condensation from vapor–gas mixture. With increasing wall temperature, the condensate liquid film thickness, the condensate liquid velocity, as well as velocity of the vapor–gas mixture at the liquid–vapor interface will decrease. However, with increasing the wall temperature, the thicknesses of the momentum, temperature, and concentration boundary layers of the vapor–gas mixture will increase.

19.1 Introduction

In this chapter, I will use the complete mathematical model presented in Chap. 18 to obtain the velocity and temperature fields of laminar free convection film condensation from vapor–gas mixture, through a system of rigorous numerical calculation.

First of all, an available approach will be proposed for determination of condensate saturated temperature of vapor at liquid–vapor interface, and an effective iterative method will be provided for a rigorous satisfaction of the set of three-point boundary physical matching conditions.

Laminar free convection film condensation of water vapor in the presence of air will be taken as an example for the numerical calculation. On these bases, the numerical calculations will be successfully completed, and a system of rigorous numerical solutions of momentum, temperature, and concentration fields of the two-phase model will be satisfyingly obtained.

From the numerical results, it will be found that the presence of noncondensable gas in the vapor–gas mixture bulk is a decisive reason for great decrease of the film condensation. With increasing gas mass fraction (or decreasing vapor mass fraction) in the vapor–gas mixture bulk, the condensate liquid film thickness, the condensate liquid velocity, and the interfacial velocity will decrease obviously. With increasing wall temperature, the condensate liquid film thickness, and the condensate liquid velocity will decrease obviously too, but the thicknesses of velocity, temperature and, concentration boundary layers of vapor–gas mixture will increase. Furthermore, with increasing the wall temperature, the effect of gas or vapor mass fraction in the vapor–gas mixture bulk on the velocity, temperature, and concentration fields of vapor–gas mixture will decrease. The shear force at the liquid–vapor interface is very small, and so if it is omitted in analysis and calculation of the laminar free convection film condensation both of pure vapor and vapor in the presence of noncondensable gas, it will never cause obvious deviation, especially for a higher wall temperature.

The investigated results of this work will lay a satisfying foundation for a successive study on heat and mass transfer of the film condensation from vapor–gas mixture.

19.2 Treatments of Variable Physical Properties

19.2.1 Treatment Methods

As presented in former chapters of this book, fluid *variable physical properties* have great effects on free convection film flows and heat transfer, so should be appropriately treated for solution of the governing equations with the boundary condition equations. For film condensation of *vapour–gas mixture*, two types of variable physical properties exist, the temperature-dependent physical properties and concentration-dependent physical properties. The former physical properties exist both in the condensate liquid film and vapor–gas mixture films, and the latter physical properties exist in vapor–gas mixture film. For treatment of temperature-dependent physical properties of liquid medium, a polynomial approach is used [1]. For treatment of the temperature-dependent physical properties of gaseous medium, the temperature parameter method will be applied [2, 3]. While, for treatment of

concentration-dependent physical properties, the analytical method in [4] will be used.

On the other hand, it is seen that all physical properties are coupled with the dimensionless governing differential equations as the forms of the related dimensionless physical property factors finally. Then, the treatment of variable physical properties for laminar free convection film condensation of vapor–gas mixture becomes treatment of these physical property factors, respectively. Based on the presentations in Chap. 5, the treatment of variable physical properties related to laminar free convection film condensation of vapor–gas mixture are given below.

19.2.2 Treatment of Temperature-Dependent Physical Properties of Liquid Film

Let me take water as example for presentation of *temperature-dependent physical properties* of liquid film. According to [1], the water variable density, thermal conductivity, absolute viscosity, and specific heat are expressed as follows for *condensate water film flow*:

$$\rho_l = -4.48 \times 10^{-3} t^2 + 999.9 \quad (19.1)$$

$$\lambda_l = -8.01 \times 10^{-6} t^2 + 1.94 \times 10^{-3} t + 0.563 \quad (19.2)$$

$$\mu_l = \exp\left(-1.6 - \frac{1150}{T} + \left(\frac{690}{T}\right)^2\right) \times 10^{-3} \quad (19.3)$$

While, the water specific heat can be taken as a constant $c_{pl} = 4, 200\text{J}/(\text{kg K})$ with temperature variation at atmospheric pressure, and then specific heat factor will be

$$\frac{1}{c_{pl}} \frac{dc_{pl}}{d\eta_l} = 0 \quad (19.4)$$

The physical property factors of water in the governing ordinary differential equations are expressed as, respectively

$$\text{Pr}_l = \frac{\mu_l \cdot c_{pl}}{\lambda_l} = \frac{\left[\exp\left(-1.6 - \frac{1150}{T} + \left(\frac{690}{T}\right)^2\right) \times 10^{-3}\right] \times 4200}{-8.01 \times 10^{-6} t^2 + 1.94 \times 10^{-3} t + 0.563} \quad (19.5)$$

$$\frac{1}{\rho_l} \frac{d\rho_l}{d\eta_l} = \frac{\left[-2 \times 4.48 \times 10^{-3} t (t_w - t_{s,\text{int}}) \frac{d\theta_l(\eta_l)}{d\eta_l}\right]}{(-4.48 \times 10^{-3} t^2 + 999.9)} \quad (19.6)$$

$$\frac{1}{\lambda_l} \frac{d\lambda_l}{d\eta_l} = \frac{\left[(-2 \times 8.01 \times 10^{-6} + 1.94 \times 10^{-3})(t_w - t_{s,\text{int}}) \frac{d\theta_l(\eta_l)}{d\eta_l} \right]}{-8.01 \times 10^{-6} t^2 + 1.94 \times 10^{-3} t + 0.563} \quad (19.7)$$

$$\frac{1}{\mu_l} \frac{d\mu_l}{d\eta_l} = \left(\frac{1150}{T^2} - 2 \times \frac{690^2}{T^3} \right) (t_w - t_{s,\text{int}}) \frac{d\theta_l(\eta_l)}{d\eta_l} \quad (19.8)$$

$$\begin{aligned} \frac{v_{l,s}}{v_l} &= \left(\frac{\mu_{l,s}}{\rho_{l,s}} \right) / \left(\frac{\mu_l}{\rho_l} \right) = \left(\frac{\mu_{l,s}}{\mu_l} \right) \left(\frac{\rho_l}{\rho_{l,s}} \right) \\ &= \frac{\exp \left[-1.6 - \frac{1150}{T_{s,\text{int}}} + \left(\frac{690}{T_{s,\text{int}}} \right)^2 \right]}{\exp \left[-1.6 - \frac{1150}{T} + \left(\frac{690}{T} \right)^2 \right]} \times \frac{-4.48 \times 10^{-3} t^2 + 999.9}{-4.48 \times 10^{-3} t_{s,\text{int}}^2 + 999.9} \end{aligned} \quad (19.9)$$

where

$$t = (t_w - t_{s,\text{int}})\theta(\eta) + t_{s,\text{int}} \quad \text{and} \quad T = t + 273$$

Thus, the dependent *physical property factors* of the governing dimensionless mathematical models become the function of dimensionless temperature under the new similarity analysis system.

19.2.3 Treatment of Concentration-Dependent Densities of Vapor–Gas Mixture

Consulting the derivation in Chap. 5 we take ρ_m as *density of vapor–gas mixture*, ρ_{mv} and ρ_{mg} as *local densities of vapor and gas* in the vapor–gas mixture, and ρ_v and ρ_g as *densities of vapor and gas*, respectively, then, we will have the following equations for their relations:

$$\rho_m = \rho_{mv} + \rho_{mg} \quad (19.10)$$

$$C_{mv}\rho_m = \rho_{mv} \quad (19.11)$$

$$\frac{\rho_{mv}}{\rho_v} + \frac{\rho_{mg}}{\rho_g} = 1 \quad (19.12)$$

The solutions of Eqs. (19.10)–(19.12) are

$$\rho_{mv} = \frac{C_{mv}\rho_v\rho_g}{(1 - C_{mv})\rho_v + C_{mv}\rho_g} \quad (19.13)$$

$$\rho_{mg} = \frac{(1 - C_{mv})\rho_v\rho_g}{(1 - C_{mv})\rho_v + C_{mv}\rho_g} \quad (19.14)$$

$$\rho_m = \frac{\rho_v\rho_g}{(1 - C_{mv})\rho_v + C_{mv}\rho_g} \quad (19.15)$$

With Eq.(19.15), the *density factor of the vapor–gas mixture* in the governing dimensional differential equations will be derived as

$$\begin{aligned} \frac{1}{\rho_m} \frac{d\rho_m}{d\eta_m} &= \frac{1}{\rho_m} \frac{d}{d\eta_m} \left(\frac{\rho_v \rho_g}{(1 - C_{mv})\rho_v + C_{m,v}\rho_g} \right) \\ &= \frac{1}{\rho_m} \frac{\rho_v \frac{d\rho_g}{d\eta_m} + \rho_g \frac{d\rho_v}{d\eta_m}}{(1 - C_{mv})\rho_v + C_{mv}\rho_g} - \frac{1}{\rho_m} \frac{\rho_v \rho_g}{((1 - C_{mv})\rho_v + C_{mv}\rho_g)^2} \\ &\quad \times \left[(1 - C_{mv}) \frac{d\rho_v}{d\eta_m} - \rho_v \frac{dC_{mv}}{d\eta_m} + C_{mv} \frac{d\rho_g}{d\eta_m} + \rho_g \frac{dC_{mv}}{d\eta_m} \right] \end{aligned}$$

i.e.

$$\begin{aligned} \frac{1}{\rho_m} \frac{d\rho_m}{d\eta_m} &= \frac{1}{\rho_g} \frac{d\rho_g}{d\eta_m} + \frac{1}{\rho_v} \frac{d\rho_v}{d\eta_m} - \frac{1}{(1 - C_{mv})\rho_v + C_{mv}\rho_g} \\ &\quad \times \left[(1 - C_{mv}) \frac{d\rho_v}{d\eta_m} - \rho_v \frac{dC_{mv}}{d\eta_m} + C_{mv} \frac{d\rho_g}{d\eta_m} + \rho_g \frac{dC_{mv}}{d\eta_m} \right] \end{aligned}$$

Then,

$$\begin{aligned} \frac{1}{\rho_m} \frac{d\rho_m}{d\eta_m} &= \frac{1}{\rho_g} \cdot \frac{d\rho_g}{d\eta_m} + \frac{1}{\rho_v} \cdot \frac{d\rho_v}{d\eta_m} - \frac{C_{mv}(\rho_v - \rho_g)}{(1 - C_{mv})\rho_v + C_{mv}\rho_g} \\ &\quad \cdot \left[\frac{1 - C_{mv}}{C_{mv}} \cdot \frac{\rho_v}{\rho_v - \rho_g} \cdot \frac{1}{\rho_v} \cdot \frac{d\rho_v}{d\eta_m} + \frac{\rho_g}{\rho_v - \rho_g} \cdot \frac{1}{\rho_g} \cdot \frac{d\rho_g}{d\eta_m} \right. \\ &\quad \left. - \frac{C_{mv,s} - C_{mv,\infty}}{C_{mv}} \cdot \frac{d\Gamma_{mv}}{d\eta_m} \right] \end{aligned} \quad (19.16)$$

where

$$C_{mv} = (C_{mv,s} - C_{mv,\infty})\Gamma_{mv} + C_{mv,\infty}.$$

Thus, the density factor $\frac{1}{\rho_m} \frac{d\rho_m}{d\eta_m}$ of the vapor–gas mixture is expressed by the gas density factor $\frac{1}{\rho_g} \frac{d\rho_g}{d\eta_m}$ and vapor density factor $\frac{1}{\rho_v} \frac{d\rho_v}{d\eta_m}$. Because $\frac{1}{\rho_g} \frac{d\rho_g}{d\eta_m}$ and $\frac{1}{\rho_v} \frac{d\rho_v}{d\eta_m}$ are temperature dependent, $\frac{1}{\rho_m} \frac{d\rho_m}{d\eta_m}$ is concentration and temperature dependent.

19.2.4 Treatment of Other Concentration-Dependent Physical Properties of Vapor–Gas Mixture

Other concentration-dependent physical properties of vapor–gas mixture are assumed as following weighted sum formulae:

$$\mu_m = C_{mv}\mu_v + (1 - C_{mv})\mu_g \quad (19.17)$$

$$\lambda_m = C_{mv}\lambda_v + (1 - C_{mv})\lambda_g \quad (19.18)$$

$$c_{p_m} = C_{mv}c_{p_v} + (1 - C_{mv})c_{p_g} \quad (19.19)$$

$$\text{Pr}_m = C_{mv}\text{Pr}_v + (1 - C_{mv})\text{Pr}_g \quad (19.20)$$

Then,

$$\begin{aligned} \frac{1}{\mu_m} \cdot \frac{d\mu_m}{d\eta_m} &= \frac{1}{\mu_m} \cdot \frac{d}{d\eta_m} [C_{mv}\mu_v + (1 - C_{mv})\mu_g] \\ &= \frac{1}{\mu_m} \left[C_{mv} \frac{d\mu_v}{d\eta_m} + \mu_v \frac{dC_{mv}}{d\eta_m} + (1 - C_{mv}) \frac{d\mu_g}{d\eta_m} - \mu_g \frac{dC_{mv}}{d\eta_m} \right] \end{aligned}$$

Consulting Chap. 5 the above equation is further changed to

$$\begin{aligned} \frac{1}{\mu_m} \cdot \frac{d\mu_m}{d\eta_m} &= \frac{1}{\mu_m} \left[C_{mv}\mu_v \frac{1}{\mu_v} \frac{d\mu_v}{d\eta_m} + (1 - C_{mv})\mu_g \frac{1}{\mu_g} \frac{d\mu_g}{d\eta_m} \right. \\ &\quad \left. + (\mu_v - \mu_g)(C_{mv,s} - C_{mv,\infty}) \frac{d\Gamma_{mv}}{d\eta_m} \right] \\ \frac{1}{\mu_m} \frac{d\mu_m}{d\eta_m} &= C_{mv} \frac{\mu_v}{\mu_m} \frac{1}{\mu_v} \frac{d\mu_v}{d\eta_m} + (1 - C_{mv}) \frac{\mu_g}{\mu_m} \frac{1}{\mu_g} \frac{d\mu_g}{d\eta_m} \\ &\quad + \frac{\mu_v - \mu_g}{\mu_m} (C_{mv,s} - C_{mv,\infty}) \frac{d\Gamma_{mv}}{d\eta_m} \end{aligned} \quad (19.21)$$

where

$$C_{mv} = (C_{mv,s} - C_{mv,\infty})\Gamma_{mv} + C_{mv,\infty}.$$

Thus, the absolute viscosity factor $\frac{1}{\mu_m} \frac{d\mu_m}{d\eta_m}$ for the vapor–gas mixture is expressed by the gas absolute viscosity factor $\frac{1}{\mu_g} \frac{d\mu_g}{d\eta_m}$ and vapor absolute viscosity factor $\frac{1}{\mu_v} \frac{d\mu_v}{d\eta_m}$.

While, $\frac{1}{\mu_g} \frac{d\mu_g}{d\eta_m}$ and $\frac{1}{\mu_v} \frac{d\mu_v}{d\eta_m}$ are temperature dependent, then, the viscosity factor of vapor–gas mixture is concentration and temperature dependent.

Similar to derivation for Eq. (19.21), the thermal conductivity factor of the vapor–gas mixture in the governing dimensionless differential equations can be expressed as by using Eq. (19.18)

$$\frac{1}{\lambda_m} \frac{d\lambda_m}{d\eta_m} = C_{mv} \frac{\lambda_v}{\lambda_m} \frac{1}{\lambda_v} \frac{d\lambda_v}{d\eta_m} + (1 - C_{mv}) \frac{\lambda_g}{\lambda_m} \frac{1}{\lambda_g} \frac{d\lambda_g}{d\eta_m} + \frac{\lambda_v - \lambda_g}{\lambda_m} (C_{mv,s} - C_{mv,\infty}) \frac{d\Gamma_{mv}}{d\eta_m} \quad (19.22)$$

Thus, the *thermal conductivity factor* $\frac{1}{\lambda_m} \frac{d\lambda_m}{d\eta_m}$ of the vapor–gas mixture is expressed by the *gas thermal conductivity factor* $\frac{1}{\lambda_g} \frac{d\lambda_g}{d\eta_m}$ and *vapor thermal conductivity factor*

$\frac{1}{\lambda_v} \frac{d\lambda_v}{d\eta_m}$. While, the physical factors $\frac{1}{\lambda_g} \frac{d\lambda_g}{d\eta_m}$ and $\frac{1}{\lambda_v} \frac{d\lambda_v}{d\eta_m}$ are temperature dependent, then, the thermal conductivity factor of vapour–gas mixture is concentration and temperature dependent.

19.2.5 Treatment of Temperature-Dependent Physical Properties of Vapor–Gas Mixture

For treatment of the above related temperature-dependent physical properties, the temperature parameter method reported in Chap. 5 will be applied, and the related vapor and gas physical property factors are expressed as follows:

For density factors we have

$$\frac{1}{\rho_v} \frac{d\rho_v}{d\eta_m} = - \frac{(T_{s,\text{int}}/T_\infty - 1)d\theta_m/d\eta_m}{(T_{s,\text{int}}/T_\infty - 1)\theta_m + 1} \quad (19.23)$$

$$\frac{1}{\rho_g} \frac{d\rho_g}{d\eta_m} = - \frac{(T_{s,\text{int}}/T_\infty - 1)d\theta_m/d\eta_m}{(T_{s,\text{int}}/T_\infty - 1)\theta_m + 1} \quad (19.24)$$

For absolute viscosity factors we have

$$\frac{1}{\mu_v} \frac{d\mu_v}{d\eta_m} = \frac{n_{\mu v}(T_{s,\text{int}}/T_\infty - 1)d\theta_m/d\eta_m}{(T_{s,\text{int}}/T_\infty - 1)\theta_m + 1} \quad (19.25)$$

$$\frac{1}{\mu_g} \frac{d\mu_g}{d\eta_m} = \frac{n_{\mu g}(T_{s,\text{int}}/T_\infty - 1)d\theta_m/d\eta_m}{(T_{s,\text{int}}/T_\infty - 1)\theta_m + 1} \quad (19.26)$$

For thermal conductivity factors we have

$$\frac{1}{\lambda_v} \frac{d\lambda_v}{d\eta_m} = \frac{n_{\lambda v}(T_{s,\text{int}}/T_\infty - 1)d\theta_m/d\eta_m}{(T_{s,\text{int}}/T_\infty - 1)\theta_m + 1} \quad (19.27)$$

$$\frac{1}{\lambda_g} \frac{d\lambda_g}{d\eta_m} = \frac{n_{\lambda g}(T_{s,\text{int}}/T_\infty - 1)d\theta_m/d\eta_m}{(T_{s,\text{int}}/T_\infty - 1)\theta_m + 1} \quad (19.28)$$

where $n_{\mu v}$ and $n_{\mu g}$ denote viscosity parameters of vapor and gas, respectively, and $\lambda_{\mu v}$ and $\lambda_{\mu g}$ denote thermal conductivity parameters of vapor and gas, respectively.

19.3 Necessity for Satisfying Whole Interfacial Balance Conditions on Reliable Solution

The interfacial matching conditions for the laminar free convection film condensation of vapor in the presence of noncondensable gas are respectively (i) velocity compo-

nent continuity, (ii) mass flow rate continuity, (iii) balance of the shear force, (iv) energy balance, (v) temperature continuity, (vi) concentration condition, and (vii) balance between the condensate mass flow rate and vapor diffusion mass transfer at the liquid–vapor interface. Compared with the laminar free convection film condensation of pure vapour, there are two additional interfacial boundary conditions (vi) and (vii) for the condensation of vapour–gas mixture. In solving the governing equations in this present work, whole above balance conditions at the liquid–vapor interface should seriously be satisfied for obtaining the reliable solutions for the velocity, temperature, and concentration fields, as well as heat and mass transfer. Otherwise, it is never possible to obtain the reliable numerical solutions of the two-phase boundary layer model, as well as reliable results of heat and mass transfer.

19.4 Numerical Calculation Approach

The numerical calculation of the two-phase boundary layer equations for free film condensation of vapor in the presence of noncondensable gas belongs to three-point boundary value problem, and is carried out numerically by two steps. In the first step, the governing ordinary differential equations for liquid film are solved with ignoring shear force at the liquid–vapor interface. The numerical calculation is done by an advanced shooting method procedure with fifth-order Runge–Kutta integration. At the beginning of the calculation, the initial values of the condensate liquid film thickness $\eta_{1\delta}$ and condensate liquid velocity component $W_{x1,s}$ should be assumed. In the second step, the governing ordinary differential equations for vapour–gas mixture film are solved by using the advanced shooting method with *seventh-order Runge–Kutta integration*. In this step of numerical calculation, the interfacial boundary conditions are divided into two groups. The first group of the interfacial boundary condition equations is the initial boundary conditions of the ordinary differential equations for the vapour–gas mixture film, and the second group is the judgment equations for convergence of the whole calculation. By means of the judgment equations, the calculation is iterated with appropriate change of the values $W_{x1,s}$ and $\eta_{1\delta}$. In each iteration, the numerical calculations of ordinary differential equations for liquid film and vapour–gas mixture film are done successively. For solving such very strong nonlinear problem, a variable mesh approach is applied to the numerical calculation programs.

The laminar free convection film condensation of water vapor in the presence of air on a vertical flat plate is taken as an example for the practical solution. The given conditions for solution are different wall temperatures T_w and the bulk vapor mass fraction $C_{mv,\infty}$ with the bulk temperature $T_\infty = 373$ K and at atmosphere as the system pressure.

Table 19.1 Physical property values for water, water vapor and air at atmosphere pressure

Term	Value		
	Water	Water vapor	Air
T_s, K	373	373	373
$c_p, \text{J}/(\text{kg K})$	4,216	2,060	1,009
$h_{fg}, \text{kJ}/\text{kg}$		2257.3	
Pr	1.76	1	0.7
$\rho, \text{kg}/\text{m}^3$	958.1	0.5974	0.946
$\mu, \text{kg}/(\text{m s})$	282.2×10^{-6}	12.28×10^{-6}	21.9×10^{-6}
$\nu, \text{m}^2/\text{s}$	0.294×10^{-6}	20.55×10^{-6}	23.13×10^{-6}
$\lambda, \text{W}/(\text{m K})$	0.677	0.02478	0.0321
$D_v, \text{m}^2/\text{s}$		0.256×10^{-4}	
n_μ		1.04 ($n_{\mu,v}$)	0.68 ($n_{\mu,g}$)
n_λ		1.185 ($n_{\lambda,v}$)	0.81 ($n_{\lambda,g}$)

19.5 Physical Property Data Applied for Numerical Calculation

For convenience, some related values of the physical properties for water, water vapor, and air used in the calculation are listed in Table 19.1. Additionally, the absolute viscosity parameters $n_{\mu,v}$ and $n_{\mu,g}$ and thermal conductivity parameters $n_{\lambda,v}$ and $n_{\lambda,g}$ of water vapor and air, respectively, obtained from Appendix A of this book are listed in Table 19.1.

19.6 Interfacial Vapor Saturation Temperature

The theoretical calculation of heat transfer of the film condensation of vapor–gas mixture depends on the calculation result of the *interfacial vapor saturation temperature* $T_{s,int}$ of the vapor–gas mixture. While, the interfacial vapor saturation temperature $T_{s,int}$ depends on the *interfacial vapor mass fraction* $C_{mv,s}$. While, the *interfacial vapor mass fraction* $C_{mv,s}$ depends on the *reference vapor saturation temperature* $T_{s,ref}$ and bulk vapor mass fraction $C_{mv,\infty}$. Here, the *reference vapor saturation temperature* refers to the saturation temperature with unity bulk vapor mass fraction (i.e. $C_{mv,\infty} = 1$) and at atmospheric pressure as the system pressure for laminar free convection film condensation of vapor–gas mixture. According to our investigation, the relationship among the above physical variables can be described by the following equation:

$$T_{s,int} = T_{s,ref} \cdot C_{mv,s}^a \quad (19.29)$$

While, the exponent “a” depends on the related vapor and gas in the mixture.

However, for laminar free convection film condensation of water vapor–air mixture, the exponent “a” equals 0.063 [4], and obviously the reference interfacial saturation temperature $T_{s,ref} = 373 \text{ K}$, then the interfacial saturation temperature can be described as

$$T_{s,int} = 373 \cdot C_{mv,s}^{0.063} \quad (19.30)$$

Take the laminar free convection film condensation of water vapor–air mixture as an example, we have obtained a system of numerical solutions on the interfacial vapor saturation temperature $T_{s,int}$, and show them in Fig. 19.1 and list some of them in Table 19.2 with variation of the reference wall subcooled grade $\frac{t_{s,ref} - t_w}{t_{s,ref}}$ and the bulk vapor mass fraction $C_{mv,\infty}$ at the bulk temperature $T_\infty = 373$ K and at atmospheric pressure as the system pressure.

It is seen from Fig. 19.1 and Table 19.2 that the interfacial vapor saturation temperature $T_{s,int}$ only depends on the bulk vapor mass fraction $C_{mv,\infty}$, but does not depend on the reference wall subcooled grade $\frac{t_{s,ref} - t_w}{t_{s,ref}}$. Then, the solutions on the interfacial vapor saturation temperature $T_{s,int}$ with the bulk vapor mass fraction $C_{mv,\infty}$ at the bulk temperature $T_\infty = 373$ K and at atmospheric pressure are formulated to the following equation for laminar free convection film condensation of water vapor–air mixture:

$$T_{s,int} = 357.06 C_{mv,\infty}^{0.063} \quad (19.31)$$

Then, it is seen that the interfacial vapor saturation temperature $T_{s,int}$ depends only on the bulk vapor mass fraction $C_{mv,\infty}$ at the special bulk temperature.

19.7 Critical Bulk Vapor Mass Fraction with the Film Condensation

From the calculation results, it is found that there is a lowest value of the bulk vapor mass fraction $C_{m,v\infty}^*$ for satisfying condition $T_{s,int} > T_w$, so that it is possible to have the film condensation. Then, if the bulk vapor mass fraction $C_{m,v\infty}$ is higher than it, i.e. $C_{m,v\infty} > C_{m,v\infty}^*$, it is possible to obtain the film condensation, since the interfacial vapor saturation temperature will be higher than the wall temperature, i.e. $T_{s,int} > T_w$ in this case. Otherwise, If the bulk vapor mass fraction $C_{m,v\infty}$ is lower than it, i.e. $C_{m,v\infty} < C_{m,v\infty}^*$, the film condensation will never happen, since the interfacial vapor saturation temperature will be lower than the wall temperature, i.e. $T_{s,int} < T_w$ in this case. This special bulk vapor mass fraction $C_{m,v\infty}^*$ is defined as the critical bulk vapor mass fraction. Obviously, special bulk vapor mass fraction $C_{m,v\infty}^*$ varies with the wall temperature T_w .

According to our numerical results on laminar free convection film condensation of water vapor–air mixture, we show the numerical results on the critical bulk vapor mass fraction $C_{m,v\infty}^*$ in Fig. 19.2 as well as Table 19.3 with the selected data for film condensation of water vapor–air mixture at $t_\infty = 100$ °C and atmospheric pressure as the system pressure.

It is seen that with increasing the *wall reference subcooled grade* $\frac{t_{s,ref} - t_w}{t_{s,ref}}$ (i.e. decreasing the wall temperature), the *critical bulk vapor mass fraction* $C_{m,v\infty}^*$

Table 19.2 Selected numerical solutions on the interfacial vapor saturation temperature $T_{s,int}$ for laminar free film condensation of water vapor–air mixture at $t_\infty = 100^\circ\text{C}$ and atmospheric pressure as the system pressure level

T_w, K	$\frac{t_{s,ref} - t_w}{t_{s,ref}}$	$C_{mv,\infty}$										
		0.0145	0.044	0.125	0.206	0.335	0.54	0.8	0.86	0.95	0.99	0.999
		$T_{s,int}$										
273	1	273.4703	293.2793	313.2198	323.2344	333.2896	343.4668	352.0778	353.6856	355.9103	356.836	357.0397
293	0.8	–	293.2793	313.2198	323.2344	333.2896	343.4668	352.0778	353.6856	355.9103	356.8362	357.0397
313	0.6	–	–	313.264	323.2344	333.2896	343.4668	352.0778	353.6856	355.9103	356.8362	357.0397
323	0.5	–	–	–	323.333	333.2896	343.4668	352.0778	353.6856	355.9103	356.8362	357.0397
333	0.4	–	–	–	–	333.4507	343.4668	352.0778	353.6856	355.9103	356.8362	357.0397
343	0.3	–	–	–	–	–	343.6265	352.0778	353.6856	355.9103	356.8362	357.0397
348	0.25	–	–	–	–	–	–	352.1055	353.6985	355.9103	356.8362	357.0397
353	0.2	–	–	–	–	–	–	–	353.9689	355.9480	356.8635	357.0623
Predicted value with Eq. (19.31)		273.4685	293.2774	313.218	323.2323	333.287	343.465	352.076	353.683	355.908	356.834	357.037

Note Sing “–” denotes the non-condensable region

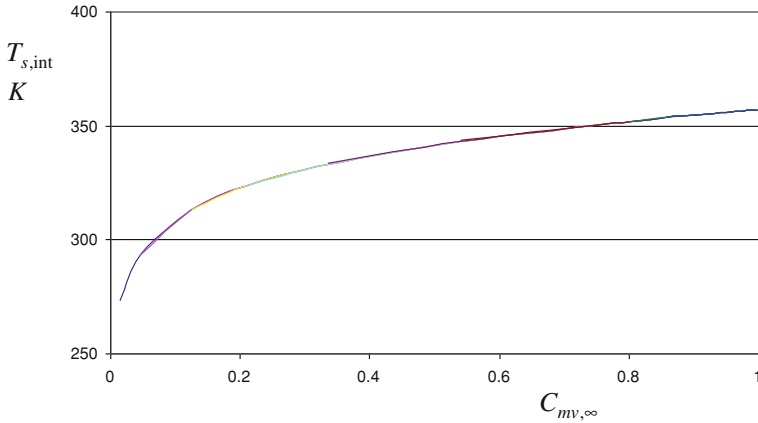
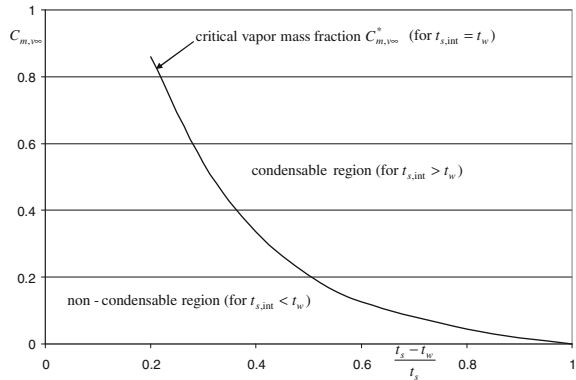


Fig. 19.1 Numerical solutions on the interfacial vapor saturation temperature $T_{s,int}$ for laminar free film condensation of water vapor–air mixture at $t_\infty = 100^\circ\text{C}$ and atmospheric pressure as the system pressure level

Fig. 19.2 Critical bulk vapor mass fraction $C_{m,v,\infty}^*$ with variation of reference wall subcooled grade $\frac{t_{s,ref}-t_w}{t_{s,ref}}$ for laminar free film condensation from water vapor–air mixture on a vertical flat plate at $t_\infty = 100^\circ\text{C}$ and atmospheric pressure as the system pressure level



decreases, and the condensable region will increase. Otherwise the condensable region will decrease.

These numerical results on the critical bulk vapor mass fraction $C_{m,v,\infty}^*$ are formulated to Eqs. (19.32) and (19.33) by using a curve-fitting method, and the results predicted by using Eqs. (19.32) and (19.33) are listed in Table 19.3 too. Comparing the numerical and predicted results on the critical bulk vapor mass fraction $C_{m,v,\infty}^*$, it is found that Eqs. (19.32) and (19.33) are pretty accurate for evaluation of the *critical bulk vapor mass fraction* $C_{m,v,\infty}^*$ for film condensation of water vapor–air mixture at $t_\infty = 100^\circ\text{C}$ and atmospheric pressure as the system pressure.

Table 19.3 Selected numerical data on critical bulk vapor mass fraction $C_{mv,\infty}^*$ with variation of reference wall subcooled grade $\frac{t_{s,ref}-t_w}{t_{s,ref}}$ for laminar free convection film condensation from water vapor–air mixture on a vertical flat plate at $t_\infty = 100^\circ\text{C}$ and atmospheric pressure as the system pressure level

$\frac{t_{s,ref}-t_w}{t_{s,ref}}$	1	0.8	0.6	0.5	0.4	0.3	0.25	0.2
$C_{mv,\infty}^*$ ^a	0.014109	0.043339	0.123615	0.203642	0.330409	0.528468	0.66494	0.833918
$C_{mv,\infty}^*$ ^b	0.0141	0.043324	0.123596	0.202104	0.325617	0.524613	0.665895	0.845224

^aDenotes numerical results

^bDenotes predicted result by using Eqs. (19.32) and (19.33) respectively

$$C_{m,v\infty}^* = 0.6381 \left(\frac{t_{s,ref} - t_w}{t_{s,ref}} \right)^2 - 1.2947 \left(\frac{t_{s,ref} - t_w}{t_{s,ref}} \right) + 0.6707 \left(0.6 \leq \frac{t_{s,ref} - t_w}{t_{s,ref}} \leq 1 \right) \quad (19.32)$$

$$C_{m,v\infty}^* = 2.194 \text{Exp} \left[-4.7694 \left(\frac{t_{s,ref} - t_w}{t_{s,ref}} \right) \right] \left(0.2 \leq \frac{t_{s,ref} - t_w}{t_{s,ref}} \leq 0.6 \right) \quad (19.33)$$

19.8 Velocity, Concentration, and Temperature Fields of the Two-Phase Film Flows

From the governing ordinary equations and their boundary conditions presented in Chap. 18, it will be expected that for the consideration of variable physical properties of the medium for liquid and vapor–gas mixture films, the velocity, temperature, and concentration fields for the two-phase film flows will depend on the temperature and concentration-dependent properties, the given wall boundary temperatures T_w , bulk temperature T_∞ , and the bulk vapor mass fraction $C_{mv,\infty}$.

With the provided numerical procedure and the related physical property factors reported, the governing ordinary Eqs. (18.28)–(18.34) with their boundary conditions, Eqs. (18.35)–(18.43) are rigorously calculated, and a system of solutions for together velocity, concentration, and temperature fields is obtained, and plotted in Figs. 19.3, 19.4, 19.5 and 19.6 with variation of the wall temperatures T_w and bulk vapor mass fraction $C_{mv,\infty}$, respectively, for the bulk temperature $T_\infty = 373\text{ K}$ and at atmospheric pressure as the system pressure of the two-phase free convection film condensation of water vapour–air mixture.

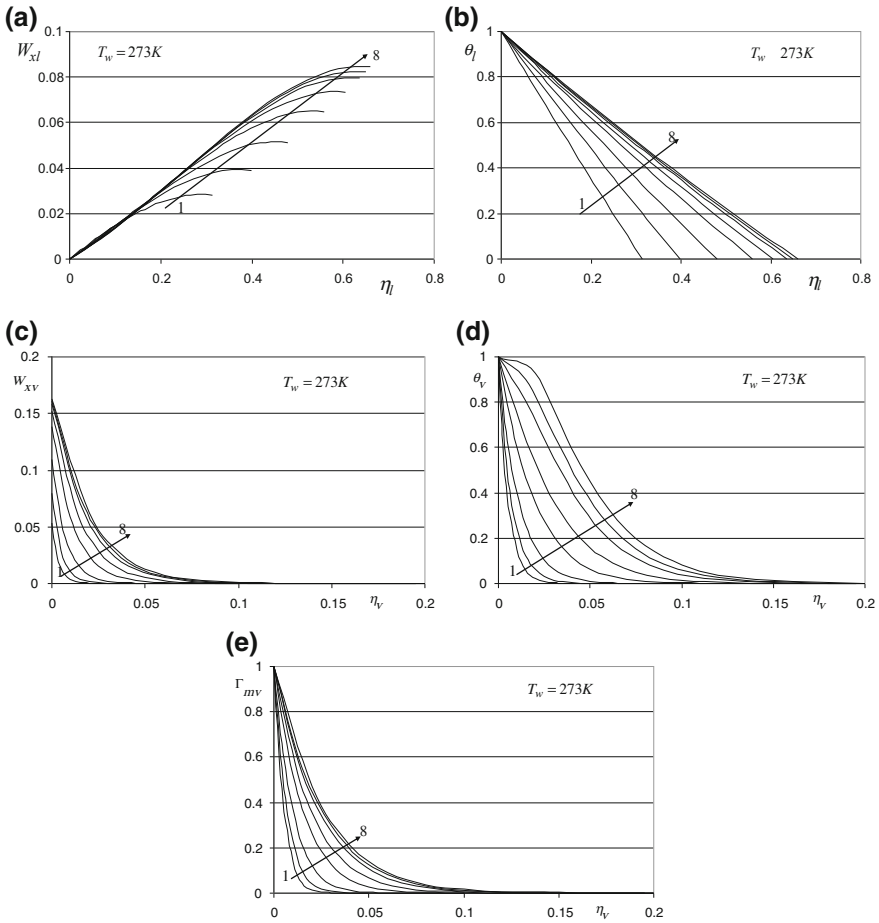


Fig. 19.3 Numerical results of **a** velocity W_{xl} , **b** temperature θ_l profiles of vapor film, **c** velocity component W_{xv} , **d** temperature θ_v , and **e** relative concentration $\Gamma_{m,v}$ profiles of vapor film for laminar free convection film condensation of water vapor–air mixture at $T_w = 273\text{ K}$, $t_\infty = 100^\circ\text{C}$, and atmospheric pressure as the system pressure level (Lines 1–8 for $C_{m,\infty} = 0.05, 0.1, 0.2, 0.4, 0.6, 0.8, 0.9$ and 0.99 respectively)

19.9 Variations of Velocity and Temperature Fields

From the numerical results the following variations of velocity and temperature fields of laminar free convection film condensation of vapour–gas mixture are found:

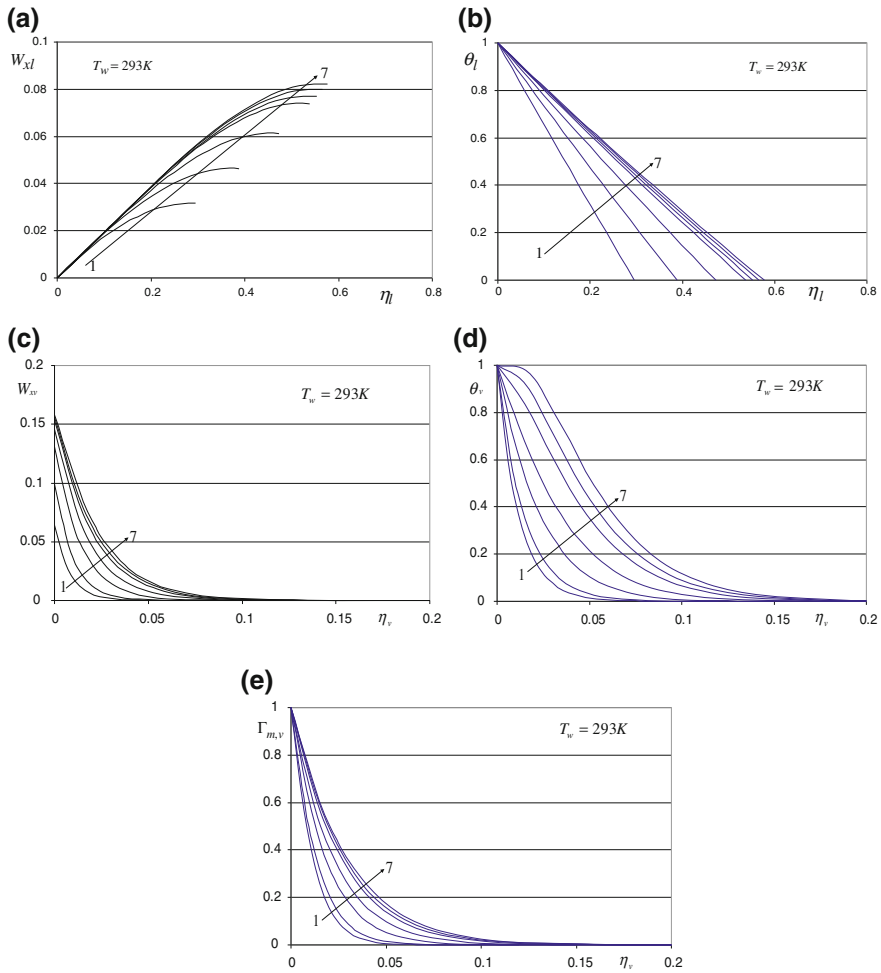


Fig. 19.4 Numerical results of **a** velocity $W_{x,l}$, **b** temperature θ_l profiles of liquid film, **c** velocity component $W_{x,v}$, **d** temperature θ_v , and **e** relative concentration $\Gamma_{m,v}$ profiles of vapor film for laminar free convection film condensation of water vapour–air mixture at $T_w = 293\text{ K}$, $t_\infty = 100^\circ\text{C}$, and atmospheric pressure as the system pressure level (Lines 1–7 for $C_{m,v,\infty} = 0.1, 0.2, 0.4, 0.6, 0.8, 0.9$ and 0.99 , respectively)

19.9.1 Variation of Film Thicknesses

From Figs. 19.3, 19.4, 19.5 and 19.6, it is seen that the condensate film liquid thickness will decrease at an accelerative pace with increasing wall temperature T_w . This phenomenon is because increasing wall temperature T_w will decrease the wall sub-cooled temperature $\Delta T_w = T_{s,int} - T_w$, and then causes decrease of the condensate

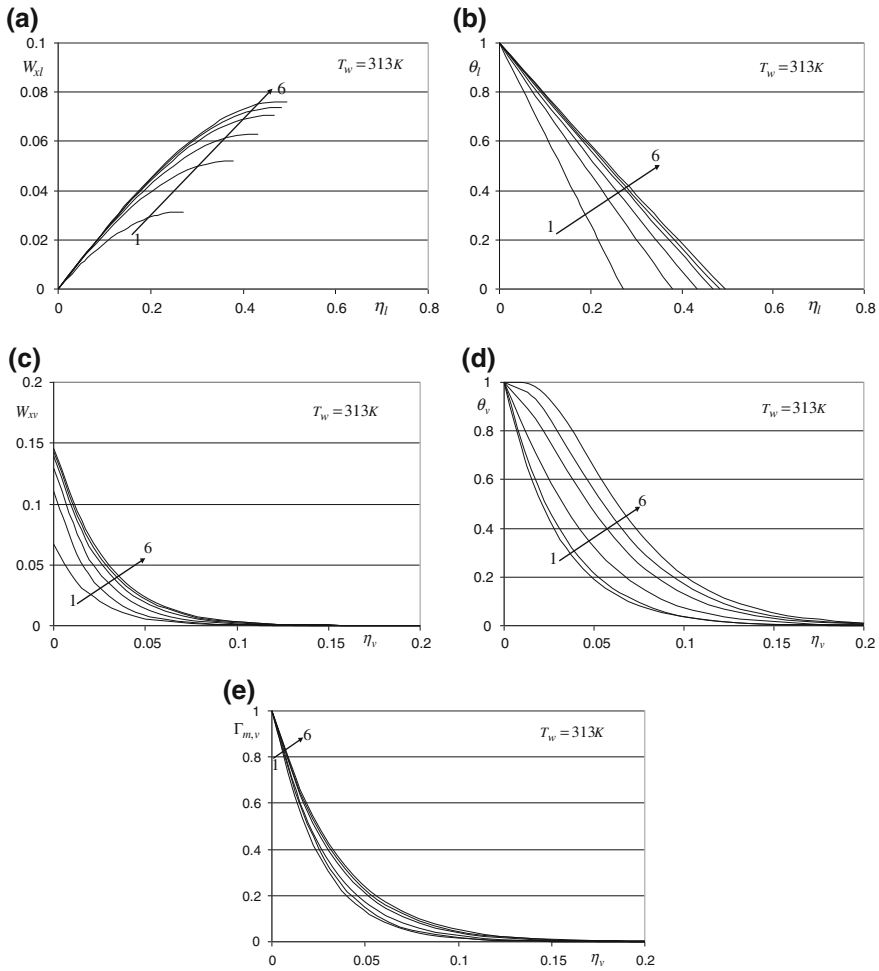


Fig. 19.5 Numerical results of **a** velocity W_{xl} , **b** temperature θ_l profiles of liquid film, **c** velocity component W_{xv} , **d** temperature θ_v , and **e** relative concentration $\Gamma_{m,v}$ profiles of vapor film for laminar free convection film condensation of water vapor–air mixture at $T_w = 313\text{ K}$, $t_\infty = 100^\circ\text{ C}$, and atmospheric pressure as the system pressure level (Lines 1–6 for $C_{m,v,\infty} = 0.2, 0.4, 0.6, 0.8, 0.9$ and 0.99 , respectively)

liquid mass flow rate. However, the vapor–gas film thickness increases with increasing wall temperature T_w .

The condensate liquid film thickness will increase with increasing the bulk vapor mass fraction $C_{m,v,\infty}$. The reason is that with increasing the bulk vapor mass fraction $C_{m,v,\infty}$, the condensate rate will speed up, which will lead to increasing the condensate liquid film thickness. Furthermore, the vapor–gas mixture film thickness will increase with increasing the bulk vapor mass fraction $C_{m,v,\infty}$.

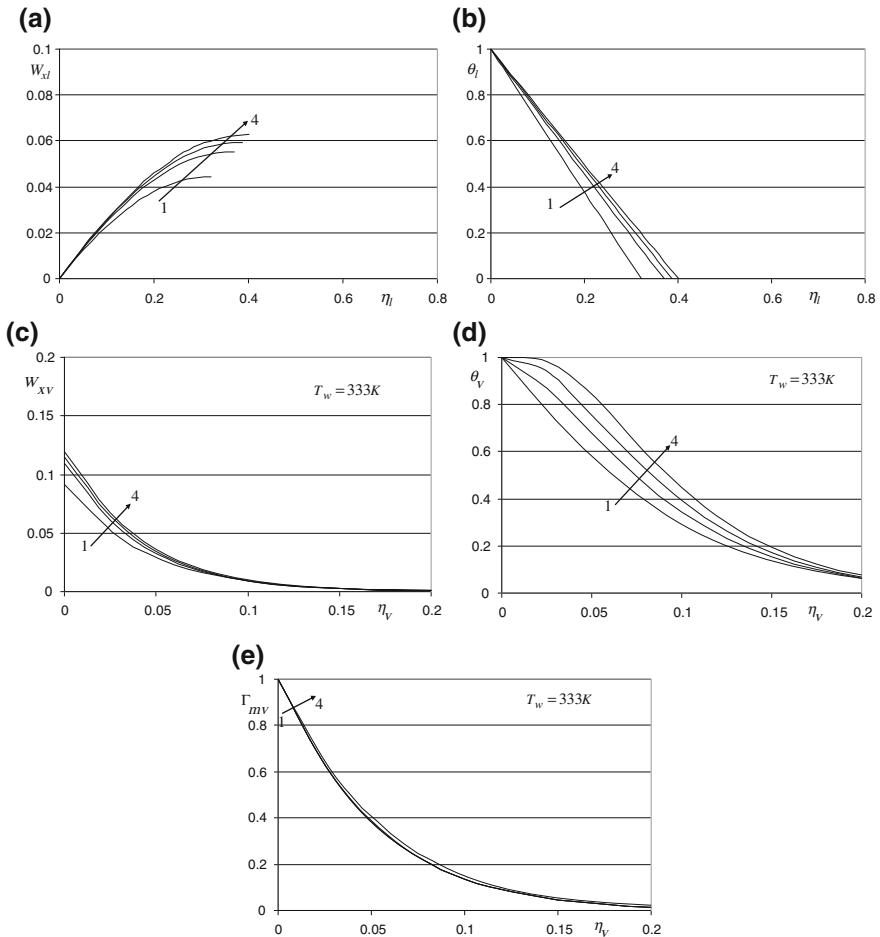


Fig. 19.6 Numerical results of **a** velocity W_{xl} , **b** temperature θ_l profiles of liquid film, **c** velocity component W_{xv} , **d** temperature θ_v , and **e** relative concentration Γ_{mv} profiles of vapor film for laminar free convection film condensation of water vapor–air mixture at $T_w = 333\text{ K}$, $t_\infty = 100^\circ\text{C}$ and atmospheric pressure as the system pressure level (Lines 1–4 for $C_{m,v\infty} = 0.6, 0.8, 0.9$ and 0.99 , respectively)

19.9.2 Variation of Velocity Fields of Condensate Liquid Film

From Figs. 19.3, 19.4, 19.5 and 19.6, it is seen that the condensate velocity components decrease with increasing the wall temperature T_w . These dependent relationships are coincident with those for the related laminar free film condensation of pure vapor reported in [6, 7].

It is seen that the condensate velocity components will increase with increasing the bulk vapor mass fraction $C_{vw,\infty}$. It will lead to increasing the interfacial velocity

components. It is because the condensate process will speed up with increasing the bulk vapor mass fraction $C_{vw,\infty}$.

19.9.3 Variation of Velocity Fields of Vapour–Gas Mixture Film

It is seen that the velocity fields of vapor–gas mixture film will decrease with increasing the wall temperature T_w , and increase with the bulk vapor mass fraction $C_{vw,\infty}$.

19.10 Remarks

A set of physical matching conditions at the liquid–vapor interface are considered and rigorously satisfied in the numerical calculation, such as those for two-dimensional velocity component balances, shear force balance, mass flow rate balance, temperature balance, heat transfer balance, concentration condition, as well as the balance between the condensate mass flow, and vapor mass diffusion. For getting reliable solutions of the three-point boundary value problem with the two-phase boundary layer model, it is necessary to consider and rigorously satisfy the physical matching conditions at the liquid–vapor interface.

By means of the example on the laminar free convection film condensation of water vapor–air mixture, a system of the interfacial vapor saturation temperature $T_{s,int}$ is found out during the numerical calculation. It is found that the interfacial vapor saturation temperature $T_{s,int}$ only depends on the bulk vapor mass fraction for a special bulk temperature. Furthermore, the numerical solutions of the interfacial vapor saturation temperature $T_{s,int}$ are formulated into a prediction equation for its practical prediction.

The laminar free convection film condensation of water vapor in the presence of air is taken as example for the numerical calculation. A system of rigorous numerical results is successfully obtained, including velocity and temperature fields of the condensate liquid film, as well as the velocity, temperature, and concentration fields of the vapor–gas mixture film. From these numerical results, it is found that with a given temperature in the vapor–gas mixture bulk, the wall temperature and the vapor (or gas) mass fraction in the bulk have decisive effects on the laminar free convection film condensation of vapor–gas mixture.

With increasing the vapor mass fraction (or decreasing the gas mass fraction) in the bulk, the condensate liquid film thickness, the condensate liquid velocity, and vapor–gas mixture velocity at the liquid–vapor interface will increase very obviously. It proved that the noncondensable gas in the vapor–gas mixture has a decisive effect on the laminar free film condensation from vapor–gas mixture.

The wall temperature has also a decisive effect on the laminar free film condensation from vapor–gas mixture. With increasing wall temperature, the condensate liquid

film thickness, the condensate liquid velocity, as well as velocity of the vapor–gas mixture at the liquid–vapor interface will decrease. However, with increasing the wall temperature, the thicknesses of the momentum, temperature, and concentration boundary layers of the vapor–gas mixture will increase.

19.11 Exercises

1. Explain the meanings of followings:
 - (i) Interfacial vapor saturation temperature;
 - (ii) Interfacial vapor mass fraction;
 - (iii) Critical vapor mass fraction;
 - (iv) Reference wall subcooled grade.
2. Please give out a detailed derivation for obtaining Eqs. (19.13)–(19.15) on description of concentration-dependent densities of vapor, gas, and vapor–gas mixture in the vapor–gas mixture.
3. Please give out a detailed derivation for obtaining Eqs. (19.16), (19.21), and (19.22) respectively on describing density factor, viscosity factor, and thermal conductivity factor of vapor–gas mixture. Which kinds of dependent physical properties do Eqs. (19.16), (19.21), and (19.22) describe?
4. Please give out a detailed derivation for obtaining Eqs. (19.23)–(19.28) respectively on related physical property factors of vapor and gas in vapor–gas mixture. Which kinds of dependent physical properties do Eqs. (19.23)–(19.28) describe?
5. Please give out a detailed derivation for obtaining Eqs. (19.6)–(19.8) respectively on describing density factor, viscosity factor, and thermal conductivity factor of condensate water film. Which kinds of dependent physical properties do Eqs. (19.6)–(19.8) describe?
6. What is the relation between the concentration-dependent and temperature-dependent physical properties of vapor–gas mixture?
7. What is the reference saturation temperature of vapor–gas mixture? What does it depend on?
8. Which kind of dependent physical properties exist in vapor–gas mixture?
9. What is the definition of critical bulk vapor mass fraction with the free film condensation of vapor–gas mixture?
10. What is the interfacial vapour saturation temperature? What does it depend on?
11. Please describe the variations of velocity, temperature, and concentration fields on laminar free convection film condensation from vapor–gas mixture.
12. Please explain why the condensate film thickness will decrease at an accelerative pace with increasing wall temperature T_w .
13. Please explain why the condensate liquid film thickness will increase with increasing the bulk vapor mass fraction $C_{m,v\infty}$.
14. Please explain why the condensate velocity components decrease with increasing the wall temperature T_w .

15. Please explain why the condensate velocity components will increase with increasing the bulk vapor mass fraction $C_{vw, \infty}$.
16. Compare the models on treatments of variable physical properties between the similarity mathematical models of laminar free convection film condensation of pure vapor, and that of vapor–gas mixture, and find out their common grounds and differences.
17. What reason causes more difficult and complicated for treatment of variable physical properties of the laminar free convection film condensation of vapour–gas mixture than that of pure vapour?
18. Further, compare the models on treatment of variable physical properties among similarity mathematical models of laminar free convection, laminar free convection film boiling, laminar free convection film condensation of pure vapor, and laminar free film condensation of vapor–gas mixture, and find out their common grounds and differences.
19. Please explain the importance for reliable determination of the interfacial vapor saturation temperature for laminar free convection film condensation of vapor–gas mixture.
20. According to Eqs. (19.30) and (19.31), please find out the relation between the interfacial vapor mass fraction and the bulk vapor mass fraction in the related conditions for laminar free convection film condensation of vapor–gas mixture.

References

1. D.Y. Shang, B.X. Wang, Y. Wang, Y. Quan, Study on liquid laminar free convection with consideration of variable thermophysical properties. *Int. J. Heat Mass Transf.* **36**(14), 3411–3419 (1993)
2. D.Y. Shang, B.X. Wang, Effect of variable thermophysical properties on laminar free convection of gas. *Int. J. Heat Mass Transf.* **33**(7), 1387–1395 (1990)
3. D.Y. Shang, B.X. Wang, Effect of variable thermophysical properties on laminar free convection of polyatomic gas. *Int. J. Heat Mass Transf.* **34**(3), 749–755 (1991)
4. D.Y. Shang, L.C. Zhong, Extensive study on laminar free film condensation from vapor–gas mixture. *Int. J. Heat Mass Transf.* **51**, 4300–4314 (2008)
5. D.Y. Shang, *Theory of Heat Transfer With Forced Convection Film Flows* (Springer, Berlin, 2010)
6. D.Y. Shang, T. Adamek, Study on laminar film condensation of saturated steam on a vertical flat plate for consideration of various physical factors including variable thermophysical properties. *Wärme- und Stoffübertragung* **30**, 89–100 (1994)
7. D.Y. Shang, B.X. Wang, An extended study on steady-state laminar film condensation of a superheated vapor on an isothermal vertical plate. *Int. J. Heat Mass Transf.* **40**(4), 931–941 (1997)

Chapter 20

Heat and Mass Transfer of Laminar Free Convection Film Condensation of Vapor–Gas Mixture

Abstract The theoretical equations on heat and mass transfer are set up for laminar free Convection film condensation of vapor–gas mixture. In the theoretical equations only dimensionless wall temperature gradient and condensate mass flow rate parameter are no-given variables respectively for prediction of heat and mass transfer rates. The laminar free Convection film condensation of water vapor in presence of air on a vertical flat plate is taken as example for the numerical solutions on condensate heat and mass transfer, including those on the dimensionless temperature gradient and mass flow rate parameter. Both by decreasing the bulk vapor mass fraction and the reference wall subcooled grade, the wall dimensionless temperature gradient will increase at accelerative pace. Both decreasing the bulk vapor mass fraction and the reference wall subcooled grade will cause decreasing the condensate mass flow rate parameter at accelerative pace. These phenomena demonstrate the decisive effect of the non-condensable gas on condensate heat and mass transfer of the laminar forced film condensation of vapor–gas mixture. The system of the rigorous key solutions on the wall dimensionless temperature gradient and the condensate mass flow rate parameter is formulated to the simple and reliable equations for the laminar free Convection film condensation of water vapor–air mixture. Coupled with these formulated equations, the theoretical equations on the condensate heat and mass transfer can be respectively used for reliable and simple prediction of heat and mass transfer rate on laminar free Convection film condensation of water vapor–air mixture. Additionally, it is found that the condensate heat transfer rate is dominated by the wall subcooled temperature $t_w - t_{s,int}$ and the wall temperature gradient, the condensate mass flow rate is dominated by the condensate mass flow rate parameter, and the condensate heat transfer rate is identical to the condensate mass flow rate. Due to the quite different condensate mechanisms, the condensate heat and mass transfer rate of the laminar free Convection film condensation from vapor in presence of non-condensable gas is quite different from that of pure vapor, even for $C_{mv,\infty} \rightarrow 0$.

20.1 Introduction

In Chaps. 18 and 19, I presented the complete similarity mathematical model and the numerical results of velocity temperature, and concentration fields on laminar free convection film condensation from vapor–gas mixture, respectively. In this chapter, further investigation will be done for heat and mass transfer on laminar free convection film condensation from vapor–gas mixture. For this purpose, the appropriate heat and mass transfer analysis will be done for providing the appropriate theoretical equations on the condensate heat and mass transfer. With these theoretical equations, the key solutions, i.e., the wall dimensionless temperature gradient and the induced condensate mass flow rate parameter become respectively the unknown variables on evaluation of condensate heat and mass transfer. While, by means of the mass transfer analysis, the condensate mass flow rate parameter consists of the dimensionless liquid film thickness, as well as the condensate interfacial velocity components. Furthermore, the key solutions on the wall dimensionless temperature gradient and the condensate mass flow rate parameter of the governing similarity mathematical model will be formulated based on the rigorous numerical results, so that the theoretical equations on condensate heat and mass transfer can be conveniently used for simple and reliable prediction.

20.2 Heat Transfer Analysis

Consulting the heat transfer analysis in Chapter 16, the *local heat transfer rate* q_x of the free convection film condensation of vapour–gas mixture at position x per unit area on the plate can be calculated by Pourier’s law as

$$q_x = -\lambda_{l,w} \left(\frac{\partial t_l}{\partial y_l} \right)_{y_l=0}$$

With Eqs. (18.17)–(18.19) the local heat transfer rate is expressed as

$$q_x = \lambda_{l,w}(t_w - t_{s,int}) \left(\frac{1}{4} Gr_{x1,s} \right)^{1/4} x^{-1} \left(-\frac{d\theta_l}{d\eta_l} \right)_{\eta_l=0} \quad (20.1)$$

where $\left(\frac{d\theta_l}{d\eta_l} \right)_{\eta_l=0}$ is dimensionless temperature gradient on the plate for the film condensation. In short, it is called wall temperature gradient.

It should be indicated in Eq.(20.1) that the value of temperature gradient $\left(-\frac{d\theta_l}{d\eta_l} \right)_{\eta_l=0}$ is positive, the value of the temperature $t_w - t_{s,int}$ is negative, and then, the value of the local heat transfer rate is negative, which means that the direction of the heat transfer rate is from the bulk vapor–gas mixture to the wall surface.

The local heat transfer coefficient on the plate, $\alpha_{x,w}$ defined as $q_x = \alpha_{x,w}(t_w - t_{s,int})$, will be given as

$$\alpha_{x,w} = \lambda_{l,w} \left(\frac{1}{4} \text{Gr}_{x1,s} \right)^{1/4} x^{-1} \left(-\frac{d\theta_1}{d\eta_1} \right)_{\eta_1=0} \quad (20.2)$$

The local Nusselt number defined as $\text{Nu}_{x1,w} = \frac{\alpha_{x,w} x}{\lambda_{l,w}}$ is expressed as

$$\text{Nu}_{x1,w} = \left(\frac{1}{4} \text{Gr}_{x1,s} \right)^{1/4} x^{-1} \left(-\frac{d\theta_1}{d\eta_1} \right)_{\eta_1=0} \quad (20.3)$$

The total heat transfer rate from position $x = 0$ to x with width of b on the plate is an integration

$$Q_x = \iint_A q_{x,w} dA = \int_0^x q_{x,w} b dx$$

where the plate area related to condensate heat transfer is described as $A = b \times x$, where b is the plate width related to heat transfer.

With Eq.(20.1), the above equation is following integration

$$Q_x = \int_0^x b \lambda_{l,w} (t_w - t_{s,int}) \left(\frac{1}{4} \text{Gr}_{x1,s} \right)^{1/4} x^{-1} \left(-\frac{d\theta_1}{d\eta_1} \right)_{\eta_1=0} dx$$

i.e.

$$Q_x = \frac{4}{3} b \lambda_{l,w} (t_w - t_{s,int}) \left(\frac{1}{4} \text{Gr}_{x1,s} \right)^{1/4} \left(-\frac{d\theta_1}{d\eta_1} \right)_{\eta_1=0} \quad (20.4)$$

The average heat transfer rate, defined as $\bar{Q}_x = Q_x / (b \times x)$ is given as

$$\bar{Q}_x = \frac{4}{3} x^{-1} \lambda_{l,w} (t_w - t_{s,int}) \left(\frac{1}{4} \text{Gr}_{x1,s} \right)^{1/4} \left(-\frac{d\theta_1}{d\eta_1} \right)_{\eta_1=0} \quad (20.5)$$

The average heat transfer coefficient $\bar{\alpha}_x$ defined as $Q_x = \bar{\alpha}_x (t_w - t_{s,int}) \cdot b \cdot x$ is expressed as

$$\bar{\alpha}_x = \frac{4}{3} \lambda_{l,w} \left(\frac{1}{4} \text{Gr}_{x1,s} \right)^{1/4} x^{-1} \left(-\frac{d\theta_1}{d\eta_1} \right)_{\eta_1=0} \quad (20.6)$$

The average Nusselt number defined as $\bar{\text{Nu}}_{x,w} = \frac{\bar{\alpha}_x x}{\lambda_{l,w}}$ is

$$\bar{\text{Nu}}_{x,w} = \frac{4}{3} \left(\frac{1}{4} \text{Gr}_{x1,s} \right)^{1/4} \left(-\frac{d\theta_1}{d\eta_1} \right)_{\eta_1=0} \quad (20.7)$$

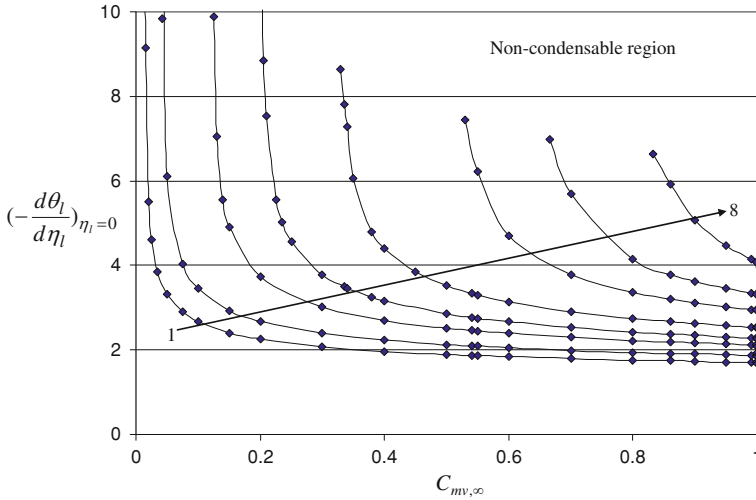


Fig. 20.1 Numerical solutions of temperature gradient $\left(-\frac{d\theta_1}{d\eta_1}\right)_{\eta_1=0}$ with variation of reference wall subcooled grade $\frac{t_{s,ref}-t_w}{t_{s,ref}}$ and bulk vapor mass fraction $C_{mv,\infty}$ for laminar free convection film condensation of water vapor–air mixture at $t_\infty = 100^\circ\text{C}$ and atmospheric pressure as the system pressure. (Note Lines 1–8 for $\frac{t_{s,ref}-t_w}{t_{s,ref}} = 1, 0.8, 0.6, 0.5, 0.4, 0.3, 0.25,$ and 0.2)

20.3 Wall Temperature Gradient

From the above heat transfer equations, it is found that the heat transfer rate is directly proportional to the wall dimensionless temperature gradient $\left(-\frac{d\theta_1}{d\eta_1}\right)_{\eta_1=0}$. Obviously, the wall dimensionless temperature gradient $\left(-\frac{d\theta_1}{d\eta_1}\right)_{\eta_1=0}$ is only one non-given variable in these heat transfer equations.

For the laminar free convection film condensation of water vapor–air mixture at $t_\infty = 100^\circ\text{C}$ and atmospheric pressure as the system pressure, a system of the numerical solutions of the wall dimensionless temperature gradient $\left(-\frac{d\theta_1}{d\eta_1}\right)_{\eta_1=0}$ obtained by the numerical calculation are plotted and listed in Fig. 20.1 and Table 20.1, respectively, with the reference wall subcooled grade $\frac{t_{s,ref}-t_w}{t_{s,ref}}$ and the bulk vapor mass fraction $C_{mv,\infty}$. Here, the reference temperature $t_{s,ref}$ denotes the saturation temperature of pure vapor with $C_{mv,\infty} = 1$.

From the numerical results it is easy to find that by decreasing the *reference wall subcooled grade* $\frac{t_{s,ref}-t_w}{t_{s,ref}}$, the wall dimensionless temperature gradient $\left(-\frac{d\theta_1}{d\eta_1}\right)_{\eta_1=0}$ will increase more and more quickly. The reason is that with decreasing the reference wall subcooled grade, the wall temperature will increase, which will lead to decrease of the wall subcooled temperature $t_{s,int} - t_w$. In this case, it will cause a

Table 20.1 Selected numerical solutions of temperature gradient $\left(-\frac{dt_h}{d\eta}\right)_{\eta=0}$ with variation of reference wall subcooled grade $\frac{t_{s,ref}-t_w}{t_{s,ref}}$ and bulk vapor mass fraction $C_{mv,\infty}$ for laminar free convection film condensation of water vapor–air mixture at $t_\infty = 100^\circ\text{C}$ and atmospheric pressure as the system pressure

T_w (K)	$\frac{t_{s,ref}-t_w}{t_{s,ref}}$	$C_{mv,\infty}$	0.0145	0.044	0.125	0.206	0.335	0.54	0.8	0.86	0.9	0.95	0.99	0.999	1
		$\left(-\frac{dt_h}{d\eta}\right)_{\eta=0}$													
0	1	11.302	3.4757	2.5118	2.2395	2.0336	1.871	1.7591	1.7403	1.7286	1.7153	1.7053	1.7031	1.5511	
20	0.8	–	11.032	3.1412	2.6544	2.3322	2.0969	1.9424	1.9171	1.9015	1.8834	1.8699	1.867	1.6679	
40	0.6	–	–	9.8836	3.6537	2.8832	2.4623	2.2194	2.1814	2.1591	2.1319	2.1128	2.1086	1.8323	
50	0.5	–	–	–	8.8454	3.4925	2.7705	2.4294	2.379	2.3487	2.3141	2.2886	2.2831	1.9450	
60	0.4	–	–	–	–	7.8191	3.3404	2.7455	2.6693	2.6246	2.5743	2.5379	2.5301	2.0789	
70	0.3	–	–	–	–	6.8981	3.3650	3.1156	3.2036	3.1156	3.0215	2.9561	2.9424	2.2685	
75	0.25	–	–	–	–	–	–	4.1412	3.7825	3.6112	3.4447	3.3349	3.3126	2.3906	
80	0.2	–	–	–	–	–	–	–	5.9454	5.0739	4.4493	4.1380	4.0822	2.5398	

Note $C_{mv,\infty} = 1$ is corresponding to the case of the related film condensation of pure vapor

decrease in the condensate liquid film thickness and then an increase in the wall dimensionless temperature gradient $\left(-\frac{d\theta_l}{d\eta_l}\right)_{\eta_l=0}$. Meanwhile, by decreasing the bulk vapor mass fraction $C_{mv,\infty}$, the wall dimensionless temperature gradient $\left(-\frac{d\theta_l}{d\eta_l}\right)_{\eta_l=0}$ will increase more and more quickly. This is because with decrease in the bulk vapor mass fraction $C_{mv,\infty}$, the condensate liquid film thickness will decrease, which leads to an increase in the wall dimensionless temperature gradient $\left(-\frac{d\theta_l}{d\eta_l}\right)_{\eta_l=0}$.

According to the rigorous numerical solutions, the formulated equations on the wall dimensionless temperature gradient $\left(-\frac{d\theta_l}{d\eta_l}\right)_{\eta_l=0}$ are created as follows for the most significant range of bulk vapor mass fraction $C_{mv,\infty}$ and all available reference wall subcooled grade $\frac{t_{s,\text{ref}}-t_w}{t_{s,\text{ref}}}$ for the laminar free convection film condensation of water vapor–air mixture:

$$\left(-\frac{d\theta_l}{d\eta_l}\right)_{\eta_l=0} = a C_{mv,\infty}^b \quad (0.8 \leq C_{mv,\infty} \leq 0.999) \quad (20.8)$$

where

$$a = 1.5152 \left(\frac{t_{s,\text{ref}} - t_w}{t_{s,\text{ref}}}\right)^{-0.5553} \quad \left(0.25 \leq \frac{t_{s,\text{ref}} - t_w}{t_{s,\text{ref}}} \leq 0.4\right) \quad (20.9)$$

$$a = 1.6976 \left(\frac{t_{s,\text{ref}} - t_w}{t_{s,\text{ref}}}\right)^{-0.4302} \quad \left(0.4 \leq \frac{t_{s,\text{ref}} - t_w}{t_{s,\text{ref}}} \leq 1\right) \quad (20.10)$$

$$b = - \left[0.3081 \left(\frac{t_{s,\text{ref}} - t_w}{t_s}\right)^{-0.8478} \right] \left(\frac{t_{s,\text{ref}} - t_w}{t_{s,\text{ref}}}\right)^{-1} \quad \left(0.25 \leq \frac{t_{s,\text{ref}} - t_w}{t_s} \leq 0.4\right) \quad (20.11)$$

$$b = -1.94 \left(\frac{t_{s,\text{ref}} - t_w}{t_{s,\text{ref}}}\right)^2 + 2.623 \left(\frac{t_{s,\text{ref}} - t_w}{t_{s,\text{ref}}}\right) - 1.1057 \quad \left(0.4 \leq \frac{t_{s,\text{ref}} - t_w}{t_{s,\text{ref}}} \leq 0.6\right) \quad (20.12)$$

$$b = 0.1667 \ln \left(\frac{t_{s,\text{ref}} - t_w}{t_{s,\text{ref}}}\right) - 0.1439 \quad \left(0.6 \leq \frac{t_{s,\text{ref}} - t_w}{t_{s,\text{ref}}} \leq 1\right) \quad (20.13)$$

Comparison of the selected numerical solutions of wall dimensionless temperature gradient $\left(-\frac{d\theta_l}{d\eta_l}\right)_{\eta_l=0}$ with the results predicted by Eqs. (20.8)–(20.13) are listed in Table 20.2 for laminar free convection film condensation of water vapor–air mixture at $t_\infty = 100^\circ\text{C}$ and atmospheric pressure as the system pressure, and it is found that their agreements are pretty good.

Table 20.2 Comparison of the selected numerical solutions with the predicted results of temperature gradient $\left(-\frac{d\theta_1}{d\eta_1}\right)_{\eta=0}$ for laminar free convection film condensation of water vapor–air mixture at $t_\infty = 100^\circ\text{C}$ and atmospheric pressure as the system pressure

T_w (K)	$\frac{t_{s,\text{ref}}-t_w}{t_{s,\text{ref}}}$	$C_{mv,\infty}$	$\left(-\frac{d\theta_1}{d\eta_1}\right)_{\eta=0}$					
			0.8	0.86	0.9	0.95	0.99	0.999
0	1	(1)	1.759115	1.7403	1.728656	1.7153	1.7053	1.7031
		(2)	1.752995	1.73485	1.72353	1.71018	1.70006	1.69784
20	0.8	(1)	1.942474	1.9171	1.901526	1.8834	1.8699	1.867
		(2)	1.945701	1.92038	1.90464	1.88608	1.87205	1.86898
40	0.6	(1)	2.2194	2.1814	2.159133	2.1319	2.1128	2.1086
		(2)	2.22573	2.18916	2.16648	2.13982	2.1197	2.11531
50	0.5	(1)	2.429476	2.379	2348701	2.3141	2.2886	2.283126
		(2)	2.43442	2.38576	2.35567	2.32037	2.29381	2.28802
60	0.4	(1)	2.745558	2.6693	2.624618	2.5743	2.5379	2.5301
		(2)	2.732659	2.6611	2.61708	2.56568	2.52715	2.51877
70	0.3	(1)	3.3650	3.2036	3.1156	3.0215	2.9561	2.9424
		(2)	3.375389421	3.23362	3.14756	3.04819	2.9745	2.95857
75	0.25	(1)	4.1412	3.7825	3.6112	3.4447	3.3349	3.3126
		(2)	4.082441471	3.79984	3.6323	3.44263	3.30463	3.2751

Note (1) Numerical solutions, and (2) results evaluated by Eqs. (20.8)–(20.13)

20.4 Variation of Condensate Heat Transfer

From heat transfer analysis, it is found that heat transfer of laminar free convection film condensation of vapor–gas mixture depends on the wall subcooled temperature $t_{s,\text{int}} - t_w$, local Grashof number, and wall dimensionless temperature gradient $\left(\frac{d\theta_1}{d\eta_1}\right)_{\eta=0}$. On this basis, the physical factors for effect on heat transfer of laminar free convection film condensation of vapor–gas mixture can be investigated.

Set $(q_{x,w})_{C_{mv,\infty}=1}$ to be the local heat transfer rater with $C_{mv,\infty} = 1$, i.e., the case for the laminar free convection film condensation of pure vapor.

Then, $\frac{q_x}{(q_x)_{C_{mv,\infty}=1}}$ is the heat transfer ratio of film condensation of vapor–gas mixture to that of the related pure vapor. From Eq. (20.1), the heat transfer ratio is expressed as

$$\frac{q_x}{(q_x)_{C_{mv,\infty}=1}} = \frac{t_w - t_{s,\text{int}}}{t_w - t_s} \cdot \left[\frac{\text{Gr}_{x1,s}}{(\text{Gr}_{x1,s})_{C_{mv,\infty}=1}} \right]^{1/4} \frac{\left(\frac{d\theta_1}{d\eta_1}\right)_{\eta=0}}{\left[\left(\frac{d\theta_1}{d\eta_1}\right)_{\eta=0}\right]_{C_{mv,\infty}=1}} \quad (20.14)$$

where $\frac{t_w - t_{s,\text{int}}}{t_w - t_s}$ is wall subcooled temperature ratio, i.e., the ratio of the wall subcooled temperature with any vapor mass fraction $C_{mv,\infty}$ (for the laminar free convection

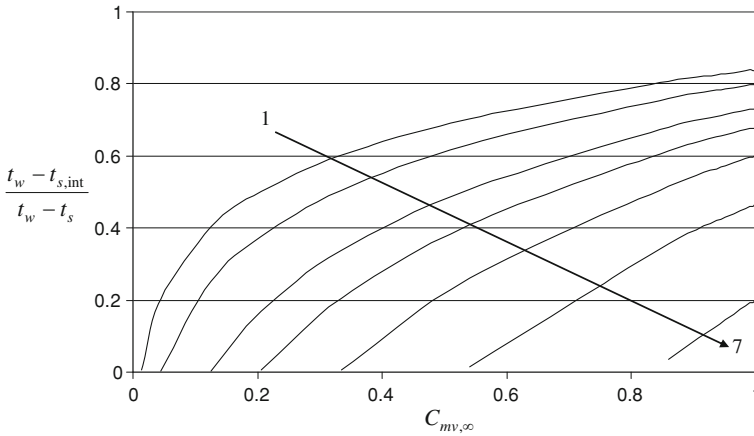


Fig. 20.2 Wall subcooled temperature ratio $\frac{t_w - t_{s,int}}{t_w - t_s}$ with variation of the reference wall subcooled grade $\frac{t_{s,ref} - t_w}{t_{s,ref} - t_s}$ and the bulk water vapor fraction $C_{mv,\infty}$ for laminar free convection film condensation of water vapor–air mixture at the bulk temperature $T_\infty = 373$ K and atmospheric pressure as the system pressure. (Note Lines 1–7 for $\frac{t_{s,ref} - t_w}{t_{s,ref} - t_s} = 1, 0.8, 0.6, 0.5, 0.4, 0.3,$ and 0.2)

film condensation of vapor–gas mixture) to that with $C_{mv,\infty} = 1$ (for the laminar free convection film condensation of pure vapor). Similarly, $\left[\frac{Gr_{xl,s}}{(Gr_{xl,s})_{C_{mv,\infty}=1}} \right]^{1/4}$ and $\frac{\left(\frac{d\theta_l}{d\eta} \right)_{\eta=0}}{\left[\left(\frac{d\theta_l}{d\eta} \right)_{\eta=0} \right]_{C_{mv,\infty}=1}}$ are local Grashof number ratio and temperature gradient ratio, respectively.

With the numerical results on the *interfacial vapor saturation temperature* $t_{s,int}$, shown in chapter 19, the *wall subcooled temperature ratio* $\frac{t_w - t_{s,int}}{t_w - t_s}$ are evaluated, and plotted in Fig. 20.2 [1] with variation of *reference wall subcooled grade* $\frac{t_{s,ref} - t_w}{t_{s,ref} - t_s}$ and bulk vapor mass fraction $C_{mv,\infty}$ at the bulk temperature $T_\infty = 373$ K and atmospheric pressure as the system pressure for laminar free convection film condensation of water vapor–air mixture.

Similarly the local Grashof number ratio can be expressed as

$$\left[\frac{Gr_{xl,s}}{(Gr_{xl,s})_{C_{mv,\infty}=1}} \right]^{1/4} = \left[\frac{\rho_{l,w} - \rho_{m,\infty}}{\rho_{l,w} - (\rho_{m,\infty})_{C_{mv,\infty}=1}} \right]^{1/4} \times \left[\frac{(\rho_{l,s})_{C_{m,v\infty}=1}}{\rho_{l,s}} \right]^{1/4} \left[\frac{(\nu_{l,s})_{C_{m,v\infty}=1}}{\nu_{l,s}} \right]^{1/2} \quad (20.15)$$

On this basis, the local Grashof number ratios $\left[\frac{Gr_{xl,s}}{(Gr_{xl,s})_{C_{mv,\infty}=1}} \right]^{1/4}$ are evaluated with the study of Ref. [1], and plotted in Fig. 20.3 with variation of reference wall sub-

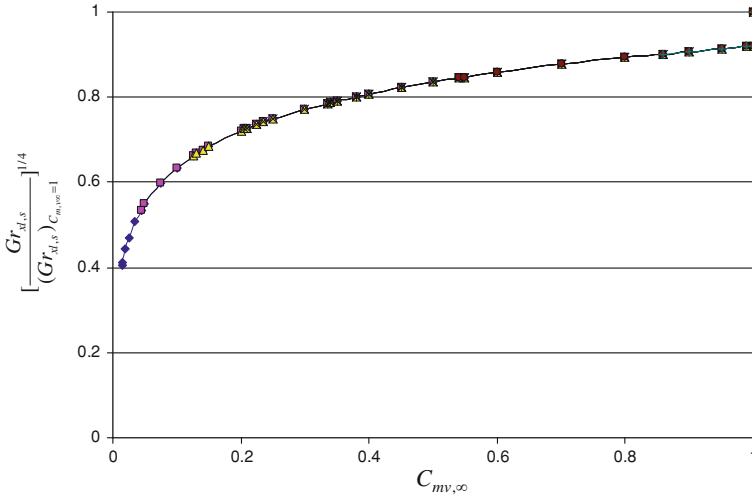


Fig. 20.3 Local Grashof number ratio $\left[\frac{Gr_{x1,s}}{(Gr_{x1,s})_{C_{mv,\infty}=1}} \right]^{1/4}$ with variation of the bulk water vapor fraction $C_{mv,\infty}$ for laminar free convection film condensation of water vapor–air mixture at the bulk temperature $T_\infty = 373$ K and atmospheric pressure as the system pressure [1]

cooled grade $\frac{t_{s,ref}-t_w}{t_{s,ref}}$ and bulk vapor mass fraction $C_{mv,\infty}$ at the bulk temperature $T_\infty = 373$ K and atmospheric pressure as the system pressure for laminar free convection film condensation of water vapor–air mixture.

With the above calculation results on the wall subcooled temperature ratio $\frac{t_w-t_{s,int}}{t_w-t_s}$, local Grashof number ratios $\left[\frac{Gr_{x1,s}}{(Gr_{x1,s})_{C_{mv,\infty}=1}} \right]^{1/4}$, and wall temperature gradient ratio $\frac{\left(\frac{d\theta_1}{d\eta}\right)_{\eta=0}}{\left[\left(\frac{d\theta_1}{d\eta}\right)_{\eta=0}\right]_{C_{mv,\infty}=1}}$, the system of values on heat transfer ratio $\frac{q_x}{(q_x)_{C_{mv,\infty}=1}}$ are evaluated, and plotted in Fig. 20.4.

It is seen that the condensate heat transfer will increase more and more quickly by decreasing the bulk vapor mass fraction $C_{mv,\infty}$, or decreasing in the reference wall subcooled grade $\frac{t_{s,ref}-t_w}{t_{s,ref}}$.

From the values shown in Figs. 20.2–20.5, it is seen that the heat transfer ratios $\frac{q_x}{(q_x)_{C_{mv,\infty}=1}}$ are very well identical to the wall subcooled temperature ratios $\frac{t_w-t_{s,int}}{t_w-t_s}$. Then, it follows that the wall subcooled temperature $t_w - t_{s,int}$ dominates the condensate heat transfer, to a great extent. While, the wall subcooled temperature is dependent on the wall temperature t_w and bulk vapor mass fraction $C_{mv,\infty}$.

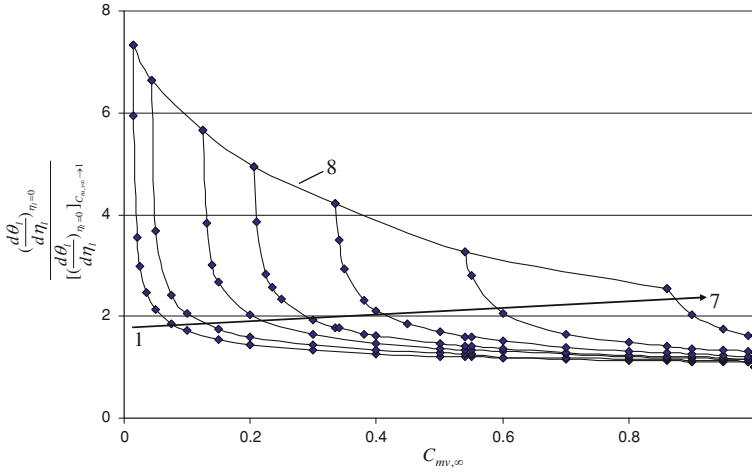


Fig. 20.4 Temperature gradient ratios $\frac{\left(\frac{d\theta_1}{d\eta}\right)_{\eta=0}}{\left[\left(\frac{d\theta_1}{d\eta}\right)_{\eta=0}\right]_{C_{mv,\infty}=1}}$ with variation of the reference wall subcooled grade $\frac{t_{s,ref}-t_w}{t_{s,ref}}$ and the bulk water vapor fraction $C_{mv,\infty}$ for laminar free convection film condensation of water vapor–air mixture at the bulk temperature $T_\infty = 373$ K and atmospheric pressure as the system pressure [1]. (Note Lines 1–7 for reference wall subcooled grade $\frac{t_{s,ref}-t_w}{t_{s,ref}} = 1, 0.8, 0.6, 0.5, 0.4, 0.3,$ and 0.2 ; Line 8 is critical condensation line with subcooled temperature $t_{s,int} - t_w \rightarrow 0$)

20.5 Condensate Mass Transfer Analysis

Set g_x to be a local condensate mass flow rate entering the liquid film at position x related to per unit area of the plate. According to the boundary layer theory of fluid mechanics, g_x is expressed as

$$g_x = \rho_{l,s} \left(w_{x1,s} \frac{d\delta_1}{dx} - w_{y1,s} \right)_s \tag{20.16}$$

With the corresponding dimensionless variables in Eqs. (18.17)–(18.21), the above equation is changed into the following one:

$$g_x = \rho_{l,s} \left[2\sqrt{g_x} \left(\frac{\rho_{l,w} - \rho_{mv}}{\rho_{l,s}} \right)^{1/2} W_{x1,s} \frac{d\delta_1}{dx} - 2\sqrt{g_x} \left(\frac{\rho_{l,w} - \rho_{mv}}{\rho_{l,s}} \right)^{1/2} \left(\frac{1}{4} Gr_{x1,s} \right)^{-1/4} W_{y1,s} \right]_s$$

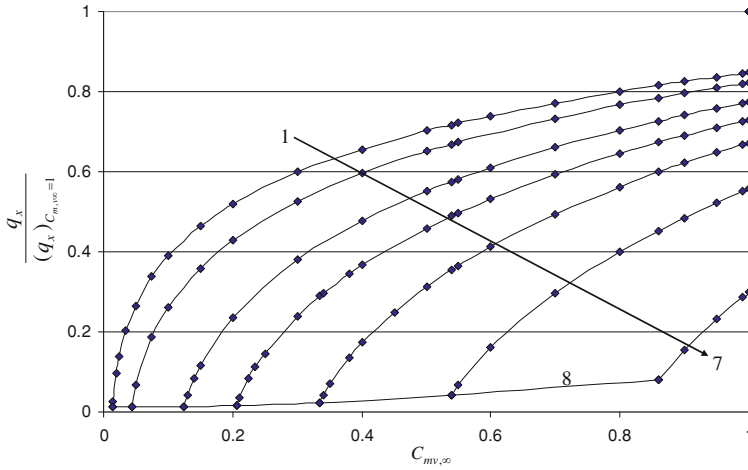


Fig. 20.5 Heat transfer ratio $\frac{q_x}{(q_x)_{C_{mv,\infty}=1}}$ with variation of the reference wall subcooled grade $\frac{t_{s,ref}-t_w}{t_{s,ref}}$ and the bulk water vapor fraction $C_{mv,\infty}$ for laminar free convection film condensation of water vapor–air mixture at the bulk temperature $T_\infty = 373\text{ K}$ and atmospheric pressure as the system pressure [1]. (Note Lines 1–7 for $\frac{t_{s,ref}-t_w}{t_{s,ref}} = 1, 0.8, 0.6, 0.5, 0.4, 0.3,$ and 0.2 ; Line 8 is critical condensation line with $t_{s,int} - t_w \rightarrow 0$)

With the definition of local Grashof number $Gr_{x1,s}$, the condensate liquid film thickness δ_l is expressed as

$$\delta_l = \eta_{l\delta} \left(\frac{1}{4} \frac{g(\rho_{l,w} - \rho_{mv,s})x^3}{\nu_{l,s}^2 \cdot \rho_{l,s}} \right)^{-1/4} x$$

or,

$$\frac{d\delta_l}{dx} = \frac{1}{4} \eta_{l\delta} \left(\frac{1}{4} Gr_{x1,s} \right)^{-1/4}$$

Then, we have

$$g_x = \left(\frac{1}{4} \frac{g(\rho_{l,w} - \rho_{mv})x^3}{\nu_{l,s}^2 \rho_{l,s}} \right)^{1/2} x^{-1} \left(\frac{1}{4} Gr_{x1,s} \right)^{-1/4} \nu_{l,s} \rho_{l,s} [\eta_{l\delta} W_{x1,s} - 4W_{y1,s}]_s$$

or

$$g_x = \mu_{l,s} x^{-1} \left(\frac{1}{4} Gr_{x1,s} \right)^{1/4} \Phi_s \tag{20.17}$$

where

$$\Phi_s = \eta_{l\delta} W_{x1,s} - 4W_{y1,s} \tag{20.18}$$

is a determinative value for local mass flow rate g_x , and defined as *condensate mass flow rate parameter*. Obviously, the mass flow rate parameter Φ_s depends on the dimensionless *condensate film thickness* $\eta_{l\delta}$ as well as interfacial *dimensionless condensate liquid velocity components* $W_{x1,s}$, and $W_{y1,s}$.

If G_x is taken to express total mass flow rate entering the liquid film for position $x = 0$ to x with width b of the plate, it should be the following integration:

$$G_x = \iint_A g_x dA = b \int_0^x g_x dx$$

where $A = b \cdot x$ is the special area of the plate related to condensate mass transfer. Then, we obtain

$$G_x = \frac{4}{3} b \cdot \mu_{1,s} \left(\frac{1}{4} Gr_{x1,s} \right)^{1/4} \Phi_s \quad (20.19)$$

20.6 Condensate Mass Flow Rate Parameter

From Eqs. (20.17) and (20.19) it is found that the condensate mass flow rate parameter Φ_s , dependent on the dimension condensate film thickness $\eta_{l\delta}$, as well as the interfacial condensate film velocity components $W_{x1,s}$, and $W_{y1,s}$, is the only one no-given variable for evaluation of the condensate mass flow rate. A system of numerical solutions of $\eta_{l\delta}$, $W_{x1,s}$, and $-W_{y1,s}$ are found out with variation of the reference wall subcooled grade $\frac{t_{s,ref}-t_w}{t_{s,ref}}$ and the bulk water vapor fraction $C_{mv,\infty}$ for laminar free convection film condensation of water vapor–air mixture at the bulk temperature $T_\infty = 373$ K and atmospheric pressure as the system pressure. Then, a series of values of the condensate mass flow rate parameter Φ_s are obtained. The numerical values of $\eta_{l\delta}$, $W_{x1,s}$, $-W_{y1,s}$, and Φ_s are plotted in Figs. 20.6, 20.7, 20.8 and 20.9 respectively. It is seen from Figs. 20.6–20.9 that by decreasing the reference wall subcooled grade $\frac{t_{s,ref}-t_w}{t_{s,ref}}$ and the bulk water vapor fraction $C_{mv,\infty}$, the dimension condensate film thickness $\eta_{l\delta}$, interfacial condensate film velocity components $W_{x1,s}$, and $W_{y1,s}$, and condensate mass flow rate parameter will decrease at an accelerative pace.

Meanwhile, the rigorous numerical results on the dimensionless condensate film thickness $\eta_{l\delta}$ are formulated to Eqs. (20.20)–(20.23) for the most significant ranges of the reference wall subcooled grade $\frac{t_{s,ref}-t_w}{t_{s,ref}}$ and the bulk water vapor fraction $C_{mv,\infty}$ for laminar free convection film condensation of water vapor–air mixture at the bulk temperature $T_\infty = 373$ K and atmospheric pressure as the system pressure. The results on the dimensionless condensate film thickness $\eta_{l\delta}$ predicted by Eqs. (20.20)–(20.23) are compared in Table 20.3 with the related rigorous numerical solutions. It is seen that their agreements are pretty good.

$$\eta_{l\delta} = a C_{mv,\infty}^b \quad (0.8 \leq C_{mv,\infty} \leq 0.999) \quad (20.20)$$

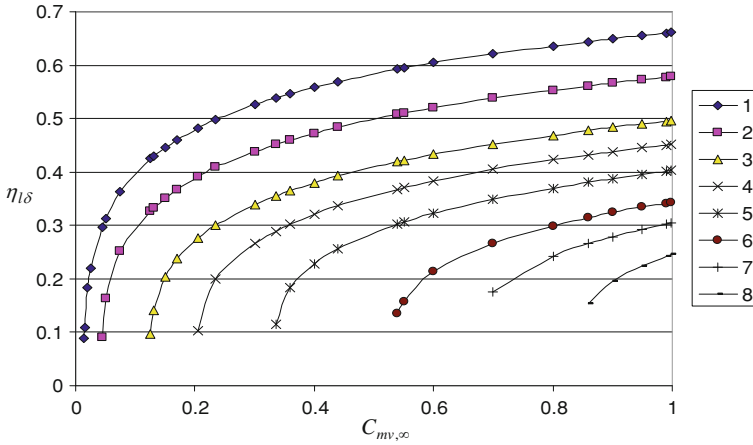


Fig. 20.6 Condensate film thickness $\eta_{1\delta}$ with variation of the reference wall subcooled grade $\frac{t_{s,ref}-t_w}{t_{s,ref}}$ and the bulk water vapor fraction $C_{mv,\infty}$ for laminar free convection film condensation of water vapor–air mixture at the bulk temperature $T_\infty = 373$ K and atmospheric pressure as the system pressure. (Note Lines 1–8 for $\frac{t_{s,ref}-t_w}{t_{s,ref}} = 1, 0.8, 0.6, 0.5, 0.4, 0.3, 0.25,$ and 0.2)

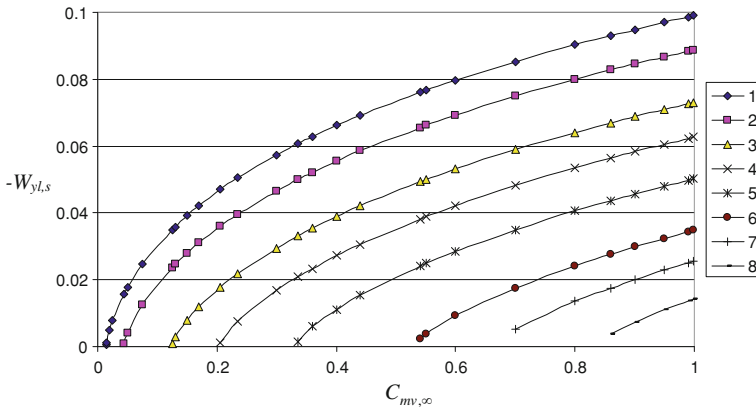


Fig. 20.7 Interfacial velocity component $-W_{x1,s}$ with variation of reference wall subcooled grade $\frac{t_{s,ref}-t_w}{t_{s,ref}}$ and bulk water vapor fraction $C_{mv,\infty}$ for laminar free convection film condensation of water vapor–air mixture at the bulk temperature $T_\infty = 373$ K and atmospheric pressure as the system pressure. (Note Lines 1–7 for $\frac{t_{s,ref}-t_w}{t_{s,ref}} = 1, 0.8, 0.6, 0.5, 0.4, 0.3, 0.25,$ and 0.2)

where

$$a = 0.6917 \left(\frac{t_{s,ref} - t_w}{t_{s,ref}} \right)^{0.585} \quad \left(0.25 \leq \frac{t_{s,ref} - t_w}{t_{s,ref}} \leq 0.4 \right) \quad (20.21)$$

$$a = 0.4248 \left(\frac{t_{s,ref} - t_w}{t_{s,ref}} \right) + 0.2377 \quad \left(0.4 \leq \frac{t_{s,ref} - t_w}{t_{s,ref}} \leq 1 \right) \quad (20.22)$$

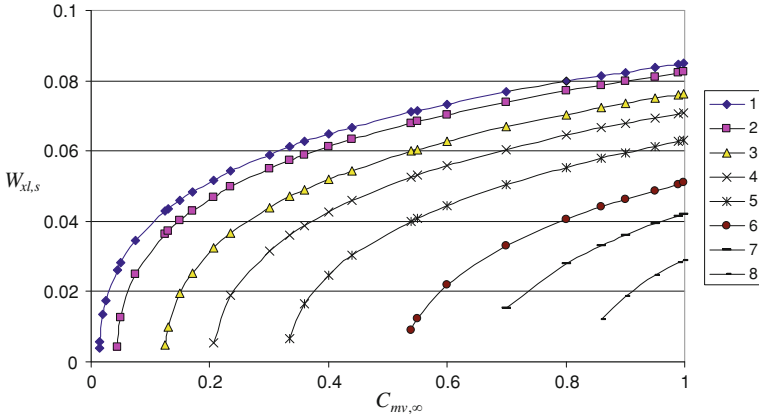


Fig. 20.8 Interfacial velocity component $W_{y1,s}$ with variation of reference wall subcooled grade $\frac{t_{s,ref} - t_w}{t_{s,ref}}$ and bulk water vapor fraction $C_{mv,\infty}$ for laminar free convection film condensation of water vapor–air mixture at the bulk temperature $T_\infty = 373$ K and atmospheric pressure as the system pressure. (Note Lines 1–7 for $\frac{t_{s,ref} - t_w}{t_{s,ref}} = 1, 0.8, 0.6, 0.5, 0.4, 0.3, 0.25,$ and 0.2)

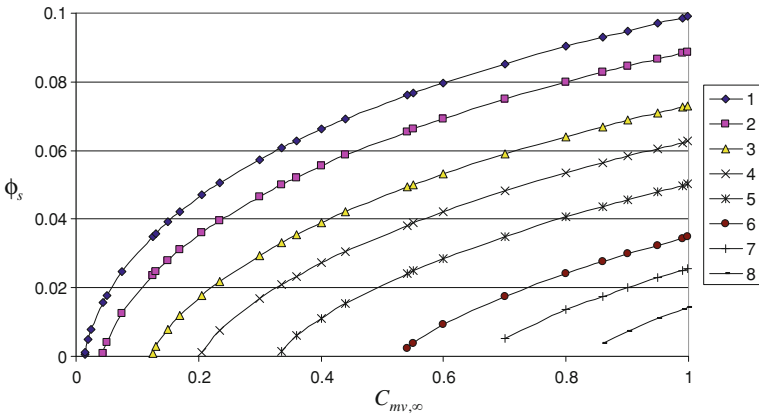


Fig. 20.9 Condensate mass flow rate parameter Φ_s with variation of the reference wall subcooled grade $\frac{t_{s,ref} - t_w}{t_{s,ref}}$ and the bulk water vapor fraction $C_{mv,\infty}$ for laminar free convection film condensation of water vapor–air mixture at the bulk temperature $T_\infty = 373$ K and atmospheric pressure as the system pressure. (Note Lines 1–7 for $\frac{t_{s,ref} - t_w}{t_{s,ref}} = 1, 0.8, 0.6, 0.5, 0.4, 0.3, 0.25,$ and 0.2)

$$b = \left[0.3222 \left(\frac{t_{s,ref} - t_w}{t_{s,ref}} \right)^{-0.818} \right] \left(\frac{t_{s,ref} - t_w}{t_{s,ref}} \right)^{-1} \quad \left(0.25 \leq \frac{t_{s,ref} - t_w}{t_{s,ref}} \leq 0.4 \right) \quad (20.23)$$

$$b = 0.1631 \left(\frac{t_{s,ref} - t_w}{t_{s,ref}} \right)^{-0.8919} \quad \left(0.4 \leq \frac{t_{s,ref} - t_w}{t_{s,ref}} \leq 1 \right) \quad (20.24)$$

Table 20.3 Selected numerical solutions on Condensate film thickness η_{δ} with variation of the reference wall subcooled grade $\frac{t_{s,ref}-t_w}{t_{s,ref}}$ and the bulk water vapor fraction $C_{mv,\infty}$ for laminar free convection film condensation of water vapor–air mixture at the bulk temperature $T_{\infty} = 373 \text{ K}$ and atmospheric pressure as the system pressure

$T_w \text{ (K)}$	$\frac{t_{s,ref}-t_w}{t_{s,ref}}$	$C_{mv,\infty}$	0.0145	0.044	0.125	0.206	0.335	0.54	0.8	0.86	0.9	0.95	0.99	0.999	1
0	1	0.088559	0.29819	0.425328	0.48355	0.539219	0.592929	0.636341	0.644249	0.649245	0.65507	0.659523	0.660499	0.73451	
20	0.8	–	0.09068	0.327584	0.392564	0.45200	0.508132	0.5531	0.561259	0.566361	0.572428	0.577030	0.578050	0.65415	
40	0.6	–	–	0.10121	0.276966	0.35475	0.419492	0.468950	0.477755	0.483090	0.4897469	0.494531	0.4956	0.57590	
50	0.5	–	–	–	0.113093	0.289342	0.368196	0.422932	0.432461	0.438385	0.445353	0.4506342	0.451788	0.53621	
60	0.4	–	–	–	–	0.127945	0.302151	0.370152	0.381190	0.387972	0.395907	0.401854	0.403152	0.49484	
70	0.3	–	–	–	–	–	0.145041	0.299236	0.314672	0.323792	0.334162	0.341775	0.343415	0.44982	
75	0.25	–	–	–	–	–	–	0.242007	0.265449	0.278231	0.291917	0.301713	0.303786	0.42496	
80	0.2	–	–	–	–	–	–	–	0.168306	0.197322	0.225193	0.242274	0.245621	0.39749	

Note $C_{mv,\infty} = 1$ is corresponding to the case of the related film condensation of pure water vapor

Furthermore, the rigorous numerical results on the condensate mass flow rate parameter Φ_s are formulated to Eqs. (20.25)–(20.30) for the most significant ranges of the reference wall subcooled grade $\frac{t_{s,\text{ref}} - t_w}{t_{s,\text{ref}}}$ and the bulk water vapor fraction $C_{\text{mv},\infty}$ for laminar free film condensation of water vapor–air mixture at the bulk temperature $T_\infty = 373\text{ K}$ and atmospheric pressure as the system pressure. The results on the condensate mass flow rate parameter Φ_s predicted by Eqs. (20.25)–(20.30) are compared in Table 20.7 with the related rigorous numerical solutions. It is seen that their agreements are pretty good.

$$\Phi_s = a C_{\text{mv},\infty}^b \quad (0.8 \leq C_{\text{mv},\infty} \leq 0.999) \quad (20.25)$$

where

$$a = 0.0518 \text{Ln} \left(\frac{t_{s,\text{ref}} - t_w}{t_{s,\text{ref}}} \right) + 0.0977 \quad \left(0.25 \leq \frac{t_{s,\text{ref}} - t_w}{t_{s,\text{ref}}} \leq 0.4 \right) \quad (20.26)$$

$$a = 0.0535 \text{Ln} \left(\frac{t_{s,\text{ref}} - t_w}{t_{s,\text{ref}}} \right) + 0.0999 \quad \left(0.4 \leq \frac{t_{s,\text{ref}} - t_w}{t_{s,\text{ref}}} \leq 1 \right) \quad (20.27)$$

$$b = \left[0.5724 \left(\frac{t_{s,\text{ref}} - t_w}{t_{s,\text{ref}}} \right)^{-0.5855} \right] \left(\frac{t_{s,\text{ref}} - t_w}{t_{s,\text{ref}}} \right)^{-1} \quad \left(0.25 \leq \frac{t_{s,\text{ref}} - t_w}{t_{s,\text{ref}}} \leq 0.4 \right) \quad (20.28)$$

$$b = 5.975 \left(\frac{t_{s,\text{ref}} - t_w}{t_{s,\text{ref}}} \right)^2 - 7.7835 \left(\frac{t_{s,\text{ref}} - t_w}{t_{s,\text{ref}}} \right) + 3.1067 \quad \left(0.4 \leq \frac{t_{s,\text{ref}} - t_w}{t_{s,\text{ref}}} \leq 0.6 \right) \quad (20.29)$$

$$b = 0.8287 \left(\frac{t_{s,\text{ref}} - t_w}{t_{s,\text{ref}}} \right)^2 - 1.7672 \left(\frac{t_{s,\text{ref}} - t_w}{t_{s,\text{ref}}} \right) + 1.3496 \quad \left(0.6 \leq \frac{t_{s,\text{ref}} - t_w}{t_{s,\text{ref}}} \leq 1 \right) \quad (20.30)$$

It is seen that decreasing the bulk vapor mass fraction $C_{\text{mv},\infty}$ and reference wall subcooled grade $\frac{t_{s,\text{ref}} - t_w}{t_{s,\text{ref}}}$ will cause decrease the condensate film thickness $\eta_{l\delta}$, interfacial velocity components $W_{x1,s}$ and $-W_{y1,s}$, and condensate mass flow rate parameter Φ_s more and more quickly.

Table 20.4 Comparison of selected numerical solutions on Condensate film thickness η_{δ} with the results evaluated by Eqs. (20.20)–(20.24) for laminar free film condensation of water vapor–air mixture at the bulk temperature $T_{\infty} = 373$ K and atmospheric pressure as the system pressure

T_w (K)	$\frac{t_{s,ref}-t_w}{t_{s,ref}}$	$C_{m,v,\infty}$	η_{δ}					
			0.8	0.86	0.9	0.95	0.99	0.999
0	1	(1)	0.636341	0.6442487	0.6492453	0.65507	0.6595225	0.660499
		(2)	0.638821993	0.6464	0.65121	0.65698	0.66141	0.66239
20	0.8	(1)	0.5531	0.5612592	0.5663613	0.5724277	0.577030	0.5780500
		(2)	0.552453113	0.56046	0.56556	0.57167	0.57639	0.57743
40	0.6	(1)	0.4689501	0.4777554	0.4830902	0.4897469	0.494531	0.4956
		(2)	0.46510248	0.47384	0.47941	0.48612	0.49131	0.49245
50	0.5	(1)	0.4229322	0.4324611	0.4383852	0.4453527	0.4506342	0.4517883
		(2)	0.42070635	0.43002	0.43597	0.44317	0.44873	0.44996
60	0.4	(1)	0.3701521	0.3811902	0.3879718	0.3959070	0.4018544	0.4031519
		(2)	0.375376288	0.38554	0.39206	0.39997	0.40611	0.40747
70	0.3	(1)	0.299236	0.314672	0.323792	0.334162	0.341775	0.343415
		(2)	0.298406976	0.31189	0.32068	0.33145	0.33991	0.3418
75	0.25	(1)	0.242007	0.265449	0.278231	0.291917	0.301713	0.303786
		(2)	0.245615697	0.26414	0.2765	0.29195	0.30431	0.3071

Note (1) denotes numerical solutions, and (2) denotes the results predicted by Eqs. (20.20)–(20.24)

20.7 Variation of Condensate Mass Flow Rate

Set $(g_x)_{C_{m,v,\infty}=1}$ to be the condensate mass transfer rate related to $C_{m,v,\infty} = 1$, which is actually corresponding to the film condensation of pure vapor. Then, $\frac{g_x}{(g_x)_{C_{m,v,\infty}=1}}$ is defined as ratio of condensate mass transfer from the vapor–gas mixture to that from pure vapor, and called condensate mass transfer ratio, for short. From Eq. (20.17), the mass transfer ratio can be expressed as

$$\frac{g_x}{(g_x)_{C_{m,v,\infty}=1}} = \frac{\mu_{1,s}}{(\mu_{1,s})_{C_{m,v,\infty}=1}} \left[\frac{Gr_{x1,s}}{(Gr_{x1,s})_{C_{m,v,\infty}=1}} \right]^{1/4} \frac{\Phi_s}{(\Phi_s)_{C_{m,v,\infty}=1}} \tag{20.31}$$

According to the calculation results in research of [1], the absolute viscosity ratios are evaluated, and plotted in Fig. 20.10 with variation of the bulk vapor mass fraction $C_{m,v,\infty}$. It is seen that the absolute viscosity ratios increase more and more quickly by decreasing the bulk vapor mass fraction $C_{m,v,\infty}$.

With the evaluated values of the mass flow rate parameters Φ_s shown in Fig. 20.9, the evaluated values of mass flow rate parameter ratio $\frac{\Phi_s}{(\Phi_s)_{C_{m,v,\infty}=1}}$ are plotted in Fig. 20.11 with variation of reference wall subcooled grade $\frac{t_s-t_w}{t_s}$ and the bulk water vapor fraction $C_{m,v,\infty}$ for laminar free film condensation of water vapor–air mixture at the bulk temperature $T_{\infty} = 373$ K and atmospheric pressure as the system pressure. It is seen that by decreasing the bulk vapor mass fraction $C_{m,v,\infty}$ and reference wall

Table 20.5 Selected numerical solutions on Condensate film thickness $W_{x1,s}$ with variation of the reference wall subcooled grade $\frac{t_{s,ref}-t_w}{t_{s,ref}}$ and the bulk water vapor fraction $C_{mv,\infty}$ for laminar free convection film condensation of water vapor–air mixture at the bulk temperature $T_\infty = 373\text{ K}$ and atmospheric pressure as the system pressure

T_w (K)	$\frac{t_{s,ref}-t_w}{t_{s,ref}}$	$C_{mv,\infty}$	0.0145	0.044	0.125	0.206	0.335	0.54	0.8	0.86	0.9	0.95	0.99	0.999	1
$W_{x1,s}$															
0	1	0.003849	0.026385	0.04293	0.051854	0.06125	0.07114	0.079762	0.081390	0.08240	0.083662	0.08462	0.08483	0.10117	
20	0.8	–	0.004092	0.03648	0.046995	0.057404	0.06803	0.077112	0.07882	0.079904	0.08119	0.082182	0.082393	0.09935	
40	0.6	–	–	0.005132	0.032345	0.047058	0.06002	0.070342	0.072251	.073545	0.074887	0.076065	0.076311	0.094743	
50	0.5	–	–	–	0.006415	0.036119	0.05249	0.064419	0.06655	.067882	0.069469	0.07067	0.07093	0.090762	
60	0.4	–	–	–	–	0.008212	0.040089	0.055347	0.057895	0.059472	0.061319	0.06272	0.063024	0.085164	
70	0.3	–	–	–	–	–	0.010548	0.040513	0.044102	0.046249	0.048713	0.050535	0.050929	0.077371	
75	0.25	–	–	–	–	–	–	0.028081	0.033161	.0360546	0.03922	0.041522	0.042015	0.0723165	
80	0.2	–	–	–	–	–	–	–	0.014155	0.0002458	0.024668	0.028266	0.028992	0.066220	

Note $C_{mv,\infty} = 1$ is corresponding to the case of the related film condensation of pure vapor

Table 20.6 Selected numerical solutions on Condensate film thickness $-W_{y1,s}$ with variation of the reference wall subcooled grade $\frac{t_{s,ref}-t_w}{t_{s,ref}}$ and the bulk water vapor fraction $C_{mv,\infty}$ for laminar free convection film condensation of water vapor-air mixture at the bulk temperature $T_\infty = 373$ K and atmospheric pressure as the system pressure

T_w (K)	$\frac{t_{s,ref}-t_w}{t_{s,ref}}$	$C_{mv,\infty}$	0.145	0.044	0.125	0.206	0.335	0.54	0.8	0.86	0.9	0.95	0.99	0.999	1
			$-W_{y1,s}$												
0	1	0.0000854	0.0019738	0.0042152	0.0055158	0.006935	0.0084849	0.0098835	0.0101537	0.0103267	0.010532	0.010690	0.010725	0.010725	0.013624
20	0.8	-	0.0000927	0.0029487	0.0044235	0.006021	0.0077586	0.0093224	0.0096236	.009815	0.010045	0.010222	0.010261	0.010261	0.013471
40	0.6	-	-	0.0001294	0.0022302	0.004090	0.0060397	0.0077713	0.0081031	0.0083116	0.008567	0.008759	0.008801	0.008801	0.012306
50	0.5	-	-	-	0.0001806	0.0025959	0.0047316	0.0065705	0.0069205	0.0071425	0.007408	0.007613	0.007658	0.007658	0.011319
60	0.4	-	-	-	-	0.000261	0.0030048	0.0050287	0.005405	0.0056428	0.005927	0.006144	0.006193	0.006193	0.010004
70	0.3	-	-	-	-	-	0.0003803	0.0030102	0.0034409	0.0037093	0.004027	0.004269	0.004322	0.004322	0.00845
75	0.25	-	-	-	-	-	-	0.0016945	0.0021915	0.0024958	0.002846	0.0031121	0.003170	0.003170	0.075178
80	0.2	-	-	-	-	-	-	-	0.0005924	0.000944	0.001384	0.001706	0.001773	0.001773	0.00648

Note $C_{mv,\infty} = 1$ is corresponding to the case of the related film condensation of pure vapor

Table 20.7 Selected numerical solutions on Condensate mass flow rate parameter Φ_s with variation of the reference wall subcooled grade $\frac{t_{s,ref}-t_w}{t_{s,ref}}$ and the bulk water vapor fraction $C_{mv,\infty}$ for laminar free convection film condensation of water vapor–air mixture at the bulk temperature $T_\infty = 373$ K and atmospheric pressure as the system pressure

T_w (K)	$\frac{t_{s,ref}-t_w}{t_{s,ref}}$	$C_{mv,\infty}$	0.0145	0.044	0.125	0.206	0.335	0.54	0.8	0.86	0.9	0.95	0.99	0.999	1
Φ_s															
0	1	0.0006824	0.0157629	0.0351201	0.0471372	0.0607671	0.0761205	0.090289	0.0930502	0.094804588	0.096932	0.0985688	0.0989301	0.1288063	
20	0.8	-	0.0007418	0.023745	0.0361425	0.0500306	0.0656026	0.079940	0.0827328	0.084514509	0.086655	0.0883094	0.0886712	0.1188738	
40	0.6	-	-	0.001037	0.0178792	0.0330538	0.0493367	0.064072	0.0669306	0.068775254	0.070943	0.0726525	0.0730237	0.1037864	
50	0.5	-	-	-	0.0014478	0.0208343	0.0382530	0.053526	0.0564622	0.058328451	0.060570	0.06222983	0.0626773	0.0939434	
60	0.4	-	-	-	-	0.0020946	0.0241321	0.040601	0.0436889	0.045644671	0.047984	0.0497802	0.0501802	0.0823025	
70	0.3	-	-	-	-	-	0.0030510	0.024163	0.0276412	0.029812256	0.032386	0.0343476	0.0347777	0.0686030	
75	0.25	-	-	-	-	-	-	0.013573	0.0175685	0.020014707	0.022832	0.0249761	0.0254435	0.0608028	
80	0.2	-	-	-	-	-	-	-	0.0047519	0.003824502	0.011091	0.0136721	0.0142130	0.0522417	

Note $C_{mv,\infty} = 1$ is corresponding to the case of the related film condensation of pure vapor

Table 20.8 Comparison of selected numerical solutions on Condensate mass flow rate parameter Φ_s with variation of the reference wall subcooled grade $\frac{t_{s,ref}-t_w}{t_{s,ref}}$ and the bulk water vapor fraction $C_{mv,\infty}$ for laminar free convection film condensation of water vapor–air mixture at the bulk temperature $T_\infty = 373\text{ K}$ and atmospheric pressure as the system pressure

$T_w, \text{ K}$	$\frac{t_{s,ref}-t_w}{t_{s,ref}}$	$C_{mv,\infty}$						
		0.8	0.86	0.9	0.95	0.99	0.999	
		Φ_s						
0	1	(1)	0.090289	0.0930502	0.09480458	0.096932	0.0985688	0.0989301
		(2)	0.0911435	0.0938939	0.09566533	0.0978154	0.0994880	0.0998589
20	0.8	(1)	0.079940	0.0827328	0.08451450	0.086655	0.0883094	0.0886712
		(2)	0.07927093	0.0819892	0.08374554	0.08588331	0.08755063	0.08792080
40	0.6	(1)	0.064072	0.0669306	0.06877525	0.070943	0.0726525	0.0730237
		(2)	0.06365283	0.06641610	0.06821423	0.07041618	0.07214351	0.07252817
50	0.5	(1)	0.053526	0.0564622	0.05832845	0.060570	0.0622983	0.0626773
		(2)	0.05362835	0.05644866	0.05829700	0.06057414	0.06237079	0.06277210
60	0.4	(1)	0.040601	0.0436889	0.04564467	0.047984	0.0497802	0.0501802
		(2)	0.04116585	0.04409133	0.04603585	0.04846038	0.05039533	0.05083014
70	0.3	(1)	0.024163	0.0276412	0.029812256	0.032386	0.0343476	0.0347777
		(2)	0.024547254	0.027623136	0.029751062	0.03249617	0.034759252	0.035276549
75	0.25	(1)	0.013573	0.0175685	0.020014707	0.022832	0.0249761	0.0254435
		(2)	0.013986615	0.017075869	0.019358228	0.022472976	0.0251818	0.025818573

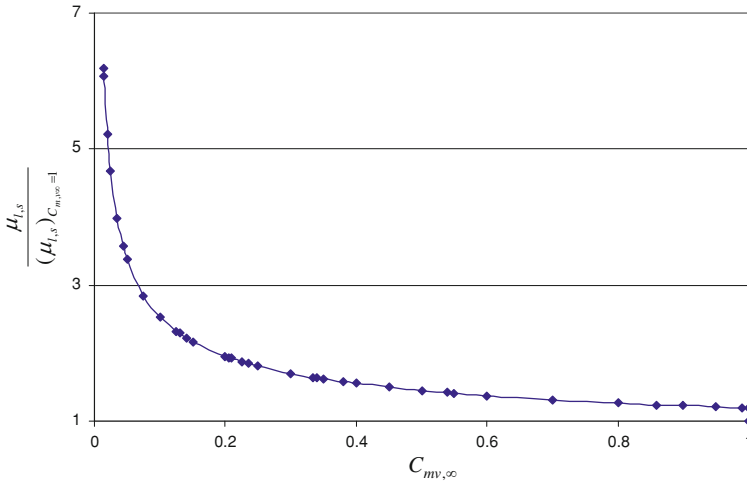


Fig. 20.10 Absolute viscosity ratio $\frac{\mu_{1,s}}{(\mu_{1,s})_{C_{mv,\infty}=1}}$ with variation of bulk vapor mass fraction $C_{mv,\infty}$ for laminar free convection film condensation of water vapor–air mixture at the bulk temperature $T_\infty = 373\text{ K}$ and atmospheric pressure as the system pressure [1]

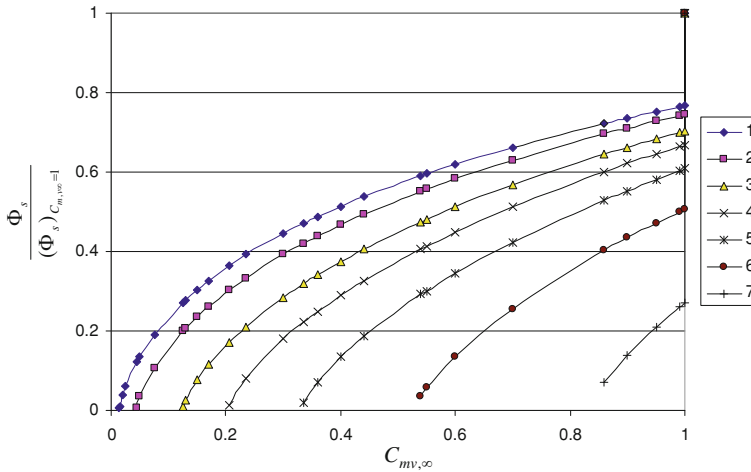


Fig. 20.11 Mass flow rate parameter ratio $\frac{\Phi_s}{(\Phi_s)_{C_{m,v\infty}=1}}$ with variation of the reference wall subcooled grade and the bulk water vapor fraction for laminar free convection film condensation from water vapor–air mixture at the bulk temperature $T_\infty = 373$ K and atmospheric pressure as the system pressure [1]. (Lines 1–7 for $\frac{t_{s,ref}-t_w}{t_{s,ref}} = 1, 0.8, 0.6, 0.5, 0.4, 0.3,$ and 0.2)

subcooled grade $\frac{t_{s,ref}-t_w}{t_{s,ref}}$, the mass flow rate parameter ratios will decrease more and more quickly.

According to the above calculation results the condensate mass flow rate ratios $\frac{g_x}{(g_x)_{C_{m,v\infty}=1}}$ are found out, and plotted in Fig. 20.12 with the variation of the bulk vapor mass fraction $C_{m,v\infty}$ and the reference wall subcooled grade $\frac{t_{s,ref}-t_w}{t_{s,ref}}$. It is seen that the condensate mass transfer ratios $\frac{g_x}{(g_x)_{C_{m,v\infty}=1}}$ decrease more and more quickly by decreasing the bulk vapor mass fraction $C_{m,v\infty}$ and the reference wall subcooled grade $\frac{t_{s,ref}-t_w}{t_{s,ref}}$.

Comparing the data of Fig. 20.5 with those of Fig. 20.12, it is seen that, like the condensate heat transfer ratio $\frac{q_x}{(q_x)_{C_{m,v\infty}=1}}$, the condensate mass transfer ratio $\frac{g_x}{(g_x)_{C_{m,v\infty}=1}}$ is also coincident to the wall subcooled temperature ratio $\frac{t_w-t_{s,int}}{t_w-t_s}$, then, it follows that, like the condensate heat transfer, the condensate mass flow rate is also dominated by the wall subcooled temperature $t_w - t_{s,int}$. However, the condensate heat transfer rate q_x is defined on the plate, and the condensate mass transfer rate g_x is defined at the liquid–vapor interface. Such deference in definition causes only very slight difference between the condensate heat transfer ratio and condensate mass transfer ratio.

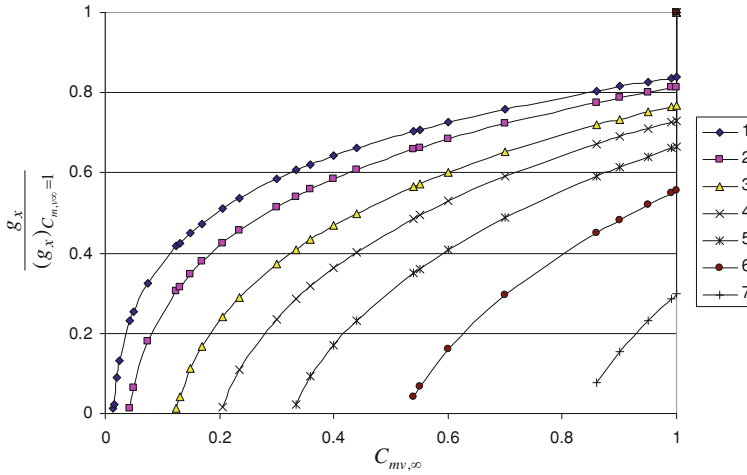


Fig. 20.12 Condensate mass flow rate ratio $\frac{g_x}{(g_x)_{C_{m,v,\infty}=1}}$ with variation of the reference wall sub-cooled grade $\frac{T_{s,ref}-T_w}{T_{s,ref}}$ and the bulk water vapor fraction $C_{m,v,\infty}$ for laminar free convection film condensation from water vapor–air mixture at the bulk temperature $T_\infty = 373$ K and atmospheric pressure as the system pressure [1]. (Lines 1–7 for $\frac{T_{s,ref}-T_w}{T_{s,ref}} = 1, 0.8, 0.6, 0.5, 0.4, 0.3,$ and 0.2)

20.8 Quite Different Film Condensations

The present work for the laminar free convection film convection of vapor in presence of non-condensable gas is based on our previous studies for laminar free convection film condensation of pure vapor presented in Chaps. 14–17. However, condensate heat and mass transfer rate of the laminar free convection film condensation from vapor in presence of non-condensable gas even for $C_{m,v,\infty} \rightarrow 1$ is quite different from that of pure vapor, which can be known from the great variations of the wall dimensionless temperature gradient and the condensate mass flow rate parameter for $C_{m,v,\infty} = 0.999$ and 1 shown in Tables 20.1 and 20.7 respectively. Such a big difference is caused by condensation mechanism. For the laminar free convection film convection of vapor in presence of non-condensable gas, the film condensation at the liquid–vapor interface is always accompanied by vapor diffusion even for $C_{m,v,\infty} \rightarrow 1$. For the laminar free convection film condensation of pure vapor, the vapor is directly condensed at the liquid–vapor interface without any mass diffusion. According to the present calculated results for $T_w = 273$ and $T_w = 353$ K, the heat transfer rates of the laminar free convection film condensation with $C_{m,v,\infty} = 0.999$ will reduce 15.3 and 70.1 % respectively, compared with the related film condensation of the pure water vapor. Meanwhile, the related condensate mass transfer rates will decrease 16.1 and 70.2 % respectively.

In order to express the difference mentioned above, the results of the heat transfer ratio $\frac{(q_x)_{C_{m,v,\infty}=0.999}}{(q_x)_{C_{m,v,\infty}=1}}$ and mass transfer ratio $\frac{(g_x)_{C_{m,v,\infty}=0.999}}{(g_x)_{C_{m,v,\infty}=1}}$ are evaluated numerically,

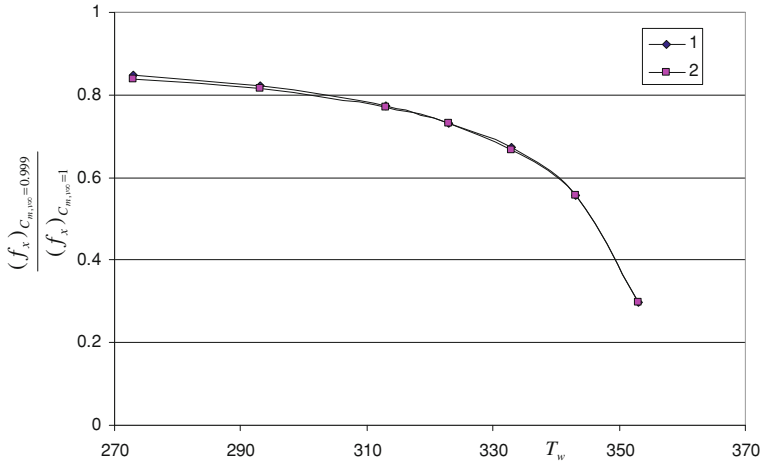


Fig. 20.13 Heat and mass transfer deviations of the case with $C_{m,v\infty} = 0.999$ to that with $C_{m,v\infty} = 1$ for laminar free film condensation from water vapor–air mixture at the bulk temperature $T_\infty = 373$ K and atmospheric pressure as the system pressure. (Line 1 for $\frac{(q_x)_{C_{m,v\infty}=0.999}}{(q_x)_{C_{m,v\infty}=1}}$ and line 2 for $\frac{(g_x)_{C_{m,v\infty}=0.999}}{(g_x)_{C_{m,v\infty}=1}}$)

and plotted in Fig. 20.13 with variation of wall temperature T_w for laminar free film condensation from water vapor–air mixture at the bulk temperature $T_\infty = 373$ K and atmospheric pressure as the system pressure. It is seen that even a very small mass fraction of non-condensable gas in the vapor–gas mixture, for example for $C_{m,g\infty} = 1 - C_{m,v\infty} = 0.001$, the condensate heat and mass transfer will be reduced very greatly compared with that for the condensation of pure vapor. Furthermore, by increasing the wall temperature T_w , such heat and mass transfer, $\frac{(q_x)_{C_{mv,\infty} \neq 1}}{(q_x)_{C_{mv,\infty} = 1}}$ and $\frac{(g_x)_{C_{mv,\infty} \neq 1}}{(g_x)_{C_{mv,\infty} = 1}}$, will decrease more and more quickly. From the present analysis and calculated results, it is found that even a very small amount of non-condensable gas in the vapor–gas mixture, will change very greatly the wall subcooled temperature, temperature gradient, condensate liquid film thickness, and the condensate liquid velocity components, and then, will greatly decrease the heat and mass transfer of the film condensation. If we take the wall subcooled temperature, temperature gradient, condensate liquid film thickness, condensate liquid velocity components, and heat and mass transfer rates as function of $C_{mv,\infty}$, i.e., function $f(C_{mv,\infty})$, such function can be mathematically described by a mathematical expression $f(C_{mv,\infty} \rightarrow 0) \neq f(C_{mv,\infty} = 0)$. It means that the function $f(C_{mv,\infty})$ is discontinuous at the point $C_{mv,\infty} = 0$. Therefore, in order to have the highest condensate heat and mass transfer rates of the film condensation, it is best to provide the pure vapor.

20.9 Summary

At present, it is the time to summarize the complete mathematical models and heat and mass equations on laminar free convection film condensation of vapor–gas mixture in Tables 20.9 and 20.10, including the two-phase film flows governing partial differential equations, similarity variables, dimensionless similarity governing equations, the physical property factor equations, and heat and mass transfer equations.

20.10 Remarks

The theoretical equations on heat and mass transfer are set up through the heat and mass transfer analysis for laminar free convection film condensation of vapor–gas mixture. In the theoretical equations only dimensionless wall temperature gradient and condensate mass flow rate parameter are no-given variables respectively for prediction of heat and mass transfer rates respectively.

The laminar free convection film condensation of water vapor in presence of air on a vertical flat plate is taken as example for the numerical solutions on condensate heat and mass transfer, including those on the dimensionless temperature gradient and mass flow rate parameter. By decreasing the bulk vapor mass fraction and reference wall subcooled grade, the wall dimensionless temperature gradient will increase at accelerative pace. Decreasing the bulk vapor mass fraction and reference wall subcooled grade will cause decrease in the condensate mass flow rate parameter quicker and quicker. These phenomena demonstrate decisive effect of the non-condensable gas on condensate heat and mass transfer of the laminar free film condensation of vapor–gas mixture.

The system of the rigorous key solutions on the wall dimensionless temperature gradient and the condensate mass flow rate parameter is formulated to the simple and reliable equations for the laminar free convection film condensation of water vapor–air mixture. With the formulated equations on wall dimensionless temperature gradient and the condensate mass flow rate parameter, the theoretical equations on the condensate heat and mass transfer can be used for reliable and simple prediction of heat and mass transfer on laminar free convection film condensation of water vapor–air mixture.

The condensate heat transfer rate is dominated by the wall subcooled temperature $t_w - t_{s,int}$. The condensate mass flow rate is dominated by the condensate mass flow rate parameter. The condensate heat transfer rate is identical to the condensate mass flow rate. Due to the different condensate mechanisms, the condensate heat and mass transfer rate of the laminar free convection film condensation from vapor in presence of non-condensable gas is quite different from that of pure vapor, even for $C_{mv,\infty} \rightarrow 0$.

Table 20.9 Summary on complete mathematical models on laminar free film condensation of vapor–gas mixture

<i>Governing partial differential equations for liquid film</i>	
Mass equation	$\frac{\partial}{\partial x}(\rho_1 w_{x1}) + \frac{\partial}{\partial y}(\rho_1 w_{y1}) = 0$
Momentum equation	$\rho_l \left[w_{x1} \frac{\partial w_{x1}}{\partial x} + w_{y1} \frac{\partial w_{x1}}{\partial y} \right] = \frac{\partial}{\partial y} \left(\mu_l \frac{\partial w_{x1}}{\partial y} \right) + g(\rho_l - \rho_{m,\infty})$
Energy equation	$\rho_l \left[w_{x1} \frac{\partial (c_{p1} t)}{\partial x} + w_{y1} \frac{\partial (c_{p1} t)}{\partial y} \right] = \frac{\partial}{\partial y} \left(\lambda_l \frac{\partial t}{\partial y} \right)$
<i>Governing partial differential equations for vapor–gas mixture film</i>	
Mass equation	$\frac{\partial}{\partial x}(\rho_m w_{xm}) + \frac{\partial}{\partial y}(\rho_m w_{ym}) = 0$
Momentum equation	$\rho_m \left(w_{xm} \frac{\partial w_{xm}}{\partial x} + w_{ym} \frac{\partial w_{xm}}{\partial y} \right) = \frac{\partial}{\partial y} \left(\mu_m \frac{\partial w_{xm}}{\partial y} \right) + g(\rho_m - \rho_{m,\infty})$
Energy equation	$\rho_m \left[w_{xm} \frac{\partial (c_{pm} t_m)}{\partial x} + w_{ym} \frac{\partial (c_{pm} t_m)}{\partial y} \right] = \frac{\partial}{\partial y} \left(\lambda_m \frac{\partial t_m}{\partial y} \right) + \frac{\partial}{\partial y} \left[\rho_m D_v (c_{pv} - c_{pe}) \frac{\partial C_{m,v}}{\partial y} - t_m \right]$
Species equation	$\frac{\partial (w_{xm} \rho_m C_{m,x})}{\partial x} + \frac{\partial (w_{ym} \rho_m C_{m,y})}{\partial y} = \frac{\partial}{\partial y} \left(D_v \rho_m \frac{\partial C_{m,v}}{\partial y} \right)$
<i>Boundary conditions of governing partial differential equations</i>	
$y = 0$	$w_{x1} = 0, w_{y1} = 0, t_1 = t_w$
$y = \delta_l$	$w_{x1,s} = w_{xm,s}$
	$\rho_{l,s} \left(w_{x1} \frac{\partial \delta_l}{\partial x} - w_{y1} \right)_{l,s} = \rho_{m,s} C_{m,vs} \left(w_{xm} \frac{\partial \delta_m}{\partial x} - w_{ym} \right)_s = g_x$
	$\mu_{l,s} \left(\frac{\partial w_{x1}}{\partial y} \right)_s = \mu_{m,s} \left(\frac{\partial w_{xm}}{\partial y} \right)_s$
	$\lambda_{l,s} \left(\frac{\partial t_1}{\partial y} \right)_{s1} = \lambda_{m,s} \left(\frac{\partial t_m}{\partial y} \right)_s + h_{fg} \rho_{m,s} C_{m,vs} \left(w_{xm} \frac{\partial \delta_m}{\partial x} - w_{ym} \right)_s$
	$t = t_{s,int}$
	$C_{m,v} = C_{m,vs}$
	$\rho_{m,s} C_{m,vs} \left(w_{xm} \frac{\partial \delta_m}{\partial x} - w_{ym} \right)_s = D_v \rho_{m,s} \left(\frac{\partial C_{m,v}}{\partial y} \right)_s$
$y \rightarrow \infty$	$w_{xm} \rightarrow 0, t_m \rightarrow t_\infty, C_{m,v} = C_{m,v\infty}$

(continued)

Table 20.9 (continued)

Similarity variables for liquid film

Dimensionless coordinate variable η

$$\eta = \left(\frac{1}{4} \text{Gr}_{x1,s}\right)^{1/4} \frac{y}{x}$$

Local Reynolds number

$$\text{Gr}_{x1,s} = \frac{g(\rho_{l,w} - \rho_{v,\infty})x^3}{\nu_{l,s}^2 \rho_{l,s}}$$

Dimensionless temperature

$$\theta_1(\eta) = \frac{t_l - t_{s,\text{int}}}{t_w - t_{s,\text{int}}}$$

Dimensionless velocity components $W_{x1}(\eta)$ and $W_{y1}(\eta)$

$$W_{x1} = \left(2\sqrt{g\bar{x}} \left(\frac{\rho_{l,w} - \rho_{m,\infty}}{\rho_{l,s}}\right)^{1/2}\right)^{-1} W_{x1}$$

$$W_{y1} = \left(2\sqrt{g\bar{x}} \left(\frac{\rho_{l,w} - \rho_{m,\infty}}{\rho_{l,s}}\right)^{1/2} \left(\frac{1}{4} \text{Gr}_{x1,s}\right)^{-4}\right)^{-1} W_{y1}$$

Similarity variables for vapor-gas mixture film

Dimensionless coordinate variable

$$\eta_m = \frac{y}{x} \left(\frac{1}{2} \text{Re}_{x,m,\infty}\right)^{1/2}$$

Local Reynolds number

$$\text{Gr}_{x,m,\infty} = \frac{g(\rho_{m,s}/\rho_{m,\infty} - 1)x^3}{\nu_{m,\infty}^2}$$

Dimensionless temperature

$$\theta_m(\eta_m) = \frac{t_m - t_\infty}{t_{s,\text{int}} - t_\infty}$$

Dimensionless velocity components $W_{x1}(\eta)$ and $W_{y1}(\eta)$

$$W_{xm} = (2\sqrt{g\bar{x}}(\rho_{m,s}/\rho_{m,\infty} - 1)^{1/2})^{-1} W_{xm}$$

$$W_{ym} = \left(2\sqrt{g\bar{x}}(\rho_{m,s}/\rho_{m,\infty} - 1)^{1/2} \left(\frac{1}{4} \text{Gr}_{x,m,\infty}\right)^{-1/4}\right)^{-1} W_{ym}$$

Vapor relative mass fraction

$$\Gamma_{mv}(\eta_m) = \frac{C_{mv} - C_{mv,\infty}}{C_{mv,s} - C_{mv,\infty}}$$

Governing ordinary differential equations for liquid film

Mass equation

$$2W_{x1} - \eta \frac{dW_{x1}}{d\eta} + 4 \frac{dW_{y1}}{d\eta} - \frac{1}{\rho_l} \frac{d\rho_l}{d\eta} (\eta W_{x1} - 4W_{y1}) = 0$$

Momentum equation

$$\frac{v_{1,s}}{v_1} \left[W_{x1} \left(2W_{x1} - \eta_1 \frac{dW_{x1}}{d\eta_1} \right) + 4W_{y1} \frac{dW_{x1}}{d\eta_1} \right] = \frac{d^2 W_{x1}}{d\eta_1^2} + \frac{1}{\mu_1} \frac{d\mu_1}{d\eta_1} \frac{dW_{x1}}{d\eta_1} + \frac{\mu_{1,s} (\rho_1 - \rho_{m,\infty})}{\mu_1} \frac{\rho_{1,w} - \rho_{m,\infty}}{\rho_1 - \rho_{m,\infty}}$$

Energy equation

$$\text{Pr}_1 \frac{v_{1,s}}{v_1} (-\eta_1 W_{x1} + 4W_{y1}) \frac{d\theta_1}{d\eta_1} = \frac{d^2 \theta_1}{d\eta_1^2} + \frac{1}{\lambda_1} \frac{d\lambda_1}{d\eta_1} \frac{d\theta_1}{d\eta_1}$$

Governing ordinary differential equations for vapor-gas mixture film

Mass equation

$$2W_{x,m} - \eta_m \frac{dW_{x,m}}{d\eta_m} + 4 \frac{dW_{y,m}}{d\eta_m} - \frac{1}{\rho_m} \frac{d\rho_m}{d\eta_m} (\eta_m W_{x,m} - 4W_{y,m}) = 0$$

Momentum equation

$$\frac{v_{m,\infty}}{v_m} \left[W_{x,m} \left(2W_{x,m} - \eta_m \frac{dW_{x,m}}{d\eta_m} \right) + 4W_{y,m} \frac{dW_{x,m}}{d\eta_m} \right] = \frac{d^2 W_{x,m}}{d\eta_m^2} + \frac{1}{\mu_m} \frac{d\mu_m}{d\eta_m} \frac{dW_{x,m}}{d\eta_m} + \frac{\mu_{m,\infty}}{\mu_m} \cdot \frac{\rho_{m,s} - \rho_{m,\infty}}{\rho_m - \rho_{m,\infty}}$$

Energy equation

$$\begin{aligned} & \frac{v_{m,\infty}}{v_m} \left[-\eta_m W_{x,m} + 4W_{y,m} \right] \frac{d\theta_m}{d\eta_m} \\ &= \frac{1}{\text{Pr}_m} \left(\frac{d^2 \theta_m}{d\eta_m^2} + \frac{1}{\lambda_m} \frac{d\lambda_m}{d\eta_m} \cdot \frac{d\theta_m}{d\eta_m} \right) \\ & - \frac{1}{v_{m,\infty}} (C_{m,v,s} - C_{m,v,\infty}) \frac{C_{p,v} - C_{p,g}}{C_{p,m}} \\ & \times \left[\frac{d\theta_m}{d\eta_m} \frac{d\Gamma_{mv}}{d\eta_m} + \left(\theta_m + \frac{t_\infty}{t_{s,int} - t_\infty} \right) \frac{d^2 \Gamma_{mv}}{d\eta_m^2} + \left(\theta_m + \frac{t_\infty}{t_{s,int} - t_\infty} \right) \frac{1}{\rho_m} \frac{d\rho_m}{d\eta_m} \frac{d\Gamma_{mv}}{d\eta_m} \right] \\ & (-\eta_m W_{x,m} + 4W_{y,m}) \frac{d\Gamma_{mv}}{d\eta_m} = \frac{1}{S C_{m,\infty}} \left(\frac{d\Gamma_{mv}}{d\eta_m^2} + \frac{1}{\rho_m} \frac{d\rho_m}{d\eta_m} \frac{d\Gamma_{mv}}{d\eta_m} \right) \end{aligned}$$

Species equation

Boundary conditions of governing ordinary differential equations

$$\eta_1 = 0: W_{y1} = 0, \theta_1 = 1$$

$$W_{x,m,s} = \left(\frac{\rho_{1,w} - \rho_{m,\infty}}{\rho_{1,s}} \right)^{1/2} (\rho_{m,s} / \rho_{m,\infty} - 1)^{-1/2} W_{x1,s}$$

(continued)

Table 20.9 (continued)

$W_{ym,s} = -\frac{1}{C_{mv,s}} \frac{\rho_{l,s}}{\rho_{m,s}} \left(\frac{v_{l,s}}{v_{m,\infty}} \right)^{1/2} \left(\frac{\rho_{l,m} - \rho_{m,\infty}}{\rho_{l,s}} \right)^{1/4}$ $\times (\rho_{m,s} / \rho_{m,\infty} - 1)^{-1/4} \left(\frac{1}{4} \eta_{\delta} W_{x1,s} - W_{y1,s} \right)^{3/4}$ $\left(\frac{dW_{xm}}{d\eta_m} \right)_s = \frac{\mu_{l,s}}{\mu_{m,s}} \left(\frac{v_{m,\infty}}{v_{l,s}} \right)^{1/2} \left(\frac{\rho_{l,w} - \rho_{m,\infty}}{\rho_{l,s}} \right)^{3/4}$ $\times (\rho_{m,s} / \rho_{m,\infty} - 1)^{-3/4} \left(\frac{dW_{x1}}{d\eta} \right)_s$ $\left(\frac{d\theta_m}{d\eta_m} \right)_s = \frac{\lambda_{l,s}(\eta_{m0})}{\lambda_{m,s}(\eta_{m0})} \left(\frac{v_{m,\infty}}{v_{l,s}} \right)^{1/2} \left(\frac{\rho_{l,w} - \rho_{m,\infty}}{\rho_{l,s}} \right)^{1/4} \frac{(\rho_{m,s} / \rho_{m,\infty} - 1)^{-1/4} \left(\frac{d\theta_1}{d\eta} \right)_s + 4h_{fg} \rho_{m,s} C_{mv,s} v_{m,\infty} W_{ym,s}}{\lambda_{m,s}(\eta_{m0})}$	$\theta_{l,s}(\eta_{\delta}) = 0, \theta_{m,s}(\eta_{m,\infty}) = 1$ $\Gamma_{mv,s}(\eta_{m0}) = 1$ $\left(\frac{d\Gamma_{mv}}{d\eta_m} \right)_s = -2S C_{m,\infty} \frac{C_{mv,s}}{C_{mv,s} - C_{mv,\infty}} W_{ym,s}(\eta_{m0})$ $W_{xm,\infty} = 0, \theta_m = 0, \Gamma_{mv,\infty} = 0$
$\eta_m \rightarrow \infty$	
<i>Treatment of variable physical on condensate liquid film</i> (for condensate water film medium) Variable physical properties	
$\rho_l = -4.48 \times 10^{-3} t^2 + 999.9$ $\lambda_l = -8.01 \times 10^{-6} t^2 + 1.94 \times 10^{-3} t + 0.563$ $\mu_l = \exp \left(-1.6 - \frac{1150}{T} + \left(\frac{690}{T} \right)^2 \right) \times 10^{-3}$ $Pr_l = \frac{\mu_l \cdot c_{pl}}{\lambda_l} = \frac{\left[\exp \left(-1.6 - \frac{1150}{T} + \left(\frac{690}{T} \right)^2 \right) \times 10^{-3} \right] \times 4200}{-8.01 \times 10^{-6} t^2 + 1.94 \times 10^{-3} t + 0.563}$	

Properties physical property factor equations

$$\frac{1}{c_p} \frac{dc_p}{d\eta} = 0$$

$$\frac{1}{\rho_l} \frac{d\rho_l}{d\eta} = \frac{[-2 \times 4.48 \times 10^{-3} t(t_w - t_s) \frac{d\theta(\eta)}{d\eta}]}{(-4.48 \times 10^{-3} t^2 + 999.9)}$$

$$\frac{1}{\lambda_l} \frac{d\lambda_l}{d\eta} = \frac{[-2 \times 8.01 \times 10^{-6} + 1.94 \times 10^{-3} (t_w - t_s) \frac{d\theta(\eta)}{d\eta}]}{(-8.01 \times 10^{-6} t^2 + 1.94 \times 10^{-3} t + 0.563)}$$

$$\frac{1}{\mu_l} \frac{d\mu_l}{d\eta} = \left(\frac{1150}{T^2} - 2 \times \frac{690^2}{T^3} \right) (t_w - t_s) \frac{d\theta(\eta)}{d\eta}$$

Treatment of variable physical on condensate liquid film on vapor-gas mixture film

Concentration-dependent physical property factors

$$\frac{1}{\rho_m} \frac{d\rho_m}{d\eta_m} = \frac{1}{\rho_v} \frac{d\rho_v}{d\eta_m} - \frac{C_{mv}(\rho_v - \rho_g)}{\rho_v \frac{d\eta_m}{d\eta_m} + C_{mv}\rho_g}$$

$$\times \left[\frac{C_{mv}}{(1 - C_{mv})} \frac{(\rho_v - \rho_g) \rho_v \frac{d\eta_m}{d\eta_m} + \rho_g}{\rho_v} + \frac{C_{mv}}{\rho_g} \frac{C_{mv,s} - C_{mv,\infty}}{C_{mv,s} - C_{mv,\infty}} \frac{d\eta_m}{d\eta_m} \right]$$

$$\frac{1}{\mu_m} \frac{d\mu_m}{d\eta_m} = \frac{\mu_v}{C_{mv}} \frac{1}{d\mu_v} + (1 - C_{mv}) \frac{\mu_g}{\rho_g} \frac{1}{d\mu_g} + \frac{\mu_m}{C_{mv}} \frac{\mu_g}{\rho_g} \frac{d\eta_m}{d\eta_m} \frac{d\Gamma_{mv}}{d\eta_m}$$

$$\frac{1}{\lambda_m} \frac{d\lambda_m}{d\eta_m} = \frac{C_{mv}}{\lambda_v} \frac{1}{d\lambda_v} + (1 - C_{mv}) \frac{\lambda_g}{\lambda_m \lambda_g} \frac{d\eta_m}{d\eta_m} + \frac{\lambda_m}{\lambda_m} \frac{\lambda_g}{\lambda_m} \frac{d\Gamma_{mv}}{d\eta_m}$$

For density factors

$$\frac{1}{\rho_v} \frac{d\rho_v}{d\eta_m} = - \frac{(T_{s,int}/T_\infty - 1)d\theta_m/d\eta_m}{(T_{s,int}/T_\infty - 1)\theta_m + 1} \frac{1}{\rho_g} \frac{d\rho_g}{d\eta_m} = - \frac{(T_{s,int}/T_\infty - 1)d\theta_m/d\eta_m}{(T_{s,int}/T_\infty - 1)\theta_m + 1}$$

For absolute viscosity factors

$$\frac{1}{\mu_v} \frac{d\mu_v}{d\eta_m} = \frac{n_{\mu,v}(T_{s,int}/T_\infty - 1)d\theta_m/d\eta_m}{(T_{s,int}/T_\infty - 1)\theta_m + 1} \frac{1}{\mu_g} \frac{d\mu_g}{d\eta_m} = \frac{n_{\mu,g}(T_{s,int}/T_\infty - 1)d\theta_m/d\eta_m}{(T_{s,int}/T_\infty - 1)\theta_m + 1}$$

For thermal conductivity factors

$$\frac{1}{\lambda_v} \frac{d\lambda_v}{d\eta_m} = \frac{n_{\lambda,v}(T_{s,int}/T_\infty - 1)d\theta_m/d\eta_m}{(T_{s,int}/T_\infty - 1)\theta_m + 1} \frac{1}{\lambda_g} \frac{d\lambda_g}{d\eta_m} = \frac{n_{\lambda,g}(T_{s,int}/T_\infty - 1)d\theta_m/d\eta_m}{(T_{s,int}/T_\infty - 1)\theta_m + 1}$$

Temperature-dependent physical property factors

Table 20.10 Summary on heat and mass transfer equations on laminar free film condensation of vapor–gas mixture

Equation for evaluation of interfacial vapor saturation temperature $t_{s,int}$

Prediction equation

$$t_{s,int} = 357.06 C_{mv,\infty}^{0.063} \quad \text{For laminar forced convection of water vapor–air mixture on a horizontal plate at } t_{\infty} = 100\text{ }^{\circ}\text{C}$$

Condensate heat transfer

Wall dimensionless temperature gradient

$$t_{\infty} = 100\text{ }^{\circ}\text{C} \quad \text{For laminar forced film condensation of water vapor–air mixture on a vertical plate at}$$

$$\left(-\frac{dh}{d\eta}\right)_{\eta=0} = a C_{mv,\infty}^b \quad (0.8 \leq C_{mv,\infty} \leq 0.999)$$

where

$$a = 1.5152 \left(\frac{t_{s,ref}-t_w}{t_{s,ref}}\right)^{-0.5553}$$

$$a = 1.6976 \left(\frac{t_{s,ref}-t_w}{t_{s,ref}}\right)^{-0.4302}$$

$$b = - \left[0.3081 \left(\frac{t_{s,ref}-t_w}{t_{s,ref}}\right)^{-0.8478} \left(\frac{t_{s,ref}-t_w}{t_{s,ref}}\right)^{-1} \right]$$

$$(0.25 \leq \frac{t_{s,ref}-t_w}{t_{s,ref}} \leq 0.4)$$

$$(0.4 \leq \frac{t_{s,ref}-t_w}{t_{s,ref}} \leq 1)$$

$$(0.25 \leq \frac{t_{s,ref}-t_w}{t_{s,ref}} \leq 0.4)$$

$$b = -1.94 \left(\frac{t_{s,ref}-t_w}{t_{s,ref}}\right)^2 + 2.623 \left(\frac{t_{s,ref}-t_w}{t_{s,ref}}\right) - 1.1057 \quad (0.4 \leq \frac{t_{s,ref}-t_w}{t_{s,ref}} \leq 0.6)$$

$$b = 0.1667 \ln \left(\frac{t_{s,ref}-t_w}{t_{s,ref}}\right) - 0.1439 \quad (0.6 \leq \frac{t_{s,ref}-t_w}{t_{s,ref}} \leq 1)$$

$$q_x = \lambda_{l,w}(t_w - t_{s,int}) \left(\frac{1}{4} Gr_{x,l,s}\right)^{1/4} x^{-1} \left(-\frac{dh}{d\eta}\right)_{\eta=0}$$

$$\alpha_x = \lambda_{l,w} \left(\frac{1}{4} Gr_{x,l,s}\right)^{1/4} x^{-1} \left(-\frac{dh}{d\eta}\right)_{\eta=0}$$

$$Nu_{x,w} = \left(\frac{1}{4} Gr_{x,l,s}\right)^{1/4} \left(-\frac{dh}{d\eta}\right)_{\eta=0}$$

Local values on heat transfer, $Nu_{x,w} = \frac{\alpha_x x}{\lambda_{l,w}}$

Table 20.10 (continued)

Average values on heat transfer,

$$\overline{Nu}_{x,w} = \frac{\overline{\alpha_{x,w}}}{\lambda_{1,w}}$$

$$\overline{Q}_x = \frac{4}{3} x^{-1} \lambda_{1,w} (t_w - t_{s,im}) \left(\frac{1}{4} Gr_{x1,s}\right)^{1/4} \left(-\frac{d\theta}{d\eta}\right)_{\eta=0}$$

$$\overline{\alpha}_x = \frac{4}{3} \lambda_{1,w} \left(\frac{1}{4} Gr_{x1,s}\right)^{1/4} x^{-1} \left(-\frac{d\theta}{d\eta}\right)_{\eta=0}$$

$$\overline{Nu}_{x,w} = \frac{4}{3} \left(\frac{1}{4} Gr_{x1,s}\right)^{1/4} \left(-\frac{d\theta}{d\eta}\right)_{\eta=0}$$

Total value on heat transfer

$$Q_x = \frac{4}{3} b \lambda_{1,w} (t_w - t_{s,im}) \left(\frac{1}{4} Gr_{x1,s}\right)^{1/4} \left(-\frac{d\theta}{d\eta}\right)_{\eta=0}$$

Prediction equation on heat transfer

$$Q_x = \frac{4}{3} b \lambda_{1,w} (t_w - t_{s,im}) \left(\frac{1}{4} Gr_{x1,s}\right)^{1/4} a C_{mv,\infty}^{0.8} \quad (0.8 \leq C_{mv,\infty} \leq 0.999)$$

where

$$a = 1.5152 \left(\frac{t_{s,ref}-t_w}{t_{s,ref}}\right)^{-0.5553}$$

$$a = 1.6976 \left(\frac{t_{s,ref}-t_w}{t_{s,ref}}\right)^{-0.4302}$$

$$b = - \left[0.3081 \left(\frac{t_{s,ref}-t_w}{t_{s,ref}}\right)^{-0.8478} \right] \left(\frac{t_{s,ref}-t_w}{t_{s,ref}}\right)^{-1}$$

$$b = -1.94 \left(\frac{t_{s,ref}-t_w}{t_{s,ref}}\right)^2 + 2.623 \left(\frac{t_{s,ref}-t_w}{t_{s,ref}}\right) - 1.1057$$

$$b = 0.1667 \ln \left(\frac{t_{s,ref}-t_w}{t_{s,ref}}\right) - 0.1439$$

$$(0.25 \leq \frac{t_{s,ref}-t_w}{t_{s,ref}} \leq 0.4)$$

$$(0.4 \leq \frac{t_{s,ref}-t_w}{t_{s,ref}} \leq 1)$$

$$(0.25 \leq \frac{t_{s,ref}-t_w}{t_{s,ref}} \leq 0.4)$$

$$(0.4 \leq \frac{t_{s,ref}-t_w}{t_{s,ref}} \leq 0.6)$$

$$(0.6 \leq \frac{t_{s,ref}-t_w}{t_{s,ref}} \leq 1)$$

Condensate mass flow rate

Mass flow rate G_x

Mass flow rate G_x

$$G_x = \frac{4}{3} b \cdot \mu_{1,s} \left(\frac{1}{4} Gr_{x1,s}\right)^{1/4} \Phi_s$$

where mass flow rate parameter $\Phi_s = (\eta_{fs} W_{x1,s} - 2 W_{y1,s})$

For laminar forced convection of water vapor–air mixture on a horizontal plate at $t_\infty = 100^\circ\text{C}$

$$\Phi_s = a C_{mv,\infty}^{0.8} \quad (0.8 \leq C_{mv,\infty} \leq 0.999)$$

(continued)

Table 20.10 (continued)

where

$$a = 0.0518 \ln \left(\frac{t_{s,\text{ref}} - t_w}{t_{s,\text{ref}}} \right) + 0.0977 \quad \left(0.25 \leq \frac{t_{s,\text{ref}} - t_w}{t_{s,\text{ref}}} \leq 0.4 \right)$$

$$a = 0.0535 \ln \left(\frac{t_{s,\text{ref}} - t_w}{t_{s,\text{ref}}} \right) + 0.0999 \quad \left(0.4 \leq \frac{t_{s,\text{ref}} - t_w}{t_{s,\text{ref}}} \leq 1 \right)$$

$$b = \left[0.5724 \left(\frac{t_{s,\text{ref}} - t_w}{t_{s,\text{ref}}} \right)^{-0.5855} \left(\frac{t_{s,\text{ref}} - t_w}{t_{s,\text{ref}}} \right)^{-1} \right] \quad \left(0.25 \leq \frac{t_{s,\text{ref}} - t_w}{t_{s,\text{ref}}} \leq 0.4 \right)$$

$$b = 5.975 \left(\frac{t_{s,\text{ref}} - t_w}{t_{s,\text{ref}}} \right)^2 - 7.7835 \left(\frac{t_{s,\text{ref}} - t_w}{t_{s,\text{ref}}} \right) + 3.1067 \quad \left(0.4 \leq \frac{t_{s,\text{ref}} - t_w}{t_{s,\text{ref}}} \leq 0.6 \right)$$

$$b = 0.8287 \left(\frac{t_{s,\text{ref}} - t_w}{t_{s,\text{ref}}} \right)^2 - 1.7672 \left(\frac{t_{s,\text{ref}} - t_w}{t_{s,\text{ref}}} \right) + 1.3496 \quad \left(0.6 \leq \frac{t_{s,\text{ref}} - t_w}{t_{s,\text{ref}}} \leq 1 \right)$$

For laminar forced convection of water vapor-air mixture on a horizontal plate
 at $t_\infty = 100^\circ\text{C}$
 $T_{s,\text{int}} = 357.06 C_{\text{inv},\infty}^{0.063}$

Evaluation of interfacial vapor saturation equations $t_{s,\text{int}}$
 Prediction equation

20.11 Calculation Examples

Example 1 A flat plate, 0.1 m in width and 0.05 m in length, is located vertically in the bulk water vapor–air mixture. The wall temperature is $t_w = 55^\circ\text{C}$, the saturation temperature of water at atmospheric pressure is $t_s = 100^\circ\text{C}$, the vapor bulk temperatures are $t_\infty = 100^\circ\text{C}$, and the bulk vapor mass fraction is $C_{m,v,\infty} = 0.95$. Please solve the following questions:

- (1) Calculate the condensate heat transfer rate on the plate;
- (2) Calculate the condensate mass flow rate on the plate.

Solution (1): Calculate the condensate heat transfer rate on the plate

- (a) The related main equations on heat transfer

With $t_w = 55$, the reference wall subcooled grade $\frac{t_{s,\text{ref}} - t_w}{t_{s,\text{ref}}} = \frac{100 - 55}{100} = 0.45$.

Then, for evaluation of the heat transfer rate on the plate, the following equations will be used:

$$Q_{x,w} = \frac{4}{3} b \lambda_{1,w} (t_w - t_{s,\text{int}}) \left(\frac{1}{4} \text{Gr}_{x1,s} \right)^{1/4} \left(-\frac{d\theta_1}{d\eta_1} \right)_{\eta=0} \quad (20.4)$$

$$\left(-\frac{d\theta_1}{d\eta_1} \right)_{\eta=0} = a C_{mv,\infty}^b \quad (0.8 \leq C_{mv,\infty} \leq 0.999) \quad (20.8)$$

$$a = 1.6976 \left(\frac{t_{s,\text{ref}} - t_w}{t_{s,\text{ref}}} \right)^{-0.4302} \quad \left(0.4 \leq \frac{t_{s,\text{ref}} - t_w}{t_{s,\text{ref}}} \leq 1 \right) \quad (20.10)$$

$$b = -1.94 \left(\frac{t_{s,\text{ref}} - t_w}{t_{s,\text{ref}}} \right)^2 + 2.623 \left(\frac{t_{s,\text{ref}} - t_w}{t_{s,\text{ref}}} \right) - 1.1057 \quad \left(0.4 \leq \frac{t_{s,\text{ref}} - t_w}{t_{s,\text{ref}}} \leq 0.6 \right) \quad (20.12)$$

- (b) Evaluation of the interfacial vapor saturation temperature

First of all, it is very important to predict the interfacial vapor saturation temperature for prediction of heat transfer of laminar free film condensation of water vapor–air mixture. With Eq. (19.31), we have

$$T_{s,\text{int}} = 357.06 C_{mv,\infty}^{0.063} = 357.06 \times 0.95^{0.063} = 355.9 \text{ K}$$

Then,

$$t_{s,\text{int}} = 82.9^\circ\text{C}$$

- (c) Prediction of the wall dimensionless temperature gradient $\left(-\frac{d\theta_1}{d\eta_1} \right)_{\eta=0} = a C_{mv,\infty}^b$

$$a = 1.6976 \left(\frac{t_{s,\text{ref}} - t_w}{t_{s,\text{ref}}} \right)^{-0.4302} = 1.6976 \times 0.45^{-0.4302} = 2.393444$$

$$\begin{aligned} b &= -1.94 \left(\frac{t_{s,\text{ref}} - t_w}{t_{s,\text{ref}}} \right)^2 + 2.623 \left(\frac{t_{s,\text{ref}} - t_w}{t_{s,\text{ref}}} \right) - 1.1057 \\ &= -1.94 \times 0.45^2 + 2.623 \times 0.45 - 1.1057 \\ &= -0.3182 \end{aligned}$$

Then,

$$\left(-\frac{d\theta_1}{d\eta_1} \right)_{\eta_1=0} = 2.393444 \times 0.95^{-0.3182} = 2.432829$$

(d) Determination of the physical property $\lambda_{1,w}$

With $t_w = 55$, we have

$$\lambda_{1,w} = 0.648 \text{ W/(m}^\circ\text{C)}$$

(e) Calculation of the local Grashof number $\text{Gr}_{x1,s}$. With Eq. (18.18), we have

$$\text{Gr}_{x1,s} = \frac{g(\rho_{1,w} - \rho_{m,\infty})x^3}{\nu_{1,s}^2 \rho_{1,s}}$$

where

$$\rho_{1,w} = -4.48 \times 10^{-3} t_w^2 + 999.9 = -4.48 \times 10^{-3} \times 55^2 + 999.9 = 986.31 \text{ kg/m}^3$$

$$\rho_{1,s} = -4.48 \times 10^{-3} t_{s,\text{int}}^2 + 999.9 = -4.48 \times 10^{-3} \times 82.9^2 + 999.9 = 970.41 \text{ kg/m}^3$$

$$\begin{aligned} \mu_{1,s} &= \exp \left(-1.6 - \frac{1150}{t_{s,\text{int}} + 273} + \left(\frac{690}{t_{s,\text{int}} + 273} \right)^2 \right) \times 10^{-3} \\ &= \exp \left(-1.6 - \frac{1150}{82.9 + 273} + \left(\frac{690}{82.9 + 273} \right)^2 \right) \times 10^{-3} \\ &= 342 \times 10^{-6} \text{ kg/(m s)} \end{aligned}$$

$$\nu_{1,s} = \mu_{1,s} / \rho_{1,s} = 342 \times 10^{-6} / 970.41 = 0.3526 \times 10^{-6} \text{ m}^2/\text{s}$$

With Eq. (19.15)

$$\rho_{m,\infty} = \frac{\rho_{v,\infty} \rho_{g,\infty}}{(1 - C_{mv,\infty}) \rho_{v,\infty} + C_{mv,\infty} \rho_{g,\infty}}$$

where $\rho_{v,\infty} = 0.5977 \text{ kg/m}^3$, and $\rho_{g,\infty} = 0.9336 \text{ kg/m}^3$ at $t_\infty = 100^\circ\text{C}$

Then,

$$\begin{aligned}\rho_{m,\infty} &= \frac{\rho_{v,\infty}\rho_{g,\infty}}{(1 - C_{mv,\infty})\rho_{v,\infty} + C_{mv,\infty}\rho_{g,\infty}} \\ &= \frac{0.5977 \times 0.9336}{(1 - 0.95) \times 0.5977 + 0.95 \times 0.9336} = 0.60865 \text{ kg/m}^3\end{aligned}$$

$$\text{Gr}_{x1,s} = \frac{g(\rho_{l,w} - \rho_{m,\infty})x^3}{\nu_{1,s}^2 \rho_{1,s}} = \frac{9.8 \times (986.3 - 0.60865) \times 0.05^3}{(0.3526 \times 10^{-6})^2 \times 970.4} = 1.0 \times 10^{10}$$

(f) Summary of the necessary physical properties in the calculation

The necessary physical properties in the calculation are summarized in Table 20.11.

(g) Calculation of the condensate heat transfer rate on the plate

The condensate heat transfer rate on the plate is

$$\begin{aligned}Q_x &= \frac{4}{3}b\lambda_{l,w}(t_w - t_{s,\text{int}}) \left(\frac{1}{4}\text{Gr}_{x1,s}\right)^{1/4} \left(-\frac{d\theta_1}{d\eta_1}\right)_{\eta=0} \\ &= \left(\frac{4}{3} \times 0.1 \times 0.648\right) \times (55 - 82.9) \times \left(\frac{1}{4} \times 1.0 \times 10^{10}\right)^{1/4} \times 2.432829 \\ &= -1311.3 \text{ W}\end{aligned}$$

The negative sign notes that the heat flux is to the wall surface from the fluids.

Solution (2): Calculate the condensate mass flow rate on the plate

With Eq. (20.17), the condensate mass flow rate on the plate is evaluated by

$$G_x = \frac{4}{3}b \cdot \mu_{1,s} \left(\frac{1}{4}\text{Gr}_{x1,s}\right)^{1/4} \Phi_s$$

where the condensate mass flow rate on the plate for the reference wall subcooled grade $\frac{(\Delta t_w)_s}{t_s} = 0.45$ and the bulk vapor mass fraction $C_{mv,\infty} = 0.95$ is calculated by

$$\Phi_s = aC_{mv,\infty}^b \quad (0.8 \leq C_{mv,\infty} \leq 0.999) \quad (20.25)$$

$$a = 0.0535 \text{Ln} \left(\frac{t_{s,\text{ref}} - t_w}{t_{s,\text{ref}}}\right) + 0.0999 \quad \left(0.4 \leq \frac{t_{s,\text{ref}} - t_w}{t_{s,\text{ref}}} \leq 1\right) \quad (20.27)$$

$$b = 5.975 \left(\frac{t_{s,\text{ref}} - t_w}{t_{s,\text{ref}}}\right)^2 - 7.7835 \left(\frac{t_{s,\text{ref}} - t_w}{t_{s,\text{ref}}}\right) + 3.1067 \quad \left(0.4 \leq \frac{t_{s,\text{ref}} - t_w}{t_{s,\text{ref}}} \leq 0.6\right) \quad (20.29)$$

Then,

Table 20.11 The related physical properties of water and water vapor

Medium	Water ($t_s = 100^\circ\text{C}$ for $C_{\text{inv},\infty} = 1$)					
Temperature ($^\circ\text{C}$)	t_w	$t_{s,\text{int}}$	t_f	$t_{s,\text{int}}$	t_∞	Water vapor
	55	82.9	68.95	82.9	82.9	
Physical properties	$\rho_{l,w}$ (kg/m^3)	$\rho_{l,s}$ (kg/m^3)	$\nu_{l,f}$ (m^2/s)	$\rho_{m,s}$	$\nu_{m,\infty}$ (m^2/s)	$\rho_{m,\infty}$
	986.3	970.4	0.3526×10^{-6}	0.000342		
		$\lambda_{l,w}$ (($\text{W}/(\text{m}^\circ\text{C})$))	h_{fg} (kJ/kg)	$\mu_{l,s}$ ($\text{kg}/(\text{m}\cdot\text{s})$)	$\nu_{m,\infty}$ (m^2/s)	$\rho_{m,\infty}$
		0.648		0.000342		

$$\begin{aligned}
 a &= 0.0535 \text{Ln} \left(\frac{t_{s,\text{ref}} - t_w}{t_{s,\text{ref}}} \right) + 0.0999 = 0.0535 \text{Ln}(0.45) + 0.0999 = 0.05718 \\
 b &= 5.975 \left(\frac{t_{s,\text{ref}} - t_w}{t_{s,\text{ref}}} \right)^2 - 7.7835 \left(\frac{t_{s,\text{ref}} - t_w}{t_{s,\text{ref}}} \right) + 3.1067 \\
 &= 5.975(0.45)^2 - 7.7835(0.45) + 3.1067 = 0.814063 \\
 \Phi_s &= a C_{\text{mv},\infty}^b = 0.05718 \times 0.95^{0.814063} = 0.05484
 \end{aligned}$$

The condensate mass flow rate on the plate is

$$\begin{aligned}
 G_x &= \frac{4}{3} b \cdot \mu_{1,s} \left(\frac{1}{4} \text{Gr}_{x1,s} \right)^{1/4} \Phi_s \\
 &= \frac{4}{3} \times 0.1 \times 0.000342 \times \left(\frac{1}{4} \times 1.0 \times 10^{10} \right)^{1/4} \times 0.05484 = 0.000559 \text{ kg/s} \\
 &= 0.000559 \text{ kg/s} \\
 &= 2.01 \text{ kg/h}
 \end{aligned}$$

20.12 Exercises

- Follow Example 1, in which only the wall temperature is changed to 75 °C, and all other conditions are kept. Please solve the following questions:
 - calculate the condensate heat transfer rate on the plate;
 - calculate the condensate mass flow rate on the plate;
 - calculate the condensate film thickness for $x = 0.01, 0.02, 0.03, 0.04,$ and 0.05 m respectively.
- Which variable dominates the condensate heat transfer on laminar free convection film condensation of vapor–gas mixture? What does this variable depend on?
- Which variable dominates the condensate mass transfer on laminar free film condensation of vapor–gas mixture? Which conditions does this variable depend on?
- In the theoretical analysis equation on condensate heat transfer of the laminar film convection condensation of vapor–gas mixture, which variable is the only one no-given condition for prediction of condensate heat transfer? Which conditions does this variable depend on?
- In the theoretical analysis equation on condensate mass transfer of the laminar film condensation of vapor–gas mixture, which variable is the only one no-given condition for prediction of condensate mass transfer? Which conditions does this variable depend on?
- Which physical variable dominates condensate heat transfer for the laminar free convection film condensation of vapor–gas mixture, why?

- 7 . Which physical variable dominates condensate mass transfer for the laminar free convection film condensation of vapor–gas mixture, why?
8. Please describe simply the effects of non-condensable gas, and wall subcooled grade on condensate heat and mass transfer of the laminar free convection film condensation of vapor–gas mixture.
9. Please explain why heat and mass transfer of the laminar free convection film condensation of vapor–gas mixture is so different from that of pure vapor?
10. What is the definition of the reference wall subcooled grade?

Reference

1. D.Y. Shang, L.C. Zhong, Extensive study on laminar free film condensation from vapor-gas mixture. *Int. J. Heat Mass Trans.* **51**, 4300–4314 (2008)

Part IV
Gravity-Driven Film Flow
of Non-Newtonian Fluids

Chapter 21

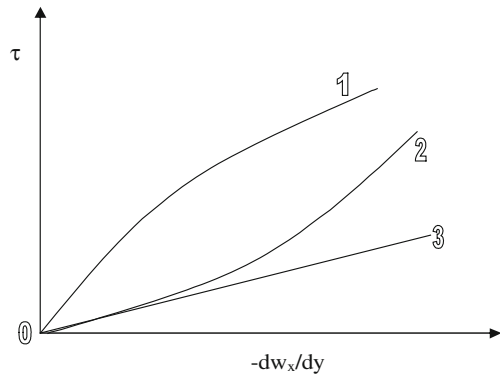
Hydrodynamics of Falling Film Flow of Non-Newtonian Power-Law Fluids

Abstract The new similarity analysis method has been applied to extensively study the gravity-driven flow of a non-Newtonian liquid film along inclined surface. The partial differential equations governing the hydrodynamics of the power-law fluid are transformed exactly into a set of two ordinary differential equations, which can be calculated numerically to an arbitrary degree of accuracy. The non-linearity of the momentum boundary layer problem for power-law fluid increases with increasing pseudo-plasticity $|1 - n|$ and the variable grid spacing is therefore increasingly important. The solutions of the system of dimensionless ordinary differential equations depends only on the single parameter n , and all other parameters, like the streamwise location x , the fluid properties K/ρ , and the component of the gravitational acceleration along the surface $g \cdot \cos\alpha$ have been combined into a generalized local Reynolds number Re_x and dimensionless velocity W_x and W_y . Various flow characteristics can thus be expressed only in term of n and Re_x . In order to determine x_0 the particular position x_0 , at which the entire freestream has been entrained into the momentum boundary layer, and the associated critical film thickness $\delta_1(x_0)$, knowledge about the total mass flow rate ρQ within the film is also required, together with the new dimensionless mass flux parameter ϕ . The latter quantity, which depends on the dimensionless boundary layer thickness η_{δ_1} and the velocity components W_{x,δ_1} and W_{y,δ_1} at the edge of the boundary layer, is generally obtained as the numerical solution of the transformed problem and turned out to be function only of the power-law index n . However, to facilitate rapid and accurate estimate of ϕ , polynomial curve-fit formulas have been developed on the basis of the new similarity analysis model.

21.1 Introduction

For heat-sensitive materials, short residence time and close temperature controls during heat transfer process are essential, which can be achieved by allowing a liquid to flow in a thin falling film along a solid surface. Such cooling techniques have

Fig. 21.1 Diagram for power-law fluids. 1 Pseudo-plastic fluid. 2 Dilatant fluid. 3 Newtonian fluid



been widely used in many industrial applications, which are especially the chemical engineering operations, food and polymer processing industries, cooling systems, distillation, evaporators, ocean thermal energy conversion systems (OTEC), molten plastics, pulps, coating equipment, etc. Such heat exchangers are characterized by high heat transfer coefficients at low mass flow rates and small temperature differences, and invite a lot of work for the extensive studies.

Fully developed laminar film flow of non-Newtonian power-law fluids along a plane surface was conducted by Astarita et al. [1], who measured the film thickness for various inclinations and flow rates. Later, Therien et al. [2] conducted a similar study, in which experimental data for the film thickness were compared with an analytical expression for the thickness of fully developed films of power-law fluids. Sylvester et al. [3] also measured the film thickness as a function of the volumetric flow rate, but they primarily focused on the onset of rippling on the film surface and the characteristics of wavy film.

Yang and Yarbrough [4, 5], Murthy and Sarma [6, 7], Tekic et al. [8], Andersson and Irgens [9] among others have used the integral method approach to study the hydrodynamics of gravity-driven power law films. Theoretical analyses of hydrodynamics of gravity-driven power-law fluid films have been studied by means of similarity analysis by Andersson and Irgens [10, 11], Yang and Yarbrough [4, 5]. Murthy and Sarma [6] extended the conventional integral analysis for Newtonian films to cover power-law fluids. Later, Murthy and Sarma [7] included the effect of interfacial drag at the liquid–vapor interface in a similar analysis, while Tekic et al. [8] presented results accounted for the streamwise pressure gradient and surface tension. Andersson and Irgens [9] explored the influence of the rheology of the film on the hydrodynamic entrance length.

A different approach was adopted by Andersson and Irgens [10, 11], namely to divide the accelerating film flow into three regions shown schematically in Fig. 21.1, the boundary layer region, the fully viscous region, and the developed flow region. While the boundary layer region is divided into a developing viscous boundary layer and an external inviscid freestream. They further demonstrated that a similarity transformation exists, such that the boundary layer momentum equation for power-law

fluids is exactly transformed into a Falkner-Skan type ordinary differential equation. The resulting two-point boundary-value problem was solved numerically with a standard shooting technique based on classical 4th-order Runge–Kutta integration in combination with a Newton iteration procedure. Numerical results were obtained for values of the power-law index n in the range $0.5 \leq n \leq 2.0$. Andersson and Irgens [11] provided a relative extensive review on the study of hydrodynamics of a falling film flow of power law fluids.

The dissolution of a soluble wall and the subsequent penetration of the solute into the non-Newtonian liquid film were considered by Astarita [12]. He provided the mass transfer rate between the wall and the hydrodynamically fully developed film, with an assumption of velocity near the wall to vary linearly with the distance from the wall. Mashelkar and Chavan [13] provided a more general solution of this problem.

More recently, Andersson and Shang [14] provided a development on formulation of a new similarity transformation for extensive studies of accelerating non-Newtonian film flow. The partial differential equations governing the hydrodynamics of the flow of a power-law fluid on an inclined plane surface are transformed into a set of two ordinary differential equations by means of the velocity component approach. Although the analysis is applicable for any angle of inclination α ($0 \leq \alpha \leq \pi/2$), the resulting one-parameter problem involves only the power-law index n . Nevertheless, physically essential quantities, like the velocity components and the skin-friction coefficient, do depend on α and the relevant relationships are deduced between the vertical and inclined cases. Accurate numerical similarity solutions are provided for n in the range from 0.1 to 2.0. The present method enables solutions to be obtained also for highly pseudo-plastic films, i.e. for n below 0.5. The mass flow rate entrained into the momentum boundary layer from the inviscid freestream is expressed in term of a dimensionless mass flux parameter ϕ , which depends on the dimensionless boundary layer thickness and the velocity components at the edge of the viscous boundary layer, which is thus an integral part of the similarity solution, turns out to decrease monotonically with n . Using this new model, they were able to determine some difficult issues, such as the mass flow rate entrained into the boundary from the free stream and the length of boundary layer region, etc.

In this chapter, before we focus on recent developments on hydrodynamics analysis for the boundary layer region, we introduce briefly the principal types of power-law fluids.

21.2 Principal Types of Power-Law Fluids

21.2.1 Newtonian Fluids

In the previous chapters, we have presented the free convection, film boiling, and film condensation, where all the fluids dealt with are Newtonian fluids. Newtonian

fluids are those which follow Newton's law, i.e.

$$\tau = -\mu \frac{dw_x}{dy} \quad (21.1)$$

for special coordinate. Here, τ is shear force, and μ is the absolute viscosity, a constant independent of shear rate. If a fluid does not follow Eq. (21.1), it is a non-Newtonian fluid. Figure 21.1 shows shear stress τ is proportional to the shear rate $-\frac{dw_x}{dy}$. The line for a Newtonian fluid is straight, the slope being μ .

However, a non-Newtonian fluid is a fluid in which the viscosity changes with the applied shear force. As a result, Non-Newtonian fluids may not have a well-defined viscosity.

21.2.2 Power-Law Fluids

Power-law fluids can be subdivided into the following types according to the range of their power-law index:

(i) Non-Newtonian pseudo-plastic fluids

For such fluids, the apparent viscosity will be reduced with rate of shear. The shape of the flow curve is shown in Fig. 21.1, and it generally can be represented by a *power-law equation* (sometimes called the *Ostwald-de Waele equation*).

$$\tau = K \left(-\frac{dw_x}{dy} \right)^n \quad (n < 1) \quad (21.2)$$

where K is coefficient of consistency, and n is the power-law index. The apparent viscosity μ_a in Eq. (21.3) is obtained from Eqs. (21.1) and (21.2) and decreases with increasing shear rate:

$$\mu_a = K \left(-\frac{dw_x}{dy} \right)^{n-1} \quad (21.3)$$

A common household example of a strongly shear-thinning fluid is styling gel, which primarily composed of water and a fixative such as a vinyl acetate/vinyl pyrrolidone copolymer (PVP/PA). The majority of non-Newtonian fluids is in this category and includes polymer solutions or melts, greases, starch suspensions, mayonnaise, biological fluids, detergent slurries, dispersion media in certain pharmaceuticals, and paints. Additionally, some colloids, clay, milk, gelatine, blood, and liquid cement also belong to pseudo-plastic fluids.

(ii) Non-Newtonian dilatant fluids

For dilatant fluids the power-law equation is often applicable, but with $n > 1$ as shown in Fig. 21.2, which means that their apparent viscosity will increase with rate of shear, i.e.

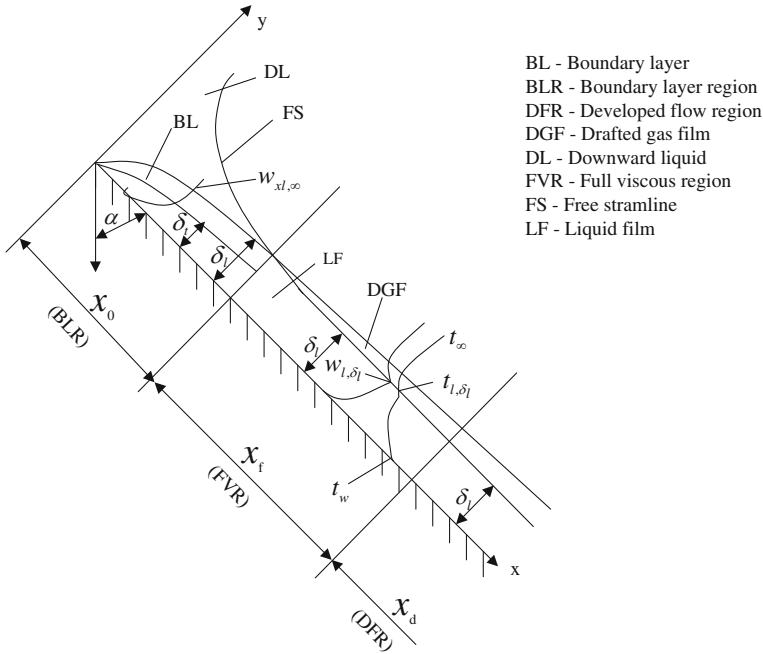


Fig. 21.2 Schematic representation of accelerating film flow

$$\tau = K \left(-\frac{dw_x}{dy} \right)^n \quad (n > 1) \tag{21.4}$$

These fluids, or shear-thickening fluids are far less common than pseudo-plastic fluids, and their flow behavior (Fig. 21.1) shows an increase in apparent viscosity with increasing shear rate.

From Eq. (21.1) it is found that Newtonian fluid is the power-law fluid with a unit power-law index, where the shear stress is directly proportional to the shear rate. Therefore, Newtonian fluids can be regarded as special *non-Newtonian power-law fluids*. In addition, Newtonian fluids include many of the most common fluids, such as water, most aqueous solutions, oils, corn syrup, glycerine, air, and other gases.

So far, the principal types of power-law fluids can be summarized as Table 21.1.

21.3 Physical Model and Governing Partial Differential Equations

Consider the accelerating laminar flow of a non-Newtonian power-law liquid film down along an inclined plane surface, as shown schematically in Fig. 21.3. The

Table 21.1 Types of power-law fluids

Name of the power-law fluid	Range of power-law index n	Example included
Pseudo-plastic fluid (majority of non-Newtonian fluids)	$n < 1$	Polymer solutions or melts, greases, starch suspensions, mayonnaise, biological fluids, detergent slurries, dispersion media in certain pharmaceuticals, paints, styling gel, some colloids, clay, milk, gelatine, blood, and liquid cement
Newtonian fluid (many of the most common fluids)	$n = 1$	Such as water, most aqueous solutions, oils, corn syrup, glycerine, air, and other gases
Dilatant fluid (far less common than pseudo-plastic fluid)	$n > 1$	Some corn flour-sugar solutions, wet beach sand, starch in water, potassium silicate in water, some solutions containing high concentrations of powder in water, an uncooked paste of cornstarch and water, concentrated solution of sugar in water, and suspensions of rice starch or corn starch

incompressible and inelastic fluid is assumed to obey the Ostwald-de-Waele power-law model and the action of viscous stresses is confined to the developing momentum boundary layer adjacent to the solid surface. The basic conservation equations for mass and momentum within the viscous boundary layer are:

$$\frac{\partial w_x}{\partial x} + \frac{\partial w_y}{\partial y} = 0 \tag{21.5}$$

$$w_x \frac{\partial w_x}{\partial x} + w_y \frac{\partial w_x}{\partial y} = g \cos \alpha + n \frac{K}{\rho} \left(\frac{\partial w_x}{\partial y} \right)^{n-1} \frac{\partial^2 w_x}{\partial y^2} \tag{21.6}$$

with boundary conditions

$$y = 0 : w_x = 0, \quad w_y = 0 \tag{21.7}$$

$$y = \delta_l : w_x = w_{x,\infty} \tag{21.8}$$

where w_x and w_y are velocity exponents in x and y directions respectively, while g and α denote the gravitational acceleration and the angle of inclination of the plane wall. Here it has been anticipated that $\frac{\partial w_x}{\partial y} \geq 0$ throughout the entire the film. The fluid physical properties ρ , c_p , K and n assumed to be constant in the present analysis are density, specific heat, coefficient of consistency, and power-law index, respectively. The two-parameter rheological model represents *pseudo-plastic or shear-thinning fluids* if the *power-law index* n smaller than unity and dilatant or shear-thickening fluids for $n > 1$. The deviation of n from unity indicates the degree of deviation from *Newtonian*

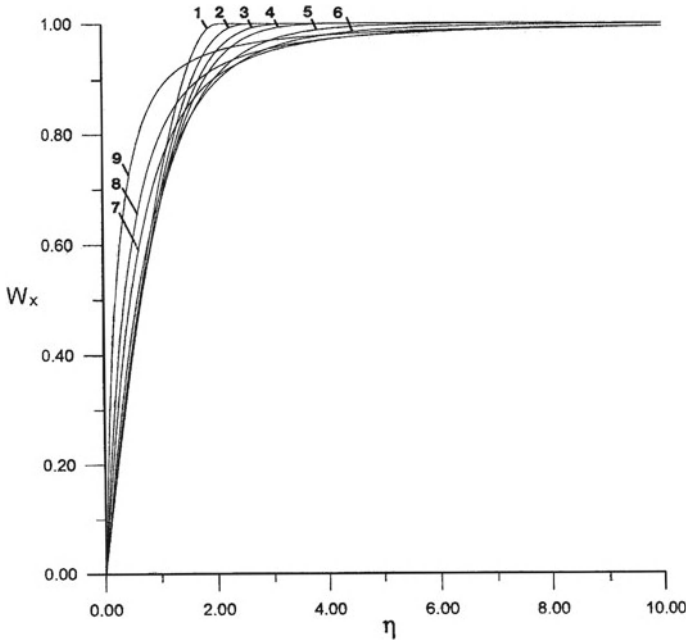


Fig. 21.3 Numerical solutions for the streamwise velocity component W_x , cited from Andersson and Shang [14] (Curves 1–9: $n = 2.0, 1.5, 1.2, 1.0, 0.7, 0.5, 0.3, 0.2, 0.1$)

rheology and the particular case $n = 1$ represents a Newtonian fluid with dynamic coefficient of viscosity K .

No-slip and impermeability at the inclined wall $y = 0$ are expressed by the boundary conditions given by Eq. (21.7), while the outer condition, Eq. (21.8), assures that the velocity component w_x within the boundary layer approaches the external velocity

$$w_{x,\infty} = \sqrt{2gx \cos \alpha} \tag{21.9}$$

at the edge $y = \delta_1$ of the boundary layer. Since the friction flow between the viscous boundary layer and the free streamline bordering the constant-pressure atmosphere is quasi-one-dimensional, the simple solution given by Eq. (21.9) is readily derived from Eq. (21.6) by assuming $w_{x,\infty} = 0$ (and infinite film thickness) at the inlet $x = 0$.

It may be worthwhile to recall that the boundary layer theory conventionally adopted in the analysis of thin-film flow may be inadequate if the Reynolds number is too low. Wu and Thompson [15] compared boundary layer theory predictions with solutions of the full Cauchy equation for flow of a shear-thinning power-law fluid past a flat plate of length L . They found that the Reynolds number Re_x (with $x = L$), below which the boundary layer approximations become inaccurate, decreased from 120 for a Newtonian fluid ($n = 1$) to 4.5 for a highly pseudo-plastic fluid ($n = 0.1$).

21.4 A New Similarity Transformation

Incidentally, as pointed out by Andersson and Iirgens [10], the external velocity, Eq. (21.9), belong to the Falkner-Skan class of freestreams $w_{x,\infty} \propto x^m$ which permits a similarity transformation of the momentum boundary layer equation even for power-law fluids. A generalized Falkner-Skan type of transformation was therefore introduced by Andersson and Iirgens [10, 11]. However, in the recent study, a new similarity analysis method is applied for transformation of governing partial differential equations of non-Newtonian power-law fluids [14], which unlike the Falkner-Skan type of approach does not involve the stream function.

Let us first introduce the related dimensionless similarity variables defined for similarity transformation of the governing partial equations.

Dimensionless similarity variables

According to the study in Ref. [14], a dimensionless similarity variable is defined as

$$\eta = \frac{y}{x} \text{Re}_x^{1/(n+1)} \quad (21.10)$$

where

$$\text{Re}_x = \frac{x^n (w_{x,\infty})^{2-n} \rho}{K} \quad (21.11)$$

is a generalized local Reynolds number. The dimensionless velocity components are defined as

$$W_x(\eta) = \frac{w_x}{\sqrt{2gx \cos \alpha}} \quad (21.12)$$

$$W_y(\eta) = \frac{w_y}{\sqrt{2gx \cos \alpha}} \text{Re}_x^{\frac{1}{n+1}} \quad (21.13)$$

for the x and y directions, respectively. These dimensionless variables analogous to the similarity transformation used in the parts 1 and 2 of this book for free convection and film flows for the particular parameter value $n = 1$.

Then, the partial differential equations given by Eqs. (21.5) and (21.6) and their boundary equations given by Eqs. (21.7) and (21.8) are now transformed as follows:

Derivation of Eq. (21.5):

From Eqs. (21.10)–(21.11), we have

$$\begin{aligned} \frac{\partial \eta}{\partial x} &= \frac{\partial}{\partial x} \left[\frac{y}{x} \text{Re}_x^{1/(n+1)} \right] \\ &= \frac{\partial}{\partial x} \left[y \left(\frac{(2g \cos \alpha)^{\frac{2-n}{2}} \rho}{K} \right)^{\frac{1}{n+1}} x^{-\frac{n}{2(n+1)}} \right] \end{aligned}$$

$$\begin{aligned}
 &= -\frac{n}{2(n+1)} \left[y \left(\frac{(2g \cos \alpha)^{\frac{2-n}{2}} \rho}{K} \right)^{\frac{1}{n+1}} x^{-\frac{n}{2(n+1)} - 1} \right] \\
 &= -\frac{n}{2(n+1)} \frac{y}{x} \left(\frac{x^n (2gx \cos \alpha)^{\frac{2-n}{2}} \rho}{K} \right)^{\frac{1}{n+1}} x^{-\frac{n+2}{2(n+1)}} x^{-\frac{n}{2(n+1)}} \\
 &= -\frac{n}{2(n+1)} \eta x^{-1} \\
 \frac{\partial \eta}{\partial y} &= \frac{1}{x} (\text{Re}_x)^{\frac{1}{n+1}}
 \end{aligned}$$

Then,

$$\begin{aligned}
 \frac{\partial w_x}{\partial x} &= \sqrt{2gx \cos \alpha} \frac{dW_x}{d\eta} \frac{\partial \eta}{\partial x} + \sqrt{\frac{g \cos \alpha}{2x}} W_x \\
 &= \sqrt{2gx \cos \alpha} \frac{dW_x}{d\eta} \left(-\frac{n}{2(n+1)} \eta x^{-1} \right) + \sqrt{\frac{g \cos \alpha}{2x}} W_x \\
 &= -\sqrt{\frac{g \cos \alpha}{2x}} \frac{dW_x}{d\eta} \frac{n}{(n+1)} \eta + \sqrt{\frac{g \cos \alpha}{2x}} W_x \\
 \frac{\partial w_y}{\partial y} &= \sqrt{2gx \cos \alpha} (\text{Re}_x)^{-1/(n+1)} \frac{dW_y}{d\eta} \frac{\partial \eta}{\partial y} \\
 &= \sqrt{2gx \cos \alpha} (\text{Re}_x)^{-1/(n+1)} \frac{dW_y}{d\eta} \frac{1}{x} (\text{Re}_x)^{\frac{1}{n+1}} \\
 &= \sqrt{\frac{2g \cos \alpha}{x}} \frac{dW_y}{d\eta}
 \end{aligned}$$

Therefore, Eq. (19.5) is changed into

$$-\sqrt{\frac{g \cos \alpha}{2x}} \frac{dW_x}{d\eta} \frac{n}{(n+1)} \eta + \sqrt{\frac{g \cos \alpha}{2x}} W_x + \sqrt{\frac{2g \cos \alpha}{x}} \frac{dW_y}{d\eta} = 0$$

Simplify the above equation we have

$$W_x - \frac{n}{n+1} \eta \frac{dW_x}{d\eta} + 2 \frac{dW_y}{d\eta} = 0 \tag{21.14}$$

Derivation of Eq. (21.6):

With Eqs. (21.12) and (21.13) we have

$$\frac{\partial w_x}{\partial y} = \sqrt{2gx \cos \alpha} \frac{dW_x}{d\eta} \frac{1}{x} (\text{Re}_x)^{\frac{1}{n+1}} = \sqrt{\frac{2g \cos \alpha}{x}} \frac{dW_x}{d\eta} (\text{Re}_x)^{\frac{1}{n+1}}$$

$$\frac{\partial^2 w_x}{\partial y^2} = \sqrt{\frac{2g \cos \alpha}{x}} \frac{d^2 W_x}{d\eta^2} \frac{1}{x} (\text{Re}_x)^{\frac{2}{n+1}}$$

Then, Eq. (21.6) is changed into

$$\begin{aligned} & \sqrt{2gx \cos \alpha} W_x \left(-\sqrt{\frac{g \cos \alpha}{2x}} \frac{dW_x}{d\eta} \frac{n}{(n+1)} \eta + \sqrt{\frac{g \cos \alpha}{2x}} W_x \right) \\ & + (\sqrt{2gx \cos \alpha} W_y) (\text{Re}_x)^{-1/(n+1)} \sqrt{\frac{2g \cos \alpha}{x}} \frac{dW_x}{d\eta} (\text{Re}_x)^{\frac{1}{n+1}} \\ & = g \cos \alpha + n \frac{K}{\rho_l} \left(\sqrt{\frac{2g \cos \alpha}{x}} \frac{dW_x}{d\eta} (\text{Re}_x)^{\frac{1}{n+1}} \right)^{(n-1)} \\ & \quad \times \sqrt{\frac{2g \cos \alpha}{x}} \frac{d^2 W_x}{d\eta^2} \frac{1}{x} (\text{Re}_x)^{\frac{2}{n+1}} \end{aligned}$$

or

$$\begin{aligned} & W_x \left(-g \cos \alpha \frac{dW_x}{d\eta} \frac{n}{(n+1)} \eta + g \cos \alpha W_x \right) + (W_y) 2g \cos \alpha \frac{dW_x}{d\eta} \\ & = g \cos \alpha + n \frac{K}{\rho} \left(\frac{dW_x}{d\eta} \right)^{(n-1)} \left(\frac{2g \cos \alpha}{x} \right)^{\frac{n}{2}} \frac{d^2 W_x}{d\eta^2} \frac{1}{x} \text{Re}_x \end{aligned}$$

The above equation is simplified to

$$\begin{aligned} & W_x \left(-\frac{dW_x}{d\eta} \frac{n}{(n+1)} \eta + W_x \right) + (W_y) 2 \frac{dW_x}{d\eta} \\ & = 1 + n \frac{K}{\rho} \left(\frac{dW_x}{d\eta} \right)^{(n-1)} \frac{2}{2gx \cos \alpha} \left(\frac{2gx \cos \alpha}{x^2} \right)^{\frac{n}{2}} \frac{d^2 W_x}{d\eta^2} \text{Re}_x \end{aligned}$$

With Eq. (21.9) the above equation is changed into

$$\begin{aligned} & W_x \left(-\frac{dW_x}{d\eta} \frac{n}{(n+1)} \eta + W_x \right) + (W_y) 2 \frac{dW_x}{d\eta} \\ & = 1 + n \left(\frac{dW_x}{d\eta} \right)^{(n-1)} \frac{K}{\rho} \frac{2}{x^n w_{x,\infty}^{2-n}} \frac{d^2 W_x}{d\eta^2} \text{Re}_x \end{aligned}$$

With the definition of local Reynolds number shown in Eq. (21.11), the above equation can be expressed as

$$W_x \left(-\frac{dW_x}{d\eta} \frac{n}{(n+1)} \eta + W_x \right) + (W_y)^2 \frac{dW_x}{d\eta} = 1 + n \left(\frac{dW_x}{d\eta} \right)^{(n-1)} 2\text{Re}_x^{-1} \frac{d^2W_x}{d\eta^2} \text{Re}_x$$

Finally, Eq. (21.6) is transformed as

$$W_x \left(-\frac{n}{(n+1)} \eta \frac{dW_x}{d\eta} + W_x \right) + 2W_y \frac{dW_x}{d\eta} = 1 + 2n \left(\frac{dW_x}{d\eta} \right)^{(n-1)} \frac{d^2W_x}{d\eta^2} \quad (21.15)$$

Thus, the governing partial differential Eqs.(21.5) and (21.6) are transformed to the dimensionless equations(21.14) and (21.15), respectively with the related dimensionless boundary conditions

$$\eta = 0: \quad W_x(\eta) = 0, \quad W_y(\eta) = 0, \quad (21.16)$$

$$\eta = \eta_{\delta_1}: \quad W_x(\eta) = 1 \quad (21.17)$$

Evidently, the power-law index n is the only explicit parameter in the transformed problem.

21.5 Numerical Solutions

The nonlinear two-point boundary value problem defined by Eqs. (21.14–21.17) was solved numerically for several values of the power-law index in the range $0.1 \leq n \leq 2.0$. Here, the shooting method was adopted. First, Eqs. (21.14) and (21.15) were written as a system of three first-order differential equations, which was solved by means of fifth-order Runge–Kutta integration. Then, a Newton iteration procedure was employed to satisfy the outer boundary condition, Eq. (21.17). Concerning the numerical procedure, the present fifth-order scheme utilizes variable grid spacing.

Some of the velocity profiles $W_x(\eta)$ computed by Andersson and Shang [14] are shown in Fig. 21.4. The power-law index appears to have a substantial effect on the velocity distribution within the boundary layer and, as observed already by Andersson and Irgens [10], the most striking feature being the monotonic thinning of the boundary layer with increasing n -values. This is fully consistent with the findings for other 2D plane flows, for instance the non-Newtonian analogue of the classical Blasius problem, i.e. flow past a semi-infinite that plate, which was first solved by Acrivos et al. [16] and more recently by Andersson and Toften [17].

The nonlinearity of the highest-order derivative in Eq.(21.15) increases with increasing deviation of the power-law index n from unity. The thickening of the boundary layer with increasing pseudo-plasticity $1 - n$, in combination with the steeper slope of the dimensionless velocity profile $W_x(\eta)$, makes the mathematical problem defined by Eqs. (21.14–21.17) increasingly stiff. In fact, the shooting method becomes gradually less attractive as the distance (in boundary layer coordinates η) from the wall to the outer edge of the calculation domain, at which the condition

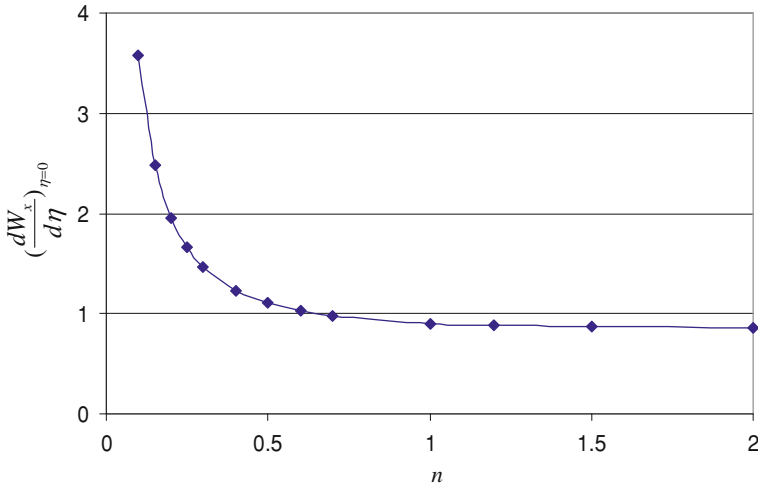


Fig. 21.4 Numerical solutions of the dimensionless velocity gradient for different values of the power-law index n

$W_x(\eta) = 1$ should be satisfied, increases. This is most likely the reason why Andersson and Irgens [10] failed to obtain converged solutions for highly pseudo-plastic fluid with $n < 0.5$. In the present study, however, this difficulty was remedied by using variable grid spacing.

21.6 Local Skin-Friction Coefficient

The gradient of the dimensionless velocity $W_x(\eta)$ at the wall $\eta = 0$ is single most important characteristic of the solution. This is because the local skin-friction coefficient $C_{x,f}$ is a dimensionless measure of the shear stress $\tau = K \left(\frac{\partial w_x}{\partial y}\right)^n$ at the wall, i.e.

$$C_{x,f} \equiv \frac{\tau_w}{\frac{1}{2}\rho w_{x,\infty}^2} = \frac{K \left[\left(\frac{\partial w_x}{\partial y}\right)_{\eta=0} \right]^n}{\frac{1}{2}\rho w_{x,\infty}^2}$$

With the dimensionless variables in Eqs.(21.10–21.13), the above equation is changed into

$$\begin{aligned}
 C_{x,f} &= \frac{K \left[\sqrt{\frac{2g \cos \alpha}{x}} \left(\frac{dW_x}{d\eta} \right)_{\eta=0} (\text{Re}_x)^{\frac{1}{n+1}} \right]^n}{\frac{1}{2} \rho w_{x,\infty}^2} \\
 &= 2 \frac{K \left[\sqrt{\frac{2g \cos \alpha}{x}} (\text{Re}_x)^{\frac{1}{n+1}} \right]^n}{\rho w_{x,\infty}^2} \left[\left(\frac{dW_x}{d\eta} \right)_{\eta=0} \right]^n
 \end{aligned}$$

where

$$\begin{aligned}
 \frac{K \left[\sqrt{\frac{2g \cos \alpha}{x}} (\text{Re}_x)^{\frac{1}{n+1}} \right]^n}{\rho w_{x,\infty}^2} &= \frac{K \left[\sqrt{\frac{2gx \cos \alpha}{x}} \right]^n}{\rho w_{x,\infty}^2} (\text{Re}_x)^{\frac{n}{n+1}} \\
 &= \frac{K}{x^n (w_{x,\infty})^{2-n} \rho} (\text{Re}_x)^{\frac{n}{n+1}} \\
 &= (\text{Re}_x)^{-1} (\text{Re}_x)^{\frac{n}{n+1}} \\
 &= (\text{Re}_x)^{-\frac{1}{n+1}}
 \end{aligned}$$

Then, with the present new dimensionless variables, the local skin-friction coefficient $C_{x,f}$ is expressed as

$$C_{x,f} \equiv \frac{\tau_w}{\frac{1}{2} \rho w_{x,\infty}^2} = 2 \text{Re}_x^{-1/(n+1)} \left[\left(\frac{dW_x}{d\eta} \right)_{\eta=0} \right]^n \tag{21.18}$$

The numerical results of the dimensionless velocity gradient at the wall $\left(\frac{dW_x}{d\eta} \right)_{\eta=0}$ are given in Table 21.2 [14] and shown in Fig. 21.4 from which it is observed that the wall gradient gradually decreases with increasing n . It is noteworthy, however, that since the local Reynolds number Re_x , as defined in Eq. (21.11), varies as $\propto x^{(n+2)/2}$, the streamwise variation of C_f becomes $C_f \propto x^{-\frac{n+2}{2(n+1)}}$, i.e. the *skin-friction coefficient* decreases in the streamwise direction, irrespective of the value of the power-law index.

In order to assess the accuracy of the present numerical results, comparisons are made with the calculations by Andersson and Irgens [10] according to the relationship

$$\left(\frac{dW_x}{d\eta} \right)_{\eta=0} = \left(\frac{3}{4} \right)^{\frac{1}{n+1}} f''(0) \tag{21.19}$$

where f denotes the Falkner-Skan type stream function and the primes signify differentiation with respect to the similarity variable adopted in their analysis. Data obtained from the approximate interpolation formula

Table 21.2 Computed variation of $\left(\frac{dW_x}{d\eta}\right)_{\eta=0}$ with power-law index n , cited from Andersson and Shang [14]

n	Ref. [14]	Eq. (21.19)	Eq. (21.20)
0.1	3.57308	–	3.6382
0.15	2.48411	–	–
0.2	1.96020	–	2.0010
0.25	1.65736	–	–
0.3	1.46275	–	1.4892
0.4	1.23218	–	–
0.5	1.10437	1.1047	1.1234
0.6	1.02613	–	–
0.7	0.97519	0.9753	–
1.0	0.89972	0.8997	0.9122
1.2	0.87902	0.8790	–
1.5	0.86592	0.8659	0.8749
2.0	0.86360	0.8636	0.8705

$$\left(\frac{dW_x}{d\eta}\right)_{\eta=0} = \frac{n+1/2}{n+1} \left[(f_0'')^{n+1} + \frac{(n+1)^2}{3n(n+1/2)} \right]^{\frac{1}{n+1}} \quad (21.20)$$

derived by Acrivos et al. [18] are also included in Table 21.2 here, f_0'' denotes the dimensionless wall shear stress for power-law boundary layer flow past a flat plate, for which data are tabulated by Acrivos et al. [18].

The comparison in Table 21.2 shows that the present numerical solutions are practically indistinguishable from the similarity solutions of Adersson and Irgens [10]. The data derived from the approximate formula given by Eq. (21.20) compares surprisingly well with the present similarity solutions and the velocity gradient at the wall is overpredicted by not more than 2% throughout the entire range of n -values considered. Here, it should be recalled that the similarity solutions could be considered as exact in the sense that they do not involve other approximations as those inherent in the boundary layer theory and the adoption of the power-law model.

21.7 Mass Flow Rate

Although the total mass flow rate within the film is constant, the partition of the mass flow rate between the viscous boundary layer and the external inviscid flow varies in the streamwise direction. As the boundary layer thickens, fluid is continuously being entrained from the freestream. Let set g_x denotes the local mass flow rate entering into an element of the boundary layer of unit streamwise extent (and unit width) of a certain position x , it can be expressed as

$$g_x = \rho \left(w_{x,\delta_1} \frac{d\delta_1}{dx} - w_{y,\delta_1} \right) \quad (21.21)$$

where δ_1 is the boundary layer thickness at the position x , and w_{x,δ_1} and w_{y,δ_1} are dimensionless velocity components in x and y directions at the edge of the boundary layer and at the position x .

Since the boundary layer thickness is given as $\delta_1 = \eta_{\delta_1} (\text{Re}_x)^{-\frac{1}{n+1}} x$, then,

$$\frac{d\delta_1}{dx} = \eta_{\delta_1} \frac{n}{2(n+1)} (\text{Re}_x)^{-\frac{1}{n+1}}$$

With Eqs. (21.12) and (21.13) and the above equation, Eq. (21.21) can be expressed as in terms of dimensionless variables

$$\begin{aligned} g_x &= \rho \left[\sqrt{2gx \cos \alpha} W_{x,\delta_1} \eta_{\delta_1} \frac{n}{2(n+1)} (\text{Re}_x)^{-\frac{1}{n+1}} - \sqrt{2gx \cos \alpha} \text{Re}_x^{-\frac{1}{n+1}} W_{y,\delta_1} \right] \\ &= \rho \sqrt{2gx \cos \alpha} (\text{Re}_x)^{-\frac{1}{n+1}} \left(\frac{n\eta_{\delta_1}}{2(n+1)} W_{x,\delta_1} - W_{y,\delta_1} \right) \end{aligned} \quad (21.22)$$

Let G_x denotes the total mass flow rate entering into the boundary layer for the area from the inlet $x = 0$ to a stream downstream position x and with the width of b of the plate, then, it should be the following integration:

$$\begin{aligned} G_x &= \iint_A g_x dA \\ &= b \int_0^x g_x dx \end{aligned} \quad (21.23)$$

where $A = b \cdot x$ is integrated area.

With Eq. (21.22), the above equation can be expressed in dimensionless form as

$$\begin{aligned} G_x &= b \int_0^x \left[\rho \sqrt{2gx \cos \alpha} (\text{Re}_x)^{-\frac{1}{n+1}} \left(\frac{n\eta_{\delta_1}}{2(n+1)} W_{x,\delta_1} - W_{y,\delta_1} \right) \right] dx \\ &= \frac{2(n+1)}{2n+1} \left(\frac{n\eta_{\delta_1}}{2(n+1)} W_{x,\delta_1} - W_{y,\delta_1} \right) \rho w_{x,\infty} b \cdot x \text{Re}_x^{-1/(n+1)} \end{aligned}$$

The above equation can be further expressed as

$$\frac{G_x \text{Re}_x^{1/(n+1)}}{\rho w_{x,\infty} b \cdot x} = \Phi \equiv \frac{2(n+1)}{2n+1} \left(\frac{n\eta_{\delta_1}}{2(n+1)} W_{x,\delta_1} - W_{y,\delta_1} \right) \quad (21.24)$$

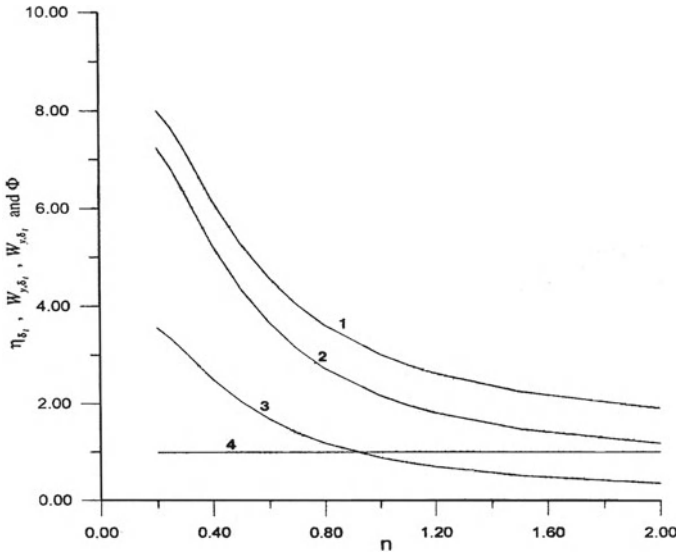


Fig. 21.5 Predicted results for mass flow rate parameter ϕ and the related dimensionless variables η_{δ_1} , W_{x,δ_1} , and W_{y,δ_1} ($1 \eta_{\delta_1}$, 2Φ , $3 -W_{y,\delta_1}$ and $4 W_{x,\delta_1}$), cited from Andersson and Shang [14]

Here, on the right-hand side, Φ defines the *mass flow rate*, η_{δ_1} is the dimensionless boundary layer thickness, and W_{x,δ_1} and W_{y,δ_1} are dimensionless velocity components in x and y directions at the edge of the boundary layer. Since the dimensionless boundary layer thickness η_{δ_1} and the *dimensionless velocity components* W_{x,δ_1} and W_{y,δ_1} may depend on the power-law index n , Φ turns out to be a function of n alone. The most frequently used definition of η_{δ_1} is the value of η_{δ_1} for which the dimensionless velocity component W_{x,δ_1} in Fig. 21.4 becomes equal to 0.99. Data for η_{δ_1} , W_{x,δ_1} , and W_{y,δ_1} obtained from the numerical similarity solutions presented are shown in Fig. 21.5. The resulting variation of the mass flow rate parameter Φ is also included and it is observed that Φ is a monotonically decreasing function of the power-law index n .

To facilitate rapid estimate of the mass flow rate parameter Φ for any value of the power-law index in the interval $0.2 \leq n \leq 2$, accurate curve-fit formulas for η_{δ_1} and W_{y,δ_1}

$$\eta_{\delta_1} = 4.9505 - 7.617(n - 0.54) + 11.214(n - 0.54)^2 + 8.703(n - 0.54)^3 - 0.37(n - 0.54)^4 \quad (0.2 \leq n \leq 1) \quad (21.25)$$

$$\eta_{\delta_1} = 2.3201 - 1.0623(n - 1.425) + 0.9962 (n - 1.425)^2 - 0.7533(n - 1.425)^3 \quad (1 \leq n \leq 2) \quad (21.26)$$

$$W_{y,\delta_1} = -1.8675 + 3.9616(n - 0.54) - 6.022(n - 0.54)^2 - 3.22(n - 0.54)^3 + 16.946(n - 0.54)^4 \quad (0.2 \leq n \leq 1) \quad (21.27)$$

$$W_{y,\delta_1} = -0.53954 + 0.5002(n - 1.425) - 0.5078(n - 1.425)^2$$

$$+ 0.3946(n - 1.425)^3 \quad (1 \leq n \leq 2) \tag{21.28}$$

are shown in Eqs. (21.25–21.28) [14] and can be used with $W_{x,\delta_1} = 0.99$ in Eq. (21.24). This curve-fit method turns out to be accurate to within 0.01 %.

21.8 Length of Boundary Layer Region

Let us now denote the total flow rate within the film, ρV , where V is the volumetric flow rate of the falling film flow. Since the viscous boundary layer develops from $x = 0$, i.e. $\delta_1(0) = 0$, the entire mass flow is initially carried by the freestream. At a certain streamwise position $x = x_0$, on the other hand, the boundary layer extends all the way to the free surface of the film and the total mass flux is within the boundary layer, i.e.

$$G_{x_0} \equiv G_x(x_0) = \rho V \tag{21.29}$$

This criterion, in combination with Eq. (21.21), can be rearranged to give the explicit relation as follows:

$$\frac{G_{x_0} \text{Re}_{x_0}^{1/(n+1)}}{\rho w_{x_0,\infty} b \cdot x_0} = \Phi$$

or

$$\frac{V \text{Re}_{x_0}^{1/(n+1)}}{w_{x_0,\infty} b \cdot x_0} = \Phi$$

i.e.

$$\frac{V \left[\frac{x^n (\sqrt{2gx_0 \cos \alpha})^{2-n} \rho}{K} \right]^{1/(n+1)}}{bx_0 \sqrt{2gx_0 \cos \alpha}} = \Phi$$

or

$$\frac{V \left[\frac{(\sqrt{2g \cos \alpha})^{2-n} \rho}{K} \right]^{1/(n+1)}}{b\sqrt{2g \cos \alpha_0}} x_0^{-\frac{2n+1}{2(n+1)}} = \Phi$$

The above equation is transformed to

$$x_0 = \left\{ \frac{V \left[\frac{(\sqrt{2g \cos \alpha})^{2-n} \rho}{K} \right]^{1/(n+1)}}{\Phi b \sqrt{2g \cos \alpha_0}} \right\}^{\frac{2(n+1)}{2n+1}}$$

i.e.

$$x_0 = \left\{ \left(\frac{V}{\Phi b} \right)^{n+1} \frac{(\sqrt{2g \cos \alpha})^{2-n} \rho}{K} \right\}^{\frac{2}{2n+1}}$$

or

$$x_0 = \left[\left(\frac{V}{\Phi b} \right)^{n+1} \frac{(2g \cos \alpha)^{(1-2n)/2} \rho}{K} \right]^{2/(2n+1)} \quad (21.30)$$

for the particular streamwise position x_0 . Since the film inlet is at $x = 0$, cf. Fig. 21.2, the characteristic coordinate value x_0 defines the streamwise length of the boundary layer region.

21.9 Critical Film Thickness

When the boundary layer extends all the way to the free surface and the freestream disappears at $x = x_0$, the film thickness equals the boundary thickness $\delta_1(x_0)$. The latter can be obtained from the definition, Eq. (21.10), of the similarity variable at the outer edge of the viscous boundary layer, i.e. $y = \delta_1(x_0)$ for $\eta = \eta_{\delta_1}$ and $x = x_0$, and expressed as

$$\delta_1(x_0) = \eta_{\delta_1} x_0 \text{Re}_{x_0}^{-1/(n+1)}$$

With the definition of local *Reynolds number* in Eq. (21.11), the above equation is changed into

$$\delta_1(x_0) = \eta_{\delta_1} x_0^{n/(2(n+1))} \left[\frac{(2g \cos \alpha)^{(2-n)/2}}{K/\rho} \right]^{-1/(n+1)} \quad (21.31)$$

It can therefore be concluded that both x_0 and $\delta_1(x_0)$ are completely determined as long as the problem characteristics n , K/ρ , Q , and $g \cos \alpha$ are known, along with the solution of the transformed problem, Eqs. (21.14–21.17), which determines Φ .

The film thickness at the particular position $x = x_0$ is a critical quantity in film flow analysis since the boundary layer concept is applicable only for range $x \leq x_0$, and in this range the local film thickness $\delta_1(x_0)$ at $x = x_0$ is largest, and named critical film thickness. Following Eq. (21.31) the boundary layer thickness $\delta_1(x)$ at any position of x in this range can be evaluated by the following equation:

$$\delta_1(x) = \eta_{\delta_1} x^{n/(2(n+1))} \left[\frac{(2g \cos \alpha)^{(2-n)/2}}{K/\rho} \right]^{-1/(n+1)} \quad (21.32)$$

21.10 Effect of Wall Inclination

It is noteworthy that the *angle of inclination* α does not appear in the transformed problem defined by Eqs. (21.14–21.17). Any solution W_x and W_y is accordingly independent of α but, nevertheless, valid for all inclinations $0 \leq \alpha \leq \pi/2$. Physically relevant quantities, on the other hand, do depend on α due to the similarity transformation, Eqs. (21.10–21.13). For a given quantity, say p , the relationship

$$\frac{P_i}{P_v} = \left(\frac{\cos \alpha_i}{\cos \alpha_v} \right)^\gamma = \cos^\gamma \alpha_i \quad (21.33)$$

between the inclined and vertical cases, identified by subscripts i and v , respectively, holds. Here, α_v , denotes the angle of inclination in the vertical case, i.e. $\alpha_v = 0$ and $\cos \alpha_v = 1$, and the exponent γ is derived as below:

For w_x

From Eq. (21.12) we can get the following equation

$$\frac{(w_x)_i}{(w_x)_v} = \left(\frac{\cos \alpha_i}{\cos \alpha_v} \right)^{1/2} = \cos^{1/2} \alpha_i$$

Then, $\gamma = 1/2$

For w_y

From Eq. (21.13) we can obtain the following equation:

$$\frac{(w_y)_i}{(w_y)_v} = \left(\frac{\cos \alpha_i}{\cos \alpha_v} \right)^{1/2} \left(\frac{(\text{Re}_x)_i}{(\text{Re}_x)_v} \right)^{-\frac{1}{n+1}}$$

where with Eq. (21.12), we have

$$\left(\frac{(\text{Re}_x)_i}{(\text{Re}_x)_v} \right)^{-\frac{1}{n+1}} = \left(\frac{(w_{x,\infty})_i}{(w_{x,\infty})_v} \right)^{-\frac{2-n}{n+1}} = \left(\frac{\cos \alpha_i}{\cos \alpha_v} \right)^{-\frac{2-n}{2(n+1)}}$$

Hence,

$$\frac{(w_y)_i}{(w_y)_v} = \left(\frac{\cos \alpha_i}{\cos \alpha_v} \right)^{1/2} \left(\frac{\cos \alpha_i}{\cos \alpha_v} \right)^{-\frac{2-n}{2(n+1)}} = \left(\frac{\cos \alpha_i}{\cos \alpha_v} \right)^{\frac{2n-1}{2(n+1)}}$$

Then, $\gamma = \frac{2n-1}{2(n+1)}$

For C_f

From Eq. (21.18) we can do the following derivation:

$$\frac{(C_f)_i}{(C_f)_v} = \left(\frac{(\text{Re}_x)_i}{(\text{Re}_x)_v} \right)^{-\frac{1}{n+1}} = \left(\frac{\cos \alpha_i}{\cos \alpha_v} \right)^{-\frac{2-n}{2(n+1)}}$$

Table 21.3 Relationship between inclined and vertical film flow

P	w_x	w_y	$C_{x,f}$	X_0	$\delta_1(x_0)$
γ	$\frac{1}{2}$	$\frac{2n-1}{2(n+1)}$	$\frac{n-2}{2(n+1)}$	$\frac{1-2n}{2n+1}$	$-\frac{1}{2n+1}$

Then, $\gamma = \frac{n-2}{2(n+1)}$

For x_0

From Eq. (21.30) we can do the following derivation:

$$\frac{(x_0)_i}{(x_0)_v} = \left(\frac{\cos \alpha_i}{\cos \alpha_v} \right)^{\frac{1-2n}{2n+1}}$$

Then, $\gamma = \frac{1-2n}{2n+1}$

For $\delta_1(x_0)$

From Eq. (21.31) we can do the following derivation:

$$\begin{aligned} \frac{(\delta_1(x_0))_i}{(\delta_1(x_0))_v} &= \left(\frac{(x_0)_i}{(x_0)_v} \right)^{\frac{n}{2(n+1)}} \left(\frac{\cos \alpha_i}{\cos \alpha_v} \right)^{-\frac{2-n}{2(n+1)}} \\ &= \left(\frac{\cos \alpha_i}{\cos \alpha_v} \right)^{\frac{n(1-2n)}{2(n+1)(2n+1)}} \left(\frac{\cos \alpha_i}{\cos \alpha_v} \right)^{-\frac{2-n}{2(n+1)}} \\ &= \left(\frac{\cos \alpha_i}{\cos \alpha_v} \right)^{-\frac{1}{2n+1}} \end{aligned}$$

Then, $\gamma = -\frac{1}{2n+1}$

For summary, exponent γ is provided in Table 21.3 for some quantities of particular interest.

21.11 Summary

So far, we have presented the recent developments on hydrodynamics of falling film flow of non-Newtonian fluids. The related equations of hydrodynamics can be summarized in Table 21.4.

21.12 Remarks

In this chapter, the new similarity analysis method has been applied to extensively study the gravity-driven flow of a non-Newtonian liquid film along inclined surface. The partial differential equations governing the hydrodynamics of the power-law fluid

Table 21.4 Summary of the related equations of hydrodynamics of falling film flow of non-Newtonian fluids

Term	Equations
<i>Governing partial differential equations</i>	
Mass equation	$\frac{\partial w_x}{\partial x} + \frac{\partial w_y}{\partial y} = 0$
Momentum equation	$w_x \frac{\partial w_x}{\partial x} + w_y \frac{\partial w_x}{\partial y} = g \cos \alpha + n \frac{K}{\rho} \left(\frac{\partial w_x}{\partial y} \right)^{n-1} \frac{\partial^2 w_x}{\partial y^2}$
Boundary conditions	$y = 0: w_x = 0, w_y = 0$ $y = \delta_1: w_x = w_{x,\infty}$
<i>Defined transformation variables</i>	
η	$\frac{y}{x} \text{Re}_x^{1/(n+1)}$
Re_x	$\frac{x^n (w_{x,\infty})^{2-n} \rho}{w_x K}$
$W_x(\eta)$	$\frac{1}{\sqrt{2gx \cos \alpha}}$
$W_y(\eta)$	$\frac{w_y}{\sqrt{2gx \cos \alpha}} \text{Re}_x^{n+1}$
<i>Governing ordinary differential equations</i>	
Dimensionless mass equation	$W_x - \frac{n}{n+1} \eta \frac{dW_x}{d\eta} + 2 \frac{dW_y}{d\eta} = 0$
Dimensionless momentum equation	$W_x \left(-\frac{n}{n+1} \eta \frac{dW_x}{d\eta} + W_x \right) + 2W_y \frac{dW_x}{d\eta}$ $= 1 + 2n \left(\frac{dW_x}{d\eta} \right)^{(n-1)} \frac{d^2 W_x}{d\eta^2}$
Boundary conditions	$\eta = 0: W_x(\eta) = 0, W_y(\eta) = 0,$ $\eta = \eta_{\delta_1}: W_x(\eta) = 1$
$w_{x,\infty}$	$\sqrt{2gx \cos \alpha}$
x_0	$\left[\left(\frac{V}{b\Phi} \right)^{n+1} \frac{(2g \cos \alpha)^{(1-2n)/2}}{K/\rho} \right]^{2/(2n+1)}$
η_{δ_1}	$4.9505 - 7.617(n - 0.54)$ $+ 11.214(n - 0.54)^2 + 8.703$ $\times (n - 0.54)^3 - 0.37(n - 0.54)^4 (0.2 \leq n \leq 1)$ $2.3201 - 1.0623(n - 0.54) + 0.9962$ $\times (n - 0.54)^2 - 0.7533(n - 0.54)^3 (1 \leq n \leq 2)$
W_{y,δ_1}	$-1.8675 + 3.9616(n - 0.54) - 6.022(n - 0.54)^2$ $- 3.22(n - 0.54)^3 + 16.946(n - 0.54)^4$ $\times (0.2 \leq n \leq 1)$ $-0.53954 + 0.5002(n - 0.54) - 0.5078$ $\times (n - 0.54)^2 + 0.3946(n - 0.54)^3 (0.2 \leq n \leq 1)$
W_{x,δ_1}	1
C_f	$2\text{Re}_x^{-1/(n+1)} \left[\left(\frac{dW_x}{d\eta} \right)_{\eta=0} \right]^n$
Φ (defined as $\frac{G_x \text{Re}_x^{1/(n+1)}}{\rho w_{x,\infty} b \cdot x}$)	$\frac{2(n+1)}{2n+1} \left(\frac{n\eta_{\delta_1}}{2(n+1)} W_{x,\delta_1} - W_{y,\delta_1} \right)$
$\delta_1(x_0)$	$\eta_{\delta_1} x_0^{n/(2(n+1))} \left[\frac{(2g \cos \alpha)^{(2-n)/2}}{K/\rho} \right]^{-1/(n+1)}$

are transformed exactly into a set of two ordinary differential equations, which can be calculated numerically to an arbitrary degree of accuracy. With the present approach, however, calculations could be accomplished also for highly pseudo-plastic liquids and the numerical results. The nonlinearity of the momentum boundary layer problem for power-law fluid increases with increasing pseudo-plasticity $|1 - n|$ and the variable grid spacing is therefore increasingly important.

It is noteworthy that the resulting system of dimensionless ordinary differential equations depends only on the single parameter n . Furthermore, all other parameters, like the streamwise location x , the fluid properties K/ρ , and the component of the gravitational acceleration along the surface $g \cdot \cos\alpha$ have been combined into a generalized local Reynolds number Re_x and dimensionless velocity W_x and W_y . Various flow characteristics can thus be expressed only in term of n and Re_x , except the particular position x_0 at which the entire freestream has been entrained into the momentum boundary layer. In order to determine x_0 and the associated critical film thickness $\delta_1(x_0)$, knowledge about the total mass flow rate ρQ within the film is also required, together with the new dimensionless mass flux parameter Φ . The latter quantity, which depends on the dimensionless boundary layer thickness η_{δ_1} and the velocity components W_{x,δ_1} and W_{y,δ_1} at the edge of the boundary layer, is generally obtained as a part of the numerical solution of the transformed problem and turned out to be function only of the power-law index n . However, to facilitate rapid and accurate estimate of Φ , polynomial curve-fit formulas have been developed on the basis of the rigorous similarity solutions.

21.13 Calculation Examples

Example: A non-Newtonian power-law fluid having a density of $1,041 \text{ kg/m}^3$ is flowing with volumetric flow rate of $0.02 \text{ m}^3/\text{s}$ along an inclined flat plate with angle of $\alpha = 30^\circ$ and width of $b = 1 \text{ m}$. The properties of the fluid are $K = 2.744 \text{ kg s}^{n-2} \text{ m}^{-1}$ and $n = 0.50$. Please calculate the followings:

- length x_0 of the boundary layer region
- critical film thickness $\delta_1(x_0)$
- local skin-friction coefficient C_f at x_0
- w_{x_0,δ_1} and w_{y_0,δ_1} corresponding to position x_0
- If the plate inclined angle is 0° (for vertical plate), calculate x_0 , $\delta_1(x_0)$, C_f , w_{x_0,δ_1} and w_{y_0,δ_1}

Solution: The given data are as follows: volumetric flow rate $V = 0.02 \text{ m}^3/\text{s}$, density $\rho = 1,041 \text{ kg/m}^3$, plate angle $\alpha = 30^\circ$ and width $b = 1 \text{ m}$, coefficient of consistency $K = 2.744 \text{ kg}/(\text{s}^{n-2} \text{ m}^{-1})$ and $n = 0.50$.

a. calculation of x_0 for $\alpha = 30^\circ$

With Eq. (21.30), x_0 is evaluated as

$$x_0 = \left[\left(\frac{V}{b\Phi} \right)^{n+1} \frac{(2g \cos \alpha)^{(1-2n)/2}}{K/\rho} \right]^{2/(2n+1)}$$

While, from Eq. (21.24) the mass flow rate parameter Φ can be evaluated as

$$\Phi = \frac{2(n+1)}{2n+1} \left(\frac{n\eta_{\delta_1}}{2(n+1)} W_{x,\delta_1} - W_{y,\delta_1} \right)$$

For $n = 0.5$, the boundary layer thickness η_{δ_1} and the velocity component W_{y,δ_1} at the edge of the boundary layer can be evaluated as:

$$\begin{aligned} \eta_{\delta_1} &= 4.9505 - 7.617(n - 0.54) + 11.214(n - 0.54)^2 \\ &\quad + 8.703(n - 0.54)^3 - 0.37(n - 0.54)^4 \\ &= 4.9505 - 7.617(0.5 - 0.54) + 11.214(0.5 - 0.54)^2 \\ &\quad + 8.703(0.5 - 0.54)^3 - 0.37(0.5 - 0.54)^4 \\ &= 5.27256 \end{aligned}$$

$$\begin{aligned} W_{y,\delta_1} &= -1.8675 + 3.9616(n - 0.54) - 6.022(n - 0.54)^2 \\ &\quad - 3.22(n - 0.54)^3 + 16.946(n - 0.54)^4 \\ &= -1.8675 + 3.9616(0.5 - 0.54) - 6.022(0.5 - 0.54)^2 \\ &\quad - 3.22(0.5 - 0.54)^3 + 16.946(0.5 - 0.54)^4 \\ &= -2.03535 \end{aligned}$$

$$\begin{aligned} \Phi &= \frac{2(n+1)}{2n+1} \left(\frac{n\eta_{\delta_1}}{2(n+1)} W_{x,\delta_1} - W_{y,\delta_1} \right) \\ &= \frac{2 \times (0.5 + 1)}{2 \times 0.5 + 1} \left(\frac{0.5 \times 5.27256}{2 \times (0.5 + 1)} \times 0.99 + 2.03535 \right) \\ &= 4.358 \end{aligned}$$

(Note: W_{x,δ_1} is defined to be 0.99 in the above equation of Φ)

Then,

$$\begin{aligned} x_0 &= \left[\left(\frac{V}{b\Phi} \right)^{n+1} \frac{(2g \cos \alpha)^{(1-2n)/2}}{K/\rho} \right]^{2/(2n+1)} \\ &= \left[\left(\frac{0.02}{4.358} \right)^{0.5+1} \frac{(2 \times 9.8 \times \cos 30^\circ)^{(1-2 \times 0.5)/2}}{(2.744/1041)} \right]^{2/(2 \times 0.5+1)} \\ &= 0.118 \text{ m} \end{aligned}$$

b. For calculation of $\delta_1(x_0)$ for $\alpha = 30^\circ$

With Eq. (21.31), $\delta_1(x_0)$ can be calculated as

$$\begin{aligned}
\delta_1(x_0) &= \eta_{\delta_1} x_0^{n/(2(n+1))} \left[\frac{(2g \cos \alpha)^{(2-n)/2}}{K/\rho} \right]^{-1/(n+1)} \\
&= 5.2726 \times 0.118^{0.5/(2 \times (0.5+1))} \left[\frac{(2 \times 9.8 \times \cos 30^\circ)^{(2-0.5)/2}}{2.744/1041} \right]^{-1/(0.5+1)} \\
&= 0.0171 \text{ m}
\end{aligned}$$

c. For calculation of C_f related to x_0 and for $\alpha = 30^\circ$

From Eq. (21.18), C_f related to x_0 and for $\alpha = 30^\circ$ can be expressed as

$$C_f = 2\text{Re}_{x_0}^{-1/(n+1)} \left[\left(\frac{dW_x}{d\eta} \right)_{\eta=0} \right]^n$$

From Table 21.4, the local Reynolds number at x_0 can be evaluated as

$$\begin{aligned}
\text{Re}_{x_0} &= \frac{x_0^n (w_{x_0, \infty})^{2-n} \rho}{K} \\
&= \frac{x_0^n (2gx_0 \cos \alpha)^{(2-n)/2} \rho}{K} \\
&= \frac{0.118^{0.5} \times (2 \times 9.8 \times 0.118 \times \cos 30^\circ)^{(2-n)/2} \times 1041}{2.744} \\
&= 219.4
\end{aligned}$$

From Table 21.2 we get

$$\left(\frac{dW_x}{d\eta} \right)_{\eta=0} = 1.10437 \text{ at } n = 0.5$$

Then,

$$\begin{aligned}
C_f &= 2\text{Re}_{x_0}^{-1/(n+1)} \left[\left(\frac{dW_x}{d\eta} \right)_{\eta=0} \right]^n \\
&= 2 \times 219.4^{-1/(0.5+1)} [1.10437]^{0.5} \\
&= 0.0578
\end{aligned}$$

d. For calculation of w_{x_0, δ_1} and w_{y_0, δ_1} for $\alpha = 30^\circ$

From Eq. (21.12) we have

$$W_{x_0, \delta_1} = \frac{w_{x_0, \delta_1}}{\sqrt{2gx \cos \alpha}}$$

i.e.

$$\begin{aligned}
 w_{x_0, \delta_1} &= \sqrt{2gx_0 \cos \alpha} W_{x, \delta_1} \\
 &= \sqrt{2 \times 9.8 \times 0.118 \times \cos 30^\circ} \times 1 \\
 &= 1.415 \text{ m/s}
 \end{aligned}$$

From Eq. (21.13) we have

$$W_{y, \delta_1} = \frac{w_{y_0, \delta_1}}{\sqrt{2gx_0 \cos \alpha}} \text{Re}_{x_0}^{\frac{1}{n+1}}$$

i.e.

$$\begin{aligned}
 w_{y_0, \delta_1} &= \sqrt{2gx_0 \cos \alpha} \text{Re}_{x_0}^{-\frac{1}{n+1}} W_{y, \delta_1} \\
 &= \sqrt{2 \times 9.8 \times 0.118 \times \cos 30^\circ} \times 219.4^{-\frac{1}{0.5+1}} \times (-2.0354) \\
 &= -0.079 \text{ m/s}
 \end{aligned}$$

e. For calculation of $x_0 \delta_1(x_0)$, C_f , w_{x_0, δ_1} for vertical plate case

According to Eq. (21.33) and Table 21.3, we have the following expression

$$(x_0)_v = (x_0)_i / \cos^\gamma \alpha$$

where

$$\text{For } x_0, \gamma = \frac{1-2n}{2n+1} = \frac{1-2 \times 0.5}{2 \times 0.5+1} = 0, \text{ then,}$$

$$\begin{aligned}
 (x_0)_v &= 0.118 / \cos^0 30^\circ \\
 &= 0.118 \text{ m}
 \end{aligned}$$

$$\text{For } \delta_1(x_0), \gamma = -\frac{1}{2n+1} = -\frac{1}{2 \times 0.5+1} = -0.5, \text{ then,}$$

$$\begin{aligned}
 (\delta_1(x_0))_v &= (\delta_1(x_0))_i / \cos^\gamma \alpha \\
 &= 0.0171 / \cos^{-0.5}(30^\circ) \\
 &= 0.0159 \text{ m}
 \end{aligned}$$

$$\text{For } C_f, \gamma = \frac{n-2}{2(n+1)} = \frac{0.5-2}{2 \times (0.5+1)} = -0.5, \text{ then}$$

$$\begin{aligned}
 (C_f)_v &= (C_f)_i / \cos^\gamma \alpha \\
 &= 0.0578 / \cos^{-0.5}(30^\circ) \\
 &= 0.05379
 \end{aligned}$$

For w_{x_0, δ_1} , $\gamma = 1/2$ then

$$\begin{aligned}
 (w_{x_0, \delta_1})_v &= (w_{x_0, \delta_1})_i / \cos^\gamma \alpha \\
 &= 1.415 / \cos^{0.5} (30^\circ) \\
 &= 1.5205 \text{ m/s}
 \end{aligned}$$

For w_{y_0, δ_1} , $\gamma = \frac{2n-1}{2(n+1)} = \frac{2 \times 0.5 - 1}{2 \times (0.5 + 1)} = 0$, then

$$\begin{aligned}
 (w_{y_0, \delta_1})_v &= (w_{y_0, \delta_1})_i / \cos^\gamma \alpha \\
 &= -0.079 / \cos^0 \alpha \\
 &= -0.079
 \end{aligned}$$

References

1. G. Astarita, G. Marrucci, G. Palumbo, Non-Newtonian gravity flow along inclined plane surface. *Ind. Eng. Chem. Fundam.* **3**, 333–339 (1964)
2. N. Therien, B. Coupal, J.L. corneille, Verification experimentale de l'epaisseur du film pour des liquides non-Newtoniens s'écoulant par gravite sur un plan incline. *Can. J. Chem. Eng.* **48**, 17–20 (1970)
3. N.D. Sylvester, J.S. Tyler, A.H.P. Skelland, Non-Newtonian film fluids: theory and experiment. *Can. J. Chem. Eng.* **51**, 418–429 (1973)
4. T.M.T. Yang, D.W. Yarbrough, A numerical study of the laminar flow of non-Newtonian fluids along a vertical wall. *ASME J. Appl. Mech.* **40**, 290–292 (1973)
5. T.M.T. Yang, D.W. Yarbrough, Laminar flow of non-Newtonian liquid films inside a vertical pipe. *Rheol. Acta* **19**, 432–436 (1980)
6. V. Narayana Murthy, P.K. Sarma, A note on hydrodynamics entrance length of non-Newtonian laminar falling films. *Chem. Eng. Ser.* **32**, 566–567 (1977)
7. V. Narayana Murthy, P.K. Sarma, Dynamics of developing laminar non-Newtonian falling liquid films with free surface. *ASME J. Appl. Mech.* **45**, 19–24 (1978)
8. M.N. Tekic, D. Posarac, D. Petrovic, A note on the entrance region lengths of non-Newtonian laminar falling films. *Chem. Sci.* **41**, 3230–3232 (1986)
9. H.I. Andersson, F. Irgens, Hydrodynamic entrance length of non-Newtonian liquid films. *Chem. Eng. Sci.* **45**, 537–541 (1990)
10. H.I. Andersson, F. Irgens, Gravity-driven laminar film flow of power-law fluids along vertical walls. *J. Non-Newtonian Fluid Mech.* **27**, 153–172 (1988)
11. H.I. Andersson, F. Irgens, Film flow of power law fluids, in *Encyclopaedia of Fluid Mechanics*, vol. 9, ed. by N.P. Chermisinoff (Gulf Publishing Company, Houston, 1990), pp. 617–648
12. G. Astarita, Mass transfer from a flat solid surface to a falling non-Newtonian liquid film. *Ind. Eng. Chem. Fundam.* **5**, 14–18 (1966)
13. R.A. Mashelker, V.V. Chavan, Solid dissolution in falling films of non-Newtonian liquids. *J. Chem. Jpn.* **6**, 160–167 (1973)
14. H.I. Andersson, D.Y. Shang, An extended study of hydrodynamics of gravity-riven film flow of power-law fluids. *Fluid Dyn. Res.* **22**, 345–357 (1998)
15. J. Wu, M.C. Thompson, Non-Newtonian shear-thinning flow past a flat plate. *J. Non-Newtonian Fluid Mech.* **66**, 127–144 (1996)
16. A. Acrivos, M.J. Shah, E.E. Peterson, Momentum and heat transfer in lamiar boundary-flows of non-Newtonian fluids past external surfaces. *AICHE J.* **6**, 312–317 (1960)
17. H.I. Andersson, T.H. Toften, Numerical solution of the laminar boundary layer equations for power-law fluids. *J. Non-Newtonian Fluid Mech.* **32**, 175–195 (1989)
18. A. Acrivos, M.J. Shah, E.E. Peterson, On the solution of the two-dimensional boundary-flow equations for a non-Newtonian power-law fluid. *Chem. Eng. Sci.* **20**, 101–105 (1965)

Chapter 22

Pseudo-Similarity and Boundary Layer Thickness for Non-Newtonian Falling Film Flow

Abstract The pseudo-similarity solutions of the thermal boundary layer of a falling film flow of power-law fluids are presented. Based on a proposed “local Prandtl number”, the dependence of the thickness of the momentum boundary layer and thermal boundary layer on the power-law index and local Prandtl number are discussed. Their variations with power-law index and local Prandtl number are also presented. The momentum layer thickness depends only on the power-law index, while the thermal boundary layer thickness depends both on the power-law index and the local Prandtl number. The momentum boundary layer thickness decreases significantly with the increase of the power-law index. While the thermal boundary layer thickness decreases slightly with increasing the power-law index and decreases with increasing the parameter local Prandtl number. With the introduction of the “local Prandtl number”, it is found that the heat transfer problem turned out to involve only two independent parameters, the power-law index and the local Prandtl number. The pseudo-similarity solution and the assumed true-similarity solution are presented for the investigation of non-similarity thermal boundary layer. The degree of non-similarity of thermal boundary layer has been determined for various values of power-law indices and local Prandtl numbers.

22.1 Introduction

Efficient heating or cooling of liquids can be achieved by allowing the fluid to flow in a thin film along a solid surface kept at a constant temperature. While the hydrodynamics of thin film flow of Newtonian liquids has been extensively studied for several decades, only modest attention has been devoted to gravity-driven films of non-Newtonian liquids.

Heat transfer from a constant temperature wall to hydrodynamically fully developed power-law films was probably first considered by Yih and Lee [1], while the corresponding mass transfer problem (i.e. solid dissolution from the wall and

diffusion into the film) has been studied by Astarita [2] and Mashelkar and Chavan [3]. For the effect of injection/suction on the heat transfer, so far there has been study by Pop et al. [4] on the steady laminar gravity-driven film flow along a vertical wall for Newtonian fluids, which is based on Falkner-Skan type transformation. A mathematical model for heat transfer of non-Newtonian falling film flow was dealt with by Ouldhadda et al. [5] on a horizontal circular cylinder. Meanwhile, Rao [6] measured experimentally the heat transfer in a fully developed non-Newtonian film flow falling down a vertical tube.

However, most of the previous theoretical models only solved the similarity momentum problem for the boundary layer region. The solution for the similarity thermal boundary layer encounters formidable difficulties when the boundary layer thickness of momentum and temperature differ significantly, which is a characteristic of non-Newtonian power-law fluids.

The solution of similarity momentum boundary layer cannot be successfully applied for solution of the heat transfer in boundary layer region, since there is no similarity solution for the energy equation related to non-Newtonian power-law fluids. The determination of exact thermal boundary layer thickness is very important, otherwise, the hydrodynamics and heat transfer analyses for the boundary layer region, fully viscous region, and the developed flow region will not produce reliable results.

Therefore, a reliable and convenient treatment approach of local non-similarity of thermal boundary layer is very important for solution for falling film flow of non-Newtonian power-law fluids. For this purpose, on the basis of Ref. [7], Shang and Andersson [8] focused on an extensive study for a systematic solution on local non-similarity of thermal boundary layer for falling-film flow of non-Newtonian power-law fluids using a pseudo-similarity approach. They provided the similarity approach for the rigorous solution of heat transfer coefficient related to the non-similarity thermal boundary layer of the non-Newtonian power-law fluids for the boundary layer region.

Furthermore, Shang and Gu [9] provided an extensive study on pseudo-similarity solutions of thermal boundary layer in falling film flow with non-Newtonian power-law fluids. Based on the newly defined “local Prandtl number” proposed by Shang and Andersson [8], it is found that the momentum boundary layer thickness decreases monotonically with power-law index, while the thermal boundary layer thickness increases slightly with power-law index and decreases significantly with the increase of the “local Prandtl number”.

In this chapter, the focus is on presentation of the recent developments on analyses of pseudo-similarity, and boundary layer thickness for non-Newtonian falling film flow. To this end, a mathematical model for thermal boundary layer in an accelerating liquid film of non-Newtonian power-law fluids is presented. A pseudo-similarity transformation method is induced for the thermal boundary layer equation. On this basis, the heat transfer problem can be solved by means of a local non-similarity approach with n and the induced local Prandtl number Pr_x being the only parameter. Based on a newly defined “local Prandtl number”, the dependence of the thickness of the momentum boundary layer and thermal boundary layer on the power-law index

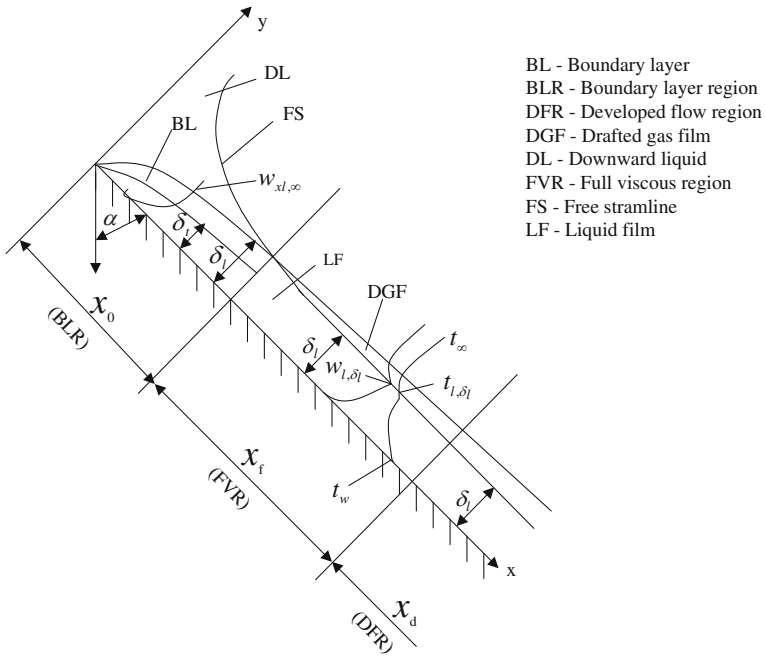


Fig. 22.1 Schematic representation of accelerating film flow

is discussed. It is found that the momentum boundary layer thickness decreases monotonically with power-law index, while the thermal boundary layer thickness increases slowly with power-law index and decreases significantly with the increase of the “local Prandtl number”. It shows that the adopted pseudo-similarity approach is capable of solving the problem of non-similarity thermal boundary layer in the falling film of a non-Newtonian power-law fluid. Meanwhile, a *critical local Prandtl number* Pr_x^* is introduced, which is a monotonically increasing function of n .

22.2 Physical Model and Governing Partial Differential Equations

Consider the accelerating laminar flow in the boundary layer region of a non-Newtonian liquid film flow down along an inclined plane surface, as shown schematically in Fig. 22.1. The incompressible and inelastic fluid is assumed to obey the Ostwald-de-Waele power-law model and the action of viscous stresses is confined to the solid surface. The basis boundary layer equations for mass, momentum, and thermal energy are:

$$\frac{\partial w_x}{\partial x} + \frac{\partial w_y}{\partial y} = 0 \quad (22.1)$$

$$w_x \frac{\partial w_x}{\partial x} + w_y \frac{\partial w_x}{\partial y} = g \cos \alpha + n \frac{K}{\rho} \left(\frac{\partial w_x}{\partial y} \right)^{n-1} \frac{\partial^2 w_x}{\partial y^2} \quad (22.2)$$

$$w_x \frac{\partial t}{\partial x} + w_y \frac{\partial t}{\partial y} = \frac{\lambda}{\rho c_p} \frac{\partial^2 t}{\partial y^2} \quad (22.3)$$

and the boundary conditions are

$$y = 0: \quad w_x = 0, \quad w_y = 0, \quad t = t_w \quad (22.4)$$

$$y = \delta_1, \quad w_x = w_{x,\infty} \quad (22.5)$$

$$y = \delta_t, \quad t = t_\infty \quad (22.6)$$

where w_x and w_y are velocity exponents in x and y directions, respectively, while g and α denote the gravitation acceleration and the angle of inclination of the plane wall. Here, it has been anticipated that $\frac{\partial w_x}{\partial y} \geq 0$ throughout the entire of the film. δ_1 and δ_t denote the thicknesses of the momentum and thermal boundary layers, respectively, while $w_{x,\infty}$ and t_∞ are velocity and temperature of the fluid outside the respective boundary layers. It is noteworthy that $w_{x,\infty}$ varies with x , and the wall temperature t_w and the external temperature t_∞ are constants as one kind of temperature conditions. The fluid physical properties λ , ρ , c_p , K , and n , which are assumed to be constant, are the thermal conductivity, density, specific heat, coefficient of consistency, and power-law index, respectively. The deviation of n from unity indicates the degree of deviation from Newtonian rheology and the particular case $n = 1$ represents a Newtonian fluid with dynamic coefficient of viscosity K .

No-slip and impermeability conditions at the inclined surface $y = 0$ are expressed by the boundary conditions (22.4), while the outer condition (22.5) assures that the velocity component w_x within the boundary layer approaches the external velocity

$$w_{x,\infty} = \sqrt{2gx \cos \alpha} \quad (22.7)$$

at the edge $y = \delta_1$ of the momentum boundary layer.

22.3 Similarity Transformation

Incidentally, as pointed out by Andersson and Irgens [10], the external velocity (22.7) belongs to the Falkner-Skan class of freestreams $w_{x,\infty} \propto x^m$, which permits a similarity transformation of the momentum boundary layer equation even for power-law fluids. A generalized Falkner-Skan type of transformation was therefore introduced

in Refs. [11, 12], while Andersson and Shang [7] devised an alternative similarity transformation. However, as we shall see, exact similarity solutions of the thermal energy equation exist only in the particular case when the power-law index n is equal to unity. In this case, Shang and Andersson derived a pseudo-similarity transformation for solution of thermal boundary layer problem in falling film flow with non-Newtonian power-law fluids [8].

According to Ref. [8], the new independent and dimensionless variables are introduced as follows:

$$\eta = \frac{y}{x} \text{Re}_x^{1/(n+1)} \quad (22.8)$$

$$\zeta = \frac{x}{x_0} \quad (22.9)$$

where x_0 is the *length of the boundary layer region* and

$$\text{Re}_x = \frac{x^n (w_{x,\infty})^{2-n} \rho}{K} \quad (22.10)$$

where Re_x is a generalized local Reynolds number.

The dimensionless velocity components are defined as

$$W_x(\eta) = \frac{w_x}{\sqrt{2gx \cos \alpha}} \quad (22.11)$$

$$W_y(\eta) = \frac{w_y}{\sqrt{2gx \cos \alpha}} \text{Re}_x^{\frac{1}{n+1}} \quad (22.12)$$

which are independent of ζ except for the particular value $n = 1$.

The dimensionless temperature is defined as

$$\theta(\eta, \zeta) = \frac{t - t_\infty}{t_w - t_\infty} \quad (22.13)$$

which depend both on η and ζ .

According to the derivations presented in Chap. 21, the partial differential Eqs. (22.1) and (22.2) are transformed into the following dimensionless equations, respectively:

$$W_x(\eta) - \frac{n}{(1+n)} \eta \frac{dW_x(\eta)}{d\eta} + 2 \frac{dW_y(\eta)}{d\eta} = 0 \quad (22.14)$$

$$\begin{aligned} W_x(\eta) \left[-\frac{n}{(1+n)} \eta \frac{dW_x(\eta)}{d\eta} + W_x(\eta) \right] + 2W_y(\eta) \frac{dW_x(\eta)}{d\eta} \\ = 1 + 2n \left(\frac{dW_x(\eta)}{d\eta} \right)^{n-1} \frac{d^2 W_x(\eta)}{d\eta^2} \end{aligned} \quad (22.15)$$

Additionally, the similarity transformation of (22.3) is done as follows:

At first, the derivative $\frac{\partial t}{\partial x}$ is expressed as

$$\frac{\partial t}{\partial x} = \frac{\partial t}{\partial \eta} \frac{\partial \eta}{\partial x} + \frac{\partial t}{\partial \xi} \frac{\partial \xi}{\partial x}$$

where

$$\begin{aligned} \frac{\partial t}{\partial \eta} &= (t_w - t_\infty) \frac{\partial \theta(\eta, \xi)}{d\eta} \\ \frac{\partial \eta}{\partial x} &= \frac{\partial}{\partial x} \left[\frac{y}{x} \text{Re}_x^{1/(n+1)} \right] \\ &= \frac{\partial}{\partial x} \left[y \left(\frac{(2g \cos \alpha)^{\frac{2-n}{2}} \rho}{K} \right)^{\frac{1}{n+1}} x^{-\frac{n}{2(n+1)}} \right] \\ &= -\frac{n}{2(n+1)} \eta x^{-1} \\ \frac{\partial T}{\partial \xi} &= (t_w - t_\infty) \frac{\partial \theta(\eta, \xi)}{\partial \xi} \\ \frac{\partial \xi}{\partial x} &= \frac{1}{x_0} \end{aligned}$$

Therefore,

$$\frac{\partial t}{\partial x} = -(t_w - t_\infty) \frac{\partial \theta(\eta, \xi)}{d\eta} \frac{n}{2(n+1)} \eta x^{-1} + \frac{1}{x_0} (t_w - t_\infty) \frac{\partial \theta(\eta, \xi)}{\partial \xi}$$

Then, the derivative $\frac{\partial t}{\partial y}$ is expressed as

$$\frac{\partial t}{\partial y} = \frac{\partial t}{\partial \eta} \frac{\partial \eta}{\partial y} + \frac{\partial t}{\partial \xi} \frac{\partial \xi}{\partial y}$$

where

$$\begin{aligned} \frac{\partial \eta}{\partial y} &= \frac{1}{x} (\text{Re}_x)^{\frac{1}{n+1}} \\ \frac{\partial \xi}{\partial y} &= 0 \end{aligned}$$

Therefore,

$$\frac{\partial t}{\partial y} = (t_w - t_\infty) \frac{\partial \theta(\eta, \xi)}{\partial \eta} \frac{1}{x} (\text{Re}_x)^{\frac{1}{n+1}}$$

Additionally,

$$\begin{aligned} \frac{\partial^2 t}{\partial y^2} &= \frac{1}{x}(t_w - t_\infty)(\text{Re}_x)^{\frac{1}{n+1}} \frac{\partial}{\partial \eta} \left(\frac{\partial \theta(\eta, \xi)}{\partial \eta} \right) \frac{1}{x} (\text{Re}_x)^{\frac{1}{n+1}} \\ &= \frac{1}{x^2}(t_w - t_\infty)(\text{Re}_x)^{\frac{2}{n+1}} \frac{\partial}{\partial \eta} \left(\frac{\partial \theta(\eta, \xi)}{\partial \eta} \right) \end{aligned}$$

On these bases, Eq. (22.3) is changed into

$$\begin{aligned} &\sqrt{2gx \cos \alpha} W_x(\eta) \left[-(t_w - t_\infty) \frac{\partial \theta(\eta, \xi)}{\partial \eta} \frac{n}{2(n+1)} \eta x^{-1} + \frac{1}{x_0}(t_w - t_\infty) \frac{\partial \theta(\eta, \xi)}{\partial \xi} \right] \\ &+ \sqrt{2gx \cos \alpha} \text{Re}_x^{-\frac{1}{n+1}} W_y(\eta) (t_w - t_\infty) \frac{\partial \theta(\eta, \xi)}{\partial \eta} \frac{1}{x} (\text{Re}_x)^{\frac{1}{n+1}} \\ &= \frac{\lambda}{\rho c_p} \frac{1}{x^2} (t_w - t_\infty) (\text{Re}_x)^{\frac{2}{n+1}} \frac{\partial}{\partial \eta} \left(\frac{\partial \theta(\eta, \xi)}{\partial \eta} \right) \end{aligned}$$

The above equation is simplified to

$$\begin{aligned} &\sqrt{2gx \cos \alpha} W_x(\eta) \left[-\frac{\partial \theta(\eta, \xi)}{\partial \eta} \frac{n}{2(n+1)} \eta x^{-1} + \frac{1}{x_0} \frac{\partial \theta(\eta, \xi)}{\partial \xi} \right] \\ &+ \sqrt{2gx \cos \alpha} W_y(\eta) \frac{\partial \theta(\eta, \xi)}{\partial \eta} \frac{1}{x} = \frac{\lambda}{\rho c_p} \frac{1}{x^2} (\text{Re}_x)^{\frac{2}{n+1}} \frac{\partial}{\partial \eta} \left(\frac{\partial \theta(\eta, \xi)}{\partial \eta} \right) \end{aligned}$$

or

$$\begin{aligned} &\sqrt{2gx \cos \alpha} W_x(\eta) \left[-\frac{\partial \theta(\eta, \xi)}{\partial \eta} \frac{n}{2(n+1)} \eta + \frac{x}{x_0} \frac{\partial \theta(\eta, \xi)}{\partial \xi} \right] \\ &+ \sqrt{2gx \cos \alpha} W_y(\eta) \frac{\partial \theta(\eta, \xi)}{\partial \eta} = \frac{\lambda}{\rho c_p} \frac{1}{x} (\text{Re}_x)^{\frac{2}{n+1}} \frac{\partial}{\partial \eta} \left(\frac{\partial \theta(\eta, \xi)}{\partial \eta} \right) \end{aligned}$$

With Eq. (22.7), the above equation can be simplified into the following form

$$\begin{aligned} &\left[-\frac{n}{2(n+1)} \eta W_x(\eta) + W_y(\eta) \right] \frac{\partial \theta(\eta, \xi)}{\partial \eta} + \xi W_x(\eta) \frac{\partial \theta(\eta, \xi)}{\partial \xi} \\ &= \frac{1}{\frac{x w_{x,\infty}}{a} (\text{Re}_x)^{-\frac{2}{n+1}}} \frac{\partial^2 \theta(\eta, \xi)}{\partial \eta^2} \end{aligned} \tag{22.16}$$

subject to the boundary conditions

$$\eta = 0: \quad W_x(\eta) = 0, \quad W_y(\eta) = 0, \quad \theta(\eta, \xi) = 1 \tag{22.17}$$

$$\eta = \eta_{\delta_1}: \quad W_x(\eta) = 1 \tag{22.18}$$

$$\eta = \eta_{\delta_t}, \quad \theta(\eta, \zeta) = 0 \quad (22.19)$$

22.4 Local Prandtl Number

The denominator $\frac{xw_{x,\infty}}{a}(\text{Re}_x)^{-\frac{2}{n+1}}$ in the diffusion coefficient in Eq. (22.16) can be defined as the local Prandtl number Pr_x , i.e.,

$$\text{Pr}_x = \frac{xw_{x,\infty}}{a} \text{Re}_x^{-2/(n+1)} \quad (22.20)$$

where $a \left(= \frac{\lambda}{\rho c_p} \right)$ denotes the thermal diffusivity.

With Eqs. (22.7) and (22.10), the above equation can be expressed as

$$\begin{aligned} \text{Pr}_x &= \frac{xw_{x,\infty}}{a} \text{Re}_x^{-2/(n+1)} \\ &= \frac{x\sqrt{2gx \cos \alpha}}{a} \left[\frac{x^n (\sqrt{2gx \cos \alpha})^{2-n} \rho}{K} \right]^{-2/(n+1)} \\ &= \frac{\sqrt{2g \cos \alpha}}{a} \left[\frac{(\sqrt{2g \cos \alpha})^{2-n} \rho}{K} \right]^{-2/(n+1)} x^{3/2} [x^{(n+2)/2}]^{-2/(n+1)} \\ &= \frac{\sqrt{2g \cos \alpha}}{a} \left[\frac{(\sqrt{2g \cos \alpha})^{2-n} \rho}{K} \right]^{-2/(n+1)} x^{(n-1)/(2(n+1))} \end{aligned}$$

Now it is readily seen that $\text{Pr}_x \rightarrow 0$ as $x \rightarrow 0$ if $n > 1$ and that $\text{Pr}_x \rightarrow \infty$ as $x \rightarrow 0$ if $n < 1$.

In the special case when the power-law index n is equal to unity, i.e., for a Newtonian liquid film, Eq. (22.20) can be simplified as

$$\text{Pr}_x = \frac{xw_{x,\infty}}{\frac{\lambda}{\rho c_p}} \left[\frac{x(w_{x,\infty})^{2-1} \rho}{K} \right]^{-2/(1+1)}$$

For Newtonian fluids, the coefficient of consistency K is replaced by the absolute viscosity μ , and then the above equation is further simplified to

$$\begin{aligned} \text{Pr}_x &= \frac{xw_{x,\infty}}{\frac{\lambda}{\rho c_p}} \left[\frac{x(w_{x,\infty}) \rho}{\mu} \right]^{-1} \\ &= \left(\frac{\rho c_p}{\lambda} \right) \left(\frac{\mu}{\rho} \right) \\ &= \frac{\mu c_p}{\lambda} \end{aligned}$$

where μ , λ , and c_p are absolute viscosity, thermal conductivity, and specific heat of the Newtonian liquid. In this case, the local Prandtl number for non-Newtonian power law fluids is simplified to Prandtl number for Newtonian fluids, the diffusion coefficient in Eq. (22.16) becomes independent of x , i.e., $\frac{\partial \theta}{\partial \xi} = 0$ and similarity can also be achieved for the temperature field. This particular case has been explored by Andersson [13].

22.5 Pseudo-Similarity for Energy Equation

Although the hydrodynamic problem admits similarity solutions, the accompanying thermal problem does not since the governing Eq. (22.16) for the temperature field exhibits explicit dependencies on both ζ and η . An accurate method for obtaining locally non-similar boundary layer solutions was suggested by Sparrow et al. [14], and applied by Shang and Andersson [8] to solutions for thermal boundary layer of non-Newtonian power-law liquids. According to Ref. [8] local pseudo-similarity transformation for the thermal boundary layer is achieved by first introducing the new variable

$$g(\eta, \zeta) = \frac{\partial \theta(\eta, \zeta)}{\partial \zeta} \tag{22.21}$$

in the actual differential equation so that the energy Eq. (22.16) becomes

$$\left[-\frac{n}{2(1+n)} \eta W_x(\eta) + W_y(\eta) \right] \frac{\partial \theta(\eta, \zeta)}{\partial \eta} + \zeta W_x(\eta) g(\eta, \zeta) = \frac{1}{Pr_x} \frac{\partial^2 \theta(\eta, \zeta)}{\partial \eta^2} \tag{22.22}$$

Differentiating Eq. (22.22) with respect to ζ , we have

$$\begin{aligned} & \left[-\frac{n}{2(n+1)} \eta W_x(\eta) + W_y(\eta) \right] \frac{\partial g(\eta, \zeta)}{\partial \eta} + W_x(\eta) g(\eta, \zeta) + \zeta W_x(\eta) \frac{\partial g(\eta, \zeta)}{\partial \eta} \\ & = \frac{\partial \left(\frac{1}{Pr_x} \right)}{\partial \xi} \left(\frac{\partial^2 \theta(\eta, \zeta)}{\partial \eta^2} \right) + \frac{1}{Pr_x} \frac{\partial}{\partial \xi} \left(\frac{\partial^2 \theta(\eta, \zeta)}{\partial \eta^2} \right) \end{aligned} \tag{22.23}$$

where

$$\frac{\partial}{\partial \xi} \left(\frac{\partial^2 \theta(\eta, \zeta)}{\partial \eta^2} \right) = \frac{\partial^2 g(\eta, \zeta)}{\partial \eta^2}$$

With Eqs. (22.7), (22.10), and (22.20), we have

$$\begin{aligned}
 \text{Pr}_x &= \frac{x\sqrt{2gx \cos \alpha}}{a} \left[\frac{x^n (\sqrt{2gx \cos \alpha})^{2-n} \rho}{K} \right]^{-2/(n+1)} \\
 &= \frac{x^{3/2} \sqrt{2g \cos \alpha}}{a} \left[\frac{x^n x^{(2-n)/2} (\sqrt{2g \cos \alpha})^{2-n} \rho}{K} \right]^{-2/(n+1)} \\
 &= \frac{x^{3/2} \sqrt{2g \cos \alpha}}{a} \left[\frac{x^{(n+2)/2} (\sqrt{2g \cos \alpha})^{2-n} \rho}{K} \right]^{-2/(n+1)} \\
 &= x^{\frac{n-1}{2(n+1)}} \frac{\sqrt{2g \cos \alpha}}{a} \left[\frac{(\sqrt{2g \cos \alpha})^{2-n} \rho}{K} \right]^{-2/(n+1)}
 \end{aligned}$$

Then

$$\begin{aligned}
 \frac{\partial \left(\frac{1}{\text{Pr}_x} \right)}{\partial \xi} &= \frac{\partial}{\partial \xi} \left\{ x^{\frac{1-n}{2(n+1)}} \left(\frac{\sqrt{2g \cos \alpha}}{a} \right)^{-1} \left[\frac{(\sqrt{2g \cos \alpha})^{2-n} \rho}{K} \right]^{2/(n+1)} \right\} \\
 &= \frac{1-n}{2(n+1)} \left\{ x_0 x^{\frac{-1-3n}{2(n+1)}} \left(\frac{\sqrt{2g \cos \alpha}}{a} \right)^{-1} \left[\frac{(\sqrt{2g \cos \alpha})^{2-n} \rho}{K} \right]^{2/(n+1)} \right\} \\
 &= \frac{1-n}{2(n+1)} \left\{ \xi^{-1} x \cdot x^{\frac{-1-3n}{2(n+1)}} x^{3/2} x^{-(n+2)/(n+1)} \left(\frac{x\sqrt{2gx \cos \alpha}}{a} \right)^{-1} \right. \\
 &\quad \left. \times \left[\frac{(x^n \sqrt{2gx \cos \alpha})^{2-n} \rho}{K} \right]^{2/(n+1)} \right\} \\
 &= \frac{1-n}{2(n+1)} \xi^{-1} \text{Pr}_x^{-1}
 \end{aligned}$$

Thus, Eq. (22.23) is changed into the following:

$$\begin{aligned}
 &\left[-\frac{n}{2(n+1)} \eta W_x(\eta) + W_y(\eta) \right] \frac{\partial g(\eta, \zeta)}{\partial \eta} + W_x(\eta) g(\eta, \zeta) \\
 &= \frac{1-n}{2(n+1)} \xi^{-1} \text{Pr}_x^{-1} \left(\frac{\partial^2 \theta(\eta, \zeta)}{\partial \eta^2} \right) + \frac{1}{\text{Pr}_x} \frac{\partial}{\partial \xi} \left(\frac{\partial^2 \theta(\eta, \zeta)}{\partial \eta^2} \right)
 \end{aligned}$$

or

$$\begin{aligned}
 &\left[-\frac{n}{2(n+1)} \eta W_x(\eta) + W_y(\eta) \right] \frac{\partial g(\eta, \zeta)}{\partial \eta} + W_x(\eta) g(\eta, \zeta) + \xi W_x(\eta) \frac{\partial g(\eta, \zeta)}{\partial \xi} \\
 &= \frac{1}{\text{Pr}_x} \left[\frac{\partial^2 g(\eta, \zeta)}{\partial \eta^2} - \frac{n-1}{2(n+1)} \xi^{-1} \frac{\partial^2 \theta(\eta, \zeta)}{\partial \eta^2} \right] \tag{22.24}
 \end{aligned}$$

where the primes have been introduced to denote differentiation with respect to η . The final step is to neglect terms involving $\left(\frac{\partial}{\partial \xi}\right)$ in the subsidiary Eq. (22.24), whereas the primary Eq. (22.22) remains intact.

We introduce the new variable

$$h(\eta, \xi) = \xi \cdot g(\eta, \xi) = \xi \frac{\partial \theta(\eta, \xi)}{\partial \xi} \quad (22.25)$$

Multiply Eq. (22.24) by ξ , and then Eq. (22.24) is simplified to

$$\begin{aligned} & \left[-\frac{n}{2(n+1)} \eta W_x(\eta) + W_y(\eta) \right] \frac{\partial h(\eta, \zeta)}{\partial \eta} + W_x(\eta) h(\eta, \zeta) \\ & = \frac{1}{\text{Pr}_x} \left[\frac{\partial^2 h(\eta, \zeta)}{\partial \eta^2} - \frac{n-1}{2(n+1)} \left(\frac{\partial^2 \theta(\eta, \zeta)}{\partial \eta^2} \right) \right] \end{aligned} \quad (22.26)$$

Likewise, $\xi \cdot g(\eta, \xi)$ in Eq. (22.25) is replaced by h . Equation (20.26) is different from the general similarity equation, and named pseudo-similarity equation.

Thus, the two-equation local pseudo-similarity model consists of the coupled second-order differential Eqs. (22.22) and (22.26) for the two unknowns $\theta(\eta, \xi)$ and $h(\eta, \xi)$. These equations can be treated as ordinary differential equations solved as a two-point boundary value problem in the single variables η with n and Pr_x being the only parameters. Boundary conditions for the subsidiary unknown h become

$$\eta = 0: \quad h(\eta, \zeta) = 0 \quad (22.27)$$

$$\eta = \eta_{\delta_t}, \quad h(\eta, \zeta) = 0 \quad (22.28)$$

after differentiation of the boundary conditions (22.17) and (22.19) for θ and respect ζ .

22.6 Critical Local Prandtl Number

The momentum boundary layer thickness η_{δ_1} and the thermal boundary layer thickness η_{δ_t} are different in most of the cases for falling film flow of power-law fluids. From Eqs. (22.14) and (22.15) it is found that the momentum boundary layer thickness η_{δ_1} only depends on the power-law index n , and it was observed in Chap. 21 that η_{δ_1} is a monotonically decreasing function of n throughout the parameter range $0.1 \leq n \leq 2$. In that study the momentum boundary layer thickness η_{δ_1} was defined in accordance with common practice in aerodynamic boundary layer theory, namely as the value of η for which the dimensionless velocity component $W_x(\eta)$ becomes equal to 0.99. For convenience, however, in the present investigation, the momentum boundary layer thickness η_{δ_1} is defined as the value of η for which $W_x(\eta)$ is practically equal to one (i.e., to within $10^{-4}\%$).

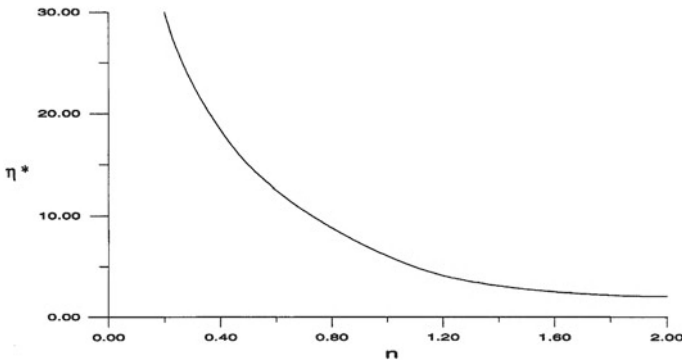


Fig. 22.2 Variation of critical momentum boundary layer thickness $\eta_{\delta_1}^*$ with power-law index n , cited from Shang and Andersson [8]

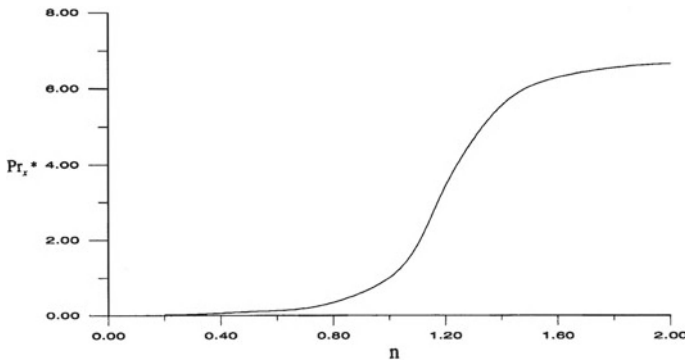


Fig. 22.3 Variation of critical Prandtl number Pr_x^* with power-law index n , cited from Shang and Andersson [8]

From Eq. (22.16) it is found that the thermal boundary thickness η_{δ_t} is observed as a part of the solution of a two-parameter problem, and it does not only depend on the power-law index n but varies also with the local Prandtl number Pr_x . In the study in [8, 9], Shang, Andersson, and Gu found that thermal boundary thickness η_{δ_t} will increase with decreasing the local Prandtl number Pr_x , and with increasing then power-law index n . For a given value of n , there should be a critical value of the local Prandtl number Pr_x , with which the thermal boundary layer thickness η_{δ_t} equals the momentum boundary layer thickness η_{δ_1} . This critical value of the local Prandtl number Pr_x is defined as the critical local Prandtl number, which is denoted by Pr_x^* . In this case, the completely identical momentum boundary layer thickness η_{δ_1} and thermal boundary layer are denoted by critical boundary layer thickness $\eta_{\delta_1}^*$.

The variations of the critical momentum boundary layer thickness $\eta_{\delta_1}^*$ and the critical value of the local Prandtl number Pr_x^* with n are displayed in Figs. 22.2 and 22.3 [8] respectively.

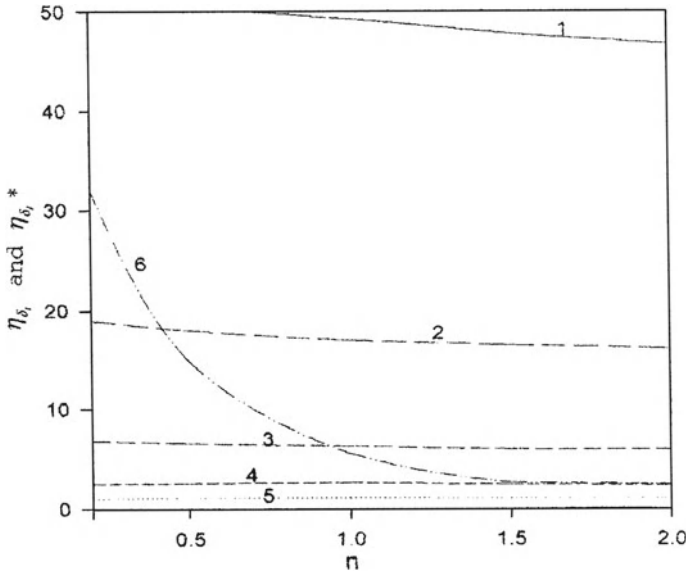


Fig. 22.4 Comparison of the thickness η_{δ_T} and $\eta_{\delta_1}^*$ together with n and Pr_x (1–5: η_{δ_T} with $Pr_x = 0.01, 0.1, 1, 10, 100$ respectively; 6: $\eta_{\delta_1}^*$), cited from Shang and Gu [9]

22.7 Analysis of Boundary Layer Thickness

22.7.1 Precautions for $Pr_x > Pr_x^*$

According to the study of Shang and Gu [9], the thickness of the thermal boundary layer η_{δ_T} , which is defined by $\partial\theta(\eta, \zeta)/\partial\eta = 0.00001$, has been determined for various local Prandtl numbers and power-law index. Figure 22.4 [9] shows a series of the related results, together with the variation of the thickness $\eta_{\delta_1}^*$ with n . From Fig. 22.4, it is seen that, for a special power-law index n , the thermal boundary layer thickness η_{δ_T} is thinner than the critical momentum boundary layer thickness $\eta_{\delta_1}^*$ for $Pr_x > Pr_x^*$. The difference between the thickness increases significantly with the increase of Pr_x , so that the temperature gradients are only confined to the innermost part of the velocity boundary layer for $Pr_x \gg Pr_x^*$. The numerical accuracy will accordingly deteriorate if the two boundary layer problems are solved simultaneously all the way from the wall ($\eta = 0$) to the edge of the momentum boundary layer ($\eta = \eta_{\delta_1}$), cf. Table 22.1. The remedy is to carry out the numerical calculation only sufficiently far so that the temperature gradient vanishes. To accomplish this, the external boundary condition for the velocity field in Eq. (22.18) is replaced with the accurately computed value of W_x at the particular position, which corresponds to the edge of the calculation domain for the temperature field. As for the specific example $n = 0.5$ and $Pr_x = 10$ in the Table 22.2, the numerical solution was obtained with

Table 22.1 Similarity solution for the velocity field for power-law index $n = 0.5$, cited from Shang and Andersson [8]

η	W_y	W_x	$\frac{dW_x}{d\eta}$
0	0	0	1.104406
0.1	-0.001811	0.105273	1.000948
0.2	-0.007129	0.200581	0.905206
0.3	-0.015776	0.286522	0.8914695
0.4	-0.027575	0.363738	0.730722
0.5	-0.042347	0.432889	0.653416
0.6	-0.059914	0.494642	0.582748
0.7	-0.080097	0.549655	0.518561
0.8	-0.102721	0.598562	0.460595
0.9	-0.127614	0.64197	0.408512
1	-0.154608	0.680448	0.361926
1.2	-0.214262	0.744686	0.28355
1.4	-0.280483	0.794992	0.222044
1.6	-0.352205	0.83441	0.17416
1.8	-0.428503	0.865373	0.137048
2	-0.508594	0.889788	0.108331
2.2	-0.591817	0.909136	0.086094
2.5	-0.721362	0.931076	0.061694
3	-0.946498	0.955015	0.036572
5	-1.179419	0.969477	0.022584
4	-1.417354	0.978569	0.014495
4.5	-1.658602	0.984503	0.009636
5	-1.9021	0.988507	0.006611
6	-2.393348	0.99328	0.003375
8	-3.384437	0.99729	0.001132
10	-4.380367	0.998791	0.000484
12	-5.37828	0.999488	0.000248
15	-6.876808	1	0.000118

$W_x(2.5) = 0.931076$ taken from Table 22.1 as outer condition for W_x , in spite of the fact that the momentum boundary layer extends all the way $\eta = 15$.

22.7.2 Precautions for $Pr_x < Pr_x^*$

For a special power-law index n , the thermal boundary layer becomes thicker than the viscous boundary layer if $Pr_x < Pr_x^*$ and in this case the ratio of the thermal boundary layer thickness η_{δ_T} to the momentum boundary layer thickness η_{δ_1} , i.e. $\eta_{\delta_T}/\eta_{\delta_1}$ increases with decreasing Pr_x . Temperature gradients thus extend far into the frictionless flow. To facilitate the numerical calculation of the thermal boundary layer problem and assure the numerical accuracy, the momentum boundary layer

Table 22.2 Local no-similarity (pseudo-similarity) solution of the heat transfer problem for $n = 0.5$ and $Pr_x = 10$, cited from Shang and Andersson [8]

η	W_y	W_x	$\frac{dW_x}{d\eta}$	$\theta(\eta, \zeta)$	$\frac{d\theta(\eta, \zeta)}{d\eta}$
0	0	0	1.104406	1.000000	-1.139345
0.1	-0.001811	0.105273	1.000948	0.886103	-1.137857
0.2	-0.007129	0.200581	0.905206	0.772716	-1.127787
0.3	-0.015776	0.286522	0.8914695	0.661083	-1.101675
0.4	-0.027575	0.363738	0.730722	0.553101	-1.054052
0.5	-0.042347	0.432889	0.653416	0.451082	-0.982272
0.6	-0.059914	0.494642	0.582748	0.357429	-0.887155
0.7	-0.080097	0.549655	0.518561	0.274286	-0.773095
0.8	-0.102721	0.598562	0.460595	0.203198	-0.647450
0.9	-0.127614	0.64197	0.408512	0.144881	-0.519255
1	-0.154608	0.680448	0.361926	0.099129	-0.397539
1.2	-0.214262	0.744686	0.28355	0.040563	-0.200474
1.4	-0.280483	0.794992	0.222044	0.013642	-0.081438
1.6	-0.352205	0.83441	0.17416	0.003704	-0.026229
1.8	-0.428503	0.865373	0.137048	0.000799	-0.006607
2	-0.508594	0.889788	0.108331	0.000135	-0.001286
2.2	-0.591817	0.909136	0.086094	0.000017	-0.000192
2.4	-0.677629	0.924559	0.068834	0.000001	-0.000022
2.5	-0.721362	0.931076	0.061694	0.000000	-0.000007

Eqs. (22.14) and (22.15) are calculated only up to η_{δ_1} . Thereafter, the velocity field is taken as

$$W_x(\eta) = 1, \tag{22.29}$$

throughout the remaining η -range from η_{δ_1} to η_{δ_T} . Meanwhile, with Eq. (22.29) and by using the relationship $\frac{dW_x(\eta)}{d\eta} = 0$, the continuity Eq. (22.14) is changed into the following one:

$$\frac{dW_y(\eta)}{d\eta} = -\frac{1}{2}$$

Integrating the above equation, we obtain the following relationship about $W_y(\eta)$:

$$W_y(\eta) = -\frac{1}{2}\eta + \text{constant} \tag{22.30}$$

By using Eqs. (22.29) and (22.30) the governing Eqs. (22.14), (22.15), (22.16), and (22.24) are further calculated. A specific example $n = 1.5$ and $Pr_x = 1$ is given in Table 22.3 and shown graphically in Fig. 22.5. Here, the analytical continuation in the range $2.7 \leq \eta \leq 5.6$.

Table 22.3 Local pseudo-similarity solution of the heat transfer problem for $n = 1.5$ and $Pr_x = 1.0$, cited from Shang and Andersson [8]

η	W_y	W_x	$\frac{dW_x}{d\eta}$	$\theta(\eta, \zeta)$	$\frac{d\theta(\eta, \zeta)}{d\eta}$
0	0	0	0.865908	1.000000	-0.485194
0.1	-0.000872	0.084788	0.829724	0.951482	-0.485141
0.2	-0.003513	0.165922	0.792848	0.902982	-0.484778
0.3	-0.007964	0.243336	0.755334	0.854547	-0.483804
0.4	-0.014265	0.316969	0.717243	0.806251	-0.481941
0.5	-0.022462	0.386768	0.678643	0.758197	-0.478929
0.6	-0.032598	0.452683	0.649610	0.710511	-0.474537
0.7	-0.044719	0.514678	0.600232	0.663342	-0.468567
0.8	-0.058871	0.572721	0.560604	0.616856	-0.460861
0.9	-0.075097	0.626794	0.520837	0.571231	-0.451305
1	-0.093438	0.676888	0.481052	0.526658	-0.439837
1.2	-0.136618	0.765174	0.401986	0.441431	-0.411192
1.4	-0.188649	0.827799	0.324677	0.362651	-0.375526
1.6	-0.249641	0.895264	0.250661	0.291595	-0.334268
1.8	-0.319506	0.938405	0.181772	0.229180	-0.289483
2	-0.397884	0.968456	0.120153	0.175877	-0.243570
2.2	-0.484046	0.987115	0.068278	0.131667	-0.198916
2.4	-0.566790	0.996604	0.028956	0.096088	-0.157574
2.6	-0.674316	0.999743	0.005337	0.068316	-0.121037
2.7	-0.724114	1	0.000493	0.057033	-0.104856
2.8	-0.774108	1	0	0.047296	-0.090137
3	-0.874108	1	0	0.031870	-0.065079
3.4	-1.074108	1	0	0.013323	-0.030914
3.8	-1.274108	1	0	0.004974	-0.012972
4	-1.374108	1	0	0.002909	-0.008021
4.4	-1.574108	1	0	0.000906	-0.002794
4.8	-1.774108	1	0	0.000243	-0.000858
5	-1.874108	1	0	0.000116	-0.000454
5.4	-2.074108	1	0	0.000016	-0.000114
5.6	-2.174108	1	0	0	-0.000054

Note The velocity field beyond $\eta = 2.7$ is obtained from the analytical continuation in Eqs. (22.29) and (22.30)

22.8 Remarks

The pseudo-similarity solutions of the thermal boundary layer of a falling film flow of power-law fluids are presented in this present work. Based on a proposed “local Prandtl number”, the dependence of the thickness of the momentum boundary layer and thermal boundary layer on the power-law index and local Prandtl number are discussed. Their changes with power-law index and local Prandtl number are also presented. The momentum layer thickness η_{δ_1} depends only on the power-law index n , while the thermal boundary layer thickness η_{δ_T} depends both on the power-law index n and the local Prandtl number Pr_x . The momentum boundary layer thickness

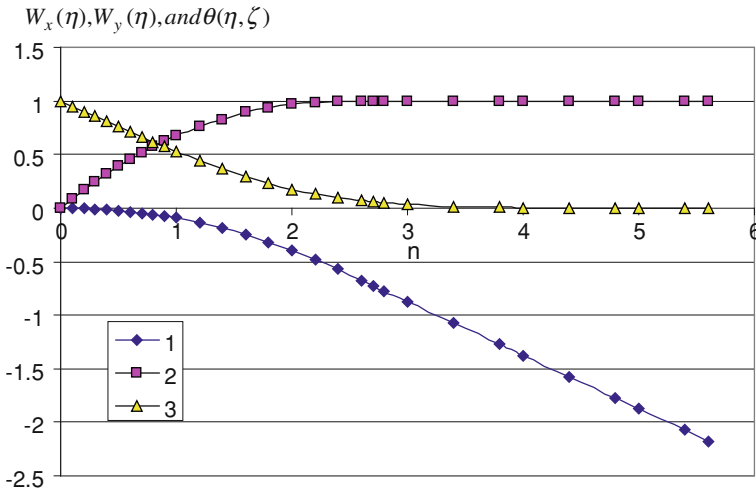


Fig. 22.5 Profiles of $W_x(\eta)$, $W_y(\eta)$ and $\theta(\eta, \zeta)$ for $Pr_x = 1$ and $n = 1.5$ Lines 1–3: for $W_y(\eta)$, $W_x(\eta)$ and $\theta(\eta, \zeta)$

η_{δ_1} decreases significantly with the increase of the parameter n , while the thermal boundary layer thickness η_{δ_t} decreases slightly with the increase of n . The thermal boundary layer thickness η_{δ_T} increases with increasing the parameter n and decreases with the increasing the parameter Pr_x , especially when $Pr_x < 1$. This analysis provides a clear identification of different regions for both $\eta_{\delta_T} > \eta_{\delta_1}^*$ and $\eta_{\delta_T} < \eta_{\delta_1}^*$.

With the introduction of the “local Prandtl number”, it is found that the heat transfer problem turned out to involve only two independent parameters, the power-law index and the local Prandtl number. In addition, the dependence of the power-law index and the local Prandtl number on the thermal boundary layer has been clarified.

The pseudo-similarity solution and the assumed true-similarity solution are presented for the investigation of non-similarity thermal boundary layer. The degree of non-similarity of thermal boundary layer has been determined for various values of power-law indices and local Prandtl numbers.

References

1. S.M. Yih, M.W. Lee, Heating or evaporation in the thermal entrance region of a non-newtonian laminar falling liquid film. *Int. J. Heat Mass Transf.* **29**, 1999–2002 (1986)
2. G. Astarita, Mass transfer from a flat solid surface to a falling non-Newtonian liquid film. *Ind. Eng. Chem. Fundam.* **5**, 14–18 (1966)
3. R.A. Mashelker, V.V. Chavan, Solid dissolution in falling films of non-Newtonian liquids. *J. Chem. Jpn.* **6**, 160–167 (1973)
4. I. Pop, T. Watanabe, H. Konishi, Gravity-driven laminar film flow along a vertical wall with surface mass transfer. *Int. Commun. Heat Mass Transf.* **23**(5), 685–695 (1996)

5. D. Ouldhadda, A. Idrissi, Laminar flow and heat transfer of non-Newtonian falling liquid film on a horizontal tube with variable surface heat flux. *Int. Commun. Heat Mass Transf.* **28**, 1125–1135 (2001)
6. B.K. Rao, Heat transfer to falling power-law fluid film. *Int. J. Heat Fluid Flow* **20**, 429–436 (1999)
7. H. Andersson, D.Y. Shang, An extended study of hydrodynamics of gravity-driven film flow of power-law fluids. *Fluid Dyn. Res.* **22**, 345–357 (1998)
8. D.Y. Shang, H. Andersson, Heat transfer in gravity-driven film flow of power-law fluids. *Int. J. Heat Mass Transf.* **42**(11), 2085–2099 (1999)
9. D.Y. Shang, J. Gu, Analyses of pseudo-similarity and boundary layer thickness for non-Newtonian falling film flow. *Heat Mass Transf.* **41**(1), 44–50 (2004)
10. H.I. Andersson, F. Irgens, Hydrodynamic entrance length of non-Newtonian liquid films. *Chem. Eng. Sci.* **45**, 537–541 (1990)
11. H.I. Andersson, F. Irgens, Gravity-driven laminar film flow of power-law fluids along vertical walls. *J. Non-Newtonian Fluid Mech.* **27**, 153–172 (1988)
12. H.I. Andersson, F. Irgens, Film flow of power law fluids, in *Encyclopaedia of Fluid Mechanics*, vol. 9, ed. by N.P. Chermisinoff, (Gulf Publishing Company, Houston, 1990), pp. 617–648
13. H.I. Andersson, Diffusion from a vertical wall into an accelerating falling liquid film. *Int. J. Heat Mass Transf.* **30**, 683–689 (1987)
14. E.M. Sparrow, H. Quack, C.J. Boener, Local nonsimilarity boundary—layer solutions. *AIAA J.* **8**, 1936–1942 (1970)

Chapter 23

Heat Transfer of the Falling Film Flow of Non-Newtonian Power-Law Fluids

Abstract A deep study is done on heat transfer from an inclined plane surface to an accelerating liquid film of a non-Newtonian power-law fluid. The new similarity analysis method for the accompanying hydrodynamic problem was adopted in combination with a local pseudo-similarity method. The resulting transformed problem turned out to involve only two independent parameters, namely the power-law index and the local Prandtl number. All other related physical properties and parameters are combined into the induced local Reynolds number, and the dimensionless velocity components. Accurate numerical results are obtained for combinations of local Prandtl number from 0.001 to 1000 and the power-law index n in the range $0.2 \leq n \leq 2$. Special treatment for the low and high local Prandtl number cases is essential in order to maintain the numerical accuracy. The calculated results obtained both by using local similarity and local pseudo-similarity methods are practically indistinguishable for $n = 1$ over the entire local Prandtl number range. Furthermore, it is found that the wall temperature gradient which depends on local Prandtl number and power-law index is the only one no-given condition for evaluation of heat transfer. With increasing the local Prandtl number, the heat transfer coefficient increases, but with increasing the power-law increase, the heat transfer coefficient decreases. A set of accurate curve-fit formulas for the wall temperature gradient is provided, so that the rapid estimates of the heat transfer rate for any combination of the local Prandtl number and power-law index within the parameter ranges considered are realized.

23.1 Introduction

There have been a number of studies on heat transfer from a constant temperature wall to hydrodynamically fully developed power-law films, such as those by Yih and Lee [1], Astarita [2], Mashelkar and Chavan [3], Pop et al. [4], Ouldhadda et al. [5], Rao [6], etc. However, only a few of recent studies of Shang, Andersson, and

Gu [7, 8] focused on a system of solutions of thermal boundary layer by using a pseudo-similarity approach, including the rigorous solutions about the heat transfer coefficient of the falling-film flow of non-Newtonian power-law fluids.

Based on the presentation in Chap. 22 for pseudo-similarity analyses of the boundary layer thickness for the non-Newtonian falling film flow, in this present chapter, a mathematical model for the flow and heat transfer in accelerating liquid film of a non-Newtonian falling film flow is further presented. For the case that the local Prandtl number Pr_x is larger than the critical Prandtl number Pr_x^* , the predicted temperature field in the boundary layer region is controlled by the velocity field of the momentum boundary layer calculated by using the governing mass and momentum equations. For the case that the local Prandtl number Pr_x is smaller than the critical Prandtl number Pr_x^* , it is difficult to directly obtain the simultaneous solutions from the equations of the momentum and thermal boundary layers, and it is necessary to apply the perfect approach presented in Chap. 22 for overcoming such difficulty.

Since the thermal boundary layer permits exact similarity solution only in the particular case when the power-law index is equal to unity, i.e. for Newtonian films, the heat transfer problem is solved by means of a pseudo-similarity approach with power-law index n and local Prandtl number Pr_x being the only parameters. The pseudo-similarity heat transfer problem is calculated numerically in the ranges $0.2 \leq n \leq 2$ and $0.001 \leq Pr_x \leq 1000$, in which the calculations for $n = 1$ are compared favorably with earlier results for Newtonian fluid films. From the numerical solutions of the pseudo-similarity energy equation of the thermal boundary layer, it is found that the effect of the power-law index n on the wall gradient of the temperature field is slight except for smaller power-law index n with larger local Prandtl number Pr_x . However, the wall gradient of the temperature field will increase with increasing the local Prandtl number Pr_x . Curve-fit formulas for the temperature gradient at the wall are provided in order to facilitate rapid and yet accurate estimates for the heat transfer coefficient and the Nusselt number.

23.2 Governing Equations

Consider the accelerating laminar flow in the boundary layer region of a non-Newtonian power-law liquid film down along an inclined plane surface, as shown schematically in Fig. 21.1. According to Chaps. 21 and 22, the governing dimensionless differential equations for mass, momentum, and energy conservations are summarized as follows for the pseudo-similarity solutions:

$$W_x(\eta) - \frac{n}{(1+n)}\eta \frac{dW_x(\eta)}{d\eta} + 2 \frac{dW_y(\eta)}{d\eta} = 0 \quad (23.1)$$

$$\begin{aligned}
W_x(\eta) \left[-\frac{n}{(1+n)} \eta \frac{dW_x(\eta)}{d\eta} + W_x(\eta) \right] + 2W_y(\eta) \frac{dW_x(\eta)}{d\eta} \\
= 1 + 2n \left(\frac{dW_x(\eta)}{d\eta} \right)^{n-1} \frac{d^2W_x(\eta)}{d\eta^2}
\end{aligned} \quad (23.2)$$

$$\left[-\frac{n}{2(1+n)} \eta W_x(\eta) + W_y(\eta) \right] \frac{\partial \theta(\eta, \zeta)}{\partial \eta} + \zeta W_x(\eta) g(\eta, \zeta) = \frac{1}{\text{Pr}_x} \frac{\partial^2 \theta(\eta, \zeta)}{\partial \eta^2} \quad (23.3)$$

$$\begin{aligned}
\left[-\frac{n}{2(n+1)} \eta W_x(\eta) + W_y(\eta) \right] \frac{\partial h(\eta, \zeta)}{\partial \eta} + W_x(\eta) h(\eta, \zeta) \\
= \frac{1}{\text{Pr}_x} \left[\frac{\partial^2 h(\eta, \zeta)}{\partial \eta^2} - \frac{n-1}{2(n+1)} \left(\frac{\partial^2 \theta(\eta, \zeta)}{\partial \eta^2} \right) \right]
\end{aligned} \quad (23.4)$$

subject to the boundary conditions

$$\eta = 0: W_x(\eta) = 0, W_y(\eta) = 0, \theta(\eta, \zeta) = 1, h(\eta, \zeta) = 0 \quad (23.5)$$

$$\eta = \eta_{\delta_l}: W_x(\eta) = 1 \quad (23.6)$$

$$\eta = \eta_{\delta_T}, \theta(\eta, \zeta) = 0, h(\eta, \zeta) = 0 \quad (23.7)$$

Here, the dimensionless coordinate variables are

$$\eta = \frac{y}{x} \text{Re}_x^{1/(n+1)} \quad (23.8)$$

$$\zeta = \frac{x}{x_0} \quad (23.9)$$

where x_0 is a characteristic length scale in the streamwise direction and the generalized local Reynolds number is

$$\text{Re}_x = \frac{x^n (w_{x,\infty})^{2-n} \rho}{K} \quad (23.10)$$

While the velocity component w_x within the boundary layer approaches the external velocity

$$w_{x,\infty} = \sqrt{2gx \cos \alpha} \quad (23.11)$$

The dimensionless velocity components are defined as

$$W_x(\eta) = \frac{w_x}{\sqrt{2gx \cos \alpha}} \quad (23.12)$$

$$W_y(\eta) = \frac{w_y}{\sqrt{2gx \cos \alpha}} \text{Re}_x^{\frac{1}{n+1}} \quad (23.13)$$

which are independent of ζ except for the particular value $n = 1$. The dimensionless temperature and the related new variables are defined as

$$\theta(\eta, \zeta) = \frac{t - t_\infty}{t_w - t_\infty} \quad (23.14)$$

$$g(\eta, \zeta) = \frac{\partial \theta(\eta, \zeta)}{\partial \zeta} \quad (23.15)$$

$$h(\eta, \xi) = \xi \cdot g(\eta, \xi) = \xi \frac{\partial \theta(\eta, \xi)}{\partial \xi} \quad (23.16)$$

which depend both on η and ζ . The local Prandtl number Pr_x is defined by a dimensionless diffusion coefficient, i.e.

$$\text{Pr}_x = \frac{x w_{x,\infty}}{a} (\text{Re}_x)^{-\frac{2}{n+1}} \quad (23.17)$$

Since the thickness η_{δ_T} of the thermal boundary layer is observed as a part of the solution of a two-parameter problem, η_{δ_T} does not only depend on n but varies also with Pr_x . For a given value of n , a *critical local Prandtl number* Pr_x^* is defined as the particular parameter value for which the thermal boundary layer thickness η_{δ_T} equals the momentum boundary layer thickness η_{δ_l} . This critical value is denoted by Pr_x^* and shown in Fig. 20.3, from which Pr_x^* can be seen to increase monotonically with n .

23.3 Heat Transfer Analysis

The heat transfer rate between the solid wall, which is maintained at temperature t_w , and the liquid film is of particular significance in industrial applications. The local heat transfer rate q_x , which is defined as follows by Fourier's law:

$$q_x = -\lambda \left(\frac{\partial t}{\partial y} \right)_{y=0} \quad (23.18)$$

where λ is the thermal conductivity of the non-Newtonian liquid. With the above defined dimensionless coordinate variable η , Eq. (23.18) can be transformed to the followings

$$q_x = -\lambda \left(\frac{\partial t}{\partial \eta} \right)_{\eta=0} \left(\frac{\partial \eta}{\partial y} \right)_{y=0}$$

With Eqs. (22.8) and (22.14), the local heat transfer rate is described as

$$q_x = -\lambda x^{-1} (t_w - t_\infty) \left[\frac{\partial \theta(\eta, \zeta)}{\partial \eta} \right]_{\eta=0} (\text{Re}_x)^{1/(n+1)} \quad (23.19)$$

where $\left[\frac{\partial\theta(\eta, \zeta)}{\partial\eta}\right]_{\eta=0}$ is the dimensionless local temperature gradient on the wall. Then, with Newtonian-Cooling law $q_x = \alpha_x(t_w - t_\infty)$, the local transfer coefficient α_x is expressed as follows:

$$\alpha_x = -\lambda x^{-1} \left[\frac{\partial\theta(\eta, \zeta)}{\partial\eta}\right]_{\eta=0} (\text{Re}_x)^{1/(n+1)} \quad (23.20)$$

or, alternately, as local Nusselt number

$$\text{Nu}_x = \frac{\alpha_x x}{\lambda} = -(\text{Re}_x)^{1/(n+1)} \left[\frac{\partial\theta(\eta, \zeta)}{\partial\eta}\right]_{\eta=0} \quad (23.21)$$

If Q_x is total heat transfer rate from the position 0 to x with the width of b on the plate, Q_x is the following integration:

$$Q_x = \iint_A q_x dA$$

where $A = b \cdot x$. Then,

$$\begin{aligned} Q_x &= b \int_0^x q_x dx \\ &= -b \int_0^x \lambda x^{-1} (t_w - t_\infty) \left[\frac{\partial\theta(\eta, \zeta)}{\partial\eta}\right]_{\eta=0} (\text{Re}_x)^{1/(n+1)} dx \\ &= -b \int_0^x \lambda x^{-1} (t_w - t_\infty) \left[\frac{\partial\theta(\eta, \zeta)}{\partial\eta}\right]_{\eta=0} \left(\frac{x^n (w_{x,\infty})^{2-n} \rho}{K}\right)^{1/(n+1)} dx \\ &= -b \int_0^x \lambda (t_w - t_\infty) \left[\frac{\partial\theta(\eta, \zeta)}{\partial\eta}\right]_{\eta=0} \left(\frac{(2g \cos \alpha)^{\frac{2-n}{2}} \rho}{K}\right)^{1/(n+1)} x^{-n/(2(n+1))} dx \\ &= -b \frac{2(n+1)}{n+2} \lambda (t_w - t_\infty) \left[\frac{\partial\theta(\eta, \zeta)}{\partial\eta}\right]_{\eta=0} \\ &\quad \times \left(\frac{(2g \cos \alpha)^{\frac{2-n}{2}} \rho}{K}\right)^{1/(n+1)} x^{(n+2)/(2(n+1))} \\ &= -b \frac{2(n+1)}{n+2} \lambda (t_w - t_\infty) \left[\frac{\partial\theta(\eta, \zeta)}{\partial\eta}\right]_{\eta=0} \left(\frac{x^n (\sqrt{2gx \cos \alpha})^{2-n} \rho}{K}\right)^{1/(n+1)} \end{aligned}$$

Then,

$$Q_x = -b \frac{2(n+1)}{n+2} \lambda (t_w - t_\infty) \left[\frac{\partial \theta(\eta, \zeta)}{\partial \eta} \right]_{\eta=0} (\text{Re}_x)^{1/(n+1)} \quad (23.22)$$

The average transfer coefficient $\bar{\alpha}_x$, defined as $Q_x = \bar{\alpha}_x (t_w - t_\infty) A$, is expressed as

$$\bar{\alpha}_x = -\frac{2(n+1)}{n+2} \lambda x^{-1} \left[\frac{\partial \theta(\eta, \zeta)}{\partial \eta} \right]_{\eta=0} (\text{Re}_x)^{1/(n+1)} \quad (23.23)$$

The average Nusselt number, defined as $\overline{\text{Nu}}_x = \frac{\bar{\alpha}_x x}{\lambda}$, is expressed as

$$\overline{\text{Nu}}_x = -\frac{2(n+1)}{n+2} \left[\frac{\partial \theta(\eta, \zeta)}{\partial \eta} \right]_{\eta=0} (\text{Re}_x)^{1/(n+1)} \quad (23.24)$$

From Eqs. (23.19) to (23.24) it is found that the local temperature gradient $\left[\frac{\partial \theta(\eta, \zeta)}{\partial \eta} \right]_{\eta=0}$ is very important for evaluation of the local heat transfer. From governing Eqs. (23.2) and (23.4) it follows that $\left[\frac{\partial \theta(\eta, \zeta)}{\partial \eta} \right]_{\eta=0}$ only depends on power-law index n and local Prandtl number Pr_x , i.e.

$$\left[\frac{\partial \theta(\eta, \zeta)}{\partial \eta} \right]_{\eta=0} = f(n, \text{Pr}_x) \quad (23.25)$$

23.4 Numerical Solution for Heat Transfer

The solutions for the pseudo-similarity equations of thermal boundary layer are obtained from the Eqs. (23.1)–(23.4) with the boundary condition Eqs. (23.5)–(23.7). Figure 23.1 shows a number of computed temperature profiles $\theta(\eta)$ with the variations of power-law index n from 0.2 to 2 and local Prandtl number Pr_x from 0.001 to 1000. While the wall temperature gradient $\left[\frac{\partial \theta(\eta, \zeta)}{\partial \eta} \right]_{\eta=0}$, which is the most important heat transfer characteristic, is listed in Table 23.1 [7] and plotted in Fig. 23.2. It is shown that the distribution of temperature $\theta(\eta)$ increases significantly with increasing local Prandtl number Pr_x from 0.001 to 1000. However, effect of the power-law index n on the wall gradient of the temperature field is slight except for smaller power-law index n together with larger local Prandtl number Pr_x . For the particular parameter value $n = 1$ the wall temperature gradient data in Table 23.1 agreed with the calculation for a Newtonian film by Andersson [9] throughout the entire Prandtl number range.

The most striking feature of Fig. 23.1 is that the local Prandtl number effect is more prominent than the influence of the rheological parameter n , except for larger local Prandtl number with smaller power-law index n . If the value of the power-law index n equals unity, the thickness of the thermal boundary layer is roughly the same

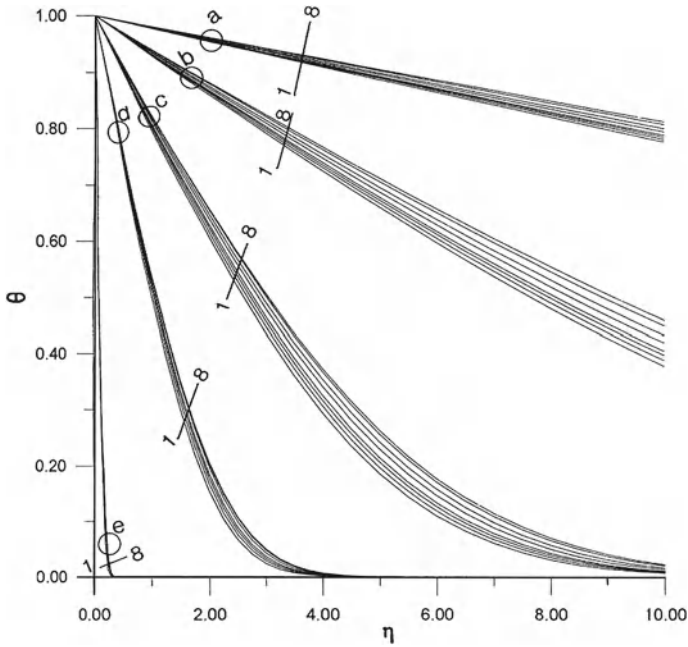


Fig. 23.1 Dimensionless temperature profile $\theta(\eta, \zeta)$ for different values of Pr_x and n , cited from Shang and Andersson [7]. **a** $Pr_x = 0.001$; curves 1–8: $n = 0.2, 0.3, 0.5, 0.7, 1.0, 1.2, 1.5$ and 2.0 , **b** $Pr_x = 0.01$; curves 1–8: $n = 0.2, 0.3, 0.5, 0.7, 1.0, 1.2, 1.5$ and 2.0 , **c** $Pr_x = 0.1$; curves 1–8: $n = 0.2, 0.3, 0.5, 0.7, 1.0, 1.2, 1.5$ and 2.0 , **d** $Pr_x = 1.0$; curves 1–8: $n = 2.0, 1.5, 1.2, 1.0, 0.2, 0.7, 0.3$ and 0.5 , **e** $Pr_x = 1000$; curves 1–8: $n = 0.2, 0.3, 2.0, 0.5, 1.5, 0.7, 1.2, 1.2$ and 1.0

as the thickness of the momentum boundary layer for $Pr_x = 1$. Moreover, for high local Prandtl number the thermal boundary layer is significantly thinner than the viscous boundary layer, while for $Pr_x \ll 1$ the thermal boundary layer extends far into the external free stream. Consequently, the thinning of the thermal boundary layer with increasing values of Pr_x makes the magnitude of the temperature gradient at the wall. The thick thermal boundary layer in the low local Prandtl number cases suggests that the temperature adjusts from T_w to T_∞ mainly in fluid with free stream velocity $w_{x,\infty}$. Thus, as a first approximation, the viscous boundary layer does not contribute to the heat flux and the temperature gradient at the wall should therefore be independent of n . However, the data for $Pr_x = 0.001$ in Table 23.1 shows that the wall temperature gradient increases slowly with n as n is varied from 0.2 to 2, the total increase being less than 8%. For $Pr_x \ll 1$ the principal effect of the viscous boundary layer on the temperature gradient at the wall stems from the displacement of the external inviscid flow away from the wall.

A qualitatively different situation occurs for high local Prandtl numbers. Due to the substantial thinning of the thermal boundary layer with increasing Pr_x , the temperature gradients are contained within the innermost part of the momentum boundary layer. Thus, the wall gradient of the temperature field is controlled by

Table 23.1 Computed values of $-\left[\frac{\partial\theta(\eta,\zeta)}{\partial\eta}\right]_{\eta=0}$ for different values of Pr_x and n , cited from Shang and Andersson [7]

n		Pr_x						
		0.001	0.01	0.1	1	10	100	1000
0.2	(1)	0.02053	0.06315	0.1863	0.5111	1.27986	2.98885	6.7598
	(2)	0.02078	0.06427	0.1838	0.5122	1.28135	2.98621	6.75929
	ε_1 (%)	-1.218	-1.77	1.34	-0.215	1.27	0.088	0.0075
	(3)	0.01897	0.05837	0.1724	0.4742	1.19263	2.78664	6.23798
	ε_2 (%)	7.60	7.57	7.46	7.226	6.82	6.77	7.72
0.5	(1)	0.020969	0.06391	0.1836	0.4793	1.13934	2.56412	5.62871
	(2)	0.020792	0.06494	0.1797	0.4782	1.13641	2.45958	5.63969
	ε_1 (%)	0.844	-1.61	2.12	0.23	0.257	4.077	-0.195
	(3)	0.020222	0.06162	0.1773	0.4638	1.10503	2.49064	5.47372
	ε_2 (%)	3.56	3.58	3.43	3.23	3.01	2.87	2.75
0.7	(1)	0.021202	0.06458	0.1847	0.4758	1.11569	2.49172	5.4554
	(2)	0.021161	0.06595	0.1812	0.4777	1.11644	2.49387	5.46885
	ε_1 (%)	0.193	-2.12	1.89	-0.399	-0.067	-0.086	-0.247
	(3)	0.02081	0.06336	0.1814	0.468	1.09865	2.4545	5.37162
	ε_2 (%)	1.85	1.89	1.79	1.64	1.53	1.49	1.54
1	(1)	0.021457	0.06536	0.1868 17	0.4776	1.10671	2.45403	5.35184
	(2)	0.021458	0.06673	0.182300	0.4773	1.10248	2.44926	5.351
	ε_1 (%)	-0.0047	-2.096	2.418	0.063	0.382	0.194	0.0157
	(3)	0.021455	0.06536	0.186817	0.4776	1.10671	2.45403	5.35184
	ε_2 (%)	0	0	0	0	0	0	0
1.2	(1)	0.021595	0.06583	0.1883	0.4804	1.10769	2.44844	5.33014
	(2)	0.021601	0.06715	0.1834	0.4803	1.10527	2.44816	5.33643
	ε_1 (%)	-0.0278	-2	2.6	0.02	0.2187	0.0114	-0.118
	(3)	0.021786	0.06641	0.1899	0.4842	1.11582	2.46617	5.37031
	(5) (%)	-0.88	-0.88	-0.85	-0.79	-0.73	-0.72	-0.75
1.5	(1)	0.021763	0.06641	0.1903	0.4853	1.11297	2.45196	5.32975
	(2)	0.021788	0.06776	0.1851	0.4847	1.10965	2.45074	5.33106
	ε_1 (%)	-0.115	-2.03	2.73	0.124	0.298	0.05	-0.0246
	(3)	0.022179	0.06767	0.1939	0.4934	1.13046	2.4897	5.41286
	ε_2 (%)	-1.91	-1.90	-1.89	-1.67	-1.57	-1.54	-1.56
2	(1)	0.022111	0.06717	0.193	0.4928	1.1246	2.46821	5.35668
	(2)	0.022099	0.06877	0.1879	0.492	1.12048	2.46717	5.35603
	ε_1 (%)	0.0543	-2.38	2.64	0.162	0.367	0.042	0.012
	(3)	0.022654	0.06922	0.1989	0.5064	1.15317	2.5297	5.49016
	ε_2 (%)	-2.46	-3.05	-3.06	-2.76	-2.54	-2.49	-2.49

Note

- (i) $-\left[\frac{\partial\theta(\eta,\zeta)}{\partial\eta}\right]_{\eta=0}$ (1) (for short as (1)) local pseudo-similarity solution
- (ii) $-\left[\frac{\partial\theta(\eta,\zeta)}{\partial\eta}\right]_{\eta=0}$ (2) (for short as (2)), result evaluated by curve-fit formula (23.26)
- (iii) Deviation ε_1 defined as Eq. (23.27)
- (iv) $-\left[\frac{\partial\theta(\eta)}{\partial\eta}\right]_{\eta=0}$ (3) (for short (3)), local similarity solution
- (v) Deviation ε_2 defined as Eq. (23.29)

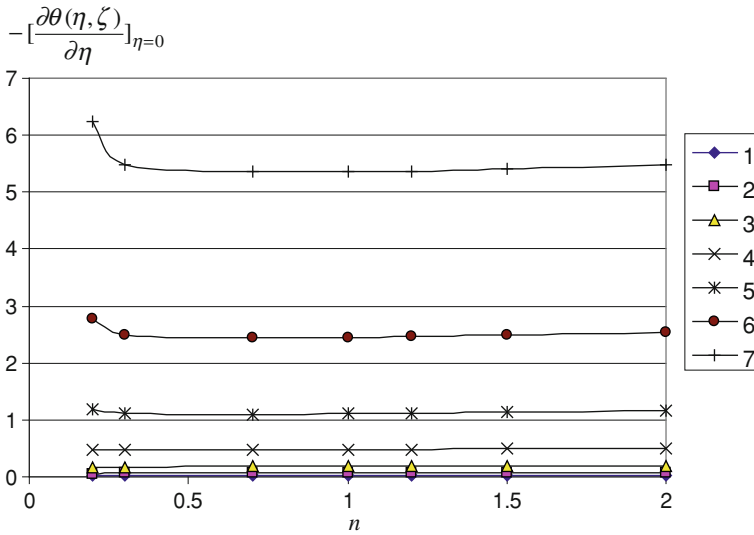


Fig. 23.2 Variation of dimensionless temperature gradient $-\left[\frac{\partial\theta(\eta,\zeta)}{\partial\eta}\right]_{\eta=0}$ at the wall $\eta = 0$ with power-law index n for different values of the local Prandtl number Pr_x . Lines 1–8 note: $Pr_x = 0.001, 0.01, 0.1, 1, 10, 100$ and 1000

the velocity gradient $dW_x/d\eta$ at the wall. The accurate numerical solution of the hydrodynamic problem in [10] showed that $dW_x/d\eta$ is practically independent of n for dilatant film but increases significantly with increasing pseudo-plasticity $1 - n$ for $n < 1$. It is therefore interesting to observe that exactly the same n -dependency is carried over to the wall gradients of the temperature field in Table 23.1.

To facilitate rapid estimates of the local heat transfer coefficient α_x or the local Nusselt number Nu_x , accurate curve-fit formulas for the wall gradient of the temperature field are provided. The optimized expressions for the coefficients a , b , and c , as obtained by Shang and Andersson [7] for matching the formula (23.26) to the data in Table 23.1, are given in Table 23.2. Predictions by means of this shot-cut method are also included in Table 23.1.

$$-\left[\frac{\partial\theta(\eta,\zeta)}{\partial\eta}\right]_{\eta=0} = a + b Pr_x^c \tag{23.26}$$

If we take the corresponding pseudo-similarity solution of temperature gradient from Eqs. (23.3) and (23.4) as $-\left[\frac{d\theta(\eta,\zeta)}{d\eta}\right]_{\eta=0}$ (1), the result evaluated by using Eq. (23.26) as $-\left[\frac{d\theta(\eta,\zeta)}{d\eta}\right]_{\eta=0}$ (2), the result of deviations ε_1 of $-\left[\frac{d\theta(\eta,\zeta)}{d\eta}\right]_{\eta=0}$ (2) from $-\left[\frac{d\theta(\eta,\zeta)}{d\eta}\right]_{\eta=0}$ (1) can be expressed as

Table 23.2 Coefficients a , b and c in the curve-fit formula (21.26), cited from Shang and Andersson [7]

Pr_x	n	a	b	c
$0.001 \leq Pr_x \leq 1$	$0.2 \leq n \leq 1$	$-0.0086 + \frac{0.0009}{n}$	$0.485 + 0.00001 \times \left(\frac{1}{n}\right)^{\frac{1}{n}}$	$0.399 + \frac{0.008}{n}$
	$1 \leq n \leq 2$	$-0.0074 - 0.00028n$	$0.47 + 0.015n$	0.407
$1 \leq Pr_x \leq 1000$	$0.2 \leq n \leq 1$	$0.0205 - 0.0845 \times \left(\frac{1}{n}\right)^{\frac{1}{3}}$	$0.518 + \frac{0.0234}{n}$	$0.3324 + \frac{0.00096}{n} \times \left(\frac{1}{n}\right)^{1.6}$
	$1 \leq n \leq 2$	$-0.12 + 0.079 \times \left(\frac{n}{n+1}\right)^{\frac{1}{2}}$	$0.541 + 0.0009n^3$	$0.3306 + \frac{0.0027}{n} \times \left(\frac{1}{n}\right)^{1.65}$

$$\varepsilon_1 = \frac{-\left[\frac{d\theta(\eta, \zeta)}{d\eta}\right]_{\eta=0} (1) - \left\{-\left[\frac{d\theta(\eta, \zeta)}{d\eta}\right]_{\eta=0} (2)\right\}}{-\left[\frac{d\theta(\eta, \zeta)}{d\eta}\right]_{\eta=0} (1)} \tag{23.27}$$

The evaluated results $-\left[\frac{d\theta(\eta, \zeta)}{d\eta}\right]_{\eta=0} (2)$ and their deviations ε_1 are listed in Table 23.1. It is found that the evaluated values of $-\left[\frac{d\theta(\eta, \zeta)}{d\eta}\right]_{\eta=0} (2)$ are very well agreement with the pseudo-similarity solutions $-\left[\frac{d\theta(\eta, \zeta)}{d\eta}\right]_{\eta=0} (1)$ over the entire parameter ranges $0.2 \leq n \leq 2$ and $0.001 \leq Pr_x \leq 1000$.

In addition, the thickness of temperature boundary layer increases with the decrease of local Prandtl number Pr_x . The related numerical solutions $h(\eta)$ are plotted in Fig. 23.3a, b, which correspond to $Pr_x = 1$ and 100 respectively. In each

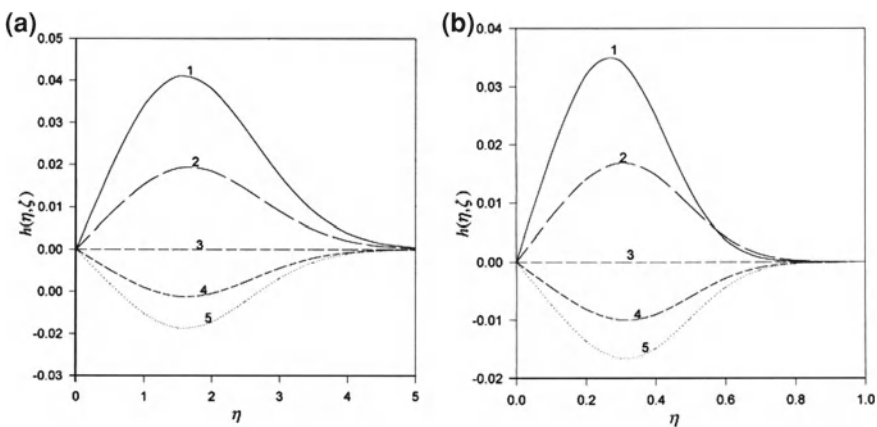


Fig. 23.3 Numerical solutions $h(\eta)$ (Curves 1–5: for $n = 0.2, 0.5, 1, 1.5$ and 2), cited from Shang and Gu [8] **a** for $Pr_x = 1$ and **b** for $Pr_x = 100$

figure the five curves correspond to $n = 0.2, 0.5, 1, 1.5,$ and $2,$ respectively. The solutions $h(\eta)$ reflect the non-similarity of the thermal boundary layer. It is shown in Fig. 23.3 that with variation of local Prandtl number $Pr_x,$ the non-similarity of the thermal boundary layer be different slightly [8]. However, with the increase of the value $|n - 1|,$ non-similarity of the thermal boundary layer increases obviously. Only when the power-law index n equals unity, true similarity solution exists. The variable $h(\eta)$ is positive for $n < 1$ and negative for $n > 1.$

23.5 Local Similarity Versus Local Pseudo-Similarity

If a true-similarity solution were assumed to exist for the thermal boundary layer, the dimensionless energy Eqs. (23.3) and (23.4) would be simplified to

$$\left[-\frac{n}{2(1+n)}\eta W_x(\eta) + W_y(\eta) \right] \frac{d\theta(\eta)}{d\eta} = \frac{1}{Pr_x} \frac{d^2\theta(\eta)}{d\eta^2} \tag{23.28}$$

A simple approach to the non-similar heat transfer problem associated with the gravity-driven power-law film would be the local similarity scheme. In that approach ξ is regarded as a known constant at any streamwise position and the dimensionless energy Eqs. (23.3) and (23.4) would be turned to Eq. (23.28). The numerical solution of the simplified version of Eq. (23.28) can then be obtained locally with Pr_x and n as parameters by means of the same calculation technique as for the local non-similar problem defined in Chap. 22.

The two-parameter *local similarity* problem was solved numerically for various combinations of n and Pr_x in the intervals $0.2 \leq n \leq 2$ and $0.001 \leq Pr_x \leq 1000.$ Results for the magnitude of the wall gradient of the dimensionless temperature field i.e. $-\left[\frac{\partial\theta(\eta,\zeta)}{\partial\eta} \right]_{\eta=0}$ are reported in Table 23.1. To facilitate the comparison between the local *pseudo-similarity* and the local similarity approach the deviation between the two sets of data, normalized with the latter, has been defined as ε_2 and included in the Table 23.1.

If we take the assumed true-similarity solution of the temperature gradient from Eq. (23.28) as $-\left[\frac{d\theta(\eta)}{d\eta} \right]_{\eta=0}$ (3), the deviations ε_2 of $-\left[\frac{d\theta(\eta)}{d\eta} \right]_{\eta=0}$ (3) from pseudo-similarity solution, $-\left[\frac{\partial\theta(\eta,\zeta)}{\partial\eta} \right]_{\eta=0}$ (1) can be expressed as in Eq. (23.29). The value of ε_2 for each n and Pr_x is shown in Table 23.1 and Fig. 23.4.

$$\varepsilon_2 = \frac{-\left[\frac{\partial\theta(\eta,\zeta)}{\partial\eta} \right]_{\eta=0} (1) - \left[-\left[\frac{d\theta(\eta)}{d\eta} \right]_{\eta=0} (3) \right]}{-\left[\frac{\partial\theta(\eta,\zeta)}{\partial\eta} \right]_{\eta=0} (1)} \tag{23.29}$$

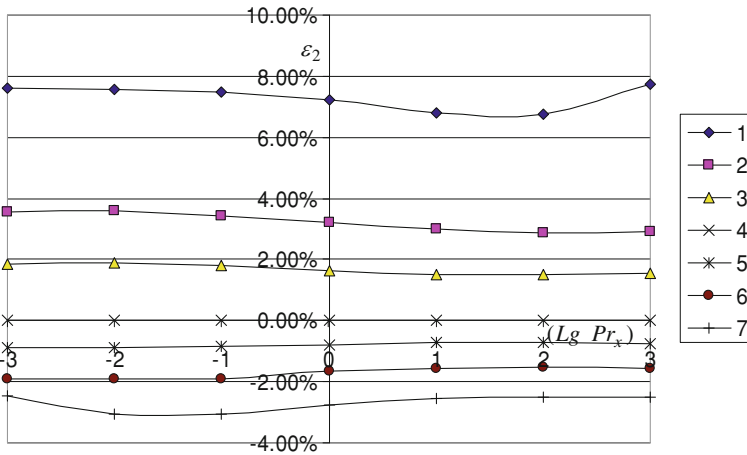


Fig. 23.4 The relative deviation ε_2 between local pseudo-similarity and local similarity solutions in the wall temperature gradient $-\left[\frac{\partial\theta(\eta,\xi)}{\partial\eta}\right]_{\eta=0}$ variation with power-law index n and local Prandtl number Pr_x (Curves 1–7: $n = 0.2, 0.5, 0.7, 1, 1.2, 1.5,$ and 2)

Let us emphasize that the two approaches become identical for $n = 1$ since the thermal boundary layer problem admits exact similarity solutions for Newtonian fluids. It is therefore not surprising that the relative deviation ε_2 in the local similarity and local pseudo-similarity solutions increases with deviation of the power-law index n from unity, i.e. with increasing non-Newtonian rheology. The deviation is moreover more significant for the most *pseudo-plastic liquids* ($n = 0.2$) than for the highly dilatant film ($n = 2$), whereas the local Prandtl number Pr_x turned out to have only a minor effect on ε_2 . It is concluded that the results obtained with the *local pseudo-similarity approach* are of good accuracy.

It is noteworthy to emphasize that the absolute value of deviation rate ε_2 equals zero for $n = 1$, increases with the increase of the absolute value $|n - 1|$. The value of ε_2 is a measure of the degree of non-similarity of the thermal boundary layer, and it is seen from Fig. 23.4 that such non-similarity for pseudo-plastic fluid (with $n < 1$) is more obvious than that of *Dilatant* fluid (with $n > 1$).

23.6 Summary

So far, we have presented the recent developments on heat transfer of falling film flow of non-Newtonian power-law fluids. The related governing equations and heat transfer expressions are summarized in Tables 23.3 and 23.4 respectively.

Table 23.3 Summary of governing equations of falling film flow of non-Newtonian power-law fluids

Term	Equations
<i>Governing partial differential equations</i>	
Mass equation	$\frac{\partial w_x}{\partial x} + \frac{\partial w_y}{\partial y} = 0$
Momentum equation	$w_x \frac{\partial w_x}{\partial x} + w_y \frac{\partial w_x}{\partial y} = g \cos \alpha + n \frac{K}{\rho} \left(\frac{\partial w_x}{\partial y} \right)^{n-1} \frac{\partial^2 w_x}{\partial y^2}$
Energy equation	$w_x \frac{\partial t}{\partial x} + w_y \frac{\partial t}{\partial y} = \frac{\lambda}{\rho c_p} \frac{\partial^2 t}{\partial y^2}$
Boundary conditions	$y = 0 : w_x = 0, w_y = 0, t = t_w$ $y = \delta_l, w_x = w_{x,\infty}$ $y = \delta_t, t = t_\infty$
<i>Similarity variables</i>	
η	$\frac{y}{x} \text{Re}_x^{1/(n+1)}$
Re_x	$\frac{x^n (w_{x,\infty})^{2-n} \rho}{K}$
Pr_x	$\frac{x w_{x,\infty}}{a} (\text{Re}_x)^{-\frac{2}{n+1}}$
$W_x(\eta)$	$\frac{w_x}{\sqrt{2g_x \cos \alpha}}$
$W_y(\eta)$	$\frac{w_y}{\sqrt{2g_x \cos \alpha}} \text{Re}_x^{\frac{1}{n+1}}$
<i>Governing ordinary differential equations</i>	
Mass equation	$W_x - \frac{n}{n+1} \eta + \frac{dW_x}{d\eta} + 2 \frac{dW_y}{d\eta} = 0$
Momentum equation	$W_x \left(-\frac{n}{n+1} \eta + \frac{dW_x}{d\eta} + W_x \right) + 2W_y \frac{dW_x}{d\eta}$ $= 1 + 2n \left(\frac{dW_x}{d\eta} \right)^{(n-1)} \frac{d^2 W_x}{d\eta^2}$
Pseudo-similarity energy equation	$\left[-\frac{n}{2(1+n)} \eta W_x(\eta) + W_y(\eta) \right] \frac{\partial \theta(\eta, \zeta)}{\partial \eta}$ $+ \zeta W_x(\eta) g(\eta, \zeta) = \frac{1}{\text{Pr}_x} \frac{\partial^2 \theta(\eta, \zeta)}{\partial \eta^2}$
Pseudo-similarity energy equation	$\left[-\frac{n}{2(n+1)} \eta W_x(\eta) + W_y(\eta) \right] \frac{\partial h(\eta, \zeta)}{\partial \eta}$ $+ W_x(\eta) h(\eta, \zeta)$ $= \frac{1}{\text{Pr}_x} \left[\frac{\partial^2 h(\eta, \zeta)}{\partial \eta^2} - \frac{n-1}{2(n+1)} \left(\frac{\partial^2 \theta(\eta, \zeta)}{\partial \eta^2} \right) \right]$
Boundary conditions	$\eta = 0 : W_x(\eta) = 0, W_y(\eta) = 0, \theta(\eta, \zeta) = 1,$ $h(\eta, \zeta) = 1$ $\eta = \eta_{\delta_t} : W_x(\eta) = 1, \theta(\eta, \zeta) = 0, h(\eta, \zeta) = 0$

23.7 Remarks

This chapter has focused on the heat transfer from an inclined plane surface to an accelerating liquid film of a non-Newtonian power-law fluid. The new similarity analysis method for the accompanying hydrodynamic problem was adopted in combination with a local pseudo-similarity method. The resulting transformed problem turned out to involve only two independent parameters, namely the power-law index n and the local Prandtl number Pr_x . All other parameters, like the streamwise location x , the fluid properties ρ, K, n, λ , and the component of the gravitational acceleration along the wall $g \cos \alpha$, have been combined into the induced Pr_x , the local Reynolds number, and the velocity components W_x, W_y , and $W_y(\eta)$. Accurate numerical results were obtained for various combinations of local Prandtl number

Table 23.4 Summary of the relate expressions on heat transfer of the falling film flow of non-Newtonian power-law fluids

α_x , defined as $\alpha_x = \frac{q_x}{(t_w - t_\infty)}$	$-\lambda_x^{-1}(\text{Re}_x)^{1/(n+1)} \left[\frac{\partial \theta(\eta, \xi)}{\partial \eta} \right]_{\eta=0}$	
$\bar{\alpha}_x$, defined as $\frac{Q_x}{(t_w - t_\infty)A}$	$\frac{2(n+1)}{n+2} \alpha_x$	
Nu_x , defined as $\frac{\alpha_x x}{\lambda}$	$-(\text{Re}_x)^{1/(n+1)} \left[\frac{\partial \theta(\eta, \xi)}{\partial \eta} \right]_{\eta=0}$	
$\bar{\text{Nu}}_x$, defined as $\frac{\bar{\alpha}_x x}{\lambda}$	$\frac{2(n+1)}{n+2} \text{Nu}_x$	
$- \left[\frac{\partial \theta(\eta, \xi)}{\partial \eta} \right]_{\eta=0}$	$a + b \text{Pr}_x^c$	
a	$-0.0086 + \frac{0.0009}{n}$	$(0.2 \leq n \leq 1, \quad 0.001 \leq \text{Pr}_x \leq 1)$
	$-0.0074 - 0.00028n$	$(1 \leq n \leq 2, \quad 0.001 \leq \text{Pr}_x \leq 1)$
	$0.0205 - 0.0845 \times \left(\frac{1}{n}\right)^{\frac{1}{3}}$	$(0.2 \leq n \leq 1, \quad 1 \leq \text{Pr}_x \leq 1000)$
	$-0.12 + 0.079 \times \left(\frac{n}{n+1}\right)^{\frac{1}{2}}$	$(1 \leq n \leq 2, \quad 1 \leq \text{Pr}_x \leq 1000)$
b	$0.485 + 0.00001 \times \left(\frac{1}{n}\right)^{\frac{1}{n}}$	$(0.2 \leq n \leq 1, \quad 0.001 \leq \text{Pr}_x \leq 1)$
	$0.47 + 0.015n$	$(1 \leq n \leq 2, \quad 0.001 \leq \text{Pr}_x \leq 1)$
	$0.518 + \frac{0.0234}{n}$	$(0.2 \leq n \leq 1, \quad 1 \leq \text{Pr}_x \leq 1000)$
	$0.541 + 0.0009n^3$	$(1 \leq n \leq 2, \quad 1 \leq \text{Pr}_x \leq 1000)$
c	$0.399 + \frac{0.008}{n}$	$(0.2 \leq n \leq 1, \quad 0.001 \leq \text{Pr}_x \leq 1)$
	0.407	$(1 \leq n \leq 2, \quad 0.001 \leq \text{Pr}_x \leq 1)$
	$0.3324 + 0.00096 \times \left(\frac{1}{n}\right)^{1.6}$	$(0.2 \leq n \leq 1, \quad 1 \leq \text{Pr}_x \leq 1000)$
	$0.3306 + 0.0027 \times \left(\frac{1}{n}\right)^{1.65}$	$(1 \leq n \leq 2, \quad 1 \leq \text{Pr}_x \leq 1000)$

Pr_x and the power-law index n covering the range of the local Prandtl numbers Pr_x from 0.001 to 1000 and for the power-law index n in the range $0.2 \leq n \leq 2$. Special treatment for the low and high local Prandtl number cases was essential in order to maintain the numerical accuracy. The calculated results obtained both by using local similarity and local pseudo-similarity methods were practically indistinguishable for $n = 1$ over the entire Pr_x range. The main findings can be summarized as follows:

The thickness of the thermal boundary layer decreases monotonically with increasing Pr_x . The thermal boundary layer extends far out in the free stream for $\text{Pr}_x \ll 1$ and is on the other hand confined to the innermost part of the momentum boundary layer for $\text{Pr}_x \gg 1$.

The local heat transfer coefficient and the local Nusselt number depend on the local Reynolds number Re_x and the wall gradient of the dimensionless temperature.

The critical local Prandtl number Pr_x^* is a very important concept for solution of thermal boundary layer, which is closely related to the solution convergence of the thermal boundary layer equation. With increasing the power-law index n , the momentum boundary layer thickness η_{δ_l} will decrease. With increasing the local Prandtl number Pr_x , the thermal boundary layer thickness η_{δ_T} will decrease too. But, with increasing the power-law index n , the thermal boundary layer η_{δ_T} will decrease. With increasing the power-law index n , the critical boundary layer thickness $\eta_{\delta_l}^*$ will decrease, meanwhile, the critical local Prandtl number Pr_x^* will increase. It is also seen that if the power-law index n tends to unity, the critical Prandtl number Pr_x^* also tends to unity with the critical boundary layer thickness $\eta_{\delta_l}^* \rightarrow 5$. It means,

when $n = 1$ and $Pr_x = 1$, the thermal boundary layer thickness η_{δ_t} is identical to the momentum boundary layer thickness η_{δ_l} , and $\eta_{\delta_t} = \eta_{\delta_l} \rightarrow 5$.

For $Pr_x \gg 1$ the wall temperature gradient is controlled by the velocity gradient at the wall, which was practically independent of n for dilatant fluids ($n > 1$) but increased with increasing pseudo-plasticity ($1 - n$).

For $Pr_x \ll 1$ the temperature gradient increased slightly with n and this modest variation was ascribed to the displacing influence of the momentum boundary layer on the external frictionless flow.

A set of accurate curve-fit formulas for the wall temperature gradient is provided in order to enable rapid estimates of the heat transfer rate for any combination of n and Pr_x within the parameter ranges considered.

A special case of the transformation method, velocity component method, used herein has been applied in the previous analysis in part 1 and part 2 of this book for the heat transfer in Newtonian liquid films with consideration of variable fluid properties. The successful generalization on non-Newtonian fluids makes us believe that the present approach should be applicable also to the analysis of heat transfer in power-law films with variable thermophysical properties.

23.8 Calculation Examples

Example:

Continue the example of Chap. 21, a non-Newtonian power-law fluid having a density of 1041 kg/m^3 is flowing with volumetric flow rate of $0.02 \text{ m}^3/\text{s}$ along an inclined flat plate with angle of $\alpha = 30^\circ$ and width of $b = 1 \text{ m}$. The properties of the fluid are thermal diffusivity $a = 13.6 \times 10^{-8} \text{ m}^2/\text{s}$, thermal conductivity $\lambda = 0.41 \text{ W}/(\text{m}^\circ\text{C})$, coefficient of consistency $K = 2.744 \text{ kg s}^{n-2} \text{ m}^{-1}$, and power-law index $n = 0.50$. The plate temperature is kept for $t_w = 60^\circ\text{C}$, and the fluid bulk temperature t_∞ is 20°C .

Calculate the total heat transfer rate Q_x in the boundary layer region. Consider the cases for $\alpha = 30^\circ$ and 0° .

Solution:

Given conditions: volumetric flow rate $V = 0.02 \text{ m}^3/\text{s}$, fluid thermal diffusivity $a = 13.6 \times 10^{-8} \text{ m}^2/\text{s}$, fluid thermal conductivity $\lambda = 0.41 \text{ W}/(\text{m}^\circ\text{C})$, fluid density $\rho = 1041 \text{ kg/m}^3$, plate inclined angle $\alpha = 30^\circ$, fluid coefficient of consistency $K = 2.744 \text{ kg}/(\text{s}^{n-2} \text{ m}^{-1})$, power-law index $n = 0.50$, wall temperature $t_w = 60^\circ\text{C}$, fluid bulk temperature $t_\infty = 20^\circ\text{C}$, and plate with $b = 0.3 \text{ m}$.

The necessary values calculated from the example in Chap. 15: the boundary layer region length $x_0 = 0.118 \text{ m}$ both for $\alpha = 30^\circ$ and 0° .

1. In the case for $\alpha = 30^\circ$

The total heat transfer rate Q_x from wall to fluid in the boundary layer region is calculated as

$$Q = \bar{\alpha}_{x_0}(t_w - t_\infty) \times b \times x_0$$

where $\bar{\alpha}_{x_0}$ is average heat transfer coefficient for the boundary layer region, b is width of the plate, and x_0 is the length of the boundary layer region.

With Eq. (23.23) the average heat transfer coefficient in the boundary layer region is expressed as

$$\bar{\alpha}_{x_0} = -\frac{2(n+1)}{n+2} \lambda x_0^{-1} \left[\frac{\partial \theta(\eta, \zeta)}{\partial \eta} \right]_{\eta=0} (\text{Re}_{x_0})^{1/(n+1)}$$

According to the previous calculated result in Chap. 21, the local Reynolds number is $\text{Re}_{x_0} = 219.4$.

With Eq. (23.17) the local Prandtl number at x_0 is calculated as

$$\begin{aligned} \text{Pr}_{x_0} &= \frac{x_0 w_{x_0, \infty}}{a} (\text{Re}_{x_0})^{-\frac{2}{n+1}} \\ &= \frac{x_0 \sqrt{2gx_0 \cos \alpha}}{a} (\text{Re}_{x_0})^{-\frac{2}{n+1}} \\ &= \frac{0.118 \times \sqrt{2 \times 9.8 \times 0.118 \times \cos 30^\circ}}{13.6 \times 10^{-8}} \times (219.4)^{-\frac{2}{0.5+1}} \\ &= 927.96 \end{aligned}$$

According to the Eq. (23.26), the temperature gradient on the plate is expressed as follows

$$-\left[\frac{\partial \theta(\eta, \zeta)}{\partial \eta} \right]_{\eta=0} = a + b \text{Pr}_{x_0}^c$$

According to Table 23.2, the coefficients a and b and exponent c can be evaluated as below with $\text{Pr}_{x_0} = 927.96$ and $n = 0.5$

$$\begin{aligned} a &= 0.0205 - 0.0845 \times \left(\frac{1}{n} \right)^{1/3} \\ &= 0.0205 - 0.0845 \times \left(\frac{1}{0.5} \right)^{1/3} \\ &= -0.08596 \\ b &= 0.518 + \frac{0.0234}{n} \\ &= 0.518 + \frac{0.0234}{0.5} \\ &= 0.5648 \\ c &= 0.3324 + 0.00096 \times \left(\frac{1}{n} \right)^{1.6} \\ &= 0.3324 + 0.00096 \times \left(\frac{1}{0.5} \right)^{1.6} \\ &= 0.33531 \end{aligned}$$

Then,

$$\begin{aligned} -\left[\frac{\partial\theta(\eta, \zeta)}{\partial\eta}\right]_{\eta=0} &= a + b \text{Pr}_{x_0}^c \\ &= -0.08596 + 0.5648 \times 927.96^{0.33531} \\ &= 5.4979 \end{aligned}$$

Therefore, average heat transfer coefficient from $x = 0$ to x_0 is evaluated as

$$\begin{aligned} \bar{\alpha}_{x_0} &= -\frac{2(n+1)}{n+2} \lambda x_0^{-1} \left[\frac{\partial\theta(\eta, \zeta)}{\partial\eta}\right]_{\eta=0} (\text{Re}_{x_0})^{1/(n+1)} \\ &= \frac{3}{2.5} \times 0.41 \times 0.118^{-1} \times 5.4979 \times (219.4)^{1/(0.5+1)} \\ &= 833.88 \text{ W/(m}^2\text{K)} \end{aligned}$$

The total heat transfer rate Q_x at $x = 0$ to x_0 for the boundary layer region is calculated as

$$\begin{aligned} Q_x &= \bar{\alpha}_{x_0} (t_w - t_\infty) \times b \times x_0 \\ &= 833.88 \times (60 - 20) \times 1 \times 0.118 \\ &= 3935.9 \text{ W} \end{aligned}$$

2. In the case for $\alpha = 0^\circ$

local Reynolds number Re_{x_0} related to x_0 is evaluated as

$$\begin{aligned} \text{Re}_{x_0} &= \frac{x_0^n (w_{x_0, \infty})^{2-n} \rho}{K} \\ &= \frac{x_0^n (2gx_0 \cos \alpha)^{\frac{2-n}{2}} \rho}{K} \end{aligned}$$

According to the previous calculated results in Chap. 21, $x_0 = 0.118$, then,

$$\begin{aligned} \text{Re}_{x_0} &= \frac{0.118^{0.5} (2 \times 9.8 \times 0.118 \cos 0^\circ)^{\frac{2-0.5}{2}} \times 1041}{2.744} \\ &= 245.11 \end{aligned}$$

Also

$$-\left[\frac{\partial\theta(\eta, \zeta)}{\partial\eta}\right]_{\eta=0} = a + b \text{Pr}_0^c$$

While,

$$\begin{aligned}
 \text{Pr}_{x_0} &= \frac{x_0 w_{x_0, \infty}}{a} (\text{Re}_{x_0})^{-\frac{2}{n+1}} \\
 &= \frac{x_0 \sqrt{2gx_0 \cos \alpha}}{a} (\text{Re}_{x_0})^{-\frac{2}{n+1}} \\
 &= \frac{0.118 \times \sqrt{2 \times 9.8 \times 0.118 \times \cos 0^\circ}}{13.6} \times 10^{-8} \times (245.11)^{-\frac{2}{0.5+1}} \\
 &= 860.2
 \end{aligned}$$

According to the above calculations, coefficients a and b , and exponent c are

$$a = -0.08596, b = 0.5648, \text{ and } c = 0.33531$$

Then,

$$\begin{aligned}
 -\left[\frac{\partial \theta(\eta, \zeta)}{\partial \eta} \right]_{\eta=0} &= a + b \text{Pr}_{x_0}^c \\
 &= -0.08596 + 0.5648 \times 860.2^{0.33531} \\
 &= 5.3578
 \end{aligned}$$

The average local heat transfer coefficient $\bar{\alpha}_{x_0}$ from $x = 0$ to x_0 is evaluated as

$$\begin{aligned}
 \bar{\alpha}_{x_0} &= -\frac{2(n+1)}{n+2} \lambda x_0^{-1} \left[\frac{\partial \theta(\eta, \zeta)}{\partial \eta} \right]_{\eta=0} (\text{Re}_{x_0})^{1/(n+1)} \\
 &= \frac{3}{2.5} \times 0.41 \times 0.118^{-1} \times 5.3578 \times 245.11^{1/(0.5+1)} \\
 &= 874.94 \text{ W}/(\text{m}^2 \text{ } ^\circ\text{C})
 \end{aligned}$$

The total heat transfer rate Q_x is calculated as

$$\begin{aligned}
 Q_x &= \bar{\alpha}_{x_0} (t_w - t_\infty) \times b \times x_0 \\
 &= 874.94 \times (60 - 20) \times 1 \times 0.118 \\
 &= 4129.72 \text{ W}
 \end{aligned}$$

References

1. S.M. Yih, M.W. Lee, Heating or evaporation in the thermal entrance region of a non-newtonian laminar falling liquid film. *Int. J. Heat Mass Transf.* **29**, 1999–2002 (1986)
2. G. Astarita, Mass transfer from a flat solid surface to a falling non-Newtonian liquid film. *Ind. Eng. Chem. Fundam.* **5**, 14–18 (1966)
3. R.A. Mashelker, V.V. Chavan, Solid dissolution in falling films of non-Newtonian liquids. *J. Chem. Jpn.* **6**, 160–167 (1973)

4. I. Pop, T. Watanabe, H. Konishi, Gravity-driven laminar film flow along a vertical wall with surface mass transfer. *Int. Comm. Heat Mass Transf.* **23**, 685–695 (1996)
5. D. Ouldhadda, A. Idrissi II, Laminar flow and heat transfer of non-Newtonian falling liquid film on a horizontal tube with variable surface heat flux. *Int. Commun. Heat Mass Transf.* **28**, 1125–1135 (2001)
6. B.K. Rao, Heat transfer to falling power-law fluid film. *Int. J. Heat Fluid Flow* **20**, 429–436 (1999)
7. D.Y. Shang, H. Andersson, Heat transfer in gravity-driven film flow of power-law fluids. *Int. J. Heat Mass Transf.* **42**(11), 2085–2099 (1999)
8. D.Y. Shang, J. Gu, Analyses of pseudo-similarity and boundary layer thickness for non-Newtonian falling film flow. *Heat Mass Transf.* **41**(1), 44–50 (2004)
9. H.I. Andersson, Diffusion from a vertical wall into an accelerating falling liquid film. *Int. J. Heat Mass Transf.* **30**, 683–689 (1987)
10. H. Andersson, D.Y. Shang, An extended study of hydrodynamics of gravity-driven film flow of power-law fluids. *Fluid Dyn. Res.* **22**, 345–357 (1998)
11. E.M. Sparrow, H. Quack, C.J. Boener, Local nonsimilarity boundary-layer solutions. *AIAA J.* **8**, 1936–1942 (1970)

Appendix A

Tables with Physical Properties

Appendix A.1 Physical Properties of Gases at Atmospheric Pressure

T (K)	ρ (Kg/m ³)	c_p [kJ/(kg °C)]	$\mu \times 10^6$ [Kg/(m s)]	$\nu \times 10^6$ (m ² /s)	λ [W/(m °C)]	$\alpha \times 10^6$ (m ² /s)	Pr
Air [1]							
100	3.5562	1.032	7.11	1.999	0.00934	2.54	0.786
150	2.3364	1.012	10.34	4.426	0.0138	5.84	0.758
200	1.7458	1.007	13.25	7.59	0.0181	10.3	0.737
250	1.3947	1.006	15.96	11.443	0.0223	15.9	0.720
300	1.1614	1.007	18.46	15.895	0.0263	22.5	0.707
350	0.9950	1.009	20.82	20.925	0.0300	29.9	0.7
400	0.8711	1.014	23.01	26.415	0.0338	38.3	0.69
450	0.7740	1.021	25.07	32.39	0.0373	47.2	0.686
500	0.6964	1.030	27.01	38.785	0.0407	56.7	0.684
550	0.6329	1.040	28.84	45.568	0.0439	66.7	0.683
600	0.5804	1.051	30.58	52.688	0.0469	76.9	0.685
650	0.5356	1.063	32.25	60.213	0.0497	87.3	0.69
700	0.4975	1.075	33.88	68.101	0.05240	98	0.695
750	0.4643	1.087	35.46	76.373	0.0549	109	0.702
800	0.4354	1.099	36.98	84.933	0.0573	120	0.709
850	0.4097	1.11	38.43	93.8	0.0596	131	0.716
900	0.3868	1.121	39.81	102.921	0.0620	143	0.720
950	0.3666	1.131	41.13	112.193	0.0643	155	0.723
1,000	0.3482	1.141	42.44	121.884	0.0667	168	0.726
1,100	0.3166	1.159	44.9	141.819	0.0715	195	0.728
1,200	0.2920	1.175	47.3	161.986	0.0763	224	0.728

(continued)

(continued)

T (K)	ρ (Kg/m ³)	c_p [kJ/(kg °C)]	$\mu \times 10^6$ [Kg/(m s)]	$\nu \times 10^6$ (m ² /s)	λ [W/(m °C)]	$a \times 10^6$ (m ² /s)	Pr
Monoxide, CO [1]							
200	1.6888	1.045	12.7	7.5201	0.017	9.63	0.781
220	1.5341	1.044	13.7	8.9303	0.0190	11.9	0.753
240	1.4055	1.043	14.7	10.4589	0.0206	14.1	0.744
260	1.2967	1.043	15.7	12.1077	0.0221	16.3	0.741
280	1.2038	1.042	16.6	13.7897	0.0236	18.8	0.733
300	1.1233	1.043	17.5	15.5791	0.025	21.3	0.730
320	1.0529	1.043	18.4	17.4755	0.0263	23.9	0.730
340	0.9909	1.044	19.3	19.4772	0.0278	26.9	0.725
360	0.9357	1.045	20.2	21.5881	0.0291	29.8	0.729
380	0.8864	1.047	21	23.6913	0.0305	32.9	0.719
400	0.8421	1.049	21.8	25.8877	0.0318	36.0	0.719
450	0.7483	1.055	23.7	31.6718	0.0350	44.3	0.714
500	0.67352	1.065	25.4	37.7123	0.0381	53.1	0.710
550	0.61226	1.076	27.1	44.2622	0.0411	62.4	0.710
600	0.56126	1.088	28.6	50.9568	0.0440	72.1	0.707
650	0.51806	1.101	30.1	58.1014	0.0470	82.4	0.705
700	0.48102	1.114	31.5	65.4858	0.0500	93.3	0.702
750	0.44899	1.127	32.9	73.2756	0.0528	104	0.702
800	0.42095	1.140	34.3	81.4824	0.0555	116	0.705
Helium, He [1]							
100	0.4871	5.193	9.63	19.77	0.073	28.9	0.686
120	0.406	5.193	10.7	26.36	0.0819	38.8	0.679
140	0.3481	5.193	11.8	33.90	0.0907	50.2	0.676
160	0.30945	5.193	12.9	41.69	0.0992	63.2	0.6745
180	0.2708	5.193	13.9	51.33	0.1072	76.2	0.673
200	0.2462	5.193	15	60.93	0.1151	91.6	0.674
220	0.2216	5.193	16	72.20	0.1231	107	0.675
240	0.20455	5.193	17	83.11	0.13	124	0.6785
260	0.1875	5.193	18	96	0.137	141	0.682
280	0.175	5.193	19	108.57	0.145	160.5	0.681
300	0.1625	5.193	19.9	122.46	0.152	180	0.68
350	0.1422	5.193	22.1	155.42	0.17	237.5	0.6775
400	0.1219	5.193	24.3	199.34	0.187	295	0.675
450	0.10972	5.193	26.3	239.70	0.204	364.5	0.6715
500	0.09754	5.193	28.3	290.14	0.22	434	0.668
600	0.083615	5.193	32	382.71	0.252	601	0.661
700	0.06969	5.193	35	502.22	0.278	768	0.654
800		5.193	38.2		0.304		
900		5.193	41.4		0.33		
1,000	0.04879	5.193	44.6	914.12	0.354	1,400	0.654
Hydrogen, H ₂ [1]							
100	0.24255	11.23	4.21	19.77	0.067	24.6	0.707
200	0.12115	13.54	6.81	26.35	0.131	79.9	0.704
300	0.08078	14.31	8.96	33.90	0.183	158	0.701
400	0.06059	14.48	10.82	41.69	0.226	258	0.695
500	0.04848	14.52	12.64	51.33	0.266	378	0.691

(continued)

(continued)

T (K)	ρ (Kg/m ³)	c_p [kJ/(kg °C)]	$\mu \times 10^6$ [Kg/(m s)]	$\nu \times 10^6$ (m ² /s)	λ [W/(m °C)]	$a \times 10^6$ (m ² /s)	Pr
600	0.0404	14.55	14.24	60.93	0.305	519	0.678
700	0.03463	14.61	15.78	72.20	0.342	676	0.675
800	0.0303	14.7	17.24	83.11	0.378	849	0.67
900	0.02694	14.83	18.65	96	0.412	1,030	0.671
1,000	0.02424	14.99	20.13	108.57	0.448	1,230	0.673
1,100	0.02204	15.17	21.3	122.46	0.488	1,460	0.662
1,200	0.0202	15.37	22.62	155.41	0.528	1,700	0.659
1,300	0.01865	15.59	23.85	199.34	0.569	1,955	0.655
1,400	0.01732	15.81	25.07	239.70	0.61	2,230	0.65
1,500	0.01616	16.02	26.27	290.14	0.655	2,530	0.643
1,600	0.0152	16.28	27.37	382.70	0.697	2,815	0.639
Nitrogen, N ₂ [1]							
100	3.4388	1.07	6.88	2.000	0.0958	2.6	0.768
150	2.2594	1.05	10.06	4.45	0.0139	5.86	0.759
200	1.6883	1.043	12.02	7.126	0.0183	10.4	0.736
250	1.3488	1.042	15.49	11.48	0.0222	15.8	0.727
300	1.1233	1.041	17.82	15.86	0.0259	22.1	0.716
350	0.9625	1.042	20	20.78	0.0293	29.2	0.711
400	0.8425	1.045	22.04	26.16	0.0327	37.1	0.704
450	0.7485	1.05	23.96	32.01	0.0358	45.6	0.703
500	0.6739	1.056	25.77	38.24	0.0389	54.7	0.7
550	0.6124	1.065	27.47	44.86	0.0417	63.9	0.702
600	0.5615	1.075	29.08	51.79	0.0416	73.9	0.701
700	0.4812	1.098	32.1	66.71	0.0499	94.4	0.706
800	0.4211	1.122	34.91	82.91	0.0548	116	0.715
900	0.3743	1.146	37.53	100.27	0.0597	139	0.721
1,000	0.3368	1.167	39.99	118.74	0.0647	165	0.721
1,100	0.3062	1.187	42.32	138.21	0.07	193	0.718
1,200	0.2807	1.204	44.53	158.64	0.0758	224	0.707
1,300	0.2591	1.219	46.62	179.93	0.081	256	0.701
Oxygen, O ₂ [1]							
100	3.945	0.962	7.64	1.936629	0.00925	2.44	0.796
150	2.585	0.921	11.48	4.441006	0.0138	5.8	0.766
200	1.93	0.915	14.75	7.642487	0.0183	10.4	0.737
250	1.542	0.915	17.86	11.58236	0.0226	16	0.723
300	1.284	0.92	20.72	16.13707	0.0268	22.7	0.711
350	1.1	0.929	23.35	21.22727	0.0296	29	0.733
400	0.962	0.942	25.82	26.83992	0.033	36.4	0.737
450	0.8554	0.956	28.14	32.89689	0.0363	44.4	0.741
500	0.7698	0.972	30.33	39.39984	0.0412	55.1	0.716
550	0.6998	0.988	32.4	46.29894	0.0441	63.8	0.726
600	0.6414	1.003	34.37	53.58591	0.0473	73.5	0.729
700	0.5498	1.031	38.08	69.26155	0.0523	93.1	0.744
800	0.481	1.054	41.52	86.32017	0.0589	116	0.743
900	0.4275	1.074	44.72	104.6082	0.0649	141	0.74
1,000	0.3848	1.09	47.7	123.9605	0.071	169	0.733
1,100	0.3498	1.103	50.55	144.5111	0.0758	196	0.736
1,200	0.3206	1.115	53.25	166.0948	0.0819	229	0.725

(continued)

(continued)

T (K)	ρ (Kg/m ³)	c_p [kJ/(kg °C)]	$\mu \times 10^6$ [Kg/(m s)]	$\nu \times 10^6$ (m ² /s)	λ [W/(m °C)]	$a \times 10^6$ (m ² /s)	Pr
1,300	0.206	1.125	58.84	285.6311	0.0871	262	0.721
Carbon dioxide, CO ₂ [1]							
220	2.4733	0.783	11.105	4.490	0.010805	5.92	0.818
250	2.1675	0.804	12.59	5.809	0.012884	7.401	0.793
300	1.7973	0.871	14.958	8.322	0.016572	10.588	0.77
350	1.5362	0.9	17.205	11.200	0.02047	14.808	0.755
400	1.3424	0.942	19.32	14.392	0.02461	19.463	0.738
450	1.1918	0.98	21.34	17.906	0.02897	24.813	0.721
500	1.0732	1.013	23.26	21.67	0.03352	30.84	0.702
550	0.9739	1.047	25.08	25.752	0.03821	37.5	0.695
600	0.8938	1.076	26.83	30.018	0.04311	44.83	0.668
Ammonia, NH ₃ [2]							
220	0.3828	2.198	7.255	18.952	0.0171	20.54	0.93
273	0.7929	2.177	9.353	11.796	0.022	13.08	0.9
323	0.6487	2.177	11.035	17.011	0.027	19.2	0.88
373	0.559	2.236	12.886	23.052	0.0327	26.19	0.87
423	0.4934	2.315	14.672	29.736	0.0391	34.32	0.87
473	0.4405	2.395	16.49	37.435	0.0476	44.21	0.84
Water vapor [2]							
380	0.5863	2.06	1.271	2.168	0.0246	20.36	1.06
400	0.5542	2.014	1.344	2.425	0.0261	23.38	1.04
450	0.4902	1.98	1.525	3.111	0.0299	30.7	1.01
500	0.4405	1.985	1.704	3.868	0.0339	38.7	0.996
550	0.4005	1.997	1.884	4.704	0.0379	47.5	0.991
600	0.3652	2.026	2.067	5.660	0.0422	57.3	0.986
650	0.338	2.056	2.247	6.648	0.0464	66.6	0.995
700	0.314	2.085	2.426	7.726	0.0505	77.2	1
750	0.2931	2.119	2.604	8.884	0.0549	88.3	1.05
800	0.2739	2.152	2.786	10.172	0.0592	100.1	1.01
850	0.2579	2.186	2.969	11.51221	0.0637	113	1.019
Gas mixture [3]							
t (°C)	ρ (Kg/m ³)	c_p [kJ/(kg °C)]	$\mu \times 10^6$ (Kg/(m s))	$\nu \times 10^6$ (m ² /s)	λ [W/(m °C)]	$a \times 10^6$ (m ² /s)	Pr
0	1.295	1.042	15.8	12.2	0.0228	12.2	0.72
100	0.95	1.068	20.4	21.47	0.0313	21.54	0.69
200	0.748	1.097	24.5	32.75	0.0401	32.8	0.67
300	0.617	1.122	28.2	45.71	0.0484	45.81	0.65
400	0.525	1.151	31.7	60.38	0.057	60.38	0.64
500	0.457	1.185	34.8	76.15	0.0656	76.3	0.63
600	0.405	1.214	37.9	93.58	0.0742	93.61	0.62
700	0.363	1.239	40.7	112.12	0.0827	112.1	0.61
800	0.33	1.264	43.4	131.52	0.0915	131.8	0.6
900	0.301	1.29	45.9	152.49	0.1	152.5	0.59
1,000	0.275	1.306	48.4	176	0.109	174.3	0.58
1,100	0.257	1.323	50.7	197.28	0.1175	197.1	0.57
1,200	0.24	1.34	53	220.83	0.1262	221	0.56

(continued)

(continued)

T (K)	ρ (Kg/m ³)	c_p [kJ/(kg °C)]	$\mu \times 10^6$ [Kg/(m s)]	$\nu \times 10^6$ (m ² /s)	λ [W/(m °C)]	$a \times 10^6$ (m ² /s)	Pr
Water vapor [2]							
380	0.5863	2.06	12.71	21.68	0.0246	20.36	1.06
400	0.5542	2.014	13.44	24.25	0.0261	23.38	1.04
450	0.4902	1.98	15.25	31.11	0.0299	30.7	1.01
500	0.4405	1.985	17.04	38.68	0.0339	38.7	0.996
550	0.4005	1.997	18.84	47.04	0.0379	47.5	0.991
600	0.3652	2.026	20.67	56.6	0.0422	57.3	0.986
650	0.338	2.056	22.47	66.48	0.0464	66.6	0.995
700	0.314	2.085	24.26	77.26	0.0505	77.2	1
750	0.2931	2.119	26.04	88.84	0.0549	88.3	1.05
800	0.2739	2.152	27.86	101.72	0.0592	100.1	1.01
850	0.2579	2.186	29.69	115.12	0.0637	113	1.019
380	0.5863	2.06	12.71	21.68	0.0246	20.36	1.06
400	0.5542	2.014	13.44	24.25	0.0261	23.38	1.04
450	0.4902	1.98	15.25	31.11	0.0299	30.7	1.01
500	0.4405	1.985	17.04	38.68	0.0339	38.7	0.996
550	0.4005	1.997	18.84	47.04	0.0379	47.5	0.991
600	0.3652	2.026	20.67	56.6	0.0422	57.3	0.986
650	0.338	2.056	22.47	66.48	0.0464	66.6	0.995
700	0.314	2.085	24.26	77.26	0.0505	77.2	1
750	0.2931	2.119	26.04	88.84	0.0549	88.3	1.05
800	0.2739	2.152	27.86	101.72	0.0592	100.1	1.01
850	0.2579	2.186	29.69	115.12	0.0637	113	1.019

Appendix A.2 Physical Properties of Some Saturated Liquid

t (°C)	ρ (Kg/m ³)	c_p [kJ/(kg °C)]	$\mu \times 10^6$ [Kg/(m s)]	$\nu \times 10^6$ (m ² /s)	λ [W/(m °C)]	$a \times 10^7$ (m ² /s)	Pr
Ammonia, NH ₃ [4]							
-50	703.69	4.463	306.11	0.435	0.547	1.742	2.6
-40	691.68	4.467	280.82	0.406	0.547	1.775	2.28
-30	679.34	4.467	262.9	0.387	0.549	1.801	2.15
-20	666.69	4.509	254.01	0.381	0.547	1.819	2.09
-10	653.55	4.564	247.04	0.378	0.543	1.825	2.07
0	640.1	4.635	238.76	0.373	0.54	1.819	2.05
10	626.16	4.714	230.43	0.368	0.531	1.801	2.04
20	611.75	4.798	219.62	0.359	0.521	1.775	2.02
30	596.37	4.89	208.13	0.349	0.507	1.742	2.01
40	580.99	4.999	197.54	0.34	0.493	1.701	2
50	564.33	5.116	186.23	0.33	0.476	1.654	1.99
Carbon dioxide, CO ₂ [4]							
-50	1156.34	1.84	137.61	0.119	0.085	0.4021	2.96
-40	1117.77	1.88	131.9	0.118	0.1011	0.481	2.45

(continued)

(continued)

t (°C)	ρ (Kg/m ³)	c_p [kJ/(kg °C)]	$\mu \times 10^6$ [Kg/(m s)]	$\nu \times 10^6$ (m ² /s)	λ [W/(m °C)]	$a \times 10^7$ (m ² /s)	Pr
-30	1076.76	1.97	125.98	0.117	0.1116	0.5272	2.22
-20	1032.39	2.05	118.72	0.115	0.1151	0.5445	2.12
-10	983.38	2.18	111.12	0.113	0.1099	0.5133	2.2
0	926.99	2.47	100.11	0.108	0.1045	0.4578	2.38
10	860.03	3.14	86.86	0.101	0.0971	0.3608	2.8
20	772.57	5	70.3	0.091	0.0872	0.2219	4.1
30	597.81	36.4	47.82	0.08	0.0703	0.0279	28.7
Sulphur dioxide, SO ₂ [4]							
-50	1560.84	1.3595	755.45	0.484	0.242	1.141	4.24
-40	1536.81	1.3607	651.61	0.424	0.235	1.130	3.74
-30	1520.64	1.3616	564.16	0.371	0.230	1.117	3.31
-20	1488.60	1.3624	482.31	0.324	0.225	1.107	2.93
-10	1463.61	1.3628	421.52	0.288	0.218	1.097	2.62
0	1438.46	1.3636	369.68	0.257	0.211	1.081	2.38
10	1412.51	1.3645	327.7	0.232	0.204	1.066	2.18
20	1386.40	1.3653	291.14	0.210	0.199	1.050	2.00
30	1359.33	1.3662	258.27	0.190	0.192	1.035	1.83
40	1329.22	1.3674	229.96	0.173	0.185	1.019	1.70
50	1299.10	1.3683	210.45	0.162	0.177	0.999	1.61
Freon 12, CCl ₂ F ₂ [4]							
-50	1546.75	0.8750	479.49	0.310	0.067	0.501	6.2
-40	1518.71	0.8847	423.72	0.279	0.069	0.514	5.4
-30	1489.56	0.8956	376.86	0.253	0.069	0.526	4.8
-20	1460.57	0.9073	343.23	0.235	0.071	0.539	4.4
-10	1429.49	0.9203	315.92	0.221	0.073	0.550	4.0
0	1397.45	0.9345	299.05	0.214	0.073	0.557	3.8
10	1364.30	0.9496	276.95	0.203	0.073	0.560	3.6
20	1330.18	0.9659	263.38	0.198	0.073	0.560	3.5
30	1295.10	0.9835	251.25	0.194	0.071	0.560	3.5
40	1257.13	1.019	240.11	0.191	0.069	0.555	3.5
50	1215.96	1.0216	231.03	0.190	0.067	0.545	3.5
C ₂ H ₄ (OH) ₂ [4]							
0	1130.75	2.294	65052.05	57.53	0.242	0.934	615
20	1116.65	2.382	21417.35	19.18	0.249	0.939	204
40	1101.43	2.474	9571.427	8.69	0.256	0.939	93
60	1087.66	2.562	5166.385	4.75	0.260	0.932	51
80	1077.56	2.650	3211.129	2.98	0.261	0.921	32.4
100	1058.50	2.742	2148.755	2.03	0.263	0.908	22.4
Mercury, Hg [4]							
0	13628.22	0.1403	1689.9	0.124	8.2	42.99	0.0288
20	13579.04	0.1394	1548.01	0.114	8.69	46.04	0.0249
50	13505.84	0.1386	1404.61	0.104	9.40	50.22	0.0207
100	13384.58	0.1373	1242.09	0.0928	10.51	57.16	0.0162
150	13264.28	0.1365	1131.44	0.0853	11.49	63.54	0.0134
200	13144.94	0.1570	1054.22	0.0802	12.34	69.08	0.0116

(continued)

(continued)

t (°C)	ρ (Kg/m ³)	c_p [kJ/(kg °C)]	$\mu \times 10^6$ [Kg/(m s)]	$\nu \times 10^6$ (m ² /s)	λ [W/(m °C)]	$a \times 10^7$ (m ² /s)	Pr
250	13025.60	0.1357	996.46	0.0765	13.07	74.06	0.0103
315.5	12847.00	0.134	864.6	0.0673	14.02	81.50	0.0083
Water, H ₂ O [2]							
0	999.9	4.217	1752.5	1.7527	0.569	0.13494	12.99
10	999.7	4.193	1299.2	1.2996	0.586	0.13980	9.30
20	998.2	4.182	1001.5	1.0033	0.602	0.1442	6.96
30	995.7	4.179	797	0.8004	0.617	0.14828	5.4
40	992.2	4.179	651.3	0.6564	0.630	0.14953	4.32
50	988.1	4.181	544	0.5450	0.643	0.15408	3.54
60	983.2	4.185	460	0.4679	0.653	0.15870	2.97
70	977.8	4.190	400.5	0.4014	0.662	0.15834	2.54
80	971.8	4.197	351	0.3612	0.669	0.16403	2.20
90	965.3	4.205	311.3	0.3225	0.675	0.16629	1.94
100	958.4	4.216	279	0.2911	0.680	0.16829	1.73
110	951.0	4.229	252.2	0.2652	0.683	0.16983	1.56
120	943.1	4.245	230	0.2439	0.685	0.17110	1.43
130	934.8	4.263	211	0.2257	0.687	0.17239	1.31
140	926.1	4.285	195	0.2106	0.687	0.17312	1.22
150	917.0	4.310	181	0.1974	0.686	0.17357	1.14
160	907.4	4.339	169	0.1862	0.684	0.17373	1.07
170	897.3	4.371	158.5	0.1766	0.681	0.17363	1.02
180	886.9	4.408	149.3	0.1683	0.676	0.17291	0.97
190	876.0	4.449	141.2	0.1612	0.671	0.17217	0.94
200	863.0	4.497	133.8	0.1550	0.664	0.17109	0.91
210	852.3	4.551	127.3	0.1494	0.657	0.16938	0.88
220	840.3	4.614	121.5	0.1446	0.648	0.16713	0.86
230	827.3	4.686	119.7	0.145	0.639	0.16483	1.185
240	813.6	4.770	111.4	0.1369	0.629	0.16208	0.85
250	799.0	4.869	107	0.1339	0.617	0.15860	0.84
260	784.0	4.985	103	0.1314	0.604	0.15455	0.85
270	767.9	5.13	99.4	0.1294	0.589	0.14952	0.86
280	750.7	5.3	96.1	0.1280	0.573	0.14402	0.89
290	732.3	5.51	93	0.1270	0.558	0.14300	0.92
300	712.5	5.77	90.1	0.1265	0.540	0.13136	0.96

Appendix A.3 Temperature Parameters of Gases [5–7]

Gas	n_μ	n_λ	$n_{\mu\lambda}$	n_{c_p}	Temperature Range, (k)	Recommended Pr
Ar	0.72	0.73	0.7255	0.01	220–1,500	0.622
He	0.66	0.725	0.69575	0.01	273–873	0.675
H ₂	0.68	0.8	0.746	0.042	220–700	0.68
Air	0.68	0.81	0.7515	0.078	230–1,000	0.7
CO	0.71	0.83	0.776	0.068	220–600	0.72
N ₂	0.67	0.76	0.7195	0.07	220–1,200	0.71
O ₂	0.694	0.86	0.7853	0.108	230–600	0.733
Water vapor	1.04	1.185	1.11975	0.003	380–800	1
Gas mixture	0.75	1.02	0.8985	0.134	273–1,173	0.63
CO ₂	0.88	1.3	1.111	0.34	220–700	0.73
CH ₄	0.78	1.29	1.0605	0.534	273–1,000	0.74
CCl ₄	0.912	1.29	1.1199	0.28	260–400	0.8
SO ₂	0.91	1.323	1.13715	0.257	250–900	0.81
H ₂ S	1	1.29	1.1595	0.18	270–400	0.85
NH ₃	1.04	1.375	1.22425	0.34	250–900	0.87

Note

1. Component of the gas mixture: CO₂ = 0.13, N₂ = 0.76, and water vapour = 0.11
2. The temperature parameters n_μ , n_λ , and n_{c_p} are defined by simple power-law of gases as follows:

$$\frac{\mu}{\mu_\infty} = \left(\frac{T}{T_\infty}\right)^{n_\mu}, \quad \frac{\lambda}{\lambda_\infty} = \left(\frac{T}{T_\infty}\right)^{n_\lambda} \quad \text{and} \quad \frac{c_p}{c_{p\infty}} = \left(\frac{T}{T_\infty}\right)^{n_{c_p}}$$

where T_∞ is a related reference temperature

3. The overall temperature $n_{\mu\lambda}$ is defined as $n_{\mu\lambda} = 0.45n_\mu + 0.55n_\lambda$

References

1. F.P. Incropera, D.P. Dewitt, *Fundamentals of Heat Transfer* (Wiley, New York, 1981)
2. T. Cebeci, P. Brabshaw, *Physical and Computational Aspects of Convective Heat Transfer* (Springer, New York, 1984)
3. S. Yang, *Heat Transfer, 2nd* (Higher Education Publisher, Beijing, 1987)
4. E.R.G. Eckert, R.M. Drake, *Heat and Mass Transfer*, 2nd edn. (Mcgraw-Hill, New York, 1959)
5. D.Y. Shang, B.X. Wang, Effect of variable thermophysical properties on laminar free convection of gas. *Int. J. Heat Mass Transf.* **33**(7), 1387–1395 (1990)
6. D.Y. Shang, B.X. Wang, Effect of variable thermophysical properties on laminar free convection of polyatomic gas. *Int. J. Heat Mass Transf.* **34**(3), 749–755 (1991)
7. D.Y. Shang, *Free Convection Film Flows and Heat Transfer* (Springer, Berlin, 2006)

Index

π -theorem, 56

A

Absolute temperatures, 75
Absolute viscosity, 48
Absolute viscosity factors, 405
Absolute viscosity of vapor–gas mixture, 370
Absolute viscosity of water, 79
Absolute viscosity ratio, 435
Accelerating laminar flow, 465
Apparent viscosity, 464
Average heat transfer coefficient, 105, 116, 129, 151, 192, 315, 321
Average heat transfer rate, 116, 129, 136, 151, 253, 315
Average Nusselt number, 112, 129, 136, 152, 192, 253, 315, 421

B

Basic dimensions, 56
Basic equations of similarity transformation for inclined case, 188, 189
Basic governing equations, 41
Boundary condition equations, 285
Boundary conditions, 47, 55, 95, 217, 221, 282
Boundary layer thickness, 473
Boundary temperature ratio, 113, 137
Boundary thickness, 478
Boussinesq approximation, 3, 46, 55, 155, 351
Boussinesq approximation solution, 133
Boussinesq solution, 113

Buckingham's π -theorem, 53
Bulk temperature, 152
Bulk vapour mass fraction, 422
Bulk water subcooled grade, 254
Bulk water vapour fraction, 427
Buoyancy factor, 100, 149
Buoyancy term, 40, 97

C

Calculation procedure, 242, 304
Coefficient of consistency, 464
Concentration-dependent densities, 78
Concentration-dependent density factor, 88
Concentration-dependent physical properties of vapor–gas mixture, 2
Concentration-dependent thermal conductivity factor, 85
Concentration-dependent viscosity factor, 89
Condensate film velocity components, 430
Condensate heat and mass transfer, 16
Condensate liquid film thickness, 429
Condensate mass-energy transformation coefficient, 330
Condensate mass-energy transformation equation, 330
Condensate mass flow rate parameter, 326, 430
Condensate mass flow rate parameter ratios, 440
Condensate mass flow rate ratios, 423
Condensate mass transfer analysis, 419
Condensate mass transfer ratios, 440
Condensate water film flow, 401

Consideration of temperature-dependent properties, 11
 Consideration of variable physical properties, 9, 10, 13
 Continuity equation, 27
 Control volume, 27, 29, 33
 Coupled effects of the variable physical properties, 12
 Critical boundary layer, 498
 Critical bulk vapor mass fraction, 408
 Critical film thickness, 478
 Critical local Prandtl number, 498
 Curve-fit equation, 263
 Curve-fit formula, 133
 Curve-fitted correlation, 18

D

Densities of vapour and gas, 402
 Density factor, 403, 405
 Density factor of the vapour–gas mixture, 386
 Dilatant fluid, 516
 Dimension condensate film thickness, 430
 Dimensionless boundary conditions, 103
 Dimensionless condensate velocity components, 321
 Dimensionless coordinate variable, 38, 59, 63, 69, 98, 218, 219, 371
 Dimensionless function variable, 190
 Dimensionless physical parameters, 55
 Dimensionless similarity parameter, 56
 Dimensionless similarity variable, 469
 Dimensionless similarity velocity components, 12
 Dimensionless temperature, 47, 69, 190, 218, 219, 286, 371, 372
 Dimensionless temperature gradient, 105, 129, 152, 253, 283
 Dimensionless temperature variable, 62, 63
 Dimensionless transformation variables, 147
 Dimensionless variable function, 9
 Dimensionless variables, 96, 123
 Dimensionless velocity component, 67, 69, 98

E

Effect of variable physical properties on heat transfer, 112, 137
 Effect of wall inclination, 479
 Effect of wall subcooled grades, 305
 Energy equation, 33
 Entire hydrodynamic entrance region, 18

F

Falkner–Skan transformation, 1, 7
 Falkner–Skan transformation related, 46
 Falkner–Skan type analysis, 5
 Falkner–Skan type transformation, 6, 8, 9, 12, 45, 46, 49
 Falling film flow of non-Newtonian fluids, 2
 Fifth-order Runge–Kutta integration, 406
 Film boiling of subcooled liquid, 216
 Film thickness, 261
 Finite difference method, 9
 Finite element method, 9
 Fluid laminar free convection on inclined plate, 188
 Formulated equations, 110
 Free convection
 boundary layer, 2
 film boiling, 2
 film condensation, 6, 15
 Free convection film condensation of vapour–gas mixture, 16
 Free film condensation of vapour–gas mixture, 16
 Free stream, 477

G

Gas density factor, 403
 Gas temperature parameters, 13
 Gas thermal conductivity factor, 404
 Gas absolute viscosity factor, 404
 Governing conservation equations, 216
 Governing dimensionless equations, 67, 124
 Governing ordinary differential equations, 103, 190, 220, 284
 Governing partial differential conservation equations, 44, 216
 Governing partial differential equations, 47, 54, 97, 123, 372
 for condensate liquid film, 369
 for vapor–gas mixture film, 367
 Grashof number, 47, 58, 219
 Gravity acceleration, 48

H

Heat transfer analysis, 128, 151, 252
 Heat transfer coefficient, 315
 Heat transfer ratio, 427
 Heat transfer under Boussinesq approximation, 137
 Highly pseudo-plastic fluids, 7

I

- Identical mathematical model, 221–222
- Independent variables, 56
- Interfacial matching conditions, 15
- Interfacial physical matching conditions, 1
- Interfacial vapour mass fraction, 16, 407
- Interfacial vapour saturation temperature, 1, 16, 407
- Interfacial velocity components, 262

K

- Kinematic viscosity, 98

L

- Laminar free convection boundary layer, 1, 10, 43
- Laminar free convection film boiling, 15, 242
- Laminar free convection film boiling of subcooled liquid, 217
- Laminar free convection film condensation, 13
- Laminar free convection film condensation of pure vapour, 6
- Laminar free convection film condensation of vapour–gas mixture, 7
- Laminar free convection film flows, 1
- Laminar free convection of gas, 97
- Laminar free film condensation of water vapour–air mixture, 16
- Laser Doppler Velocimeter (LDV), 166
- Limitations of the Falkner–Skan type transformation, 49
- Liquid film, 217, 219, 281, 283
- Liquid film flow, 372
- Liquid free convection, 86
- Liquid subcooled grade, 243
- Liquid–vapour interface, 10
- Liquid–vapour interfacial shear force, 352
- Local condensate mass flow rate, 428
- Local densities, 78
- Local densities of vapour and gas, 402
- Local Grashof number, 58, 98, 218, 283, 371, 372, 419
- Local Grashof number ratio, 426
- Local heat transfer coefficient, 104, 128, 136, 151, 191, 252, 257, 421
- Local heat transfer rate, 104, 111, 128, 136, 151, 191, 252, 257, 314, 318, 420
- Local mass flow rate, 259, 474
- Local Nusselt number, 104, 112, 128, 136, 151, 191, 252, 257, 314, 318, 421
- Local Prandtl number, 17, 494

Local pseudo-similarity approach, 516

Local Reynolds number, 468

Local Schmidt number, 373

Local skin-friction coefficient, 472

M

- Mass flow rate, 474
- Mass flow rate parameter, 320, 321, 326, 461
- Mass flow rate parameter ratio, 435
- Measurement of velocity field of the boundary layer, 18
- Momentum boundary layer thickness, 490
- Momentum equation (Navier–Stokes equations), 29, 38
- Momentum, heat and mass transfer between inclined and vertical cases, relationships of, 191
- Monatomic and diatomic gases, 76

N

- New similarity analysis method, 1, 12, 15, 53, 54, 95, 98
- New similarity variables, 1
- Newtonian fluids, 463
- Newton iteration procedure, 108
- Newton–Raphson shooting method, 107
- Noncondensable gas, 16
- Non-linear governing equations, 152
- Non-linear two-point boundary value problem, 471
- Non-Newtonian dilatant fluids, 464
- Non-Newtonian fluid flow, 7
- Non-Newtonian liquid film flow, 489
- Non-Newtonian power-law fluid, 3, 7, 465, 468
- Non-Newtonian power law liquid film, 465
- Non-Newtonian pseudoplastic fluids, 464
- Non-Newtonian rheology, 516
- Numerical calculation, 152, 242, 406
- Numerical results, 109, 243
- Numerical solution, 110, 129, 304
- Nusselt number, 53, 57

O

- Ordinary differential equations, 47
- Ostwald-de-Waele power-law model, 487

P

- Partial differential equations, 43
- Particulate generator, 167

- Physical property factors, 12, 13, 15, 80, 106, 128, 150, 240, 401, 402
- Polyatomic gases, 122
- Polynomial method, 76, 79, 241
- Polynomials, 150
- Power-law equation, 464
- Power-law fluids, 464
- Power-law index, 464
- Power-law model, 466
- Practical prediction equation
 - of heat transfer, 111, 136
 - on boiling heat transfer, 257, 264
 - on boiling mass transfer, 264
 - on condensation heat transfer, 318
 - on condensation mass transfer, 328
 - on wall dimensionless temperature gradient, 316
- Prandtl number, 53, 58, 76
- Pseudoplastic fluids, 464, 465
- Pseudo-similarity equations, 510
- Pseudo-similarity solution, 515
- Pseudo-similarity transformation, 495
- Q**
- Quantitative grade analysis, 37
- R**
- Ratio of condensate mass transfer, 435
- Rectangular coordinate system, 43
- Reference wall subcooled grade, 408, 422, 424, 434, 435, 440
- Reynolds number, 53, 507
- Runge–Kutta iteration, 107, 471
- Runge–Kutta integration, 107, 471
- S**
- Seventh-order Runge–Kutta integration, 406
- Shear rate, 464
- Shear stress, 470
- Shooting method, 152
- Similarity analysis method, 9, 11, 12, 45, 53, 54, 69
- Similarity intermediate function variable, 45
- Similarity transformation, 123, 147, 148
- Similarity variables, 218, 283
- Simple-power law, 13
- Special bulk vapor mass fraction, 408
- Specific heat of vapor–gas mixture, 470
- Specific heat parameter, 75, 76
- Stream function, 46, 48
- Streamwise length of the boundary layer region, 478
- Subcooled liquid, 217
- Subcooled temperature, 221
- Superheated grade, 239, 242, 248, 251, 254, 261, 262, 271, 301, 310, 313, 321, 326, 341, 353
- T**
- Temperature, 48
- Temperature gradient, 136
- Temperature parameter, 106
- Temperature parameter method, 13, 73, 75, 240
- Temperature-dependent expressions, 150
- Temperature-dependent physical properties, 2, 73, 241, 401
- Thermal and momentum boundary layers, 18
- Thermal boundary layer thickness, 500
- Thermal conductivity, 48
- Thermal conductivity factor, 107
- Thermal conductivity parameter, 75
- Thermal conductivity factor of vapor–gas mixture, 403
- Total heat transfer, 129, 136, 192
- Total heat transfer rate, 104, 112, 129, 136, 151, 192, 252, 258, 314, 319, 320, 421
- Total mass flow rate, 260, 430, 475
- Treatment of temperature-dependent physical properties of liquid film, 401
- Treatment of variable physical properties, 75, 150, 240, 302
- Two-dimensional basic conservation equations, 45
- Two-dimensional boundary layer, 46
- Two-phase boundary layer, 283
- Two-phase flow phenomenon, 11
- Two-phase laminar film condensation, 15
- Two-point boundary value problem, 46, 107
- Typical experimental data, 79
- V**
- Vapor bulk superheated grade, 326
- Vapor density factor, 403
- Vapor film, 218, 283, 417
- Vapor mass diffusion coefficient in the non condensable gas, 370
- Vapor mass fraction, 370, 407
- Vapor relative mass fraction, 372
- Vapor saturation temperature, 407
- Vapor superheated grade, 310, 316

Vapor thermal conductivity factor, 404
Vapor viscosity factor, 404
Vapor–gas mixture, 370, 390, 402
Vapor–gas mixture film, 372
Vapor–gas mixture film flows, 15, 373
Vapourid film, 282
Variable physical properties, 1, 12, 54, 241, 400
Variable physical properties of liquids, 150
Variable temperature-dependent properties, 10
Variable thermophysical properties, 4
Velocity and temperature fields, 243
Velocity fields of liquid film, 305
Viscosity factor, 85
Viscosity factor of vapour–gas mixture, 404
Viscosity parameter, 75

W

Wall dimensionless temperature gradient, 315, 422, 424
Wall subcooled grade, 310, 316, 326
Wall subcooled temperature, 425, 427
Wall subcooled temperature ratio, 426, 427
Wall superheated grade, 242, 243, 261
Wall temperature, 153
Wall temperature gradient, 510
Wall temperature gradient ratio, 427
Water subcooled grade, 242, 243, 254, 263
Water vapor superheated grade, 305
Whole physical variables, 55